AN INVESTIGATION OF THE INFLUENCE OF RHEOLOGICAL FACTORS ON THE RELEASE OF DRUGS FROM PHARMACEUTICAL SEMISOLIDS

by

MADHUSUDAN SAVCHAND KHANDERIA

615.0153 KHA
203621 - 1 APR 1977

A Thesis submitted for the Degree of

Doctor of Philosophy

in the Department of Pharmacy of

The University of Aston in Birmingham

September 1976

ABSTRACT

Many factors can affect the release of a drug from an ointment base. Some authors have suggested that rheological properties can be an important consideration. Unfortunately the literature is not clear on this point. In all studies where 'viscosity' has been implicated, the formulated bases contained various complex components and it is not sensible to ascribe observed changes in release rate to rheological properties alone.

In order to clarify the role of rheological factors the release of salicylates from liquid paraffin-polyethylene gels (Plasti-bases) has been studied. These bases were chosen on the grounds that the drug-vehicle interactions were minimal and that bases of variable rheological properties were available. At a given concentration, the chemical potential of the drug in the base was constant and thus changes in release rate depended solely on rheological factors.

The ointment bases were viscoelastic and rheological properties were characterised using continuous shear, creep and oscillatory testing. Various relationships between apparent viscosity, yield value, dynamic viscosity, dynamic modulus and polyethylene content of the bases were obtained. Methods of altering rheological parameters in the design of topical preparations were also investigated.

The release of the drug *in vitro* into an aqueous sink was linearly related to the reciprocals of the apparent viscosity and the dynamic viscosity (measured at low test frequency) when the drug was

in suspension in the base (salicylic acid). In vitro drug release was independent of viscosity when the drug was in solution in the base (methyl salicylate). These results were confirmed by in vivo studies on human volunteers from skin irritation and urinary excretion data.

It was concluded that the viscosity of the base became an important factor when dissolution of the drug in the vehicle was a rate determining factor. The rheological environment as seen by the diffusing drug molecule was different to that determined using a conventional viscometer or fundamental methods (creep and dynamic testing), however, simple relationships between microviscosity and macroviscosity were derived.

ACKNOWLEDGEMENTS

I am grateful to Professor S S Davis for the supervision of this work. I am also grateful for the encouragement given by Professor M R W Brown and Dr J B Kayes.

I thank the University of Aston in Birmingham for the award of the research studentship held during the course of this work. I would also like to thank Messrs E R Squibb & Sons for the generous supply of Plastibases and Dr B Warburton of the School of Pharmacy, University of London, for providing facilities for the oscillatory testing of Plastibases.

I also wish to acknowledge the help of the following:- Mrs Griffiths of RAPRA for carrying out Differential Scanning Calorimetry of Plastibases, Mr S Ludlow for obtaining X-ray diffraction photographs of Plastibases, Mrs C A Preston for an independent assessment of *in vivo* skin irritation reactions and Mr M Williams and Mr Howard for technical assistance.

Finally, I would like to thank Miss M Stevens for typing this thesis.

MEMORANDUM

This thesis, which is being submitted for the Degree of Doctor of Philosophy of the University of Aston in Birmingham, is an account of the work carried out in the Department of Pharmacy of the University of Aston in Birmingham under the supervision of Professor S S Davis.

Except where acknowledged by reference in the text, the work described herein is claimed to be original and has not been submitted for any other award.

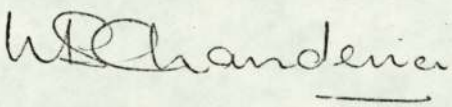

M S Khanderia

September 1976

CONTENTS

PART B

RHEOLOGICAL CHARACTERISATION OF PLASTIBASES AND THE EFFECT OF FORMULATION ON THE CONSISTENCY OF THESE VEHICLES

PART C

RELEASE OF DRUGS FROM PLASTIBASES

PART A

GENERAL INTRODUCTION

1 INTRODUCTION

1.1 Role of Rheological Investigation in Formulation of Pharmaceutical Semisolids

Many pharmaceutical products take the form of 'semisolids'. Examples include ointments (non-aqueous), creams and gels. The important physical properties of these systems can be defined by various fundamental rheological parameters that define deformation and flow (elasticity and viscosity) although in general discussion it is helpful to employ a more subjective term 'consistency' to describe in qualitative terms the 'thickness' or 'thinness' or 'body' of a semisolid material. Investigation of rheological properties of semisolid pharmaceutical preparations has been the subject of considerable research in the last few years. Such investigations can provide information that will be of great value in evaluating

(i) the rheological character of basic raw materials (ingredients) prior to formulation;

(ii) the effect of formulation factors and of ingredients on consistency;

(iii) the effect of production scale-up processes, e.g. stirring, mixing, milling, pumping, etc., on consistency;

(iv) the physical stability of formulated and final product on storage;

(v) the quality of raw materials used as ingredients and the final product for control purposes;

(vi) the effect of sterilisation processes on the consistency of a product, e.g. γ irradiation;

(vii) the behaviour of the material under use conditions and

sensory assessment of the product, e.g. spreadability, skin adherence, etc.;

(viii) the effect of consistency on drug release and availability to body tissues and fluids (bioavailability).

While much work has been published in this area, attention has not often been drawn to the fact that a thorough investigation of rheological properties is essential at almost each and every stage of the design, development and manufacture as illustrated in Table 1 of the semisolid dosage form.

1.2 Assessment of Consistency for Elegance or Efficacy?

The assessment of consistency in the formulation of a semisolid pharmaceutical product had, all too often, simply been directed at improving the cosmetic acceptability of the finished product. For example, Langenbucher et. al. (1) have emphasised that "the final purpose of a rheological consistency assessment is the establishment of simple correlation between physical quantities and the sensory response of the average consumer". Martin et. al. (2) have reported that "no class of pharmaceutical product is subjected to a closer or more critical evaluation by the consumer in the course of their use than are ointments, creams, pastes and gels. The pharmaceutical elegance of all topical semisolid preparations is most directly related to consistency". In a similar fashion, Worthington (3) considers that "an important feature of elegant semisolid preparations is that they have the right 'viscosity'*. Products should spread readily when applied by

---

* In pharmaceutical literature, the term 'viscosity' is often used to describe the 'consistency' of a semisolid product. The reference to

TABLE 1

STAGES IN THE DESIGN, DEVELOPMENT AND MANUFACTURE OF PHARMACEUTICAL SEMISOLIDS

WHERE RHEOLOGICAL EVALUATION IS CONSIDERED NECESSARY

PREFORMULATION	DESIGN, FORMULATION AND EVALUATION	PILOT PLANT AND PRODUCTION SCALE-UP PROCESSES	PILOT PLANT AND PRODUCTION SCALE-UP QUALITY CONTROL
1. Characterisation of ingredients. 2. Stability of ingredients.	1. Design and formulation of test products. 2. Physical stability of test products. 3. Sterilisation of test product. 4. Bioavailability. 5. Sensory Assessment.	Identify effect on rheological properties of product due to:- (i) Heat exchange (ii) Pumping (iii) Stirring (iv) Mixing (v) Milling (vi) Aeration (vii) Extrusion and filling (viii) Sterilisation	1. Quality control of ingredients. 2. Characterisation of products. 3. Storage stability. 4. Consumer sensory assessment. 5. Therapeutic evaluation.

hand to inflamed or damaged skin surfaces and yet be sufficiently viscous at skin temperatures so as not to run off the skin surface after application. The viscous properties should also allow convenient withdrawal of the product from the pack (usually a tube). Careful selection of the type, grade and proportions of ingredients used in topical preparations allows these demanding rheological criteria to be met". Thus it is that much of the work carried out on the assessment of consistency has been aimed, directly or indirectly, at improving the pharmaceutical and cosmetic elegance of the product.

While it cannot be denied that the pharmaceutical elegance of a product is an important factor to the pharmacist and the patient, it is improper to formulate primarily for elegance. Semisolid products are designed to deliver therapeutic agents and as such the therapeutic effectiveness of these products must be of prime concern. Hence the investigation of the consistency of semisolids must also relate to the therapeutic effectiveness of the product.

1.3 Influence of Rheological Factors on Drug Availability - Literature Search

Reference has often been made in literature to the influence the rheological properties of a semisolid product may have on drug release and bioavailability. Eros et. al. (4) stated that "suitable rheological characteristics are very important as they will determine the manner in which an effective agent is liberated from the ointment

---

'viscosity' in this context is a misnomer and henceforth where such usage is encountered, it will be referred to as 'viscosity' (i.e. in inverted commas).

and depending on this, suitable therapeutic effect can be expected". Similarly Martin and others (5) have commented that "the rheology of a particular product, which can range in consistency from fluid to semisolid to solid, can affect its patient acceptability, physical stability and even biological availability".

Van Abbe (6) and Idson (7) have stated that the choice of a vehicle should take into account physical properties such as 'viscosity' as this is a drug vehicle factor of importance. Van Abbe (6, 8) considers that a less 'viscous' vehicle will be able to have a more intimate contact with sebum thus enhancing penetration however when a fairly thick layer is applied to the skin, there is no likelihood that the drug in the upper regions of this layer will have any affect at all; 'viscosity' is therefore a relevant factor. Skauen et. al. (9) were among the first to report that the consistency of semisolid vehicles could influence the release of drugs which they contain. "A greater release of active ingredients was generally possible from a softer, less 'viscous' base". In a review article, Munzel (10) has stated that viscosity enhancing agents that are used to modify consistency and permeability to obtain greater physical stability can retard drug absorption.

Higuchi (11), Wurster (12), Wagner (13) and Gibaldi (14) have all drawn attention to the Stokes-Einstein inverse relationship between viscosity and the diffusion coefficient. Wurster (12) has emphasised that although the relationship may not hold rigidly for the complex systems used in ointment bases, it can be assumed that a decrease in the 'viscosity' would yield an increased diffusion coefficient for the drug in the ointment base.

Sherman (15) has observed that a relationship exists between the water content, degree of dispersity, rheology and drug release characteristics of water/oil emulsions. He says "that when a standard procedure is used to prepare a water/oil emulsion based product, the degree of dispersity depends upon the water content. It is highest when the water concentration is at its lowest level, and it decreases as the water content increases. Release of medicament improves as the degree of dispersity decreases. Since the degree of dispersity influences the rheological properties of an emulsion, the latter should also directly influence the rate of medicament release".

Temperature, through its effect on consistency, has also been noted to affect drug release from semisolids. Larry and Hymnimen (16) have observed that under cold weather conditions, petrolatum base ointments are difficult to extrude from an ointment tube and when instilled into the eye by application to the lower eyelid they exhibit poor drug release of the medicament. Barr (17) considers that an increased absorption due to an increase in temperature probably results due to a lowering of the viscosity of the sebum which would facilitate its mixing with the innuncted preparation.

Katz and Poulsen (18) have stated that "when a poorly soluble drug is suspended in an ointment vehicle, relatively minor changes in vehicles composition, to reduce the 'viscosity' (thus favourably changing the diffusion coefficient and/or increasing the solubility) may markedly increase the release rate".

Occasionally reports concerning lack of correlation between the 'viscosity' of pharmaceutical products with their therapeutic activity have also appeared in literature. Giroux and Schrenzel (19) investigating organogel type bases showed no correlation between 'viscosity' of the base and drug release. Brocades Pharmaceuticals on their product De-Nol state that the 'viscosity' of the product is of no significance in terms of the therapeutic properties of the product (20, 20a). Nogami and Hanano (21) used benzene-vehicle partition coefficients to correlate vehicle effects to in vivo percutaneous absorption of salicylic acid, and found that 'viscosity' of the vehicle had no effect on the absorption.

While much has been said of the influence of the 'viscous' character of the product in determining drug release and absorption, few, if any, reports of original fundamental work relating the parameters have appeared in literature. This is somewhat surprising as a comprehensive literature survey reveals that separate interests in studying rheological properties of and drug release from semisolid pharmaceuticals has not been lacking. The reports gathered from literature of attempts at correlating the two sets of parameters have been listed in Table 2. In order to make the list comprehensive details of rheological parameters measured, the drug-vehicle system used, the drug release method and the statement on correlation attained have all been included. Some references relating to non-semisolid systems have also been included for comparison.

From a detailed analysis of the studies listed in Table 2, several points are clear:-

TABLE 2

REPORTS INFERRING SUCCESSFUL CORRELATION OF RHEOLOGICAL PROPERTIES AND DRUG RELEASE PARAMETERS

AUTHOR	DRUG-VEHICLE SYSTEMS	RHEOLOGICAL METHOD AND PARAMETERS	DRUG RELEASE METHOD	AUTHOR'S COMMENTS ON 'VISCOSITY'-DRUG RELEASE CORRELATION
Wood J.A. et. al. (22)	Various combinations of S.A.A., P.E.G., Liquid Paraffin, sterylalchol, preserved water. Salicylic acid and sodium salicylate.	Brookfield Synchro-lectric viscometer. Apparent viscosity.	In vitro Diffusion cell.	The rate of diffusion was very closely related to the 'viscosity' of the medium.
Khristov K. (23)	Emulsion ointment bases prepared with cottonseed oil, Ca^{++} soap and petrolatum. Chloralhydrate.	Rotational visco-meter PR-4. Yield value, plastic viscosity.	In vivo Using rats.	The relation between structural-rheological indexes of the bases and rate of absorption of medicaments showed that the rate of absorption increased with decreasing values of the indexes.
Norn M. (24)	Dyes.	Not stated.	Not stated.	The therapeutic action and any side effects of a drug depend on the consistency of the vehicle.
Levy & Jusko W.J. (25)	Ethanol, salicylic acid and methyl-cellulose solutions.	Epprecht Rheomat "15".	In vivo Stomach of rats.	It was found that both the rate of movement of drug molecules to the absorption membrane and the rate of G.I. transit of the solution were decreased with increasing viscosity.
Khristov K. (26)	Emulsion ointment bases: petrolatum/ Tween systems. Salicylic acid.	Rotational visco-meter PR-4. Yield value, plastic viscosity.	Agar plate method.	There exists a close relationship between the structural-rheological properties of vaseline and its mixtures with Tween 80 on the one hand and the release rate of the drug on the other. With decrease in the yield values and plastic viscosity values, the release rate of the drug increased.
Khristov K. & Draganova L. (27)	Emulsion ointment bases prepared with goat fat, cotton-seed oil and lanolin.	Rotational visco-meter PR-4. Yield value, plastic viscosity.	Agar plate method.	The velocity of drug release clearly rises with a decrease in the static viscosity, i.e. they are inversely proportional.
Cid E. (28)	Emulsion ointment bases prepared with Tweens, alchol, liquid paraffin, propylene glycol and water. Tetracaine.	Not described.	In vivo method Rabbits - local anaesthetic effect. In vitro Through cellophane membrane.	When the study of the influence of 'viscosity' in the diffusion of tetracaine took place, it was possible to verify that the diffusion of tetracaine decreases when the medium 'viscosity' increases. The influence of the tensioactive would be due more to the change in the 'viscosity' of the medium than to the nature of the tensioactive.
Voigt R. & Falk G. (29)	Suppositories. 35 drugs.	Subjective rheological evaluation.	In vitro Diffusion cell.	The addition of a 2% viscosity increasing additive such as Arlacel 161, Aluminium stearate or Aerosil had an inhibiting effect on the release of very soluble drugs but only a slight effect or none on the hard to dissolve drugs.
Khristov K., Cluzman M. & Levitskaya I. (30)	Emulsion ointment bases prepared with Ca^{++} soap, liquid paraffin/hydroxy-propylmethyl-cellulose gel.	Rotational visco-meter PR-4. Yield value, plastic viscosity.	Agar plate method.	An inverse correlation exists between values of the rheo-logical parameters of the base and the release rate of medical substances.
Khristov K. (31)	Emulsion ointment base with oil phase: liquid paraffin/ cottonseed oil/castor oil/sunflower oil. Iodine, chloral hydrate.	Rotational visco-meter PR-4. Yield value, plastic viscosity.	Agar plate method and radioactive isotope method.	A strong correlation between rheological parameters of ointments and the rate of liberation and absorption of drugs incorporated in them was found. The lower the 'viscosity' of an ointment, the higher the rate of liberation.
Khristov K. (32)	Bone fat.	Rotational visco-meter PR-4. Yield stress, plastic viscosity.	Agar plate method.	The base had low rheology indices which enabled a very fast release of medicinal compounds.
Block L.H. & Lamy P.P. (33)	Na^{+}CMC, gastric mucin, hydroxypropyl cellulose. Salicylic acid, Antipyrine, Aminopyrine.	Ostwald Capillary viscometer and Rotovisco.	In vitro model due to LAMY (34) PhD Thesis 1964 Philadelphia College of Pharmacy, Philadelphia, Pennsylvania.	The viscosity of the cellulosic ether solutions appeared to play a predominant role in the depression of drug transfer rate.

TABLE 2 (continued)

AUTHOR	DRUG-VEHICLE SYSTEMS	RHEOLOGICAL METHOD AND PARAMETERS	DRUG RELEASE METHOD	AUTHOR'S COMMENTS ON 'VISCOSITY'-DRUG RELEASE CORRELATION
Khristov K., Gluzman M., Todorova P. & Daschevskaja I. (35)	Emulsion ointment bases prepared with polyethylene glycols/ hydroxypropylmethyl-cellulose. Zinc oxide, Boric acid and Bismuth gallate or nitrate.	Rotational viscometer PB-4. Yield value, plastic viscosity.	Agar plate method.	The 'viscosity', flow point and cloud point of the ointments decreased and the medicament release rate increased as the proportion of hydroxypropylmethylcellulose-water hydrogel in the compositions increased.
Baichwal M.R. & Lohit T. (36)	Cocoa butter mixtures for suppository bases. Salicylic acid, Boric acid and copper sulphate.	Stormer viscometer. Viscosity index for pseudoplastic flow.	In vitro Saline flow over suppository on cotton wool plug.	Drug release from suppositories was related inversely to the consistency of the bases.
Eros I. et. al. (4)	Propylene glycol emulsion bases. Sulphadimidine, chloramphenicol.	Rotovisco. Extrusion force, spreadability, adhesiveness.	Microbiological method.	Sulphadimidine and chloramphenicol ointments of optimal rheological properties have been prepared; their release rates complied with the requirements.
Popovicia A. & Ionescu N. (37)	Five ointment bases. Hydrocortisone acetate.	Penetrometer and Extensiometer.	In vivo Anti-inflamatory effect on the granulation tissue induced by subcutaneous implant.	The adequate rheological properties of ointment bases influence the penetration of corticosteroids. From Short & Rhodes (38) Pharmazie 1973, 28/8, 509. "The Rheological Properties of Ointment Bases Influenced Corticosteroid Absorption".
Whitworth C.W.& Stephenson R.E. (39)	Four multi-component ointment and emulsion vehicles. Atropine.	Brookfield Synchrolectric viscometer. Brookfield viscosity units.	In vitro Polyethylene cup - membrane - water.	The 'viscosity' of each mixture was determined and in some instances, appeared to correlate with the diffusion rates.
Eros I. & Kedvessy G. (40)	Ointment bases comprising petrolatum and microcrystalline paraffin. Salicylic acid.	Parallel plate Plastometer. Structure - viscosity index and yield stress.	Agar plate method.	In the case of the ointments tested, a direct relationship exists between structure-viscosity index, yield stress and diameter of the ring indicating diffusion of the drug.
Ritschel W.A. et. al. (41)	Sodium-carboxymethylcellulose solutions. Sodium phenobarbitol.	Not stated.	L.D. 50 in male white Swiss mice.	In reporting L.D. 50 data, it is essential to state the exact composition of the vehicle because by using viscosity increasing agents as dissolution or suspension media the L.D. 50 decreases.
Whitworth C.W.& Stephenson R.E. (42)	Four multi-component emulsion vehicles. Atropine.	Brookfield Synchrolectric viscometer Model RVT. Brookfield viscosity units.	In vitro Polyethylene cup - membrane - water.	The 'viscosity' of each mixture was determined and in some instances appeared to correlate with diffusion results.

(a) Drug-Vehicle Systems Used

(i) Most studies have employed complex multi-component vehicles disregarding the possibility of inter-component interactions.

(ii) The nature and character of the formulations being compared have often differed, e.g. simple and multi-component bases have been compared with water/oil or oil/water emulsion bases.

(iii) There would often appear to be no rationale exercised in the choice of drug or drugs used in the studies, e.g. familiarity and ready availability seem to have been the deciding factors in preference to physicochemical considerations.

(b) Rheological Parameters Measured For Correlation

(i) Instruments such as the Brookfield viscometer, penetrometer, etc., used for the measurement of rheological parameters have often been of empirical nature.

(ii) Parameters measured such as Brookfield viscometer units, penetration depths, etc., have had no fundamental significance when applied to semisolids.

(iii) The technique of measurement has not corresponded to the conditions of use, e.g. Brookfield viscometer units have no significance in relation to the undisturbed state of a semi-solid or the behaviour of the material under use conditions.

(c) Drug Release Test Method

(i) Studies have not been appropriate for the release process

being investigated, e.g. microbiological and agar plate methods have been used to simulate the process of percutaneous absorption.

(ii) The treatment of results has often overlooked fundamental considerations, e.g. similar treatment of drug release from simple and emulsion ointment bases with the drug either in solution or suspension has made the results invalid.

The above mentioned points are best illustrated by considering a few specific examples. For instance Figure 1 is a plot of diffusion rate constants derived from drug release experiments on four semisolid vehicles each comprising up to six different components, versus 'viscosity' of the vehicles determined using the Brookfield viscometer. The authors (39) of this work claim that "the 'viscosity' of each mixture was determined and in some instances, appeared to correlate with the diffusion rates". Two vehicles used in this work were of emulsion type and the other two were of ointment type. No attempt was made to distinguish between the emulsion and ointment vehicles in the analysis of the results. In several investigations of physical properties of ointment bases (23, 26, 29, 30, 31, 34) Khristov and associates have reported an inter-relationship between rheological characteristics and drug release. Figure 2 illustrates one such report (29) where yield stress and plastic viscosity are correlated with the diffusion of drug in agar gel. Mixtures of hydroxypropylmethylcellulose, water, calcium soap, liquid paraffin and cotton seed oil in various proportions were used as vehicles. Rheological parameters in this study were measured using a rotational viscometer and appear to bear no fundamental significance. The authors of this work state that "an inverse

FIGURE 1

RELATIONSHIP BETWEEN DIFFUSION CONSTANTS AND 'VISCOSITY'

After Stephenson and Whitworth, 1971. (39)

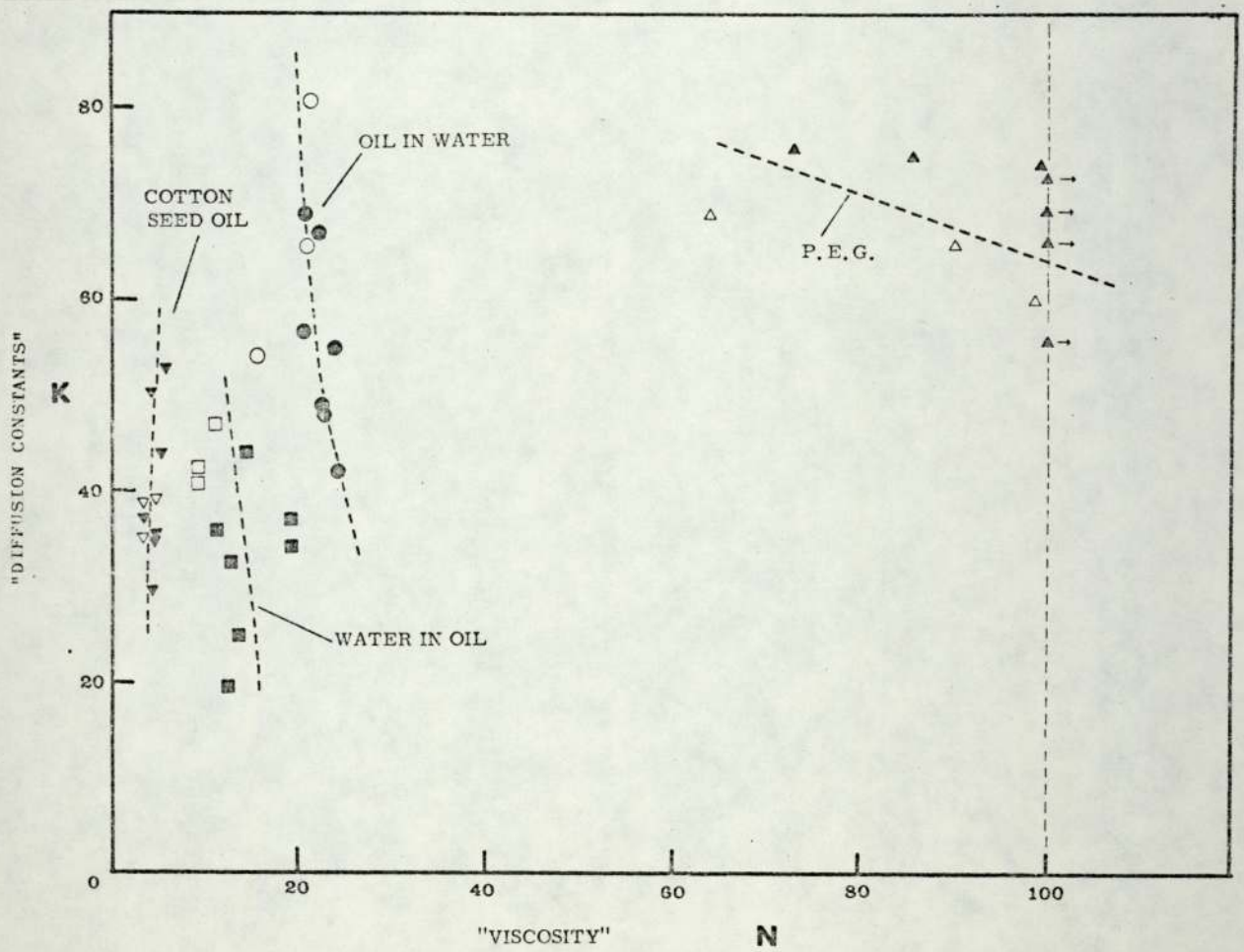

FIGURE 2

RELATIONSHIP BETWEEN STRUCTURAL-RHEOLOGICAL

INDEXES AND DRUG RELEASE

After Khristov et. al. (29)

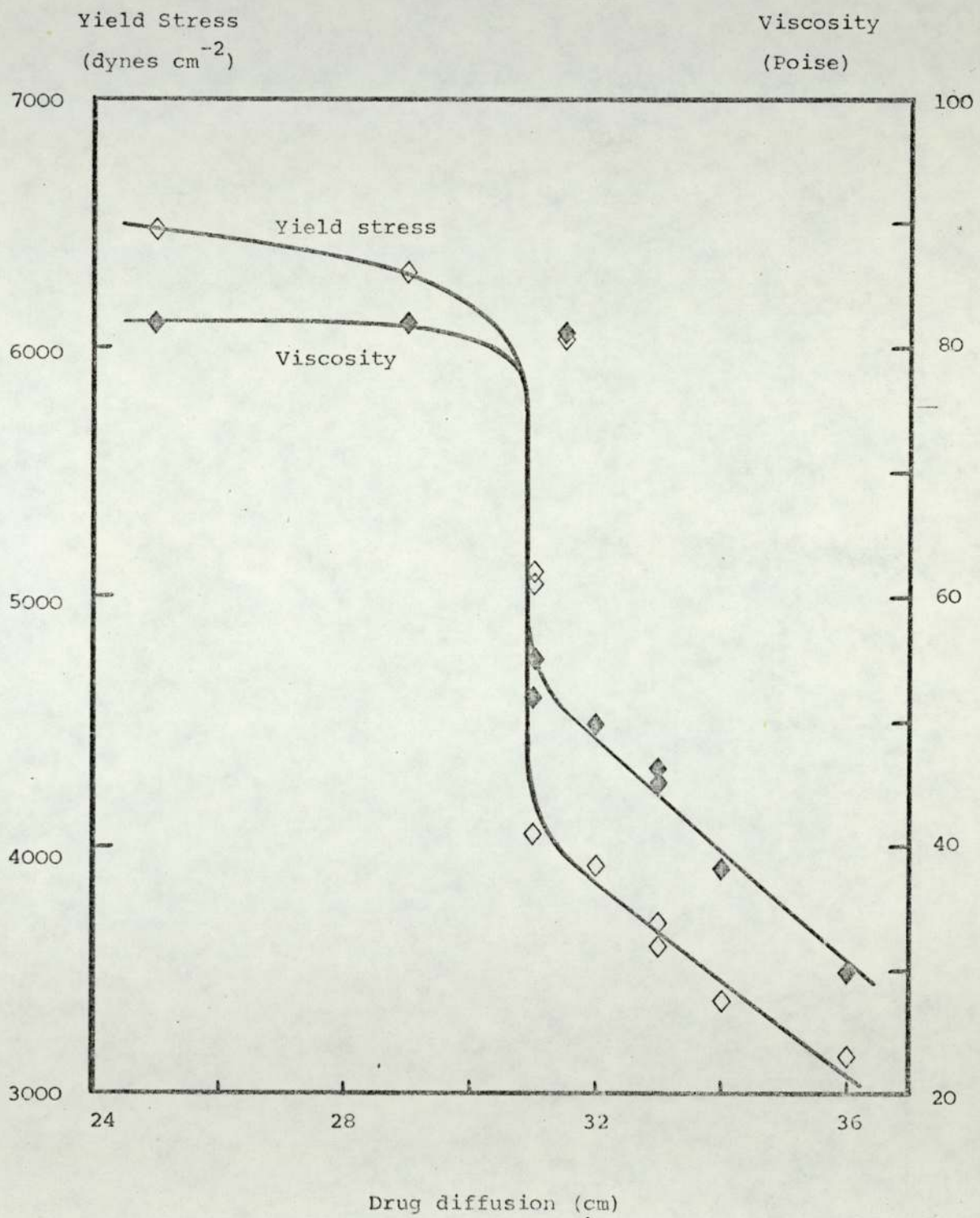

correlation exists between the values of the rheological parameters and the release rate of medical substances". Finally Figure 3 illustrates the work of Eros and Kedvessy (40) showing "a direct relationship between structure-viscosity index, yield stress and diameter of ring indicating diffusion of salicylic acid in agar gel". Rheological parameters in this study were measured using a form of a parallel plate plastometer and appear to bear no fundamental significance.

The three examples quoted above are typical of all the studies listed in Table 2. It is evident that the complex composition of the vehicles, the character of the formulations and the physical state of the drug in the base introduce drug-ointment base interactions which make it difficult, if not impossible, to delineate any changes in drug diffusion and release due to rheological factors. Moreover it would appear that in none of these studies has any attempt been made to answer the fundamental question "What is the real rheological environment as seen by a diffusing drug molecule and how can it be determined?" Thus it is not surprising that the results of these studies have not been conclusive.

It is interesting to note however that while no quantitative mathematical relationships have been proposed correlating rheological parameters with drug availability, the fact that the studies listed in Table 2 have yielded any trends at all must signify the importance of rheological contribution in drug release. It is clear therefore that in order to determine and define the nature and extent of rheological effects in drug release, a fundamental investigation comprising rheological characterisation and drug release behaviour of 'model' semi-solid systems must be undertaken.

FIGURE 3

RELATIONSHIP BETWEEN STRUCTURE-VISCOSITY

INDEX, YIELD STRESS AND DRUG RELEASE

After Eros and Kedvessy, 1972. (40)

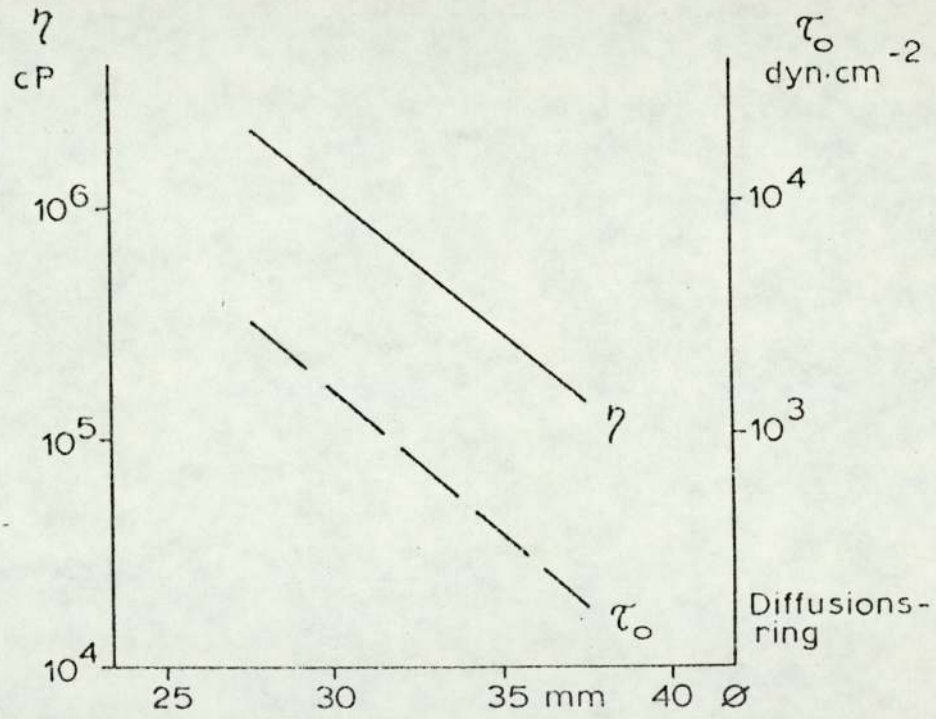

2 RHEOLOGICAL CONSIDERATIONS

2.1 Nature of Semisolids

Semisolid materials exhibit complex rheological properties that comprise both liquid and solid behaviour. In no way can they be said to exhibit ideal (Newtonian or Hookean) characteristics. The non-ideal behaviour exhibited by these materials is referred to as visco-elasticity. Characterisation of these materials is thus not simple as derivation of meaningful results invariably involves the determination of a multipoint consistency curve or the study and definition of constituent characteristics. Unfortunately, in much published work the dominant viscoelastic nature of materials such as ointments and creams has not been recognised or has simply been ignored and rheological testing has been performed on the implicit assumption that these materials are at the most anomalous liquids, i.e. non-Newtonian fluids (43).

2.2 Measurement of Rheological Properties of Semisolids

Martin (5) has reported that the subjective testing of "proper consistency" by trained personnel has often been the method of evaluation used in many industries. However, the variability of subjective tests at different times under varying conditions is well recognised. A more serious objection from a scientific standpoint is the failure of subjective methods to distinguish the various properties which comprise the total consistency of the product.

For the same reason, the use of a 'one-point' instrument to characterise a semisolid can be quite meaningless. It is sometimes

argued that although a 'one-point' measurement cannot characterise the rheological properties of a system, it does provide a reproducible value with sufficient precision for industrial control purposes. Green (44) has insisted that this argument is spurious and Martin (2) has shown that the 'one-point' method is inadequate even for controlling the quality of successive batches of a product of a definite rheological class.

Empirical instruments have often been used in the investigation of the rheological properties of semisolid pharmaceuticals. They usually operate on the principle of squeezing the material from an irregularly shaped tube, allowing a weighted object to fall on the surface of the mass, or drawing a plate across the material under test (2). The significance of the results obtained from these instruments is not known. The methods often yield results which are difficult, if not impossible, to replicate and they suffer by comparison with fundamental methods since the former do not lend themselves to mathematical characterisation nor do they permit a study of product behaviour under a variety of conditions (45). There is therefore no justification in the use of these instruments in rheological characterisation.

In any serious scientific investigation of semisolids, it is apparent that specially designed instruments which will allow the individual physical-rheological properties to be studied and defined are essential. Several instruments have been designed for this purpose and they can be broadly classified as follows:-

(i) those that will measure inter-relationships between shear stress and shear rate;

(ii) those that will characterise the undisturbed structure of the product.

Instruments that belong to category (i) do not allow fundamental characterisation, however they will permit mathematical definition and as such they have found enormous popularity as general purpose control instruments for preliminary investigations of semisolid structure. Typical of these instruments are the concentric cylinder and the cone and plate viscometers. There are however some viscometers of mathematically undefinable geometry that can be included in the first category, e.g. the paddle type of instrument (46). The use of such equipment must be avoided in serious investigations as the data yielded cannot be corrected for various errors inherent in the design and are therefore rendered almost meaningless. Martin (2) has cautioned that instruments of different designs may produce significantly different flow diagrams however he has pointed out that once some knowledge of rheology has been acquired, these inconsistencies cause no difficulty; they can, in fact, be turned to good use.

To gain an insight into the undisturbed structure of the product, small strain tests must be employed which will enable the examination of the material in its "rheological ground state", i.e. when the test method does not alter the structure of the product (47). The results may be interpreted on the basis of the theory of visco-elasticity and correlated with the other physical properties of the semisolid in order to derive a true picture of the behaviour of the product under normal usage conditions. Criticisms that have been levelled at this form of analysis are that the equipment is often very

expensive, that setting up procedures are complex, the analysis of results is time consuming, and the mathematics often quite forbidding. While it is true that, for instance, the Weissenberg Rheogoniometer can be quite expensive, cheaper and simpler viscometers are available, e.g. the concentric cylinder creep viscometer (48). The main and irrefutable argument in favour of the use of these instruments is that no other form of analysis will provide the necessary fundamental information.

2.3 Theory Concerning Instruments used in this Study

2.3.1 Continuous Shear Viscometry

Cone and plate viscometers are widely used for continuous shear measurements of Newtonain and non-Newtonian materials, the main advantage of these instruments being that they allow uniform shearing conditions to operate throughout the whole sample. A general discussion of the theory and mode of operation of these viscometers has been given by McKennell (49 - 51) and Van Wazer et. al. (52). The following treatment of the calculation of the shear parameters is due to Van Wazer et. al. (52).

Let a torque T (Newton metre) be applied to a cone of radius R (metres) and angle α (radians) which causes it to rotate at an angular velocity Ω (radians sec^{-1}). Then the shear stress σ (Newtons $metre^{-2}$) is given by:-

$$\sigma = 3T/2\pi R^3 \quad \ldots (1)$$

and the rate of shear, $\dot{\gamma}$ (sec^{-1}) is given by:-

$$\dot{\gamma} = \frac{\Omega}{\alpha} \qquad \ldots (2)$$

for Newtonian fluids. The viscosity, η (Newton sec $metre^{-2}$) is thus given by:-

$$\eta = \frac{\sigma}{\dot{\gamma}} = \frac{3T\alpha}{2\pi R^3 \Omega} \qquad \ldots (3)$$

For Equation (1) to (3) to be applicable, the following assumptions must hold (53):-

(i) the sample material must be incompressible;

(ii) the motion of the sample material must be laminar;

(iii) streamlines of flow are circles on the horizontal plane perpendicular to the axis of rotation, that is, radial and axial flow are assumed to be zero;

(iv) the motion is steady;

(v) there is no relative movement between the viscometer elements and the sample material in immediate contact with them, that is, no slippage;

(vi) the motion is two dimensional;

(vii) the system is isothermal.

It is evident that a viscoelastic semisolid material exhibiting complex rheological behaviour may not comply with several of these assumptions at any given time in the shear cycle and therein lies

the limitations of this method. Hutton (54) and Davis (55) have pointed out that the most serious of these limitations is the phenomena of shear fracture where the sample fractures and is expelled from in between the measuring surfaces.

In this work it was demonstrated that flow patterns of the semisolids were relatively simple. Any flow irregularities were of secondary importance.

2.3.2 The Nature of Viscoelastic Behaviour

Polymer scientists have adopted and exploited viscoelastic theory and techniques to great advantage. As a result of their work pharmaceutical and cosmetic scientists have become aware of and interested in the viscoelastic properties of topical semisolids. A suitable explanation of the nature of viscoelastic behaviour can be based on the work of Leaderman (56), Ferry (57) and Barry (46).

Classical theories of elasticity and hydrodynamics are usually applied in the analysis of behaviour of elastic solids and viscous liquids respectively. For small deformations, according to Hooke's law for real solids, stress is directly proportional to strain but is independent of the rate of strain itself. Similarly for real liquids, according to Newton's law, stress is directly proportional to the rate of strain but is independent of the strain itself. These are idealisations however, and although the behaviour of many solids and liquids approaches the ideal at infinitesimal strains and strain rates, deviations are observed under other conditions. Two types of deviations have been distinguished.

The first of these is stress dependent. In this case, the strain in a solid or the strain rate in a liquid is not proportional to the stress but depends on the stress in a more complicated manner.

The second of these is time dependent. In this case the stress depends on both the strain and the rate of strain. This is the characteristic of linear viscoelastic behaviour, i.e. when the ratio of stress to strain is a function of time alone and not the stress magnitude.

Where stress and time dependent behaviour coexist, non-linear viscoelasticity is exhibited. Most materials in large deformations exhibit non-linearity however for small deformations in a set range, which must be determined experimentally, the relationship between the viscous and/or elastic deformation and the applied stress may be considered a linear function (58). The small strain behaviour may then be interpreted according to the linear theory of viscoelasticity.

(a) Constitutive Equations of Linear Viscoelasticity

The relation between stress, strain and their time dependencies are in general described by simple "constitutive equations". The equations are based on the principle that the effects of sequential changes in strain are additive (57).

$$\sigma(t) = \int_{-\infty}^{t} G(t - t')\dot{\gamma}(t')dt' \qquad \ldots (4)$$

$$\gamma(t) = \int_{-\infty}^{t} J(t - t')\dot{\sigma}(t')dt'$$

... (5)

where σ (t) and γ (t) are stress and strain at time t respectively, t' is all past times, G (t - t') is the relaxation modulus and J (t - t') is the creep compliance, $\dot{\gamma}$ is the rate of strain and $\dot{\sigma}$ is given by $\frac{d\sigma}{dt}$. In a recent publication, the mathematical interpretation of the constitutive equations has been discussed extensively (59).

(b) Mechanical Model Representation of Linear Viscoelastic Behaviour

An alternative to "constitutive equations" is the representation of linear viscoelastic behaviour by means of mechanical models comprising assemblies of elastic elements (Hookean springs) and viscous elements (dashpots imagined as pistons moving in Newtonian oil), Figures 4 and 5. The force applied to the terminals of the model is analogous to shear strain and the rate of displacement is analogous to the rate of change of strain. While the mathematical analogy of the mechanical model is satisfactory (57) it must be said that this is only one of a number of equivalent representations. Alfrey (60) has emphasised that the use of models does not necessarily imply anything concerning the molecular mechanisms responsible for the observed behaviour. Models such as these, however help one to visualise the fundamental processes which are involved in viscoelasticity (15) and individual elements can sometimes

be identified qualitatively with definite processes at a molecular level (61).

The two extremes of behaviour, the elastic solid and the viscous liquid are represented simply by a spring and a dashpot respectively. The force and displacement across a Hookean spring, Figure 4 (a), are related by:-

$$\sigma = G\gamma \qquad \ldots (6)$$

where σ is the stress, G the modulus and γ the strain. The strain and stress have a similar time relation. The force and displacement across a Newtonian dashpot, Figure 4 (b), are related by:-

$$\sigma = \eta\dot{\gamma} \qquad \ldots (7)$$

where η is the viscosity and $\dot{\gamma} = d\gamma/dt$. The application of a constant stress to the dashpot terminal brings about a linear increase in strain until such time as the stress is removed, when there is no recovery. The strain-time relationship is characterised by the gradient of the slope.

In between the two extremes lies the semisolid and this is represented by model assemblies of springs and dashpots.

(i) The Maxwell Model

The Maxwell element, Figure 4 (c), consists of a spring of

FIGURE 4

MECHANICAL MODEL REPRESENTATION OF VISCOELASTIC BEHAVIOUR I

(a) Hookean Spring

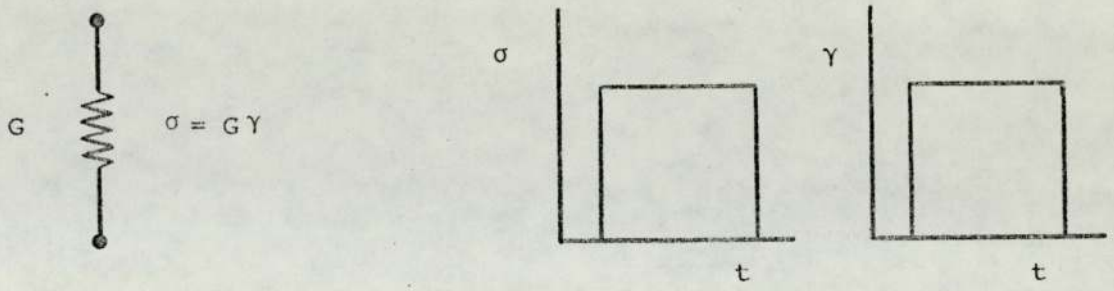

(b) Newtonian dashpot

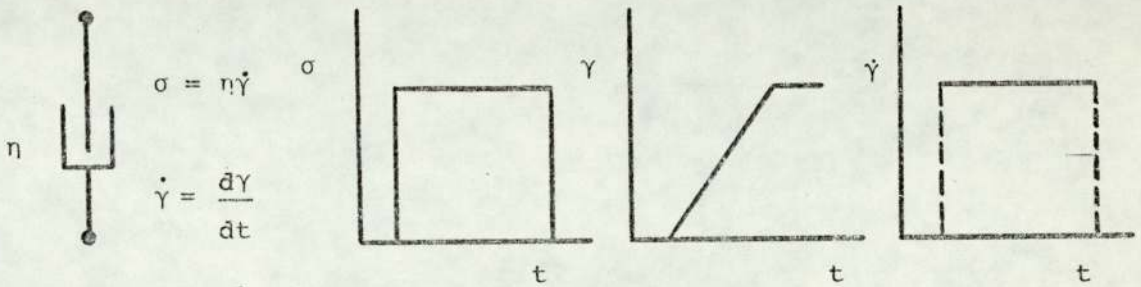

(c) Maxwell element

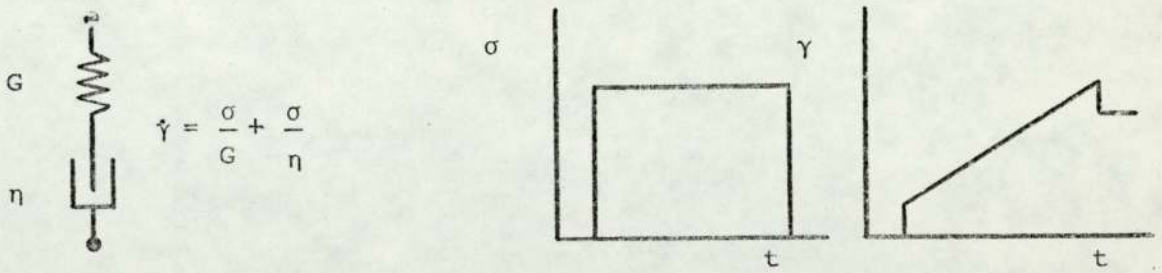

(d) Kelvin (Voigt) element

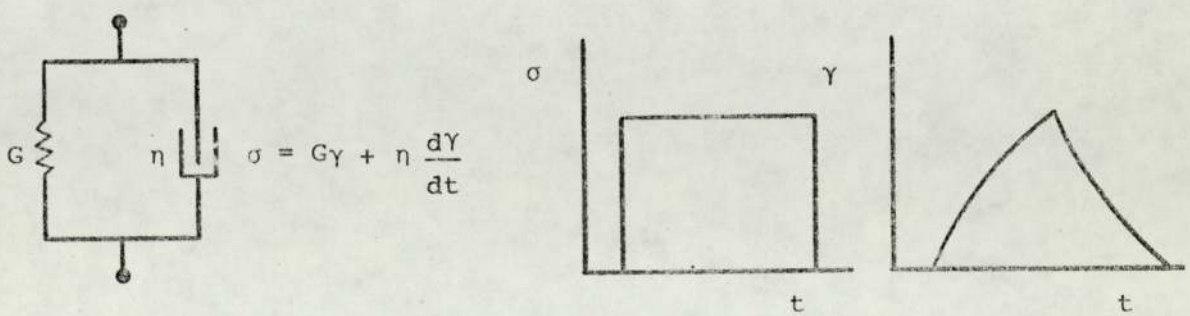

modulus G in series with a dashpot containing an oil of viscosity η. When a shear stress (σ) is applied to the element terminal, the forces across the spring and the dashpot are equal and the total displacement is the sum of the individual displacements. Thus the force due to a constant total displacement γ imposed at time t = o relaxes exponentially and is given by (58):-

$$\sigma = \gamma G \exp\left(-\frac{Gt}{\eta}\right) = \gamma G \exp\left(-\frac{t}{\tau}\right) \quad \ldots (8)$$

where the ratio of shear viscosity to shear modulus has the dimensions of time, and is called the relaxation time τ, i.e. $\tau = \eta/G = \eta J$.

A Maxwell model consists of a number of Maxwell elements in parallel, Figure 5 (a). The displacement of each element will be the same, and the total force will be the sum of that contributed by each element. The stress relaxation for a Maxwell model will therefore be of the form (58):-

$$G(t) = \sum_{i=1}^{n} G_i \exp\left(-\frac{t}{\tau_i}\right) \quad \ldots (9)$$

The Maxwell model is particularly useful for representing stress relaxation phenomena, in which a body is constrained

FIGURE 5

MECHANICAL MODEL REPRESENTATION OF VISCOELASTIC BEHAVIOUR II

(a) The Maxwell model

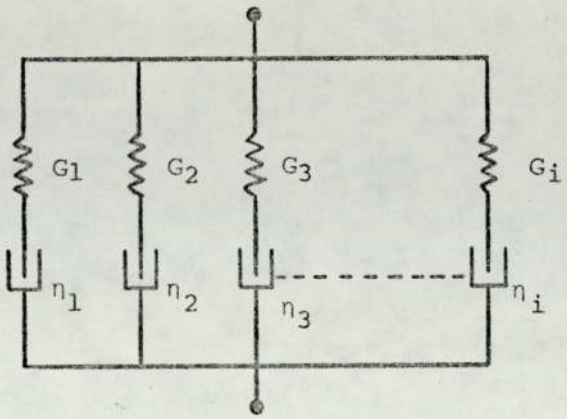

$$G(t) = \sum_{i=1}^{n} G_i \exp\left(-\frac{t}{\tau_i}\right)$$

(b) The Kelvin (Voigt) model

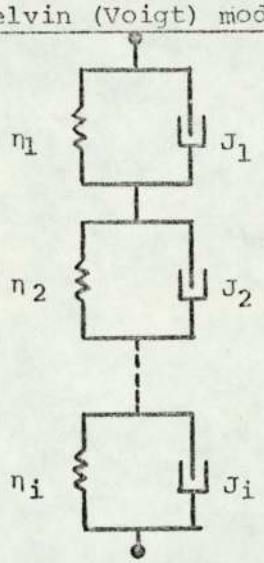

$$J(t) = \sum_{i=1}^{n} J_i\{1 - \exp(-\frac{t}{\tau_i})\}$$

(c) Generalised Viscoelastic Behaviour

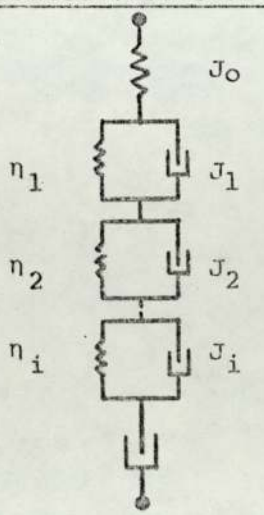

$$J(t) = J_o + \sum_{i=1}^{n} J_i\{1 - \exp\left(-\frac{t}{\tau_i}\right)\} + \frac{t}{\eta_b}$$

at constant deformation, and the stress required to maintain this deformation diminishes or relaxes with time (46).

(ii) The Voigt (Kelvin) Model

The behaviour of systems used in this work was analysed according to the Voigt (Kelvin) model and hence this has been dealt with more fully. The following derivation is based on that of Warburton and Barry (62).

The Voigt element consists of a spring and dashpot in parallel, Figure 4 (d). When a shear stress is applied to the element terminal, the strain γ in the spring equals that in the dashpot and the total stress, σ, is the sum of the stress in the spring and in the dashpot. Thus applying Hooke's law and Newton's law:-

$$\sigma = G\gamma + \eta\frac{d\gamma}{dt} \qquad \ldots (10)$$

A Voigt model consists of a number of elements connected in series, Figure 5 (b). In shear, the stress in the ith element at time (t) will be σ_i, the strain γ_i, the shear compliance of the spring Ji, corresponding to a shear modulus Gi and the Newtonian viscosity of the dashpot η_i. Substituting in Equation (10):-

$$\sigma_i = G_i\gamma_i + \eta_i\frac{d\gamma_i}{dt} \qquad \ldots (11)$$

Rearranging:-

$$\frac{d\gamma_i}{\sigma_i - \gamma_i G_i} = \frac{1}{\eta_i} dt$$

... (12)

If the retardation time for the ith element is defined as:-

$$\tau_i = \frac{\eta_i}{G_i} = \eta_i J_i$$

... (13)

Equation (12) becomes:-

$$\frac{d\gamma_i}{\frac{\sigma_i}{G_i} - \gamma_i} = \frac{dt}{\tau_i}$$

... (14)

On integration without limits:-

$$- \ln \left\{ \frac{\sigma_i}{G_i} - \gamma_i \right\} = \frac{t}{\tau_i} + k_1$$

... (15)

When experiment commences, $t = o$, $\gamma_i = 0$; thus:-

$$k_1 = - \ln \{ \sigma_i J_i \}$$

... (16)

Substituting Equation (16) in Equation (15) and rearranging:-

$$\ln \left\{ \frac{\sigma_i J_i - \gamma_i}{\sigma_i J_i} \right\} = -\frac{t}{\tau_i} \qquad \ldots (17)$$

hence

$$\gamma_i = \sigma_i J_i \left\{ 1 - \exp \left(-\frac{t}{\tau_i} \right) \right\} \qquad \ldots (18)$$

and

$$J_i(t) = J_i \left\{ 1 - \exp \left(-\frac{t}{\tau_i} \right) \right\} \qquad \ldots (19)$$

The total strain in a generalised model, $\gamma(t)$, is the sum of the strains in the individual elements, and thus compliances in series are additive. Hence:-

$$J(t) = \sum_{i=1}^{n} J_i \left\{ 1 - \exp \left(-\frac{t}{\tau_i} \right) \right\} \qquad \ldots (20)$$

Pharmaceutical materials may be classified into either viscoelastic liquids or viscoelastic solids. When examined in creep, the former eventually reach a state of steady flow (linearly increasing deformation with time), while viscoelastic solids

approach an equilibrium deformation or zero strain rate. It is conventional among non-rheologists for both types to be called semisolids; most typical semisolids which have been investigated belong to the subsection of viscoelastic liquids (46). The Voigt model as defined by Equation 20 represents a viscoelastic solid; to simulate real, viscoelastic liquids, the Equation may be extended to include at the limits $\tau = 0$ and ∞ . In the first case a Voigt element degenerates to an elastic spring of modulus Go (or compliance Jo). The inclusion of such an element in the generalised Voigt model corresponds to a certain amount of instantaneous elastic compliance in the material. In the second case a Voigt element degenerates to a viscous dashpot of compliance $J_N(t) = t/\eta$. The inclusion of this element corresponds to a viscoelastic liquid, which exhibits unlimited Newtonian flow.

Thus for a real viscoelastic liquid, the mathematical analogy of the mechanical representation, Figure 5 (c), is:-

$$J(t) = Jo + \sum_{i=1}^{n} J_i \{1 - \exp\left(-\frac{t}{\tau_i}\right)\} + \frac{t}{\eta_o} \qquad \ldots (21)$$

where J(t) is the observed creep compliance and the first and the last terms on the right hand side represent the shear compliances due to the degenerate models.

(c) The Boltzman Superposition Principle

The Boltzman Superposition Principle states that the effects of mechanical history are linearly additive where the stress is described as a function of strain history or rate of strain history or alternatively the strain is described as a function of the history of rate of change of stress (56, 57).

Thus for a material to exhibit linear viscoelasticity, it must also obey the Boltzman Superposition Principle. The "constitutive equations", Equations (4) and (5), are two of the many possible expressions of the principle.

The Boltzman Superposition Principle can be illustrated by the case where the strain is defined in terms of the stress history (56). For instance, when a simple shear stress σ_i is applied at time u_i to a previously unloaded mechanical model consisting of Voigt elements in series, together with degenerate Voigt elements (an isolated spring and dashpot), the shear strain at a subsequent time t is given, from Equation (5), by:-

$$\gamma(t) = \sigma_i J(t - u_i) \qquad \ldots (22)$$

where J(t) is the creep compliance. If instead, a series of stress increments σ_i are applied at times u_i, where $u_i < t$, the resultant total strain at time t is the sum of the shear strains which would be observed at time t if each increment were applied independently. Thus:-

$$\gamma(t) = \sum_{u_i=-\infty}^{u_i=t} \sigma_i \, J(t - u_i) \qquad \ldots (23)$$

In a creep experiment, when the material has been deformed under constant stress for a period of time and the stress is suddenly removed, reverse deformation called creep recovery is observed. The removal of the stress in this instance is analogous to the application of a negative stress of equal magnitude and consideration of the above Equation indiciates that creep recovery will occur.

2.3.3 Measurement of Linear Viscoelastic Behaviour

(a) The Creep Test

In this test, the experimental system is subjected to a sudden instantaneous shear stress which is maintained constant for a considerable period of time. The measured time dependent strain response is known as the creep curve. Figure 6 illustrates a typical creep curve and its mechanical model analogy.

The region A-B in the Figure represents the instantaneous elastic compliance, Jo, which is independent of time and is simulated mechanically by a Hookean spring. This region is said to represent the elastic stretch between the bonds of the primary structural units (15). This elastic stretch is completely recoverable when the stress is removed as is shown by the region D-E.

FIGURE 6

MODEL CREEP CURVE AND MECHANICAL MODEL ANALOGY

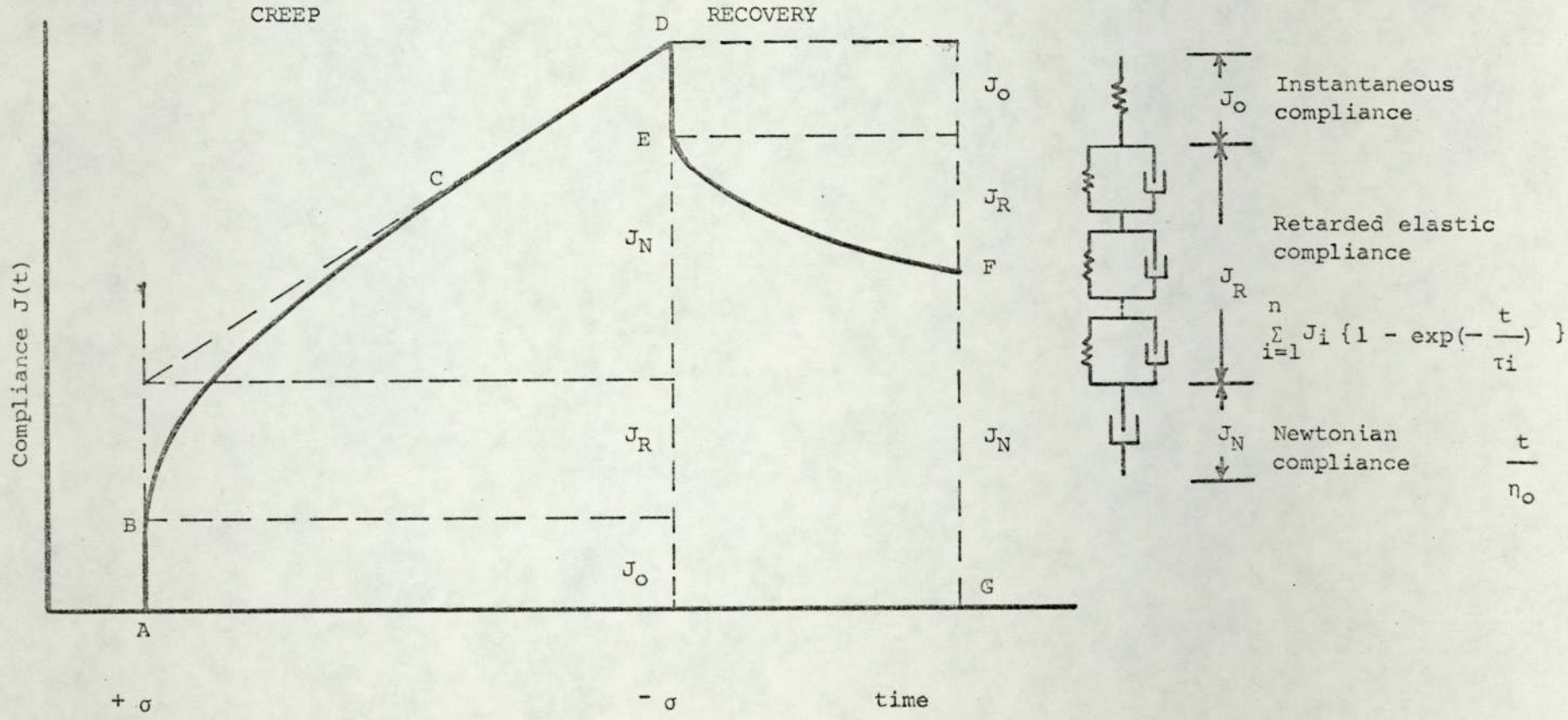

The region B-C in the Figure represents the retarded elastic compliance, J_R, which is time dependent and is simulated by a number of Voigt units in series. This represents the region where the bonds break and reform. All bonds do not break and reform at the same rate. The weaker bonds break at shorter time intervals than the stronger bonds (15). The retarded elastic compliance is also recovered with time when the stress is removed as is shown by the region E-F in the Figure.

The region C-D represents the Newtonian compliance simulated by a dashpot. Here some of the bonds have been ruptured and as their time of reformation is longer than the test time, the particles or units flow past one another exhibiting true viscous flow (15). This is the non-recoverable part of the creep curve and is due to irreversible viscous flow.

A creep curve, such as the one in Figure 6, may be represented mathematically by Equation (21). An experimentally observed creep curve can in principle be fitted with any desired degree of accuracy by taking n sufficiently large in Equation (21). This would amount to determining a discrete spectrum of "lines", each with a location, τ_i and intensity, Ji (57). In practice, this form of analysis of experimental data is difficult and it is not possible to resolve more than a few lines. This difficulty may be avoided by deriving instead a continuous spectra of retardation times.

If the number of Voigt elements in the mechanical model is made infinite in extent, it represents a continuous spectrum of

retardation times, L (57), defined by the continuous analogue of Equation (21).

$$J(t) = Jo + \int_{-\infty}^{+\infty} L\{ 1 - \exp\ (-\frac{t}{\tau}) \}d\ln\tau + \frac{t}{\eta_o}$$

... (24)

The continuous spectrum of retardation times, L, refers to deformation in simple shear and has the dimensions of compliance although they have the nature of distribution function. Maxima in the spectra represent a concentration of retardation processes, measured by their contributions to compliance. While L is not essential to the treatment of linear viscoelastic behaviour, the spectra is useful qualitatively in gauging the distribution of retardation mechanisms in different regions of the time scale.

(b) Oscillatory (Dynamic) Test

Transient methods, such as creep, are limited at short times by inertial effects and by the impossibility of having an instantaneous application of stress at the beginning of the experiment (63). Thus these tests can be supplemented by oscillatory (dynamic) tests which provide information corresponding to very short times. Oscillatory experiments are conducted by varying the stress or strain periodically usually with a sinusoidal alternation at a frequency N in cycles/sec (Hz) or ω ($=2\pi f$) in radians/sec. A periodic experiment at frequency ω is qualitatively equivalent to a transient experiment at time $t = 1/\omega$ (57).

If a material under examination behaves as a real solid, then the strain and stress will be in phase and of the same amplitude. If the material is a real liquid, then the strain and stress will be 90% out of phase with each other. A linear viscoelastic material exhibits a stress-strain relationship that lies in between the two extremes and the ratio of the stress-strain amplitude is a constant. This is illustration in Figure 7 (a). The following derivation of this relationship is based on that of Ferry (57):-

$$\gamma = \gamma_o \sin \omega t \qquad \ldots (25)$$

where γ_o is the maximum amplitude of the strain. Then

$$\dot{\gamma} = \omega \gamma_o \cos \omega t \qquad \ldots (26)$$

substituting into Equation (4), denoting $t - t'$ by s,

$$\sigma = \int_o^\infty G(s)\, \omega \gamma_o \cos \{ \omega (t - s) \}\, ds$$

$$= \gamma_o \{ \omega \int_o^\infty G(s) \sin \omega s\, ds \} \sin \omega t$$

$$+ \gamma_o \{ \omega \int_o^\infty G(s) \cos \omega s\, ds \} \cos \omega t \qquad \ldots (27)$$

The quantities in the brackets are functions of frequency but not of elapsed time, hence the above equation can be rewritten as:-

FIGURE 7

(a) Stress-Strain relationship for materials undergoing forced sinusoidal oscillation.

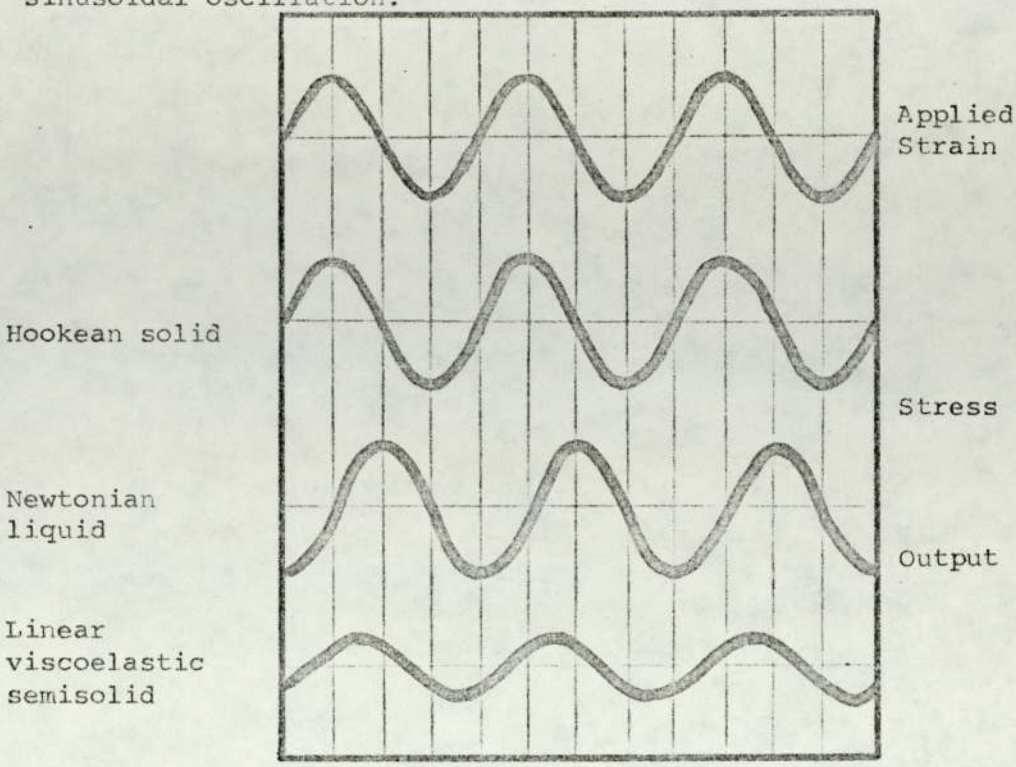

(b) Vectorial resolution of complex modulus and compliance.

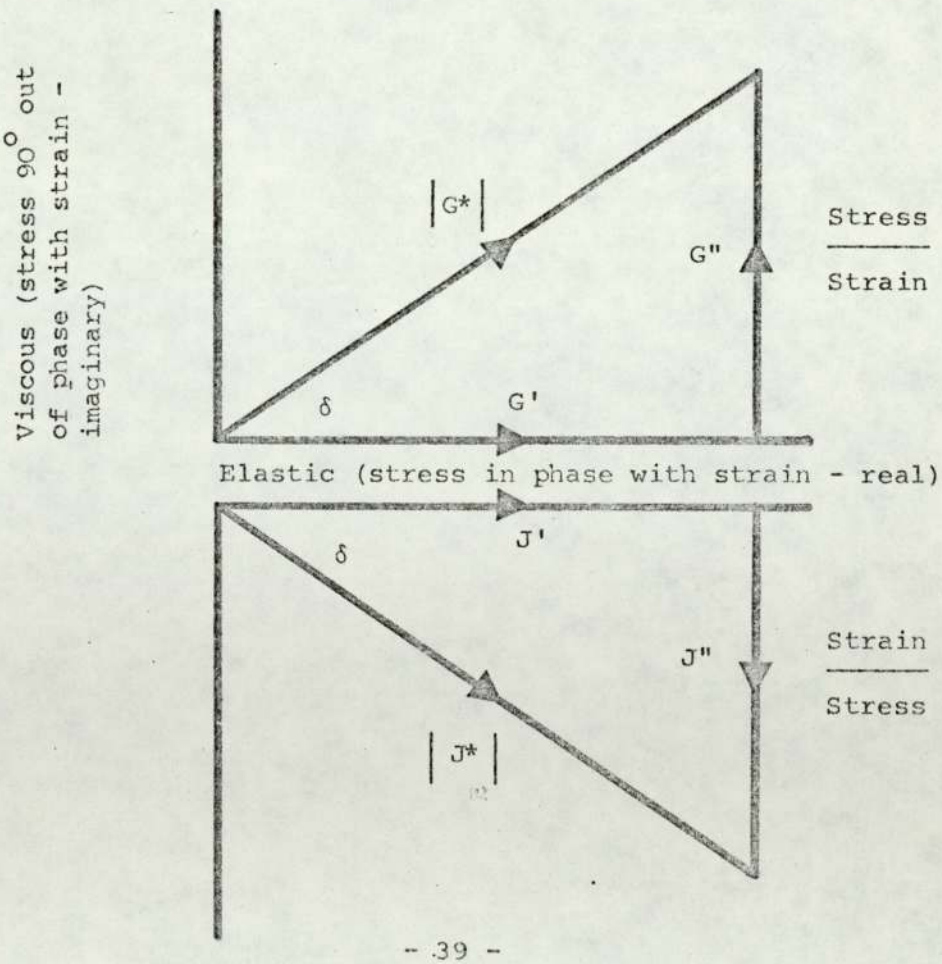

$$\sigma = \gamma_o \, (G' \mathrm{Sin}\, \omega t + G'' \mathrm{Cos}\, \omega t)$$

... (28)

thus defining the two frequency dependent functions - the shear storage modulus G' and the shear loss modulus G".

The stress can be redefined in an alternative form to include amplitude σ_o and the phase angle δ between stress and strain. From trigonometric relations,

$$\sigma = \sigma_o \mathrm{Sin}\, (\omega t + \delta)$$

$$= \sigma_o \mathrm{Cos}\ \delta \mathrm{Sin}\ \omega t + \sigma_o \mathrm{Sin}\ \delta \mathrm{Cos}\ \omega t$$

... (29)

Comparison of Equations (29) and (30) yields:-

$$G' = \left(\frac{\sigma_o}{\gamma_o} \right) \mathrm{Cos}\, \delta$$

... (30)

$$G'' = \left(\frac{\sigma_o}{\gamma_o} \right) \mathrm{Sin}\, \delta$$

... (31)

$$\frac{G''}{G'} = \tan \delta$$

... (32)

The sinusoidally varying stress is often expressed as a complex quantity. The corresponding modulus is also complex and is given by:-

$$\frac{\sigma^*}{\gamma_o} = G^* = G' + i\,G'' \qquad \ldots (33)$$

where $i = \sqrt{-1}$.

The absolute modulus $|G^*|$ is defined as the ratio of peak stress to peak strain and is given by:-

$$|G^*| = \frac{\sigma_o}{\gamma_o} = \sqrt{(G')^2 + (G'')^2} \qquad \ldots (34)$$

The complex compliance is also similarly expressed:-

$$J^* = \frac{\gamma^*}{\sigma_o} = \frac{1}{G^*} = J' - iJ'' \qquad \ldots (35)$$

and the absolute compliance $|J^*|$, defined as the ratio of peak strain to peak stress is given by:-

$$|J^*| = \sqrt{(J')^2 + (J'')^2} \qquad \ldots (36)$$

The vectorial resolution of Equations (34) and (36) is illustrated in Figure 7 (b). It is evident that G' is the ratio of the

stress in phase with the strain to the strain and J' is the ratio of the strain in phase with the stress to the stress. These two represent the elastic contribution and are the 'real' components of their complex counterparts. The storage modulus G' and compliance J' are thus so named because they are associated with energy storage and release in the periodic deformation. G'' is the ratio of the stress 90^{o} out of phase with the strain to the strain and J'' is the ratio of the strain 90^{o} out of phase with the stress to the stress. These represent the viscous contributions and are the 'imaginary' components of their complex counterparts. The loss modulus G'' and compliance J'' are associated with the dissipation or loss of energy as heat.

Although the complex compliance and modulus are inversely related ($J^* = 1/G^*$) their individual components are not. The relations between the components are presented by Ferry as follows (57):-

$$J' = \frac{G'}{(G')^2 + (G'')^2} = \frac{1/G'}{1 + \tan^2\delta} \qquad \ldots (37)$$

$$J'' = \frac{G''}{(G')^2 + (G'')^2} = \frac{1/G''}{1 + (\tan^2\delta)^{-1}} \qquad \ldots (38)$$

$$G' = \frac{J'}{(J')^2 + (J'')^2} = \frac{1/J'}{1 + \tan^2\delta} \qquad \ldots (39)$$

$$G'' = \frac{J''}{(J')^2 + (J'')^2} = \frac{1/J''}{1 + (\tan^2\delta)^{-1}} \qquad \ldots (40)$$

Walters (64) derived the following equation of state for a linear viscoelastic material undergoing forced harmonic oscillation of small amplitude

$$\sigma = 2\eta^*\dot{\gamma} \qquad \ldots (41)$$

where σ is the shear stress, η^* the complex dynamic viscosity which is a function of the frequency of oscillation ω rad sec^{-1} and $\dot{\gamma}$ the shear rate. It is usual to express η^*, which is a ratio of the complex stress (σ^*) to the complex rate of strain ($\dot{\gamma}^*$) in the form:-

$$\eta^* = \frac{\sigma^*}{\dot{\gamma}^*} = \eta' - \frac{iG'}{\omega} \qquad \ldots (41A)$$

where η' is the dynamic viscosity, G' the storage modulus and $i = \sqrt{-1}$. The dynamic viscosity represents energy lost or dissipated as heat per cycle and the storage modulus measures the energy stored and recovered per cycle.

The loss modulus G'' is a measure of the energy dissipated or lost as heat per oscillatory cycle and has been defined by Van Wazer et. al. (52) as:-

$$G'' = \eta'\omega \qquad \ldots (42)$$

The imaginary component of the dynamic viscosity η'' may be derived from the equation (57):-

$$G' = \omega\eta'' \qquad \ldots (43)$$

2.4 Rationale in the Choice of Suitable Rheological Methods and Parameters for Correlation

In rheological evaluation of topical semisolids there has been considerable debate concerning the choice and measurement of suitable rheological parameters that would lead to a useful interpretation. The argument has been whether the measurement of rheological parameters should reflect the undisturbed structure of the product or whether it should reflect the shear behaviour under use conditions. It is thought that the mode of application of the semisolid could conceivably affect the structure of the product to a degree where this would be the important factor determining the efficacy of the product. In this case the study of the behaviour of the product under continuous shear is clearly indicated. On the other hand it is arguable that since the topical product is in situ for a time which is infinitely longer than the time the product is subjected to shear on application, it is the undisturbed structure of the product that the rheological parameters should reflect and in this case small strain measurement of rheological parameters is indicated.

In this work both continuous shear and small strain measurements have been undertaken. In small strain measurements both transient and dynamic tests to cover a wide time scale have been carried out and

interconversion of the data has been made possible through approximation methods. Ferry (57) observed that since each of the characteristic viscoelastic functions, mentioned in the previous Section 2.3, can be calculated from any other it is an arbitrary matter which is chosen to depict the behaviour of a system. The question however arises whether the arbitrarily chosen function which in itself depicts a specific molecular mechanism truly represents the physical-rheological environment seen by the diffusing drug molecule. It would seem logical to suppose that one or more of these functions would reflect the rheological environment more closely than the others.

It is thus clear that the fundamental rheological characterisation of the topical semisolids in itself is not adequate. A thorough appreciation of the fundamentals of the semisolid dosage form and the diffusion of drug molecules therein is also necessary in this case, to enable appropriate choice of suitable rheological methods and parameters.

3 FUNDAMENTAL CONSIDERATIONS OF THE SEMISOLID DOSAGE FORM

3.1 Topical Drug Delivery

Semisolid medicaments applied to the skin have been mainly used for the superficial and local effect that they produce. While the systemic absorption of drugs that results from topical applications has been known for a long time, this knowledge has rarely been exploited for any therapeutic purposes. A distinctive feature of topical drug administration has been the usual lack of precision in the quantity of drug administered (65). Consequently, correlation between the physicochemical characteristics of the dosage form and its effect in a clinical situation has often been difficult.

More recently however, with interest focusing on new and novel ways of formulating and administering drugs, it has been recognised that topical drug delivery for local and systemic effects has considerable advantages over the more conventional oral, rectal and parental forms. Programmes have been initiated to study and control the local and systemic administration of medicines through the skin (66 - 69).

For a local effect, Stoughton (70) has reported that the unbelievably rich prospect of controlling normal and abnormal cutaneous biologic functions by topical applications is already "on the shelf". Local topical therapy provides a unique opportunity to deliver the drug directly to the disease site in high concentrations with a minimal potential for the provocation of systemic side effects (18). Gaggi and Del Mastro (71) have demonstrated that of the equiactive oral, interperitoneal and topical dosage of oxyphenbutazone for its anti-inflamatory potency, the topical application permitted the attainment of effective high

concentration of the drug in the inflamed tissue while being potentially less toxic because of the lower circulating levels of the drug.

Systemic administration of drugs, on the other hand, via the topical route has several advantages. Unlike the orally administered drug, topically administered drug does not have to survive drug-nutrient interactions and digestive enzymes in the stomach. The drug is delivered directly to the general circulation, bypassing the efficient filtering plant, the liver. The drug is released and absorbed slowly and predictably over a period of hours or days and it is possible to achieve a time-course of drug in the blood which is similar to that obtained after oral absorption (68, 72). This method of delivery is particularly useful for drugs which are poorly absorbed in the GI tract or which cause GI disturbances like for instance insulin for diabetes, vasodilators for heart disease, analgesics, and antinausea compounds (66, 68). This route of administration is convenient for the patient and also provides maximum safety; if necessary the medication could be removed and the therapy promptly terminated.

It is apparent thus that topical drug delivery offers a desirable, controllable form of target therapy that will enable a substantial reduction in the concentration of drugs required for beneficial effects, local or systemic, thus minimizing deleterious side effects. An important consideration in the design of the topical dosage form must necessarily be the extent of bioavailability desired.

3.2 Bioavailability Considerations

Poulsen (65) considers that "the definition of what constitutes

bioavailability for a drug applied to the skin is somewhat ambiguous. According to a recent report of the American Pharmaceutical Association Academy of Pharmaceutical Sciences(73) 'bioavailability is a term used to indicate measurement of both the relative amount of an administered drug that reaches the general circulation and the rate at which this occurs'. This definition as intended by the authors of the Academy report, applies to drugs which are distributed by the general circulation to the target tissue. Perhaps the major distinction between drugs applied for a topical effect and those administered systemically by the oral, rectal or parental routes is that for a topical drug the general circulation does not distribute the drug to the target tissue - it instead removes it from the site of action. Nonetheless, in most cases the rate and the total amount of drug or drug metabolite(s) reaching the systemic circulation following topical application should be a reliable indicator of bioavailability".

A distinction must be made between topical delivery for superficial effect (for the control of normal and abnormal cutaneous biology (reactions)) and for systemic effect. In this context and in relation to topical drug delivery as described in Section 3.1 it is clear that the term bioavailability used in the context of topically administered drugs has a particular significance.

3.3 Percutaneous Absorption

The process of drug absorption via the topical route is generally referred to as percutaneous absorption and has been defined as the penetration of substances from the outside into the skin and through the skin into the bloodstream (74). In relation to topical administration this may be defined as a three phase process:-

(i) drug release from vehicle;

(ii) intracutaneous absorption of drug through the entire thickness of the epidermal layers and into the connective tissue, and

(iii) systemic absorption.

Hlynka et. al. (75) have pointed out that the degree of intracutaneous and systemic absorption intended may vary depending on the reason for initiating percutaneous absorption.

Analysis of the process of percutaneous absorption must take into account physicochemical and biopharmaceutical aspects of the topical dose formulation as well as the physiological and pathological condition of the skin. Despite the large amount of work that has been carried out in this area to elucidate the extent of the factors influencing percutaneous absorption, the exact mechanism of this process is still not fully explained. Thus a logical approach in understanding the process is to rationalise and identify the drug; the vehicle and the skin effects.

3.3.1 Skin Effects

Numerous reviews of the anatomical structure of the skin may be found in literature (76, 77). For clarity of the following discussion, a diagram of the structure of the skin is included, Figure 8.

(a) Barrier Function of the Skin

The film on the surface of the skin is composed of sebum, sweat and desquamating stratum corneum. It is discontinuous and offers little

FIGURE 8

DIAGRAM OF THE STRUCTURE OF THE SKIN

After Katz & Poulsen

1971 (76)

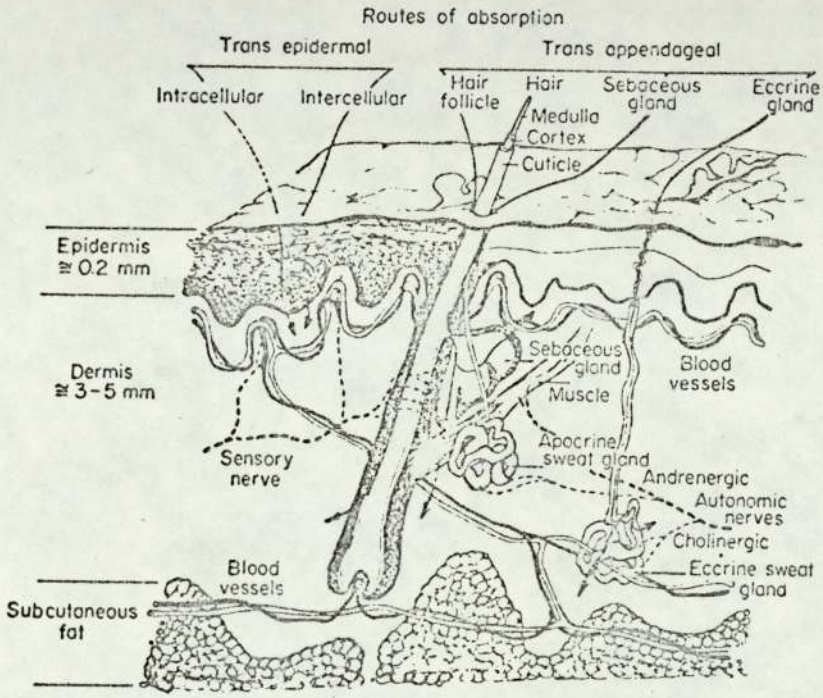

resistance to a penetrating molecule (78). The barrier function of the skin resides almost entirely in the stratum corneum (79, 80). The effective performance of the barrier function appears to depend on the chemical composition of the stratum corneum which has been shown to consist principally of keratin fibrils and lipids (81). The permeability of the barrier has been inversely related to the thickness of the stratum corneum (82, 83, 84). Molecules which do penetrate the barrier layer are either bound by the living epidermis, the dermis, or carried away by the tissue fluid to the lymphatic and blood vessels (85) into the general circulation.

(b) Routes of Penetration of the Barrier Layer

The two possible routes of penetration of intact human skin are transepidermal and transappendageal. Transepidermal absorption is said to occur through the cells of the stratum corneum or alternatively along the intercellular channels. Transappendageal absorption is known to occur via the hair follicle, the sebaceous gland and the eccrine sweat gland. While there is little agreement in literature concerning the preferred route of penetration, it is generally accepted that all the avenues take part in the transfer of substances through the skin (86). It is reasoned however that transappendageal absorption usually predominates until a steady state of penetration is reached after which due to the vastly greater surface area involved, transepidermal absorption is the major route of penetration (87).

(c) Integrity of the Skin

Percutaneous absorption is increased in diseases characterised by defective stratum corneum formation (88 - 90). Abrasion, e.g. stripping

and chemical injury, e.g. acids or alkalies can damage the barrier layer and this will dramatically enhance the absorption of almost any substance (91, 92).

(d) Effect of Regional Variation

Variation in penetration of the skin in different regions of the body occurs due to differences in thickness of the barrier layer and the distribution of the appendages. The rate of penetration of the skin has been shown to increase in the following anatomical order: plantar anterior forearm, instep, scalp and ventral thigh, scrotum and posterior auricular (18).

(e) Skin Age

Relationship of age to skin permeability has rarely been investigated (93) though it is observed that foetal and infant skin appears to be more permeable than adult skin (94) and that percutaneous absorption of topical steroids occurs more readily in children than adults (95). The significant dermal atrophy and gross epidermal changes in the elderly denote, to some extent, absorption influence (93, 96).

(f) Species Variation

Human and animal skin display wide differences in physical characteristics such as the number of appendageal openings per unit area and the thickness of the stratum corneum (93, 97). The penetration pathways and the penetration resistance of the skins of different species could vary and this is the main consideration guiding the choice of model

membranes for *in vitro* studies.

(g) State of Hydration

Several investigators have shown that an increased moisture content of the skin promotes percutaneous absorption (98 - 103). Normal hydration of the stratum corneum is maintained by the water diffusing from the underlying epidermal tissues. The moisture content of the skin can be increased by the occlusive effect of an ointment or a plastic covering as for example has been beneficially used in steroid therapy. Drugs such as estrogens have also been reported to increase skin hydration. Occlusion prevents evaporation of the sweat and of insensible perspiration, resulting in the endogenous hydration of the stratum corneum from a normal 5 - 15% moisture content up to as much as 50% water (83).

The mechanism of transport of a drug through the normal and hydrated stratum corneum may be quite different (83). The water in the stratum corneum is believed to hydrate the keratin fibres, thus loosening the compact network and allowing an easier and more rapid penetration. Recent work (104) has suggested that the water is retained in the intercellular space in association with macromolecules possibly of a mucopolysaccharide nature thus it is possible that for water soluble drugs, this provides a continuous aqueous pathway through the skin.

(h) Temperature

Under normal *in vivo* conditions, substances penetrate the skin only within a narrow range of temperatures (83). Any variation in

temperature results chiefly from occulusion or solvent evaporating effects. When conducting *in vitro* experiments however, temperature can be varied to cover a wide range, the main assumption in these studies being that the cutaneous barrier remains unchanged (83, 100, 105, 106). From the evidence in literature, it would appear that there is a direct relationship between temperature and skin permeability *in vitro*, however the practical importance of temperature effects in topical therapy is considered to be of minor importance (76).

3.3.2 Drug Effects

(a) Skin Reaction and Permeability to Drugs

Epidermal, dermal and vascular changes produced by certain drugs can affect the permeability of the skin. This is illustrated by the following examples:-

(i) Keratolysis

Salicylic acid, for example, in concentrations greater than five per cent can soften excessively keratinised tissue by endogenous hydration and a lowering of the pH thus enabling the removal of the cornified tissue (77, 107) which in turn would facilitate increased penetration of the drug (108).

(ii) Hydration

Steroids such as estrogens have been reported to cause swelling of the collagen fibres and produce a beneficial effect on ageing skin by hydrating the skin (76). As has been discussed, hydration of stratum corneum dramatically increases the permeability of the skin.

(iii) Circulatory Effects

Nicotinic acid esters are known to be potent vasodilators. Corticosteroids are known to be potent vasoconstrictors. These drugs can bring about vascular changes in the dermal capillaries that will affect their rate of clearance and the clearance of other concomitantly administered drugs from the dermis via the systemic route. This would affect the concentration gradient between the skin surface and the deeper tissues and logically, it is thought that this may influence the permeability of the skin (93, 108).

(b) Drug Metabolism by Skin

Very little is known about the metabolism of most drugs by the skin in spite of the accessibility of the skin relative to other body organs (18). Fredriksson showed that parathion is metabolised to paraoxon which is then degraded to non-toxic metabolites within the skin (109, 110). Studies of this nature have not indicated whether these represent enzymatic activity or are straightforward chemical interactions.

(c) Binding of Drugs by Skin

Many drugs have been known to interact with the skin. The interactions range from weak physical attractions of the Van der Waals type to chemical reactions producing strong chemical bonds (18). The existence in the skin of a depot or reservoir for topical corticosteroids was first demonstrated using the return of vasoconstriction after occulusion as a physiological marker (111). The reservoir has

subsequently been shown to exist for several other groups of drugs (112). The therapeutic significance of the reservoir effect has been evaluated (113) and discussed (112, 114).

(d) Solubility and Partition Coefficient

Lipid soluble substances generally penetrate the skin more readily than polar substances (115). Increased lipid solubility has often been associated with increased rate of absorption (80, 116). Other workers have also found a correlation between the vasoconstrictor potency of a series of topical corticosteroids with partition coefficient and aqueous solubility (117). In order to explain the importance of lipid and water solubilities in the passage of any substance through the skin, the Meyer-Overton theories of absorption through a lipid or lipid-protein cell membrane structure have been invoked (108, 118). These theories imply that substances which are lipid soluble may penetrate the stratum corneum because of its lipid content, while the hydration of the keratin leaves the stratum corneum permeable to water-soluble substances.

It is also recognised that the relative solubility, the partition coefficient of the drug in the vehicle and the stratum corneum is important as this will reflect the tendency of the drug to remain in or diffuse out of the vehicle (98). It has often been considered that substances having an oil/water partition coefficient of unity will have the highest penetration rate (17, 78, 98). Poulsen (65) has cautioned that this conclusion is not strictly correct and its general acceptance has led to erroneous assumptions regarding the importance and significance of the partition coefficient.

Many workers have shown some correlation between a compound's partition coefficient in model systems such as benzene/water, oil/water, ether/water and its ability to penetrate the skin (98, 117, 120 - 2). The validity of the use of these models has been questioned and it is said that realistically, the only partition coefficient measurement for a drug that can be exactly related to its rate of diffusion through the skin is the value determined for the equilibrium distribution of the drug between the vehicle and the stratum corneum (76). Measurements of this type, using excised stratum corneum/water systems have been made by Scheuplein. He found that while the permeability coefficients were proportional to the partition coefficients for a series of simple aliphatic alchols (80), they were not proportional for a range of steroids (123). The main criticisms levelled at these studies is that water does not adequately simulate the complex nature of the vehicle and any similarity between the two is purely coincidental (76). In addition, water tends to hydrate the stratum corneum and this tends to increase the steady state permeability constants by a factor of 2 or 3 (105). The method also does not distinguish between the amount of drug actually partitioned into the stratum corneum and the amount that has interacted with the skin.

(e) Concentration

The role of concentration effects in percutaneous absorption has often not been adequately investigated and Feldmann & Maibach (124) have reported that in much investigative dermatology standard concentration figures have been arbitrarily drawn on the basis of precedent rather than pharmacologic dose range studies.

Higuchi (11) has reported that the amount of drug percutaneously absorbed per unit surface area per time interval will usually increase as the concentration of the drug in the vehicle is increased. The positive penetrative effects of increased concentration have been demonstrated with various steroids and other drugs (125, 126) Skog and Wahlberg (127) have observed that increasing the concentration of various compounds in guinea pigs increased penetration up to a certain point, at which a plateau was reached indicating that the barrier layer was not influenced by diffusion gradients but merely acted as an absolute limiting step, limiting the total amount of drug passing through in unit time. This further suggested that for true steady state diffusion, permeability constants were independent of concentration (118).

It is interesting to note that reports indicating negative effect of increased concentration have also appeared in literature. Strakosch and Clark (128) observed that increasing the concentration of sulphonamide from one to ten per cent in the vehicle caused no increase in their absorption when applied to the skin. For substances having a caustic effect on the skin, e.g. phenol in high concentration (129) or hydrogen sulphide gas (130), the negative penetrative effect of increased concentration has been explained as being due to the formation of a crust which impedes further penetration.

From a physicochemical point of view only the dissolved drug is capable of diffusing from the vehicle phase into the skin and therefore the concentration of drug in solution in the vehicle will be critical. As a general rule (76) penetration is faster from a vehicle

in which the drug is in solution or in which a poorly soluble drug is completely solubilised compared with the same vehicle in which the drug is in suspension. Physical models of diffusion processes occurring when a drug is in solution or suspension in a topical vehicle have been defined by Higuchi (11) and these have been outlined in Section 3.4.3.

(f) Miscellaneous Effects

(i) Molecular Characteristics of the Drug

Chemical structure of the drug is important because of its influence on the water/lipid partition coefficient and on the interaction between the drug and the stratum corneum (81). For instance, in an homologous series of compounds, a more polar molecule will exhibit increased attraction with the polar sites within the stratum corneum thus decreasing its mobility.

Over a large range of molecular sizes, an inverse relationship appears to exist between the absorption rate and the molecular weight (83, 121, 131), however over a narrow range, size does not appear to be relevant.

(ii) Particle Size

A reduction in the particle size of a suspended drug is thought to promote the rate of dissolution and release. Barrett et. al. (132) have demonstrated that percutaneous penetration of fluocinolone acetonide was significantly improved on micronising the steroid.

(iii) Polymorphism

Since polymorphs of the same drug entity may differ significantly in many of their physical properties, including solubility, careful consideration must be given to this phenomena in any pharmaceutical delivery system in which the drug exists in the solid state (18, 133).

3.3.3 Vehicle Effects

(a) Effect on Hydration

One of the factors determining the efficiency of a vehicle in aiding penetration is the effect the vehicle will have on the stratum corneum hydration. For instance, greases and oils, e.g. the paraffins, are the most occlusive vehicles and induce the greatest hydration through sweat accumulation at the skin-vehicle interface (99). Emulsions generally are less occulusive than the greases and of the water/oil and oil/water types, the latter are more occulusive than the former. Certain emulsifiers and humectants which have a high affinity for water dehydrate the stratum corneum and decrease penetration (76). On the other hand, solvents such as tetrahydrofurfuryl alchol and propylene glycol have been postulated to reduce the barrier function of the stratum corneum promoting an increase in water loss and allowing an easier passage of the corticosteroids (118, 134).

(b) Defatting Solvents

The passage of a drug through the lipid barrier either in the outer layer or through the follicular route represents a major diffusional pathway. Removal of part of this lipid material by organic

solvents like ether or chloroform is said to make the skin permeable to water soluble substances diminishing the penetration of lipid soluble compounds (74). Wurster and Kramer (98) have reported that the disruption or partial elimination of the lipid pathway normally used by methyl salicylate produced a 27% decrease in its absorption. Scheuplein and Blank have however shown that delipidisation of stratum corneum produces a fairly porous, non-selective membrane which allows a more rapid and easier passage of a penetrant due to an effective reduction in the diffusional pathway (135).

(c) Aprotic Solvents

Various aprotic materials such as urea, dimethylsulphoxide, dimethylformamide and dimethylacetamide on their own or in combination with other vehicles have been found to accelerate percutaneous penetration. Of these materials, DMSO a dipolar aprotic solvent, miscible with water and other common organic solvents, is widely studied and is best known for its ability to enhance percutaneous absorption (76, 81, 101, 118, 135 - 9). Not only does DMSO enhance percutaneous absorption, it also promotes the formation of a reservoir in the skin (140, 141).

DMSO has been shownto exhibit an unusual concentration dependent-accelerant effect (143 - 5). In low concentrations, DMSO does not appear to enhance percutaneous absorption appreciably. At least 60% DMSO is required for a measurable increase in penetration rate. Beyond this concentration, penetration increases very rapidly. Sweeney et. al. (142) showed that from a twofold increase in penetration at 60%, at 80% and 90% the increase was tenfold and ninety-fold respectively.

The mechanism of the accelerant effect of DMSO is still not clearly defined. It is clear that the accelerant effect observed *in vivo* is not due to increased skin circulation (143) (a) because this can be increased without increasing the penetration rate; (b) because accelerants do not increase the skin clearance rate; and (c) the effect can be observed *in vitro* with isolated non-perfused skin preparations. It has been suggested that DMSO, due to its strong hygroscopic properties, increases the water content of the stratum corneum thus increasing its permeability (146). Tees (147) considers that only high concentrations of DMSO are effective because they increase the hydration of the stratum corneum beyond the maximum reversible extent thus disrupting the membrane structure. Rammler and Zaffaroni (148) have attributed the increased permeability to the possible reversible configurational changes in protein structure brought about by substitution of internal water molecules by DMSO. Vinson et. al. (149) and Montes et. al. (150) have shown that accelerants can extract structural material from the stratum corneum and this has been shown to leave permeable channels (143, 151). Elfbaum & Laden (152) and Allenby et. al. (143) have shown that some accelerants can cause the stratum corneum to swell thus reducing its diffusional resistance (153). The results of the above mentioned workers suggest that accelerants such as DMSO owe their effectiveness to a lowering of the barrier properties of the stratum corneum brought about by hole formation and a reduction in diffusional resistance. Accelerant/water partition coefficient is also thought to play a significant role in determining the increase in the rate of percutaneous penetration (143, 154).

(d) Surface Active Agents

Surface active agents are often included in topical pharmaceutical formulations and may play a part in promoting skin penetration. The effect on penetration due to, and the penetrant action of, surface active agents has often been reported and reviewed (17, 81, 118, 135, 153). The penetration and penetrant action of the surface active agents is said to be of the following order: anionics > cationics > nonionics (118, 135). The nonionics in general are thought to have very little influence on the stratum corneum and consequently on permeation.

Surface active agents lower the surface tension of aqueous solution and further aid in the emulsification and subsequent removal of the surface lipids of the skin. Bettley (155) has shown that lowering the surface tension of water is not an important factor in enhancing skin permeability. The removal of the surface lipids would however aid the penetration of the surfactants.

Dilute solutions of anionic and cationic surfactants are effective in damaging the skin thus causing an alteration in the barrier function of the skin (135). Increasing the concentration of the surfactant has been shown to increase the rapidity and the severity of the damage. The removal of the surfactant causes the progressive penetration and damage of the skin to stop.

The influence of surfactants on skin penetration, particularly of anionic-type materials, appears to be related to their ability to increase the permeability of the skin to water by altering the physical

state of water in the skin, in such a way as to permit greater freedom to the passage of charged hydrophilic substances (118, 135, 156).

(e) Vehicle pH

The pH of an aqueous vehicle influences percutaneous absorption principally by determining the state of ionisation of the penetrant. In the case of ionic compounds only the un-ionised form of the drug may penetrate the skin to any degree (18). Arita et. al. (106) reported that *in vivo*, altering the pH of the skin to either side of neutrality increased absorption. They attributed the low absorption at neutral pH to a higher degree of ionisation at this pH more than at more acid or alkaline pH values. Katz & Poulsen (76) have pointed out that the skin keratin being a protein with an isoelectric point of 3.7 - 4.5, the pH of topically applied vehicles might also affect its hydration state significantly.

(f) 'Viscosity'

The part played by 'viscosity' of a vehicle in influencing drug release from a semisolid has been discussed at length in an earlier Section 1.1.3. It was shown that the nature and extent of this influence seems somewhat uncertain. Several workers have attempted correlation of rheological parameters with drug release data however these studies have largely been empirical and inconclusive. In most cases, the important fundamental question "What is the rheological environment seen by the diffusing drug molecule and how

can it be determined?" has been ignored or left unanswered.

(g) Nature of Formulation

Various aqueous or oily, single phase or biphasic, topical vehicles are used in practice. The vehicle composition, the nature and character of the fomulation play an important role in determining drug release. For instance, in an emulsion ointment, the distribution coefficient of the drug between the internal and external phases as well as the total concentration, defines the concentration gradient between the vehicle and the skin surface (18). A knowledge of the concentration gradient will thus aid the understanding of the drug release characteristics of the emulsion ointment base. Koizumi and Higuchi (157, 158) have carried out an extensive study of drug diffusion through emulsion systems.

Consideration of the changes that may occur in the vehicle formulation on application of the vehicle to the skin is also very important. Loss of a volatile component, uptake of water from the skin or atmosphere, phase inversion of an emulsion - all are factors that may produce an entirely different effective drug concentration so far as drug transport into the skin is concerned (18). Concentration changes due to loss of a volatile component in the vehicle were exploited by Coldman (159) et. al. to facilitate steroid penetration.

3.4 Theory of Topical Drug Absorption

It is generally accepted that the process of topical drug release and absorption is a passive diffusional process and that no

active transport mechanism is involved. Various physical-mathematical models have been developed in order to predict and explain the drug release characteristics of topical dosage fomulations. The following treatment is based on that of Barrer (160), T Higuchi (11) and Lueck (161).

3.4.1 Permeation

Tha main characteristics of a penetrating agent which determine its rate of entry through the skin are its effective partition coefficient and diffusivity in the barrier phase. The product of these two is often spoken of as the permeability constant (11).

Permeability constant = Partition coeff (P.C.) x Diffusivity (D)

... (44)

(a) Partition Coefficient

The partition coefficient, represented by the symbol P.C., is indicative of the quantity of the penetrant available for permeation. For dilute, ideal solutions at a given temperature and pressure, this may be defined as the ratio of the concentrations of the penetrant at equilibrium in phase I and II respectively.

$$PC = \frac{C1}{C2} = \text{constant}$$

... (45)

(b) Diffusivity

The diffusivity of the penetrant defines the rate of movement of the agent through the medium. The mechanism of transfer of the penetrant in a continuous medium is a diffusional process. The laws which are applied to this diffusional process were first proposed by Fick in 1855. Fick's first general law of unidirectional diffusion states that the driving force which causes the transfer of a substance from regions of high to regions of low concentration is proportional to the concentration gradient. This first law is written as:-

$$\frac{dQ}{dt} = - D \left(\frac{dc}{dx} \right) \qquad \ldots (46)$$

where Q represents the amount of penetrant crossing a plane of unit area, t the time of diffusion, $\frac{dc}{dx}$ is the concentration gradient and D the diffusion constant.

The application of the first law requires the determination of the flux $\frac{dQ}{dt}$ and the concentration gradient $\frac{dc}{dx}$. The fact that the law specifies a constant concentration gradient implies the establishment of a steady state.

In some experiments, the conditions of steady state can be arrived at experimentally. However often this is not possible. Where the concentration changes only slightly with time, i.e.

$$\left\{ \frac{dc}{dt} \right\}_x \approx 0 \qquad \ldots (47)$$

the condition of quasi-steady state is said to occur, and the application in this case of Fick's first law for unidirectional diffusion will not introduce any serious errors.

Where the concentration gradient is changing relatively rapidly, it becomes necessary to determine the change of concentration with time resulting from the non-stationary state diffusion. This leads to Fick's second law which is usually written as(162):-

$$\frac{dc}{dt} = D\frac{d^2c}{dx^2} \qquad \ldots (48)$$

assuming in this case that D is constant. Treating D as a constant is a specialisation not always valid and it is necessary to treat D as a variable in deriving an expression for the change of concentration with time. Thus Fick's second law can be rewritten as:-

$$\frac{dc}{dt} = \frac{d}{dx}\left(D\frac{dc}{dx}\right) \qquad \ldots (49)$$

Integration of the above equation can yield D in a fixed frame of reference from measurements of either $\frac{dc}{dx}$ or c as a function of x and t.

Often it is of greater importance to know the length of time required to establish the steady state within the barrier than to know the subsequent rate of flow. This period, the well known 'lag time' of Barrer (160) is defined by the expression

$$L = \frac{h^2}{6D}$$

... (50)

where L refers to the 'lag time' and h, the effective thickness of the skin barrier. Thus the experimental determination of L permits estimation of the diffusion constant D. Flynn and Roseman (163) have questioned the applicability of Equation (50) to complex, hetrogenous membranes such as stratum corneum. They have pointed out that protein binding of the penetrant in the stratum corneum occurs frequently, thus considerably increasing the lag time and drastically reducing the estimates of diffusion coefficient.

The mathematical solution to any problem of non-stationary state diffusion depends upon the successful integration of Fick's second law. The numerical analysis of the resulting differential equations can be quite complex. For this reason experimental conditions are often adjusted to yield steady state or quasi-steady state conditions for diffusion.

3.4.2 Case where Diffusion across the Skin is rate limiting

Several expanded forms of Fick's first law of diffusion have been developed. Higuchi (11) has proposed the following equation where the rate limiting step in penetration is diffusion across the skin barrier.

$$\frac{dQ}{dt} = \frac{D\ (PC)\ CvA}{h}$$

... (51)

Cv represents the concentration of the drug dissolved in the vehicle and A is the effective cross-sectional area over which diffusion occurs. Equation (51) is only valid for the steady state penetration of the rate limiting skin barrier.

3.4.3 Case where Diffusion through the Vehicle is rate limiting

The properties of the skin can be ignored where diffusion and release of the drug from the vehicle is rate limiting. The skin can be regarded as a perfect sink which plays no part in determining the rate at which the diffusing drug penetrates the skin (65). Of particular interest in such a situation are the following general cases.

(a) Release of Uniformly Dissolved Drug

Higuchi (11) derived from Fick's laws the following equation for the amount of drug released from (one side of) a layer of ointment in which the drug is initially dissolved in a uniform manner.

$$Q = hCo \left\{1 - \frac{8}{\pi^2} \sum_{m=o}^{\infty} \frac{1}{(2m+1)^2} \exp\left(-\frac{D(2m+1)^2 \pi^2 t}{4h^2}\right)\right\} \quad \ldots (52)$$

where Q = amount of drug released per unit area of application, h = thickness of layer, Co = initial concentration of drug in ointment, D = diffusion coefficient of drug in the ointment, t = time after application and m = integer with values from 0 to ∞ .

W I Higuchi (164) has pointed out that the following assumptions must hold for Equation (52) to be applicable.

(i) Only a single drug species is important in the ointment.

(ii) The diffusion constant is independent of the time and position in the ointment layer.

(iii) The composition of the vehicle remains constant and only the drug diffuses out of the vehicle.

(iv) The drug reaching the receptor side of the ointment layer is removed rapidly.

Furthermore he has pointed out that for most practical applications when the ointment layer is sufficiently thick and the percentage of drug released is $\lesssim$ 30%, a simplified form of Equation (52) may be successfully used.

$$Q = 2Co \left(\frac{Dt}{\pi} \right)^{\frac{1}{2}} \qquad \ldots (53)$$

This square root relationship provides an easy and a practical method for the determination of D.

(b) Release from Suspensions

Higuchi (11, 165) has deduced the following equation for the release of a drug uniformly suspended in an ointment base:-

$$Q = (2Co - Cs) \left\{ \frac{Dt}{1 + \frac{2(Co - Cs)}{Cs}} \right\}^{\frac{1}{2}} \qquad \ldots (54)$$

where Cs is the solubility of the drug in the external phase of the ointment and the other symbols are as before.

The Equation is derived for a system described as follows:-

(i) the suspended drug is in a fine state such that the particles are much smaller in diameter than the thickness of the applied layer;

(ii) the amount of drug Co per unit volume is substantially greater than Cs; and

(iii) the surface to which the drug ointment is applied is immiscible with respect to the ointment and constitutes a perfect sink for the released drug.

Equation (54) further simplifies, for a common suspension case where Cs << Co to:-

$$Q = (2CoDCst)^{\frac{1}{2}} \quad \ldots (55)$$

In this case the square root relationship again holds and simplifies the evaluation of D. Higuchi and Higuchi have also evaluated the hetrogenous barrier behaviour of a suspension ointment to diffusion (166).

(c) Release from Emulsions

More recently the theoretical analysis of drug diffusion

through emulsion systems have been extensively studied and reported (157, 158, 166). Equations (52) to (55) were derived on the assumption that D must be constant with respect to both time and position. Koizumi and Higuchi (157, 158) have shown that in many situations involving emulsions, the diffusion coefficient is not constant but is a function of concentration. They have derived from Equation (49), in the following manner, the expression for the release of a drug from an emulsion system.

From Equation (49), applying Boltzman's method (160), the following expression for the effective concentration C may be derived:-

$$C = a \int_o^{\lambda} \frac{1}{D} \exp \left(- \int_o^{\lambda} \frac{\lambda}{2D} d\lambda \right) d\lambda \qquad \ldots (56)$$

$$a = \frac{Co}{\int_o^{\infty} \frac{1}{D} \exp \left(- \int_o^{\lambda} \frac{\lambda}{2D} d\lambda \right) d\lambda} \qquad \ldots (57)$$

where $\lambda = x/\sqrt{t}$ and x is the co-ordinate.

The non steady state drug release rate per unit area, G, is given by:-

$$G = \left(D \frac{dc}{dx} \right)_{x=o} \qquad \ldots (58)$$

Integration of Equation (58) using Equations (56) and (57) gives:-

$$\left(D \frac{dc}{dx}\right)_{x = o} = \frac{1}{\sqrt{t}} \left(D \frac{dc}{d\lambda}\right)_{\lambda = o} \quad \ldots (59)$$

thus

$$Q = 2a \sqrt{t} \quad \ldots (60)$$

where Q is the amount of drug released per unit area, and a is the constant defined by Equation (57).

Koizumi and Higuchi have thus pointed out that even if D is concentration dependent, the release pattern is exactly the same as the constant D case and the "square root" relationship still holds.

3.4.4 Relationship of the Diffusion Coefficient to Other Physical Quantities

The diffusion constant, D, is an index of the resistance of the medium to movement of the penetrant molecule through it (76). The relative magnitude of this term in the vehicle and skin phases is a reliable indicator of whether penetration is rate limited by release from the vehicle or by the diffusional resistance of the skin (65).

The diffusion coefficient, D, is related to other measurable physical quantities by the Stokes-Einstein relation

$$D = \frac{kT}{6\pi\eta r} \qquad \ldots (61)$$

where k is the Boltzman constant, T, the absolute temperature, η the viscosity and r is the hydro-dynamic radius of the diffusing drug molecule. The above relation is applicable for low concentrations of drug molecules which should be roughly spherical, electrically neutral and large compared with the solvent molecules. Despite the limitations imposed upon this equation by the above assumptions, it has found rather wide usage with better than moderate success (76).

The Stokes-Einstein relation has thus related the diffusion coefficient to the temperature, the size of the drug molecule and the viscosity of the medium. As has been pointed out earlier, temperature is of minor importance in topical therapy. Wurster (12) has pointed out that the dependence of the diffusion coefficient on molecular weight is minimal since relatively large changes in molecular weight are required to affect significantly the mean radius. Thus it is the 'viscosity' of the medium that plays an important role in determining the effective diffusion coefficient.

3.5 Methods of Studying Percutaneous Absorption

The methods of studying percutaneous absorption have been extensively reviewed in several excellent articles on the subject (17, 76, 81, 97, 118, 167 - 70). These can be broadly classified into two categories: the *in vitro* simulation of drug absorption and the *in vivo*

experiments on animals and humans. It is not the intention in the following discussion to give detailed experimental descriptions of the methods used to study percutaneous absorption, but instead to point out in general terms the principles involved in the design of experimental methods and the limitations of these methods.

3.5.1 In Vitro Methods

From an academic viewpoint these methods are of great interest as they allow absolute control of experimental conditions thus facilitating the study, individually, of the various factors affecting percutaneous absorption. It is true however that these methods do not correspond entirely with the conditions of clinical application of the product and that the final results in the study of the effectiveness of these preparations must be obtained by *in vivo* evaluation. *In vitro* methods will however enable certain general conclusions to be made which are useful when studying these preparations under *in vivo* conditions.

(a) Diffusion Models without Membranes

These models can be represented as comprising a diffusion cell or a well filled with the semisolid medicament from which the drug diffuses into a diffusion medium (usually agar (171, 172) or gelatin gel (76) but more recently chloroform (173) and isopropyl myristate (174) have also been used) said to simulate skin. No membrane divides the diffusion cell or well from the diffusion medium. The fact that such a model does not truly represent skin absorption may be judged from several points:-

(i) the diffusion medium (receptor phase) cannot adequately simulate the two phase process of drug absorption into and through the skin.

(ii) The aqueous nature of the agar and gelatin gels that have been the most popular receptor phases do not resemble the lipoidal nature of the skin.

(iii) There is no membrane to simulate the barrier function of the skin.

(iv) Until recently, when chloroform and isopropyl myristate were introduced as receptor phases for these models, they were rather limited in their application to drugs of the antimicrobial type.

While these models are in some instances useful for studying drug release from vehicles, they are so far removed from real conditions of the skin that Hadgraft (175) has stated that they are unlikely to indicate the behaviour of the preparation on skin surface.

(b) Diffusion Models with Membranes

These models basically consist of two compartments divided by a membrane. The diffusion cell holds the medicament and the release of the drug from the cell is modulated through a membrane into the diffusion fluid (the receptor phase).

The number of variables an investigator has to cope with in his task of designing a two compartment diffusion model are illustrated in Figure 9 and discussed in a subsequent section in Part C. Given the large number of variables, it is perhaps not surprising that numerous

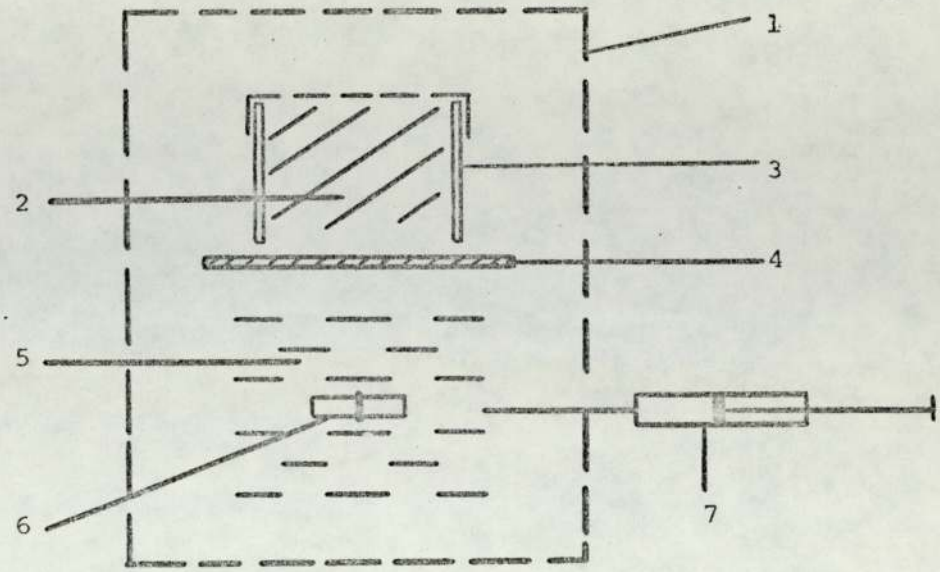

FIGURE 9

FACTORS TO BE CONSIDERED IN DESIGNING A SUITABLE

IN VITRO DIFFUSION CELL

1. Temperature
2. Form of medicament
3. Type of diffusion cell
4. Type of membrane
5. Diffusion fluid
6. Stirring conditions
7. Sampling method

variations of a diffusion model have been reported in literature (102, 159, 167, 176 - 82). Inevitably, this has produced studies that have often been irreproducible and incomparable and the results of these studies have sometimes been confusing and contradictory. This has further hindered the design and development of a simple standard *in vitro* diffusion model for percutaneous absorption studies.

3.5.2 In Vivo Methods

Of numerous methods proposed, the practical *in vivo* test methods that can be employed readily in routine analysis are somewhat limited and in addition these methods fail to provide a separate quantitative measure of the extent of intra-cutaneous and systemic absorption of the penetrant. Objection has also been raised to the use of animals in studying percutaneous absorption and Marzulli et. al. (97) have drawn attention to the differences in physical and biochemical characteristics of human and animal skin, which if not recognised could lead to erroneous interpretation of animal data (76). The main objection however to the use of live human or animal models has been that these studies measure penetration by an indirect means, e.g. through urinary recovery. Barr (17) has emphasised that *in vivo* methods give a more accurate picture of percutaneous absorption and this is the most significant reason for carrying out *in vivo* studies. Perhaps the most desirable technique in studying percutaneous absorption is to obtain complementary *in vitro* and *in vivo* data.

The following discussion of *in vivo* techniques is based on the classification proposed by Blank (170).

(a) Loss of Penetrating Substance from Surface

This method involves the measurement of decrease in the concentration of a given penetrant from a fluid chamber open to the skin. The measurement may involve analysis of the fluid in the diffusion chamber or the record of the disappearance of radioactivity from labelled compounds applied to skin surface (183). The drawbacks of this method are that where the amount of material penetrating the skin is a very small percentage of the applied material, this is difficult to measure accurately due to relative large errors of measurement involved and secondly the radioactive disappearance method has an inherent 5 - 15% error due to the subdued emissions from agents that have passed into the stratum corneum (169).

(b) Histochemical Methods

These methods are useful for demonstrating the absorption, route of penetration and passage time of drugs into and through the skin (184). The presence and position of the drug in the skin is usually detected from histological sections made from biopsies taken from the site of application. Dyes, flourescent compounds and radio labelled compounds have been used to trace the movement of the drug through the skin. The method presupposes that the tracer and the penetrant act similarly and do not become separated during penetration, however this is not always the case. The major limitation of these methods is that their application demand considerable expertise of histochemical techniques and even then, it cannot be guaranteed that the cutting, staining and handling of tissue will not displace or remove the penetrant from the tissue (169).

(c) Elicitation of Biological Response

Arbitrary ranking of biological reaction elicited by the penetrant provides a simple and practical method for evaluating percutaneous absorption. Biological responses such as vasoconstriction (185), vasodilation (121), wheal formation (186), local anaesthesia (187) and changes in sebum secretion (188) can be visually evaluated for pharmacologically active substances. The major drawback of this form of evaluation is that quantitation of the rates of absorption of biologically active compounds is difficult however comparative estimations of absorption of a given agent in such varying environmental circumstances as humidity and temperature can be meaningful (169). A great deal of information regarding comparative effectiveness of topically applied steroids has been derived from this approach (189 - 90). For instance, Place et. al. (192) have demonstrated that strict control of experimental variables yields a vasoconstrictor assay of extreme sensitivity and high precision.

(d) Body Fluids or Tissue Analysis

While skin specimens obtained by biopsy may be analysed for drug concentration, the most common method of studying percutaneous absorption *in vivo* is the detection of the drug in blood (188), urine (98) and faeces (193) at different intervals following application of the material to the skin surface. The inherent limitations of these methods are obvious for substances which are normal body constituents and for compounds so poorly absorbed as to be diluted beyond detection in body tissues or fluids. However, in many instances, radioactive labelled compounds can overcome some of these problems (76). The objection to the use of these methods has been that a drug recovered

in blood or urine will not necessarily reflect the total original amount penetrating the skin as the amount of drug distributed, stored or metabolised by the tissues cannot be accounted for. However the objection can be overcome to some extent by animal "calibration" (194) and controlled excretion and recovery of the drug and metabolites and Stoughton (169) has confirmed that this type of study can be very useful for comparing absorption of a given agent in a given individual in variable conditions.

4 AIMS AND OBJECTS OF THE PRESENT INVESTIGATION

Despite the fact that numerous studies have been carried out in the past on rheological and drug release characterisation of pharmaceutical semisolids, there is limited information in literature concerning the influence of rheological properties on drug release and bioavailability. Several workers have attempted correlation of rheological parameters with drug release however these studies have largely been empirical and inconclusive. The main reason for the lack of definition arising out of these studies has been that they have failed to yield meaningful rheological data that could be interpreted at a molecular level in terms of the viscous resistance experienced by the diffusing drug molecule. Furthermore the complexity of the systems used in these studies has made it difficult to delineate any changes in drug release due to rheological factors. Finally rationalisation in the design of *in vitro* and *in vivo* experimental systems to suit the interest of the investigators has led to situations where the results obtained have often been unrepeatable, incomparable and sometimes even contradictory.

All these factors have thus contrived to make the picture concerning the influence of rheological properties on drug release and bioavailability from pharmaceutical semisolids somewhat confusing. It was the aim of this investigation to attempt to clarify this situation by providing a rational and fundamental approach to the problem. This objective necessitated the following three-fold investigation:-

(a) A fundamental investigation of the rheological properties of "model" semisolid vhicles. This part of the investigation

required:-

(i) choice of suitable "model" semisolid vehicles;

(ii) rheological characterisation of the "model" semisolid vehicles;

(iii) evaluation of the effects of formulation on the consistency of the "model" semisolid vehicles.

(b) Investigation *in vitro* and *in vivo* of drug release from the "model" semisolid vehicles. This part of the investigation required:-

(i) choice of suitable "model" drugs;

(ii) development and characterisation of simple reproducible *in vitro* method of assessing drug availability;

(iii) development of a simple *in vivo* method of assessing drug availability;

(iv) *in vitro* and *in vivo* drug release characterisation of the "model" semisolid vehicles.

(c) Investigation of the influence of rheological characteristics of a product in determining drug release by a correlation of rheology and drug release data for the "model" semisolid vehicles.

PART B

RHEOLOGICAL CHARACTERISATION OF PLASTIBASES

AND THE EFFECT OF FORMULATION ON THE

CONSISTENCY OF THESE VEHICLES

1 INTRODUCTION

1.1 Plan of Rheological Investigation

The object of this part of the investigation was to determine meaningful rheological characteristics of semisolid systems that could be employed in correlation of drug release data at a later stage.

Rheological characterisation of 'model' semisolid systems was carried out using continuous shear, small strain creep and dynamic tests. Continuous shear tests were employed in order to assess parameters that would reflect the shear behaviour of the systems under conditions of application. The fundamental rheological characteristics of the systems were evaluated using small strain creep and oscillatory (dynamic) tests. Dynamic tests were particularly useful for vehicles with relatively 'thin' consistencies which could not be characterised adequately by the creep method. Interconversion of creep and dynamic data was undertaken in order to provide a complete set of values for correlation with drug release data.

It is clear that the final consistency of a product is not only dependent on the rheological ground state of the vehicle(s) but also on factors concerned with the formulation and manufacture of the product. For this reason the effects of formulation on the consistency and physical properties of 'model' vehicles were studied.

1.2 'Plastibases'* as model semisolid vehicles within the

---

* 'Plastibases' - Trade name for polyethylene-mineral oil gels manufactured by E R Squibb & Sons Limited, Wirral, Cheshire.

1.2.1 Criteria governing the choice of 'suitable' model semisolid vehicles

The choice of semisolid vehicles used in the context of this work as 'model' systems was based on two sets of criteria.

For the rheological part of this study, the 'model' systems were expected to meet the following requirements:-

(i) the vehicles are relatively simple in composition and structure;

(ii) the consistency characteristics of the vehicles are within the control of the manufacturer such that vehicles exhibiting a range of consistencies may be produced;

(iii) the vehicles remain stable over the normal range of temperatures, 0^{o} to 50^{o}, encountered in practice.

For the drug release part of this study, the 'model' systems were expected to meet the following requirements:-

(i) comprise a simple composition such that the chemical potential of a drug of standard specifications and given concentration incorporated in the 'model' vehicles does not alter from one vehicle to another;

(ii) the vehicles are inert in order that drug-vehicle interactions are reduced to a minimum. This would make it possible to delineate changes in drug release due to rheological factors;

(iii) the vehicles do not cause an inflamatory or sensitizing response on application to the skin. This is an important consideration when conducting in vivo studies.

'Plastibases' fulfilled the above listed requirements for 'model' vehicles in this study and their selection from the range of pharmaceutical semisolid vehicles available is discussed in the next Section.

1.2.2 Possible 'model' vehicles

Martin et. al (5) have classified the various types of semisolid vehicles used in present day practice into three categories, namely organogels, hydrogels and emulsion type semisolids. Due to the biphasic character of the emulsion type semisolids, these were obviously not suitable as 'model' vehicles in the context of this thesis.

The hydrogels were also considered unsuitable due to the number of technical difficulties that have been reported to have been encountered in their use (8), notable amongst these being instability, incompatibility and drying of the vehicles.

The organogels were thus carefully evaluated for their potential use as 'model' vehicles. Several types of organogels are available in practice. Of these, the animal and vegetable fat bases are well known for the ease with which they go rancid (195). The hydrophilic organogels, e.g. Carbowax, polyethyleneglycol, although still a popular component of several ointment vehicles, have the dis-

advantage of not absorbing more than about three per cent of water before becoming fluid and of softening due to complex formation (5, 196) in the presence of salicylates, benzoates, phenols and phenolates. In addition they have also been said to cause dehydration of the skin thereby reducing percutaneous absorption (76). Thus the hydrocarbon type of organogels were found to be most promising as potential 'model' vehicles.

The paraffins are the most common and most widely used hydrocarbon type organogels. Typical of these is white soft paraffin, a two phase colloidal system of oil and wax, the latter component comprising a crystalline portion and a "protosubstance" (197). The crystalline portion provides rigidity to the system while the "protosubstance" which is partially amorphous and acts as a gel former prevents the separation of the liquid from the solid hydrocarbon (198). The physical properties of the soft paraffins are dependent upon the proportions of n-, iso- and cyclic paraffins (199). The composition of the paraffins can vary with the source of the crude oil, method of refining and blending processes which may occur after the petrolatum has been refined (200) and thus considerable difference in physical properties such as consistency may be exhibited between batches and grades of petrolatum.

In order to produce a product of consistent quality attempts have been made to gel mineral oil with crystalline or amorphous wax alone (198), but these have met with little success. The crystalline wax produced a granular mixture and the amorphous wax produced a thick, heavy, stringy mass. It was clear thus that both amorphous and crystalline fractions were essential prerequisites of a gelling agent

for producing a mineral oil gel.

Polyethylene, a high molecular weight hydrocarbon with a high melting point and a relatively flat temperature viscosity curve, is one such gelling agent containing both crystalline and amorphous fractions. It is a synthetic substance and hence subject to very close control (198). It has been found highly suitable for use as a gelling agent for mineral oil to form unctuous base compositions useful in the preparation of ointments and creams. These preparations are manufactured by E R Squibb & Sons Limited and are sold under the trade name Plastibase (201). Closely controlled manufacturing conditions of these preparations ensure consistent quality standard. These vehicles complied with the criteria set down in Section 1.2.1 and a considerable amount of information concerning their formulation was available in the literature. Plastibases were thus chosen within the context of this thesis as 'model' semisolid vehicles.

1.2.3 The Plastibases (202)

Plastibase was originally introduced by Research Products Corporation, Madison, Wisconsin, (203- 205) under the trade name Jelene 50W (206). It was subsequently manufacturered by E R Squibb & Sons under its present trade name. There are six Plastibase formulations available commercially and these are listed below:-

Plastibase 5W

Polyethylene	5g
Mineral oil q.s.	1000g

Plastibase 10W

Polyethylene	10 g
Mineral oil	1000 g

Plastibase 20W

Polyethylene	20 g
Mineral oil q.s.	1000 g

Plastibase 30W

Polyethylene	30 g
Mineral oil q.s.	1000 g

Plastibase 50W (Jelene 50W)

Polyethylene	50 g
Mineral oil q.s.	1000 g

Plastibase Hydrophilic

Polyethylene	56.4 g
Glyceryl Mono-oleate	60.0 g
Tenox 2 (R)	1.0 g
Propyl Parahydroxybenzoate	0.5 g
Methyl Parahydroxybenzoate	0.5 g
Mineral oil q.s.	1000 g

Plastibase has been described (202) as a smooth, soft, homogeneous, colourless, odourless, neutral, non-irritating, non-sensitizing and an extremely stable base. It can be used for a wide variety of formulations including aerosols. It allows rapid and easy compounding, exhibits a wide range of compatibility and a uniform

dispersion of drugs, even at elevated temperatures. It maintains consistent softness even at high concentrations of solids and in extremes of temperatures. Comparatively, Plastibase is said to demonstrate a faster, greater, more regular and more thorough release of medicaments. The base is easily applied, exhibits remarkable spreadability, is "non-running" at body temperatures, imparts a velvety, non-greasy feel to the skin and is readily removed.

(a) Preparation of Plastibases (198, 202)

Polyethylene of molecular weight 21,000 is dissolved in heavy mineral oil (Saybolt viscosity 340 sec) by heating the mixture to 130°C and holding the mixture at this temperature for three hours with constant agitation. The hot solution is allowed to cool to a temperature just above its cloud point (95° - 100°C) and is then shockcooled at the rate of 10°C per second to a temperature just below its gel point (about 50°C). Strict control of the manufacture and cooling conditions should ensure consistent gel quality. Schultz and Kassem (207) and Huttenrauch et. al. (208 - 210) have investigated the influence of temperature of solution, solution time and the rapidity of cooling on the structure and physical properties of polyethylene-mineral oil gels. Other methods for the preparation of polyethylene-mineral oil gels have been reported by Thau and Fox (211 - 2) and Backer (213).

(b) Structure of Plastibases

Phase contrast microscopy has revealed that polyethylene in mineral oil precipitates as small crystallites surrounded by long fibrous amorphous filaments which intermesh and produce a sponge-like

structure resulting in a three dimensional lattice responsible for the gel structure (198, 207, 210).

The number of crystallites present in a five per cent gel are determined partly by the degree of crystallinity of the polyethylene (198). Rapid chilling is necessary to produce the gel structure while a slowly cooled gel results in a grainy, slushy, pourable mixture containing 'lumps' of polyethylene (198, 207, 210). Huttenrauch et. al. (210) observed that polyethylene forms large spherulites on slow cooling. The degree of crystallinity in polyethylene varies with the polymerisation process, the best polyethylene-mineral oil gels are formed with polyethylene of molecular weight 21,000 (202).

Thau and Fox (211) have reported that their proposed high shear method of preparation of polyethylene-mineral oil gels yields a finer dispersion of the polyethylene resulting in more compact gels with smaller pore size and of greater rigidity. Furthermore, the consistencies of gels produced by this high shear method are independent of cooling rates. Backer (213) has determined that with his proposed method of preparation of these gels, the particle size of polyethylene in the gel was less than 0.8 micron.

(c) Consistency of Plastibases

Several reports concerning consistency measurements of Plastibases are found in the literature (198, 202, 207 - 11, 214 - 220). While most of these report the measurement of consistency of Plastibase using the penetrometer, the exceptions are the reports of Chun (216), Schultz and Kassem (207, 219, 220) and that of Squibb (202).

The measure of consistency of the gels as determined by the penetrometric method has usually been expressed in terms of penetration depth. The rheological parameters controlling penetration depth are not defined and as such this form of empirical measurement bears little fundamental significance (221). Chun (216), using the modified Stormer viscometer, has determined the plastic viscosity and the thixotropic index as a function of temperature for Jelene 50W. Schultz and Kassem (207, 219, 220) have derived the structure-viscosity index, the plastic viscosity, the practical yield value and the area of the hysteresis loop from the rheograms obtained for 1, 2, 3, 4 and 5% polyethylene-mineral oil gels with increasing temperature using the Haake Rotovisco rotational viscometer. Squibb (202) have also reported the temperature-viscosity relationship for Plastibase 50W, 20W, 10W, 5W determined using the Brookfield Synchrolectric viscometer.

A characteristic feature of polyethylene-mineral oil gels that has been reported by several of the above mentioned investigations is that these gels apparently exhibit relatively little change in consistency over a wide range of temperatures from -15°C to 60°C. This has been known to have the important advantage that while the gels remain extrudable and spreadable at low temperatures, they do not liquify when applied to the skin nor do they melt or undergo segregation of the ingredients at summer heat. Foster et. al. (214) and Thau and Fox (211) have attributed this remarkable temperature-viscosity relationship to the relatively low thermal coefficient of viscosity exhibited by these bases. Schultz and Kassem (219) reported that the temperature coefficient of plastic viscosity for a 5% polyethylene gel was ten times lower than that for Dutch natural vaselin. Interpreting the results of Chun (216), Martin et. al. (5)

have, however, stated that both Plastibase and white soft paraffin exhibit about the same temperature coefficient of plastic viscosity; it is the alteration of the thixotropic index with temperature that differentiates and characterises Plastibase from other bases. They consider that since thixotrophy is a consequence of gel structure, the waxy matrix of petrolatum is probably broken down considerably as the temperature is raised, whereas the resinous structure of Plastibase is able to withstand temperature changes over the range encountered in practice.

As the physical properties of the polyethylene-mineral oil gels are highly dependent on their structure, determined by the rate of cooling in their preparation (197, 207, 210), of particular interest has been the effect on the gels of the disruption of the structure. Multimer et. al. (198) have reported that polyethylene gels are sufficiently resistant to mechanical working and shear to allow for cold compounding, and furthermore the ointments may be mixed, milled and mechanically packed with very little, if any, effect on the gel stability. In contrast, Squibb (202) have reported that Plastibase products show a decrease in viscosity as the rate of shear is increased. This sensitivity to shear resembles pseudoplastic behaviour (202, 220), but excessive shear causes a reduction in viscosity which is not completely recoverable (202, 214, 218). It has thus been recommended that high shear mixing or milling should be used only in the preparation of concentrates which are then diluted to final weight or volume in low shear mixers.

Consistency related physical properties of the polyethylene-mineral oil gels such as spreadability, tube extrusion pressure,

capacity to suspend for solids, stability of ointments and handling and manufacturing characteristics have been evaluated (202, 220) in comparison with white soft paraffin. In all instances Plastibase formulations have been shown to have superior qualities.

(d) Other Relevant Physical and Biological Characteristics

(i) Absorption

The absorption characteristics of the polyethylene-mineral oil gels are modified by the incorporation of oil soluble emulsifiers (198, 202, 205, 223) just before the cooling process. Plastibase hydrophilic described in an earlier Section is one such commercially available preparation. Water, when added to this preparation, forms a stable water-in-oil emulsion. The emulsion is also reported to be consistency stable over the normally encountered temperature range (202). Leszczynska-Bakal et. al. (224), investigating absorptive and emulsive ointment bases made from polyethylene gel, have reported that these bases are stable, non-irritant, compatible with a wide range of active agents, and release the active agents well.

(ii) Stability

Polyethylene and mineral oil are known to be inert and the chemical stability of the ointments prepared from polyethylene-mineral oil gels are reported to be entirely dependent on the nature of the active ingredients (198).

The gels alone are reported to be physically stable when stored at normally encountered temperature extremes for a period of time (217, 225). The phenomena of 'bleeding' associated with gels due to contraction of structure and separation of oil has been recently investigated with polyethylene-mineral oil gels (226, 227). It is reported that both the dispersing method and concentration of polyethylene had a strong effect on the bleeding of these gels. Increase in temperature accelerated bleeding and increase in viscosity of the oil decreased the velocity of the initial bleeding however had little effect on the ultimate oil separation.

(iii) Compatibility

Plastibase vehicles have been reported to be compatible with most active ingredients which are in themselves stable (202). High concentrations of active ingredients, soluble in Plastibase, do however have the tendency to reduce the consistency of the ointments considerably. For instance, coal tar is said to produce an ointment too soft to prevent separation (218). Aqueous and alcholic solutions of drugs are not compatible with Plastibase due to its nonpolar nature and hence for this purpose Plastibase Hydrophilic has been suggested as a suitable base.

(iv) Irritation and Sensitivity

A wide range of studies that have been carried out to assess the toxicological properities of Plastibases for topical, ophthalmic and parental uses are reported (202).

Robinson (228,229) has reported a negative response to primary irritation due to Plastibase and Plastibase Hydrophilic in three hundred patients on whom routine patch-tests were performed. The sensitizing properties of Plastibase and Plastibase Hydrophilic were determined to be extremely low following normal "usage" tests.

In testing eye irritation in rabbits (202), Plastibase was shown to have no more irritative effect than other hydrocarbon bases. Plastibase Hydrophilic was however shown to produce marked eye irritation. Slight irritation has also been reported following intramuscular or subcutaneous injection of Plastibase 50W. Intraperitoneal administration of Plastibase 5W has been reported to produce no irritation or other adverse effects from the injection.

Robinson (228, 229) has evaluated Plastibase and Plastibase Hydrophilic and found these to have application in a wide range of skin conditions from inflamed dermatoses to dry scaly lesions.

(e) Drug Release Characteristics

Various *in vitro* and *in vivo* methods of investigation have been reported in the evaluation of the drug release characteristics of Plastibases and these have been listed in Table 3. By and large these investigations have usually been confined to the comparative evaluation of Plastibase 50W and Plastibase Hydrophilic with other vehicles. Other Plastibase formulations are not reported to have been evaluated for their

TABLE 3

METHODS EMPLOYED IN DRUG RELEASE CHARACTERISATION OF PLASTIBASE

METHOD	DRUG	REFERENCE
Microbiological	Thiomersal, Ammoniated Mercury, Liquified Phenol	Billups & Sager (230)
	Sulphanilamide, Sulphathiazole	Foster et. al. (214)
	Iodine, Yellow Mercuric Oxide, Ammoniated Mercury, Boric Acid	Kolstad & Lee (231)
	Dichloramine-T, Chloroazodin, Trichloromelamine	Taub et. al. (232)
Diffusion model — type unspecified	Pilocarpine hydrochloride	Jurgens & Becker (225)
	Sodium Salicylate	Leszczyńska-Bakal et. al. (224)
Diffusion model without membrane	Salicylic Acid	Foster et. al. (214)
	Intracaine, Salicylic Acid	Mutimer et. al. (222)
Diffusion model with membrane	Salicylic Acid	Billups & Patel (233)
	Amberlite (CG-50 AR) resin	Billups & Sager (230)
	Citric Acid, Boric Acid, Ascorbic Acid, Salicylic Acid, Potassium Iodide, Sodium Sulphathiazole, Phenylbutazone, Oxytetracycline, Pilocarpine, Amberlite (IRC-50) resin	Golucki (234)
	Boric Acid, Salicylic Acid, Mercuric Oxycyanide, Chloramphenicol, Tetracycline	Grzesiczak (235)
	Amberlite (XE-64) resin	Mutimer et. al. (222)
Biological	Radioactive Sodium Iodide	Ruggiero & Skauen (236)
	Salicylic Acid, Sodium Salicylate, Vitamin A, Potassium Bichromate, Phenol, Ammoniated Mercury Sulphur	Flesch et. al. (237)
In vivo skin biopsy	Sulphanilamide, Sodium Iodide, Sodium Chloride	Sheinaus et. al. (238)
In vivo skin blanching	Betamethasone 17 - benzoate	Pepler et. al. (239)
In vivo skin irritation	Salicylic Acid	Robinson (228, 229)
	Not specified	Blank (240)

drug release characteristics.

While direct comparison of results of the studies listed in Table 3 is difficult due to vast differences in experimental techniques, conditions and treatment of results, general observations concerning the relative drug release efficacy of Plastibase 50W and Plastibase Hydrophilic in comparison with other types of vehicles can be made.

In vitro findings indicate that the release of active ingredients from Plastibase Hydrophilic occurs at a faster and greater rate than Plastibase 50W (222, 230, 237). In general it would appear that the emulsion type bases (222, 233) and the hydrogels (231) exhibit superior drug release characteristics to Plastibases. Of the organogels, the hydrocarbon type of bases, e.g. Plastibases are superior to the hydrophilic organogels like the Carbowax and Macrogol bases.

The results of in vivo evaluation of ointment vehicles have generally corroborated the in vitro findings. Pepler et. al. (239) found that absorption, as indicated by the intensity and duration of vasoconstriction (blanching), due to Betamethasone-17-Benzoate from Plastibase was considerably greater than from the Macrogel bases though white soft paraffin with five per cent propylene glycol or isopropyl myristate as vehicles allowed a greater absorption of the steroid. Blank (240), using skin irritation as a criterion of drug release, demonstrated that the emulsion type base prompted the greatest irritation, followed by Plastibase and then by petrolatum. Robinson (228, 229) has reported that when three per cent concentrations of salicylic acid in Plastibase Hydrophilic, white petrolatum, Aquaphor, Carbowax and vanishing cream were applied to the back of a volunteer and left in

place for twenty four hours, only Plastibase Hydrophilic and Aquaphor ointments gave a positive reaction.

From all these studies, the most interesting finding has been the apparent superiority of Plastibase over white soft paraffin in its drug release characteristics. Foster et. al. (214) and Mutimer et. al. (198, 222) have attributed this finding to the unique structure of Plastibase which allows constant migration of oil within the gel matrix presenting a continually changing interface to the skin, thereby permitting a release of active ingredient much superior to petrolatum and approaching the emulsion type ointment.

2 CONTINUOUS SHEAR VISCOMETRY OF PLASTIBASES

2.1 Introduction

The consistency characteristics of Plastibases reported in the literature have been discussed in Section 1.2.3(e). The theory concerning continuous shear tests was discussed in the first part of this thesis. The purpose of this Section of the investigation was to determine:-

(i) the rheological characteristics exhibited by the five grades of Plastibase;

(ii) the influence of temperature on these rheological characteristics;

(iii) the effect of heating, melting and slow cooling on the consistency of a single batch of Plastibase 50W;

(iv) the cause of the hysteresis loops obtained in continuous shear experiments of all grades of Plastibase, i.e. whether they were due to thixotropy or irreversible shear breakdown or simply instrumental effects such as expulsion of materials from the sample gap;

(v) the inter-batch variation within a particular grade of Plastibase.

2.2 Materials

The Plastibases used in this study were supplied by E R Squibb & Sons Limited (Wirral). Following is a list of Plastibases employed:-

Plastibase 50W	Batch Numbers	118, 2298, 2310, 1148, 2363
Plastibase 30W	Batch Number	Not given
Plastibase 20W	Batch Number	Not given
Plastibase 10W	Batch Number	2122
Plastibase 5W	Batch Number	1280

2.3 Experimental

2.3.1 Ferranti Shirley Viscometer

(a) Description

Continuous shear investigation of the Plastibases was carried out using the Ferranti Shirley cone and plate viscometer. The complete viscometer assembly comprised the measuring unit, Figure 10 (241), an automatic gap setting unit, an amplifier unit, a control and indicator unit and an X-Y recorder. Temperature control of the plate was maintained with the aid of a laboratory thermocirculator with a variable heat control (Churchill Inst. Co., Middlesex). A general discussion of the principles and operation of the viscometer has been given by McKennell (49 - 51) and Van Wazer et. al. (52). The following description is based on that of Van Wazer et. al. (52).

The Ferranti Shirley viscometer has a stationary flat plate and a conical rotating disc driven by a variable speed motor through a gear train and torque spring. The tension due to viscous drag is measured by a potentiometer on the spring which sends a signal to the dial indicator and the X-Y

FIGURE 10

SCHEMATIC DIAGRAM OF THE FERRANTI SHIRLEY VISCOMETER

After Davis 1973 (241)

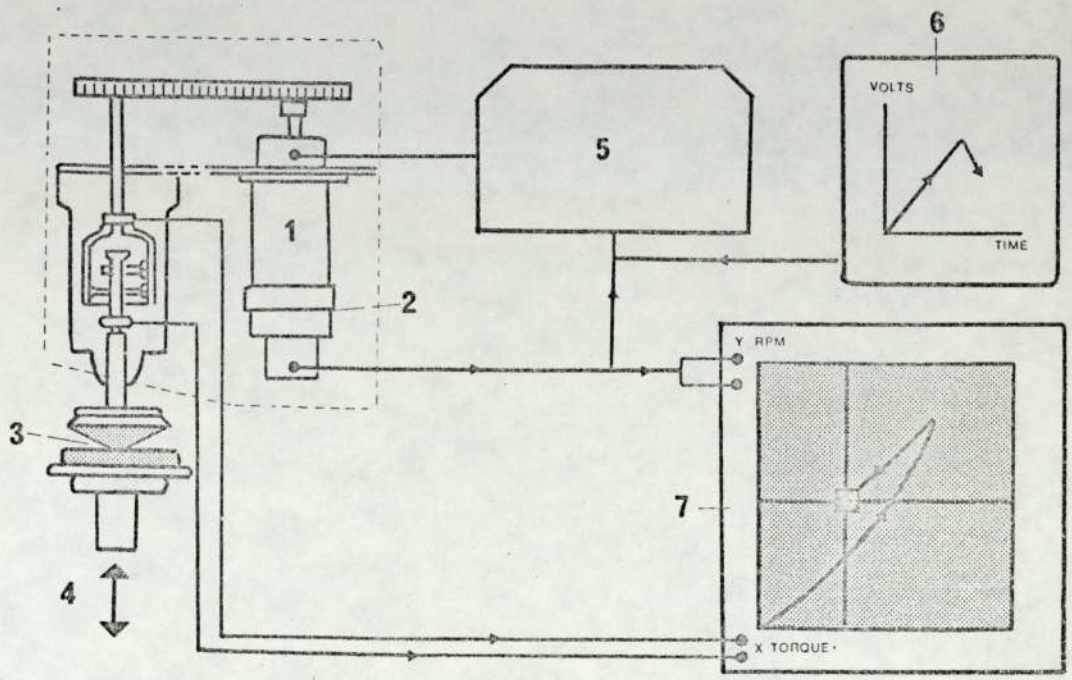

1. Motor
2. Tachogenerator
3. Cone and plate
4. Gap setting arrangement
5. Amplifier
6. Control Unit
7. X - Y Recorder

recorder. The d.c. motor-generator is a velocity servo-mechanism which produces a speed virtually independent of the viscous drag on the cone. A tachometer fitted to the d.c. motor-generator feeds a signal to the X-Y recorder. The control unit generates a voltage linearly increasing with time, which when applied to the motor via the amplifier allows a predetermined programme of acceleration and deceleration of cone angular velocity. Eight such programmes may be selected in a time ranging from 10 to 600 sec., taking the cone velocity from zero to the maximum speed of 10, 100 or 1000 revs. per minute (r.p.m.). Intermediate maximum speeds may be accurately selected by means of a ten-turn helical potentiometer. The 'Check Speed' control allows a direct check of the cone angular velocity as indicated by the dial indicator. A rapid, full-scale sweep of the speed range may be achieved in about 1 sec. with the 'Fast Up - Fast Down' control. The cone angular velocity can be held constant at a preset value with the aid of the 'Hold Speed' control for any desired length of time before deceleration is initiated. The temperature of the test material in the sample gap may be determined during a run with the aid of three thermocouples imbeded in the lower plate. The instrument is supplied with three different size cones which allows a wide range of shear rates to be applied - specifications for these are included in the Appendix.

(b) Operation and Calibration

In the initial setting up of the instrument, the operating

instructions as outlined in the instrument manual were followed. The gear ratio combination in the moving train gear box was adjusted to allow cone velocities varying from 0 - 100 r.p.m. in the 'Low Gear' position and 0 - 1000 r.p.m. in the 'High Gear' position. On each subsequent, separate occasion the viscometer was used, the following setting up and calibration procedure was adopted:-

(i) a suitable length of time (approximately thirty minutes) was allowed between switching the instrument on and any experimental work, for the warming up, stabilization and temperature equilibriation of the instrument.

(ii) The rotational velocity of the cone was checked, and adjusted if necessary to ensure that it agreed to within one per cent of the programmed cone velocity.

(iii) The sweep time produced by the X-Y recorder was checked and adjusted if necessary to ensure that it agreed to within one per cent of the preset sweep time.

(iv) The cone and plate gap was set manually, following the recognised procedure for this.

(v) The instrument was then switched to automatic control and zeroed if necessary, with the Zero Speed Control.

(vi) Appropriate gear setting, cone velocity, scale range and sweep time were selected.

(vii) The X-Y recorder was adjusted to 0 and 100% on the r.p.m. and torque axes.

(viii) The recorded cone velocity (r.p.m.) was checked and adjusted if necessary to within one per cent of the programmed r.p.m.

(ix) The recorded torque was checked with the applied torque as indicated by the dial indicator, and again adjusted if necessary.

(x) A final check on the calibration of the viscometer was made with the aid of a sample of liquid paraffin (1.572 poise at $25^{o}C \pm 0.005^{o}C$) calibrated by the National Physical Laboratory.

The instrument thus calibrated was left set for use in the automatic mode. The sample material was transferred to the viscometer plate with the help of a small spatula ensuring that the sample was disturbed as little as possible. The viscometer plate was raised to the operating position and left for exactly two minutes for temperature equilibriation during which time any excess sample round and between the cone and plate was wiped off. The sample was then subjected to 0 to 460 to 0 $sec.^{-1}$ in 240 secs. shear cycle. Each sample was tested in this manner at least twice and mean values of the rheological parameters derived were accepted.

(c) Derivation of Rheological Parameters

Figure 11 shows a representative flow diagram derived using the Ferranti Shirley viscometer for the Plastibase 50W. The rheogram comprises an anticlockwise hysteresis loop indicating thixotropic or irreversible shear breakdown of structure and exhibits the following measurable characteristics:-

FIGURE 11

A REPRESENTATIVE FLOW DIAGRAM FOR PLASTIBASE 50W OBTAINED USING THE FERRANTI SHIRLEY VISCOMETER

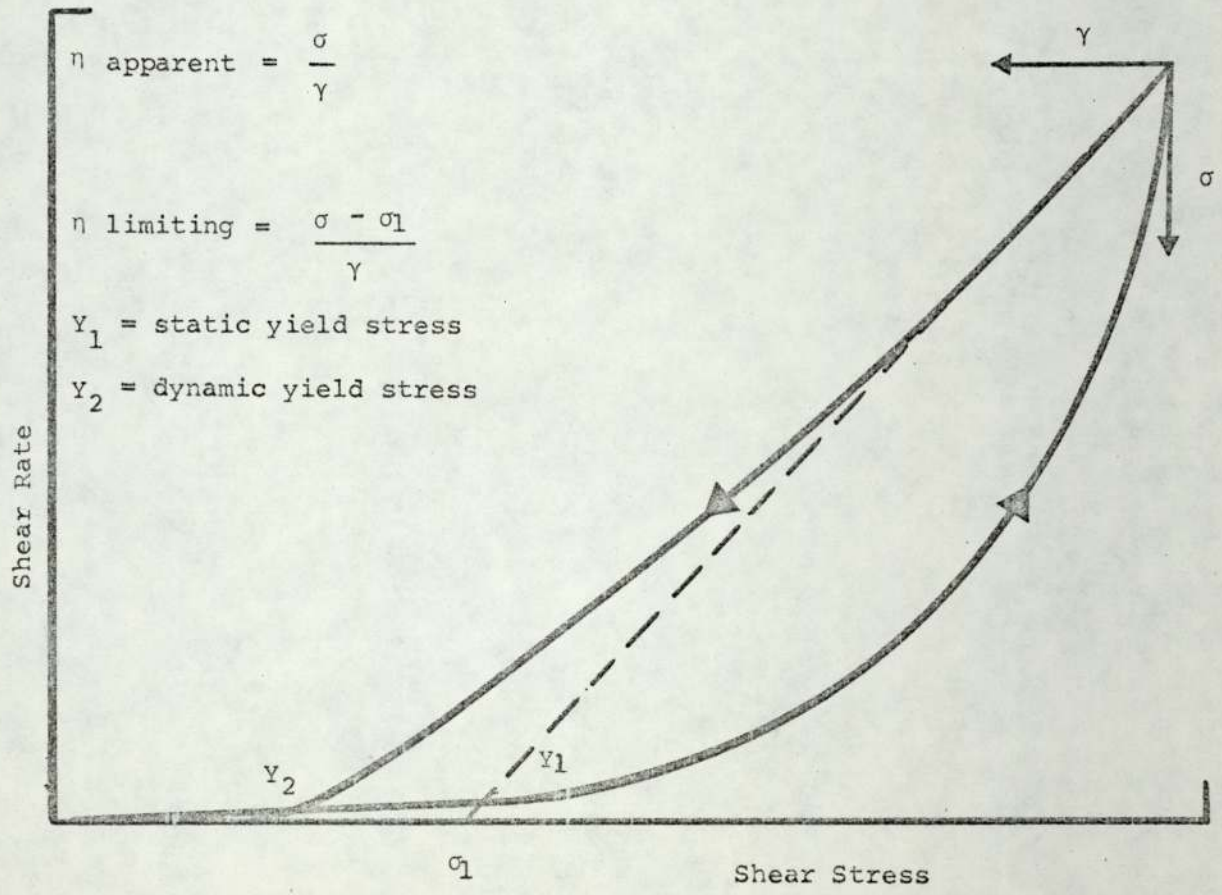

(i) the static yield value (Y1) (on the initial part of the upcurve) expressed in Nm^{-2}.

(ii) The apparent viscosity at the apex of the rheogram (ratio of the shear stress to shear rate at the maximum shear rate) expressed in Poise.

(iii) The limiting viscosity (the reciprocal of the slope of the linear portion of the downcurve) expressed in Poise.

(iv) The dynamic yield value (Y2) (residual yield effect on the downcurve) expressed in Nm^{-2}.

(v) The loop area expressed in m^2.

For the purpose of characterising the systems under study, several of the above mentioned parameters were evaluated subsequently for comparative purposes, only apparent viscosity and static yield stress values were evaluated.

2.3.2 Procedure

The Ferranti Shirley viscometer was used for the continuous shear investigation of Plastibases. The viscometer was employed in the automatic mode as described in the previous Section, with a sweep time of 120 secs. and a maximum shear rate of 460 sec^{-1}.

The five grades of Plastibase described in Section 2.2 were characterised over a temperature range 20°C to 45°C. The five batches of Plastibase 50W described in the same Section were characterised at 25°C and 37°C.

In order to determine the cause of the hysteresis loops exhibited by all Plastibase systems in continuous shear experiments, the following investigation was undertaken. A sample of Plastibase 50W was loaded on to the viscometer with the medium cone attached in such a manner that the sample gap was very slightly underfilled. The sample at 25°C was then subjected to the shear cycle described at the beginning of this Section. The same sample was held undisturbed in the viscometer at 25°C for forty eight hours and another rheogram was then obtained.

The effect of heating, melting and slow cooling on the consistency of a single batch of Plastibase 50W was determined in the following manner. A 100g sample was heated in an evaporating dish until it had all melted and was then stirred until cold. A portion of the sample was then examined on a glass slab held against a dark background, immediately on cooling, twenty four hours later, and a week later. The sample was characterised twenty four hours after cooling using the Ferranti Shirley viscometer over a temperature range 20°C to 45°C.

2.4 Results

The Ferranti Shirley viscometer gave anticlockwise hysteresis loops for all Plastibase systems at all temperatures as shown in Figures 12 and 13. Measurable static and dynamic yield values were demonstrated by samples of Plastibase with 2 - 5 per cent polyethylene (PPE); those with lower PPE exhibited hysteresis loops approaching Newtonian flow with very small static yield values at low temperatures. Apparent viscosity and limiting viscosity data derived from the rheograms of the five grades of Plastibase at temperatures from 20°C to

45°C are given in Table 4. The static yield stress data derived for the five grades of Plastibase at 25°C are also included in Table 4. Plots of percentage polyethylene in the Plastibases versus apparent viscosity, limiting viscosity and static yield stress are shown in Figures 14 to 16. Static and dynamic yield stress data for Plastibase 50W at temperatures from 20°to 45°C are given in Table 5. Apparent viscosity, limiting viscosity and static yield stress data derived from rheograms obtained at temperatures from 20°C to 45°C for a sample of Plastibase 50W, twenty four hours after it had been heated, melted and cooled are given in Table 6. The latter sample, when examined on a glass slab immediately on cooling and twenty four hours later, did not show any evidence of lump formation. The sample appeared more glossy but did not show any signs of bleeding. A week later, when the sample was again examined, there was still no evidence of any lumps, however the sample appeared to be 'bleeding'.

The apparent viscosity, limiting viscosity and yield stress data derived from temperature studies of all the samples mentioned above were used in the Arrhenius type plots, Figures 17 to 19. Activation energy values for the viscous flow of the various Plastibases were derived from the Arrhenius plots and listed in Table 7. The curvilinear relationship between the activation energy values and the percentage polyethylene is shown in Figure 20. For comparative purposes, activation energy values have also been calculated from the viscosity-temperature relationships reported in literature for polyethylene-mineral oil gels and these values have been listed in Table 8.

The rheograms obtained in the investigation to determine the cause of the hysteresis loops are shown in Figure 21.

FIGURE 12

ILLUSTRATION OF CONTINUOUS SHEAR RHEOGRAMS OF PLASTIBASES OBTAINED AT 20°C

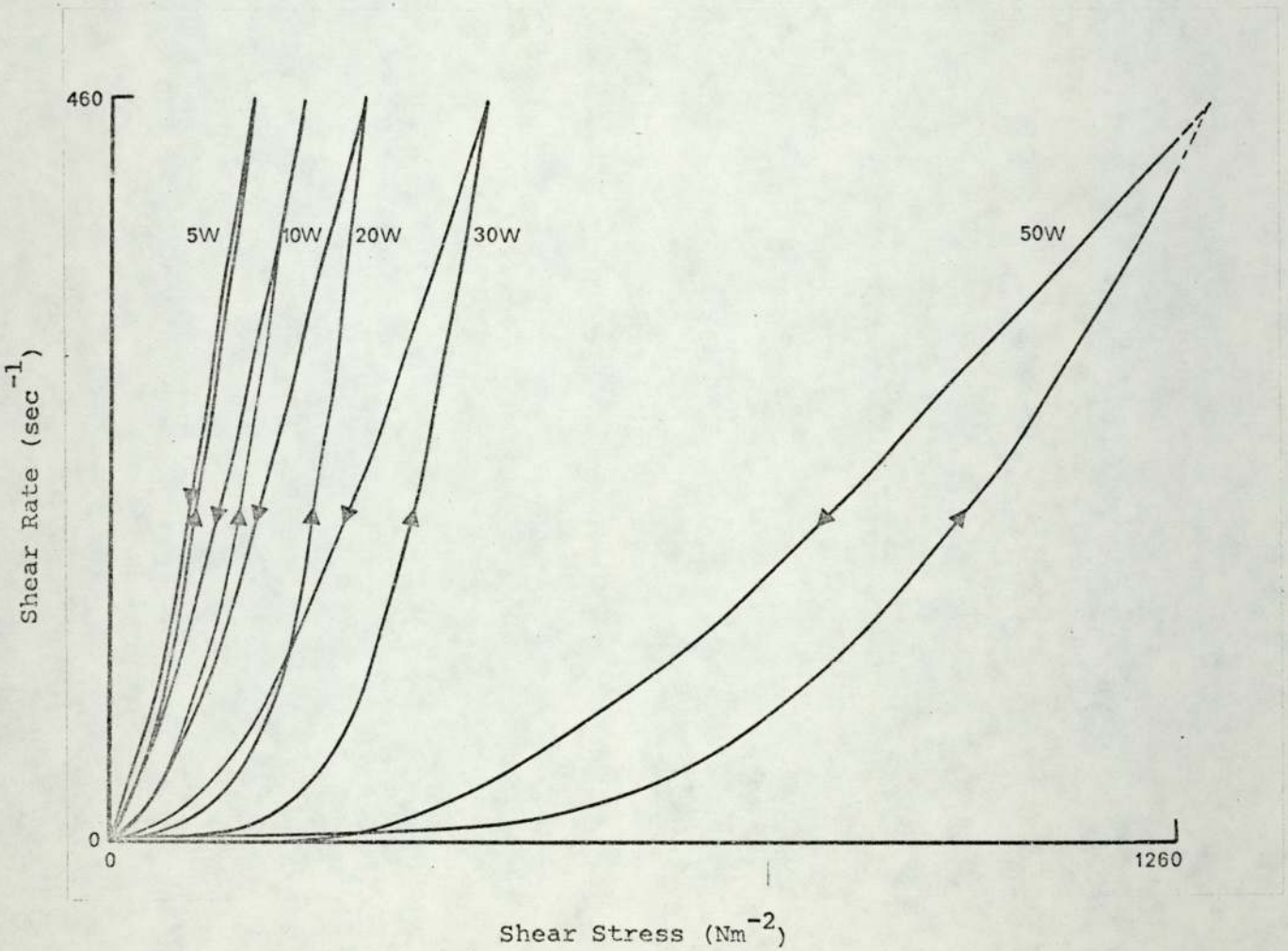

FIGURE 13

ILLUSTRATION OF THE EFFECT OF TEMPERATURE ON THE CONTINUOUS SHEAR RHEOGRAMS OF PLASTIBASE 50W

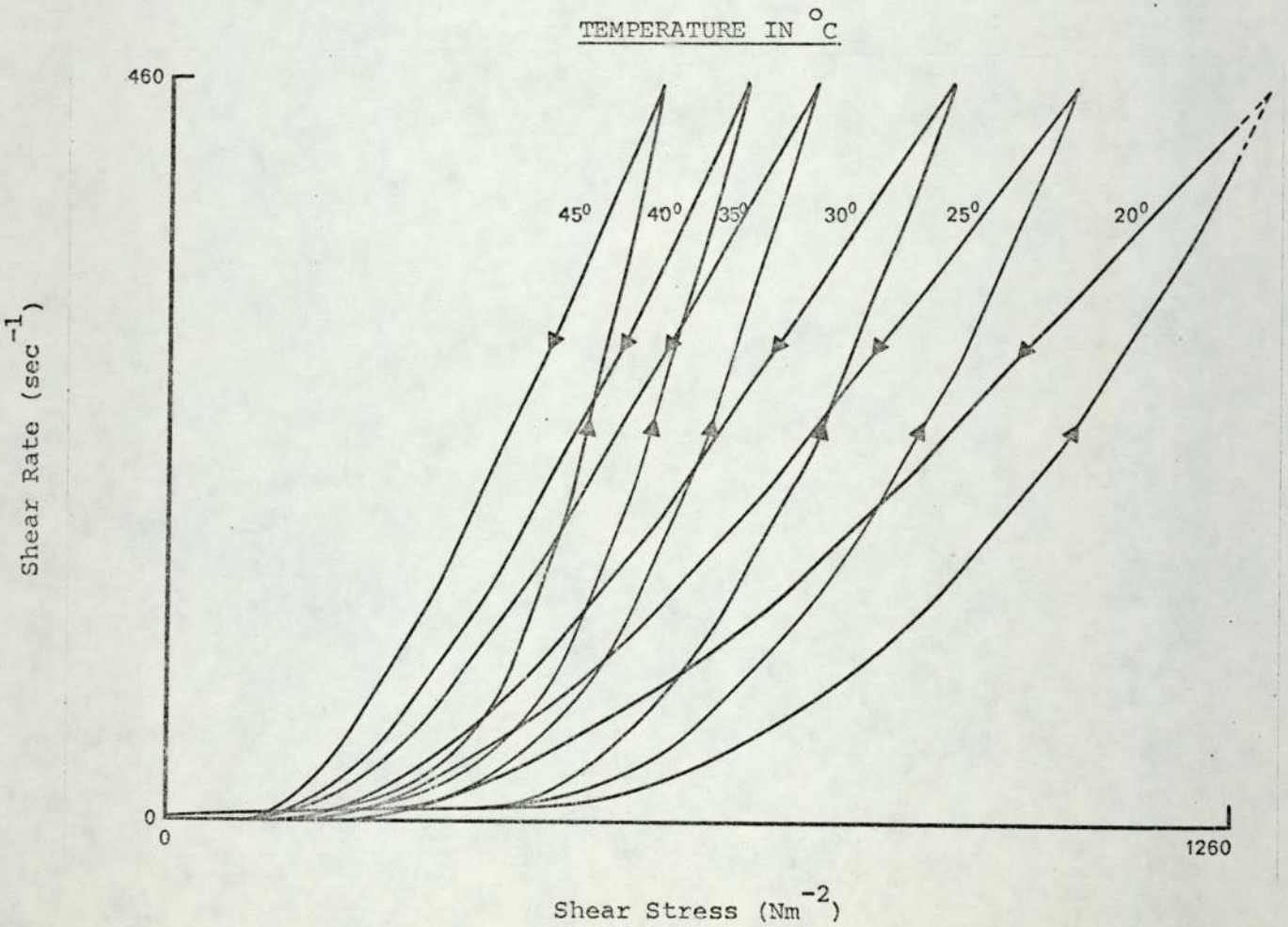

TABLE 4

APPARENT VISCOSITY, LIMITING VISCOSITY AND YIELD STRESS DATA DERIVED FROM CONTINUOUS SHEAR VISCOMETRY OF FIVE GRADES OF PLASTIBASE (APPARENT AND LIMITING VISCOSITIES IN POISE (10^{-1} Ns m^{-2}))

Plastibase	20°		25°		30°		35°		40°		45°		Static Yield stress at 25°C Nm^{-2}
Grade	η app	η limit	η app	η limit	η app	η limit	η app	ηlimit	η app	η limit	η app	η limit	
50W	27.96	17.94	23.06	14.81	20.04	13.29	17.02	11.11	14.41	9.86	12.49	8.39	425.0
30W	9.27	6.61	7.29	5.17	5.49	4.05	4.99	3.39	3.97	3.01	3.27	2.47	139.9
20W	5.98	5.41	4.57	4.24	3.43	3.21	2.72	2.67	2.16	2.06	1.69	1.80	18.7
10W	4.67	4.55	3.18	3.16	2.61	2.57	1.88	2.00	1.52	1.62	1.18	1.28	2.9
5W	3.63	3.47	2.32	2.38	1.68	1.76	1.30	1.44	1.00	1.09	0.713	0.843	1.8

FIGURE 14

PLOTS OF LOG APPARENT VISCOSITY DATA OBTAINED

FROM CONTINUOUS SHEAR TESTING OF PLASTIBASES

VS PERCENTAGE POLYETHYLENE

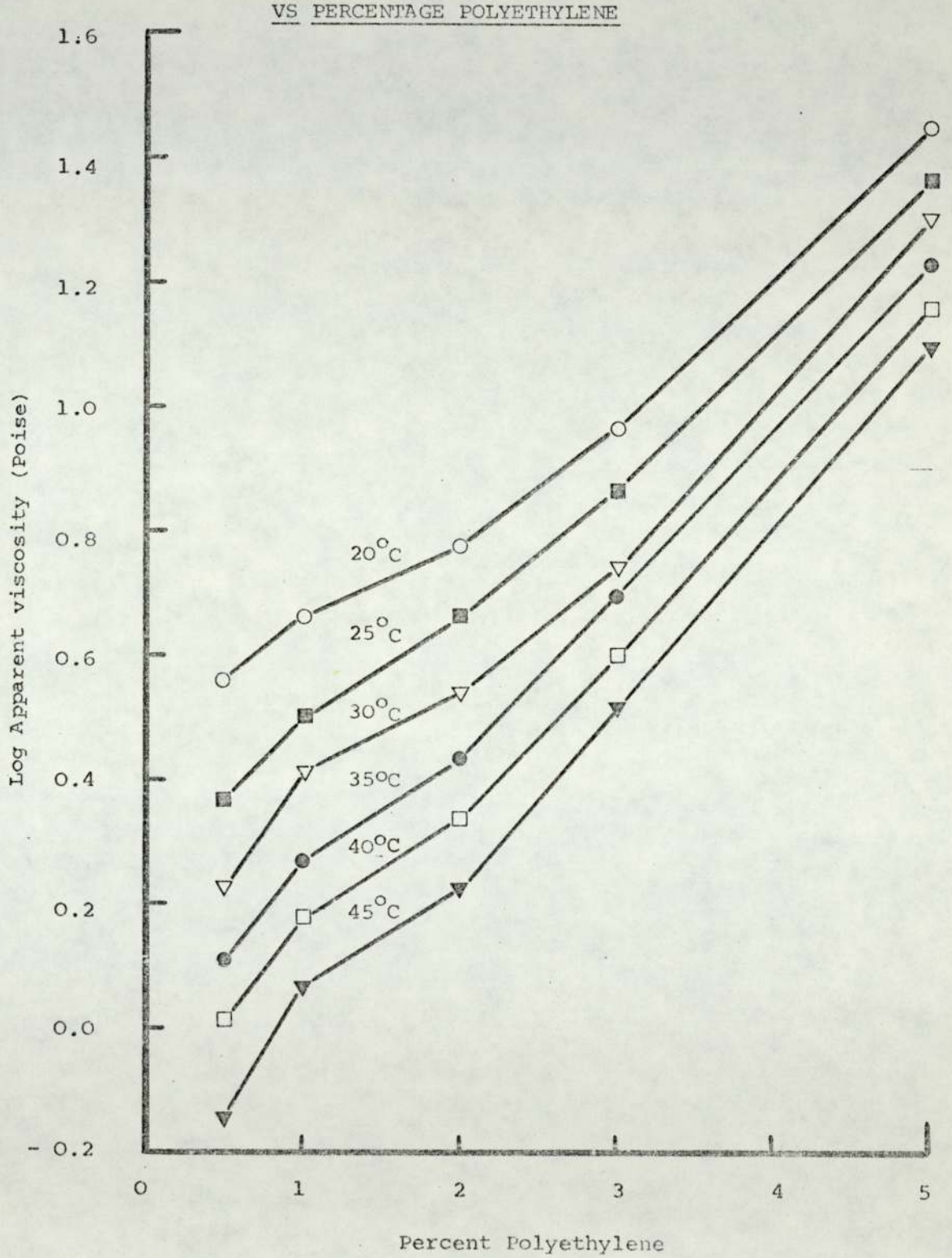

FIGURE 15

PLOTS OF LOG LIMITING VISCOSITY DATA OBTAINED

FROM CONTINUOUS SHEAR TESTING OF PIASTIBASES

VS PERCENTAGE POLYETHYLENE

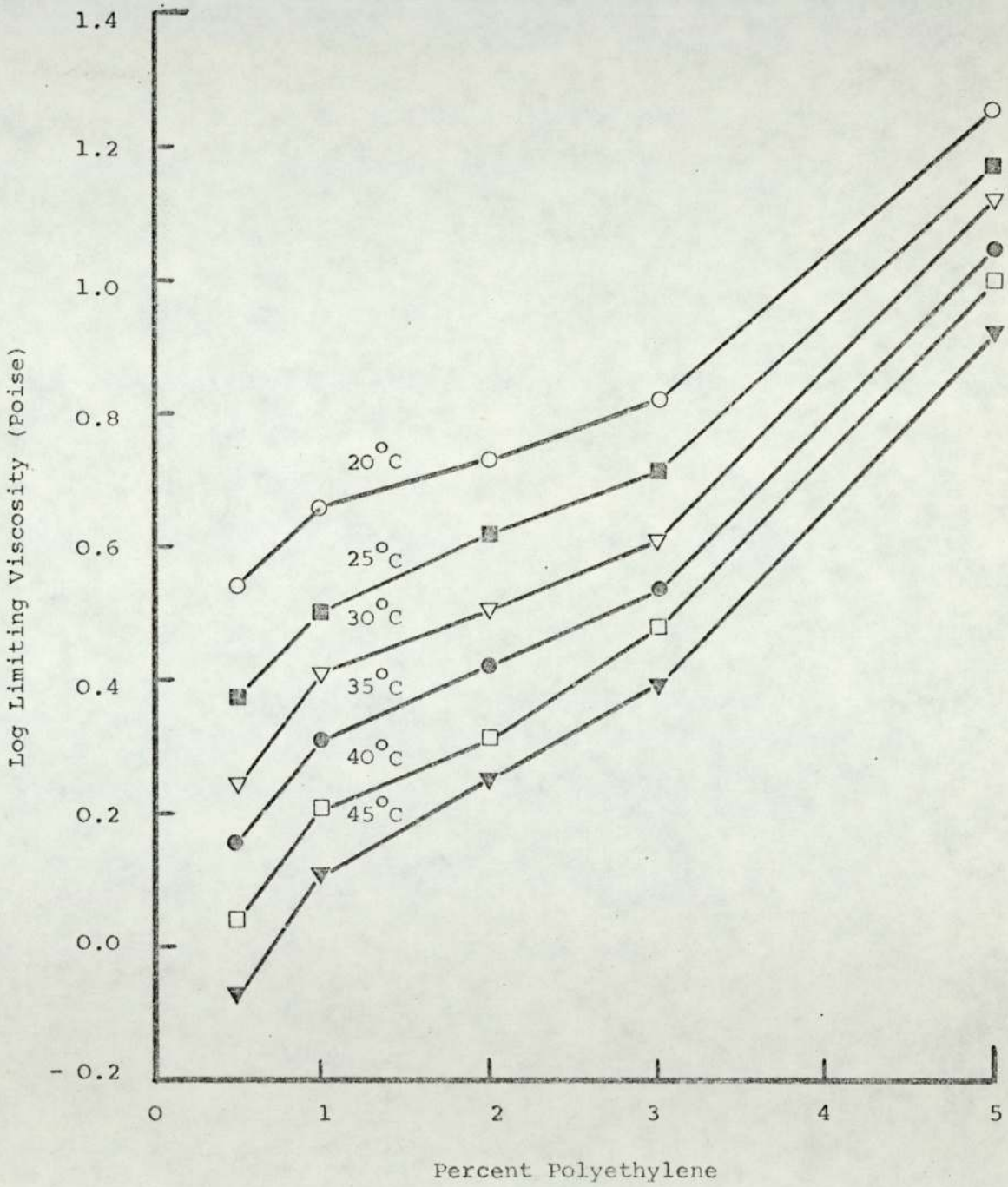

FIGURE 16

PLOT OF LOG STATIC YIELD STRESS DATA OBTAINED

AT 25°C FOR PLASTIBASES VS

PERCENTAGE POLYETHYLENE

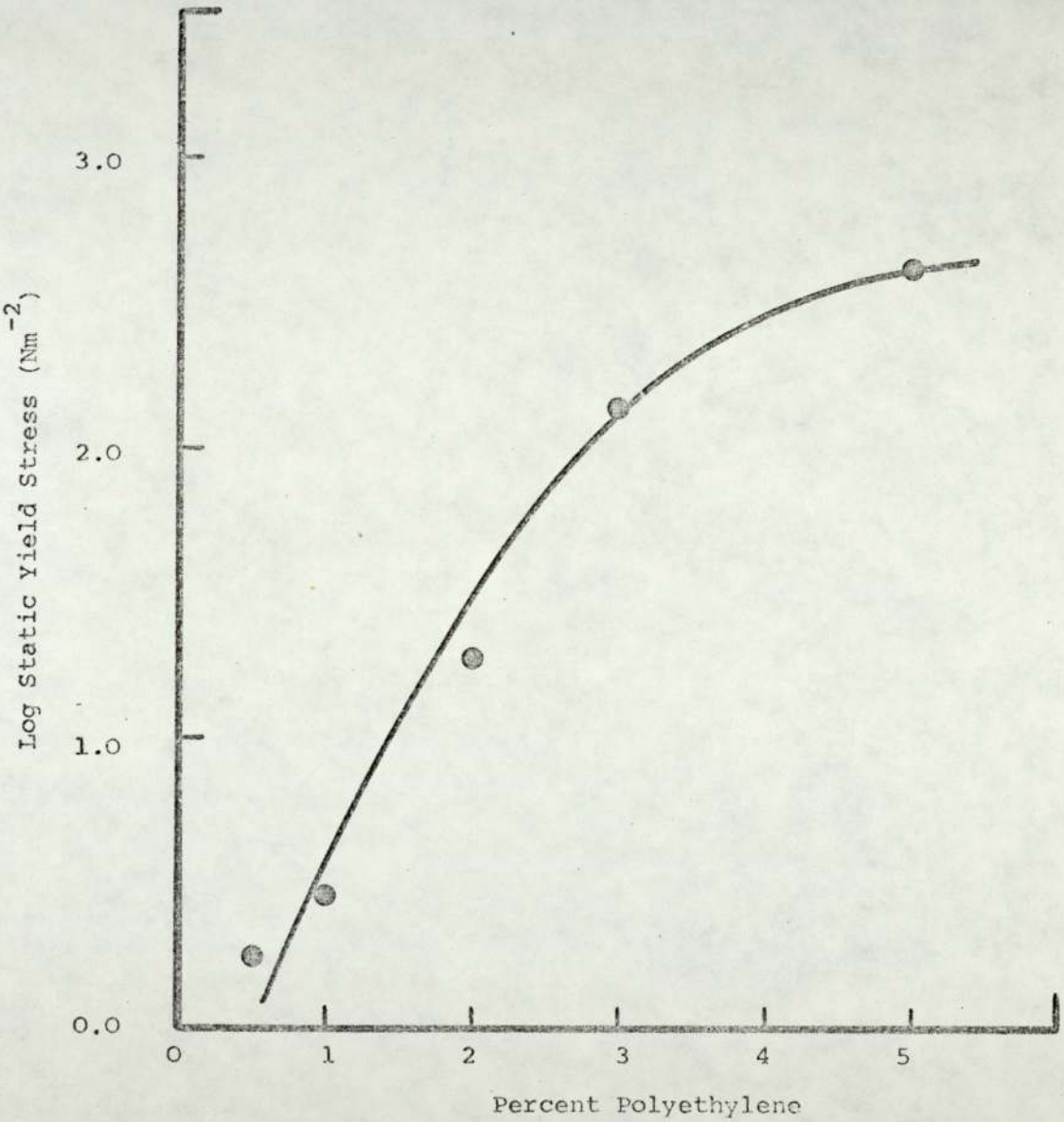

TABLE 5

STATIC AND DYNAMIC YIELD STRESS DATA

FOR PLASTIBASE 50W

Temperature ^{o}C	Static Yield Value Nm^{-2}	Dynamic Yield Value Nm^{-2}
20°	480.0	205.0
25°	425.0	180.0
30°	405.0	157.5
35°	315.0	125.0
40°	300.0	115.0
45°	270.0	105.0

TABLE 6

APPARENT VISCOSITY, LIMITING VISCOSITY AND STATIC YIELD VALUE DERIVED FROM CONTINUOUS SHEAR TESTING OF PLASTIBASE 50W, 24 HOURS AFTER IT BEEN HEATED, MELTED AND COOLED

Temperature °C	η app (Poise) (10^{-1} Ns m^{-2})	η limiting (Poise) (10^{-1} Ns m^{-2})	Static Yield Stress Nm^{-2}
20°	15.78	13.94	135.0
25°	12.35	11.27	112.5
30°	9.88	8.99	100.0
35°	8.24	7.35	85.0
45°	6.04	5.61	45.0

FIGURE 17

ARRHENIUS-TYPE PLOTS OF APPARENT VISCOSITY DATA OBTAINED

IN CONTINUOUS SHEAR TESTING OF PLASTIBASES

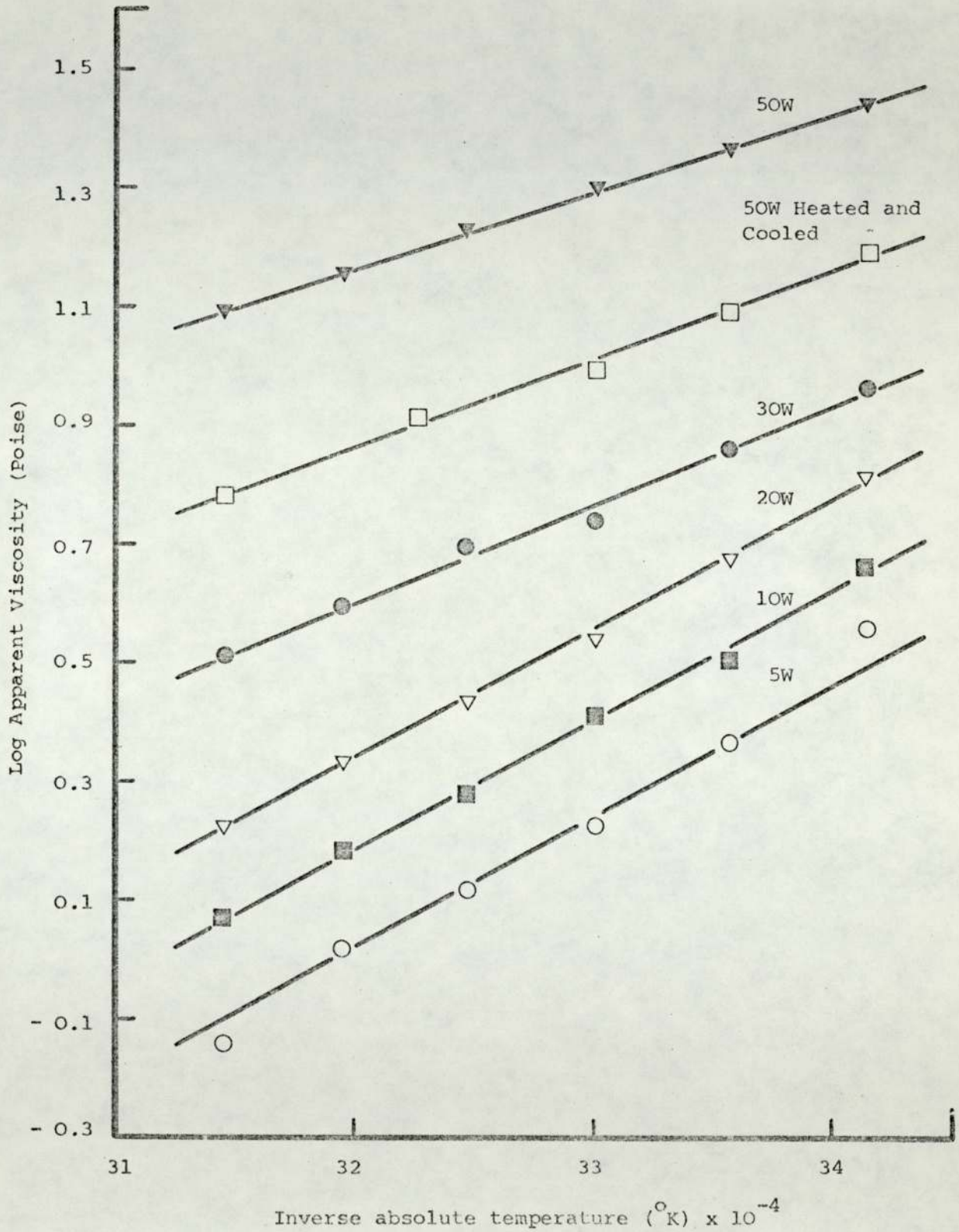

FIGURE 18

ARRHENIUS-TYPE PLOTS OF LIMITING VISCOSITY DATA OBTAINED

IN CONTINUOUS SHEAR TESTING OF PLASTIBASES

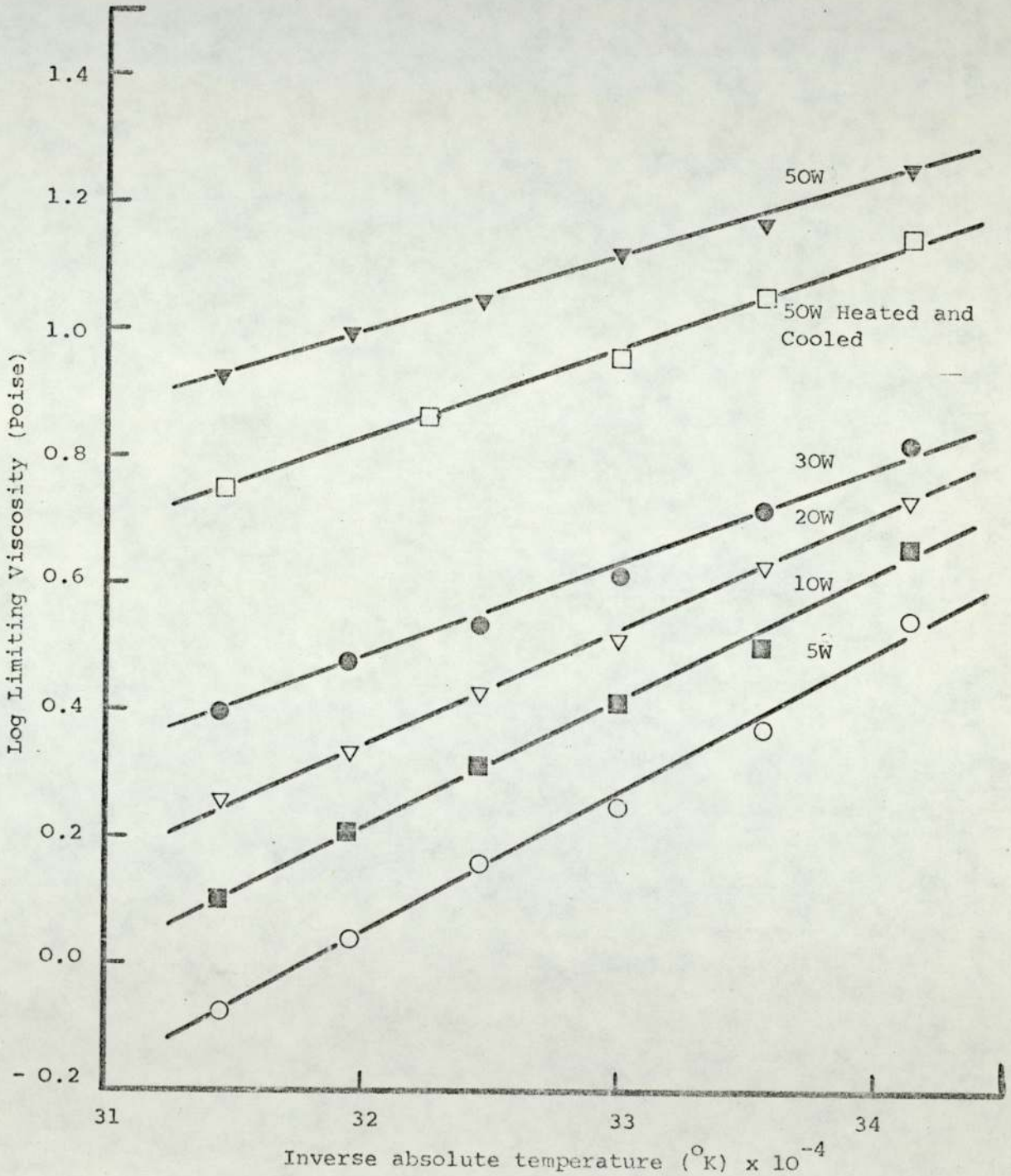

FIGURE 19

ARRHENIUS-TYPE PLOTS OF YIELD STRESS DATA OBTAINED IN CONTINUOUS SHEAR TESTING OF PLASTIBASES

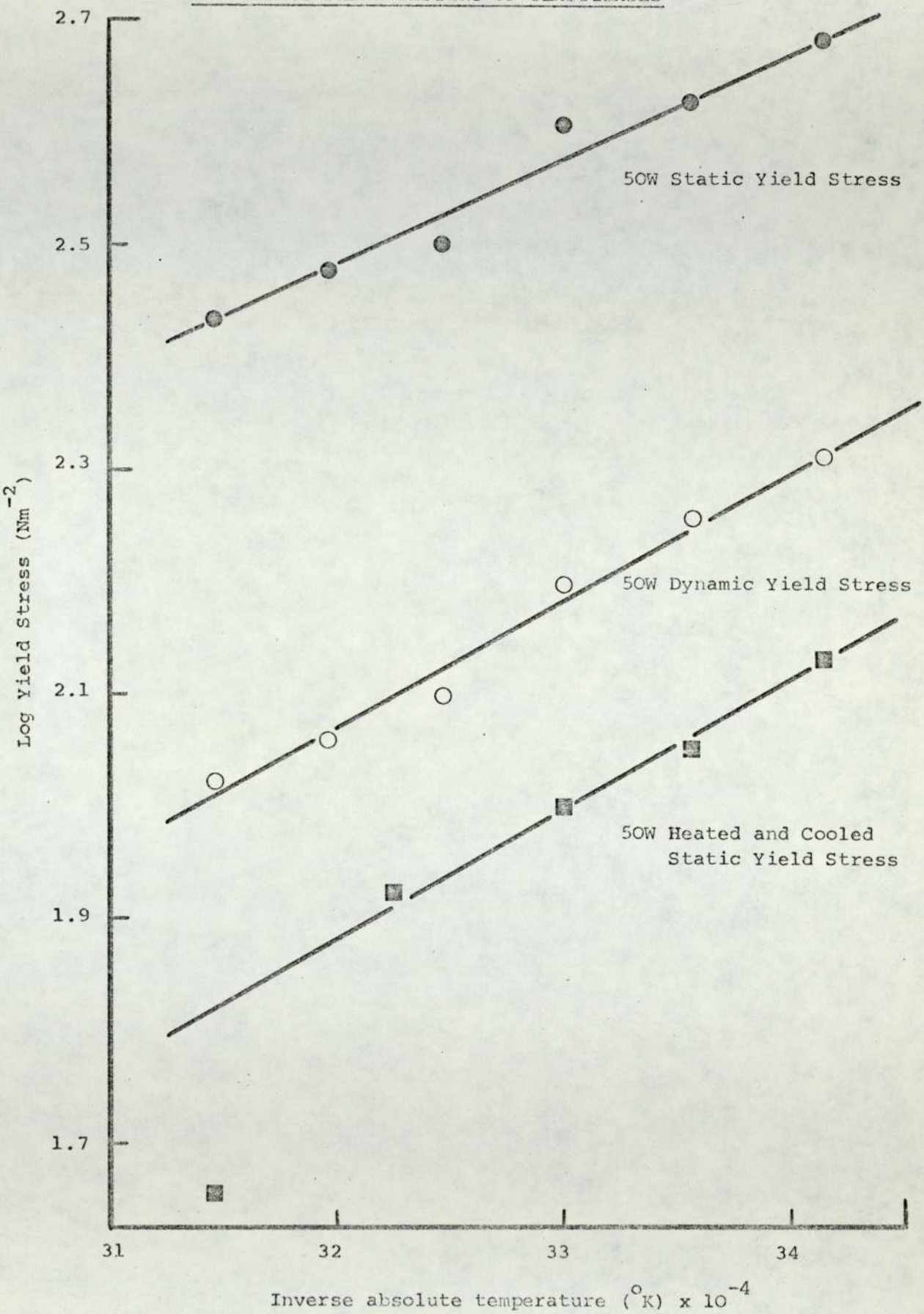

TABLE 7

ACTIVATION ENERGY VALUES FOR THE VISCOUS FLOW OF PLASTIBASES DERIVED FROM CONTINUOUS SHEAR RESULTS

Plastibase Grade	Δ E values derived from η app KJ mol^{-1}	Δ E values derived from η limiting KJ mol^{-1}
50W	25.1	23.4
30W	31.9	30.5
20W	40.3	35.6
10W	42.3	38.9
5W	48.9	43.1
50W Heated and cooled	29.5	28.5

FIGURE 20

GRAPHICAL REPRESENTATION OF ACTIVATION ENERGY VALUES

DERIVED FOR ALL FIVE GRADES OF PLASTIBASES FROM ARRHENIUS-TYPE

PLOTS OF APPARENT AND LIMITING VISCOSITY

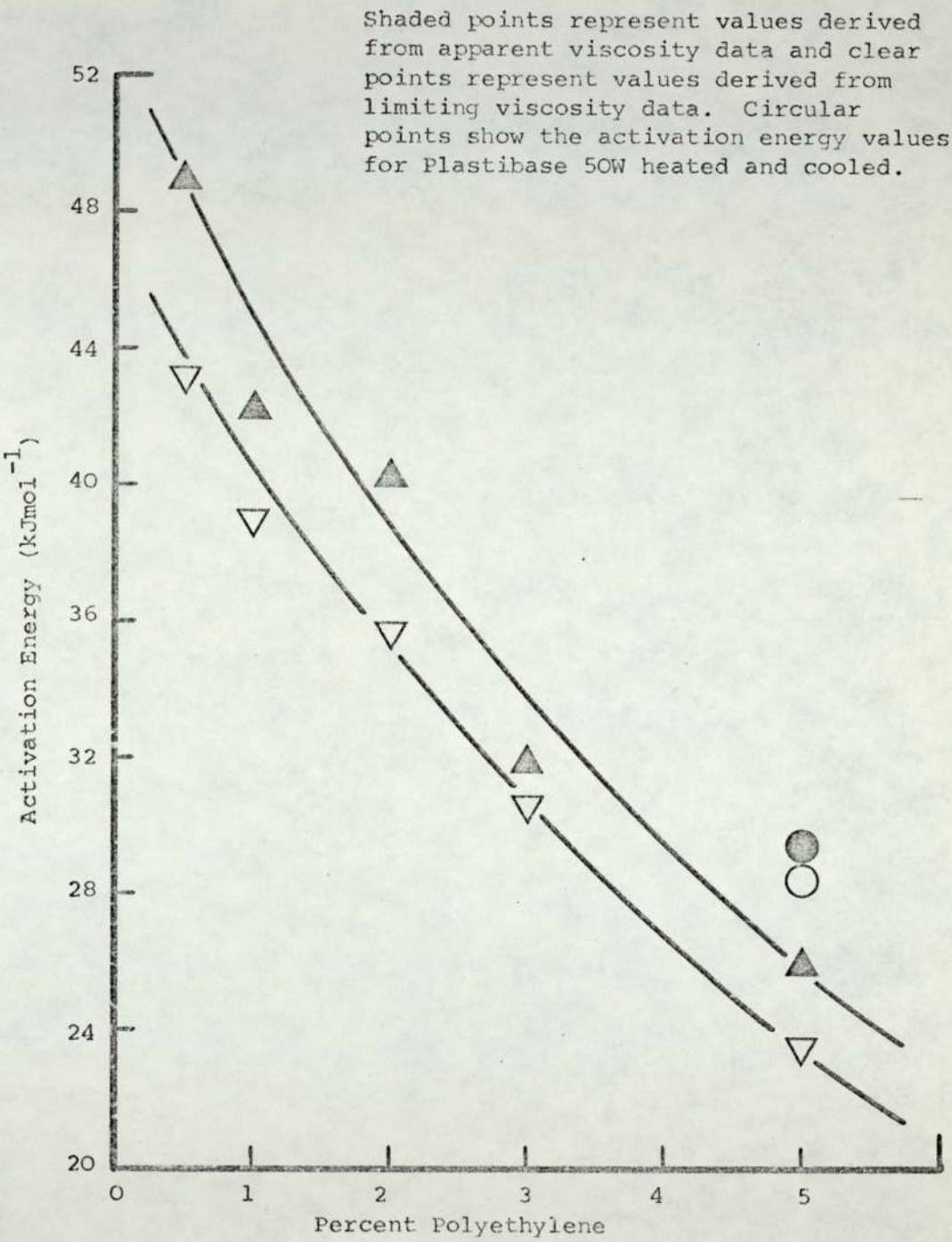

TABLE 8

ACTIVATION ENERGY VALUES DEDUCED FROM THE VISCOSITY-TEMPERATURE RELATIONSHIPS

REPORTED IN LITERATURE FOR POLYETHYLENE-MINERAL OIL GELS

Reference	Viscometer employed	Δ E values (KJ mol^{-1}) for gels containing the following concentrations of polyethylene					
		20%	5%	3%	2%	1%	0.5%
Plastibase Bulletin (202)	Brookfield	-	14.2	-	20.3	26.6	44.8
Foster et. al. (214)	Penetrometer	-	16.1	-	-	-	-
Chun (216)	Stormer	-	36.7	-	-	-	-
Schultz & Kassem (207)	Haake Rotovisco	-	11.4	-	-	19.5	-
Huttenrauch et. al. (209)	Penetrometer	8.4	-	-	-	-	-

FIGURE 21

ILLUSTRATION OF THE RESULT OF THE EXPERIMENT ON PLASTIBASE 50W TO DETERMINE THE CAUSE OF HYSTERESIS LOOPS OBTAINED IN CONTINUOUS SHEAR TESTING OF PLASTIBASES

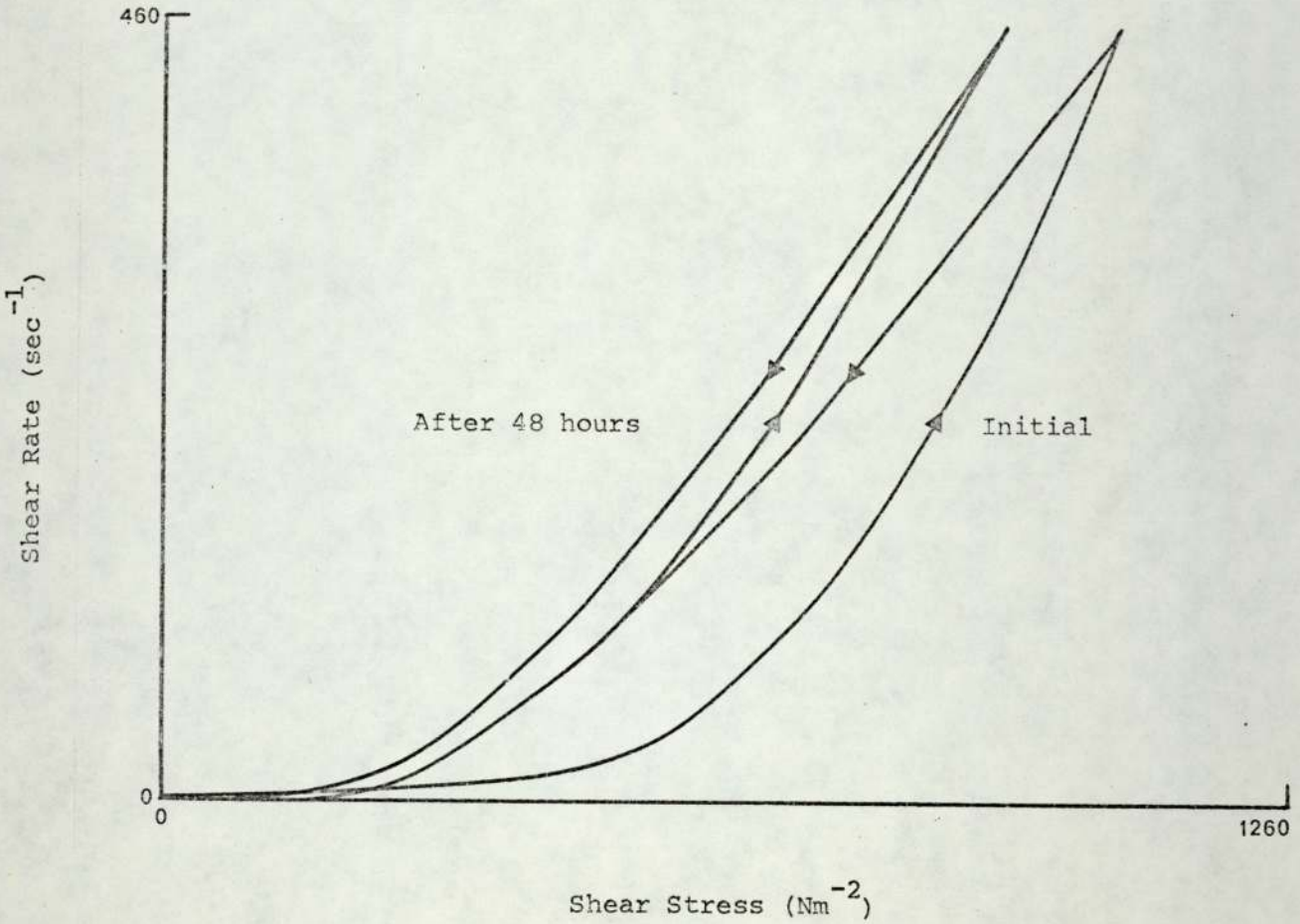

Apparent viscosity and yield stress data, derived from rheograms obtained in the study of inter-batch variation of Plastibase 50W, are listed in Table 9.

2.5 Discussion

Plastibase systems yield anticlockwise hysteresis loops, typical of time dependent materials, in continuous shear experiments. The samples are not visibly ejected from between the cone and plate during the course of a shear cycle and from the rheograms obtained, there is no evidence of shear fracture or slippage effects. The rheograms obtained are considered satisfactory and no smoothing is required or necessary in their interpretation. Reproducibility of the rheograms was found to be remarkably good enabling reliable derivation of rheological parameters. None of the usual difficulties experienced in the continuous shear viscometry of semisolid materials were encountered and from this standpoint Plastibase systems appear to serve as excellent models for continuous shear investigations.

The first part of a typical Plastibase 50W rheogram, the upcurve, is characterised by a static yield point indicating the minimum shear stress required to cause the material to flow. Below this point the material is behaving as a solid. Beyond this point the upcurve is smooth and demonstrates a pseudoplastic characteristic. The upcurve in its upper section is rather steep indicating that subsequent to the initial structural damage, increasing the shear rate does not promote a corresponding increase in the rate of structural breakdown. It is possible that the latter effect is a subtle reflection of a limited amount of shear fracture occurring within the material leading to a

TABLE 9

INTERBATCH VARIATION DATA FOR PLASTIBASE 50W

Batch Number	25°C	25°C	25°C	37°C	37°C	37°C
	Static Yield Value Nm^{-2}	Dynamic Yield Value Nm^{-2}	η app Poise (10^{-1} Ns m^{-2})	Static Yield Value Nm^{-2}	Dynamic Yield Value Nm^{-2}	η app Poise (10^{-1} Ns m^{-2})
BN 118	425.0	180.0	23.06	310.0	120.0	15.67
BN 2298	495.0	200.0	20.59	385.0	140.0	14.01
BN 2363	425.0	180.0	20.59	325.0	135.0	13.65
BN 2310	475.0	190.0	19.04	351.0	130.0	13.02
BN 1148	400.0	150.0	18.91	300.0	95.0	12.04

small increase in the slope of the upcurve. This effect is however not sufficiently gross to warrant serious consideration. The down-curve follows a linear path over a considerable part of its length, ending in a residual yield effect termed the dynamic yield stress. The shapes of Plastibase rheograms obtained with the Ferranti Shirley viscometer compare well with the polyethylene-mineral oil gel rheograms obtained by Schultz and Kassem (207) using the Haake Rotovisco viscometer.

In the experiment to determine the cause of the hysteresis loops, the sample of Plastibase 50W did not show any apparent signs of structural recovery during the forty eight hours time course of the experiment, Figure 21. This indicated that the extent of hysteresis as demonstrated by the loop area was largely a result of the structural breakdown due to the shear treatment. The sensitivity of Plastibases to shear has been reported by several workers (202, 214, 218) and this has been discussed in Section 1.2.3(c). This shear sensitivity of Plastibases can be attributed to its unique structure resulting from the rapid cooling process employed in its manufacture. It is logical to assume that the mechanically disrupted three dimensional gel matrix composed of intermeshed fibrous amorphous filaments and crystallites will not reform in its original framework, thus accounting for the decrease in consistency and the negligible recovery observed under experimental conditions.

Of particular interest in these rheograms has been the effect of temperature on the size of the hysteresis loop. It is significant to note, Figure 13, that the loop area does not change to any great extent with increasing temperature. A similar finding has been reported by Schultz and Kassem (207) and Martin et. al. (5); the latter workers

reasoned that this was due to the resinous structure of Plastibase which was able to withstand temperature changes over the range encountered in practice. This may well explain the viscostatic consistency behaviour of Plastibases reported by several authors (5, 202, 207, 214). It must be pointed out however that loop area has no fundamental significance in relation to consistency behaviour at a molecular level and hence caution must be exercised in order to avoid erroneous assumptions in the interpretation of consistency behaviour based on the loop area parameter.

Static and dynamic yield values were readily determined from the rheograms for Plastibase 50W, 30W and 20W. The lower consistency Plastibases, namely 10W and 5W, did not exhibit any yield effects at the higher temperatures and at lower temperatures, these effects were somewhat obscured by the instrumental effect associated with the method of torque measurement (241). For this reason, the yield stress values for these two bases were determined at 25°C using the method due to Boardman and Whitmore (242). The yield stress values increase with an increase in the concentration of polyethylene in the gel but decrease with an increase in the test temperature of the sample, Table 5. A semilog plot of static yield stress using percentage polyethylene (PPE) in the gel, Figure 16, shows an initial rather steep increase in the yield stress with increasing PPE indicating a very rapid build up of the gel structure even at low polyethylene concentrations.

The apparent and limiting viscosities increase with an increase in the concentration of polyethylene in the gel, Table 4. The limiting viscosity as derived from the downcurve of the rheogram was found to have a lower value than the apparent viscosity determined at the maximum

rate of shear. The exceptions are Plastibase 5W and 10W which, at higher temperatures, exhibit anomolous relatively high limiting viscosity values in comparison with the apparent viscosity values. This is due to an instrumental rewind effect which obscures the very beginning of the rheogram. The limiting viscosity of the Plastibase systems reflect to a large degree the extent of structual change due to the shear treatment and thus it is only logical that these values are lower than the apparent viscosity values. A semilog plot of the apparent and limiting viscosity versus percent polyethylene yields a more or less linear relationship between the two, Figures 14 and 15. At 25°C, regression analysis (correlation coefficient 0.92) yields the following relationship between percentage polyethylene (PPE) and the apparent viscosity:-

$$\log \eta_{app} = 0.22PPE + 0.23 \qquad \ldots (62)$$

The apparent and limiting viscosity data yielded linear Arrhenius type plots over the temperature range investigated in continuous shear, Figures 17 and 18. From these plots using the viscosity modification of the Arrhenius equation:-

$$\eta = A \exp\left(\frac{E}{RT}\right) \qquad \ldots (63)$$

or

$$\log \eta = \log A + \frac{E}{2.303\ RT} \qquad \ldots (64)$$

where η is the coefficient of viscosity, A a constant, R the molar gas constant, T the absolute temperature and E the energy of activation for viscous flow. E values were determined for all the

five Plastibases.

The viscosity modification of the Arrhenius equation is a rate process expression containing an exponential term involving an activation energy value. Glasstone et. al. (243) proposed an explanation for this expression which is based upon a lattice structure for a liquid containing some unoccupied sites or holes. According to these authors, under an applied stress, molecules in such a liquid which overcome an energy barrier E jump from site to site in the direction which relieves stress thus initiating viscous flow. The energy E , k $Jmol.^{-1}$, required to initiate this process is thus referred to as the activation energy for viscous flow. The expression does not contain a term representing the free volume change of the liquid with temperature and this has sparked off some controversy concerning the validity of activation energy values derived (53, 244, 245). The modified Arrhenius equation has been successfully applied by several workers for the evaluation of the energy of activation for the viscous flow of semisolid materials (246, 247) though in all cases it is not certain as to what entities of the semisolid material the value represents energising. Huttenrauch et. al. (209) have further modified the viscosity modification of the Arrhenius equation to enable the calculation of the energy of activation directly from cone penetration data.

In this work, the activation energy values evaluated for the five Plastibases, Table 7, Figure 20, decreased with increasing concentration of polyethylene in the gel. The low polyethylene content gels are demonstrating flow characteristics similar to liquid paraffin and are showing a much greater relative change in viscosity with

increasing temperature than are the high polyethylene content gels. Consequently a decrease in temperatue coefficient of viscosity with an increase in the concentration of polyethylene is reflected by a decrease in the energy of activation for viscous flow. This can be tentatively explained on the basis of molecular and segmental flow (248). The low polyethylene content gels behaving in a similar manner to liquid paraffin are demonstrating complete molecular flow requiring a higher energy of activation. The high polyethylene content semisolid gels are demonstrating segmental molecular flow, where the viscous flow takes place by successive jumps of segments of a molecular entity instead of the whole entity thus requiring a relatively lower energy of activation.

The activation energy values derived from limiting viscosity data are somewhat lower than the values derived from apparent viscosity data, Table 7, Figure 20. This is as would be expected with a shear thinning material and may be associated with the dynamic motion of small and larger molecular segments of the material.

There are several reports in literature concerning the influence of temperature on the consistency of polyethylene-mineral oil gels, however as the viscosity parameter and the method of measurement have differed in all cases, direct comparison of the published data has been difficult. The energy of activation values calculated from the published temperature-viscosity plots, Table 8, assuming in all cases that the measured viscosity parameter reflected to some degree the consistency character of the product have thus provided a useful comparative measure of the thermal behaviour of the materials. There is good correlation between the activation energy values determined for the five Plastibases

in this investigation and those values determined from the published viscosity-temperature plots for polyethylene-mineral oil gels. It is interesting to note that both sets of values indicate a similar decrease in the activation energy with an increase in concentration of polyethylene in the gel. The small numerical difference in the activation energy values determined in this investigation for Plastibases and those determined from published data for gels of similar composition may be explained as resulting from differences in the method of viscosity parameter measurement and the nature of the gels due to a variation in the average molecular weight polyethylene used and the method of preparation of the gels.

The static and dynamic yield values for Plastibase 50W decreased with an increase in temperature and yielded linear Arrhenius type plots, Figure 19. Similar linear Arrhenius plots relating yield values to inverse absolute temperature have been reported by several workers for related pharmaceutical semisolids (247, 249). Davis (246) has cautioned that yield values obtained in continuous shear are a function of the method of testing rather than a fundamental property of the material. Barry and Grace (247) have reasoned that whilst yield stress may not have fundamental significance, the linearity of the Arrhenius plots tends to confirm that yield values are a function of some property of the material and may be of use in comparative testing procedures such as quality control. In view of the fact that yield values are usually unaffected by any flow irregularities which may occur in continuous shear viscometry of semisolids, it is suggested here that Arrhenius plots using yield stress data from which can be derived the value of the activation energy required to initiate viscous flow may be more meaningful than Arrhenius plots of arbitrary

viscosity parameters.

A sample of Plastibase 50W on heating, melting and slow cooling did not show any evidence of lump formation. The glossy nature of the gel indicated however that perhaps not all of the mineral oil was again immobilised in the gel matrix and this suspicion was confirmed when bleeding of the sample was recorded a week later. From this was concluded that the dispersion of polyethylene in the reformed gel was reduced due to the formation of larger entities of the material (though not large enough to be evident as lumps) resulting in a more condensed gel network which could not accommodate all the mineral oil. The consistency of the treated sample was greatly reduced and this was reflected in a considerable reduction of the apparent viscosity, limiting viscosity and yield values as derived from Ferranti Shirley rheograms of the sample tested over the 20°C to 45°C temperature range, Table 6. These findings are consistent with those of several other workers (198, 207, 210). Linear Arrhenius plots, Figures 17, 18 and 19, were obtained using the apparent viscosity, limiting viscosity and static yield stress data. Activation energy values derived from the Arrhenius plots for the viscosity data were, as expected, higher than the values derived for untreated Plastibase 50W and this may be reasoned as being due to the dynamic motion of larger entities of polyethylene as compared with that of smaller entities present in untreated Plastibase 50W. From polarising ligh microscopy of polyethylene-mineral oil gels, Huttenrauch et. al. (210) have proposed that a reduction of cooling rate in manufacture of the gels produces a change in the structure of the gels from a microcrystalline network of polyethylene to that comprising large spherulites, resulting in reduced consistency and

increased bleeding tendency. The latter two features of the gel are highly undesirable and tend to promote instability of formulated products. Thus in product formulations using Plastibases, procedures which require heating and cooling of the vehicles are contraindicated (202). Similarly, experimental testing procedures either for characterisation or quality control which require heating and cooling of the sample cannot be adopted as the results will not truly reflect the character of the original product.

Inter-batch variation study for five batches of Plastibase 50W yielded a ten per cent scatter in the measured parameters. Huttenrauch et. al. (210) have reported that on repeating the rheological measurements on polyethylene gels, they found a maximum of $\pm$ 5% variation in the results. In this work, however, as the reproducibility of the continuous shear rheograms was very good the inter-batch variation cannot be attributed to this. Squibb have quoted that there can be up to $\pm$ 10% variation in the polyethylene content of the Plastibases (202). It is also possible that there may have been some variation in the cooling rates of thes batches leading to a varying degree of crystallinity in the structure of these bases. Finally, as the date of manufacture of these bases was not known, it is possible that the variation in the rheological parameters of the five batches may simply be attributable to age differences.

3 SMALL STRAIN CREEP INVESTIGATION OF PLASTIBASES

3.1 Introduction

The object of this Section of the study was to determine fundamental rheological characteristics of Plastibases by examining them in their 'ground state' using nondestructive tests. The theory of small strain creep analysis has been discussed in Part A of this thesis.

The desired objective of this Section necessitated:-

(a) the construction and calibration of a suitable viscometer which would permit creep investigation of Plastibases;

(b) creep investigation of Plastibases. This involved the determination of :-

(i) viscoelastic properties of Plastibases;

(ii) the influence of temperature on the viscoelastic properties of Plastibases;

(iii) inter-batch variation within a single grade of Plastibase.

3.2 Materials

The Plastibases used in this study were supplied by E R Squibb & Sons Limited (Wirral). Following is a list of Plastibases employed:-

Plastibase 50W	Batch Number	118, 2298, 2310, 1148, 2363
Plastibase 30W	Batch Number	Not given
Plastibase 20W	Batch Number	Not given
Plastibase 10W	Batch Number	2122

3.3 Experimental

3.3.1 Concentric Cylinder Creep Apparatus

(a) Construction

Small strain viscoelastic analysis of Plastibases was carried out using a concentric cylinder creep apparatus. The design and construction of the apparatus were based on the modification, by Barry and Grace (250), of the concentric cylinder air turbine viscometer of Davis et. al. (48) and Davis (251). The apparatus employs the principle of an air bearing turbine system to centre, support and apply a constant torque to the inner cylinder. The strain response is measured from the rotation of the inner cylinder. Figure 22(a) shows a photograph of the main components of the apparatus as set up by the author. A schematic diagram of the complete apparatus is given in Figure 22(b).

The important feature of the apparatus is the Westwind Model 134 (P.C.B.3) Turbine Powered Bearing Spindle (Federal Mogul Westwind Air Bearings Limited, Poole) incorporating both a radial and thrust air bearing. The thrust bearing consists of a diametrically extended section on the upper end of the rotor supported by a cushion of air. This bearing completely supports the rotor and its attachments and there is no physical connection between the stator and rotor of the turbine. Air enters the turbine by crossing a very small air gap. The turbine rotor is driven by the ejection of air from holes drilled in the rotor head. Interaction of turbine and

FIGURE 22(a)

PHOTOGRAPH OF THE CONCENTRIC CYLINDER CREEP APPARATUS AS SET UP BY THE AUTHOR

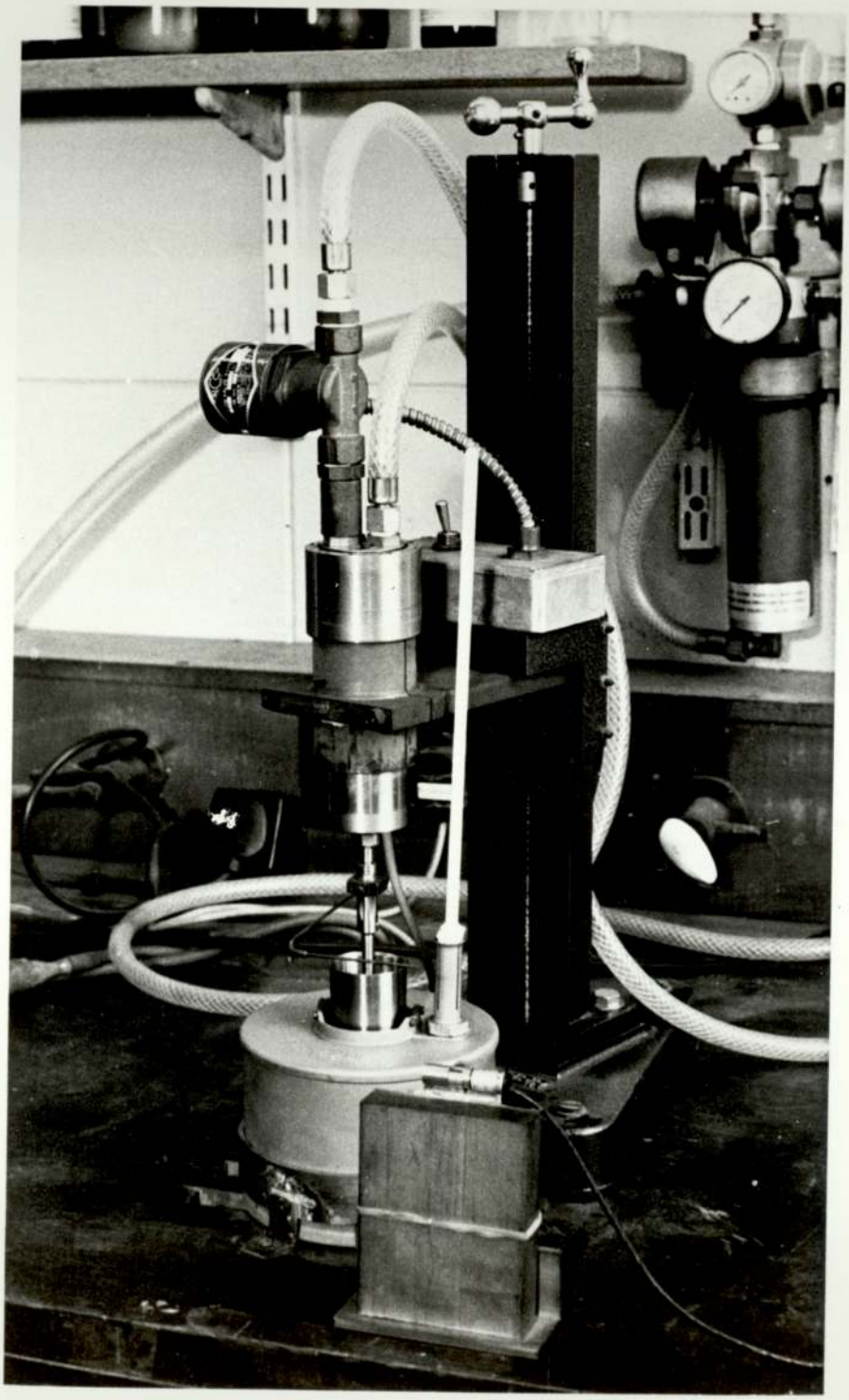

FIGURE 22 (b) SCHEMATIC DIAGRAM OF THE CONCENTRIC CYLINDER CREEP APPARATUS AS SET UP BY THE AUTHOR

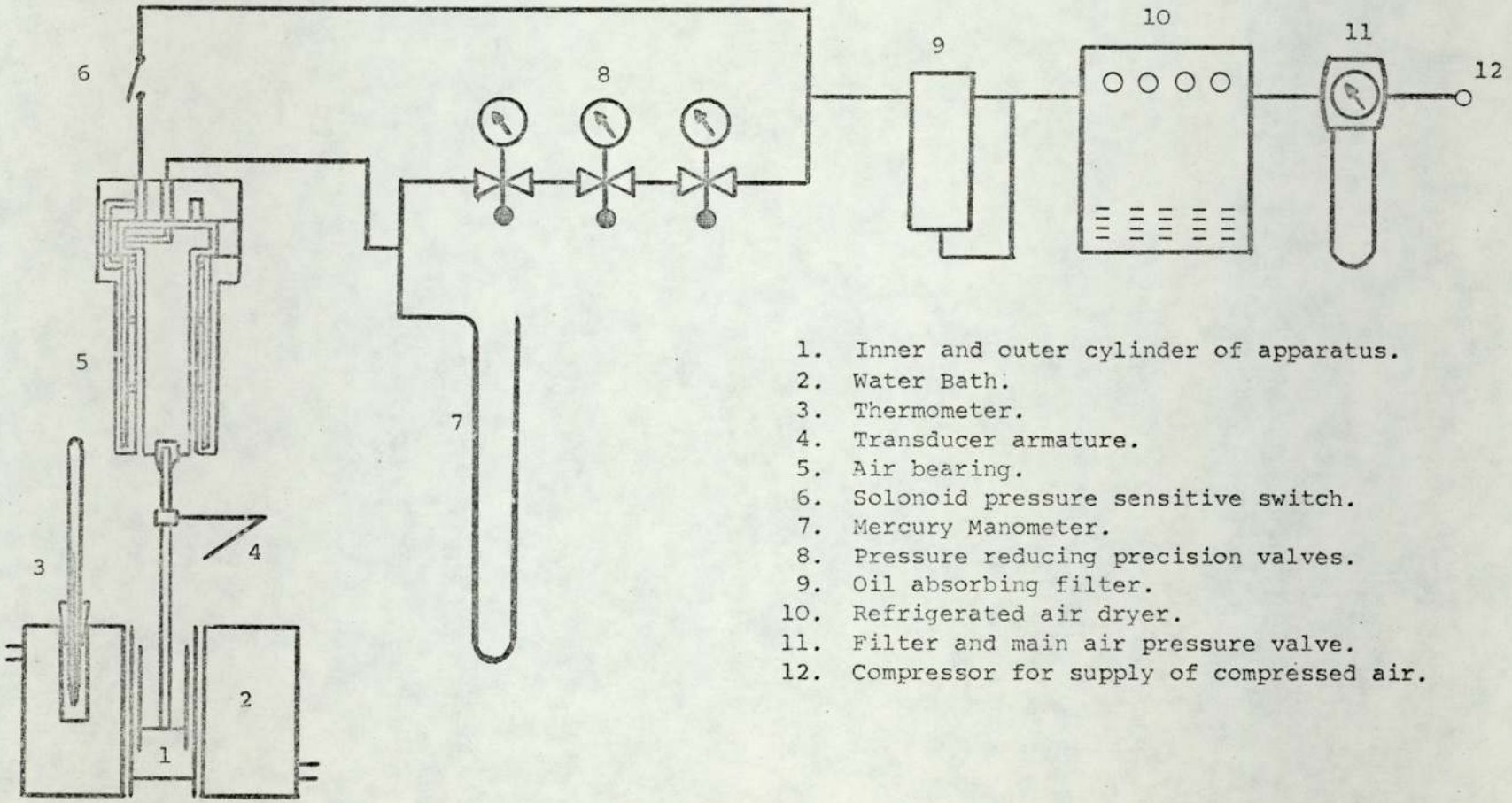

1. Inner and outer cylinder of apparatus.
2. Water Bath.
3. Thermometer.
4. Transducer armature.
5. Air bearing.
6. Solonoid pressure sensitive switch.
7. Mercury Manometer.
8. Pressure reducing precision valves.
9. Oil absorbing filter.
10. Refrigerated air dryer.
11. Filter and main air pressure valve.
12. Compressor for supply of compressed air.

bearing air exhausting from the top of the bearing is minimal and consequently the standing friction in the bearing is very low.

A Hydrovane compressor model 9PU fitted with a three phase motor (Oscott-Air, Birmingham) was used for the supply to the bearing spindle of compressed air at approximately 690 K Nm^{-2}. The air drawn from the compressor was passed through a filter containing a 5 x 10^{-6} m element and incorporating the main air pressure valve (Aerostyle, London), a refrigerated air dryer (Model No 2, Ingersoll-Rand, London) and an oil absorbing filter (Aerostyle, London), all of which were connected in series in the supply line in order to remove and filter from the air, contaminants such as oil, dust and condensed water. The oil absorbing filter directed through a T-junction the bearing and turbine air. A pressure regulator in the oil absorbing filter allowed coarse adjustment of the turbine drive pressure. Accurate and fine adjustment and measurement of the turbine drive pressure were made with the aid of a precision valve (0 to 138 KNm^{-2}) (Watts, Stroud, London) and a mercury manometer. Instantaneous application and removal of the turbine drive pressure was facilitated by a solonoid pressure sensitive switch (Alexander Controls, Sutton Coldfield) fitted into the turbine air line.

The inner cylinder of the apparatus was machined from stainless steel to the dimensions of the Haake Rotovisco MV II cylinder. The spindle of the cylinder was modified to fit the collet of the air bearing, and it was fitted with a boss. The outer cylinder and water-bath of the apparatus were adopted from those used on the Rotovisco viscometer.

The bearing with the inner cylinder attached was mounted on a heavy, vertically adjustible rack and pinion stand (Palmer). A split cylinder clamp was built and fitted to the rack of the stand to hold and prevent torsional movement of the bearing during operation.

The symetery of rotation of the inner cylinder attached to the bearing was checked using a dial indicator. The inner and outer cylinder were positioned to be concentric with the aid of wire gauges and a dial indicator. The whole assembly was thus rigidly and permanently positioned.

Loading of the outer cylinder into the waterbath was facilitated through a recess made in the bench beneath the assembly. Vertical movement of the rack and pinion stand allowed the inner cylinder to be raised out of and lowered into the outer cylinder. In use, the bearing and the inner cylinder were always lowered to the same preset vertical height.

The temperature of the waterbath and the sample were maintained by circulation of water through a laboratory thermocirculator with a variable heat control (Churchill Inst. Co., Middlesex). A cooler unit (Model CC20 Grant Instruments Limited, London) was employed where temperatures below ambient were required. The temperature of the sample was determined with the aid of an N.P.L. calibrated thermometer (Griffin and George) immersed in liquid paraffin in a socket in the waterbath.

The rotational movement of the inner cylinder was measured with the aid of an inductance displacement transducer with free-

unguided armature type 'A' (Sangamo Western Controls Limited, Bognor Regis). The transducer armature was fitted at right angles to a 10cm support arm attached to the boss on the spindle of the inner cylinder. The transducer core was held on a non magnetic moveable stand. When correctly positioned, the armature inserted into the core did not touch the sides of the core; displacement was measured by a change in inductance across the air gap. The transducer output was fed into a direct reading A.C. modular carrier amplifier system (Sangamo Western Controls Limited, Bognor Regis) which gave full scale deflections corresponding to 0.0635, 0.635, 2.54, 6.35 25.4, 254 cm x 10^{-3} displacement of the transducer armature relative to the coil and depending on the scale setting. The amplifier output was fed through an attenuating network to a single point variable speed chart recorder (Pye Unichem).

(b) Calibration of Concentric Cylinder Apparatus

(i) Transducer and Amplifier System

In the initial setting up of the transducer-amplifier system, the operating instructions in the instrument manual were followed. Two additional calibration checks were made. The chart expansion "Factor Control" was calibrated and the linearity of the amplifier-meter response to input signals was checked. These two calibrations were performed in the following manner.

A vernier scale mounted on a stand was placed in contact with the end of the transducer armature. Contact between the armature and the vernier scale was maintained by applying a

torque to the inner cylinder with the aid of the air turbine. The amplifier meter was set on the lowest chart expansion "Factor" and the least sensitive "Scale Range Factor". The amplifier meter was coarsely zeroed by a suitable adjustment of the transducer coil relative to the armature. The meter was then accurately zeroed with the "Fine" adjustment control. The vernier scale setting was altered by a screw adjustment and the armature was allowed to move out of the coil under the influence of the applied torque until the meter indicated a full scale deflection. The ratio of the displacement of the transducer armature relative to the coil, as indicated by the vernier scale, to the displacement indicated by the "Scale Range Factor" gave the order of expansion corresponding to the chart expansion "Factor". The above procedure was carried out for all the four chart expansion "Factors", and the corresponding order of chart expansions determined are given in Table 10.

In order to determine the linearity of response of the amplifier meter, the above procedure was repeated for a range of input signals corresponding to which were obtained from zero to full scale deflection a range of meter readings and a range of readings on the chart recorder. In each case the amplifier meter reading was compared with the vernier scale reading and the chart recorder reading. Plots of vernier scale reading and chart recorder reading against transducer meter reading were drawn. An example of the data obtained and its graphical representation are given in

TABLE 10

ORDER OF CHART EXPANSION DETERMINED CORRESPONDING

TO CHART EXPANSION 'FACTORS'

Expansion Factors	Multiply Indicated Factor by
2	½
4	1
8	2
16	4

Table 11 and Figures 23 and 24. At all "Scale Range Factors", the amplifier meter exhibited a linear response to the input signals. The relative movement of the armature as measured to three decimal places by the vernier scale and the distance moved indicated by the meter agreed to within one per cent up to three decimal places. The amplifier meter and the recorder output agreed to within one per cent of the meter full scale deflection. The 0.25×10^{-3} and the 0.025×10^{-3} scale ranges were not used and therefore not calibrated.

(ii) Recorder

The transducer-amplifier system was adjusted to a zero position and the recorder was zeroed mechanically. The full scale deflection of the amplifier meter was set up with the aid of the "CAL" control and the variable resistors of the attenuation network built into the recorder were adjusted to give a full scale deflection of the recorder. Linearity between zero and full scale deflection was checked using various input signals from the meter, Table 11 and Figure 24, and was within one per cent of full scale deflection of the recorder. The recorder calibration procedure was repeated on each separate occasion the creep apparatus was used.

(iii) Air Bearing Turbine System

The pulley and weights method has been popular in the calibration of the Air Bearing Turbine System (48, 53, 251, 252). With this method, the bearing is either calibrated

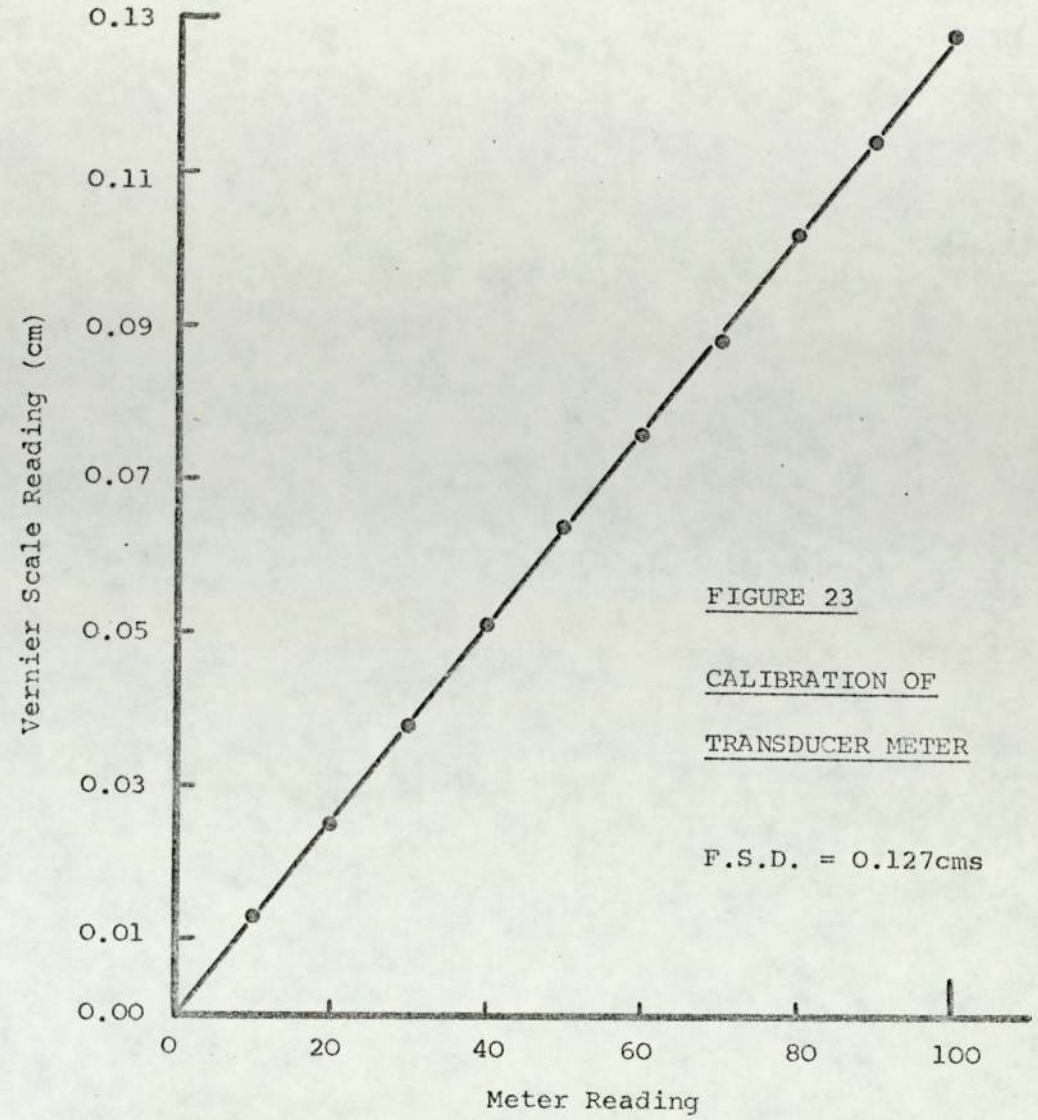

FIGURE 23

CALIBRATION OF

TRANSDUCER METER

F.S.D. = 0.127cms

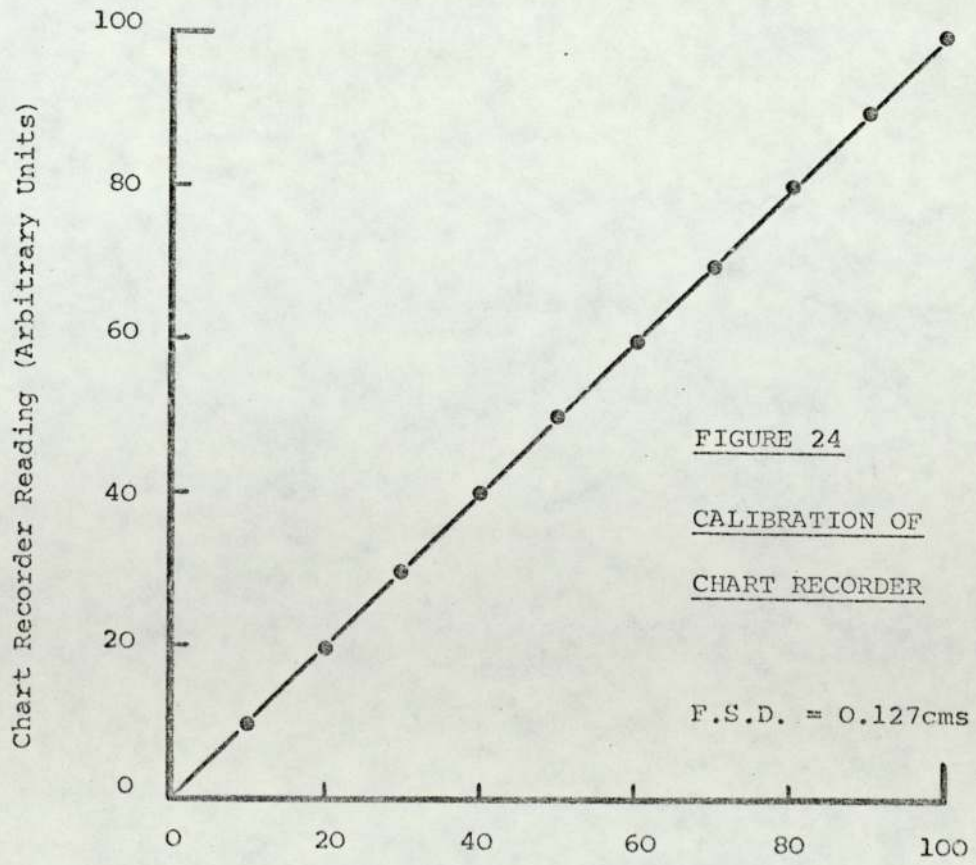

FIGURE 24

CALIBRATION OF

CHART RECORDER

F.S.D. = 0.127cms

TABLE 11

EXAMPLE OF DATA OBTAINED ON CALIBRATION OF AMPLIFIER METER AND CHART RECORDER AT CHART EXPANSION FACTOR 2

SCALE RANGE FACTOR 100

Meter	Vernier (cm)	Recorder (arbitrary units)
0	0	0
10	0.013	9.6
20	0.025	19.6
30	0.038	29.5
40	0.051	39.7
50	0.064	49.9
60	0.076	59.8
70	0.088	69.9
80	0.102	80.0
90	0.114	89.9
100	0.128	100.0

in the vertical or the horizontal position. In the horizontal position, the angular position of the air bearing is reported to affect the calibration (53). For calibration in the vertical position, weights cannot be applied directly to the turbine rotor and therefore a special air bearing has to be constructed, to function as a frictionless pulley wheel (252). The special features of this air bearing have been described by Barry and Saunders (252) who have also reported that the movement of the bearing from the horizontal to the vertical position brought about an under two per cent alteration in the calibration result and have since recommended that the bearing be calibrated in its final working position.

In this work the applied turbine pressure was calibrated in terms of torque with the bearing in its final working assembly using standard silicon oils of viscosity 1×10^{-4} m^2s^{-1}, 5×10^{-4} m^2s^{-1}, 1×10^{-3} m^2s^{-1} and 1.25×10^{-2} m^2s^{-1} in the following manner.

The viscometer was loaded with a standard oil. Turbine pressures ranging from 0 to 133,000 Nm^{-2} were applied keeping the bearing pressure constant at $517KNm^{-2}$. The resulting rates of rotation of the inner cylinder of the viscometer were recorded with a stopwatch. Figure 25 shows that plots of revs. min^{-1} vs the applied turbine pressure were linear over the whole pressure range tested and this was further confirmed on the computer analysis of the results which yielded linear regression correlation coefficient of

FIGURE 25

CALIBRATION PLOTS FOR THE AIR BEARING

TURBINE SYSTEM

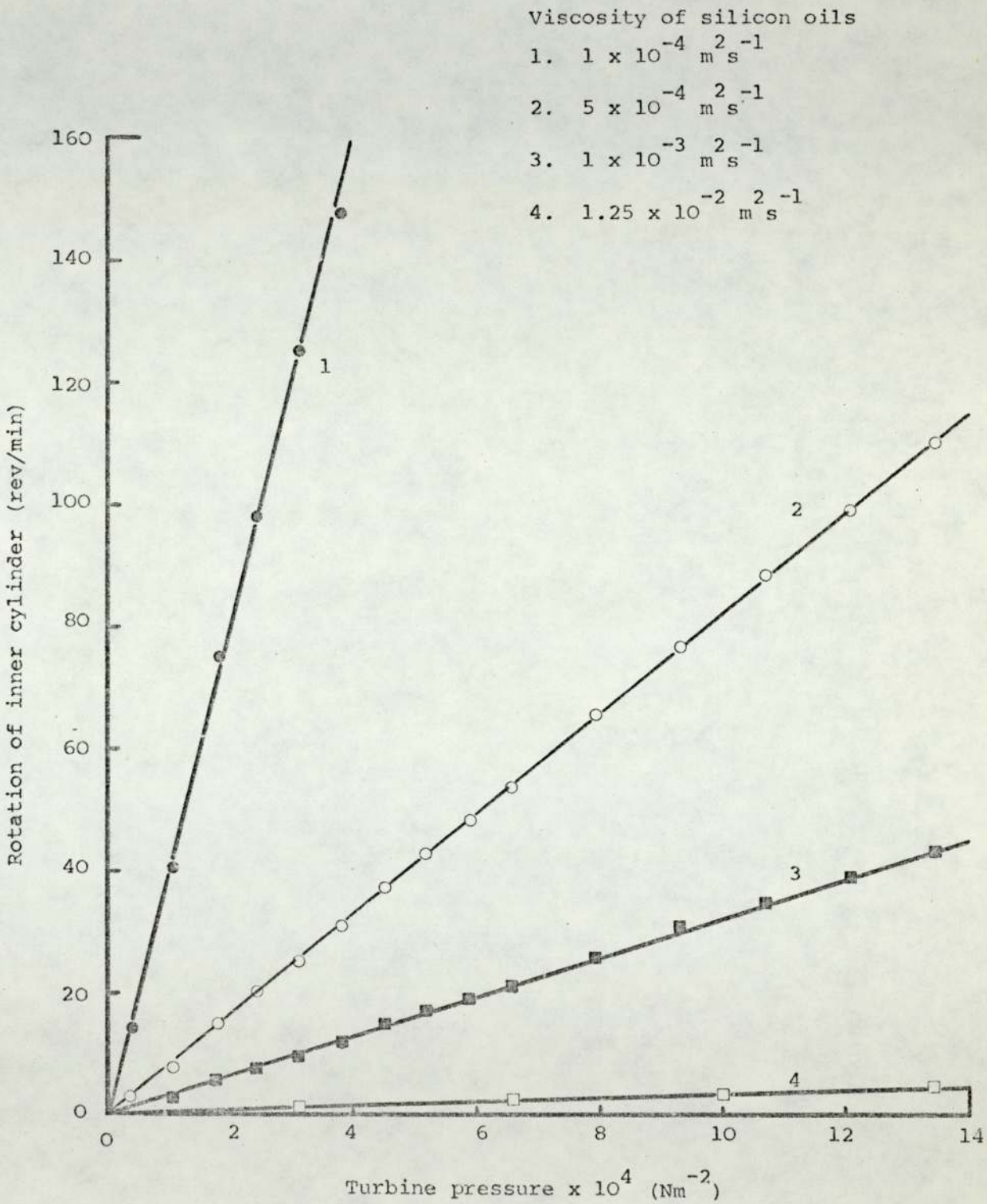

between 0.9980 and 0.9999 for each plot of the standard oil. The plots did not pass through the origin but instead gave a small intercept on the abscissa, the average value of which was $\approx 439 Nm^{-2}$. This value is attributed to a small standing friction in the bearing caused by the incorrect alignment of the air jets, often referred to as the windmill effect. Davis (251) and Barry and Saunders (252) have reported for this model of the air bearing, standing friction values of $399 Nm^{-2}$ and $183.5 Nm^{-2}$ respectively. Correction for the turbine pressure required to overcome the standing friction is not usually made due to the relatively large turbine pressures used in practice.

The instrumental shear rate and shear stress constants for the concentric cylinder geometry have been given by Dinsdale and Moore (253). The arithmetic mean of the shear stress calculated at the surfaces of the inner and outer cylinder is given by the expression

$$\sigma_m = \frac{T(R_1^2 + R_2^2)}{4 \pi h R_1^2 R_2^2} \qquad \ldots (65)$$

for which the corresponding shear rate is

$$\dot{\gamma}_m = \frac{(R_2^2 + R_1^2)\,\theta'}{(R_2^2 - R_1^2)} \qquad \ldots (66)$$

The shear strain between concentric cylinders for small movement has been given by Sherman (15, 254) as

$$\gamma = \frac{R_1 \theta}{R_2 - R_1} \qquad \ldots (67)$$

where T is the applied torque (Nm^{-2}),

R_1 is the radius of the inner cylinder (1.85 cm),

R_2 is the radius of the outer cylinder (2.10 cm),

h is the height of the inner cylinder (6.00 cm),

θ' is the angular velocity of the inner cylinder (radians sec^{-1}), and

θ is the angular deflection (radians) of the inner cylinder.

From a knowledge of the viscosity of the silicon oils, the slopes of the calibration plots, Figure 25, and the shear rate constant, the torque constant was calculated to be 3.126×10^{-4}. The applied torque was thus the product of this constant and the turbine air pressure measured in Nm^{-2}

$$\sigma = Nm^{-2} \times 3.126 \times 10^{-4} \qquad \ldots (68)$$

In creep studies, the strain was thus calculated from Equation (67) assuming that the amplifier meter gave a full scale deflection for the transducer armature movement of 2.54×10^{-3} cm. Thus

$$\gamma = \frac{X \times 1.85 \times 2.54 \times 10^{-3} \times \text{Range Factor}}{100 \times 10 \times 0.25} \qquad \ldots (69)$$

where X represents the "chart reading" and the range factor

combines the "chart expansion factor" and "scale range".

Creep compliance, J(t), was thus obtained by a combination of Equations (68) and (69).

$$J(t) = \frac{X \times 6.0128 \times 10^{-2} \times \text{Range Factor}}{Nm^{-2}} \quad \ldots (70)$$

(iv) Thermometers

The thermometers used were supplied by Griffin and George (Birmingham) and were calibrated to a tenth of a degree by the National Physical Laboratory.

(c) Loading and Operation of the Concentric Cylinder Creep Apparatus

Plastibase systems have been reported to undergo considerable structual changes on heating, melting and slow cooling (207, 210), and this has been further confirmed in the previous Section on continuous shear viscometry. The creep apparatus was thus loaded with the samples at room temperature in the following manner.

About 50g of the sample was introduced into the outer cylinder taking great care to ensure that no unnecessary stresses were imposed on the sample. The outer cylinder was then loaded into the waterbath maintained at the test temperature. The inner cylinder fitted to the bearing was gently lowered into the outer cylinder up to the preset mark on the vertical arm of the stand, thus ensuring that it was always

lowered to the same depth. Excess sample extruding from between the inner and outer cylinder was removed. In the whole loading procedure, particular care was taken to ensure that no air was entrapped in the sample other than at the base of the inner cylinder. The transducer core was then positioned with the armature inserted into it without touching the sides of the core. The whole assembly so positioned was left overnight for the stresses introduced in loading to relax.

In order to perform a creep test on the sample, the amplifier and the chart recorder were switched on and allowed to warm up for thirty minutes. The compressor was turned on and the bearing air was set at $517 KNm^{-2}$. The coarse valve on the turbine outlet from the oil filter, the first turbine air reducing valve, was set at $207 KNm^{-2}$. The transducer core was adjusted relative to the armature, without moving the armature, to give a zero reading on the amplifier meter set on the least sensitive scale. The meter was then set to the desired sensitivity. The amplifier meter was zeroed using the "Fine" setting control. The recorder chart paper was next calibrated as stated in Section 3.3.1 (b)(ii). The complete assembly was thus left to stabilize until a steady recorder base line was obtained.

A check for linear behaviour was then made on the sample by applying increasing stresses and measuring the strain response corresponding to each stress at short arbitrary times. In the linear viscoelastic region of the sample, the ratio of strain to stress (i.e. compliance) remained constant and it was in this linear region that the creep test was subsequently performed. A constant shear stress was suddenly applied to the sample and maintained until the strain curve on

the recorder was linear for a fair proportion of its length. The stress was then removed and a strain recovery curve was recorded which allowed an additional check on the linear viscoelastic behaviour of the sample.

(d) Derivation of Rheological Parameters from an Analysis of Creep Curves

The theory of the creep test in examining viscoelastic behaviour of a semisolid has been given in Section 2.3.3(a) of Part A. Here has also been detailed the line spectrum Voigt model representation of the creep compliance J(t) as a function of time (Equation 24, Figure 6).

Figure 26 shows a typical experimentally determined creep and recovery curve plotted according to convention of compliance vs time. From such a curve, the analysis of the instantaneous elastic compliance, the retarded viscoelastic compliance and the linear viscous compliance will yield several characteristic viscoelastic parameters for the material.

The instantaneous elastic compliance Jo may be measured directly at the onset of the applied shear stress. The steady state viscosity, otherwise termed as the residual Newtonian viscosity may be measured at long times, when all the Voigt units are fully extended and the creep curve tends to a linear, non-recoverable region of viscous flow associated with a Newtonian dashpot.

The retarded viscoelastic compliance, associated with several Voigt elements in series, may be analysed to yield a discrete or a

continuous spectrum of retardation times.

(i) Discrete Spectrum Analysis

Graphical methods for the discrete spectral analysis of creep curves have been given by Inokuchi (255), Warburton and Barry (62) and Sherman (15). A computer modification of the analysis procedure described by Warburton and Barry (62) has been proposed by Davis and Warburton (256). In this work the following graphical method of analysis as outlined by Barry (46) has been used.

The retarded viscoelastic compliance, J_R, is given, as shown in Figure 6, by

$$J_R(t) = \sum_{i=1}^{n} J_i \left(1 - \exp\left(-t/\tau_i\right)\right) \quad \ldots (71)$$

In the above equation let

$$Q = \sum_{i=1}^{n} J_i \exp\left(-\frac{t}{\tau_i}\right) \quad \ldots (72)$$

so that Q represents at any time the distance between the extrapolated linear portion of the creep curve and the curved portion. Logarithmically, dropping the summation sign

$$\ln Q = \ln J_i - \frac{t}{\tau_i} \quad \ldots (73)$$

From the creep curve in Figure 26, compliance Q was derived at various times 't' and plotted on a $\log_{10}$ graph paper against time 't'. Compliance data were normally plotted on a $\log_{10}$ graph paper and in calculations converted to $\log_e$ mathematically. At large values of 't', a straight line was obtained. From Equation (73), the intercept of the linear portion on the ordinate corresponded to J_1 and the slope of the linear portion corresponded to $^1/\tau_1$. For small values of t, the plot was not linear indicating the presence of more than one Voigt unit.

The properties of a second Voigt unit were determined by plotting $\ln(Q - J_1 \exp(-^t/\tau_1))$ against t on a $\log_{10}$ graph paper, Figure 28. The values of $(Q - J_1 \exp(-^t/\tau_1))$ for different values of t were obtained from the extrapolated linear and the curved region of the lnQ vs t plot. From the linear region of the plot J_2 and τ_2 were obtained. The process was repeated until all the data were exhausted. Thus for the creep curve in Figure 26, a group of three Voigt elements were identified by the derivation of three discrete retardation times and their associated spectral compliances, Figures 27 to 29, Table 12. The viscosities associated with the compliances may be determined from Equation (13).

The accuracy of all derived discrete parameters was checked from a reconstitution of the creep data by insertion of the discrete parameters in Equation (21). The above procedure was carried out with the aid of an I.C.L. 1904S computer for

FIGURE 26

AN EXPERIMENTAL CREEP CURVE

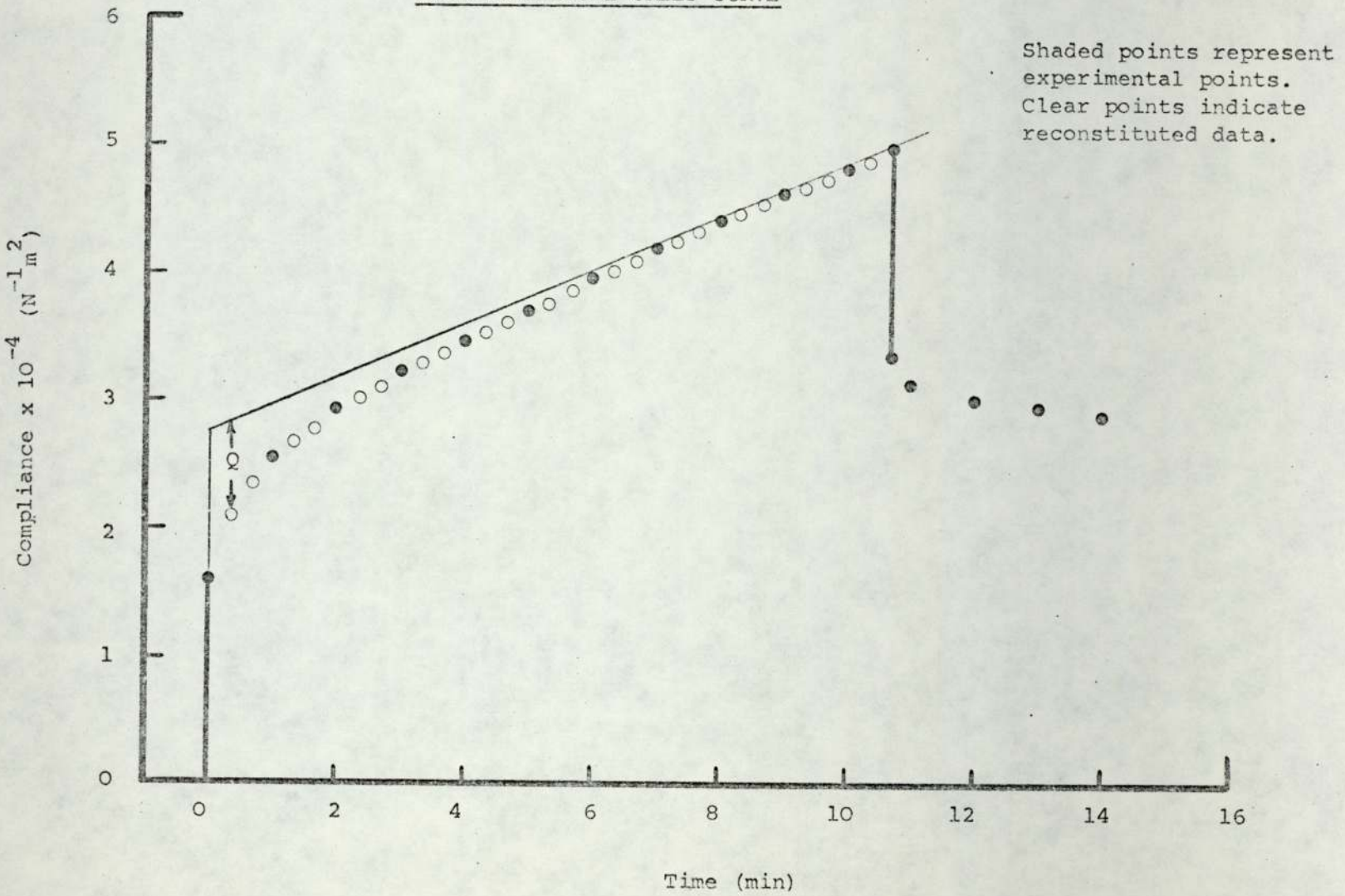

FIGURE 27

DISCRETE SPECTRUM ANALYSIS OF CREEP CURVE IN FIGURE 26

Plot of data derived from Figure 26 to determine parameters of first Voigt unit

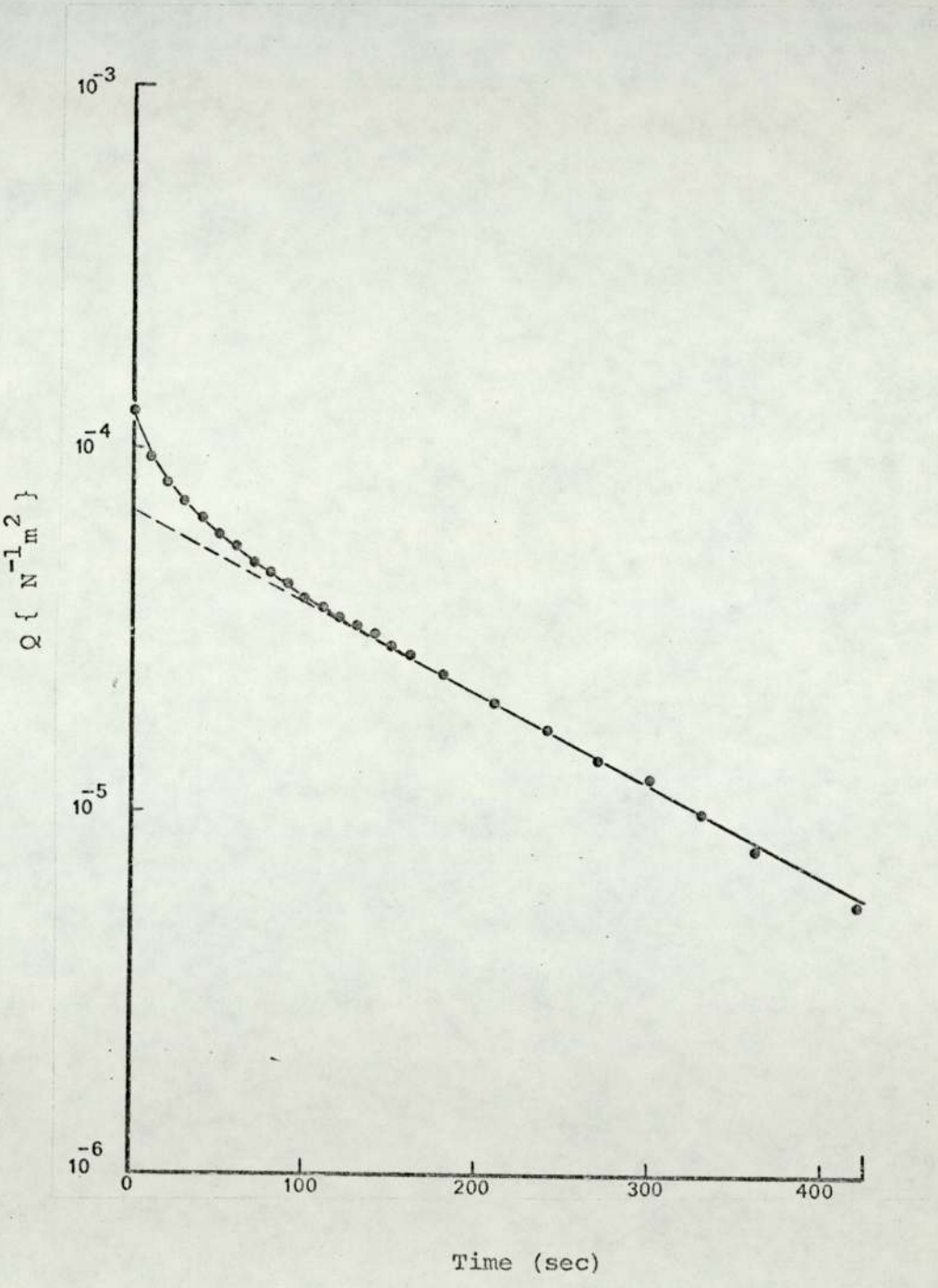

FIGURE 28

DISCRETE SPECTRUM ANALYSIS OF CREEP CURVE IN FIGURE 26

Plot of data derived from Figure 27 to determine

parameters of second Voigt unit

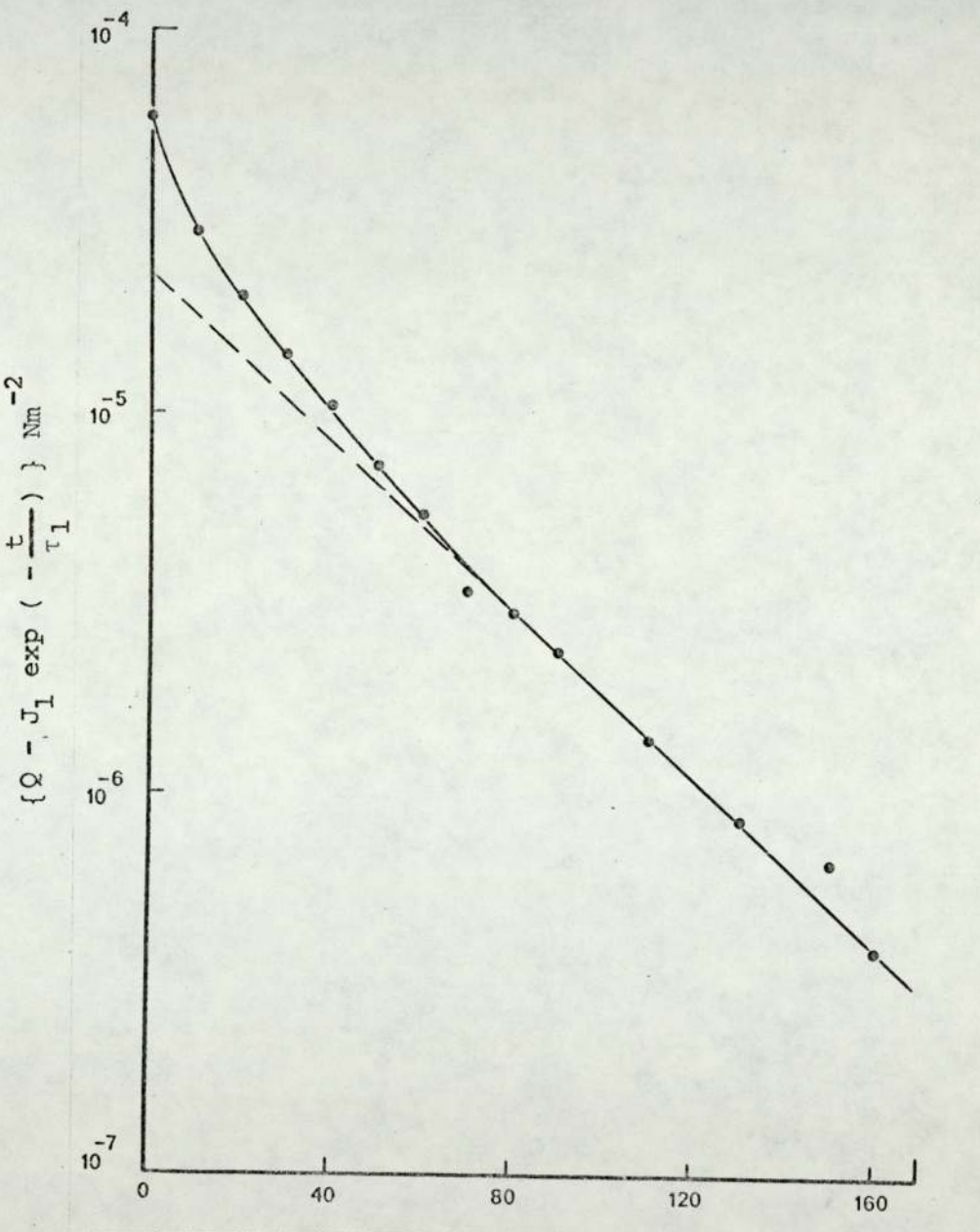

FIGURE 29

DISCRETE SPECTRUM ANALYSIS OF CREEP CURVE IN FIGURE 26.

Plot of data derived from Figure 28 to determine parameters of third Voigt unit

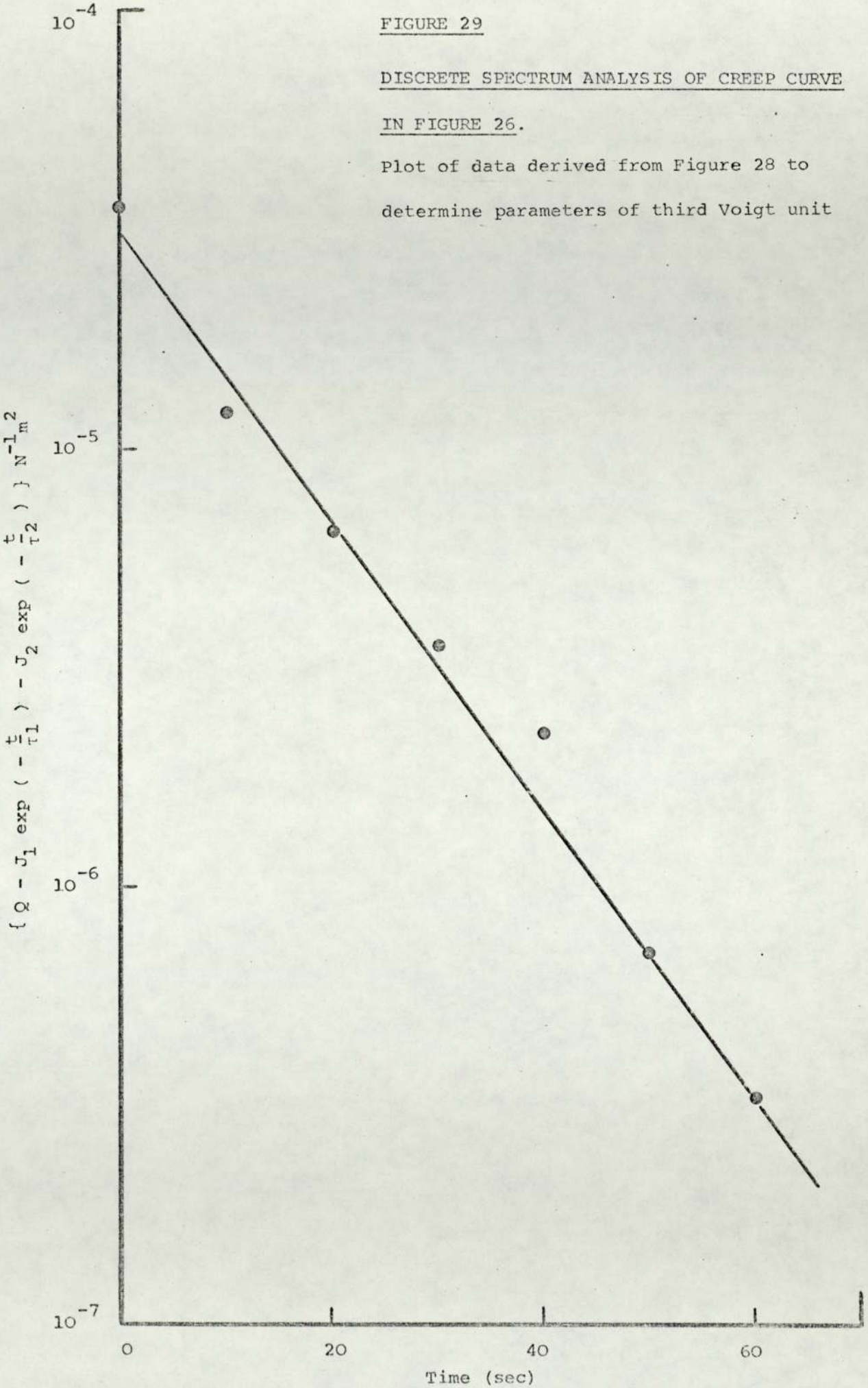

TABLE 12

DISCRETE SPECTRAL DATA DERIVED BY GRAPHICAL ANALYSIS

OF THE CREEP CURVE IN FIGURE 26

J_o	J_1	J_2	J_3	τ_1	τ_2	τ_3	η_o
$N^{-1}m^2 \times 10^{-5}$				secs			Poise $\times 10^7$
16.11	6.8	2.3	3.25	171.5	39.4	13.0	3.09

which the programme was written in ALGOL (Appendix). The discrete spectral data were accepted when the reconstituted creep data agreed to within two per cent of the original.

(ii) Continuous Spectrum Analysis

Continuous retardation spectrum $L(\tau)$ defined by Equation (24) given in Section 2.3.3(a) of Part A, can be determined using one of several approximation techniques (56, 257 to 261). In this work the approximation method due to Schwarzl (258) and Schwarzl and Staverman (259, 260) has been used. According to this method, the following first order approximation gives the value of the distribution function at any specified time

$$L(\tau) \simeq \frac{d}{d\ln t} \left\{ J(t) - \frac{t}{\eta_o} \right\} \Big|_{t = \tau} \quad \ldots (74)$$

The value of $(J(t) - t/\eta_o)$ determined from the creep curve at various values of t is plotted as a function of $\log_{10} t$, Figure 30. The gradient of this curve at various times, t, plotted as a function of $\log_{10} t$ after mathematical treatment to convert $\log_e$ yields a continuous spectrum of retardation times, Figure 30.

While the first order approximation yields the overall shape of the spectra, it does not give great details of the maxima at which retardation processes are taking place. For this reason, approximations of the higher order are generally

FIGURE 30

CONTINUOUS SPECTRUM ANALYSIS OF CREEP CURVE

SHOWN IN FIGURE 26

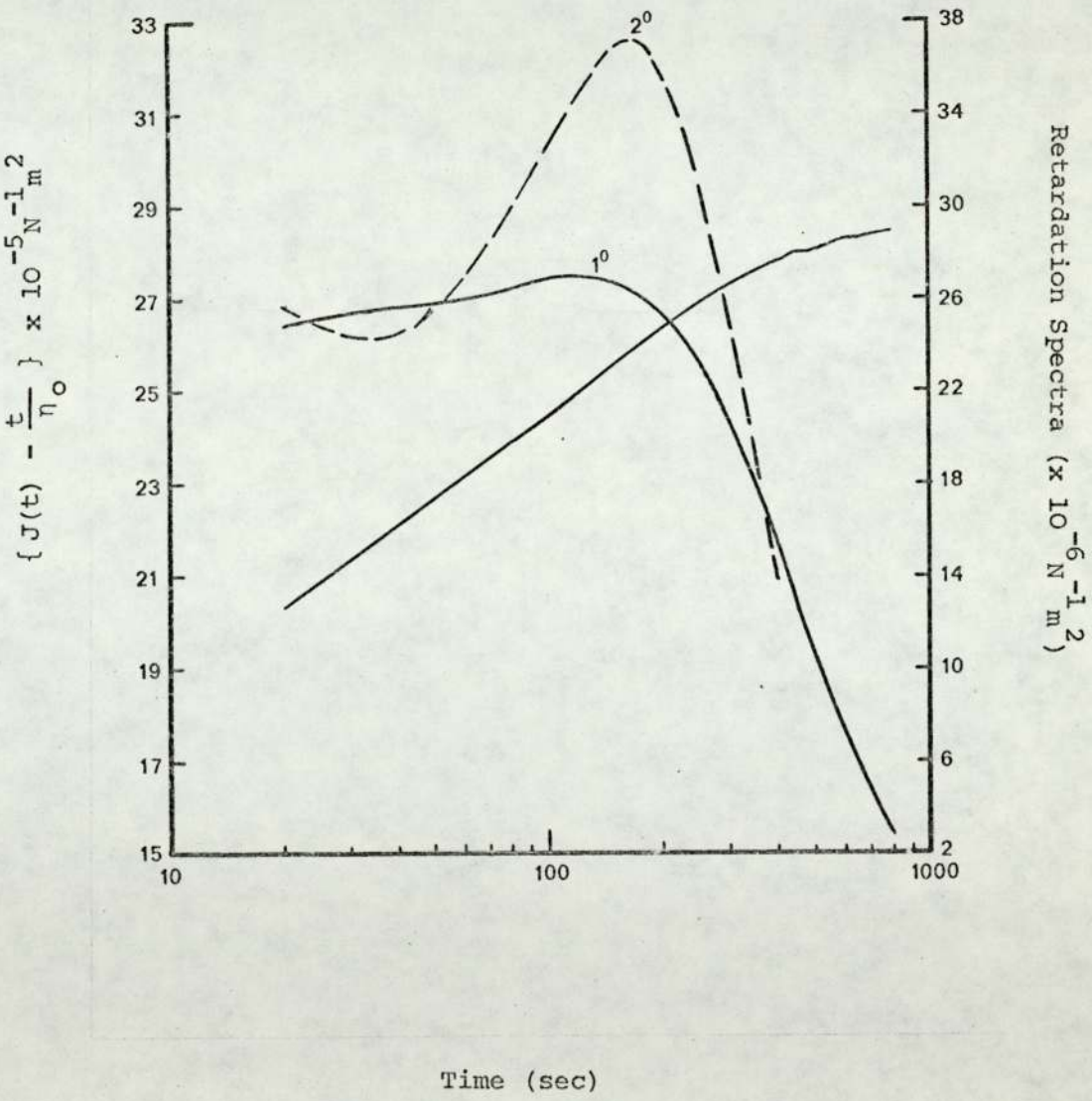

preferred in the derivation of continuous spectra. The following second order approximation has found favour in pharmacy (262 - 5)

$$L(\tau) = \left\{ \frac{d\,J(t)}{d\ln t} - \frac{d^2\,J(t)}{d\ln t^2} \right\} \Bigg|_{t = 2\tau} \quad \ldots (75)$$

due to the fact that the viscous contribution to compliance does not have to be known and thus continuous spectra may be obtained for materials which have not attained a steady state of flow. In practice, Leaderman (56) has pointed out that substitution of $(J(t) - {}^{t}/\eta_0)$ for $J(t)$ does not change Equation (75). Thus, where greater clarity is required, a second order approximation of the continuous spectra can be derived directly from the first order spectra as is shown in Figure 30. The second order approximation has been used for all continuous spectral analysis in this thesis.

3.3.2 Procedure employed in Concentric Cylinder Creep Analysis of Plastibases

The concentric cylinder apparatus constructed for the purpose of small strain creep investigation of Plastibases was operated and the results evaluated as described in the previous Section 3.3.1.

With all samples, linearity checks were made before performing creep tests. Creep analysis was attempted on all the five grades of Plastibase over a temperature range $10^{\circ}C$ to $45^{\circ}C$.

Changes in viscoelasticity due to interbatch variation were investigated by performing creep tests on four batches of Plastibase 50W over a temperature range 10°C to 45°C.

3.3.3 Thermo-microscopy of Plastibase 50W

Thermomicroscopy of Plastibase 50W was undertaken in order to investigate the cause of a discontinuity observed in the Arrhenius type plots of residual viscosity and modulus verses inverse absolute temperature.

(a) Phase Contrast

Plastibase 50W was examined using a Kofler Micro Hot Stage (Optische Werke A.G., Austria) attached to a Wild microscope (Wild Heerbugg Limited, Switzerland) with phase contrast accessories and achromatic lenses over a temperature range 20°C to 70°C. A simple smear technique was used in the preparation of the slides.

(b) Polarising Light

Plastibase 50W was examined using a Kofler Micro Hot Stage attached to a Zeiss Photomicroscope Model 2 (Carl Zeiss, Obercochen Ltd., London.) with polarising accessories and achromatic lenses over 20°C to 70°C temperature range. A simple smear technique was used in the preparation of the slides.

3.3.4 Calorimetric Analysis of Plastibases

Calorimetric analysis of Plastibases was undertaken in order to assess the nature of any transistions occurring within the

material which may be related to the discontinuity observed in the Arrhenius type plots of residual viscosity and modulus versus inverse temperature.

(a) Differential Thermal Analysis

This form of analysis was carried out under nitrogen using a Standard DTA Cell plugged into the Du Pont 900 Cell Base (Du Pont Instruments, Hitchin, Herts.). The sample material and a reference material placed in disposable glass tubes were heated at the rate of $3^{o}C$ per minute. Thermocouples inserted into the tubes measured the temperature difference between the sample and reference material (liquid paraffin) and this was monitored as a function of temperature by an X-Y recorder. The thermogram thus obtained was scanned for signs of any endothermic or exothermic changes.

(b) Differential Scanning Calorimetry

DTA at high sensitivity was hampered by electronic noise. It was believed that perhaps the transistion endotherms were rather small and thus indistinguishable at high sensitivity from noise effects. Thus in order to extend the investigation to the high sensitivity scale, samples of Plastibases were sent to RAPRA (Shrewsbury) for analysis where DSC was carried out using a Perkin-Elmer model DSC-1 differential scanning calorimeter. The Plastibase thermograms were again scanned for signs of endothermic or exothermic changes.

3.4 Results

Experimental difficulties prevented creep testing of Plasti-

base 20W, 10W and 5W, owing to the 'thin' consistencies of these vehicles. Plastibase 20W exhibited linear behaviour over a very small stress range at low temperatures, however the reproducibility of the creep curves in this linear region was inconsistent. Plastibase 10W and 5W exhibited non-linear behaviour with the smallest stress that could be applied using the concentric cylinder viscometer and hence these materials could not be subjected to creep analysis.

Viscoelastic linearity plots for Plastibase 50W and 30W are shown in Figures 31 and 32. The effect of temperature on the creep behaviour of these bases is shown in Figures 33 and 34. Discrete spectral data and second order continuous retardation spectra, derived from creep curves of Plastibase 50W and 30W determined over a temperature range 10°C to 45°C are given in Tables 13 and 14, and shown in Figures 35 and 36 respectively.

Arrhenius type plots of residual viscosity and instantaneous compliance vs inverse absolute temperature are shown in Figures 37 and 38. Both plots show an inflection in the 25°C to 30°C temperature range indicating a temperature dependent change in the flow properties of the material. These figures also include batch to batch variation data for Plastibase 50W.

Photomicrographs obtained from phase contrast and polarising light thermo-microscopy of Plastibase 50W are included in Figures 39 and 40.

The traces resulting from the differential thermal analysis and differential scanning calorimetry of Plastibase 50W, 30W and 5W

FIGURE 31

VISCOELASTIC LINEARITY PLOT FOR PLASTIBASE 50W

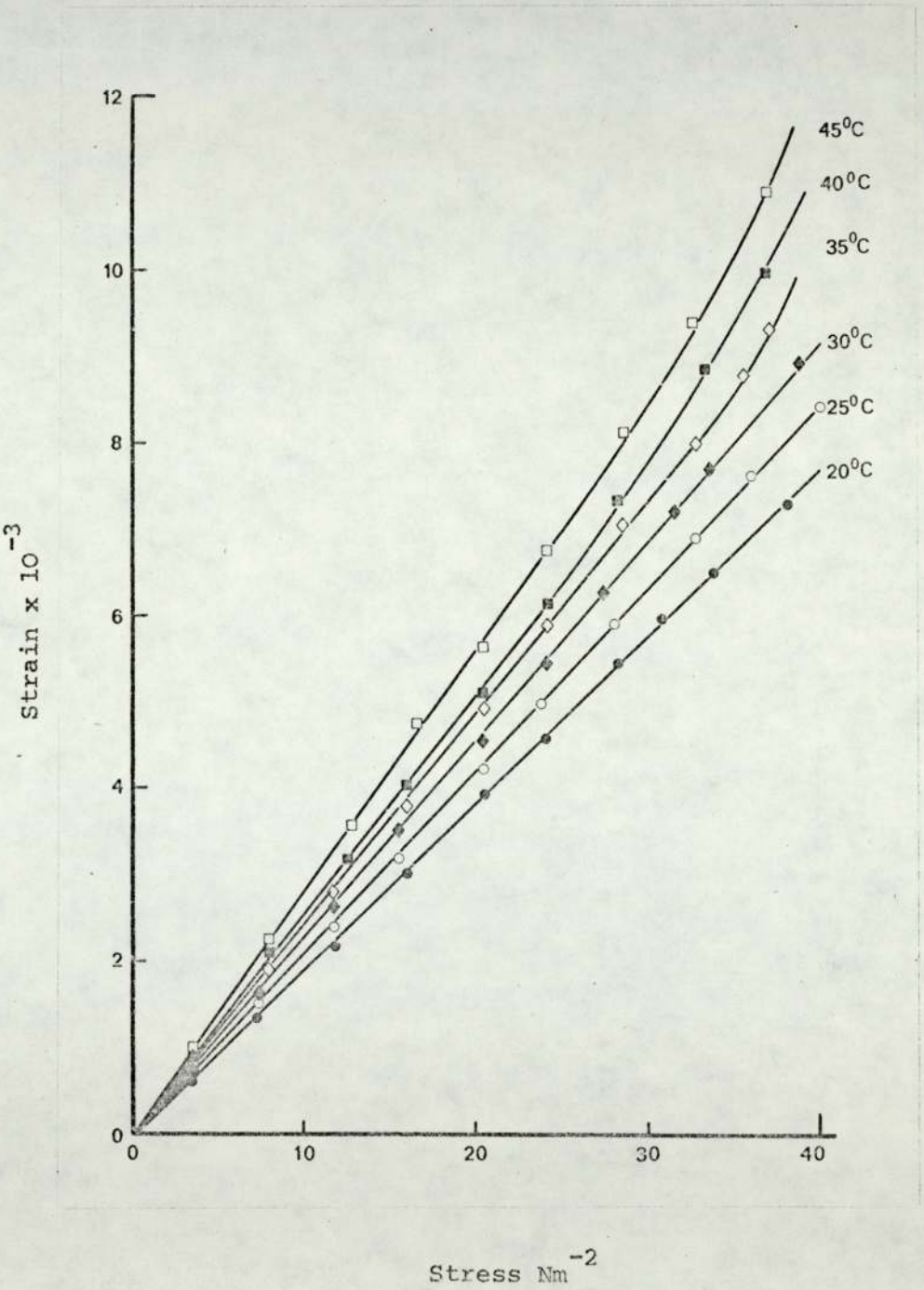

FIGURE 32

VISCOELASTIC LINEARITY PLOT

FOR PLASTIBASE 30W

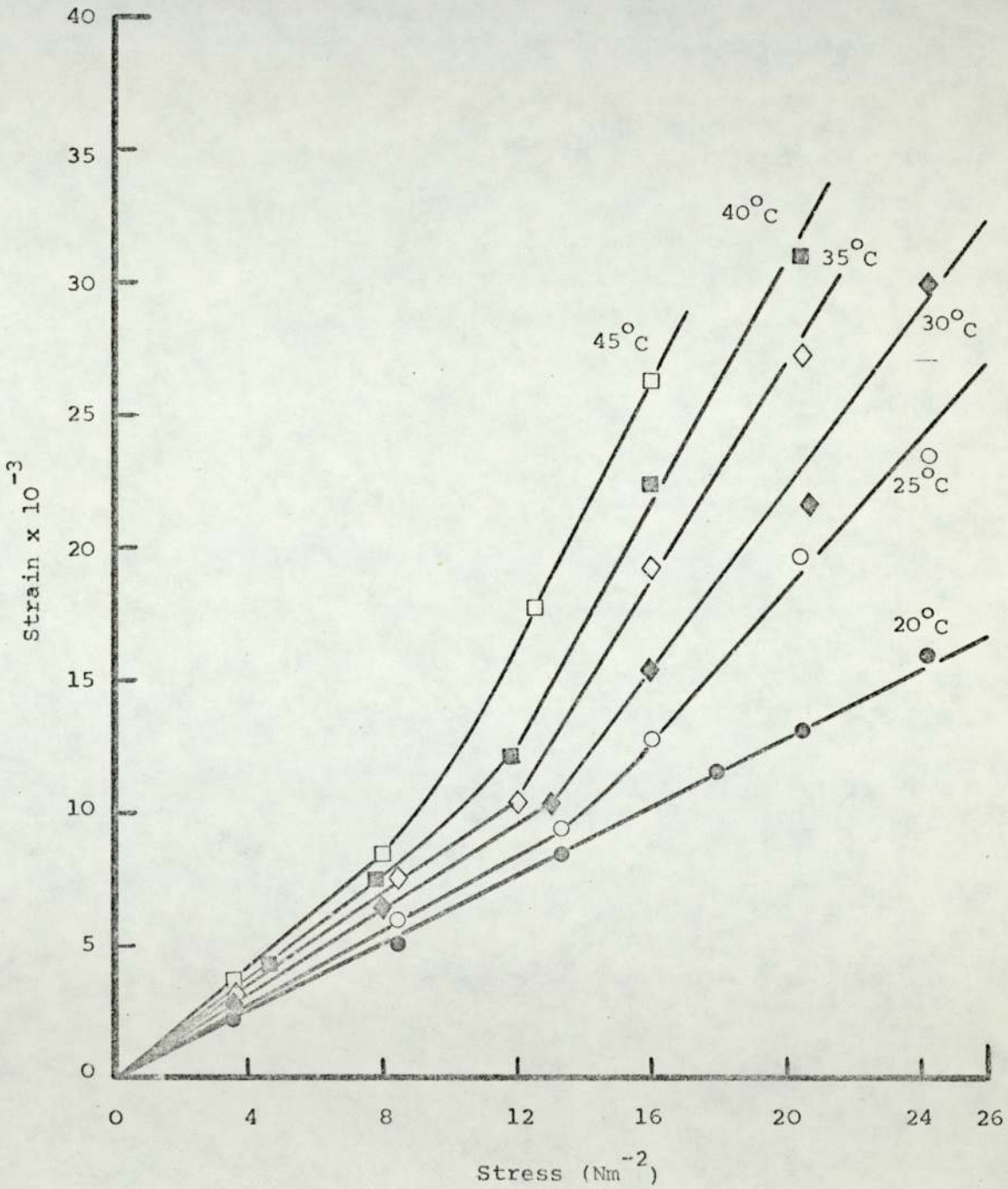

FIGURE 33

CREEP CURVES AND CORRESPONDING MECHANICAL MODEL ANALOGIES ILLUSTRATING THE EFFECT OF TEMPERATURE ON THE VISCOELASTIC PROPERTIES OF PLASTIBASE 50W

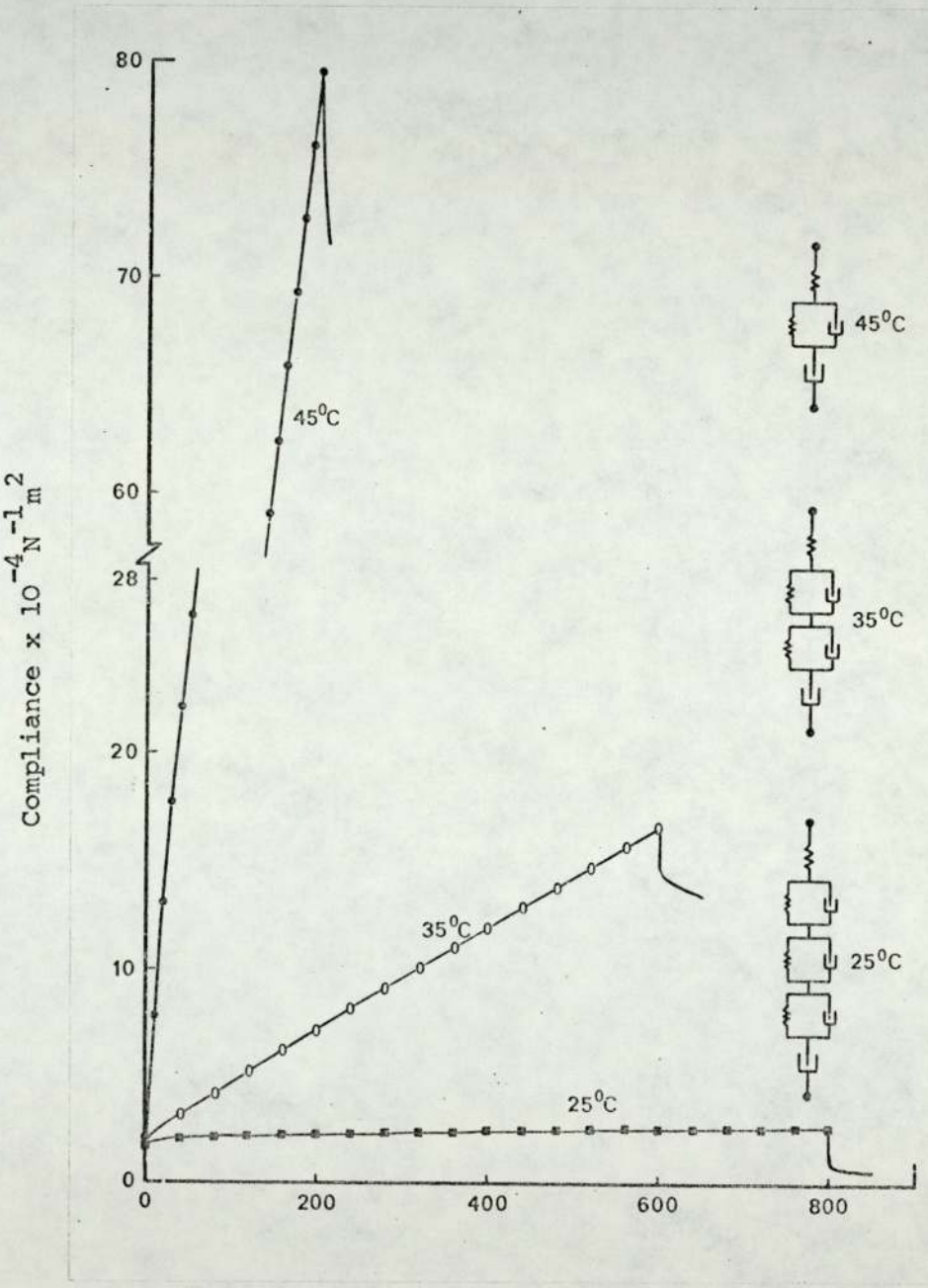

FIGURE 34

CREEP CURVES AND CORRESPONDING MECHANICAL MODEL ANALOGIES ILLUSTRATING THE EFFECT OF TEMPERATURE ON THE VISCOELASTIC PROPERTIES OF PLASTIBASE 30W

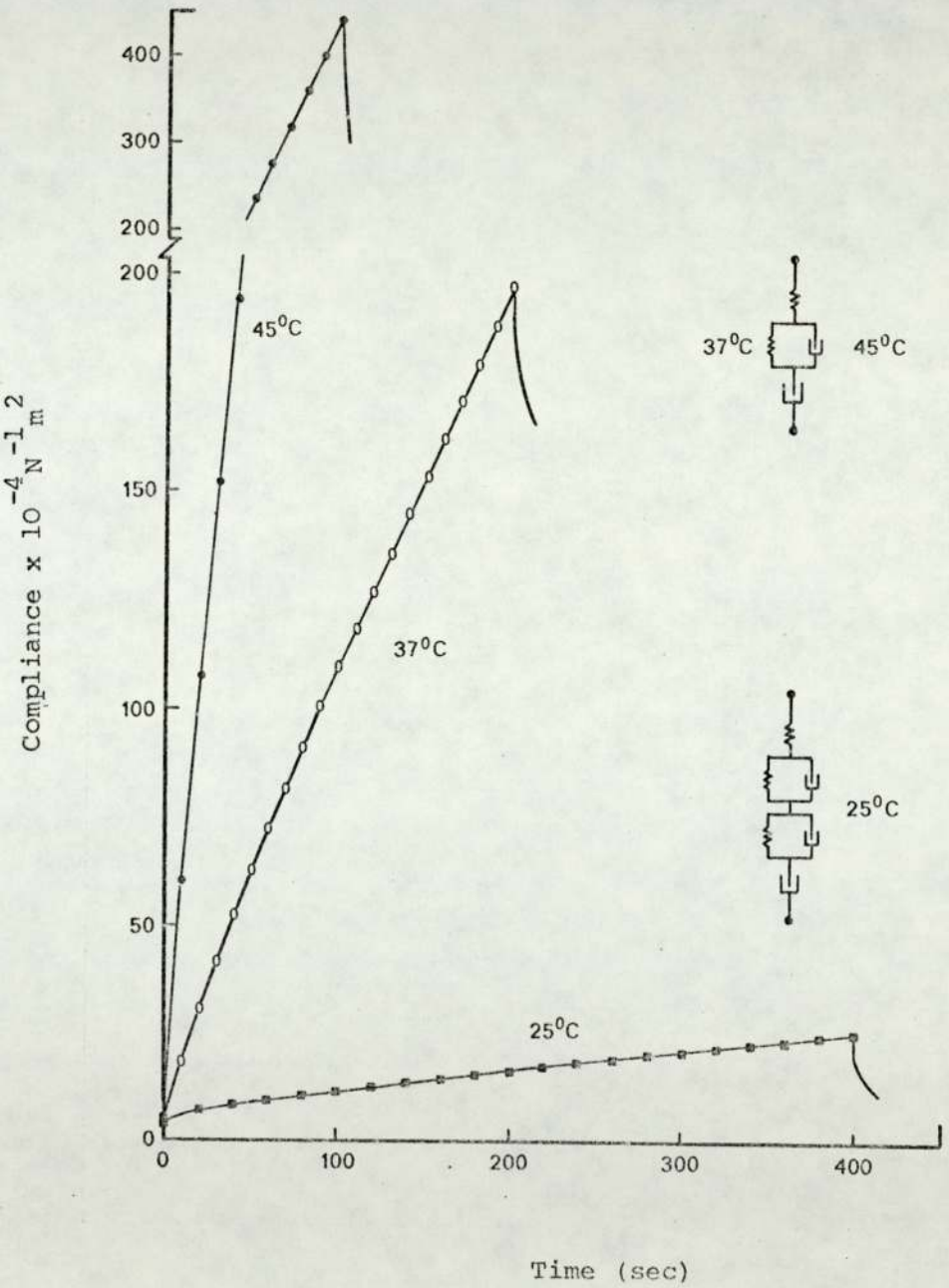

TABLE 13

DISCRETE SPECTRAL ANALYSIS DATA FOR PLASTIBASE 50W

Temperature	10°C	15°C	20°C	25°C	30°C	35°C	40°C	45°C
	Compliance x 10^{-5} m^2N^{-1}							
J_o	11.89	13.12	14.37	16.84	18.57	19.61	20.77	21.05
J_1	1.28	1.69	2.38	3.07	3.72	3.97	26.76	94.67
J_2	1.01	1.24	1.44	1.57	2.24	2.73	-	-
J_3	0.81	1.19	1.20	2.18	-	-	-	-
J_4	1.10	1.39	1.50	-	-	-	-	-
	Retardation times (sec)							
τ_1	293	249	203	157	132	130	47	35
τ_2	55	28.9	28.2	26.5	16	14	-	-
τ_3	11	4.3	4.0	4.0	-	-	-	-
τ_4	4	2.8	2.2	-	-	-	-	-
	Viscosity x 10^6 Poise (10^{-1} Nsm^{-2})							
η_o	544.7	504.4	456.0	252.9	75.9	4.3	0.91	0.29
η_1	228.9	147.3	85.3	51.1	35.5	32.7	1.8	0.37
η_2	54.5	23.3	19.6	16.9	7.1	5.1	-	-
η_3	13.6	3.6	3.3	1.8	-	-	-	-
η_4	3.6	2.0	1.5	-	-	-	-	-

TABLE 14

DISCRETE SPECTRAL ANALYSIS DATA FOR PLASTIBASE 30W

Temperature	10°C	15°C	20°C	25°C	30°C	35°C	40°C	45°C
	Compliance x 10^{-5} m^2N^{-1}							
J_o	28.2	33.0	38.0	46.2	49.4	51.8	55.4	57.3
J_1	37.9	33.0	35.0	36.0	43.0	190.0	230.0	270.0
J_2	2.5	6.9	11.4	14.3	-	-	-	-
J_3	7.5	-	-	-	-	-	-	-
	Retardation times (sec)							
τ_1	110	143	136	134	38	36	25	14
τ_2	11	18	16	12	-	-	-	-
τ_3	3	-	-	-	-	-	-	-
	Viscosity x 10^5 Poise (10^{-1} x Nsm^{-2})							
η_o	37.8	42.9	34.4	25.6	5.5	1.16	0.54	0.25
η_1	29.0	43.3	38.9	37.2	8.8	1.9	1.1	0.52
η_2	44.0	26.1	14.0	8.4	-	-	-	-
η_3	4.0	-	-	-	-	-	-	-

FIGURE 35

CONTINUOUS RETARDATION SPECTRA

FOR PLASTIBASE 50W

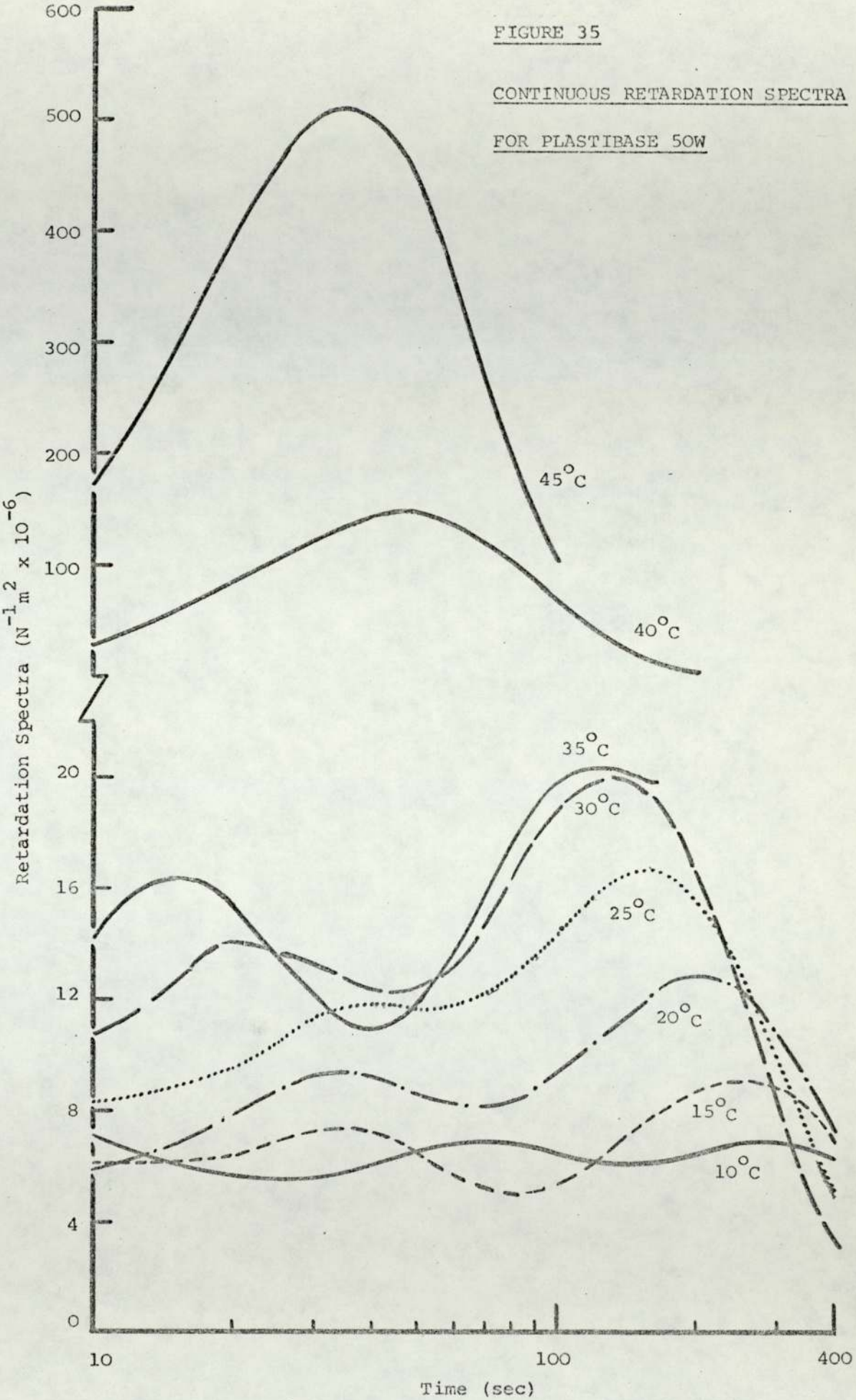

FIGURE 36

CONTINUOUS RETARDATION SPECTRA FOR PLASTIBASE 30W

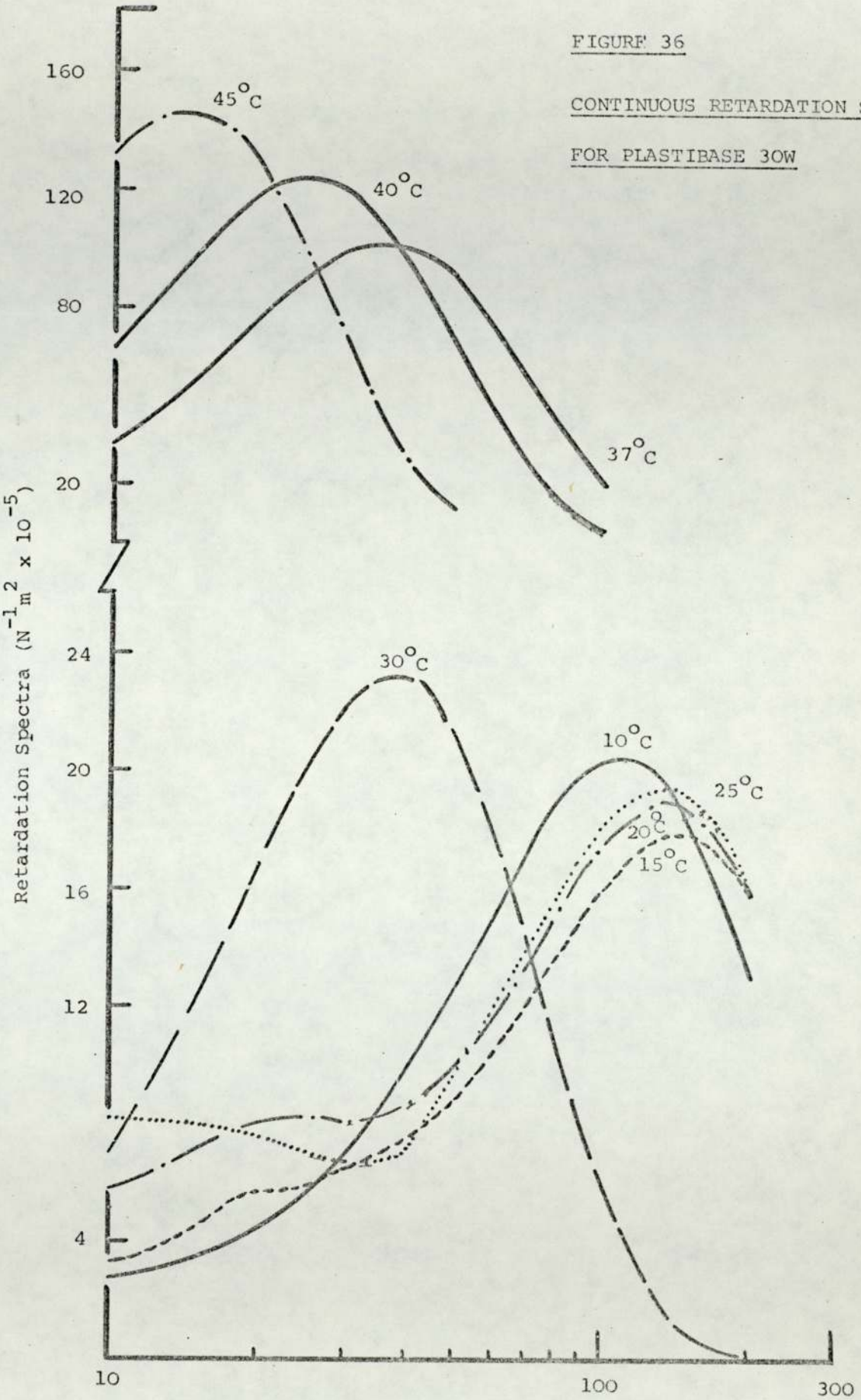

FIGURE 37

ARRHENIUS-TYPE PLOTS OF RESIDUAL NEWTONIAN VISCOSITY DATA DERIVED FOR FOUR BATCHES OF PLASTIBASE 50W AND PLASTIBASE 30W FROM CREEP TESTS

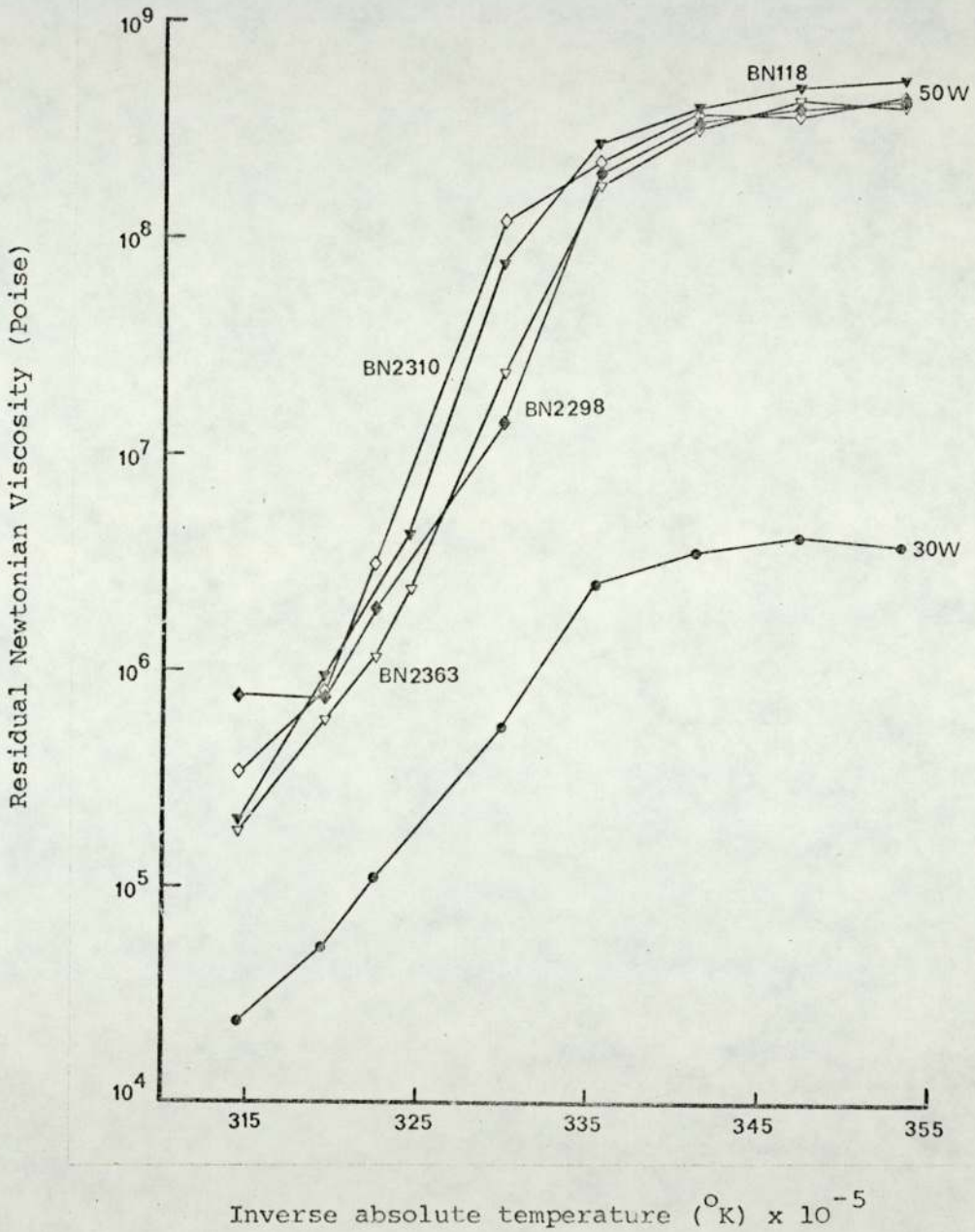

FIGURE 38

ARRHENIUS-TYPE PLOTS OF INSTANTANEOUS SHEAR MODULUS DATA DERIVED FOR FOUR BATCHES OF PLASTIBASE 50W AND PLASTIBASE 30W FROM CREEP TESTS

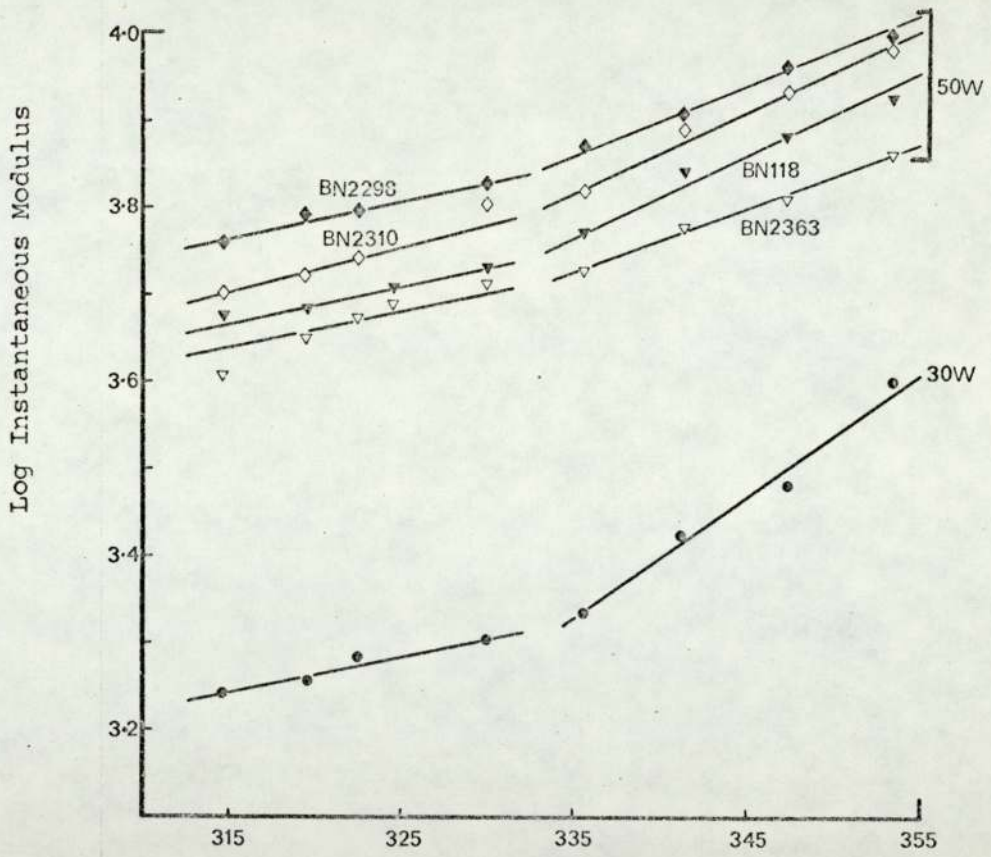

FIGURE 39

PHOTOMICROGRAPH IN PHASE CONTRAST OF PLASTIBASE 50W

(magnified 1600 times)

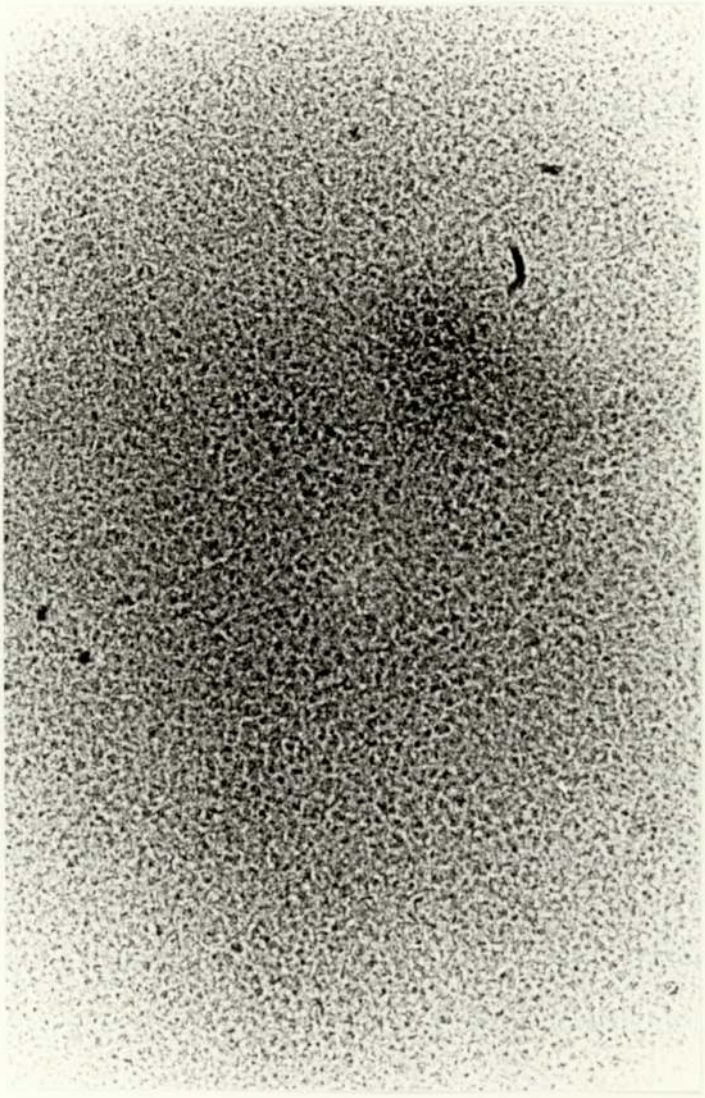

FIGURE 40

PHOTOMICROGRAPH IN CROSS POLARISED LIGHT OF PLASTIBASE 50W

(magnified 1600 times)

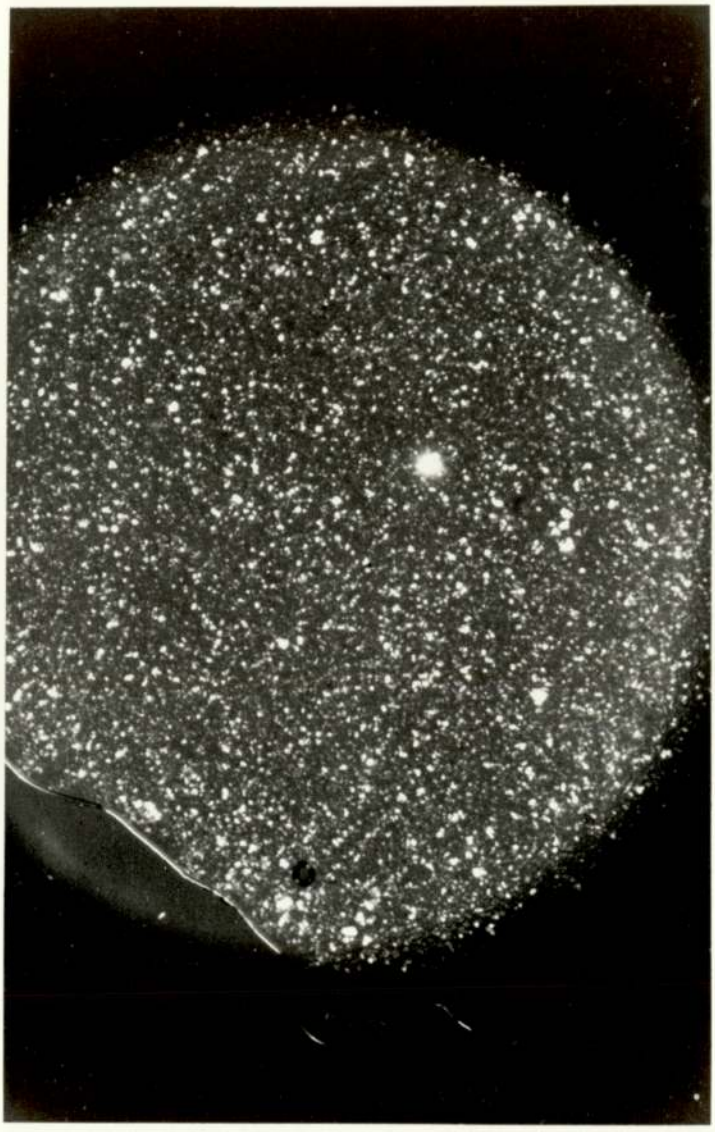

are illustrated in Figures 41 and 42.

3.5 Discussion

A combination of instrumental limitation and non-linear viscoelasticity exhibited by the 'thin' Plastibases prevented creep analysis of these bases. Other workers have reported encountering similar difficulties in creep testing of 'thin' mucoid fluids (241, 266). The linear behaviour of Plastibase 50W and 30W over a temperature range 20°C to 45°C was determined from strain response of these materials to increasing stresses of up to 40Nm^{-2} and 25Nm^{-2} respectively, Figures 31 and 32.

Plastibase 50W at temperatures up to and including 30°C demonstrated linear viscoelastic behaviour over the entire 0 - 40 Nm^{-2} stress range. At 35°C, the onset of non-linear behaviour for this material occurred at approximately 35Nm^{-2}, and over the 40°C to 45°C temperature range at approximately 25Nm^{-2}.

At 20°C Plastibase 30W exhibited linear behaviour over the entire 0 - 26Nm^{-2} stress range. From 25°C to 35°C, the material exhibited linear behaviour up to 12Nm^{-2} applied stress and over the temperature range 40°C to 45°C, up to approximately 8Nm^{-2} applied stress.

Creep curves for Plastibase 50W and 30W, Figures 33 and 34, show that the viscoelastic properties of the materials change in a characteristic way with an increase in temperature. Discrete spectral data for Plastibase 50W and 30W indicate that with an increase in temperature while the derived compliances generally increased, the

FIGURE 41

DIFFERENTIAL THERMAL ANALYSIS THERMOGRAMS FOR PLASTIBASES

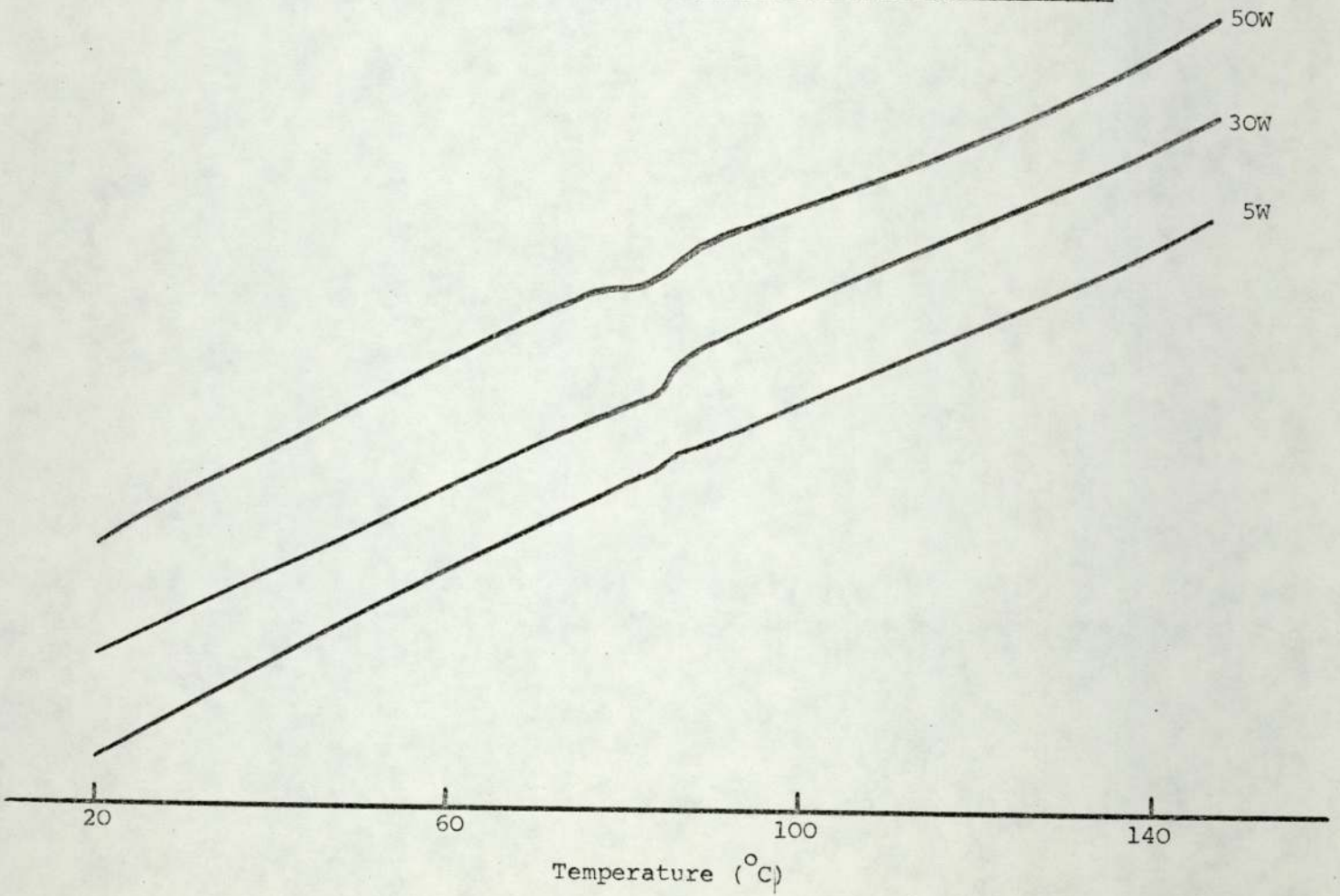

FIGURE 42

DIFFERENTIAL SCANNING CALORIMETRY THERMOGRAM FOR PLASTIBASE 50W

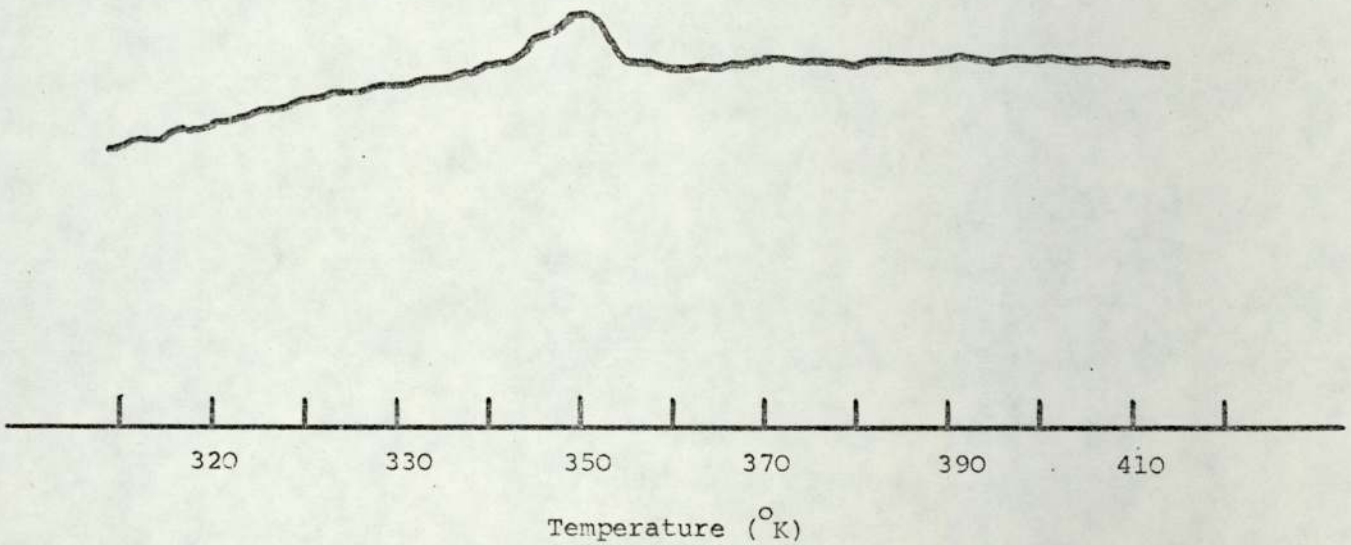

retardation times and viscosities decreased. Viscoelastic properties of Plastibase 50W can be characterised by four retardation times over 10°C to 20°C, three retardation times at 25°C, two retardation times from 30°C to 35°C and one retardation time at 40°C and 45°C. The corresponding mechanical model representation of this behaviour for Plastibase 50W is one Maxwell element in series with four Voigt (Kelvin) elements from 10°C to 20°C, three Voigt (Kelvin) elements at 25°C, two Voigt (Kelvin) elements from 30°C to 35°C and one Voigt (Kelvin) element from 40°C to 45°C. Viscoelastic properties of Plastibase 30W can be characterised by three retardation times at 10°C, two retardation times from 15°C to 25°C and one retardation time from 30°C to 45°C. The corresponding mechanical model representation being one Maxwell element in series with three Voigt (Kelvin) elements at 10°C, two Voigt (Kelvin) elements from 15°C to 25°C and one Voigt (Kelvin) element from 30°C to 45°C.

The continuous retardation spectra for Plastibase 50W, Figure 35, demonstrates two maxima at temperatures below 35°C and one maxima at temperatures above 35°C. The spectra for Plastibase 30W, Figure 36, demonstrates two maxima at temperatures below 25°C and one maxima at temperatures above 25°C. The creep behaviour for Plastibase 30W at 10°C would appear to be anomalous, probably due to an experimental error resulting from temperature fluctuations. Overall, the peak heights of all the spectra increased with increase in temperature indicating a decrease in the consistency of the Plastibases and a progressive concentration of retardation processes. With increase in temperature, there is also a gradual tendency for the maxima in the retardation spectra to move to shorter times. This movement, which represents an overall increase in the rate at which strain

occurs, suggests that the basic structure of the product is changing at a molecular level with the temperature increase. This is particularly evident in the 25°C to 35°C temperature range where the transition in the structure is characterised by a marked shift of the longer time maxima to the shorter time resulting in a spectra with a single shorter time maxima.

Arrhenius type plots, Figures 37 and 38, of residual viscosity and elastic modulus for four different batches of Plastibase 50W and one batch of Plastibase 30W also exhibited a discontinuity in the 25°C to 30°C temperature range. This further confirmed that Plastibases appear to undergo a structural-rheological change in the 25°C to 35°C temperature range. Barry and Grace (247) have reported finding a similar discontinuity in the 25°C to 35°C temperature range when investigating the rheological characteristics of white soft paraffin. It was reported (53) that a relationship probably exists between temperature, rheological properties and infra red transmittance, however the evidence was not conclusive.

Phase contrast and polarising light thermomicroscopy of Plastibase did not yield any information concerning a structural transition. Phase contrast photomicrographs, Figure 39, of Plastibase 50W show an anisotropic dispersion of polyethylene in mineral oil. This dispersion appears to remain stable until 55°C when the melting of the polyethylene is observed to commence yielding an isotropic solution at 70°C. The resolving capacity of the microscope in phase contrast microscopy of Plastibases is limited and therefore it is difficult to determine the exact character of the polyethylene dispersion in Plastibase. Polarising light microscopy, however, yielded a much clearer

picture, Figure 40, showing that the gel network in Plastibase is composed of a microcrystalline dispersion of polyethylene and that there is no evidence of any spherulite formation. Huttenrauch et. al. (210) have reported a similar structure for a rapidly chilled polyethylene gel like Plastibase. They have, however, observed that for a slow cooled polyethylene gel, the structure is largely composed of spherulites. Once again, polarising light thermo-microscopy yielded the information that the polyethylene gel network appears to remain stable until 55°C when melting commences leaving an apparently isotropic solution at 70°C. The microscopic evidence thus suggests that there may not be any melting phenomena associated with the discontinuity in the rheological properties.

Kato and Saito (267) have reported observing a peak between 27°C and 35°C in the differential thermal analysis of white petrolatum. Calorimetric investigation in this work did not yield any such peaks for Plastibases in the stated temperature range, Figures 41 and 42. Differential thermal analysis of Plastibase 50W, 30W and 5W shows only one melting endotherm at 82°C corresponding to the eutectic melting point. Similarly, differential scanning calorimetry of Plastibase 50W shows only one melting transition at around 77°C. The calorimetric studies thus indicate that the structural transition in Plastibases in the 25°C to 35°C temperature range does not involve any heat exchange, suggesting that the change occurring is of a 'morphological nature' involving intralamellar motions or motions within crystalline regions (268, 269).

It is known that long chain paraffinic molecules may undergo temperature dependent structural transitions accompanied by volume

changes (270). It is also known that most semi-crystalline polymers and especially polyethylene, undergo three transitions commonly referred to as α, β and γ transitions (271). The α transition in polyethylene which is related to some form of second order transition in the crystalline structure occurs over a temperature range which corresponds with that at which the discontinuity in the rheological properties of Plastibases is observed. Bearing in mind the work of Barry and Grace (247), it is suggested that the discontinuity in the rheological properties of Plastibase occurring in the 25°C to 35°C temperature range may be explained as resulting due to a temperature dependent crystalline transition phenomena which may be associated with volume changes in the material. Further investigation of this phenomena is necessary. It is suggested that dilatometric measurements may help to establish the volume changes that accompany any transitions in the 25°C to 35°C temperature range.

Figures 37 and 38 show that the interbatch transition in Plastibase 50W is considerable. Once again, as has been discussed in Section 2.5 of Part B, the batch to batch variation may be explained as resulting from a possible variation in polyethylene concentration, crystalline fraction and/or age.

In comparing creep and continuous shear parameters, several correlations may be drawn. Davis (221) has suggested that in creep studies the stress required for the onset of non-linear behaviour can be regarded as representing a type of yield value and has reported a correlation between the ratio of these values and the ratio of the static yield stress values found in continuous shear tests of lard and shortening. It is interesting to note that a similar correlation can

be drawn between the two ratios for Plastibase 50W and Plastibase 30W at 25°C, Table 15. A similar correlation can also be drawn between the two ratios from parameters measured at 25°C and 45°C (1.6:1) for Plastibase 50W.

Davis (246) and Barry and Grace (250) have reported a correlation between yield stress values found in continuous shear tests and long retardation times obtained from creep studies. In this work it was found that the ratio of the second retardation times was somewhat close to the ratio of the yield stress values, Table 15, and from this it would seem that some correlation may be drawn between the two sets of parameters.

Van den Tempel (272) has shown that hardness (modulus) values obtained using sophisticated methods gave a correlation coefficient with penetrometer yield values of the order of 0.9 or better. Davis (221) has shown that penetrometer yield values of the Haighton (273) type may be correlated with the static yield values obtained from the Ferranti-Shirley viscometer and thus it may be reasoned that a correlation between the yield stress values obtained from continuous shear and the instantaneous modulus values obtained from creep studies should be possible. On theoretical grounds as both the yield value and the instantaneous modulus are a function of the crystalline gel network, such a correlation would seem logical. Thus it is gratifying to note that in this work a correlation was found between the yield stress values and instantaneous modulus values for Plastibase 50W and 30W, Table 15. No correlation however could be drawn between the apparent and residual viscosities derived from continuous shear and creep studies respectively.

TABLE 15

COMPARISON OF CONTINUOUS SHEAR AND CREEP DATA DERIVED AT 25°C FOR PLASTIBASES 50W AND 30W

Method of Measurement	Rheological Parameters	Plastibase 50W	Plastibase 30W	Ratio of Parameters
Continuous Shear	Yield Stress (Nm^{-2})	425	140	3.04
	App Viscosity (Poise)	23.06	7.29	3.16
Creep	Onset of Nonlinearity (Nm^{-2})	≃ 40	12.5	3.20
	G_o (Nm^{-2})	5.95×10^3	2.16×10^3	2.75
	G_1 (Nm^{-2})	32.2×10^3	2.78×10^3	11.60
	G_2 (Nm^{-2})	62.5×10^3	6.99×10^3	8.90
	τ_1 (sec)	157.0	134.0	1.17
	τ_2 (sec)	26.5	12.0	2.20
	η_o (Poise)	252.9×10^6	2.56×10^6	98.8

4 OSCILLATORY (DYNAMIC) TESTING OF PLASTIBASES

4.1 Introduction

Small strain creep experiments provided valuable fundamental information concerning the rheological characteristics of Plastibase 50W and Plastibase 30W. These tests are however limited at short times by inertial effects and by the impossibility of applying a truly instantaneous stress at the beginning of the experiment. Furthermore, experimental difficulties restricted creep investigation by the concentric cylinder creep apparatus of the relatively 'thin' Plastibases (20W, 10W and 5W) in the linear viscoelastic region. Dynamic tests were thus undertaken in order to complete the rheological characterisation of the five grades of Plastibases. The theory concerning oscillatory (Dynamic) testing is discussed in Part A. As a periodic experiment of frequency ω (rads/sec) is qualitatively equivalent to a creep experiment of time $t = {}^{1}/\omega$, interconversion of creep and dynamic data allowed comparison and completion of fundamental rheological parameters over a wide time scale for subsequent correlation with drug release data for all Plastibases.

4.2 Materials

The Plastibases used in this study were supplied by E R Squibb & Sons Limited (Wirral). Following is a list of Plastibases employed:-

Plastibase 50W	Batch Number	118, 2298, 2310, 1148, 2363
Plastibase 30W	Batch Number	Not given
Plastibase 20W	Batch Number	Not given
Plastibase 10W	Batch Number	2122

4.3 Experimental

4.3.1 The Weissenberg Rheogoniometer

(a) Description

A detailed description of the Rheogoniometer assembly has been given previously by Van Wazer et. al. (52), Warburton & Davis (274), Watson (275) and Solatron Electronics (276).

The Rheogoniometer employed in this study was the model R14 (Sangmo Controls Limited, Sussex) modified to R16 standards. Data collection was simplified by the use of a Solatron Digital Transfer Function Analyser (DTFA) model JM 1600 and a Mechanical Reference Synchroniser (MRS) model JX 1606 (Solatron Electronics Group Limited, Farnborough) coupled to the Rheogoniometer. Parallel plate (7.5 cm diameter) geometry was used in this study. Two torsion bars, $^{1}/_{16}$" (0.15875 cm) diameter and $^{1}/_{8}$" (0.3175 cm) diamter, were employed for lower and higher consistency Plastibases respectively. For clarity of discussion a diagram of the Rheogoniometer assembly, Figure 43, is included.

(b) Principle of Operation

The test material, held in a suitable geometry (cone and plate, parallel plates or concentric cylinder), is subjected to a small sinusoidal shear strain by oscillating one member of the measuring unit in contact with the material. The other member, also in contact with the test material, is constrained by a torsion bar. In the linear

FIGURE 43

SCHEMATIC DIAGRAM OF THE WEISSENBERG RHEOGONIOMETER

After Barry, 1974. (46)

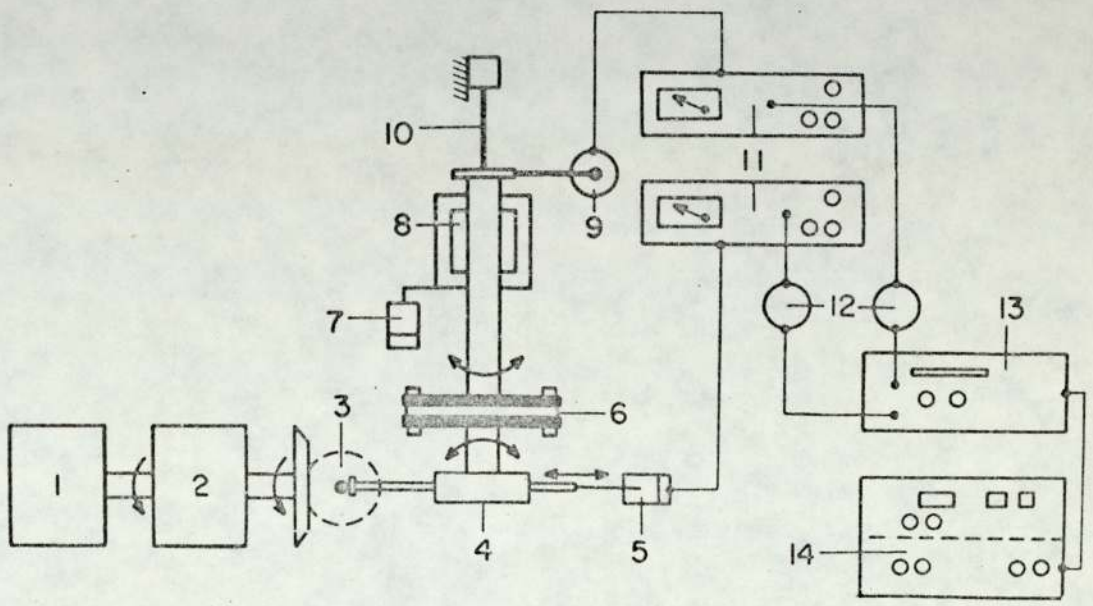

1. Motor;
2. Gear Box;
3. Variable Sine Wave Generator;
4. Worm Screw;
5. Input oscillation (strain) transducer;
6. Platens containing sample;
7. Gap setting transducer;
8. Air bearing;
9. Output oscillation (stress) transducer;
10. Torsion bar;
11. Transducer meters;
12. 1 - KHz matched filters;
13. Mechanical reference synchroniser;
14. Digital transfer function analyser.

viscoelastic region of the test material, the constrained member also oscillates sinusoidally with an amplitude proportional to that of the forced member, but with a phase lag between the waves (Figure 7a). Transducers fitted to the measuring unit will yield information concerning the amplitude and phase characteristics of the output waveform and the input waveform. This information is either recorded with a pen recorder, an ultraviolet recorder or an oscilloscope and evaluated manually, or fed to a Digital Transfer Function Analyser coupled to a Mechanical Reference Synchroniser which will provide a direct digital readout of the amplitude ratio and the phase shift of the two waveforms. These test material characteristics obtained as a function of frequency may then be converted mathematically into standard viscoelastic functions.

(c) Calibration of the Rheogoniometer

(i) The Electronic System

The input and output signals on the Rheogoniometer were measured by displacement transducers F51 and fed to Boulton Paul direct reading transducer meters (type C51). The signals from the meters were then passed via B.P.A. electronics filter units to the DTFA and MRS. The signals were not passed through the Sangamo twin filter networks normally used in oscillatory testing (274).

It was Bogie and Harris (277) who originally pointed out that considerable phase shift between the two transducer circuits may occur and that the attenuation of each circuit may not be identical. They reported that errors may arise due

to these effects in evaluating the mechanical properties of materials and recommended that each instrument be individually analysed for accuracy of results. This view was further substantiated by Davis (278) who found considerable differences in the measured and quoted calibration data and instrument constants.

In this work the electronic system was calibrated in the manner outlined by Davis (278). Tables 16 and 17 give the derived values of phase shifts and the apparatus constants required to convert the ratio of the transducer meter output voltages to amplitude ratio for a range of frequencies. The mean apparatus constant 0.2862 derived using a $^{1}/16$" (0.15875 cm) diameter torsion bar is under one per cent greater than the mean apparatus constant 0.2838 derived using a $\frac{1}{8}$" (0.3175 cm) diameter torsion bar however this slight difference is not thought to be significant. These values are however considerably smaller than the value 0.325 quoted in the instrument manual (279). There is an average fourteen per cent difference between the measured and the quoted instrument constants.

As the amplitude ratio constant is the ratio of the effective radius of the drive shaft worm wheel to the radius of the torque transducer arm, the most likely explanation of the discrepancy in the derived and quoted instrument constant is attributable to the incorrect measurement of either of the above mentioned components (280).

TABLE 16

ELECTRONIC PHASE SHIFTS AND ATTENUATIONS.

Calibration data for Rheogoniometer obtained with 1/16" (0.15875 cm) diameter torsion bar.

(DFTA cut off frequency = 100 Hz).

Frequency (Hertz)	Phase Shift (°)	Amplitude Ratio constant
25.0	0° 10'	0.2866
19.9	- 0° 40'	0.2908
15.8	0° 20'	0.2866
12.6	- 0° 20'	0.2873
10.0	- 0° 10'	0.2857
7.91	- 0° 50'	0.2861
2.5	2° 0'	0.2862
0.791	- 1° 0'	0.2870
0.25	- 1° 10'	0.2871
0.0791	- 1° 30'	0.2871
0.025	- 2° 50'	0.2801
0.00791	- 1° 20'	0.2855
0.0025	- 0° 50'	0.2854
	Average	0.2862

TABLE 17

ELECTRONIC PHASE SHIFTS AND ATTENUATIONS.

Calibration data for Rheogoniometer obtained with ⅛"

(0.3175 cm) diameter torsion bar.

(DFTA cut off frequency = 100 Hz).

Frequency (Hertz)	Phase Shift (°)		Amplitude Ratio constant
25.0	0° 10'		0.2796
7.91	- 2° 0'		0.2796
2.5	- 0° 40'		0.3045
0.791	- 0° 30'		0.2805
0.25	- 0° 5'		0.2818
0.0791	- 0° 35'		0.2793
		Average	0.2838

(ii) Calibration of the Torsion Bars

The torsion bars were calibrated using Newtonian fluids over a range of frequencies, Table 18 and 19. The results, Figures 44 and 45, show the expected changes in the amplitude ratio (υ) and the phase angle (δ) with frequency (N).

For the $^{1}/_{16}$" (0.15875 cm) diameter torsion bar which has a resonant frequency of 10.2Hz, δ approaches -90^{o} phase lag and υ remains small at low frequencies. As the frequency of oscillation however approaches the resonant frequency of the torsion bar, δ approaches 0^{o} and υ increases. Beyond the resonant frequency δ approaches $+90^{o}$ phase lead and υ decreases. Similar plots have been reported by Davis (278) for several Newtonian fluids.

For the $^{1}/_{8}$" (0.3175 cm) diameter torsion bar which has a resonant frequency of 48Hz, δ and υ are simply seen to increase over the 7.91×10^{-2} to 25Hz frequency range studied.

At low frequencies, the double log plot of υ vs N is linear with a slope of approximately 1.00. It is from this part of the plot that the torsion bar constant was determined at each frequency using the following equation due to Harris and Wilkinson (281)

$$\eta = \frac{Bk\upsilon}{2\pi N} \qquad \ldots (76)$$

TABLE 18

VARIATION OF AMPLITUDE RATIO AND PHASE ANGLE WITH FREQUENCY FOR LIQUID PARAFFIN OF VISCOSITY 1.572 POISE AT 25°C DETERMINED USING THE 1/16" (0.15875 CM) DIAMETER TORSION BAR

Frequency (N) Hz	Amplitude Ratio (υ)	Phase Angle (δ) (°)
0.025	2.0×10^{-4}	- 86° 40'
0.0791	5.3×10^{-4}	- 88° 20'
0.25	1.6×10^{-3}	- 89° 50'
0.791	5.1×10^{-3}	- 87° 30'
2.5	1.6×10^{-2}	- 92° 0'
7.91	9.2×10^{-2}	- 82° 0'
10.0	2.0×10^{-1}	- 75° 30'
12.6	5.3×10^{-1}	60° 0'
15.8	1.3×10^{-1}	84° 10'
19.9	7.3×10^{-2}	88° 30'
25.0	4.7×10^{-2}	91° 0'
Gradient-double log plot at low frequency (υ vs N)	0.9887	

TABLE 19

VARIATION OF AMPLITUDE RATIO AND PHASE ANGLE WITH FREQUENCY FOR SILICON OIL OF VISCOSITY 29.1 POISE AT 25°C DETERMINED USING ⅛" (0.3175 CM) DIAMETER TORSION BAR

Frequency (N) Hz	Amplitude Ratio (υ)	Phase Angle (δ) (°)
0.0791	7.5×10^{-4}	- 91° 10'
0.25	2.3×10^{-3}	- 87° 30'
0.791	7.3×10^{-3}	- 89° 20'
2.5	2.2×10^{-2}	- 87° 40'
7.91	7.4×10^{-2}	- 84° 40'
25.0	3.1×10^{-1}	- 69° 10'
Gradient - double log plot at low frequency (υ vs N)	0.9938	

FIGURE 44

CALIBRATION OF 1/16" (0.15875cm) AND ⅛" (0.3175cm) DIAMETER TORSION BARS USING LIQUID PARAFFIN AND SILICON OIL RESPECTIVELY

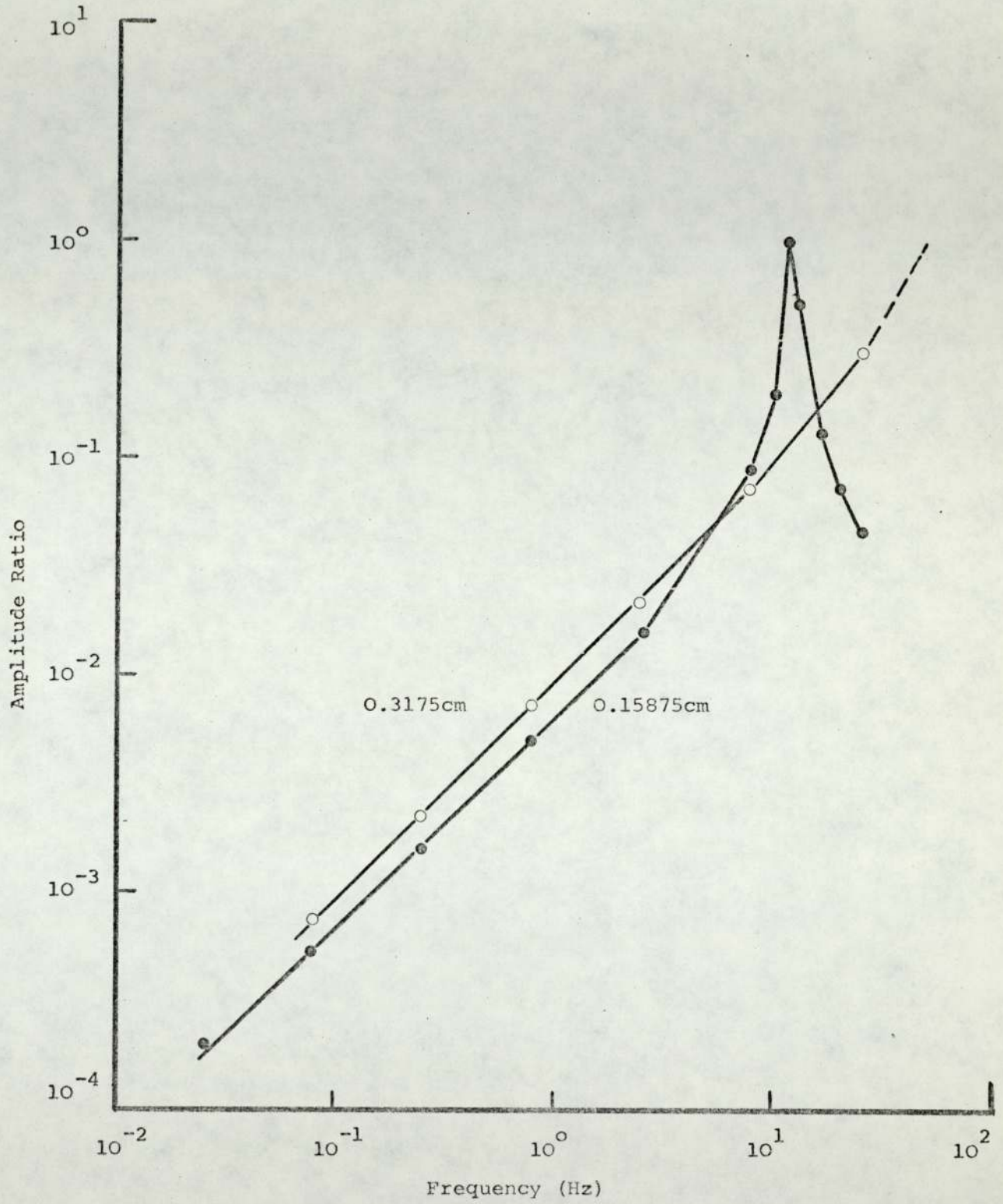

FIGURE 45

CALIBRATION OF 1/16" (0.15875cm) AND ⅛" (0.3175cm) DIAMETER TORSION BARS USING LIQUID PARAFFIN AND SILICON OIL RESPECTIVELY

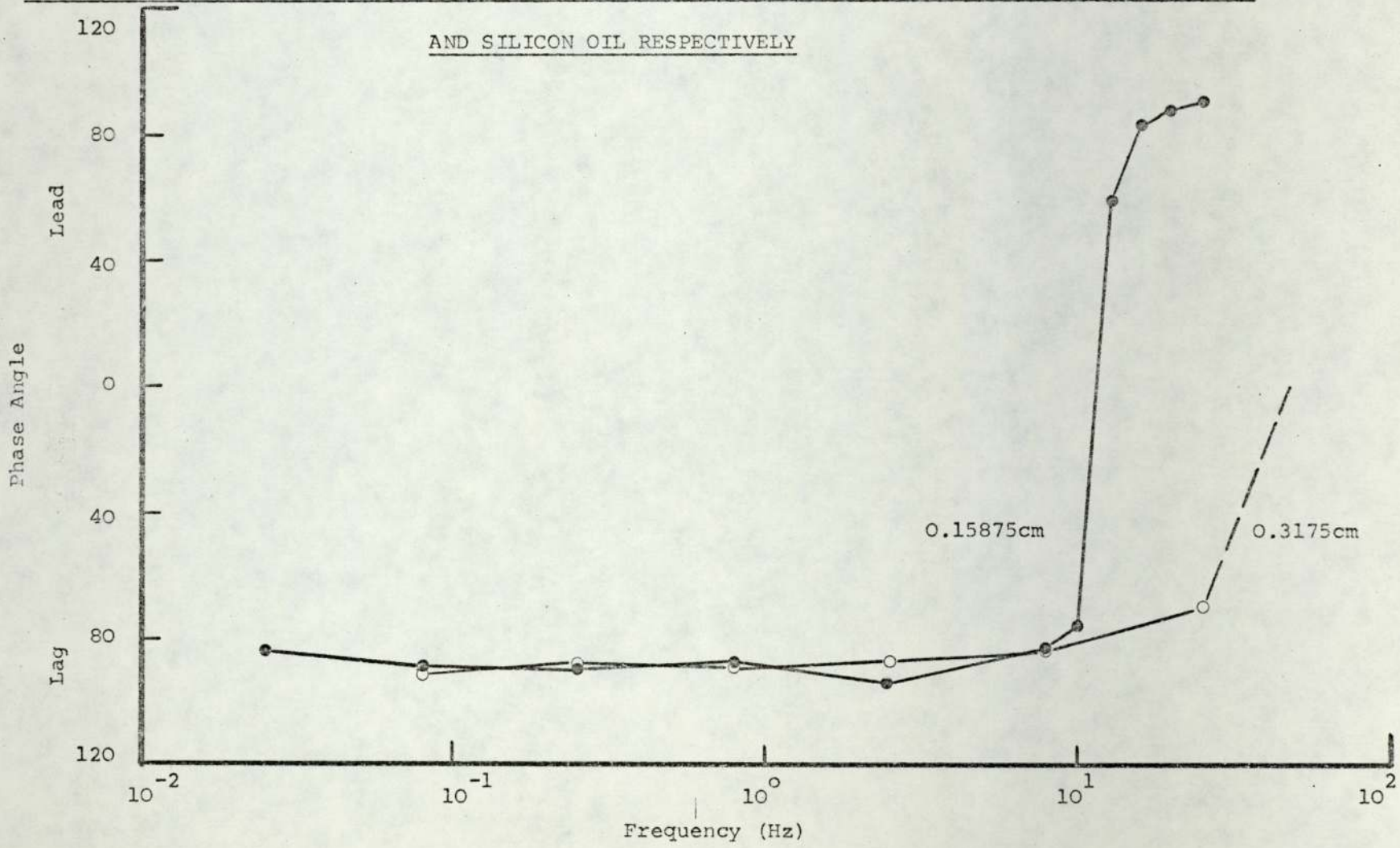

where $B = 2h/\pi R^4$, h being the gap thickness (0.06096 cm), R the plate radius (3.75 cm) and K the torsion bar constant.

The average torsional constant for the $^1/16$" (0.15875 cm) diameter torsion bar was thus determined to be 7.76×10^6 dyne cm rad.$^{-1}$ (0.776 Nm rad.$^{-1}$). This value was found to be $\approx$ 15% smaller than the value 8.91×10^6 dyne cm rad.$^{-1}$ (0.891 Nm rad.$^{-1}$) quoted by the manufacturer. With the $\frac{1}{8}$" (0.3175 cm) diamter torsion bar the average torsional constant was determined to be 1.0564×10^8 dyne cm rad.$^{-1}$ (10.564 Nm rad.$^{-1}$) and the quoted constant was 1.3041×10^8 dyne cm rad.$^{-1}$ (13.041 Nm rad.$^{-1}$), a difference of 23%.

It has been suggested that the discrepancies observed in the derived and quoted torsion bar constants arise as a result of a substantial twist in the drive shaft, between the wheel and the lower plate, and in the upper plate shaft, between the plate and the transducer arm (280). These observed discrepancies further emphasise the need for the individual calibration of the instrument.

(d) Derivation of Standard Viscoelastic Functions

The raw data in terms of amplitude ratio and phase angle obtained from a dynamic study may be used as such to characterise a system however the conversion of this data to standard viscoelastic functions is usually more satisfactory. For a parallel plate rheogomometer geometry, Walters (64) has derived the following equations:-

$$S = \frac{2}{\pi R^4 h \rho}\left(\frac{K}{4\pi^2 N^2} - I\right)$$

... (77)

$$\eta' = \frac{-2\pi N \rho S h^2 \upsilon \sin\delta}{(\upsilon^2 - 2\upsilon\cos\delta + 1)}$$

... (78)

$$G' = \frac{4\pi^2 N^2 S h^2 \rho \upsilon(\cos\delta - \upsilon)}{(\upsilon^2 - 2\upsilon\cos\delta + 1)}$$

... (79)

where S = shear stress parameter

K = torsion bar constant

I = the moment of inertia of the constrained member about its axis

R = radius of the plates

h = gap thickness

N = frequency of oscillation

η' = real dynamic viscosity

ρ = density of sample

υ = amplitude ratio

δ = phase angle

G' = storage modulus

The two standard viscoelastic functions η' and G' were thus calculated using the above equations. From these two functions and employing Equations (32), (37), (38), (42) and (43), the other dynamic viscoelastic functions namely G'' , J' , J'' , η'' and

tan δ were evaluated.

A computer programme in ALGOL for I.C.L. 1904S computer was written in order to execute all the above calculations. This programme has been included in the Appendix.

(e) Interconversion of Creep Data to Dynamic Data

The theory of linear viscoelasticity allows the interconversion of creep and dynamic data by application of linear integral transformations (282). The application of these transformations to experimental data is often difficult and tedious, and thus various approximation procedures have been proposed for this purpose (56, 282, 283, 284). Schwarzl (282) has derived a number of formulae of increasing complexity but decreasing relative error, based on a simple numerical approximation, for the interconversion of creep compliance to storage and loss compliances. The calculation in these formulas is based upon values of creep compliance J(t), at times which are equally spaced on a logarithmic time scale; the ratio between two successive times being a factor of two. Avoiding the infinite series, the following two formulas are the most accurate though complex for the calculation of storage (J') and loss (J'') for compliances respectively.

$$J'(\omega) \sim J(t) - 0.000715\{J(32t) - J(16t)\} - 0.0185 \{J(16t) - J(8t)\} + 0.197\{J(8t) - J(4t)\} - 0.778 \{J(4t) - J(2t)\} - 0.181\{J(t) - J(t/2)\} - 0.049\{J(t/4) - J(t/8)\} \quad \ldots (80)$$

$$J''(\omega) \sim -0.470\{J(4t) - J(2t)\} + 1.674\{J(2t) - J(t)\}$$
$$+ 0.198\{J(t) - J(t/2)\} + 0.620\{J(t/2) - J(t/4)\}$$
$$+ 0.012\{J(t/4) - J(t/8)\} + 0.172\{J(t/8) - J(t/16)\}$$
$$+ 0.043\{J(t/32) - J(t/64)\} + 0.012\{J(t/128) - J(t/256)\}$$

... (81)

where ω (rad sec^{-1}) = 1/t secs.

The two formulae listed above were used in this work for the numerical calculation of storage and loss compliances from creep compliance data. The values of J(t) required in the calculations could have been read directly from the experimental creep curves however this is a tedious procedure. As the discrete spectral data were available for the creep curves, a computer programme was written in ALGOL for the I.C.L. 1904S computer, which used the discrete spectral information to compute the values of compliances, J(xt), and thus evaluate $J'(\omega)$ and $J''(\omega)$ corresponding to various times. The programme written was also devised to evaluate the other dynamic viscoelastic functions namely G', G'', η', η'' and $\tan \delta$ employing Equations (32), (39), (40), (42) and (43). The inter-converted data was subsequently unified with the experimentally derived dynamic data.

4.3.2 Procedure employed in the Dynamic Testing of Plastibases

The Weissenberg Rheogoniometer employed in this study has been described in Section 4.3.1 (a). All tests were carried out in the following manner at 25 $\pm$ 0.5°C.

Each sample was loaded on to the lower plate and after a short period of equilibration, the upper plate was lowered into position and excess sample was removed. The plate gap was set at 0.0635 cm on each occasion using a displacement transducer connected to a digital voltmeter calibrated to display gap width directly. Each grade of Plastibase was tested initially for linearity by increasing the amplitude of oscillation at representative experimental frequencies. The amplitude ratio and phase shifts were determined at each frequency. Departure from linearity was indicated by an abrupt change in these values. The Plastibases were subsequently examined in their linear viscoelastic region by applying a sinusoidally varying shear strain at frequencies ranging from 2.5×10^{-3} to 25Hz. The amplitude ratio and the phase shift were determined at each frequency and converted to standard viscoelastic functions.

4.4 Results

Plastibase 20W, 10W and 5W exhibited linear viscoelastic behaviour for small amplitudes and a 0.0635 cm plate gap when examined with the Rheogomometer assembled with a $^{1}/16$" diameter torsion bar. With this assembly however, Plastibase 30W and 50W, even at low frequencies, yielded very small ($> 1^{o}$) phase angles demonstrating a rigid solid type behaviour. This difficulty could have been resolved by increasing the gap between the plates however Warburton and Davis (274) have advised against adopting this procedure. Thus in order to complete the characterisation of all Plastibases, the Rheogomometer was next assembled with a $\frac{1}{8}$" diameter torsion bar and all Plastibases were retested.

Figures 46 and 47 show the change in storage modulus G' and real viscosity η' with frequency, determined using $^1/16$" diameter torsion bar, for Plastibase 20W, 10W and 5W. Figures 48 to 54 show plots of storage and loss modulus G' and G'', storage and loss compliance J' and J'', real and imaginary components of viscosity η' and η'' and the loss tangent tan δ versus frequency derived using $\frac{1}{8}$" diameter torsion bar for the five grades of Plastibase. All dynamic viscoelastic functions derived are tabulated in the Appendix. Figures 48 and 52 also include plots of G' and η' versus frequency for the five dilutions of Plastibase 50W. The discussion of the plots of the diluted Plastibase 50W is included in Section 5.3. Figure 55 shows transformed creep data unified with experimental dynamic data for Plastibase 50W and 30W. The transformed data are plotted over a frequency range 10^{-8} to 10^{-2} and the experimental data are plotted over a frequency range 10^{-3} to 10^{2}. G', G'', J', J'', η', η'' and tan δ obtained by transforming creep data are included in the Appendix. The relationship between log η', log G' and percent polyethylene in the gels is shown in Figures 56 and 57. The interbatch variation within a single grade of Plastibase 50W is shown in Figure 58.

4.5 Discussion

Plastibase 20W, 10W and 5W show a characteristic change in the storage modulus G' and the real viscosity η', determined using the Rheogoniometer fitted with the $^1/16$" torsion bar, with frequency, Figures 46 and 47. At low frequencies the dynamic viscosity is high but falls more or less monotonically with an increase in the frequency of oscillation. The storage modulus exhibits a very slight gradual increase with an increase in the frequency of oscillation. In the proximity of

FIGURE 46

VARIATION IN STORAGE MODULUS WITH FREQUENCY DETERMINED FOR THREE GRADES OF PLASTIBASE USING THE 1/16" (0.15875cm) DIAMETER TORSION BAR IN THE RHEOGONIOMETER ASSEMBLY

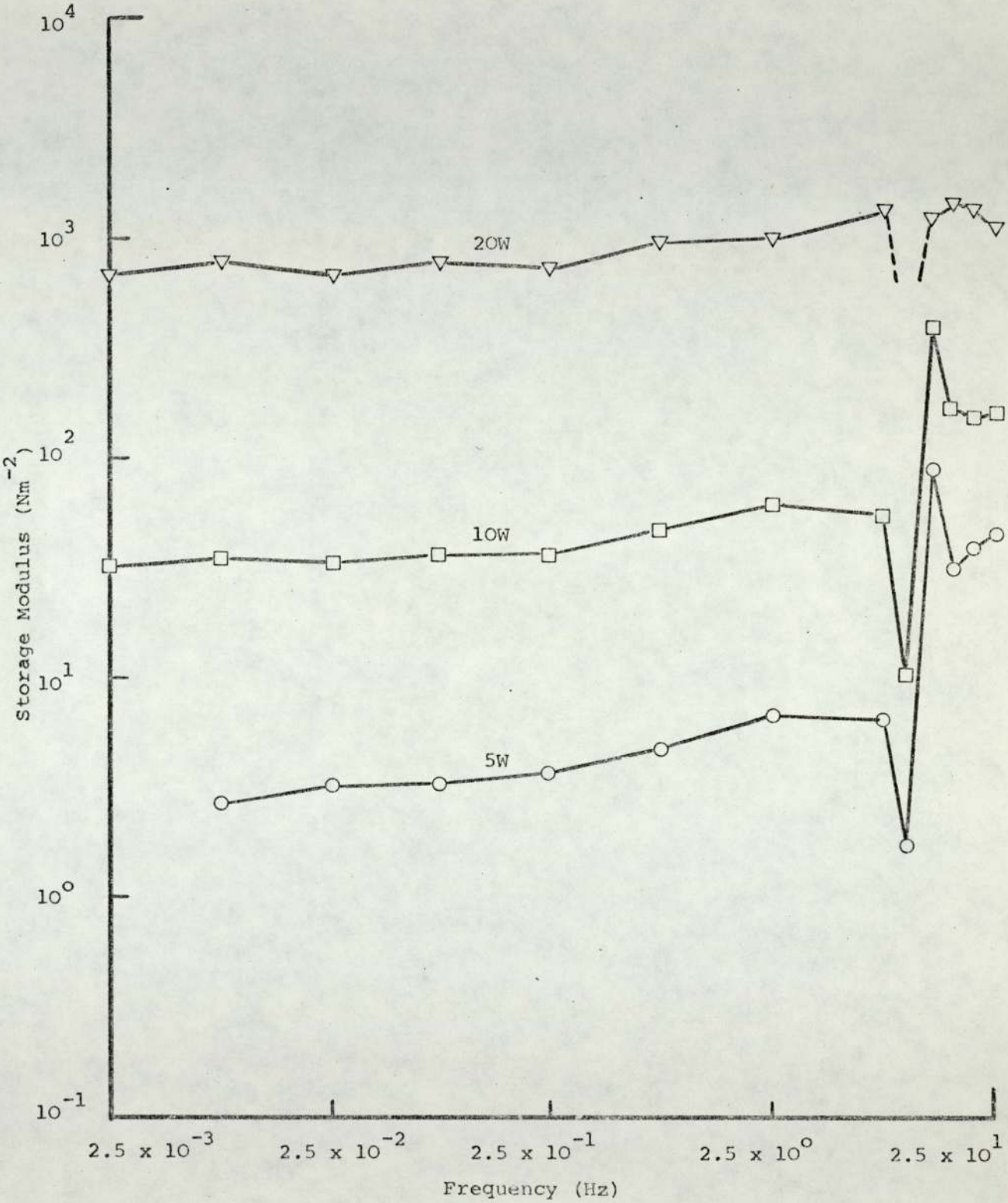

FIGURE 47

VARIATION IN DYNAMIC VISCOSITY WITH FREQUENCY DETERMINED FOR THREE GRADES OF PLASTIBASE AND LIQUID PARAFFIN USING THE 1/16" (0.15875) DIAMETER TORSION BAR IN THE RHEOGONIOMETER ASSEMBLY

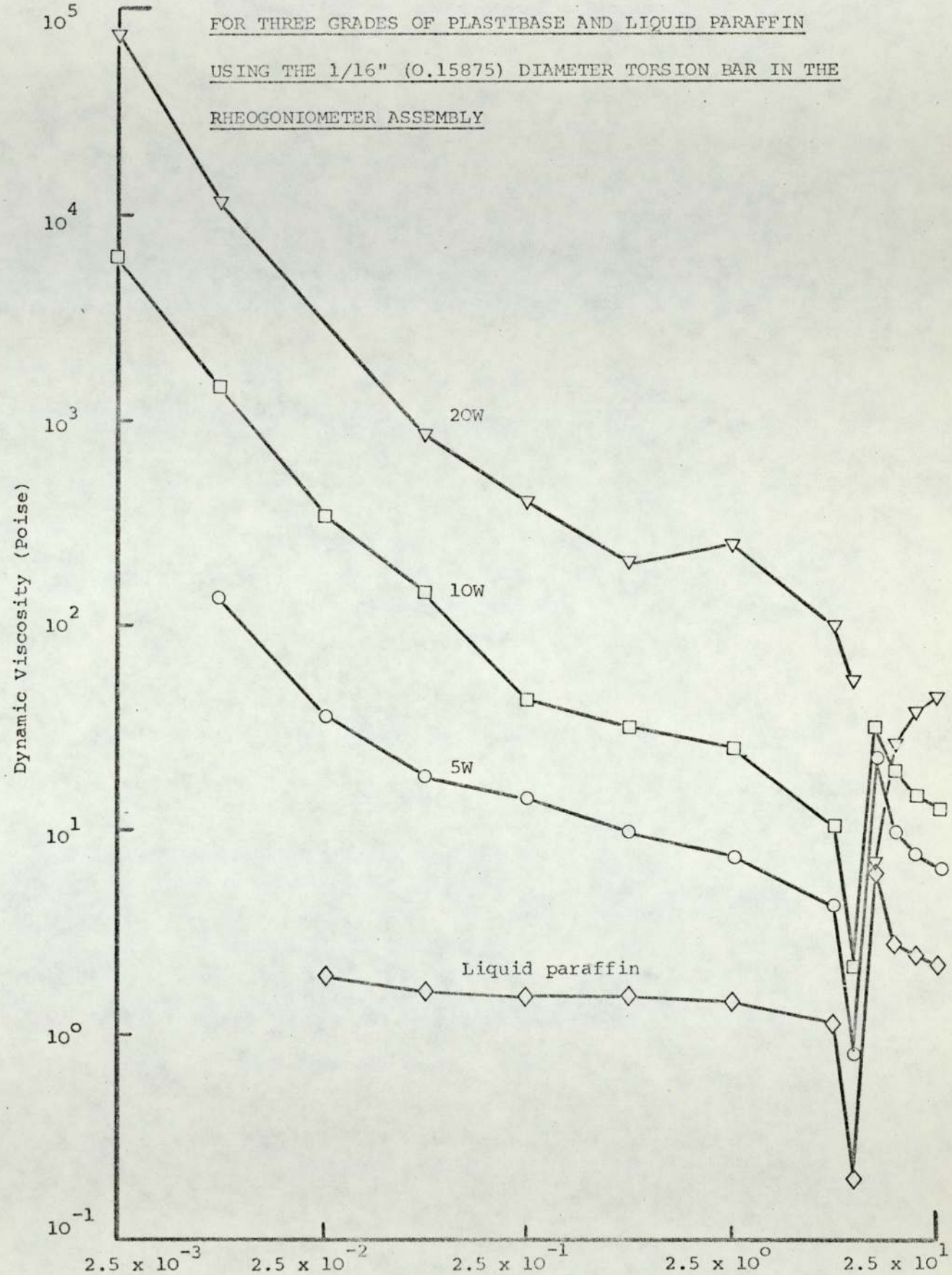

FIGURE 48

VARIATION IN STORAGE MODULUS WITH FREQUENCY DETERMINED FOR PLASTIBASES USING THE ⅛" (0.3175cm) DIAMETER TORSION BAR

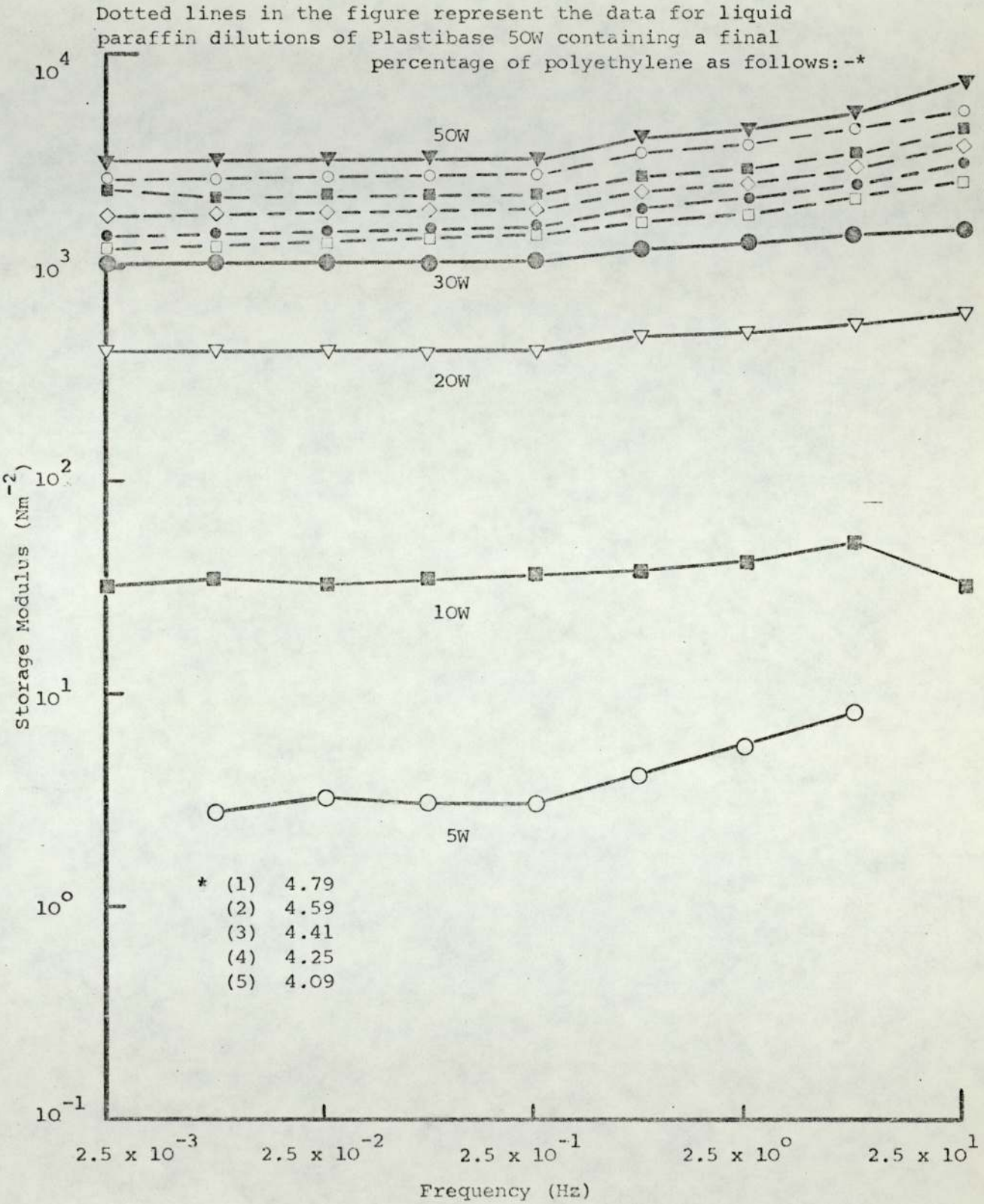

FIGURE 49

VARIATION IN LOSS MODULUS WITH FREQUENCY DETERMINED FOR PLASTIBASES USING THE ⅛" (0.3175cm) DIAMETER TORSION BAR IN THE RHEOGONIOMETER ASSEMBLY

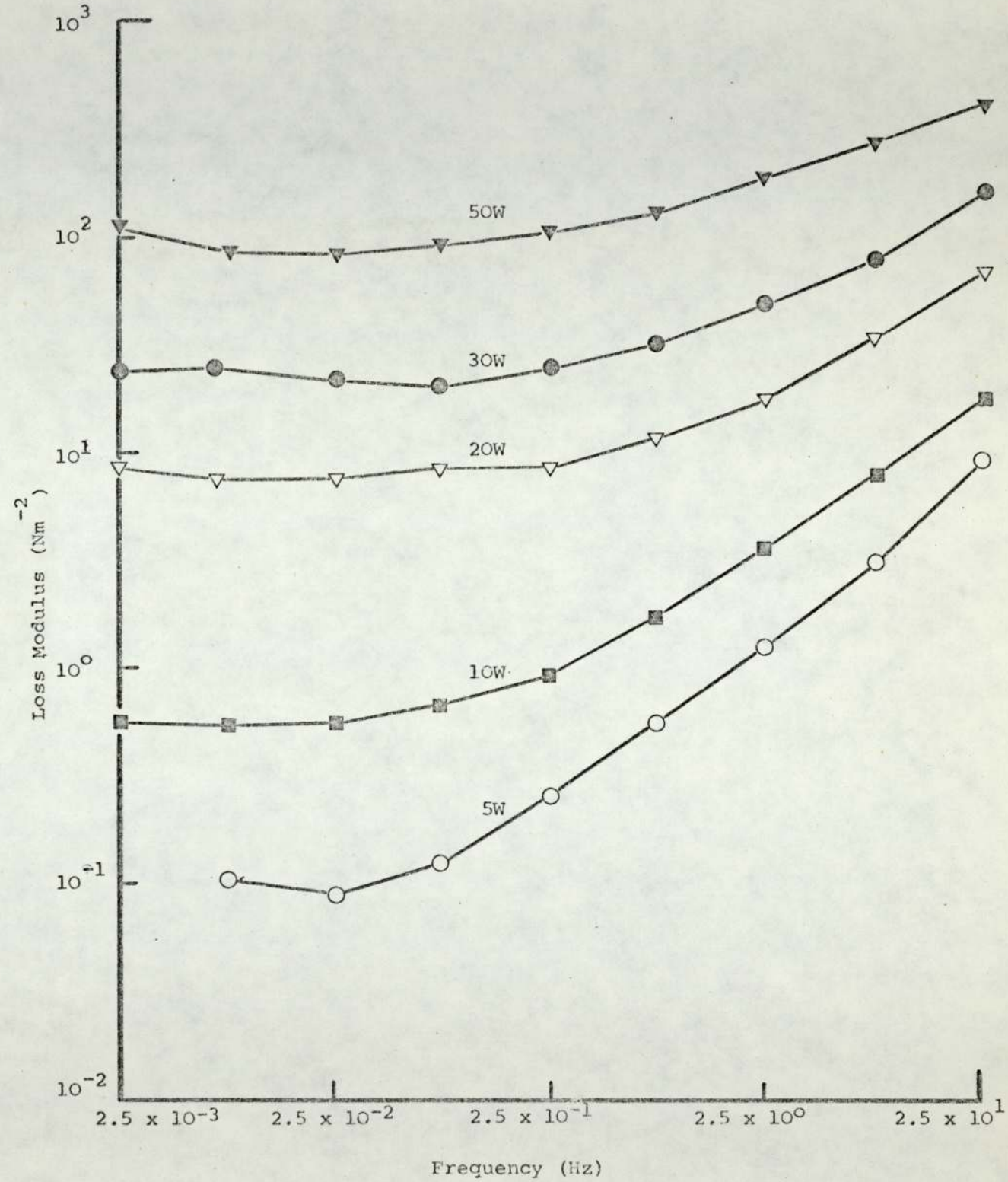

FIGURE 50

VARIATION IN STORAGE COMPLIANCE WITH FREQUENCY DETERMINED FOR PLASTIBASES USING THE ⅛" (0.3175cm) DIAMETER TORSION BAR IN THE RHEOGONIOMETER ASSEBLY

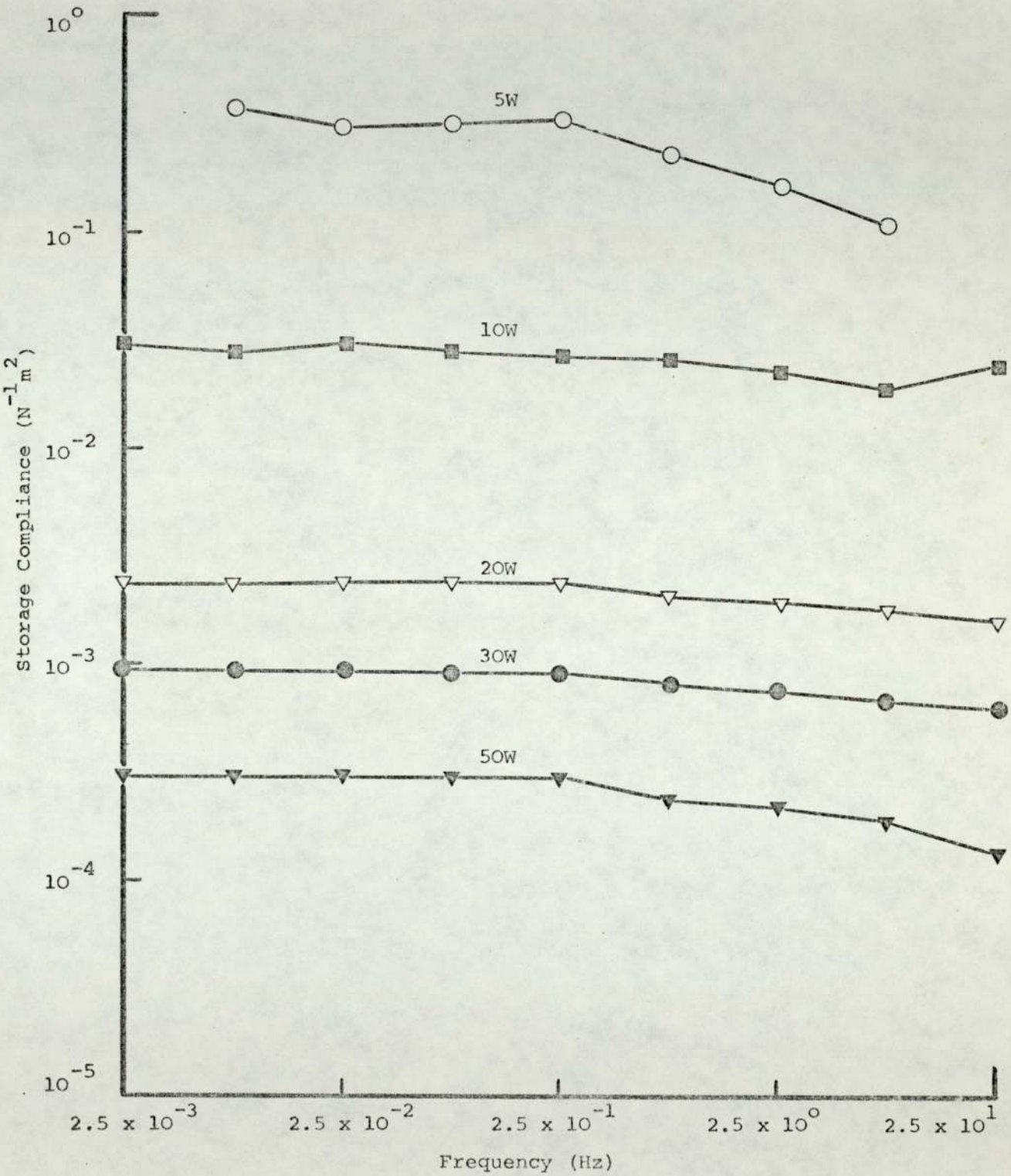

FIGURE 51

VARIATION IN LOSS COMPLIANCE WITH FREQUENCY DETERMINED FOR PLASTIBASES USING THE ⅛" (0.3175cm) DIAMETER TORSION BAR IN THE RHEOGONIOMETER ASSEMBLY

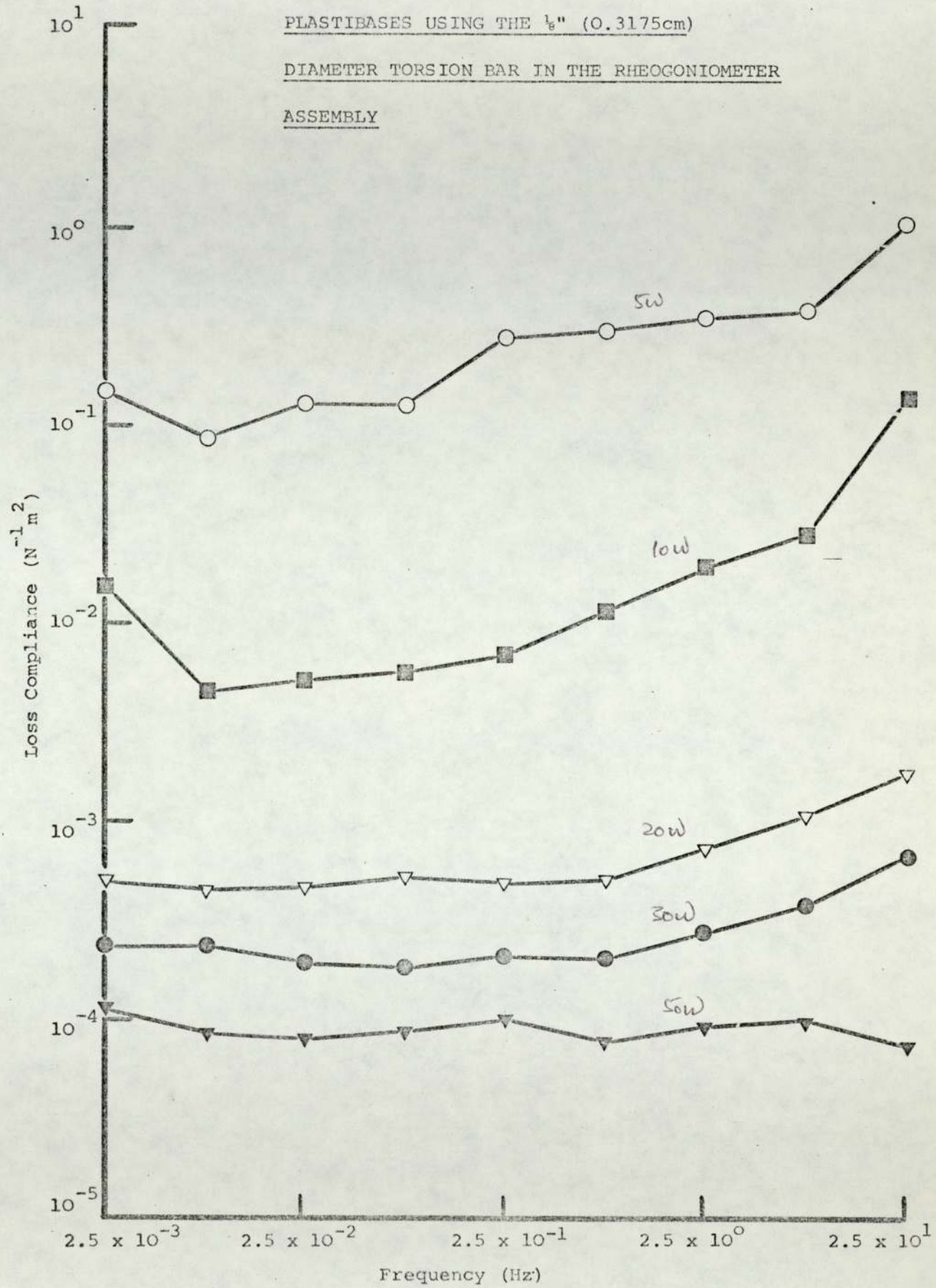

FIGURE 52

VARIATION IN DYNAMIC VISCOSITY WITH FREQUENCY DETERMINED FOR PLASTIBASES USING THE ⅛" (0.3175cm) DIAMETER TORSION BAR IN THE RHEOGONIOMETER ASSEMBLY

Dotted lines represent the data (as in Figure 48) for liquid paraffin dilutions of Plastibase 50W

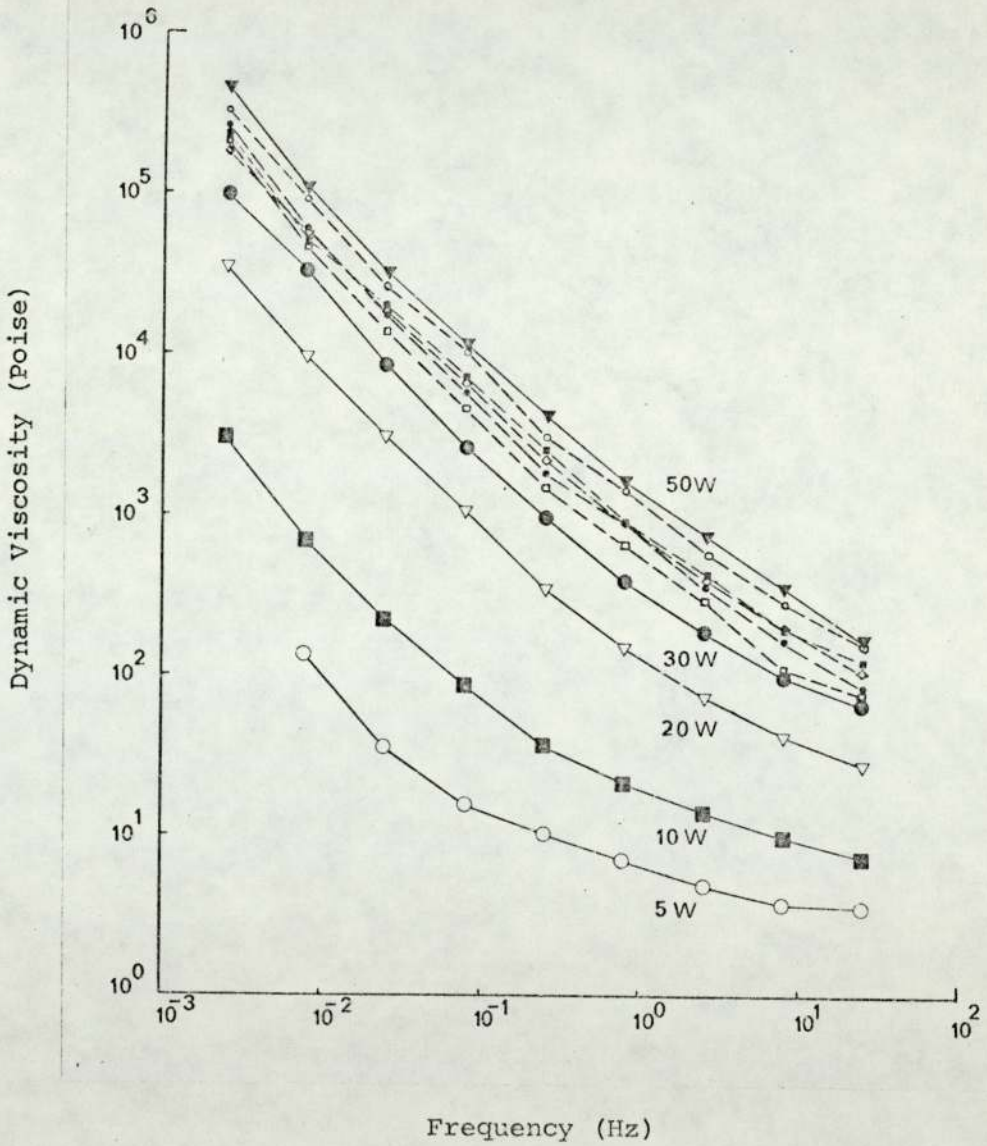

FIGURE 53

VARIATION IN THE IMAGINARY COMPONENT OF VISCOSITY WITH FREQUENCY DETERMINED FOR PLASTIBASES USING THE ⅛" (0.3175cm) DIAMETER TORSION BAR IN THE RHEOGONIOMETER ASSEMBLY

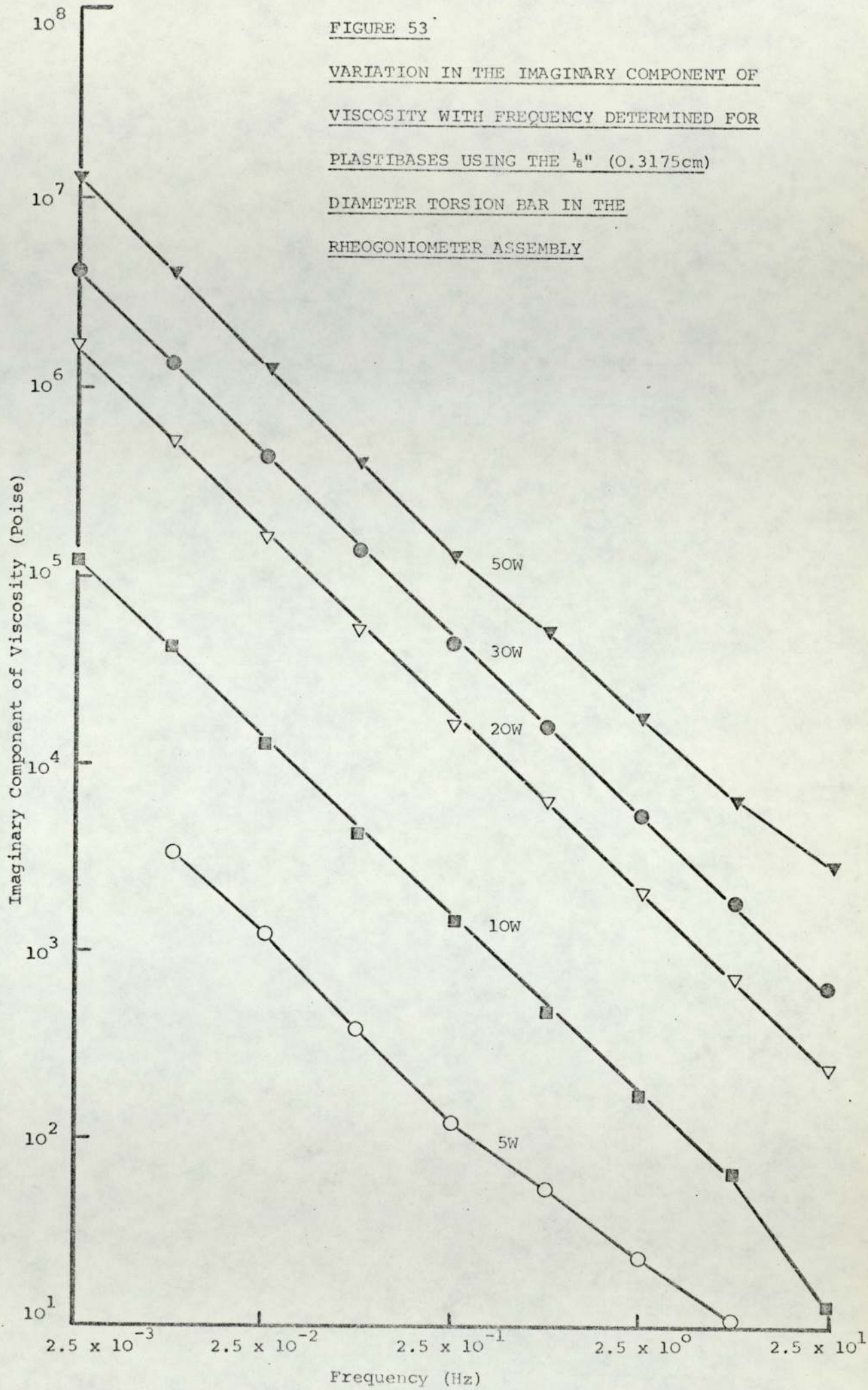

FIGURE 54

VARIATION IN LOSS TANGENT WITH FREQUENCY DETERMINED FOR PLASTIBASES USING THE ⅛" (0.3175cm) DIAMETER TORSION BAR IN THE RHEOGONIOMETER ASSEMBLY

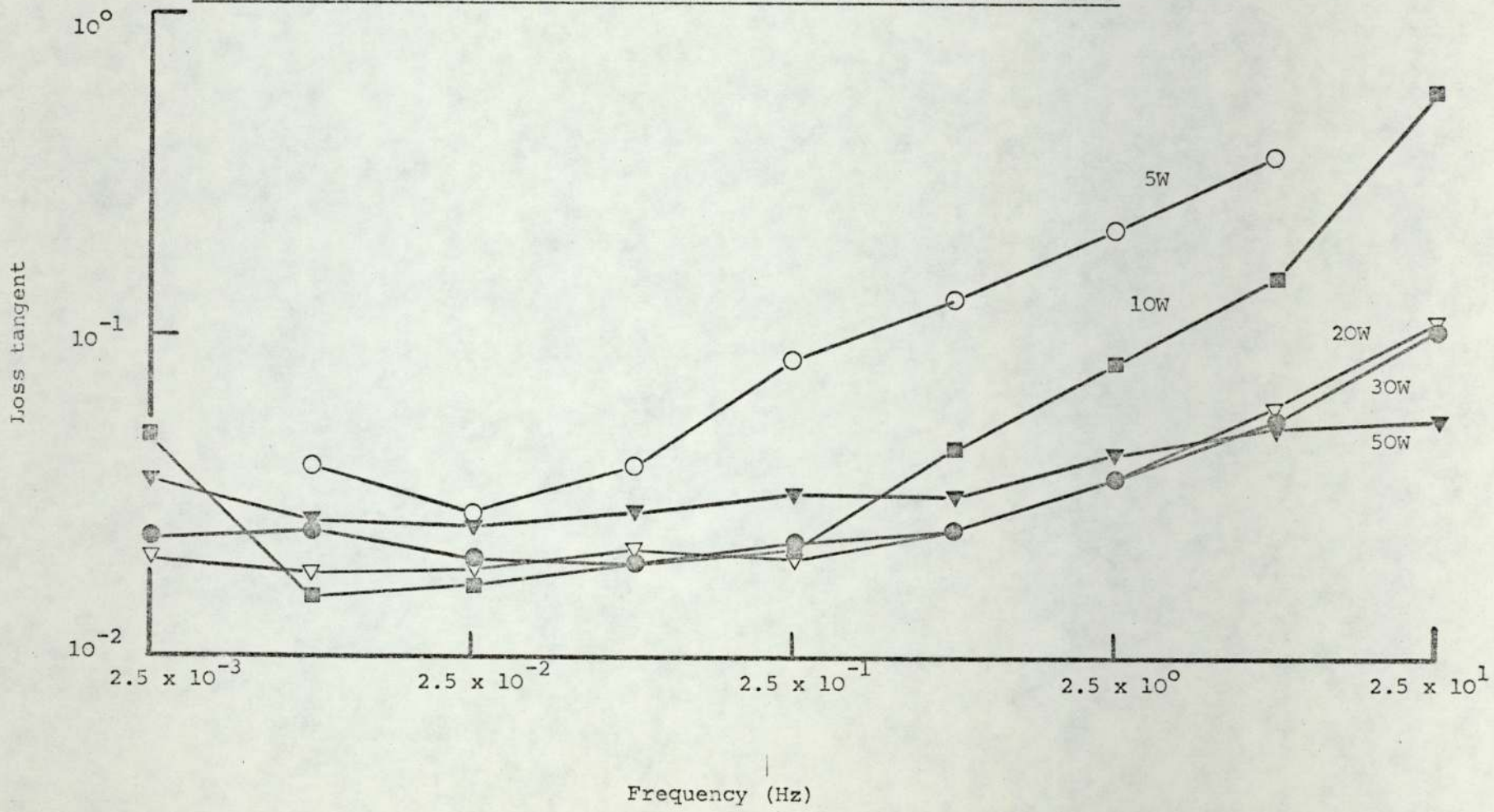

FIGURE 55

UNIFICATION OF DYNAMIC AND TRANSFORMED CREEP DATA FOR PLASTIBASE 50W AND 30W

Shaded points represent dynamic data and open points represent transformed creep data. Broken lines indicate the position of dynamic data derived for the lower consistency Plastibase by the extrapolation method.

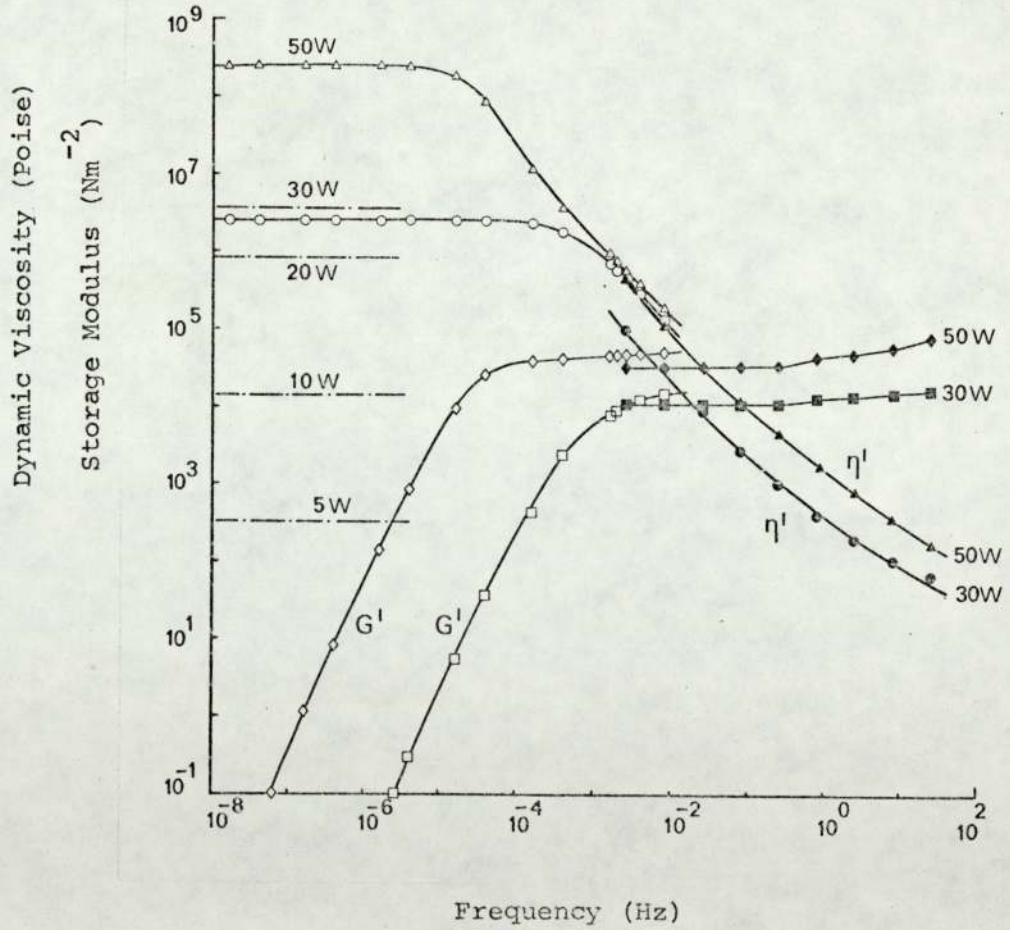

FIGURE 56

VARIATIONS IN DYNAMIC VISCOSITY (DERIVED OVER A RANGE OF FREQUENCIES) WITH INCREASE IN THE PERCENTAGE OF POLYETHYLENE

Broken line shows the extrapolated plot at 2.5×10^{-8} Hz frequency

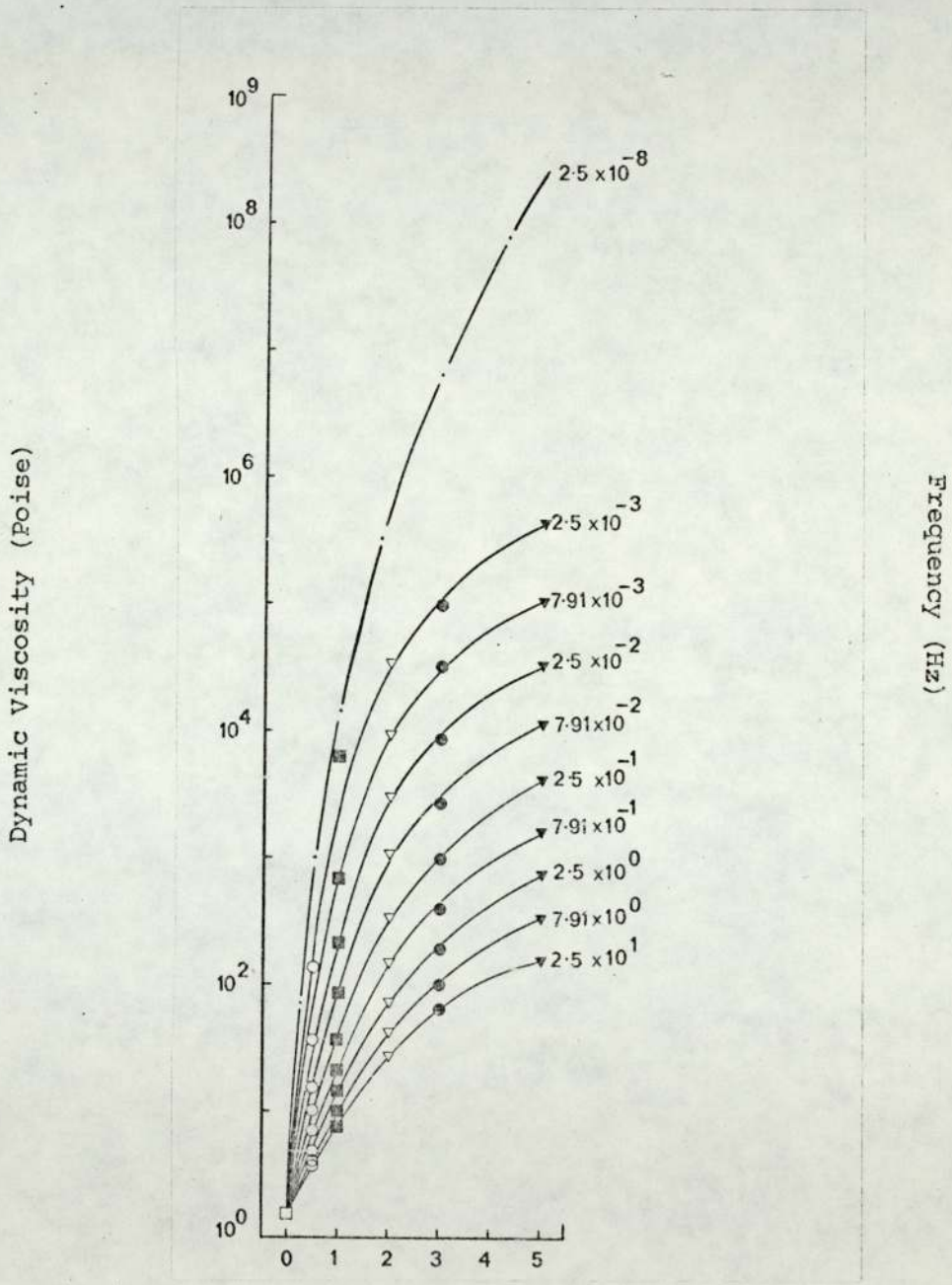

FIGURE 57

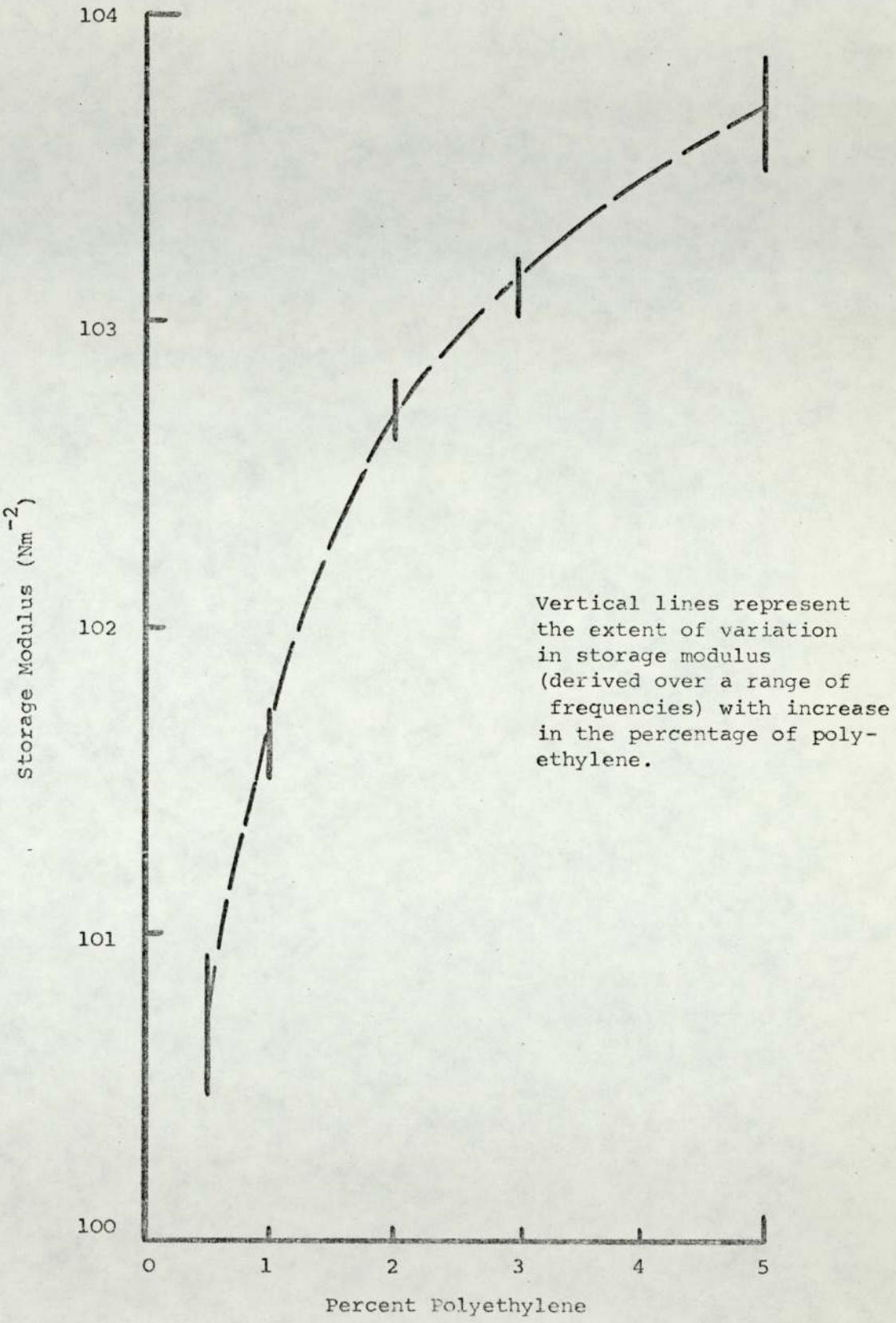
104
103
102
101
100
Storage Modulus (Nm^{-2})
0
1
2
3
4
5
Percent Polyethylene
Vertical lines represent the extent of variation in storage modulus (derived over a range of frequencies) with increase in the percentage of polyethylene.

FIGURE 58

PLOTS SHOWING THE BATCH TO BATCH VARIATION LIMITS

FOUND IN THIS WORK FOR PLASTIBASE 50W

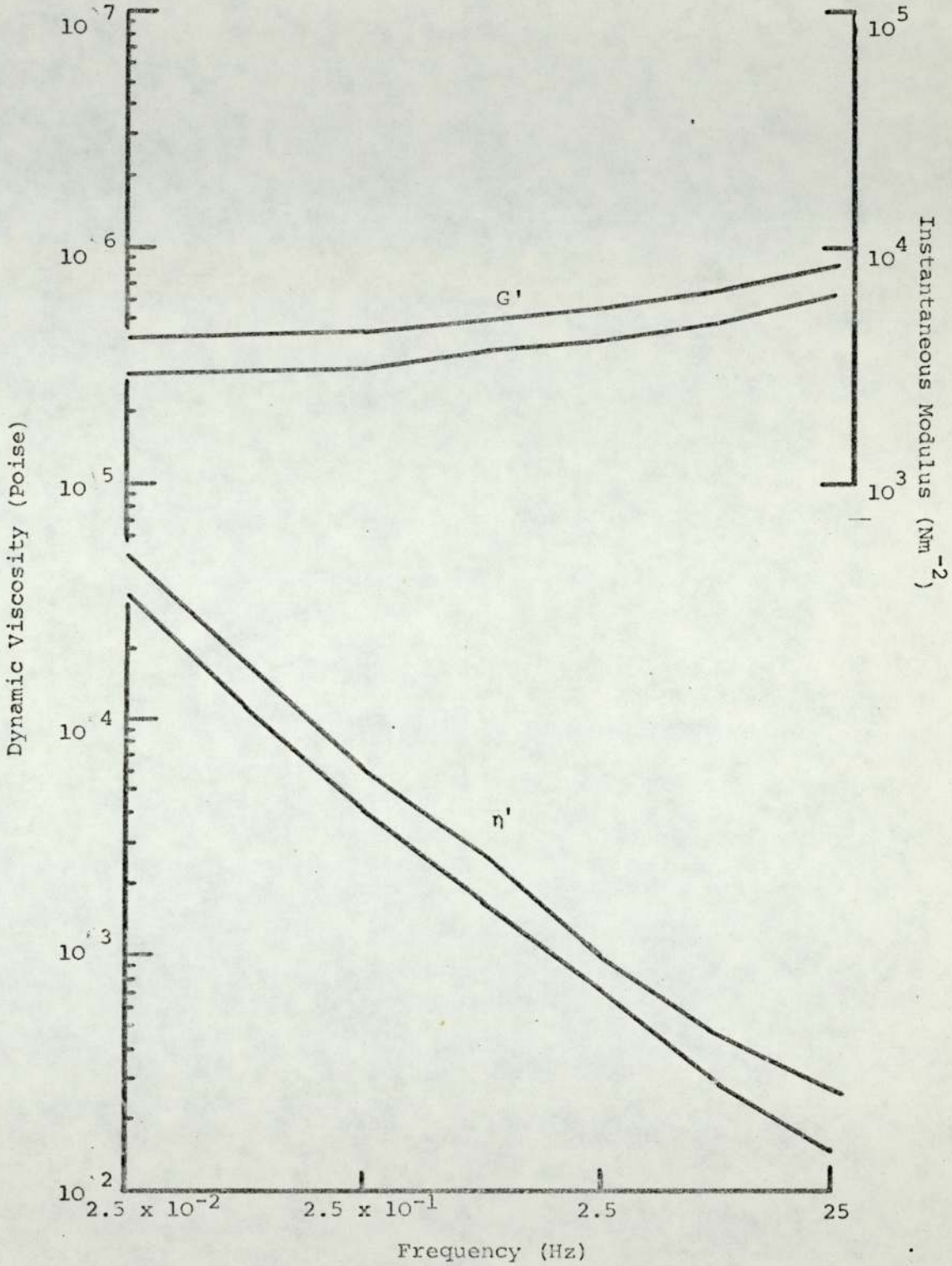

the resonant frequency of the torsion bar (10.2Hz), the amplitude ratio approaches unity and the phase angle passes through zero. This phenomena is characterised by a discontinuity in the η', G' vs frequency plots. Jones and Walters (285) have postulated that it is the magnification of small experimental errors at frequencies close to resonance that leads to this anomalous behaviour and as such it can be discounted. In the experiments using a ⅛" diameter torsion bar which had a resonance frequency of 48Hz, no anomaly in the behaviour of the samples was evident over the frequency range tested. It must be noted however that at low frequencies, both the 1/16" diameter and the ⅛" diameter torsion bars yielded essentially similar viscoelastic parameters.

All the five grades of Plastibase exhibited linear viscoelastic behaviour over the frequency range tested. The viscoelastic parameters derived for the five Plastibases were plotted against frequency to determine the characteristic behaviour of these bases in dynamic experiments, Figures 48 to 54.

In sinusoidally oscillating deformations, the storage modulus G' is a measure of the energy stored and recovered per cycle and the loss modulus G'' is a measure of the energy dissipated or lost as heat per cycle (57). The plots of G' verses frequency for all Plastibases are essentially similar and placed in ascending order of Plastibase with increasing percentage of polyethylene throughout the measured frequency range, Figure 48. G'' verses frequency plots also follow a similar ascending pattern, Figure 49. The storage modulus G' verses frequency plots show a very small gradual increase in G' with an increase in frequency for all the Plastibases. This reflects a largely elastic

behaviour with a comparatively small dissipation of energy. Thus the G'' plots in the measured frequency range are lower than the G' plots. At high frequencies, elastic behaviour should predominate as there is little time available for viscous deformation and G'' should approach zero however in practice this situation is seldom achieved (57).

The storage compliance J' is defined as a measure of the energy stored and recovered per cycle of sinusoidal deformation and the loss compliance J'' is defined as a measure of the energy dissipated or lost as heat per cycle of sinusoidal deformation (57). The plots of J' verses frequency over a range of measured frequencies for all the five Plastibases are essentially similar and placed in the ascending order of decreasing concentration of polyethylene in the Plastibase, Figure 50. The J'' verses frequency plots also follow a similar ascending pattern, Figure 51. At low frequencies, viscous behaviour becomes increasingly prominent and this is characterised by a small increase in J' with a reduction in frequency. At higher frequencies, increasing elastic predominance is reflected in a drop in J'. The J'' verses frequency plots exhibit several small, broad maxima which are thought to be associated with the configurational re-arrangements of the network structure of the Plastibases.

The real and imaginary parts of the complex dynamic viscosity η^* , η' and η'' respectively, Figures 52 and 53, decreased monotonically with an increase in frequency of oscillation. The plots of η' verses frequency are of particular interest as at very low frequencies η' approaches η_b the residual Newtonian viscosity derived from creep studies (57). At high frequencies, the predominant elastic

behaviour is reflected in the low η' values.

The loss tangent tan δ is a dimensionless parameter and is defined as a measure of the ratio of energy lost to energy stored in a cyclic deformation (G''/G' or J' /J'', (57)). This parameter is of considerable practical interest as it provides a comparative measure of both the elastic and viscous contributions and Davis (286) has referred to plots of tan δ versus frequency as being the 'consistency spectra'. In this work, plots of tan δ verses frequency, Figure 54, exhibit a steep rise in tan δ at higher frequencies and several small broad maxima in the intermediate and low frequency range associated possibly with retardation mechanisms.

Comparison of the plots of the viscoelastic functions, Figures 48 to 54, with published data (57) yields an interesting insight into the structure of Plastibases. It appears that the behaviour of Plastibases resembles very closely that of a very lightly cross-linked amorphous polymer with a molecular weight between cross-linking points of about 23,000. This observation is largely based on the tan δ verses frequency plot, Figure 54, which shows that tan δ attains an extremely small value at low frequencies, of the order of 0.01 and exhibits a small maximum in the low frequency range associated with losses involved in entanglement slippage. The resemblence in the behaviour of Plastibase with that of a lightly cross-linked polymer is also evident from the remarkable similarity in the J', J'', G', G'', η' , η'' vs frequency for the two systems. No cross-linking is involved in the Plastibase systems and this is confirmed from the residual Newtonian viscosity obtained in creep experiments on the material indicating that Plastibase is behaving as a viscoelastic liquid. It

would seem however that the quenching process in the production of Plastibases imposes a rigidity of structure which is analogous to the rigidity imposed by the formation of cross-links in a polymer. This finding is consistent with the report that crystallites in polyethylene serve as extensive pseudo-cross-linking regions (287) and also offers an explanation for the high degree of elasticity exhibited by the Plastibases.

The unification of creep and dynamic data for Plastibase 50W and 30W is shown in Figure 55. In general, there is good agreement between experimentally determined dynamic data and that derived from creep data using the Schwarzl transformations. It would appear from an upward shift in the transformed viscoelastic parameters, Table 20, that the samples tested by the creep method were of a somewhat higher consistency than those tested under dynamic conditions. As materials of the same batch had been used for both tests, it is proposed that the apparent differences in the consistencies measured are largely a function of the method of testing and the approximations in the transformation (288). The unified plots for η' and G' versus frequency show that at high frequencies, η' falls monotonically and G' exhibits a plateau effect. At low frequencies, as expected η' levels off at a high value and approaches η_o the residual Newtonian viscosity determined from creep tests. G' on the other hand falls rapidly at low frequencies and viscoelastic theory predicts that for an uncross-linked polymer, the G' plot should approach a slope of 2.0 on a double logarithmic scale (57). The data included in Table 20 shows that there is good agreement between the theoretical value of the slope and that determined experimentally. Unification of creep and dynamic data is thus seen to allow a compilation of rheological properties of the material over a wide frequency or time

TABLE 20

COMPARISON OF VISCOELASTIC DATA DERIVED AT 25°C

FUNCTION	PLASTIBASE 50W	PLASTIBASE 30W
G' (Dynamic) at 2.5×10^{-3} Hz in Nm^{-2}	3.18×10^{3}	1.04×10^{3}
G' (Creep transformed) at 2.5×10^{-3} Hz in Nm^{-2}	4.64×10^{3}	1.01×10^{3}
η' (Dynamic) at 2.5×10^{-3} Hz in Poise	4.49×10^{5}	9.87×10^{4}
η' (Creep transformed) at 2.5×10^{-3} Hz in Poise	5.55×10^{5}	4.28×10^{5}
η_o (Creep) at $(1/2 \times 3.142 \times 2.5 \times 10^{-8})$ sec in Poise	2.53×10^{8}	2.56×10^{6}
η' (Creep transformed) at 2.5×10^{-8} Hz in Poise	2.46×10^{8}	2.49×10^{6}
Slope of G' plots at low frequencies (theoretical value = $2.0 Nm^{-2}Hz^{-1}$)	2.19	2.12

scale.

While it was possible to collate creep and dynamic data for Plastibase 50W and 30W, this could not be done for Plastibase 20W, 10W and 5W as experimental difficulties had prevented creep analysis of these vehicles. Dynamic tests could not be performed on these vehicles at low frequencies due to the limiations of the Rheogoniometer and the Transfer Function Analyser. In order however to derive rheological data at low frequencies for Plastibase 20W, 10W and 5W, the following methods were pursued:-

(a) Ways of linearising the data plotted in Figure 56 were investigated. The functions employed included logarithmic, inverse, square root, squared, etc. The object in pursuing this method was to derive a linear relationship between f' (η') and f' (percentage polyethylene - PPE) which could then be employed, knowing the values of η' for 0.5, 1, 2 and 3 PPE over the low frequency region.

(b) Derivation of a model to fit the data shown in Figure 56. It was envisaged that based on the model, a family of plots of the type shown in Figure 56 may be derived at representative frequencies over the range 2.5×10^{-3}Hz to 2.5×10^{-8} Hz. The following types of models were investigated.

(i) Parabolic

(ii) Exponential and modified exponential

(iii) Polynomial and modified polynomial

(c) Derivation of a model to fit the data shown in Figure 55. It was envisaged that based on the model, it may be possible to extend the 5W, 10W, 20W and 30W plots of log (η') vs

log N to the low frequency region.

Several of the above methods were fraught with difficulties largely due to the basic assumptions which have to be made in order to extrapolate the required data. It was found that of the methods listed above the following involving the derivation of a polynomial model to represent the relationship between η' and PPE provided a satisfactory means of extrapolating the data.

Initially, plots of log η' verses PPE at representative frequencies in the range 2.5×10^{1} to 2.5×10^{-3} were drawn, Figure 56. A third degree polynomial of the form

$$y = a + bx - cx^2 + dx^3 \qquad \ldots (82)$$

corresponding to each plot was determined using a standard curve fitting programme (Aston Computer Library). Based on the coefficients a, b, c and d (listed in the Appendix) of this family of equations, a series of coefficients were next substituted in turn in Equation (82) and a polynomial Equation (83) was deduced which gave values identical with known values of log (η') corresponding to 0 PPE and 5 PPE.

$$\log(\eta') = 0.1965 + 5.39PPE - 1.6PPE^2 + 0.17PPE^3 \qquad \ldots (83)$$

Using Equation (83) a plot of log (η') verses PPE at 2.5×10^{-8}Hz frequency was generated and values of η' for the five grades of Plastibase were deduced, Table 21. These values of η' are

TABLE 21

DYNAMIC VISCOSITY VALUES FOR THE FIVE GRADES

OF PLASTIBASE DEDUCED BY EXTRAPOLATION

Frequency at $\approx 2.5 \times 10^{-8}$ Hz

PLASTIBASE	25°C	37°C
50W	2.49×10^{8}	4.47×10^{6}
30W	3.60×10^{6}	1.86×10^{5}
20W	8.64×10^{5}	7.59×10^{4}
10W	1.43×10^{4}	2.14×10^{3}
5W	3.26×10^{2}	6.33×10^{1}
Liquid Paraffin	1.572	0.398

shown in dotted lines in Figure 55.

In a manner similar to that mentioned above, the following polynomial was deduced relating log (η') and PPE at 37°C.

$$\log (\eta') = - 0.4 + 5.16PPE - 1.6PPE^2 + 0.17PPE^3 \quad \ldots (84)$$

Using Equation (84), η' values for the five grades of Plastibase at 37°C were deduced, Table 21. G' exhibits a similar curvilinear relationship, Figure 57, which may also be represented by a third degree polynomial.

While the above method provides a useful and satisfactory means of deriving η'values for Plastibase 30W, 20W, 10W and 5W in a frequency region not otherwise accessible in this work, it must be borne in mind that this does not remove the main objections often raised in the use of extrapolation methods. The reasons for such objections are clear. In attempting extrapolation, it is assumed that the relationship between the two given variables does not alter in the extrapolated region. This may not necessarily be true. Secondly, it is often not possible to give limits within which the extrapolated values may be true and thus it is difficult to predict the accuracy of the extrapolated results. A more satisfactory method would obviously be to derive the data experimentally where possible. Further work on the relatively 'thin' Plastibases may show that it is possible to carry out creep studies on these vehicles using alternative methods of creep measurement (289, 290 - 1). Transformation of such data would not only yield the required

dynamic data but would also indicate the relative accuracy of the extrapolation method described above.

Dynamic tests further confirm the interbatch variation in Plastibase 50W that was recorded by continuous shear and creep methods. As before, it is thought that this variation may be attributed to differences in polyethylene concentration, crystalline structure and/or age.

Comparison of continuous shear, creep and dynamic data for Plastibase 50W and 30W at 25^{o}C shows that a correlation may be drawn between yield stress, instantaneous modulus and dynamic modulus parameters obtained using the three methods of measurement respectively. This further adds weight to the suggestion (272) that yield values may be usefully employed for rapid analysis of semisolids. The other parameters derived by the three methods cannot be correlated.

5 INVESTIGATION OF THE EFFECTS OF FORMULATION ON THE CONSISTENCY CHARACTERISTICS OF PLASTIBASE 50W

5.1 Introduction

The final consistency of a topical semisolid product is often a function of the formulation and manufacturing operations it has undergone in its production. Though considerable work is reported to have been done in determining the influence of formulation on the rheological properties of petrolatum and other semisolids (263, 292 - 296), few reports can be found concerning the effects of formulation on the rheological properties of Plastibases. Shoemaker et. al. (203 - 205) and Thau & Fox (211, 212) have discussed in detail the methods of manufacture of polyethylene-mineral oil gel products containing one or several other ingredients but have not established the relative effects of these additions on the gel consistency. Jones and Lewicki (218) reported that Plastibase dissolved substances such as menthol, methyl salicylate and camphor with the result that ointments containing these chemicals became 'too soft'. They did however carry out penetrometric measurements on samples of Plastibase 50W passed through a roller mill and an ointment mill and observed that the 'viscosity' of the sample passed through the ointment mill had decreased considerably as a result of excessive shear. Mutimer et. al. (198), Singiser & Beal (217) and Schultz & Kassem (207) have all since confirmed the high sensitivity to shear of polyethylene-mineral oil gels. Leszczynska-Bakal et. al. (224) investigating the properties of absorption and emulsion ointment bases comprising polyethylene gel and other constituents have reported from penetrometic measurements an overall decrease in the consistency of the emulsion bases when compared with the polyethylene gels.

It is evident from the reports mentioned above that further consideration of the processes employed in the formulation of Plastibase products, and their effect on the consistency of Plastibase, is necessary. The previous three Sections in this work have detailed an investigation of the rheological properties of manufactured Plastbases. The purpose of the work reported in this Section was to investigate the effects of the following formulation and manufacturing processes on the rheological properties of Plastibase 50W:

(i) shear effects and work softening;

(ii) dilution effects on addition of liquid paraffin;

(iii) emulsification;

(iv) irradiation.

It was thought that in studying the above processes, ways may be found in which subtle changes in the rheological properties of Plastibase may be effected. This would then provide the means of extending the range of available model Plastibase systems in any future further investigations of the effects of consistency on drug release.

5.2 Shear Effects and Work Softening

5.2.1 Introduction

In the extemporaneous incorporation of an active ingredient into a base at bench level, the method most commonly adopted is that of levigation by parts. On a larger scale a semisolid mixer may be used followed by passage through an ointment mill. All these processes shear the sample to a different degree, e.g.,from low shear on levigation or mixing to high shear on milling. Previous workers (198) have reported

that polyethylene gels are sufficiently resistant to mechanical working and shear to allow cold compounding however excessive shear causes a reduction in viscosity which is only partly reversible. This phenomena was investigated in this work by evaluation of the effect on the consistency of Plastibase 50W due to levigation, mixing and milling operations.

5.2.2 Experimental

(a) Materials

Plastibase 50W Batch Numbers BN118 and 2363

(b) Procedure

A 100 g sample of Plastibase 50W was levigated on an ointment slab with the aid of a spatula for fifteen minutes. Twenty four hours later, the levigated sample was subjected to continuous shear and creep analysis at 25°C and 37°C.

A large quantity of Plastibase 50W was subjected to a low agitation mixing process in a Peerless planetary mixer (Peerless and Ericsson, Birmingham) with a paddle attachment and a variable speed control. Samples were withdrawn from the mixer at fifteen minutes, thirty minutes, forty five minutes and ninety minutes and subjected to continuous shear viscometry at 25°C and 37°C.

Finally four 100 g samples of Plastibase 50W were milled, once, twice, four times and eight times respectively in a triple roll mill (Pascall Model No 1). Twenty four hours later these samples were

subjected to continuous shear and creep testing at 25°C and 37°C.

The Ferranti Shirley viscometer was employed as described in Section 2 for continuous shear investigations. The viscometer was fitted with a medium cone and the samples were subjected to a 0 to 460 to 0 sec^{-1} in 240 secs shear cycle at 25°C and 37°C.

The creep apparatus was employed as described in Section 3. The materials were tested at 25°C and 37°C and the initial elastic compliance and the residual Newtonian viscosity were determined from each creep curve. Creep curves for the milled samples at 25°C were further analysed for discrete and continuous spectra of retardation times.

5.2.3 Results

Continuous shear and creep data for levigated and unlevigated Plastibase 50W are given in Tables 22 and 23. Both sets of data indicate a very small decrease in rheological parameters of the levigated Plastibase.

Figure 59 shows rheograms for Plastibase 50W subjected to the mixing process. Data derived from these rheograms are given in Table 24. These indicate a small progressive decrease in yield value and apparent viscosity with an increase in mixing time, however the overall decrease in the values of these parameters after ninety minutes is not great.

Figure 60 shows rheograms for milled and unmilled Plastibase

TABLE 22

CONTINUOUS SHEAR DATA FOR THE LEVIGATED PLASTIBASE 50W;

APPARENT VISCOSITY (η APP) IN POISE AND

YIELD STRESS (Y_1) IN Nm^{-2}

	25°C		37°C	
	Y_1	η app	Y_1	η app
Plastibase 50W (2363)	425.0	20.59	325.0	13.65
Levigated	405.0	20.17	312.5	12.61

TABLE 23

CREEP DATA FOR THE LEVIGATED PLASTIBASE 50W; INSTANTANEOUS COMPLIANCE (Jo) IN m^2N^{-1} AND RESIDUAL NEWTONIAN VISCOSITY (η_o) IN POISE

	25°C		37°C	
	Jo	η_o	Jo	η_o
Plastibase 50W (2363)	1.86×10^{-4}	1.75×10^{8}	2.10×10^{-4}	1.16×10^{6}
Levigated	1.82×10^{-4}	1.53×10^{8}	2.09×10^{-4}	1.11×10^{6}

FIGURE 59

CONTINUOUS SHEAR RHEOGRAMS OF PLASTIBASE 50W ILLUSTRATING A PROGRESSIVE SMALL DECREASE IN RHEOLOGICAL PARAMETERS WITH AN INCREASE IN THE TIME OF MIXING

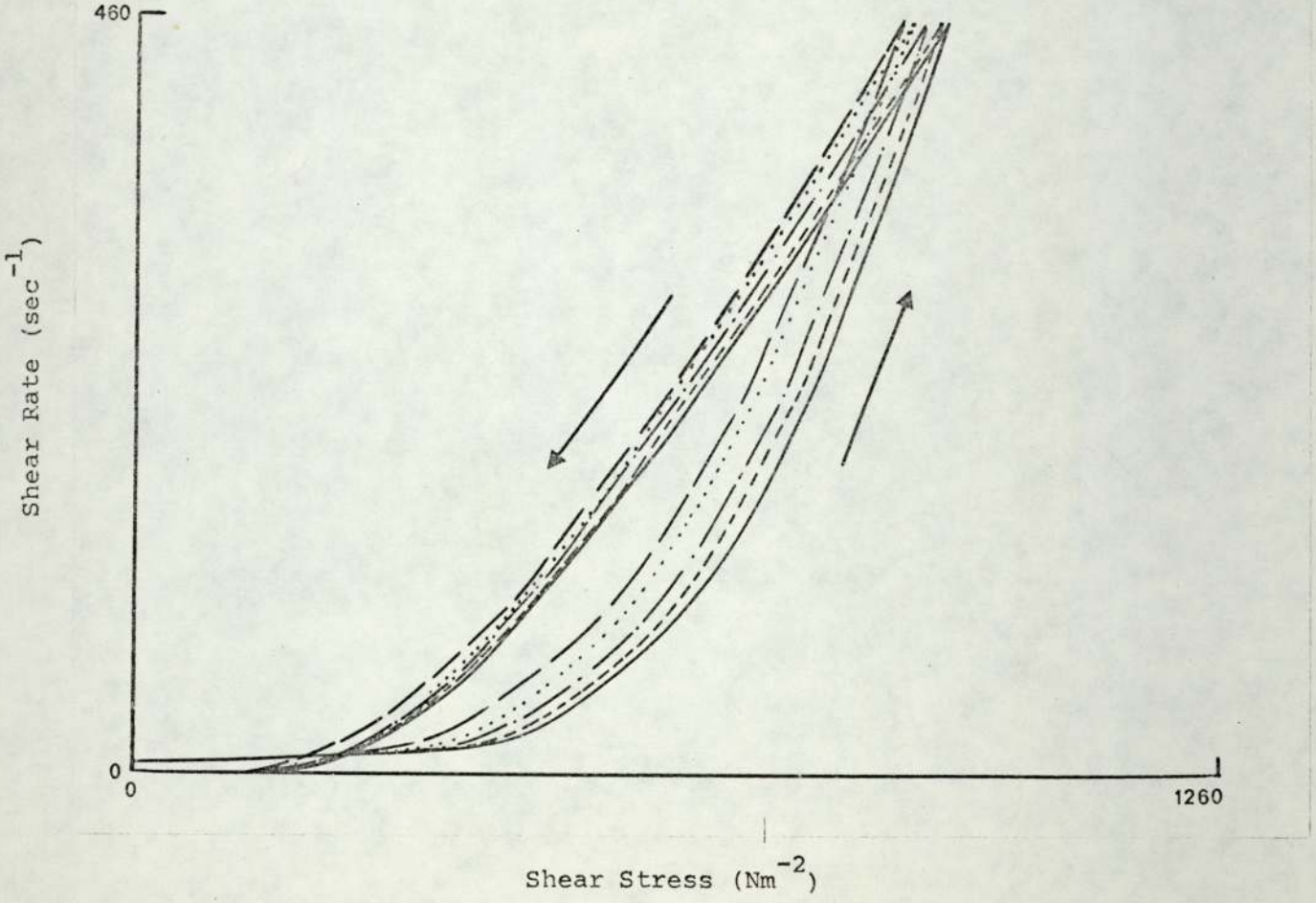

TABLE 24

CONTINUOUS SHEAR DATA FOR PLASTIBASE 50W SUBJECTED TO MIXING PROCESS; η APP IN POISE AND Y_1 IN Nm^{-2}

Plastibase 50W (2363)	25°C		37°C	
Time mixed	Y_1	η app	Y_1	η app
0 mins	425.0	20.59	325.0	13.65
15 mins	396.4	20.04	308.3	13.18
30 mins	389.0	19.77	298.5	13.03
45 mins	381.6	19.48	286.3	12.63
90 mins	371.9	19.22	278.9	12.22

FIGURE 60

CONTINUOUS SHEAR RHEOGRAMS OF PLASTIBASE 50W ILLUSTRATING A MARKED CHANGE IN RHEOLOGICAL CHARACTERISTICS ON MILLING OF THE MATERIAL

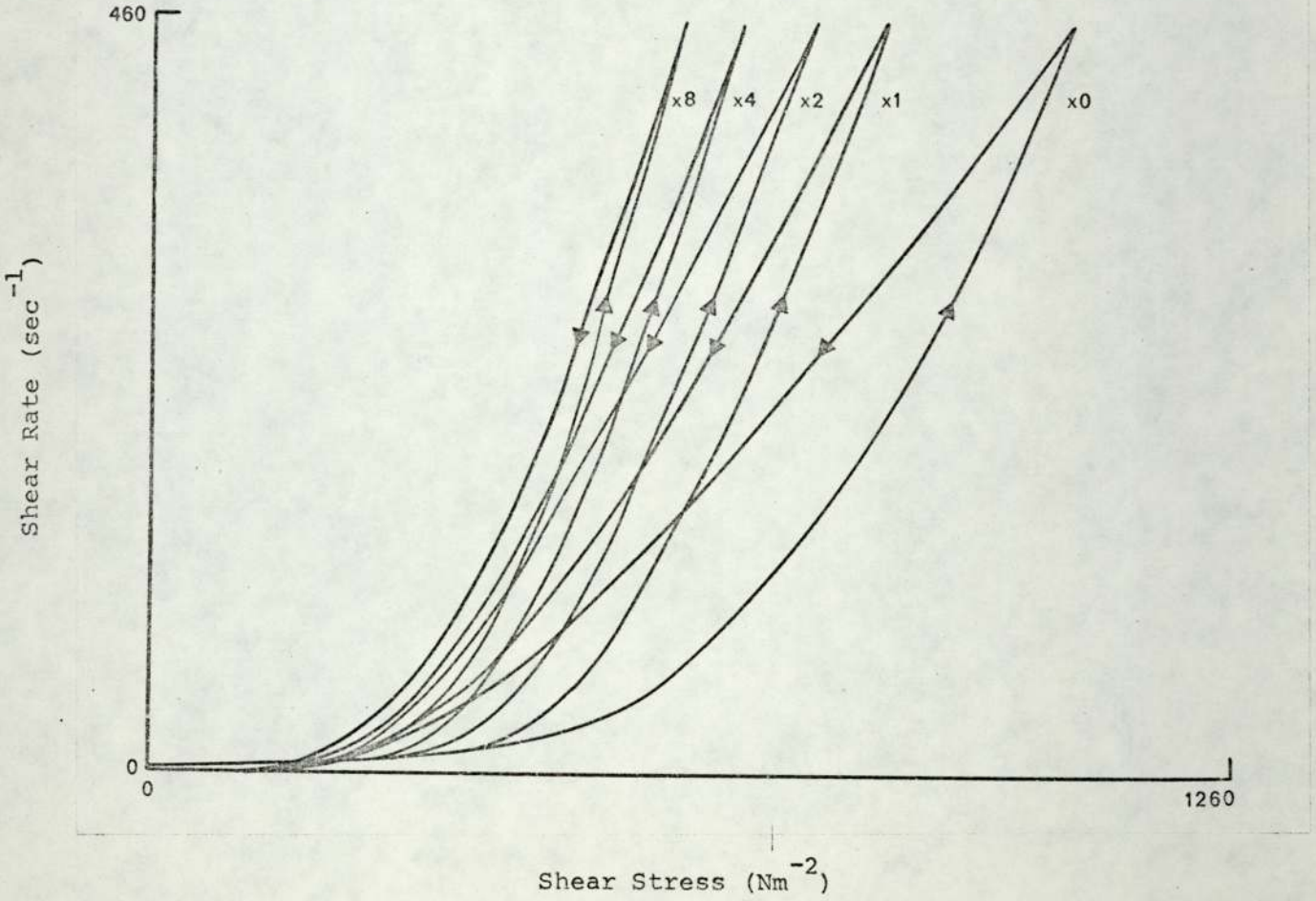

TABLE 25

CONTINUOUS SHEAR DATA FOR MILLED PLASTIBASE 50W;

η APP IN POISE AND Y_1 IN Nm^{-2}

Plastibase 50W (118)	25°C		37°C	
Times milled	Y_1	η app	Y_1	η app
None	425.0	23.06	310.0	15.67
x 1	382.5	19.05	310.0	12.46
x 2	345.0	17.37	280.0	11.06
x 4	285.0	15.27	230.0	9.66
x 8	265.0	13.73	210.0	8.54

FIGURE 61

GRAPHICAL REPRESENTATION OF CONTINUOUS SHEAR AND CREEP DERIVED FOR UNMILLED AND MILLED PLASTIBASE 50W

TEMPERATURE IN ^{o}C

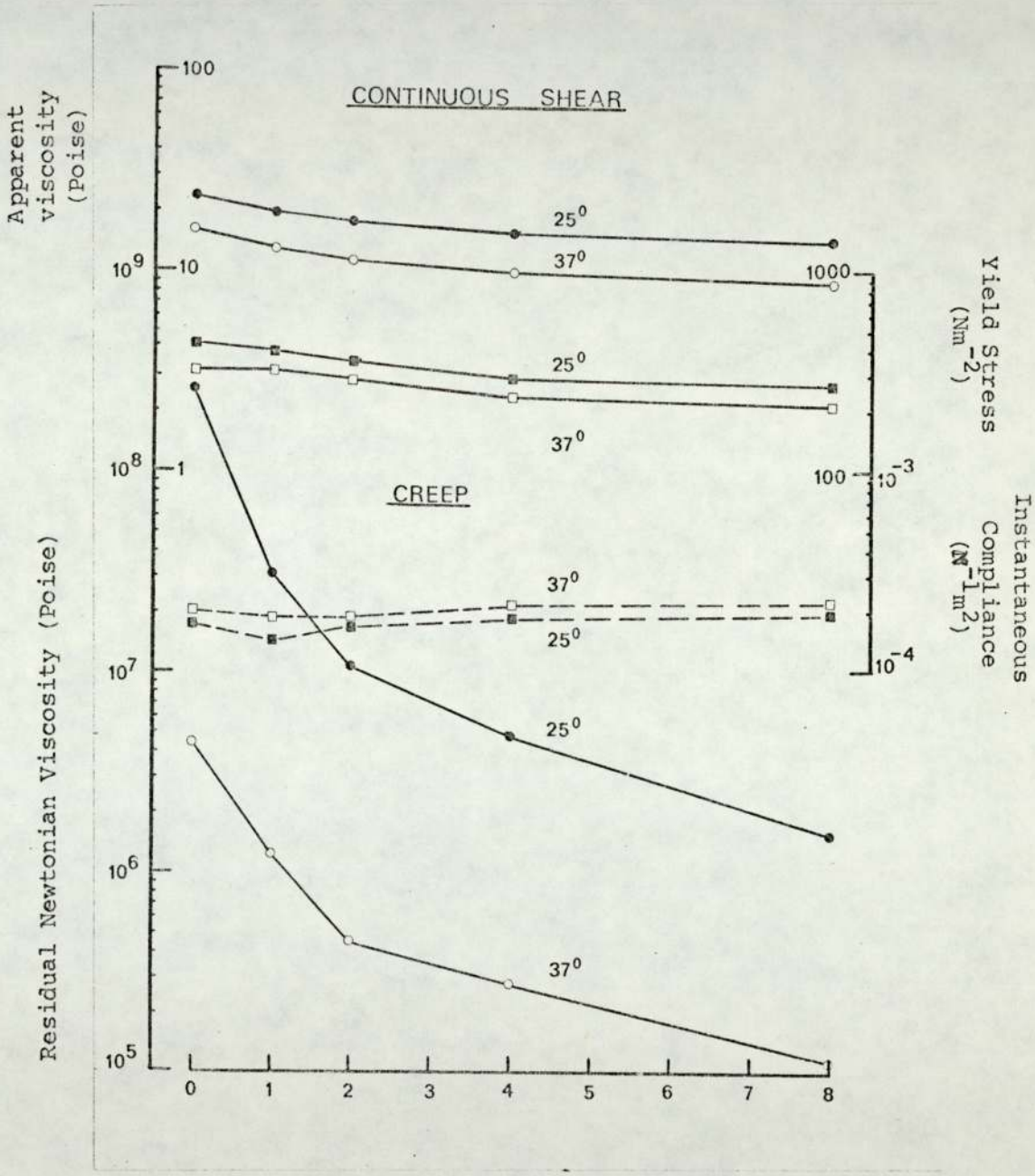

TABLE 26

CREEP DATA FOR MILLED PLASTIBASE 50W (118)

COMPLIANCES ARE IN m^2N^{-1}, RETARDATION TIMES IN SECS AND VISCOSITIES IN POISE

	25°C					37°C				
	M x 0	M x 1	M x 2	M x 4	M x 8	M x 0	Mx1	M x 2	M x 4	M x 8
						35°C				
$J_o \times 10^{-4}$	1.68	1.40	1.64	1.81	1.93	1.96	1.84	1.84	2.11	2.23
$J_1 \times 10^{-5}$	3.07	8.97	10.41	11.70	28.75	3.97	-	-	-	-
$J_2 \times 10^{-5}$	1.57	4.21	3.37	6.54	-	2.73	-	-	-	-
$J_3 \times 10^{-5}$	2.18	-	-	-	-	-	-	-	-	-
τ_1	157.0	161.0	220.0	65.3	63.0	130.0	-	-	-	-
τ_2	26.5	19.8	21.2	6.7	-	14	-	-	-	-
τ_3	4.0	-	-	-	-	-	-	-	-	-
$\eta_o \times 10^6$	252.9	30.50	10.20	4.62	1.51	4.3	1.22	0.441	0.271	0.114
$\eta_1 \times 10^6$	51.1	18.02	21.13	5.58	2.19	32.7	-	-	-	-
$\eta_2 \times 10^6$	16.9	4.70	6.29	1.02	-	5.1	-	-	-	-
$\eta_3 \times 10^6$	1.8	-	-	-	-	-	-	-	-	-

FIGURE 62

CONTINUOUS RETARDATION SPECTRA ILLUSTRATING THE CHANGE IN THE VISCOELASTIC PROPERTIES OF PLASTIBASE 50W ON MILLING

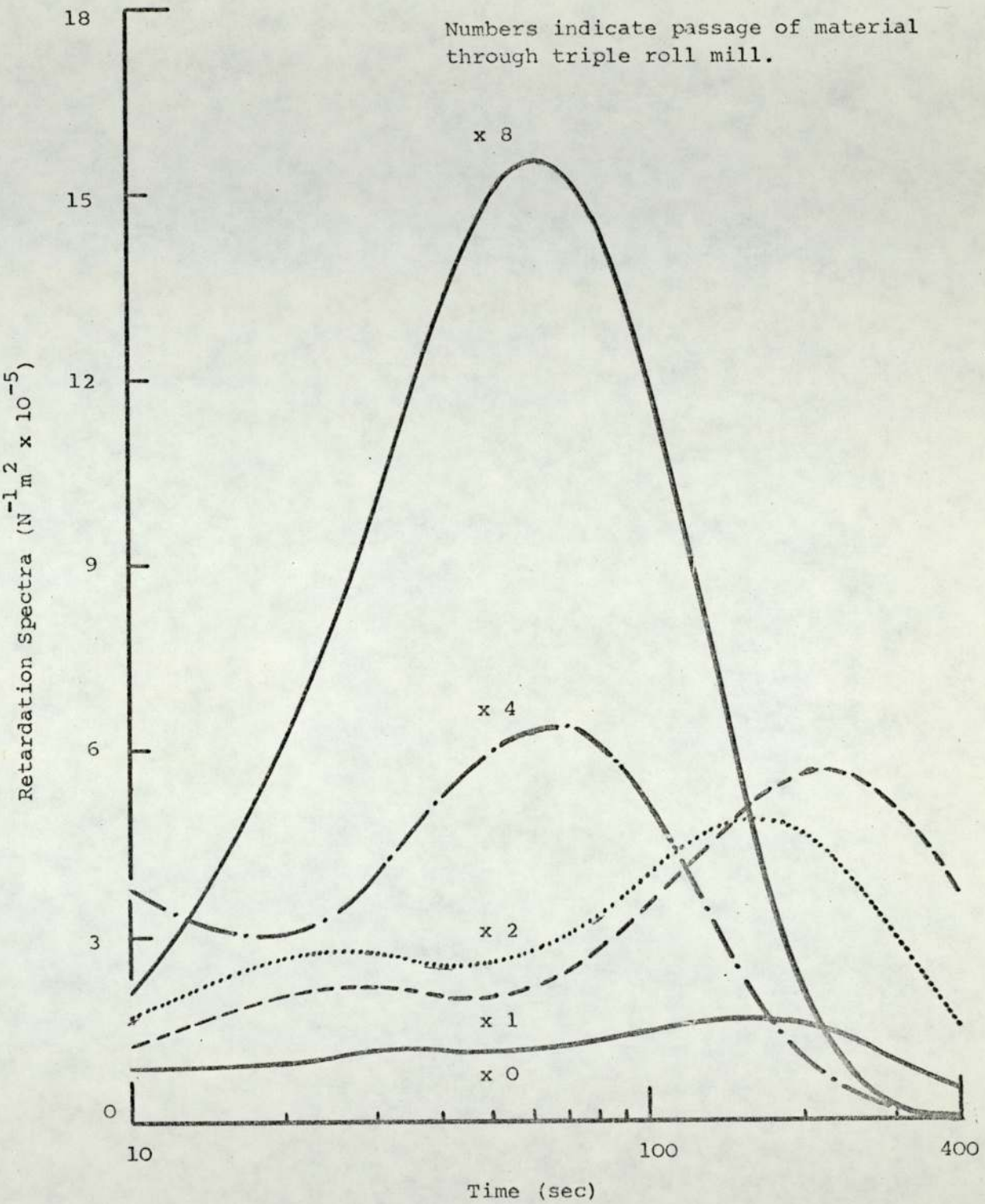

50W. Data derived from these rheograms are given in Table 25 and plotted in Figure 61. Decrease in the consistency of Plastibase 50W on milling is indicated by a considerable decrease in yield values and apparent viscosities. Creep data for milled and unmilled Plastibase 50W are given in Table 26 and the instantaneous complicane Jo and the residual viscosity η_0 for each material are plotted in Figure 61. An overall increase in compliances and a decrease in residual viscosities indicates a decrease in consistency of Plastibase 50W on milling. Discrete spectral data, Table 26, indicate a progressive decrease in the number of retardation times required to characterise the viscoelastic properties of milled Plastibase 50W. The continuous spectra of retardation times for milled and unmilled Plastibase 50W are shown in Figure 62. Except for the material milled eight times, all other milled and unmilled materials exhibit a bimodal retardation spectra with one maxima at long times and one at short times. The material milled eight times shows a single maxima at short times. As the number of times Plastibase 50W was milled increased, the spectra increased in height and the larger maxima at longer times moved to shorter times.

5.2.4 Discussion

In allowing twenty four hours to elapse before commencing rheological measurements, it was ensured that the samples subjected to levigation, mixing and milling had recovered, if any recovery was possible, to a more or less equilibrium state. Thus any alteration in rheological properties measured was taken to represent irreversible shear breakdown related to the shear (working) procedure.

Continuous shear and creep data for the levigated Plastibase 50W indicated a tiny reduction in the consistency of the material reflecting some small changes or disruption in its structure owing to perhaps a breaking of the weak secondary bonds. These changes are however so small that in practice they are unlikely to be of any significance.

Plastibase 50W subjected to the mixing process also showed a progressive drop in consistency with an increase in the time for which it was mixed; once again indicating some disruption of structure. As the overall reduction in the apparent viscosity and yield value were not great, it is considered that the disruption of structure occurred largely due to the breaking of weak secondary bonds. It should be realised that the shear breakdown of Plastibase 50W will vary depending on the type of mixer used and the length of time the process of mixing proceeds. Thus in any large scale or industrial mixing operation of the material, the effect of this procedure must be carefully evaluated. In this work, it was seen from the above two experiments that low shear working procedures produced relatively minor alterations in the consistency characteristics of Plastibase 50W.

In contrast, milling a high shear working procedure had a profound effect on the consistency of Plastibase 50W. From continuous shear rheograms of unmilled and milled Plastibase 50W, it is possible to see in qualitative terms the extent of structural damage as is illustrated by the progressive drastic reduction in the extent of hysteresis (loop area) after successive milling. This is accompanied by a rapid reduction in the apparent viscosity and yield value.

In creep study it was seen that the viscous properties of Plastibase 50W were most affected by the milling process. The first two runs through the triple roll mill appear to have had the greatest effect on the structual-rheological properties of the material. Milling Plastibase 50W four and eight times does not lead to as great a drop in the residual viscosity of the material as the initial two runs through the mill. Discrete spectra show that in the mechanical model representation of the viscoelastic behaviour of Plastibase 50W on milling the number of Voigt (Kelvin) elements are reduced. This corresponds with a reduction in the number of maxima in the continuous retardation spectra for the material indicating that with an increase in the number of times Plastibase 50W is milled, there is a gradual decrease in the types of retardation mechanisms within the material. An increase in the elastic compliance of the material on milling is seen by the increase in the height of the spectra and the shift of the maxima to lower times indicates an increase in the rate at which strain occurs. From the above observations it is evident that a profound irreversible disruption in the structure of Plastibase 50W occurs after milling.

A possible explanation of this behaviour may be offered by comparison with that of petrolatum, which comprises n-, iso-, and cyclic paraffins. The presence of iso-paraffins in this gel allows the formation of smaller crystals of n-paraffin (210) with the result that the consistency of this material is relatively high. The thixotropic breakdown of this material does not resemble a rapid sol-gel transformation but instead leads to a more permanent structural change (15) and the original structure and consistency of this material are

only partly recovered (15, 264); the recovery being aided greatly by the presence of the iso-paraffins (220). The high pressure polyethylene used in the manufacture of Plastibase is largely an amorphous polymer and the crystallinity in Plastibase is largely a function of the manufacturing conditions. Shear breakdown of Plastibase 50W resembles petrolatum in that the material suffers a gross structural change. Plastibase 50W however shows negligible recovery over a period of time due possibly to the irreversible rupture of a large number of secondary bonds. This was seen in Section 2 when the cause of the hystersis loop in continuous shear tests was investigated and again in this Section when even after low shear treatment, the material did not demonstrate a regeneration of consistency after twenty four hours. Schultz and Kassem (220) have suggested that the structure of polyethylene-mineral oil gels does not regenerate after shear breakdown due to the low iso-paraffin content of these gels. A more likely explanation of this behaviour is that the high shear process ruptures the three dimensional matrix of the gel to the extent that the crystallites are freed from the matrix and the amorphous filaments are reorientated. The material cannot revert to the original network and this effect is manifested in a reduced consistency of the material.

5.3 Investigation of Dilution Effects on Addition of Liquid Paraffin

5.3.1 Introduction

Though several workers have reported the effects of dilution of petrolatum with liquid paraffin (249, 263, 297 - 9), the study of the physical properties of polyethylene-mineral oil gels has largely been

confined to determining the most suitable polyethylene for geling and its effect in various concentrations on the consistency of the product (198, 203 - 5, 207). Indeed an investigation of the dilution effects on the gel would seem unnecessary in view of the fact that polyethylene-mineral oil gels are available in different consistency grades ranging from mobile liquids to rigid semisolids. Moreover Squibb (202) have warned that "no attempt should be made to dilute Plastibase products or influence their 'viscosities' since the stability of the gels depends on the insolubility of the polyethylene in the mineral oil at normal temperatures". While this as it is, the work reported in this Section was prompted for the following two reasons:

(i) It is recognised (218) that the incorporation of a liquid medicament or one that dissolves in Plastibase can have a profound effect on the consistency and stability of the product; the extent of these effects needs to be evaluated.

(ii) It was considered that the process of dilution could be usefully employed in extending the range of available model vehicles, with different consistencies for instance between Plastibase 50W and Plastibase 30W which could be used in future drug release correlation studies.

5.3.2 Experimental

(a) Materials

Plastibase 50W Batch Number 2363 and liquid paraffin B.P.

(b) Procedure

5ml, 10ml, 15ml, 20ml, 25ml, 30ml, 40ml and 50ml of liquid paraffin were incorporated by a process of levigation on an ointment slab into eight 100g samples of Plastibase 50W respectively. Continuous shear and creep tests were performed on each sample twenty four hours after preparing at 25°C and 37°C. Oscillatory tests were performed on all samples at 25°C.

The Ferranti Shirley viscometer fitted with a medium cone was employed as described in Section 2 for continuous shear tests. The samples were subjected to a 0 to 460 to 0 sec^{-1} in 240 secs shear cycle. The creep apparatus was employed as described in Section 3. Creep curves for all the samples were analysed for the initial elastic compliance (Jo) and the residual Newtonian viscosity (η_o). The Weissenberg Rheogoniometer was employed as described in Section 4 for oscillatory tests on the samples. The dynamic viscosity (η') and the storage modulus (G') were derived over a range of frequencies for each sample.

5.3.3 Results

Samples are described in Table 27 in terms of the concentration of polyethylene they contain, i.e., corresponding to each dilution. Continuous shear data for the diluted Plastibase 50W are given in Table 27 and plotted in Figure 63. The progressive decrease in the consistency of the materials on dilution is reflected in a decrease in the yield values and apparent viscosities.

Creep data for the diluted and undiluted Plastibase 50W are

TABLE 27

CONTINUOUS SHEAR DATA FOR PLASTIBASE 50W DILUTED WITH LIQUID PARAFFIN. THE APPARENT VISCOSITY (η APP) IS GIVEN IN POISE AND THE YIELD STRESS IS GIVEN IN Nm^{-2}

Percent Polyethylene in the sample	25°C		37°C	
	Y_1	η app	Y_1	η app
5.0 (BN2363)	425.0	20.59	325.0	13.65
4.79	310.0	18.49	225.0	11.76
4.59	267.5	16.87	190.0	10.85
4.41	210.0	15.47	140.0	9.80
4.25	165.0	14.43	115.0	8.96
4.09	140.0	12.95	95.0	8.12
3.95	115.0	12.74	75.0	7.98
3.69	-	10.64	-	6.44
3.46	-	9.52	-	5.74

FIGURE 63

GRAPHICAL REPRESENTATION OF CONTINUOUS SHEAR DATA DERIVED FOR PLASTIBASE 30W, 50W AND SAMPLES OF PLASTIBASE 50W DILUTED WITH LIQUID PARAFFIN

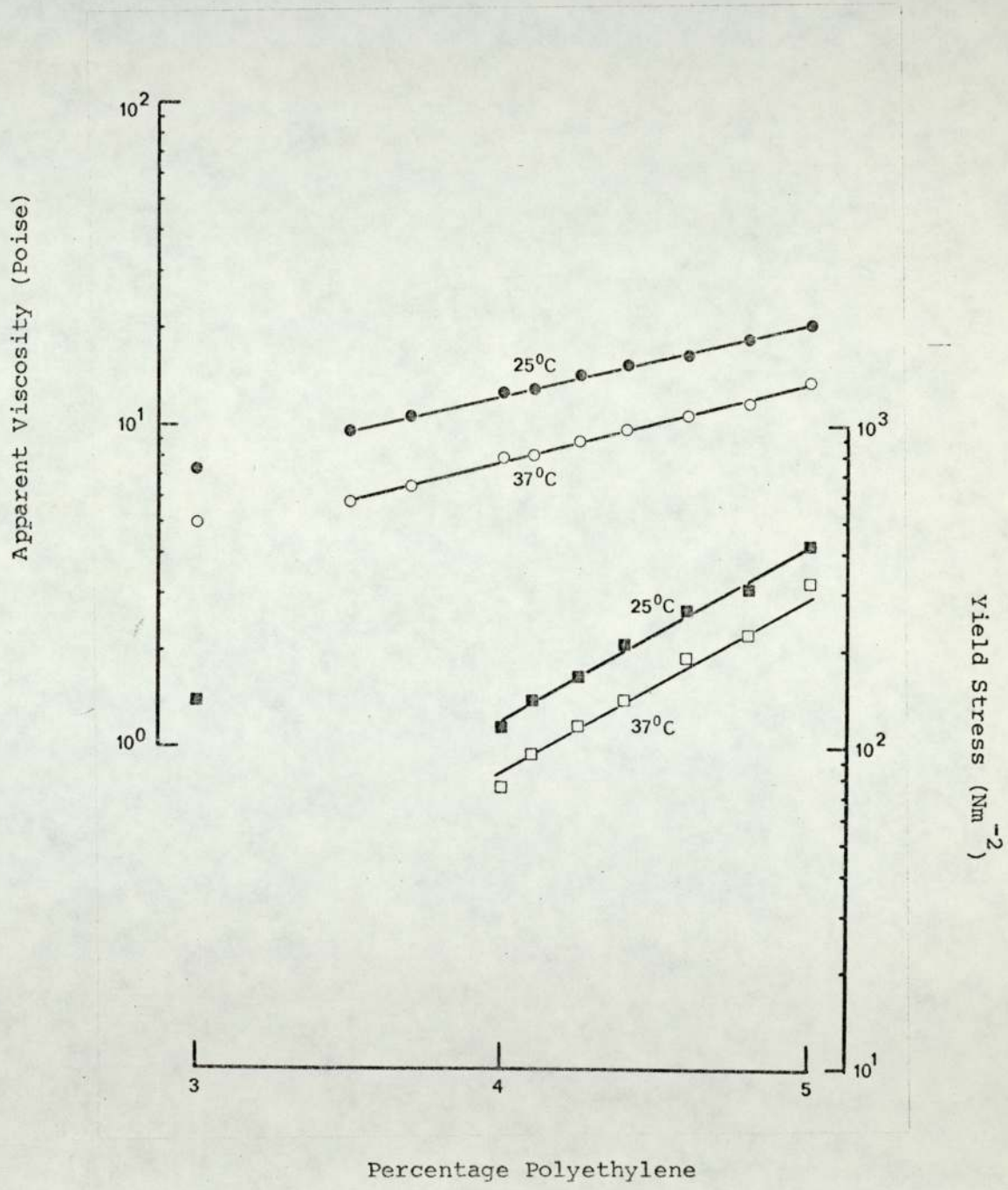

TABLE 28

CREEP DATA FOR PLASTIBASE 50W (2363) DILUTED WITH LIQUID PARAFFIN.

THE INSTANTANEOUS COMPLIANCE (Jo) IS GIVEN IN m^2N^{-1} AND RESIDUAL NEWTONIAN VISCOSITY (η_o) IN POISE

Percent Polyethylene in the sample	25°C		37°C	
	Jo	η_o	Jo	η_o
5.0	1.86×10^{-4}	1.75×10^{8}	2.10×10^{-4}	1.16×10^{6}
4.79	2.07×10^{-4}	7.01×10^{7}	2.23×10^{-4}	4.46×10^{5}
4.59	2.58×10^{-4}	3.06×10^{7}	2.98×10^{-4}	2.11×10^{5}
4.41	3.40×10^{-4}	1.04×10^{7}	4.10×10^{-4}	7.24×10^{4}
4.25	3.97×10^{-4}	5.84×10^{6}	4.77×10^{-4}	4.07×10^{4}
4.09	4.47×10^{-4}	3.00×10^{6}	5.38×10^{-4}	1.89×10^{4}

FIGURE 64

GRAPHICAL REPRESENTATION OF CREEP DATA DERIVED FOR PLASTIBASE 30W, 50W AND SAMPLES OF PLASTIBASE 50W DILUTED WITH LIQUID PARAFFIN

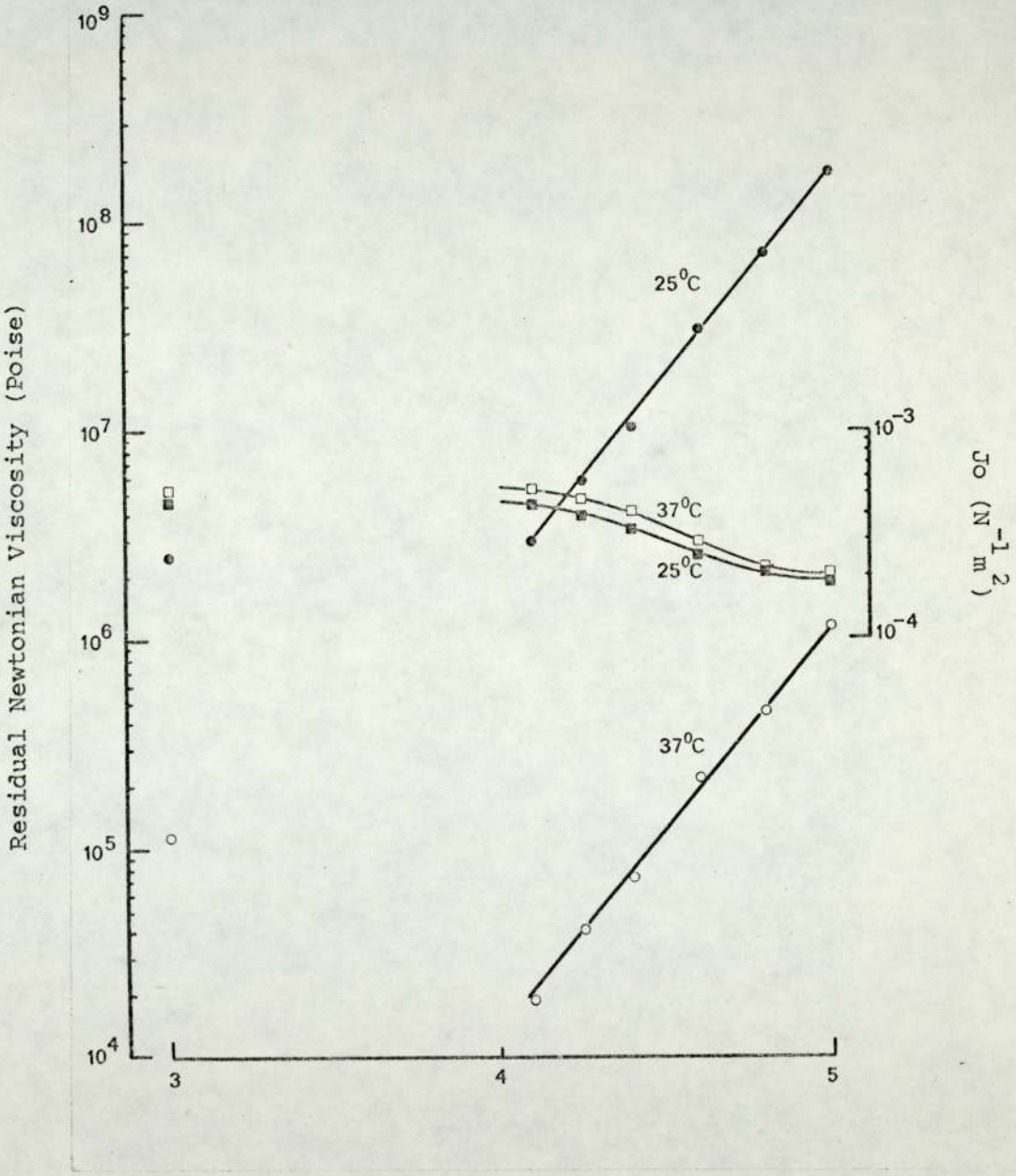

FIGURE 65

GRAPHICAL REPRESENTATION OF DYNAMIC DATA DERIVED AT A FREQUENCY OF OSCILLATION 2.5×10^{-1} HZ FOR PLASTIBASE 30W, 50W AND SAMPLES OF PLASTIBASE 50W DILUTED WITH LIQUID PARAFFIN

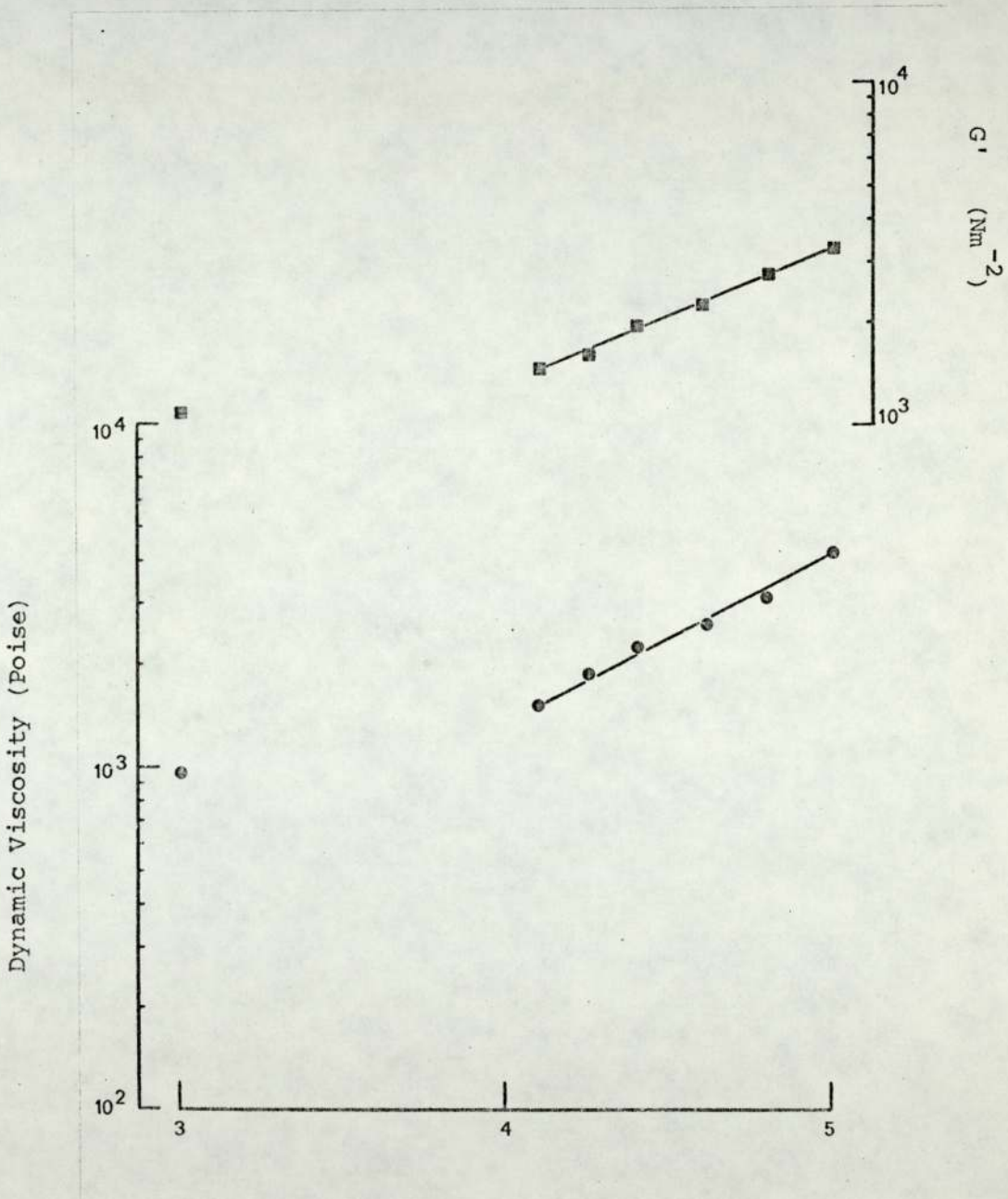

given in Table 28 and plotted in Figure 64. The low consistency of the samples diluted with 30ml, 40ml and 50ml of liquid paraffin did not permit creep testing. Creep data on the five dilutions of Plastibase 50W show an increase in initial compliance and a decrease in residual viscosity indicating once again a progressive decrease in the consistency of Plastibase 50W on dilution.

Data for the dynamic tests on the five dilutions of Plastibase 50W are given in the Appendix and shown in Figures 48 and 52 of Section 4. Figure 65 illustrates the decrease in the storage modulus G' and real viscosity η' for the five dilutions at 2.5×10^{-1}Hz frequency.

5.3.4 Discussion

In allowing twenty four hours to elapse before commencing the measurement of rheological parameters, it was ensured that the diluted samples of Plastibase 50W had sufficient time to reach an equilibrium state following the stresses imposed on the materials in the incorporation by levigation of liquid paraffin. In the previous Section it was seen that only minor changes occur in the consistency of Plastibase 50W following levigation. It was thus assumed that any changes in the rheological properties of the material represented the effects of dilution.

All measured rheological parameters indicate a progressive decrease in the consistency of Plastibase 50W after dilution. Log-linear plots of rheological parameters *vs* the percentage of polyethylene show a linear relationship. The dilutions of Plastibase 50W show a much

steeper decline in the rheological parameters than that observed in the five grades of Plastibase indicating a much greater relative change in the consistency of the material even after small dilutions. There are two possible explanations for this. Firstly, Mutimer et. al. (198) have proposed that at five per cent polyethylene concentration, the crystallites in Plastibase are just close enough together to allow the long filaments of amorphous polyethylene to intermesh and produce a three dimensional structure which entraps and holds the mineral oil. It can be reasoned thus that increase in the concentration of mineral oil is likely to produce a disruption of the long filaments at the point of intermesh leading to a considerable reduction in the consistency of the material. The second explanation of this behaviour is that as in the case of petrolatum, where the liquid phase contains more dissolved solid paraffins than may be explained by solubility alone (297), the mineral oil in Plastibase contains some dissolved polyethylene leading to the 'thickening' of the continuous phase of the gel. Dilution of such a system would lead to a 'thinning' of the continuous phase and this would be manifested by a reduction in the consistency of the material. Either of the above mentioned effects, individually or collectively, will have a significant effect on the viscous and elastic properties of a material and this is seen to occur in this work. In a system such as Plastibase, gross structural-rheological changes after dilution will be characterised by the tendency of the material to bleed considerably on storage. This effect was clearly evidenced after four weeks storage in Plastibase samples diluted to contain less than four per cent of polyethylene.

Comparison of continuous shear, creep and oscillatory data, Table 29, shows that a correlation may possibly be drawn between the

TABLE 29

COMPARISON OF CONTINUOUS SHEAR, CREEP AND OSCILLATORY DATA FOR PLASTIBASE 50W AND PLASTIBASE 50W DILUTED WITH LIQUID PARAFFIN ($\equiv$ 4.09% POLYETHYLENE)

Method of Measurement	Rheological Parameter	Ratio of Parameters	
		at 25°C	at 37°C
Continuous Shear	Yield Stress	3.04	3.42
	Apparent Viscosity	1.59	1.68
Creep	Initial Shear Modulus	2.40	2.56
	Residual Viscosity	58.33	61.38
Oscillatory	Storage Modulus*	2.23	-
	Real Viscosity*	2.80	-
	* at 2.5×10^{-1} Hz frequency		

yield stress values, initial shear modulus values and storage modulus values. The ratios of the apparent viscosities and the real dynamic viscosities for undiluted and diluted Plastibase 50W are also sufficiently close to predict a possible correlation of the parameters derived from the two methods.

From the results of this work it is evident that even small dilutions of Plastibase can lead to profound changes in the consistency of the material and this will have a bearing on the stability of the product. Design of additional model systems based on the dilution of Plastibase 50W is possible provided the extent of dilution is not too great so as to reduce the concentration of polyethylene in the gel to below four per cent. The decrease in consistency of these diluted vehicles does not follow the characteristic decrease exhibited by the five grades of Plastibase.

5.4 Investigation of Emulsified Plastibase 50W Systems

5.4.1 Introduction

The absorption characteristics of Plastibase are altered by the addition of glyceryl mono-oleate to the Plastibase formulation resulting in a hydrophilic ointment base capable of absorbing several times its weight of water to form a water in oil emulsion (202). Plastibase Hydrophilic (formula included in Section 1) is such a system. Shoemaker (205) has reported that while the concentration of the emulsifier is not critical and may vary within wide limits, amounts of about one per cent to twenty five per cent, based on the weight of the mineral oil, are satisfactory for most uses. Mutimer et. al. (198) have recommended an emulsifier concentration of six per cent and

Leszczynska-Bakal et. al. (224) found that five per cent of "Lanocerylt" (Wool-wax alchols) or two per cent of Span 60 were sufficient to stabilise emulsions of polyethylene-mineral oil gel and water. The proportion of water incorporated in the Plastibase Hydrophilic systems has varied and emulsions with a phase volume of approximately 0.5 have been reported. The effect of changing emulsifier concentration or phase volume ratio on the consistency characteristics of Plastibase Hydrophilic have not been reported. The purpose of the work reported in this Section was to determine using a cold compounding method and a heating method of preparation of Plastibase emulsions, the effect on the consistency and stability of the systems due to an alteration of emulsifier concentration and phase volume ratio.

5.4.2 Experimental

(a) Materials

(i) Plastibase 50W Batch Number 2363

(ii) Distilled water from an all glass still

(iii) Atmos 300 (a commercial sample from Honywill-Atlas Limited, Surrey).

Glyceryl monooleate could not be obtained commercially and hence Atmos 300 which is nominally mono- and diglycerides of fat forming fatty acids in the form of a clear yellow liquid with an HLB of 2.8 was used as the surfactant. The manufacturer's specifications are given in Table 30. The surfactant was used as such without any further analysis.

TABLE 30

HONEYWILL-ATLAS SPECIFICATIONS FOR ATMOS 300

General Characteristics	
Classification	Food Emulsifier
Form at 25°C	Clear yellow liquid (may cloud at low temperatures)
Viscosity at 25°C	Approx. 130 cps.
Specific Gravity at 25°/25°C	Approx. 0.96
Odour and Taste	Bland
Total Monoglycerides (α & β forms)	Approx. 57%
Hydrophile-Lipophile Balance Rating	2.8

Standard Specifications	
Free fatty acid, % as oleic	1.0 max.
Moisture, %	1.0 max.
Clear Point, °C	24 max.
Monoglyceride content (α form), %	46 min.

Solubilities

(a) Soluble in cottonseed oil, mineral oil and isopropylalchol.

(b) Insoluble in water.

(b) Procedure

The compositions of various emulsion bases prepared according to the following techniques are listed in Table 31.

(i) Cold Compounding

Emulsions identified by numbers EM 1 to 12 were prepared by this technique. The surfactant was first incorporated into Plastibase 50W by a process of levigation on an ointment slab. To this was added water and the resulting emulsion was thoroughly levigated until homogenous. The whole process was carried out over a set period of time.

(ii) Hot Compounding

Emulsions identified by numbers EM1H to EM4H were prepared by this technique. The surfactant and the Plastibase 50W were heated in an evaporating basin to 85°C. The mixture was held at this temperature until all the Plastibase 50W had melted. Water at 85°C was then added and the emulsion was stirred until cold.

Emulsions 1 to 12 were subjected to continuous shear and creep tests at 25°C and 37°C, twenty four hours after the preparation of each sample. Emulsions 1H to 4H were subjected to continuous shear and creep tests at 25°C, twenty four hours after the preparation of each sample.

The Ferranti Shirley viscometer fitted with a medium cone was employed as described in Section 2 for continuous shear tests. The samples were subjected to a 0 to 460 to 0 sec^{-1} in 240 secs shear cycle.

TABLE 31

COMPOSITION OF EMULSION BASES

System Number	Constituents %			
	Plastibase	Atmos 300	Water	% S.A.A.
				in oil phase
EM1 + EM1H	88.2	1.8	10	
EM2 + EM2H	78.4	1.6	20	2%
EM3 + EM3H	58.8	1.2	40	
EM4 + EM4H	39.2	0.8	60	
EM5	86.4	3.6	10	
EM6	76.8	3.2	20	4%
EM7	67.6	2.4	40	
EM8	38.4	1.6	60	
EM9	84.6	5.4	10	
EM10	75.2	4.8	20	6%
EM11	56.4	3.6	40	
EM12	37.6	2.4	60	

The creep apparatus was employed as described in Section 3. Creep curves for all the samples were analysed for the initial elastic compliance (Jo) and the residual Newtonian viscosity (ηo). The creep curved for emulsions 1 to 12 at 25°C were further analysed for discrete and continuous spectra of retardation times.

Emulsions 1 to 4 and 1H to 4H were examined microscopically using a Wild microscope (Wild Heerbrugg, Switzerland). A simple smear technique was used in the preparation of the slides. Improved Neubauer Counting Chamber (Hawkesley, England) was used for the slide in order to ensure a constant thickness of the emulsion being examined. The slide and coverslips were treated with silicon fuild (MS 200/1000 cs. 2% solution in xylene. Hopkins and Williams) in order to prevent wetting.

5.4.3 Results

Continuous shear rheograms for the emulsion systems were similar to the Plastibase rheograms. These comprised simple reproducible anticlockwise hysteresis loops, demonstrating a static and in some instances a dynamic yield point, from which reliable data could be derived. The continuous shear data for all the emulsion systems are given in Table 32 and shown in Figures 66 to 68. The emulsions prepared by the hot compounding method demonstrated a considerably lower consistency than those of similar compositions prepared by the cold compounding method. All emulsion systems demonstrated a decrease in yield value with an increase in the surfactant concentration and phase volume ratio. The apparent viscosity for all the systems decreased with an increase in surfactant concentration but

TABLE 32

CONTINUOUS SHEAR DATA FOR PLASTIBASE 50W EMULSION SYSTEMS

APPARENT VISCOSITY (η APP) GIVEN IN POISE AND YIELD STRESS (Y_1) IS GIVEN IN Nm^{-2}

System Number	25°C		37°C	
	Y_1	η app	Y_1	η app
EM1	262.8	18.70	172.2	11.48
EM2	207.9	18.49	153.6	11.20
EM3	171.0	19.33	104.1	11.76
EM4	131.0	21.85	66.5	12.88
EM1H	107.0	10.99	-	-
EM2H	96.6	11.48	-	-
EM3H	74.6	13.58	-	-
EM4H	-	14.36	-	-
EM5	239.0	17.93	164.1	11.16
EM6	196.2	17.72	140.4	10.92
EM7	156.1	18.91	96.2	11.41
EM8	116.1	21.29	62.0	12.18
EM9	227.7	17.37	155.9	10.83
EM10	183.0	17.02	118.9	10.57
EM11	143.4	18.07	86.1	11.06
EM12	105.1	20.66	44.1	11.76

FIGURE 66

GRAPHICAL REPRESENTATION OF APPARENT VISCOSITY DATA DERIVED AT 25°C FROM CONTINUOUS SHEAR TESTING OF THE PLASTIBASE EMULSION SYSTEMS PREPARED BY THE COLD COMPOUND METHOD

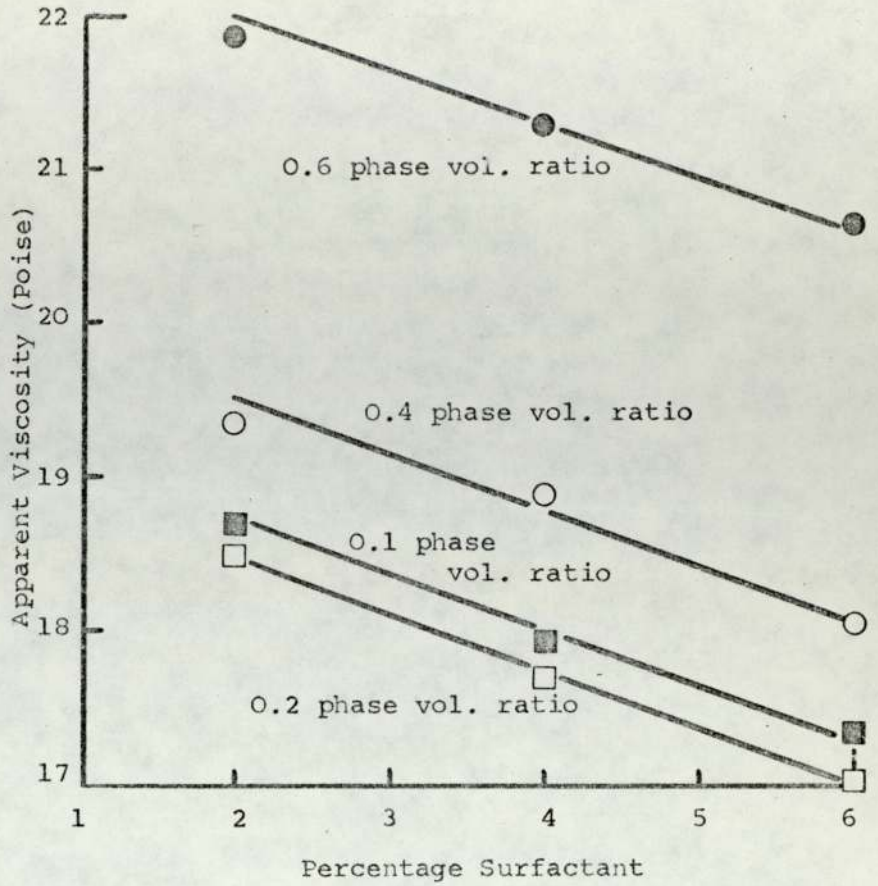

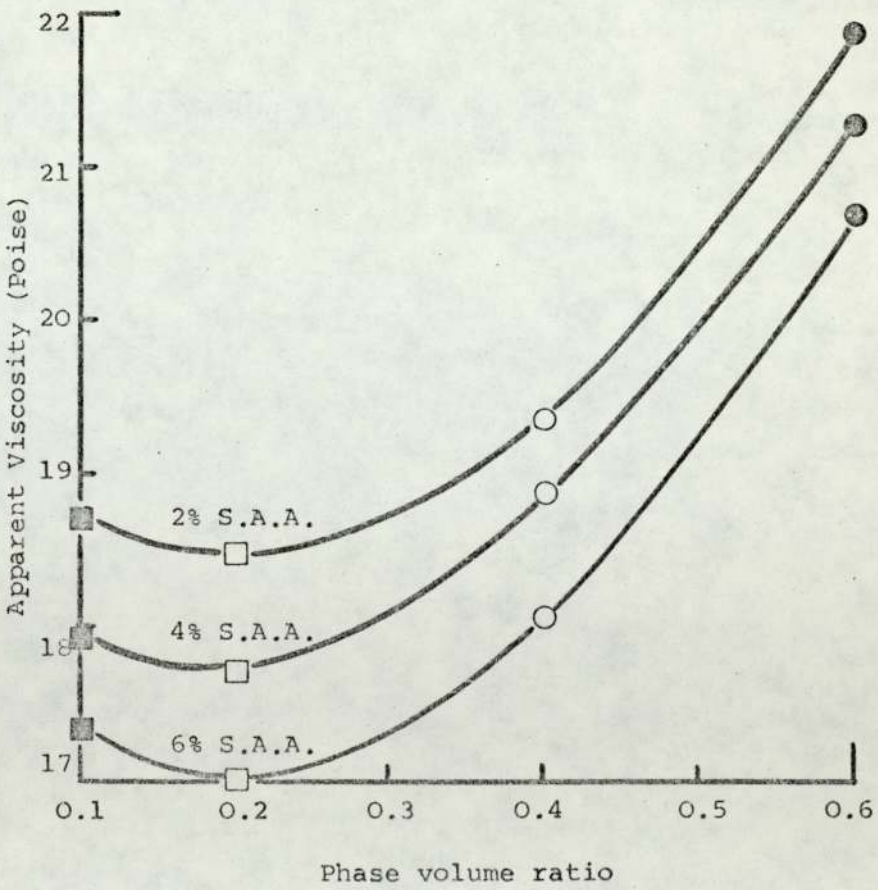

FIGURE 67

GRAPHICAL REPRESENTATION OF YIELD STRESS DATA DERIVED AT 25°C FROM CONTINUOUS SHEAR TESTING OF THE PLASTIBASE EMULSION SYSTEMS PREPARED BY THE COLD COMPOUNDING METHOD

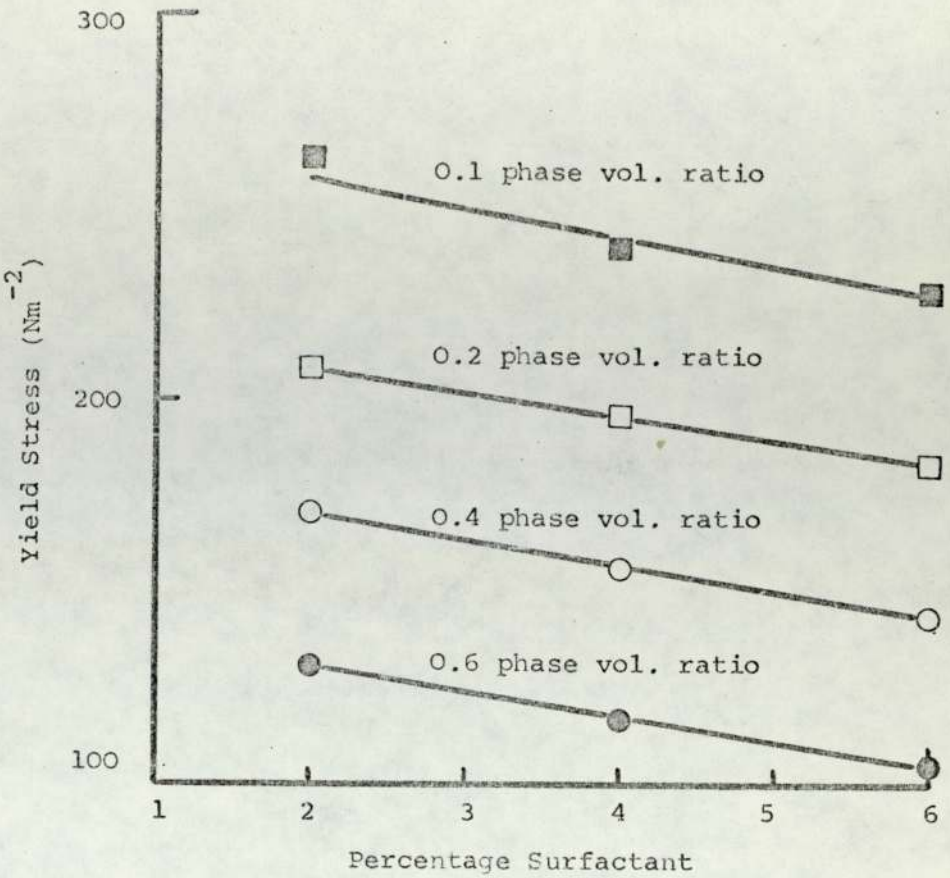

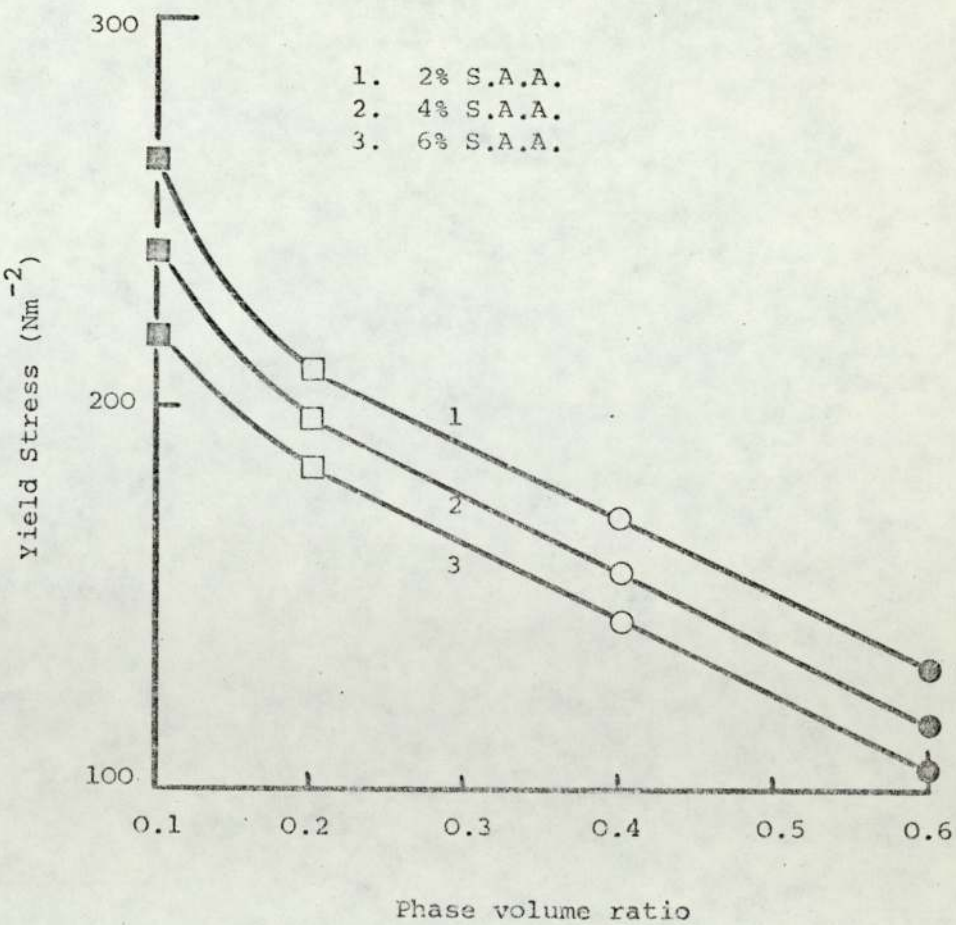

FIGURE 68

GRAPHICAL REPRESENTATION OF CONTINUOUS SHEAR DATA DERIVED AT 25°C FOR THE PLASTIBASE EMULSION SYSTEMS PREPARED BY THE HOT COMPOUNDING METHOD

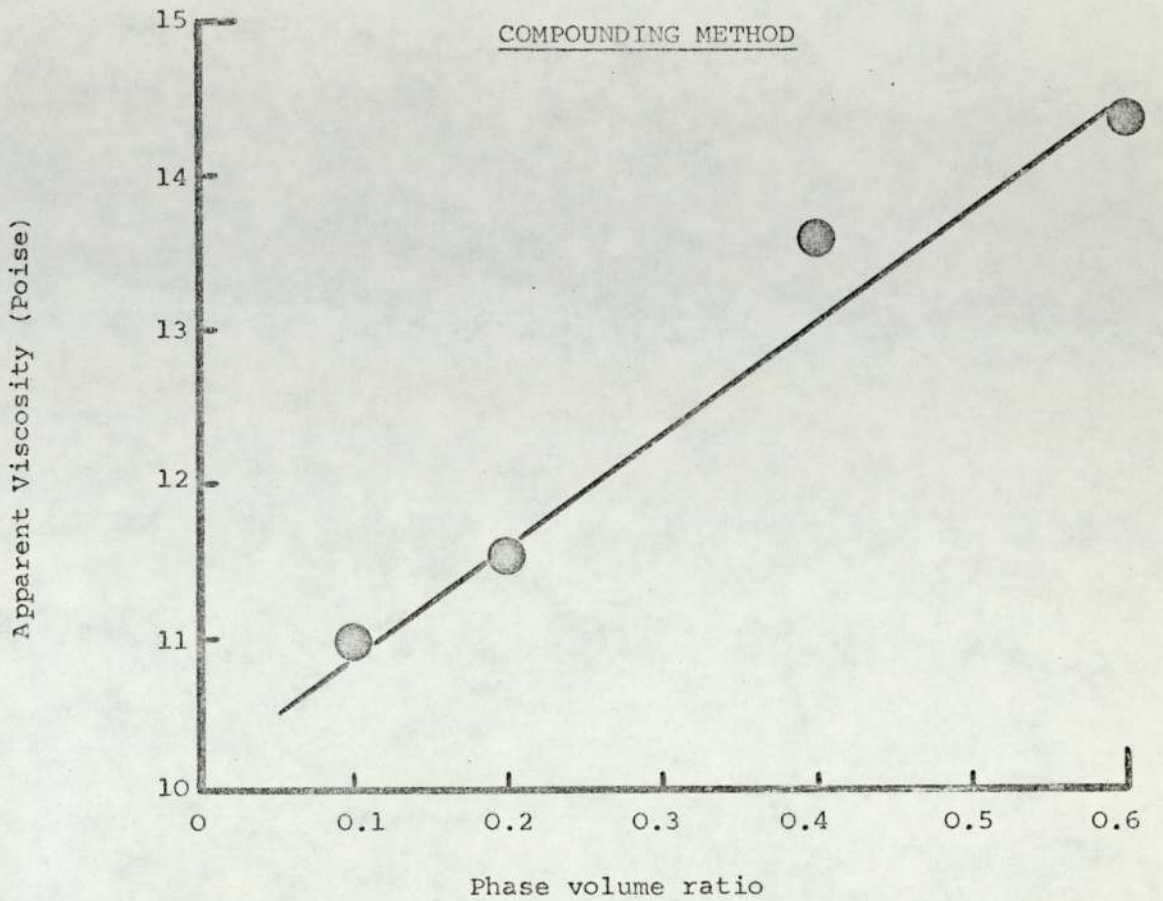

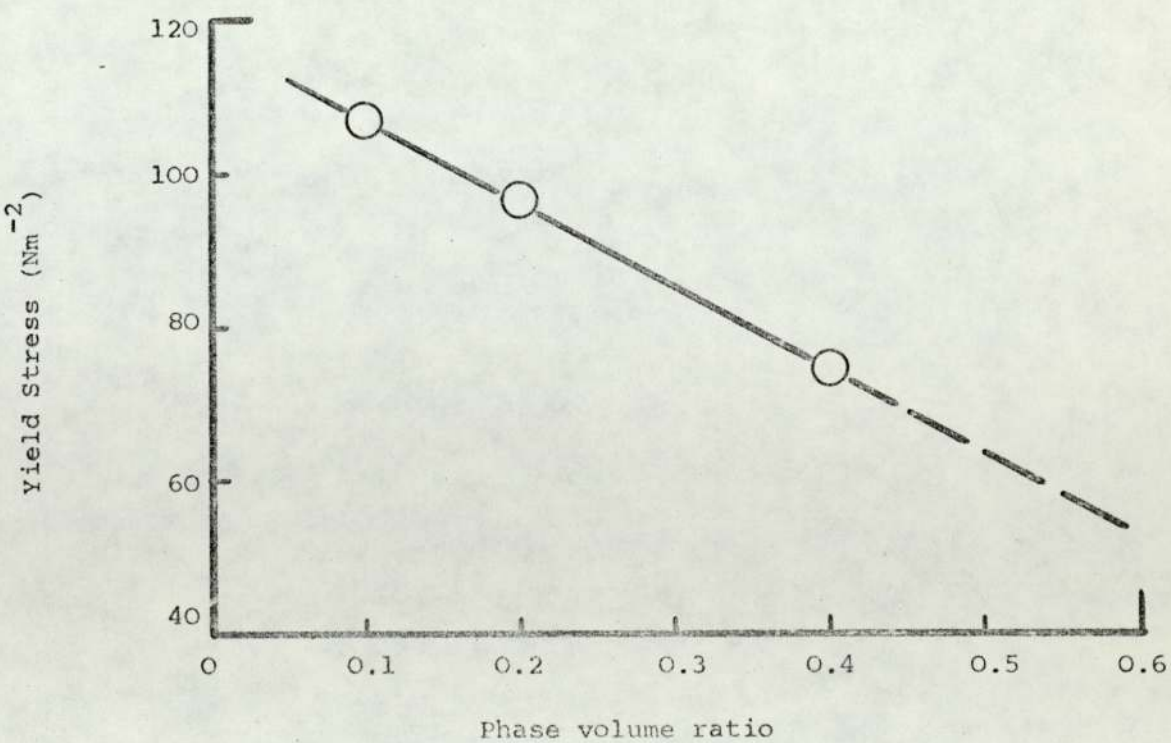

TABLE 33

CREEP DATA FOR PLASTIBASE 50W EMULSION SYSTEMS AT 25°C. INSTANTANEOUS COMPLIANCES ARE GIVEN IN m^2N^{-1}, RESIDUAL VISCOSITIES IN POISE AND RETARDATION TIMES IN SECS

	EM1	EM2	EM3	EM4	EM5	EM6	EM7	EM8	EM9	EM10	EM11	EM12
$J_o \times 10^{-4}$	2.39	2.72	5.36	15.01	2.17	2.50	4.67	14.44	1.93	2.47	4.32	10.31
$J_1 \times 10^{-4}$	7.67	10.31	16.09	17.15	7.36	10.00	11.26	17.90	7.00	8.25	9.01	9.24
τ_1	29	22	31.8	72.8	19.7	27.5	43.8	72.4	14.9	18.6	35.2	48.1
$\eta_o \times 10^4$	9.48	11.70	20.61	49.5	8.23	9.85	18.0	44.5	7.64	8.77	13.65	32.50
$\eta_1 \times 10^4$	37.81	21.34	19.76	42.49	26.77	27.50	38.90	40.45	21.29	22.55	39.07	52.06

TABLE 34

CREEP DATA FOR PLASTIBASE 50W EMULSION SYSTEMS AT 37°C. INSTANTANEOUS COMPLIANCES (Jo) ARE GIVEN IN m^2N^{-1} AND RESIDUAL NEWTONIAN VISCOSITIES (η_o) IN POISE

	EM1	EM2	EM3	EM4	EM5	EM6	EM7	EM8	EM9	EM10	EM11	EM12
$Jo \times 10^{-4}$	2.89	3.30	5.98	16.22	2.65	3.09	5.77	15.88	2.41	2.89	5.54	11.14
$\eta_o \times 10^{4}$	2.70	3.46	5.75	9.70	2.62	3.01	4.84	8.83	2.57	3.00	4.51	8.49

TABLE 35

CREEP DATA FOR PLASTIBASE 50W EMULSION SYSTEMS

EM1H TO EM4H AT 25°C.

INSTANTANEOUS COMPLIANCES (Jo) ARE GIVEN IN $m^2 N^{-1}$

AND RESIDUAL NEWTONIAN VISCOSITY (η_o) IN POISE

	EM1H	EM2H	EM3H	EM4H
$Jo \times 10^{-4}$	6.87	6.95	8.88	23.10
$\eta_o \times 10^{4}$	1.25	2.13	5.23	10.24

FIGURE 69

GRAPHICAL REPRESENTATION OF CREEP DATA DERIVED

FOR THE PLASTIBASE EMULSION SYSTEMS

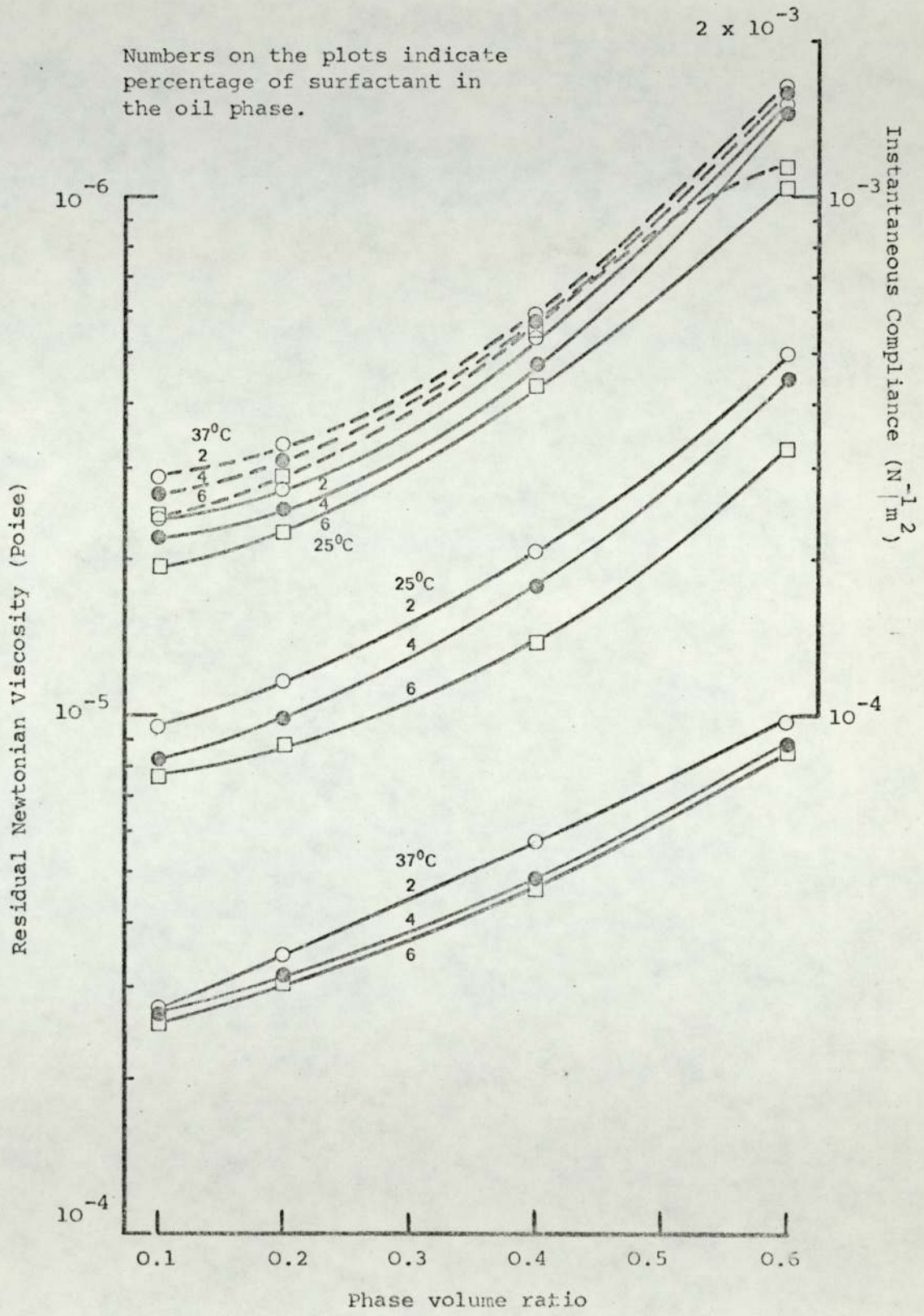

FIGURE 70 (a) CONTINUOUS RETARDATION SPECTRA OF THE PLASTIBASE EMULSION SYSTEMS

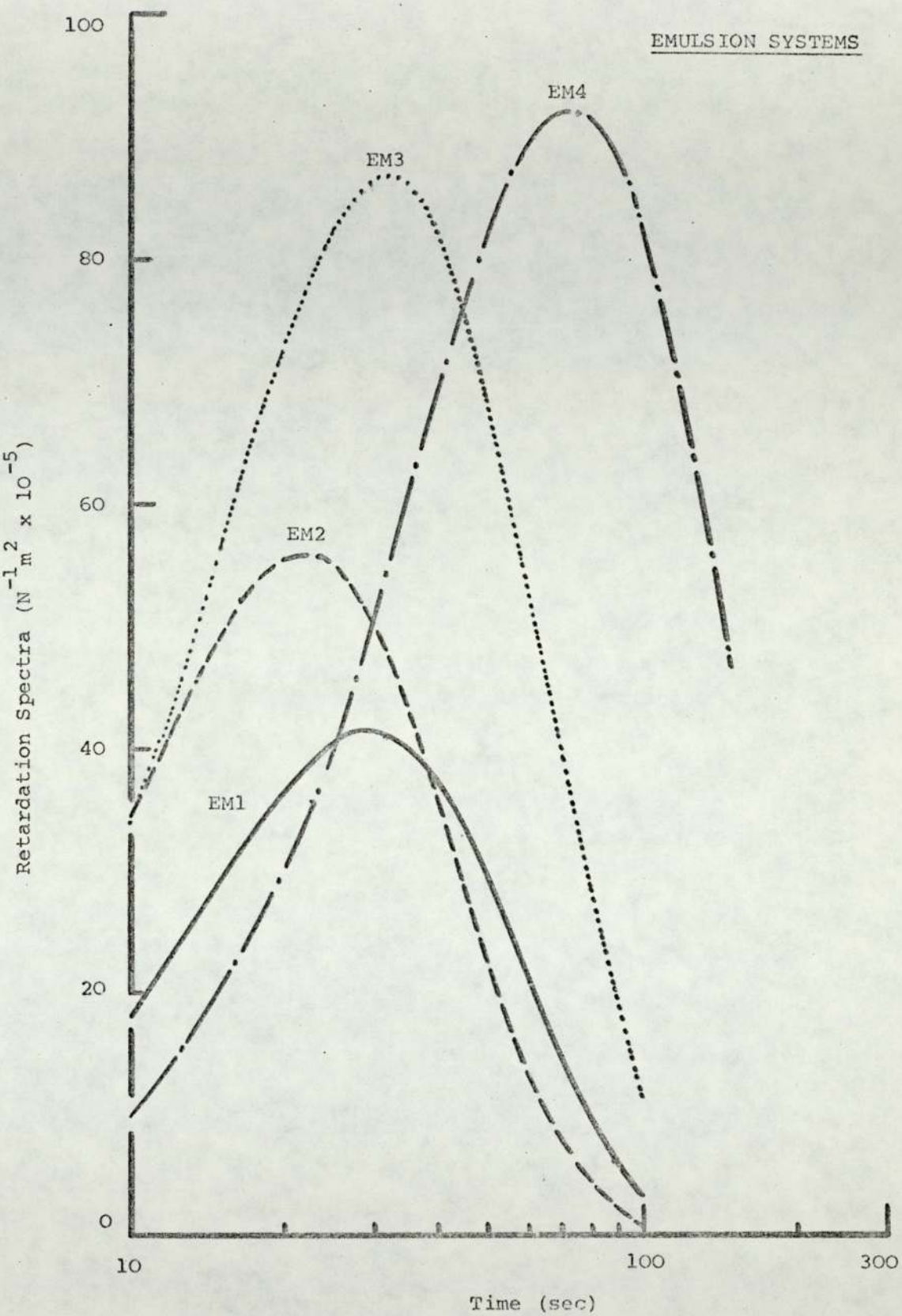

FIGURE 70 (b) CONTINUOUS RETARDATION SPECTRA OF THE PLASTIBASE EMULSION SYSTEMS

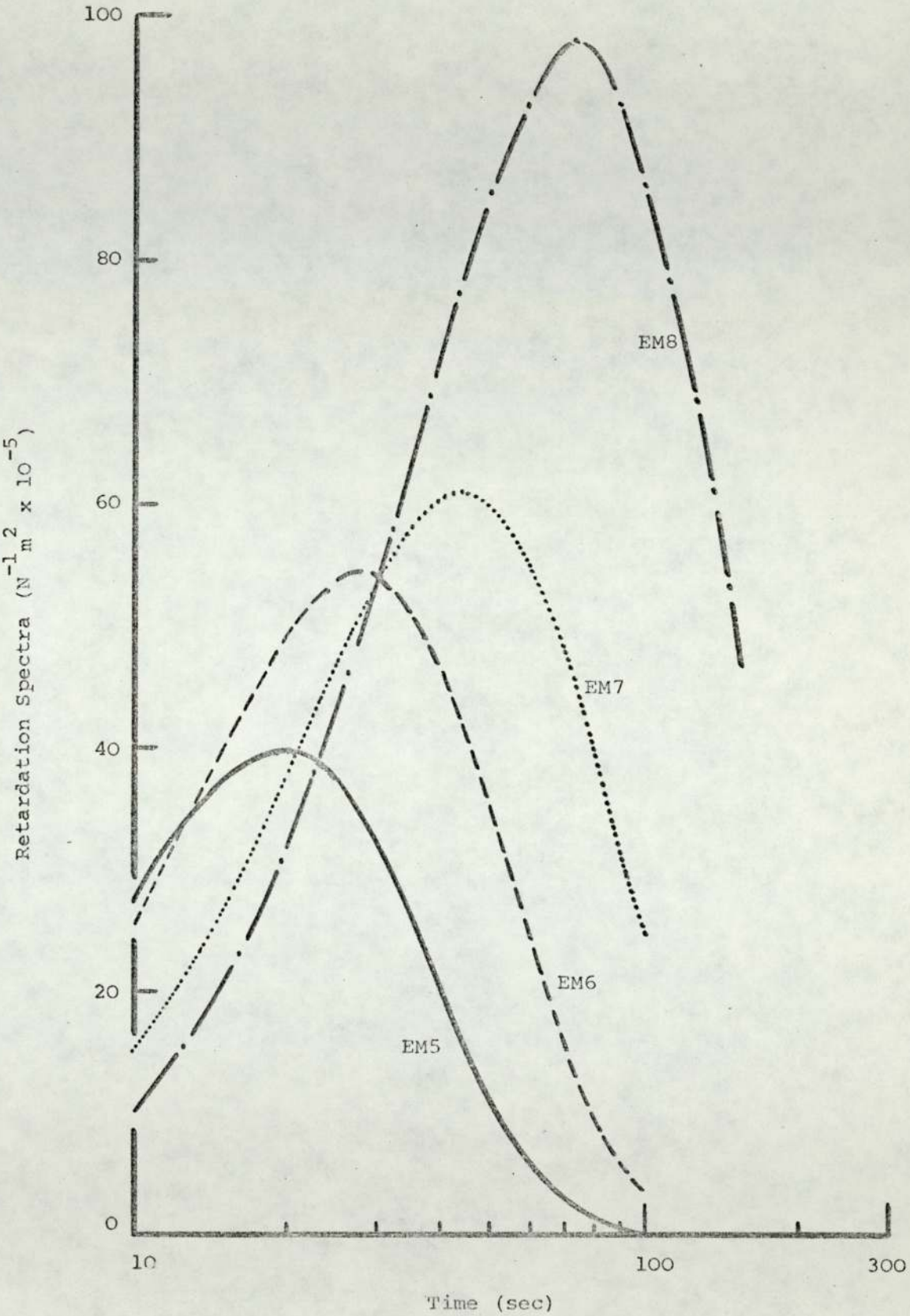

FIGURE 70 (c)

CONTINUOUS RETARDATION SPECTRA OF THE

PLASTIBASE EMULSION SYSTEMS

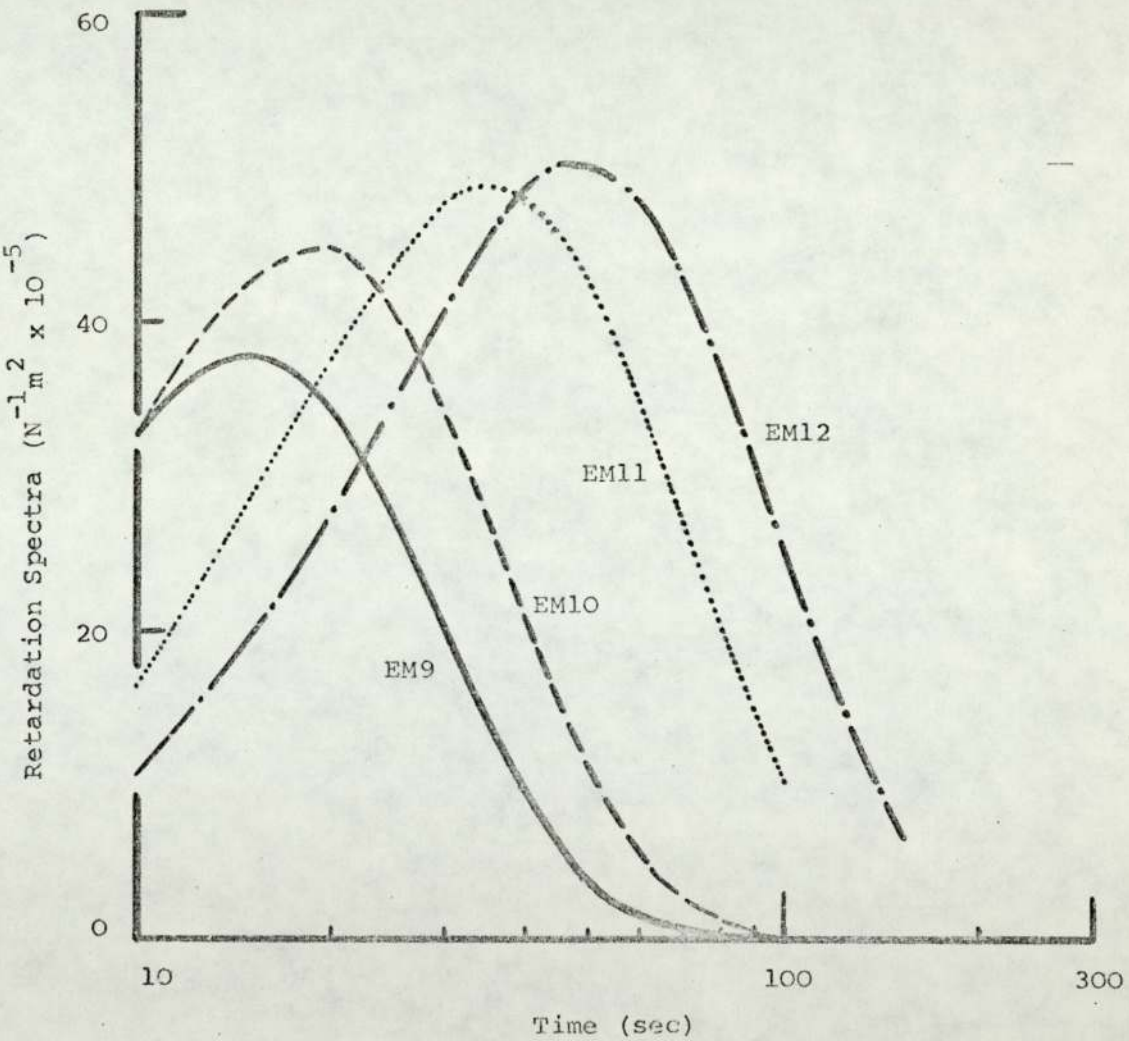

FIGURE 71

PHOTOMICROGRAPHS OF PLASTIBASE 50W EMULSION SYSTEMS

(magnified 1600 times)

Emulsions prepared by the cold compounding method

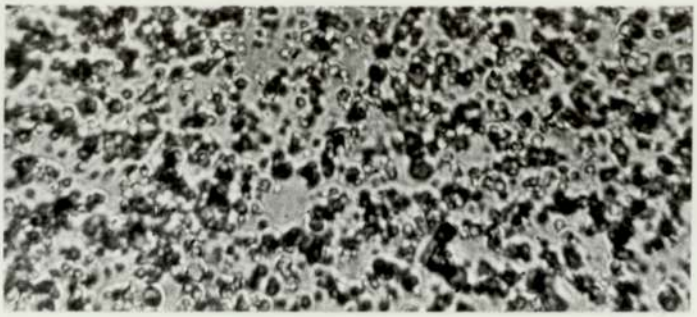

EM1

EM4

Emulsions prepared by the hot compounding method

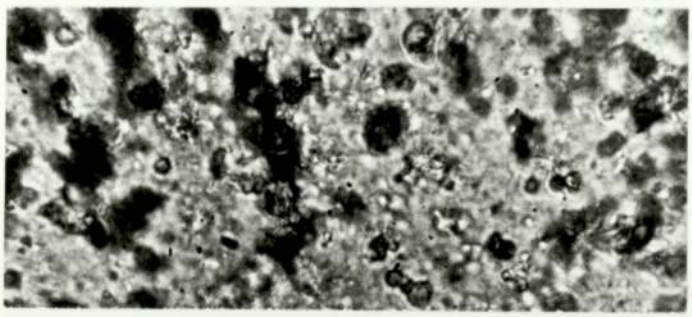

EM1H

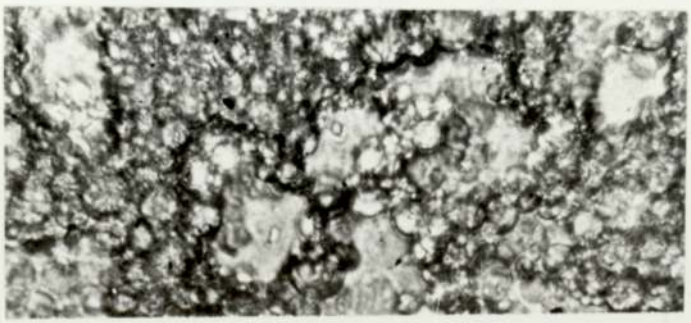

EM4H

increased with an increase in the phase volume ratio. The emulsions prepared by the hot compounding method were not tested at 37°C because of the rather low consistencies of these systems at this temperature.

Creep data for all the emulsion systems are given in Tables 33 to 35. The instantaneous compliance Jo and the residual viscosity η_o for emulsions 1 to 12 are plotted in Figure 69. Discrete spectral data, Table 33, show that the viscoelastic properties of all the emulsion systems may be characterised by one retardation time. Continuous spectra of retardation times for emulsions 1 to 12 at 25°C are shown in Figure 70. All the spectra show a single maxima which decreases in height with an increase in the surfactant concentration and moves to longer times with an increase in the phase volume ratio. The low consistencies of emulsions 1H to 4H prevented creep study of these at 37°C.

Microscopy of the emulsions revealed that the disperse phase globules were trapped in the three dimensional matrix of Plastibase 50W, Figure 71. The dispersed globules were much larger in the emulsions prepared by the hot compounding method than in those of similar compositions prepared by the cold compounding method.

None of the emulsions showed any signs of instability when examined twenty four hours after preparation. A week later however emulsions 3H, 4H, 4, 8 and 12 had cracked. A month later emulsions 1H, 2H, 3, 7 and 11 were also showing signs of cracking.

5.4.4 Discussion

Water/oil emulsion systems were produced by the incorporation of water in Plastibase 50W containing in the oil phase 2%, 4% and 6% Atmos 300. In allowing twenty four hours to elapse after the preparation of these systems and before commencing experimental measurements, it was ensured that the emulsions had reached an equilibrium state and that the measured parameters were a property of the systems alone.

Photomicrographs of the emulsions, Figure 71, show that there is a marked difference in the structure of emulsions prepared by the cold and hot compounding methods. In both cases the use of siliconised slide and coverslip as recommended by Barry et. al. (300) enabled a considerable reduction in the distortion of the emulsion particles. While it was not possible to carry out particle size analysis of the systems, it is evident from the photomicrographs that the mean particle size of the emulsions prepared by the cold compounding method is much smaller than that of emulsions prepared by the hot compounding method. In all cases the disperse phase particles appear to be flocculated, the extent of flocculation increasing with increase in the phase volume ratio.

Rheological properties of emulsions prepared by the cold and hot compounding methods are also markedly different. The emulsions prepared by the hot compounding method exhibit poor stability and a considerably lower consistency than those made by the cold compounding method. There are two reasons for this behaviour. Firstly, as was demonstrated in Section2, heating and slow cooling leads to a considerable reduction in the consistency of Plastibase 50W due to an alteration in the

structure of the material and this will affect the consistency of the emulsions. Secondly, the relatively large mean particle size exhibited by emulsions 1H to 4H will lead to reduced stability and relatively lower emulsion consistencies. It was thus evident that apart from shock cooling the hot emulsion mixture, the only other satisfactory method of preparing Plastibase emulsions was by a cold compounding method and emulsion 5 to 12 were subsequently made by the cold compounding method.

Continuous shear tests show a decrease in yield stress with an increase in both the surfactant concentration and the phase volume ratio of the emulsion systems. The apparent viscosity values, derived from continuous shear rheograms, decrease with an increase in surfactant concentration but increase with an increase in the phase volume ratio. Similarly, creep results for the emulsion systems show that the measured compliances and the residual viscosities increase with an increase in the phase volume ratio but decrease with an increase in the surfactant concentration. This behaviour is reflected in the continuous retardation spectra where increase in the elastic compliance is seen by an increase in the height of the spectra and an increase in viscosity is seen by a shift of the maxima to longer time indicating a decrease in the rate at which strain occurs (265). Continuous shear and creep results may be explained as follows.

The decrease in rheological parameters observed with an increase in the surfactant (in liquid form) concentration is largely a dilution effect and thus easily explained. The decrease in yield value and elastic modulus with an increase in the phase volume ratio of the systems may be explained as resulting from an increased penetration of the gel matrix by

the disperse phase particles which would lead to a weakening of the gel structure. The classical Einstein (301) equation and various other derivations relating viscosity with the concentration of the disperse phase indicate that increase in the phase volume ratio will lead to an increase in the 'viscosity' of the emulsion systems (i.e. up to phase inversion). Kostenbauder and Martin (298) have reported similarly a decrease in yield value and an increase in the plastic viscosity on addition of water to hydrophilic petrolatum.

Subjectively, the decrease in elastic modulus and an increase in the residual viscosity of the emulsions with an increase in the phase volume ratio is seen in an increased mobility of the systems. This is interesting as it reflects a reduced consistency of the material and will be measured as such by empirical methods of measurements such as the penetrometer. The results of such investigations (penetrometric) are likely to lead to the false impression that the 'viscosity' of the material is decreasing. This further demonstrates the ineptness of using empirical methods in rheological assessment.

Emulsions 1H to 4H prepared by the hot compounding method demonstrated very poor stability and demulsification of these systems was seen to occur relatively rapidly. Emulsions with a phase volume ratio of 0.6 prepared by the cold compounding method also demonstrated poor stability possibly owing to the rather high concentration of the disperse phase. The results of this study indicate that stable Plasti-base 50W emulsions may be prepared using a cold compounding method provided the phase volume ratio is kept between 0.2 to 0.3 and the Atmos 300 concentration in the oil phase is kept to between 2% to 6%.

5.5 Investigation of the Effects of γ - Irradiation of Plastibase 50W

5.5.1 Introduction

Microbial contamination of products can be a serious problem in the manufacture of semisolid pharmaceuticals. With the present day requirement that all ophthalmic ointments be sterile, the manufacture of sterile semisolid products is being closely scrutinised. Due to the thermolabile nature of the semisolid products, sterilisation by conventional heating techniques of the sealed final containers is not possible. Production units have been set up for the aseptic manufacture and filling of sterile ointments (302) however experience has shown that even these are not without their shortcomings and perfect sterility of the product manufactured by these units cannot be guaranteed (303). Moreover this form of aseptic production is rather costly. In these events, γ-irradiation sterilisation of pharmaceutical semisolids provides an attractive alternative (304), as this form of sterilisation procedure is accurately controllable, no initial aseptic handling is required and the temperature rise due to the sterilisation dose is very small - about $4^{o}C$ (305). Ionising radiation is however known to produce adverse physical and chemical changes in various materials (305) and an A.B.P.I. investigation of the effects of irradiation on pharmaceutical products (306) led to the conclusion that in many instances, 2.5×10^{6} rad dose required to ensure sterility produces changes that may make the preparation unacceptable for administration or presentation. Thus one of the objects of this study was to determine the effects of increasing γ - irradiation dose on the properties of Plastibase 50W.

γ-irradiation has been shown to retard the release of Quinidine from PVC matrix (307) and modify the physical properties of

hydrocarbon ointments (308). The other object of this study was to determine whether γ - irradiation would enable subtle changes in the rheological properties of Plastibase to be effected thereby providing the means of extending the range of available model Plastibase vehicles which could then be employed in drug release correlation studies.

5.5.2 Experimental

(a) Materials

Plastibase 50W Batch Number 2363

(b) Procedure

Seven 100g samples of Plastibase 50W were packed in 120g plain glass ointment jars and sent to the Atomic Energy Research Establishment at Harwell for irradiation treatment. The seven jars were subjected to 0, 0.5, 1.0, 2.0, 4.0, 8.0 and 16.0 megarad γ-irradiation doses respectively at the rate of 0.5 megarad per hour. On their return the samples were examined for any physical changes and were subsequently subjected to continuous shear and creep tests at 25°C and 37°C.

The Ferranti Shirley viscometer fitted with a medium cone was employed as described in Section 2 for continuous shear measurements. The samples were subjected to 0 to 460 to 0 sec^{-1} in 240 secs shear cycle. The creep apparatus was employed as described in Section 3. Creep curves for all samples were analysed for the initial elastic compliance (Jo) and the residual Newtonian viscosity (η_o).

The control and the 16.0 megarad irradiated samples were subjected to an X-ray diffraction study and the resulting diffraction patterns were examined for any changes in the crystalline structure between the irradiated and unirradiated Plastibase 50W.

5.5.3 Results

The colour of the clear glass jars in which Plastibase 50W was packed changed to brown on irradiation. This darkening in colour increased with increasing doses of irradiation. All irradiated samples showed a tendency to bleed and a bubbly effect indicating an evolution of a gas.

Continuous shear data for irradiated Plastibase 50W are given in Table 36 and shown in Figure 72. The yield stress and apparent viscosity appear to change in a regular manner with increasing doses of irradiation.

Creep data for irradiated Plastibase 50W are given in Table 37 and shown in Figure 72. Small changes in the initial compliance and residual viscosity are recorded with increasing doses of irradiation. A small increase in consistency is marked by an increase in the residual viscosity with a corresponding decrease in the initial compliance and vice versa. There appears to be a good correlation between the changes in consistency as determined from continuous shear tests and creep tests.

Figure 73 shows the X-ray diffraction pattern for the irradiated control and the 16.0Mrad irradiated Plastibase 50W. The diffraction pattern shows sharp rings superimposed on diffuse haloes.

TABLE 36

CONTINUOUS SHEAR DATA FOR IRRIDIATED PLASTIBASE 50W.

APPARENT VISCOSITY (η APP) IS GIVEN IN POISE AND

YIELD STRESS (Y_1) IS GIVEN IN Nm^{-2}

Radiation Dose M. Rad.	25°C		37°C	
	Y_1	η app	Y_1	η app
Control	414.0	20.87	290.9	13.57
0.5	392.7	20.15	268.2	12.88
1.0	313.9	18.63	208.2	12.04
2.0	415.3	21.85	267.7	13.30
4.0	422.8	22.69	311.6	14.29
8.0	329.5	19.82	218.6	12.74
16.0	449.1	22.13	307.5	13.73

FIGURE 72

GRAPHICAL REPRESENTATION OF CONTINUOUS SHEAR AND CREEP DATA DERIVED FOR UNIRRADIATED AND IRRADIATED PLASTIBASE 50W

TEMPERATURE IN ^{o}C

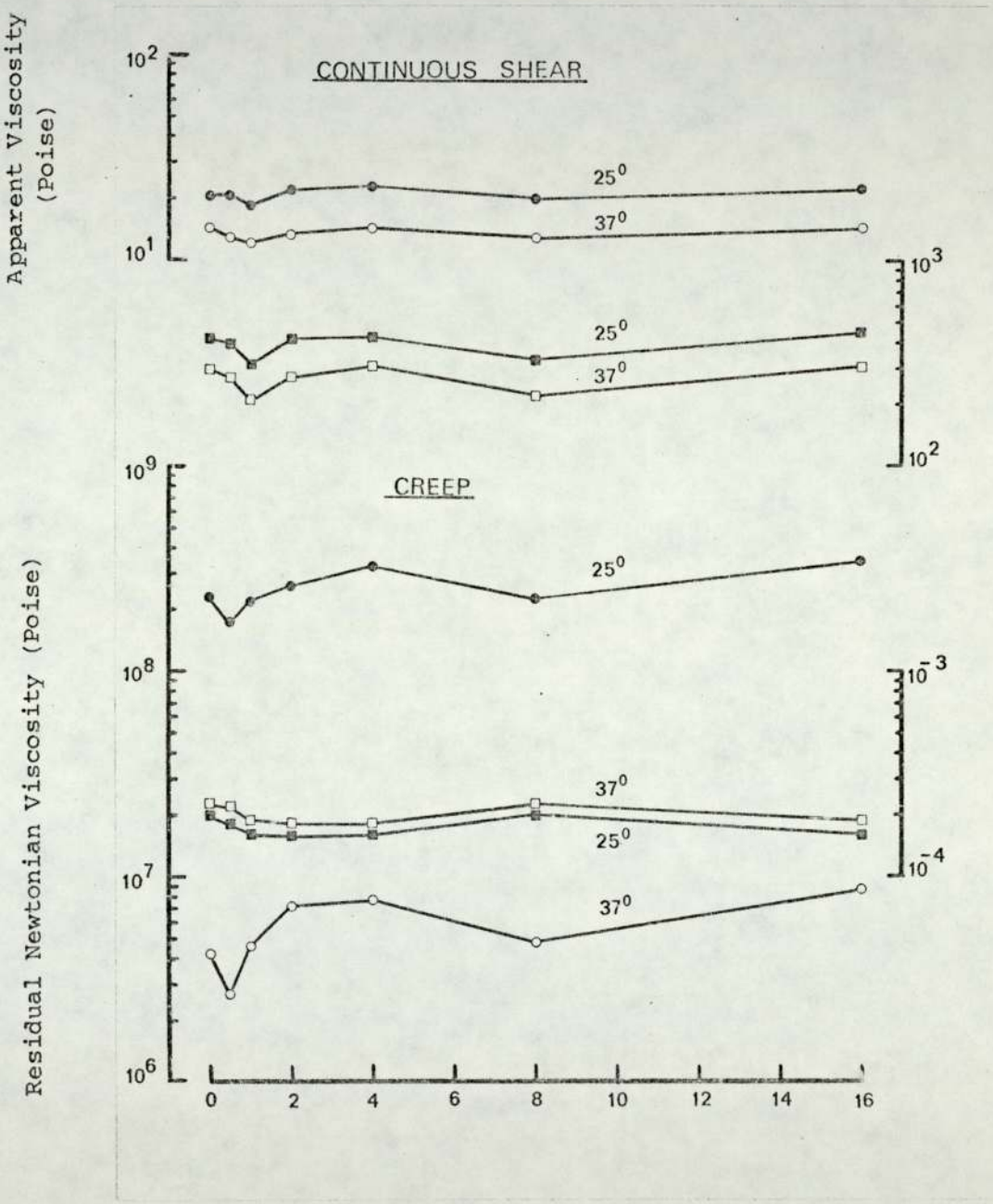

TABLE 37

CREEP DATA FOR IRRIDIATED PLASTIBASE 50W. INSTANTANEOUS COMPLIANCE (Jo)

IS GIVEN IN $m^2 N^{-1}$ AND RESIDUAL NEWTONIAN VISCOSITY IS GIVEN IN POISE

Radiation Dose M. Rad.	25°C		37°C	
	Jo	η_o	Jo	η_o
Control	2.00×10^{-4}	2.30×10^{8}	2.28×10^{-4}	4.26×10^{6}
0.5	1.78×10^{-4}	1.74×10^{8}	2.23×10^{-4}	2.67×10^{6}
1.0	1.61×10^{-4}	2.21×10^{8}	1.88×10^{-4}	4.60×10^{6}
2.0	1.59×10^{-4}	2.60×10^{8}	1.83×10^{-4}	7.28×10^{6}
4.0	1.61×10^{-4}	3.26×10^{8}	1.83×10^{-4}	7.76×10^{6}
8.0	2.03×10^{-4}	2.29×10^{8}	2.28×10^{-4}	4.80×10^{6}
16.0	1.61×10^{-4}	3.42×10^{8}	1.88×10^{-4}	8.75×10^{6}

FIGURE 73

X-RAY DIFFRACTION PHOTOGRAPHS

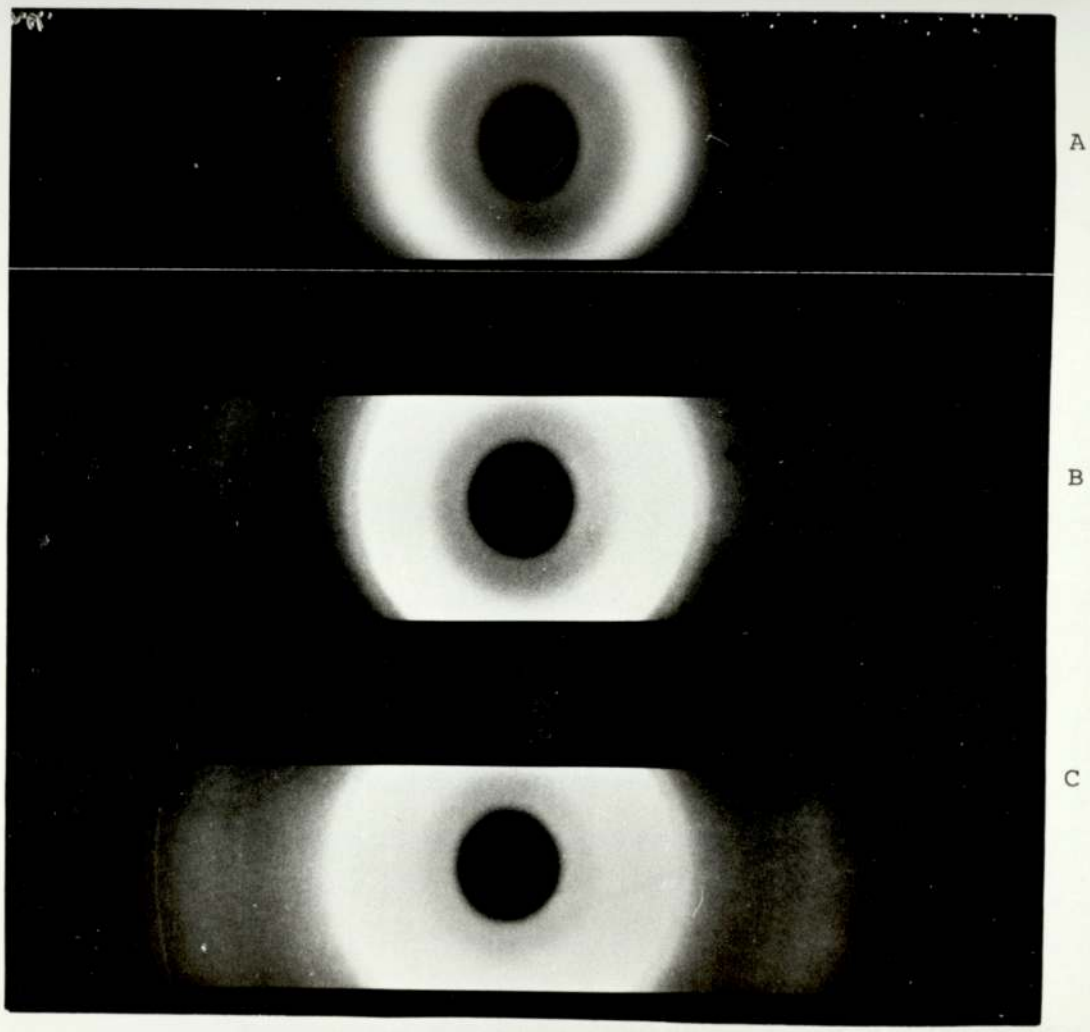

A Liquid Paraffin

B Plastibase 50W

C Irradiated Plastibase 50W (16.0 megarad)

5.5.4 Discussion

Visual physical changes observed after irradiation of Plastibase 50W are characteristic features of the effects of irradiation. Colour changes occurring in neutral glass are widely reported and indeed small pieces of glass are often included within packages as indicators of irradiation treatment (305). The evolution of gaseous and liquid fraction indicates release of hydrogen and low molecular weight hydrocarbons from the material (309).

In discussing the effects of irradiation on Plastibase 50W it is useful to draw a comparison with irradiation effects on paraffins and in particular polyethylene. The following major effects said to be observed (309, 310) when polyethylene is irradiated are analogous to those produced in low molecular weight paraffins:-

(i) Gases such as hydrogen and some low molecular weight hydrocarbons are evolved.

(ii) Crosslinking occurs by formation of C - C bonds between molecules.

(iii) There is an increase in unsaturation.

(iv) Crystallinity in the material may be destroyed by large doses of irradiation.

(v) Extensive exposure to irradiation may lead to colour changes.

(vi) In the presence of oxygen, oxidative reactions may cause polymer degredation and this would offset the effect of cross-linking.

Much of the reported work on polyethylene has been carried out at high doses of irradiation and thus direct comparison of work reported with work carried out at low doses of irradiation is difficult. However, on the basis of the reported work, it is possible to appreciate in some cases the phemenological changes occurring at low doses of irradiation.

Rheological data for unirradiated and irradiated Plastibase 50W show that there is a good correlation between continuous shear and creep data. There was no significant difference in the shape of the continuous shear rheograms for unirradiated and irradiated Plastibase 50W. Plots of rheological parameter verses irradiation dose show two minima and two maxima indicating four specific irradiation effects. The first minima occurs at 0.5 to 1.0 megarad and the second minima occurs at 8.0 megarad. The first maxima occurs at 3.0 megarad and the second maxima is indicated in the plots by a shoulder in the 16.0 megarad region. These effects may be tentatively explained in the following manner.

At low doses of irradiation, the only major physical change in Plastibase 50W comprises some evolution of a gas and a tendency to bleed indicating a possible disruption or reorientation of structure resulting in a decrease in consistency of the material. Increase in the irradiation dose to 3.0 megarad may lead to the formation of some cross-links in polyethylene. The major effect of this low degree of cross-linking in the material would be an increase in the degree of branching and in the average molecular weight (310). Irradiated Plastibase 50W however still behaves as a viscoelastic liquid and this is confirmed from the residual viscosity obtained in creep tests. The

effective increase in the molecular weight and degree of branching in polyethylene results in an increase in the consistency of Plastibase 50W. This maxima at 3.0 megarad corresponds to a maxima reported in the swelling measurements of low density polyethylene (310) at the same irradiation dose providing some evidence of the possible occurrence of cross-links. It has been shown that in polyethylene during irradiation, cross-linking and main chain fracture can occur simultaneously, at random and in proportion to the radiation dose, with cross-linking predominating (310). It is suggested in this work that increasing the irradiation dose beyond 3.0 megarad promotes oxidative degradation of the main polyethylene chain resulting in a reduction in consistency of the Plastibase. This is manifested in the minimum at 8.0 megarad. The consistency of Plastibase at this point corresponds to the consistency of the control. The consistency of Plastibase 50W is largely dependent on the extent of crystallinity in the material. Irradiation is known to bring about a reduction in the crystallinity of a material. X-ray diffraction patterns obtained for unirradiated and irradiated Plastibase 50W both show a sharp ring pattern superimposed on diffuse haloes. The sharp ring pattern for the irradiated Plastibase is seen to become somewhat weaker but there is no marked change in their spacing. These changes indicate a very small decrease in the crystallinity of the samples. This should produce a corresponding small decrease in the consistency of Plastibase 50W. Instead the plots of rheological parameter vs irradiation dose show an increase in consistency approaching a maxima in the 16.0 megarad region. It is proposed that the positive effects of cross-linking on increasing the dose of irradiation predominate over the combined negative effects of oxidative degradation and reduction in crystallinity, thus showing an increase in the consistency of Plastibase 50W. This latter observation is confirmed by

the work of Huttenrauch et. al. (308). They have reported a consistent increase in the 'viscosity' of polyethylene-mineral oil gels with an increase in the irradiation dose.

The results in this work show that irradiation of Plasti-base 50W does not lead to any gross adverse physical change in the material. Irradiation does bring about small changes in the rheological properties of the material which depends largely on the balance between the cross-linking effect on one hand and oxidative degradation and reduction in crystallinity on the other.

PART C

RELEASE OF DRUGS FROM PLASTIBASES

1. INTRODUCTION

1.1 Plan of Drug Release Investigation

The object of this part of the study was to determine the release characteristics of 'model' drugs incorporated in Plastibases and thereby determine what influence rheological properties have on the release of drugs from Plastibases.

The drug release study was carried out using *in vitro* and *in vivo* methods. A simple *in vitro* method of evaluating drug release from Plastibases was designed for this work. *In vivo* drug release was evaluated in human volunteers from skin irritation and urinary excretion data. *In vitro* and *in vivo* drug release data have been compared and subsequently correlated with rheological data.

1.2 'Salicylates' as 'Model' Drugs within the context of this work

Salicylic acid, methylsalicylate and ethylsalicylate were chosen in this work as 'model' drugs for the following reasons:-

(i) The drugs have the desired solubility characteristics in Plastibases. Salicylic acid exhibits poor solubility in Plastibase. Methyl- and ethylsalicylate on the other hand are completely miscible in Plastibase. The respective solubility of these drugs would enable their release to be studied in light of current theories relating to the release of a uniformly suspended and a uniformly dissolved drug from a semisolid vehicle (Part A. Section 3.4.3).

(ii) The drugs are capable of rapid and accurate analysis.

(iii) They are known drugs with relatively low toxicity. This was an important consideration as it ensured that *in vivo* studies in human volunteers would not create any practical difficulties.

In addition to the above considerations, salicylic acid, methyl- and ethylsalicylate are well known to be absorbed through the skin (311, 312, 115). These drugs have the advantage that their analysis and their actions, metabolism and elimination in humans and animals have been extensively studied (313, 314). It was thus considered that the 'salicylates' were suitable model compounds for this study.

2. IN VITRO DRUG RELEASE FROM PLASTIBASES

2.1 Introduction

Several workers have previously studied the release of various drugs from Plastibase 50W and Plastibase Hydrophilic (Table 3). A large proportion of this work has been of a comparative nature aimed at determining the relative efficacy of Plastibase 50W and Plastibase Hydrophilic compared with other vehicles. Seldom has any attempt been made to fit a model to the drug release data in order to explain the relative release characteristics of the vehicles. Study of the release of drugs from the lower consistency Plastibases (30W, 20W, 10W and 5W) has largely been ignored.

The purpose of the work reported in this Section was to study the release characteristics of salicylic acid, methylsalicylate and ethylsalicylate from all five grades of Plastibase and thereby determine what influence rheological properties have on the release of a drug from these vehicles. This objective required the:-

(i) design, setting up and characterisation of a simple *in vitro* drug release model;

(ii) determination of the drug release characteristics of the five grades of Plastibase, and

(iii) determination of the influence of rheological properties of Plastibases on the *in vitro* release of a drug which is in the form of a suspension and one that is in solution from these vehicles.

2.2 Materials

Plastibase 50W	Batch Numbers 2363 and 118
Plastibase 30W	Batch Numbers Not given
Plastibase 20W	Batch Numbers Not given
Plastibase 10W	Batch Numbers 2122
Plastibase 5W	Batch Numbers 1280

Salicylic acid, methylsalicylate and ethyl salicylate were all of analytical grade (B.D.H.)*. Other materials were as described below.

2.3 Experimental

2.3.1 In vitro drug release apparatus

(a) Design

The design of the drug release apparatus in this study, Figure 74, is a modification of the method proposed by Billups & Patel (233). The apparatus is simple in design, easy to set up and quick to assemble in routine use. It comprises basically of two compartments separated by a membrane; the quantity of drug diffusing out of the ointment and into the diffusion fluid (receptor phase) being measured spectrophotometrically. The choice of various components of the apparatus is dicussed below:-

---

* Salicylic acid was sieved through a No. 85 (315) sieve prior to each occasion it was used. The same batch of salicylic acid was used throughout this work.

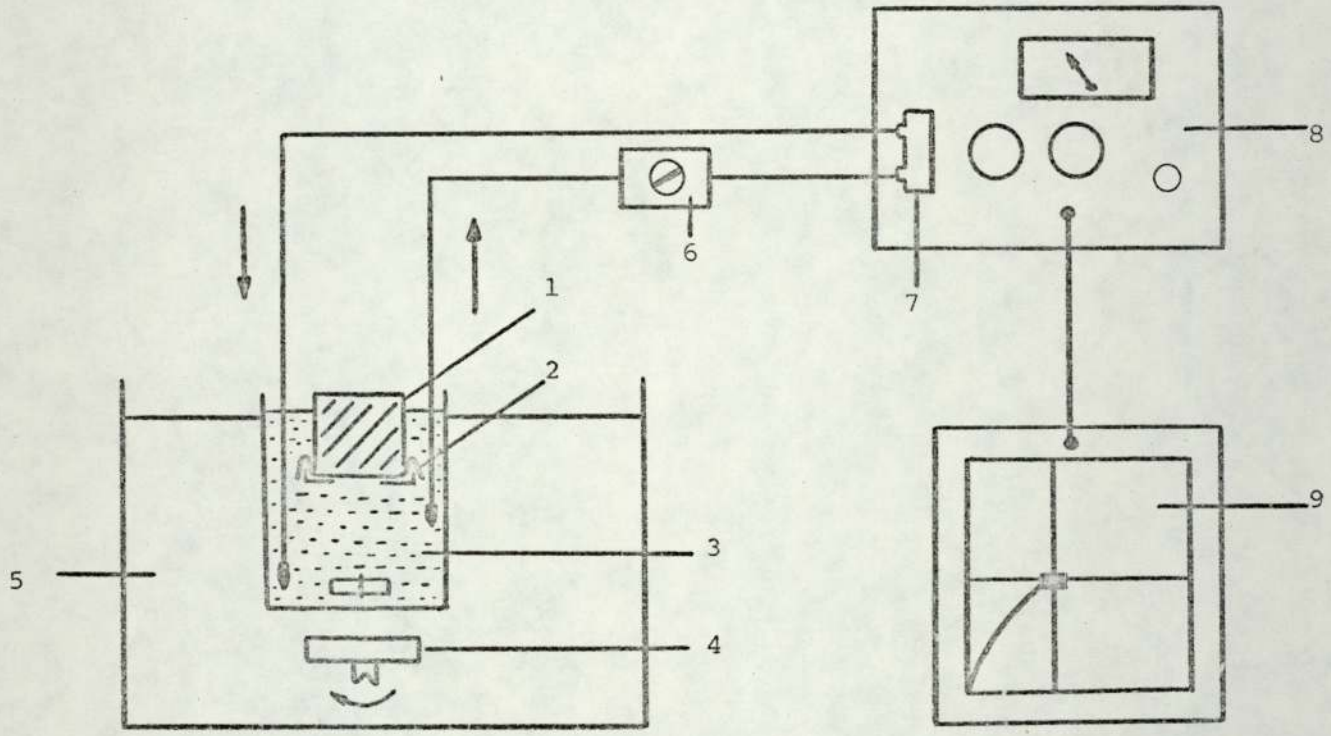

FIGURE 74

A SCHEMATIC DIAGRAM OF THE IN VITRO DRUG RELEASE APPARATUS

1. Ointment jar containing sample. 2. Membrane. 3. Diffusion fluid (receptor phase) - Saline.

4. Magnetic stirrer. 5. Water bath. 6. Peristaltic pump. 7. Flow-through cell.

8. UV Spectrophotometer. 9. Graph plotter.

(i) Diffusion Cell

A 25g ointment jar with a circular aperture (2.8575 cm diameter) made in the cap was used as a diffusion cell. It served the purpose of holding the ointment in place (as some of the ointments were somewhat mobile) and ensuring that the diffusion of the drug from the ointment was modulated through a constant surface area (6.4 cm^2). The preparation of the diffusion cell for an experimental run is illustrated in Figure 75 and described below.

The ointment was packed into the jar until full and the surface levelled with a spatula. A membrane was next placed over the mouth of the jar. A cardboard washer ensured that when the cap was screwed on, the membrane did not rupture or wrinkle. Finally, a strip of "Parafilm" was used to seal the side of the jar in order to ensure that the drug did not leak out from the side.

(ii) Membrane

There is a growing tendency in investigative work of this type to used excised human skin as the membrane (76, 100, 316, 317). In this work, initial studies of organising a procedure for the use of excised skin as the membrance have highlighted several difficulties. These include establishing a constant source of supply of human skin (particularly difficult in this country as collaborative research interests between hospitals and schools of pharmacy are somewhat scarce), ensuring that the techniques of excision and separation of the required

FIGURE 75

AN ILLUSTRATION OF THE PREPARATION OF THE DIFFUSION CELL

thickness does not have harmful effects on the morphology of the skin, arriving at standards (freezing, thickness, treatment, etc.,) to reduce interbatch variation in membranes and ensuring that the integrity of the membrance is maintained during the time course of the experiment. A considerable number of the above mentioned histological studies would have to be carried out routinely in conjunction with the in vitro experimental runs. This would thus further complicate the work and make it particularly time consuming. Finally, the results of in vitro work using excised skin would have to be correlated with the in vivo situation. On reflection, it was considered that there was no greater benefit to be gained in using excised human or animal skin in this work and thus these studies were curtailed. Indeed, it was found that the use of artifical membranes has distinct advantages. These membranes are uniform, reproducible and easy to use. Moreover, they do not deteriorate during the time course of an experiment.

Artificial membranes most commonly used in drug diffusion studies are those made of cellulose derivative, e.g. cellophane (22, 172, 233, 318, 319), or silicon rubber, e.g. polydimethylsiloxane (Trade Name Silastic) (177, 181, 320 - 3). Drug transport in a cellophane membrane occurs by a process of dialysis through pores present in the membrane (118, 177). The drawback of these membranes being that there is little selectivity in the transport of material through the pores, e.g. solvent and solute may both be transported through the pores provided that their size is smaller than

the size of the pores (177) or the diffusion fluid may permeate into the ointment compartment and form an aqueous solution of the drug in the diffusion cell with the result that subsequent release of drug from the ointment compartment would be through an aqueous solution rather than the base (181, 319). Drug transport in a silastic membrane occurs by a process of partitioning of the drug into and diffusion through the membrane (181, 322). This process is akin to drug transport through the skin and indeed Nakano & Patel (181) have reported that "based on the agreement of *in vitro* release pattern with *in vivo* data (324), a silicon membrance appears to be ideal for investigating drug release from diverse bases".

Silastic membranes with labelled thickness of 0.127mm (Batch Number HH0939) were used in this study. These membranes are made by Dow Corning Corp., Michigan and supplied through Lepetit Pharmaceuticals Limited, Maidenhead. The same batch of membranes was used throughout this study in order to avoid any interbatch variation that may result due to an alteration in filler content (325), etc. The membranes were soaked in warm water for half an hour prior to use in order to clean and remove the sodium bicarbonate that is dusted on the membranes by the manufacturers to facilitate handling. After each experimental run the membranes were discarded and were not re-used.

(iii) Diffusion fluid (receptor phase)

Normal saline (Polyfusor, Boots) was used as the diffusion fluid in this work. 400ml of saline was used per experimental

FIGURE 76

AN ILLUSTRATION OF THE CLOSED CELL USED FOR METHYL SALICYLATE RELEASE

run, providing 'sink' conditions for drug diffusion. Two types of receiving compartments were employed. Where release of salicylic acid from semisolid vehicles was being investigated, a 500ml beaker was used as the receiving compartment. Where release of methyl salicylate was being investigated however, due to the volatile nature of methyl salicylate, a closed cell was required in order to reduce to a minimum loss of the drug by evaporation. For this reason a "Kilner" jar was used as the receiving compartment and the drug release cell was assembled as illustrated in Figure 76. The diffusion fluid in the receiving compartments was stirred with a teflon coated magnetic stirring rod which was driven by a synchronous motor. The stirring speed was checked regularly with the help of a stroboscope.

(iv) Sampling and Assay

All the drugs obeyed the Beer-Lambert relationship at their wavelength of maximum absorption within the concentration range tested, Figures 77 to 79. Concentration of a drug in the diffusion fluid (receptor phase) was thus determined after recording its absorbance by referring to the respective plot of absorbance versus concentration.

Sampling was carried out continuously with the use of a flow-through cell (Pye Unichem Part No. 681223). The diffusion fluid was pumped at a predetermined rate (400ml/hr) with the aid of a peristaltic pump (MHRE Mk III, Watson-Marlow Limited, Falmouth) in a closed circuit through the cell assembled in the

FIGURE 77

BEER-LAMBERT PLOT FOR SALICYLIC ACID OBTAINED AT

λ = 295nm USING A 10mm PATH LENGTH AND NORMAL SALINE

AS SOLVENT

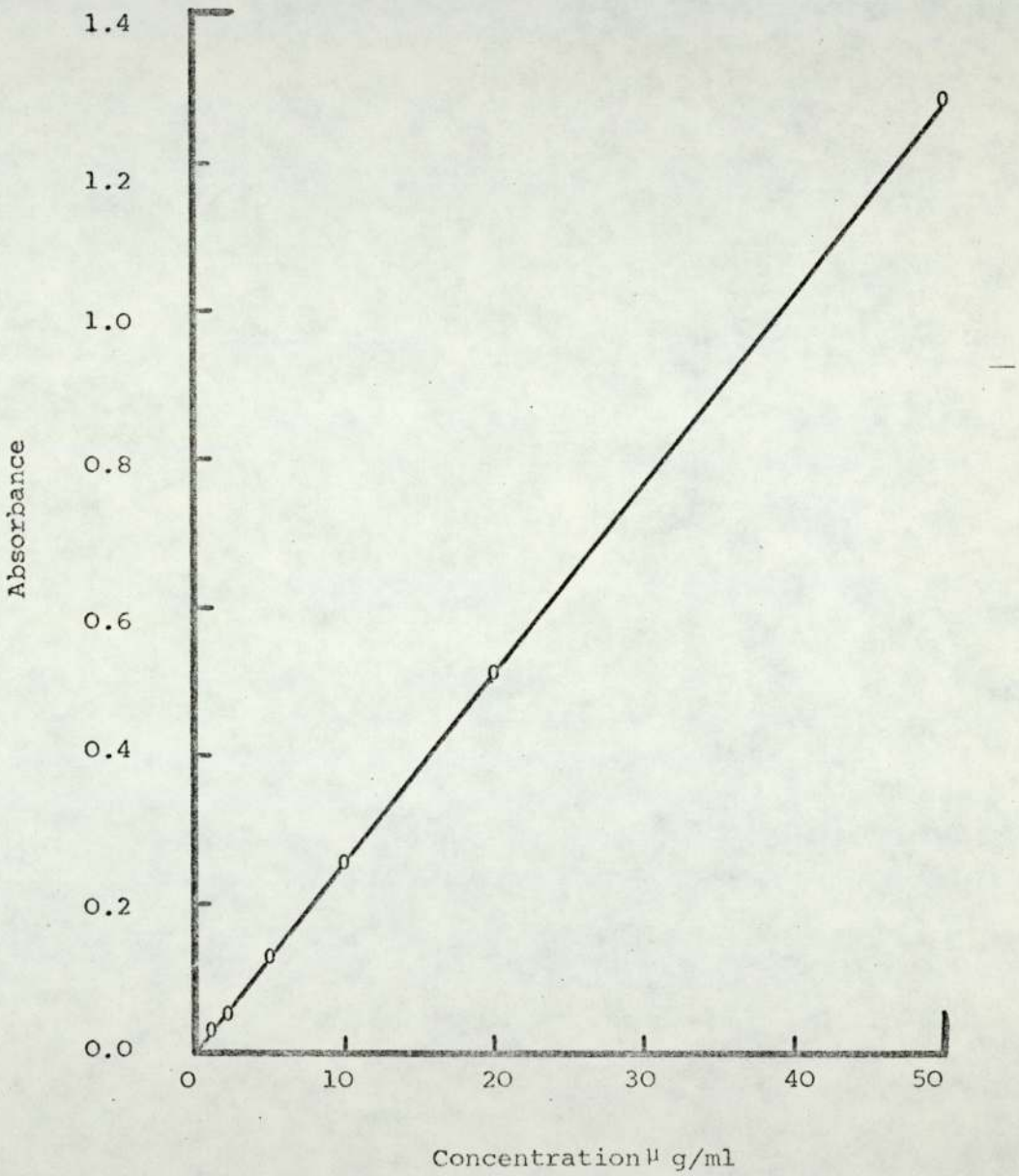

FIGURE 78

BEER-LAMBERT PLOT FOR METHYL SALICYLATE OBTAINED AT

λ = 302nm USING A 10mm PATH LENGTH AND

NORMAL SALINE AS THE SOLVENT

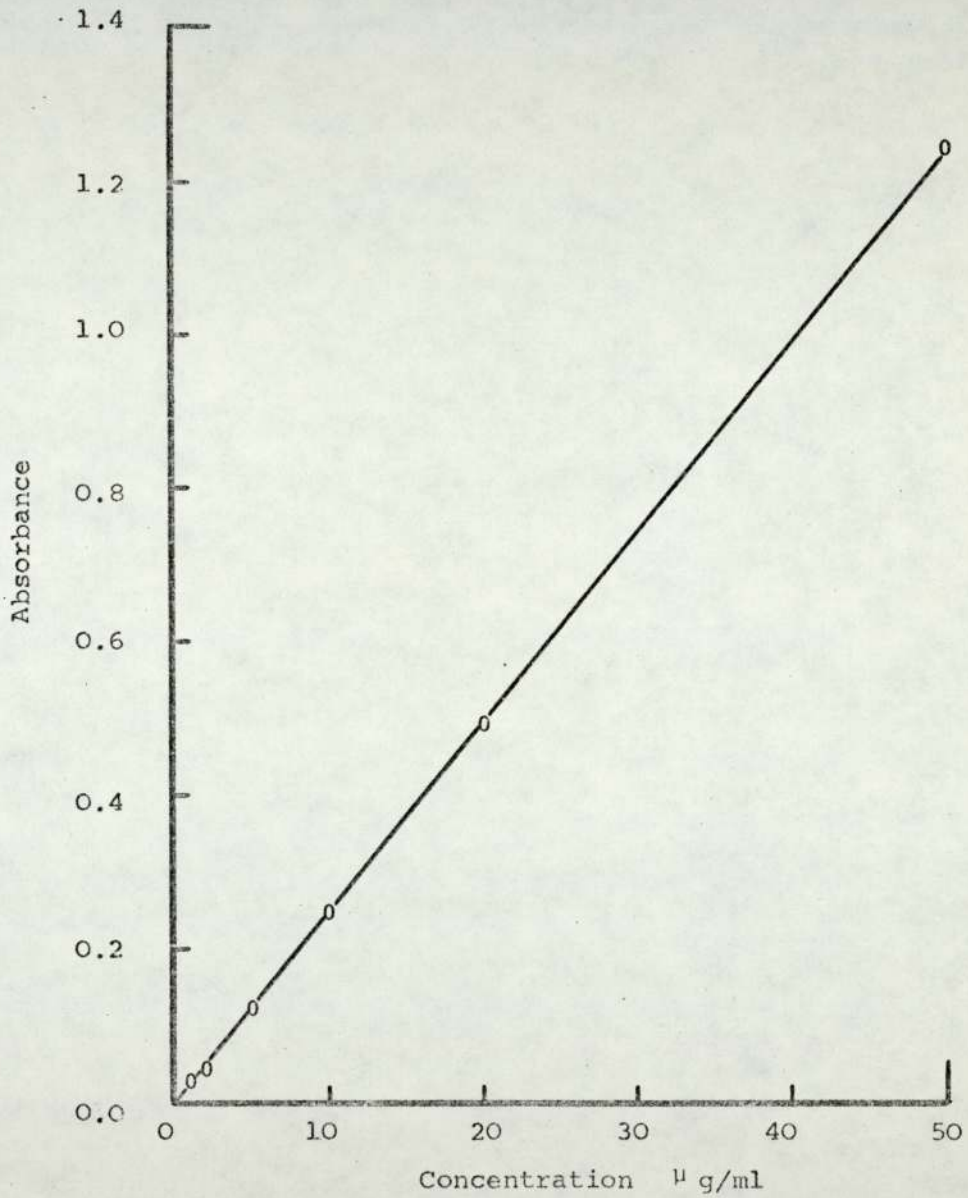

FIGURE 79

BEER-LAMBERT PLOT FOR ETHYL SALICYLATE OBTAINED

USING A 10mm PATH LENGTH AND NORMAL SALINE AS THE SOLVENT

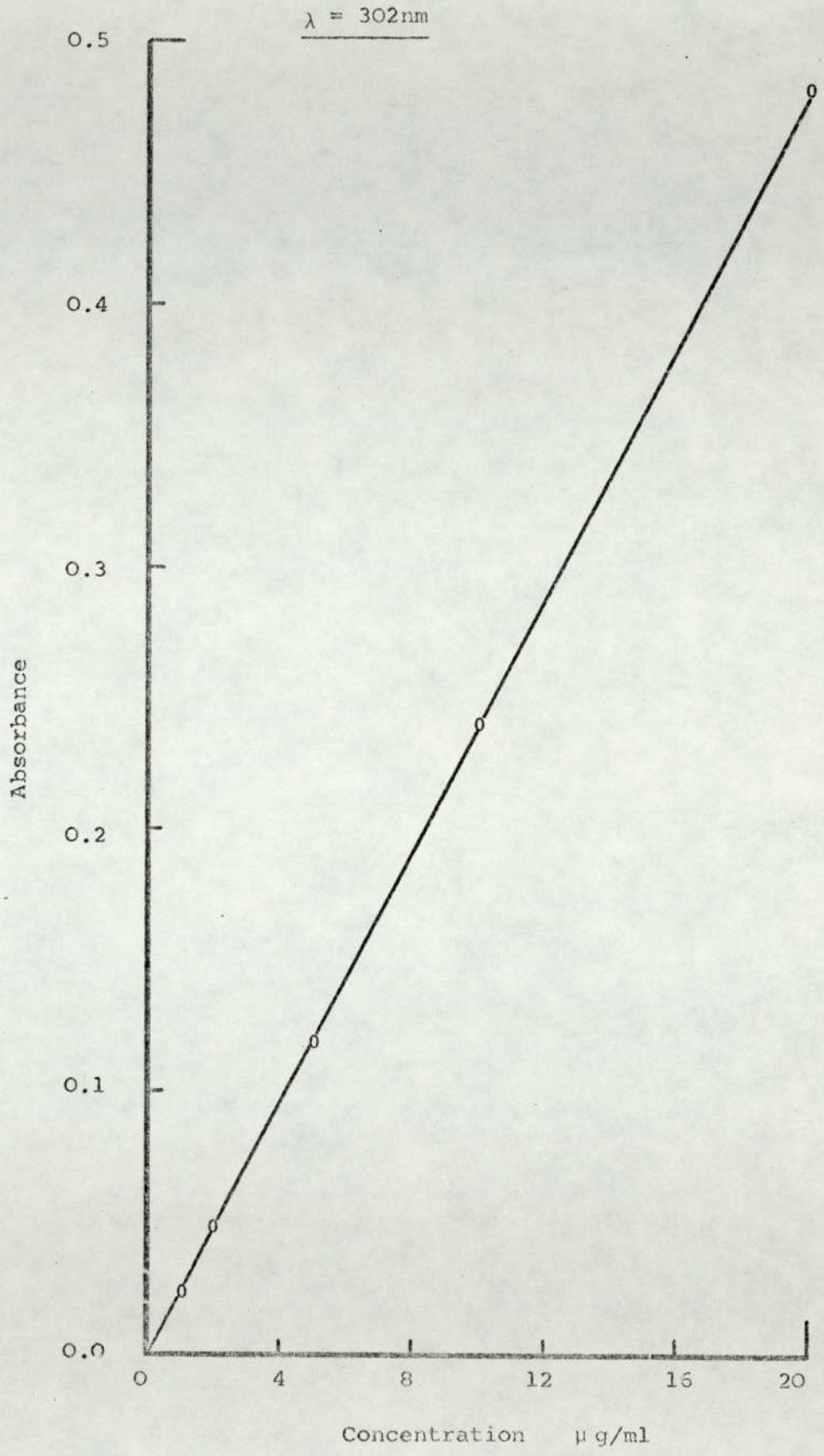

cell housing of a UV Spectrophotometer (SP 500 Series 2, Pye Unichem). The absorbance of the solution flowing through the cell was recorded at regular time intervals and converted to concentration by referring to the Beer-Lambert plots.

(v) Temperature

Temperature control of the drug release cell was achieved by using a thermostatically controlled water bath (Grant Instruments).

(b) Routine use of drug release apparatus

In routine use the apparatus was assembled as shown in Figure 74 in the following manner.

400ml of diffusion fluid contained in the receiving compartment of the drug release cell was allowed to equilibrate in a thermostatically controlled water bath at the test temperature. The diffusion fluid was stirred with a teflon coated magnetic stirring rod which was driven by a synchronous motor. After a suitable period of equilibration, circulation of the diffusion fluid through the spectrophotometer cell was started and the spectrophotometer was zeroed. The diffusion cell was next prepared as stated in Section 2.3 (a)(i). At zero time the diffusion cell was lowered into the diffusion fluid up to three quarters of its height. The absorbance of the diffusion fluid flowing through the spectrophotometer cell was measured at regular intervals and converted to concentration by reference to the Beer-Lambert plot.

(c) Reproducibility characterisation of the apparatus

The reproducibility of drug release studies was tested by studying the release of salicylic acid ($\simeq$ 10%) from Plastibase 50W (Batch No. 2363) at 37°C. Two drug release studies were performed on each of five days. The same batch of ointment was used for all ten experiments. The results of this study are shown in Table 38. Analysis of these results shows that at no point during the course of the experiment the standard error of the mean exceeds 1.5%.

(d) Derivation of the diffusion coefficient from drug release data

Diffusion coefficients were derived from drug release data according to the models proposed by T. Higuchi and W.I. Higuchi (11, 164, 165) as outlined in Section 3.4.3 of Part A. For clarity, the derivation of the diffusion coefficient from a model drug release plot illustrated in Figure 80 is detailed below:-

(i) Release of a uniformly dissolved drug

The diffusion coefficient of a uniformly dissolved drug was found (326) by rearranging Equation (53):

$$D = \left\{ \frac{Q}{\sqrt{t}} \cdot \frac{\sqrt{\pi}}{2Co} \right\}^2 \qquad \ldots (85)$$

where Q = drug release in g/cm^2 and Co = initial concentration in g/cm^3.

Assuming that Figure 80 represents the release of a uniformly dissolved drug, then:

TABLE 38

REPRODUCIBILITY CHARACTERISATION OF THE APPARATUS

Time (hr)	Drug release measured in absorbance units										Mean Absorbance	Standard error of the mean
	Day 1		Day 2		Day 3		Day 4		Day 5			
	Run 1	Run 2	Run 3	Run 4	Run 5	Run 6	Run 7	Run 8	Run 9	Run 10		
0.0	0.0000	0.0000	0.0000	0.0000	0.0000	0.0000	0.0000	0.0000	0.0000	0.0000	0.0000	$\pm$ 0.0000
1.0	0.0800	0.0810	0.0800	0.0740	0.0825	0.0850	0.0790	0.0815	0.0825	0.0815	0.0807	$\pm$ 9.14×10^{-4}
2.0	0.1460	0.1490	0.1440	0.1420	0.1460	0.1430	0.1420	0.1460	0.1450	0.1470	0.1450	$\pm$ 7.15×10^{-4}
3.0	0.2040	0.2070	0.1990	0.1980	0.1940	0.1905	0.1955	0.1980	0.1940	0.1980	0.1978	$\pm$ 1.53×10^{-3}
4.0	0.2600	0.2600	0.2440	0.2430	0.2395	0.2390	0.2450	0.2480	0.2450	0.2515	0.2475	$\pm$ 2.38×10^{-3}
5.0	0.3030	0.3040	0.2910	0.2850	0.2820	0.2830	0.2880	0.2910	0.2895	0.2970	0.29135	$\pm$ 2.45×10^{-3}
6.0	0.3470	0.3480	0.3330	0.3240	0.3220	0.3230	0.3300	0.3305	0.3340	0.3400	0.33315	$\pm$ 2.96×10^{-3}
7.0	0.3870	0.3900	0.3720	0.3640	0.3600	0.3620	0.3680	0.3690	0.3690	0.3830	0.3724	$\pm$ 3.35×10^{-3}
8.0	0.4240	0.4300	0.4120	0.4040	0.4010	0.4040	0.4020	0.4050	0.4010	0.4190	0.4102	$\pm$ 3.34×10^{-3}
9.0	0.4610	0.4700	0.4520	0.4440	0.4400	0.4430	0.4420	0.4470	0.4420	0.4580	0.4499	$\pm$ 3.18×10^{-3}

FIGURE 80

(a) Model Drug Release Plot

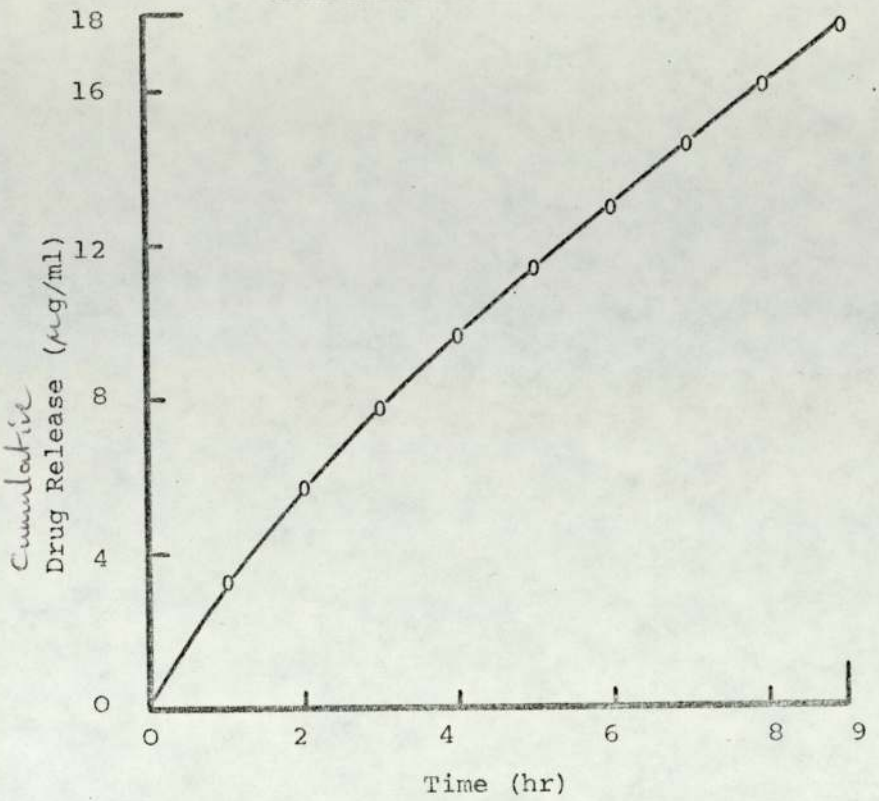

(b) Drug Release plotted as a function of square root of time

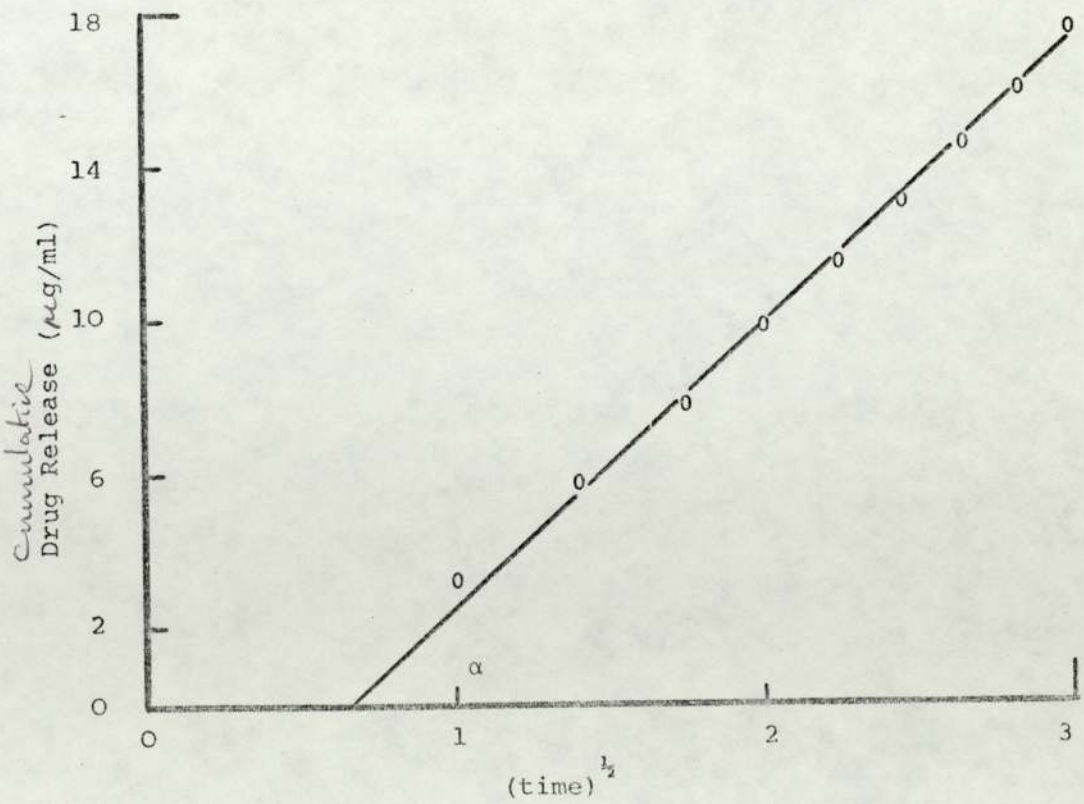

$$\frac{Q}{\sqrt{t}} = \{\frac{\tan \alpha \times 400}{60 \times 6.4 \times 10^6}\} \text{ g/cm}^2\text{sec}^{\frac{1}{2}}$$

... (86)

since tan α = slope of the square root of time plot and the release of the drug is modulated through a surface area of 6.4cm^2 into 400mls of saline. Substituting Equation (86) in Equation (85):

$$D = \{ \frac{\tan \alpha \times 400}{60 \times 6.4 \times 10^6} \cdot \frac{\sqrt{\pi}}{2Co} \}^2$$

... (87)

Thus the diffusion coefficient was calculated from a knowledge of the initial concentration of the drug in the vehicle and the slope of drug release plotted as a function of square root of time.

(ii) Release of a Suspended drug

The diffusion coefficient of a drug uniformly suspended in Plastibase was found in a similar manner by rearranging Equation (55):

$$D = \{ \frac{Q}{\sqrt{t}} \cdot \frac{1}{\sqrt{2CoC_s}} \}^2$$

... (88)

where Q = drug release in g/cm^2, Co = initial concentration in g/cm^3 and C_s = solubility of the drug in the vehicle in g/cm^3. In the case of salicylic acid C_s was taken as 0.495mg/cm^3 according to Washitake et. al. (327). As before (Equation (86)):

$$\frac{Q}{\sqrt{t}} = \frac{\tan \alpha \times 400}{60 \times 6.4 \times 10^6} \quad g/cm^2 sec^{\frac{1}{2}}$$

... (89)

assuming in this case that Figure 80 represents a plot of drug release from a suspension ointment. Substituting Equation (89) in Equation (88):

$$D = \left\{ \frac{\tan \alpha \times 400}{60 \times 6.4 \times 10^6} \cdot \frac{1}{\sqrt{2C_0C_s}} \right\}^2$$

... (90)

The diffusion coefficient for a suspension ointment was thus calculated from a knowledge of the initial concentration, the saturation solubility of the drug and the slope of drug release plotted as a function of square root of time.

2.3.2 Procedure employed in the Drug Release Characteriation of Plastibases

All ointments were prepared extemporaneously on an ointment slab twenty four hours prior to commencing an experimental run. The drug release apparatus was assembled as described in Section 2.3.1. All studies were carried out over a nine hour time period. The following drug release studies were conducted.

(i) The effect of concentration on drug release

The release characteristics of salicylic acid and methyl salicylate individually at concentrations of 2%, 5% and 10% from Plastibase 50W ointments into saline were studied at 37°C.

(ii) The influence of rheological properties on drug release

The release characteristics of salicylic acid into saline from ointments prepared with all five grades of Plastibase containing 10% salicylic acid were studied at 25°C and 37°C. The release characteristics of methyl salicylate and ethyl salicylate from ointments containing 2% of the drug, and prepared with all the five grades of Plastibase, into saline were studied at 37°C.

(iii) The effect of temperature on drug release

The release characteristics of salicylic acid into saline were studied at 20°C, 25°C, 30°C, 35°C, 40°C and 45°C from a Plastibase ointment containing 10% salicylic acid. The release characteristics of methyl salicylate from a 2% Plastibase 50W ointment were also studied at the above temperatures.

2.4 Results

The release rate of salicylic acid and methyl salicylate at concentration of 2%, 5% and 10% from Plastibase 50W ointments is shown in Figures 81 (a) and 82 (a). The relationship between the release rate of the drug and the initial concentration in the ointment illustrated in Figures 81 (b) and 82 (b) is more or less linear. The diffusion coefficients derived from the drug release plots, Figures 81 (a) and 82 (a), are given in Table 39.

The release of salicylic acid from the five grades of Plastibase determined at 25°C and 37°C is shown in Figures 83 and 84

FIGURE 81

PLOTS SHOWING THE INFLUENCE OF CONCENTRATION ON THE RELEASE OF SALICYLIC ACID FROM PLASTIBASE 50W AT 37°C

(a)

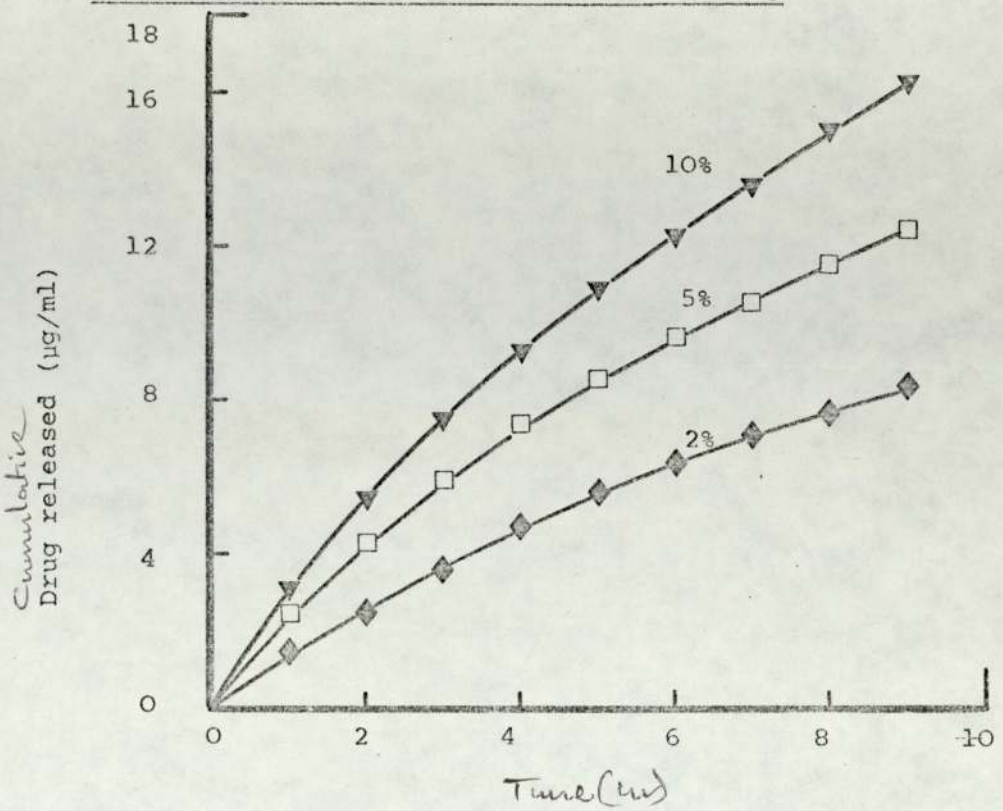

(b)

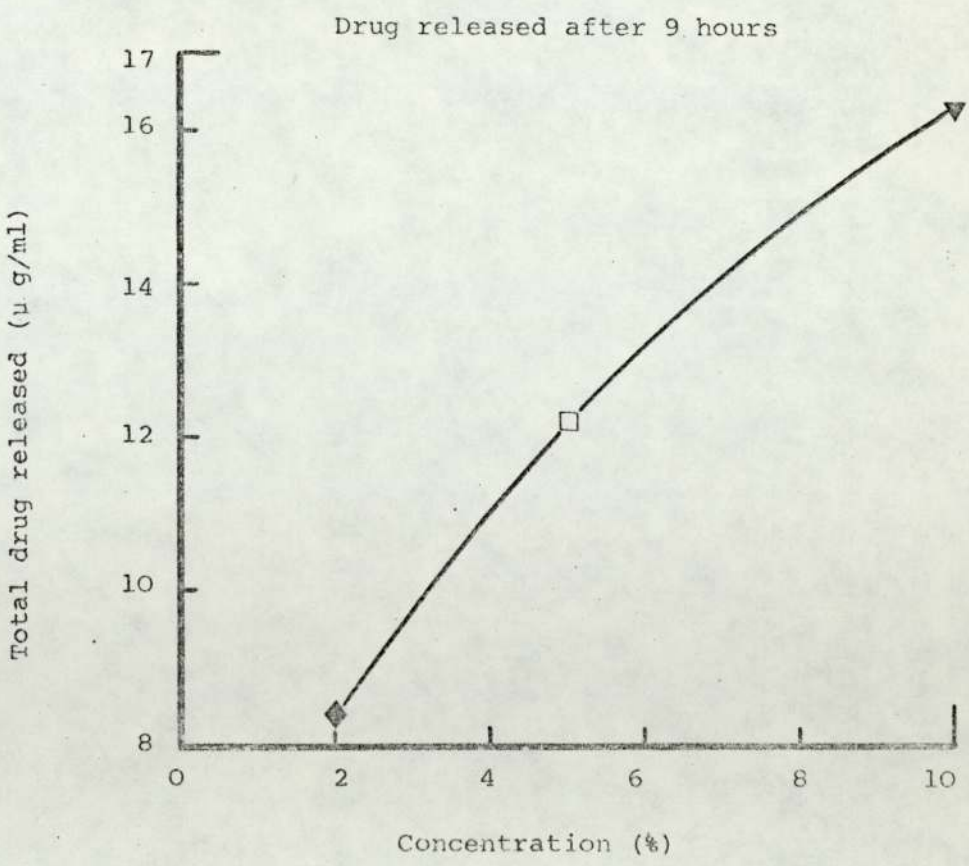

FIGURE 82

PLOTS SHOWING THE INFLUENCE OF CONCENTRATION ON THE RELEASE OF METHYL SALICYLATE FROM PLASTIBASE 50W AT 37°C

(a)

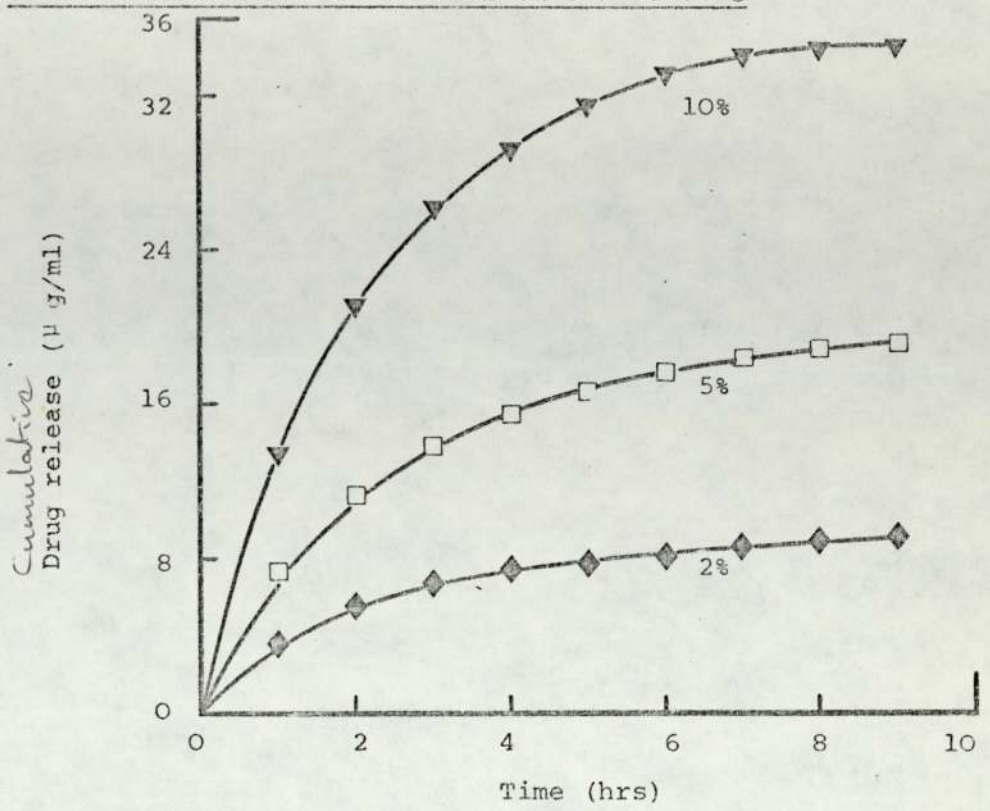

(b)

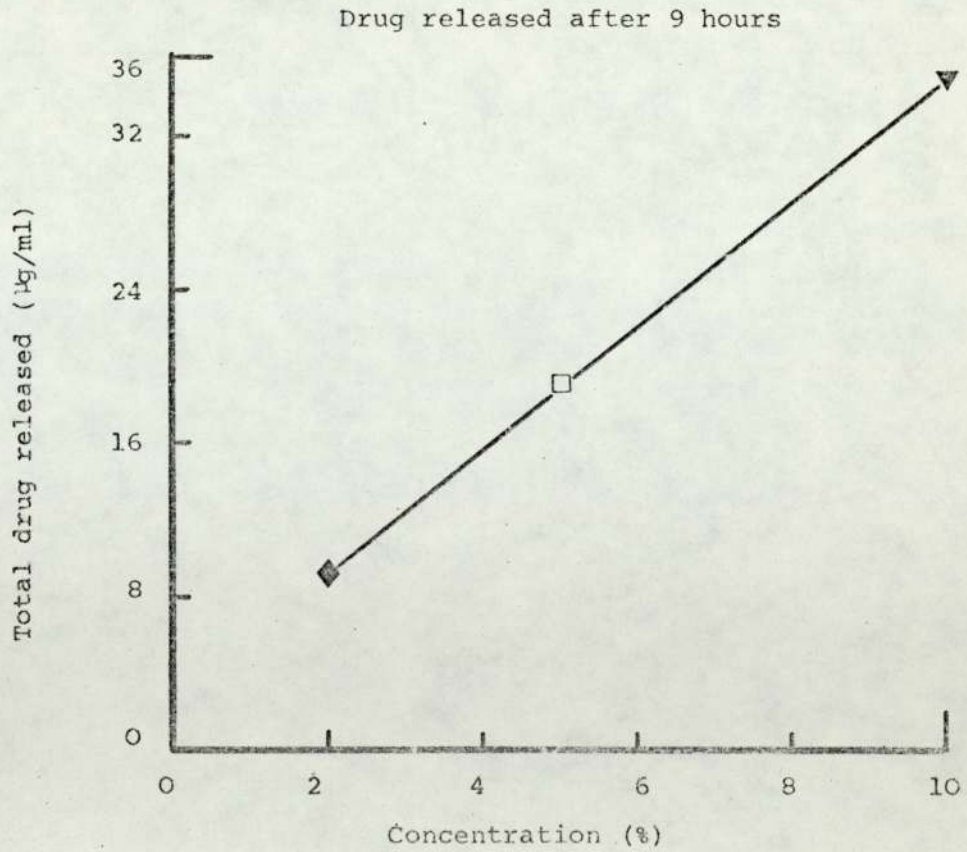

TABLE 39

APPARENT DIFFUSION COEFFICIENTS FOR SALICYLATES AT 37°C

IN PLASTIBASE 50W OINTMENTS CONTAINING A RANGE OF CONCENTRATIONS

Drug Concentration in Plastibase 50W ointment	Salicylic Acid D $cm^2/sec \times 10^{-8}$	Methyl Salicylate D $cm^2/sec \times 10^{-8}$
2%	74.70	3.62
5%	59.13	2.82
10%	56.40	2.82

TABLE 40

APPARENT DIFFUSION COEFFICIENTS FOR THE SALICYLATES IN THE

FIVE GRADES OF PLASTIBASE

Platibase Grade	Salicylic Acid 10% D $cm^2/sec \times 10^{-8}$		Methyl Salicylate D cm^2/sec	Ethyl Salicylate D cm^2/sec
	25°C	37°C	37°C	37°C
50W	10.88	56.40		
30W	13.11	69.65		
20W	15.30	93.97	3.93×10^{-8}	4.89×10^{-9}
10W	20.97	129.42		
5W	27.66	170.24		

TABLE 41

APPARENT DIFFUSION COEFFICIENTS FOR SALICYLIC ACID IN PLASTIBASE

50W AT VARIOUS TEMPERATURES

10% Salicylic Acid in Plastibase 50W	Temperature					
	20°C	25°C	30°C	35°C	40°C	45°C
D $cm^2/sec \times 10^{-8}$	4.06	10.88	27.08	44.25	83.27	151.32

FIGURE 83

SALICYLIC ACID RELEASE FROM THE FIVE GRADES OF PLASTIBASE OINTMENTS CONTAINING 10% SALICYLIC ACID AND FROM LIQUID PARAFFIN AT 25°C

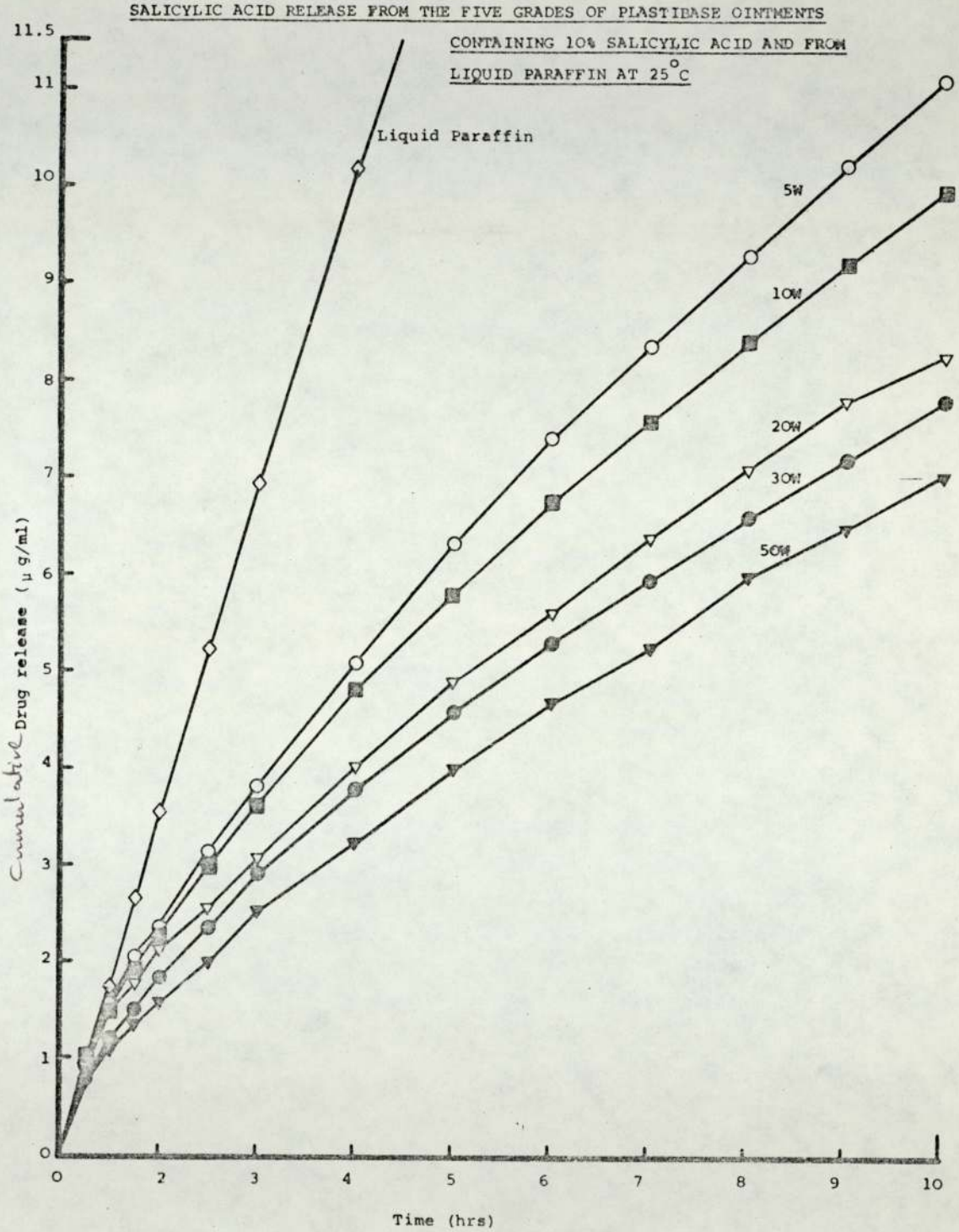

FIGURE 84

SALICYLIC ACID RELEASE FROM THE FIVE GRADES OF PLASTIBASE OINTMENTS CONTAINING 10% SALICYLIC ACID AT 37°C

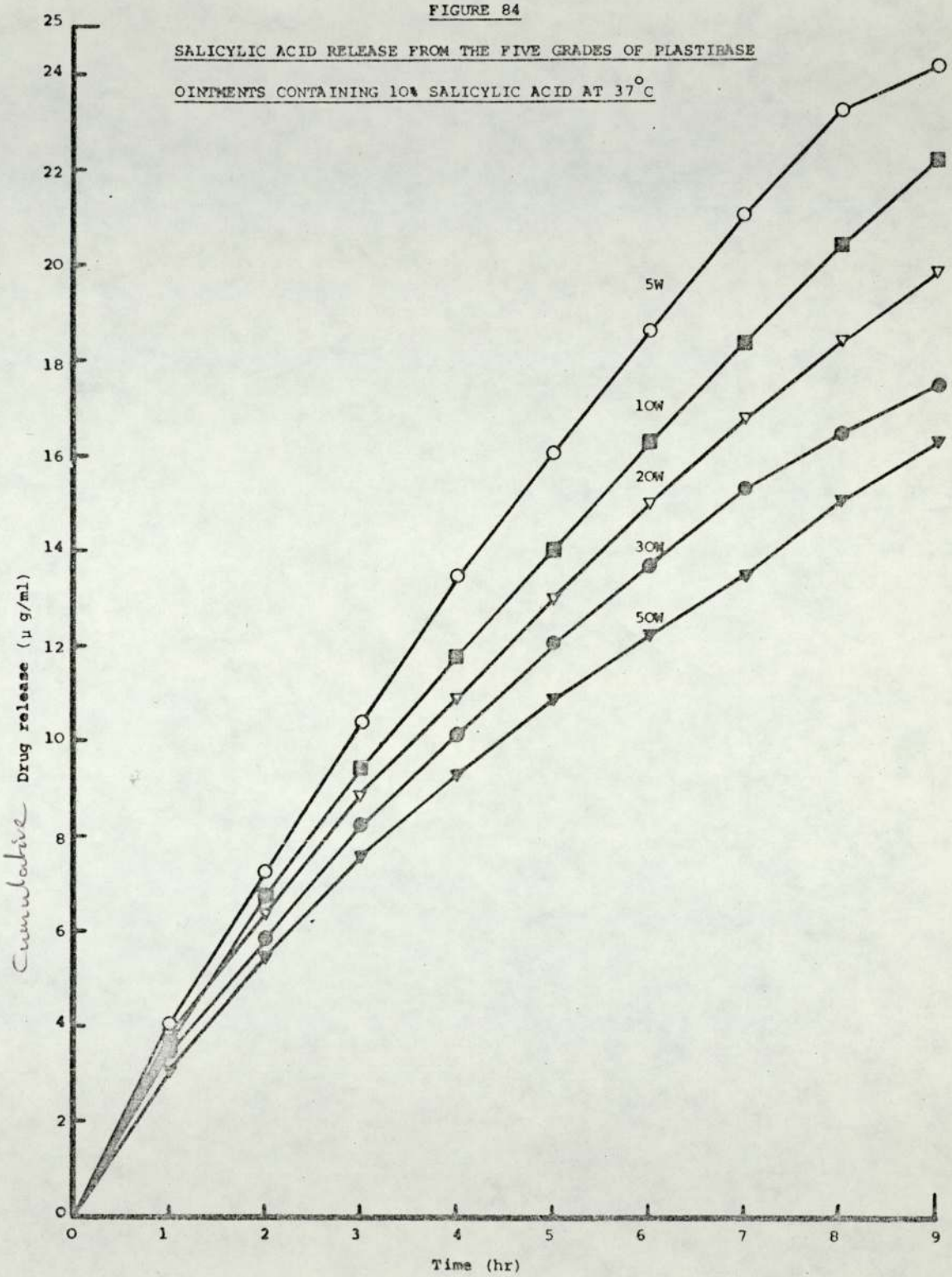

respectively. These results indicate that with a decrease in the rheological properties of the vehicle, there is an overall increase in the release rate of salicylic acid. The release of methyl and ethyl salicylate, Figure 85, would appear to be largely unaffected by the rheological properties of the vehicles. The diffusion coefficients derived from the drug release plots shown in Figures 83 to 85 are given in Table 40.

The release of salicylic acid at various temperatures from Plastibase 50W ointment containing 10% salicylic acid is shown in Figure 86. Increase in temperature is seen to lead to an increase in the rate of release of salicylic acid. The release of methyl salicylate with an increase in temperature, however appears to be unpredictable, Figure 87. The diffusion coefficients derived from the drug release plots shown in Figure 86 are given in Table 41.

2.5 Discussion

Recently, Whitworth & Asker (328) have drawn attention to the fact that different small scale techniques of ointment preparation may result in different drug release profiles. Comparing mechanical incorporation and fusion methods, they have explained that two respective release profiles result due to a 'viscosity' effect and a different degree of wetting produced by the two methods. Hersey & Cook (329) have drawn attention to the important problem of achieving dose uniformity in topical preparations and Chowhan & Pritchard (330) have pointed out that "changes in concentration due to nonhomogeneity or any other reason could also result in differences in release profiles". In the light of this debate it is considered necessary to point out that

FIGURE 65

METHYL SALICYLATE AND ETHYL SALICYLATE RELEASE ASSESSED SEPARATELY FROM THE FIVE GRADES OF PLASTIBASE OINTMENTS CONTAINING 2% OF THE DRUG AT 37°C

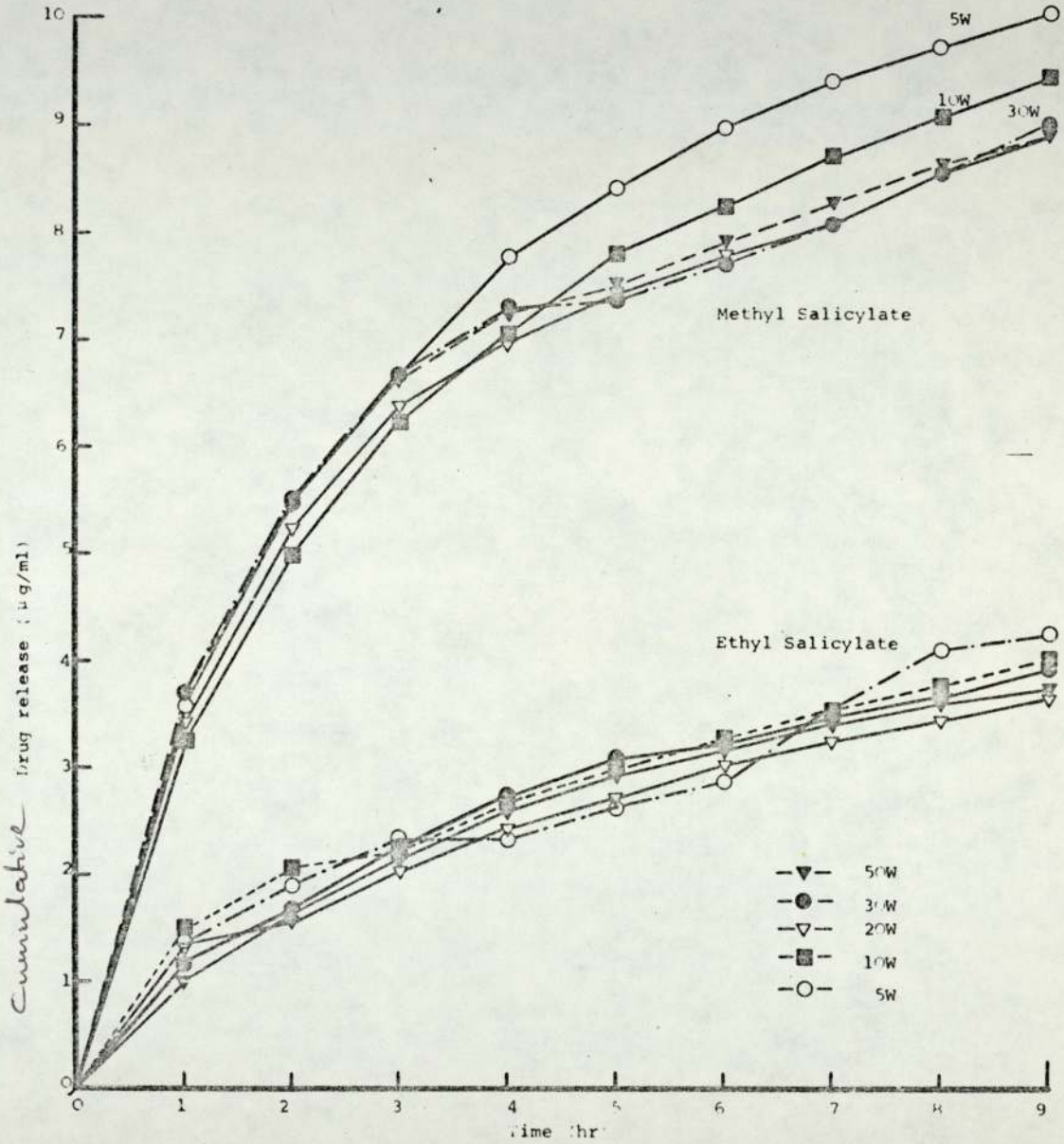

FIGURE 86

SALICYLIC ACID RELEASE FROM PLASTIBASE 5%W

OINTMENT CONTAINING 1% OF THE DRUG

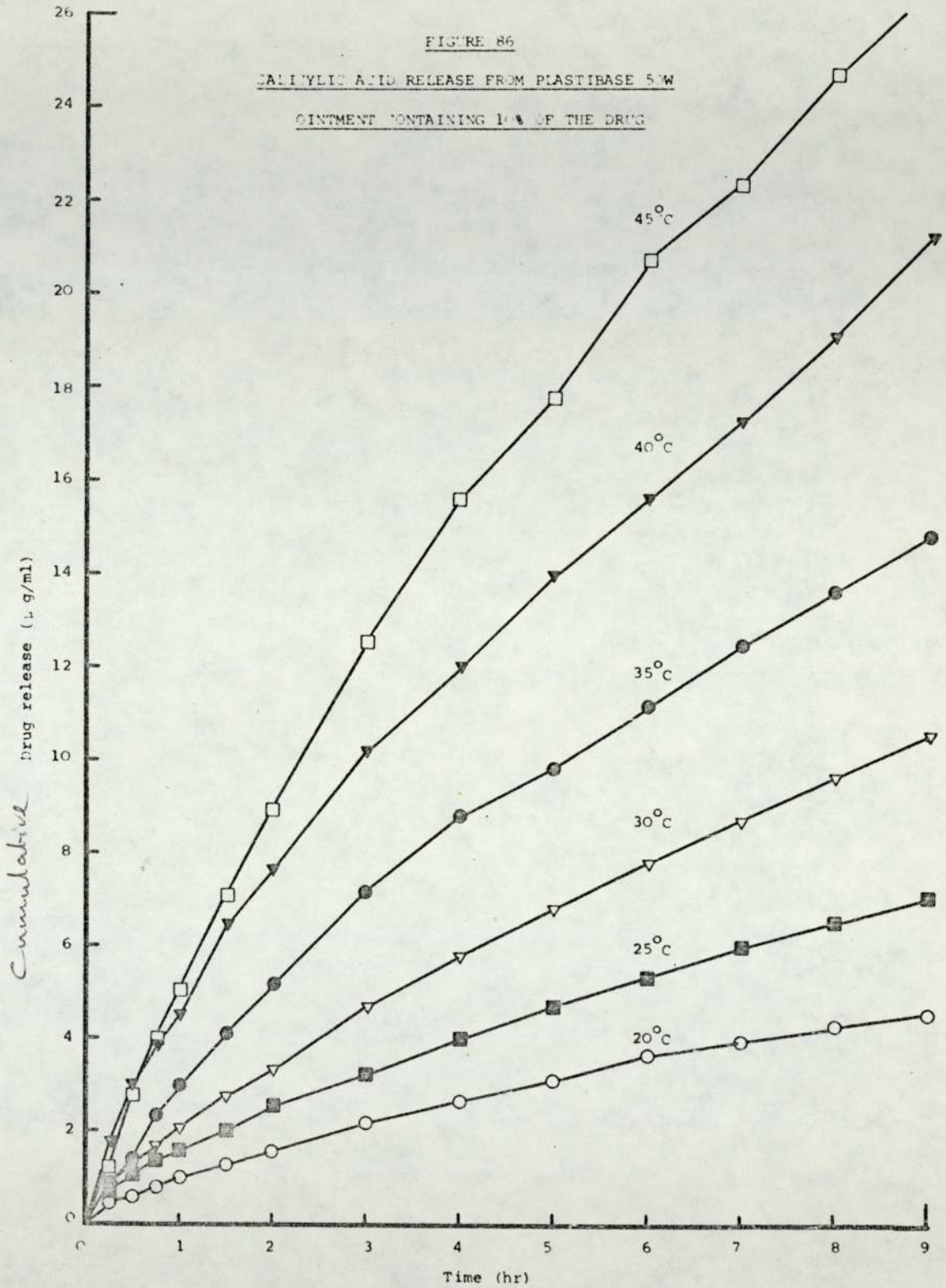

FIGURE 87

METHYL SALICYLATE RELEASE FROM PLASTIBASE 50W OINTMENTS

CONTAINING 2% OF THE DRUG

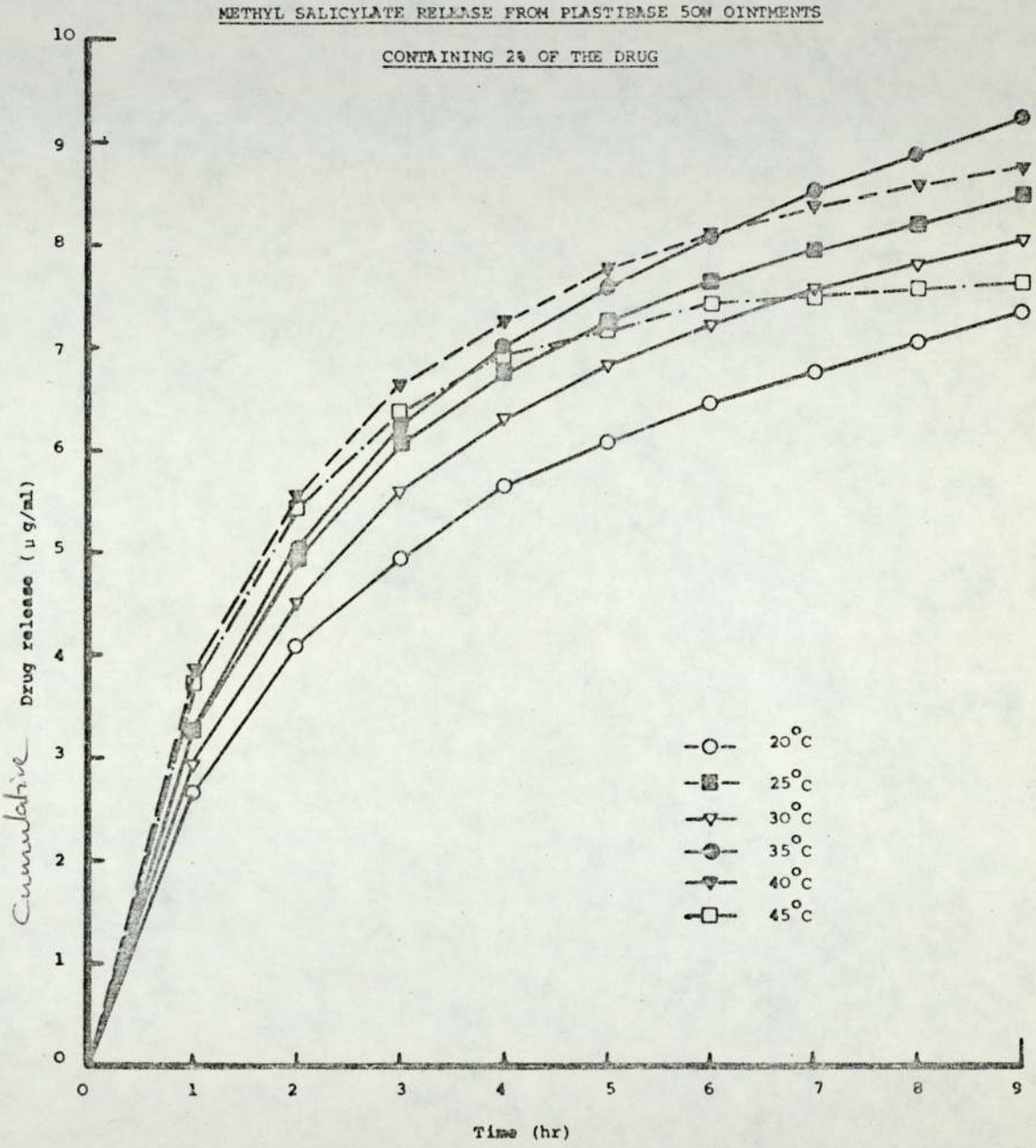

only the mechanical incorporation method of ointment preparation was used in this work. The ointments were prepared twenty four hours before commencing an experimental run giving the dispersed drug and/or drug in solution time to reach an equilibrium state. This procedure was also necessary to ensure that the stresses imposed on the ointment by the process of levigation had relaxed and that from a rheological standpoint the material had reached an equilibrium state. The reproducibility results, Table 38, indicate from the low standard errors that a good dispersion of the drug in Plastibase was achieved using the method adopted in this work.

The release of salicylic acid from Plastibase comprising dissolution in the base, diffusion through the base and diffusion through the membrane into the receptor phase is illustrated in Figure 88. Release of methyl and ethyl salicylate simply involves diffusion through the base and membrane as the drugs are already in solution. From the "square root of time relationship" the release of all three drugs was seen to be in agreement with the reported diffusional models. The salicylic acid plots showed an initial nonlinear portion indicating a lag time. This phenomena has been reported in the release measurements of various drugs from semisolids (319, 326, 330 - 1). As the quasi-steady state diffusion is reflected in the slope of the linear portion of these plots, the lag times seen were neglected. The methyl salicylate "square root of time" plots were characterised by a discontinuity in the slopes after four hours of release time showing a reduction in the diffusion coefficient reflecting a saturation effect.

Increase in the concentration of both salicylic acid and methyl salicylate led to a proportional increase in the release of these drugs.

FIGURE 88

AN ILLUSTRATION OF THE RELEASE MECHANISM OF SALICYLIC ACID FROM PLASTIBASE

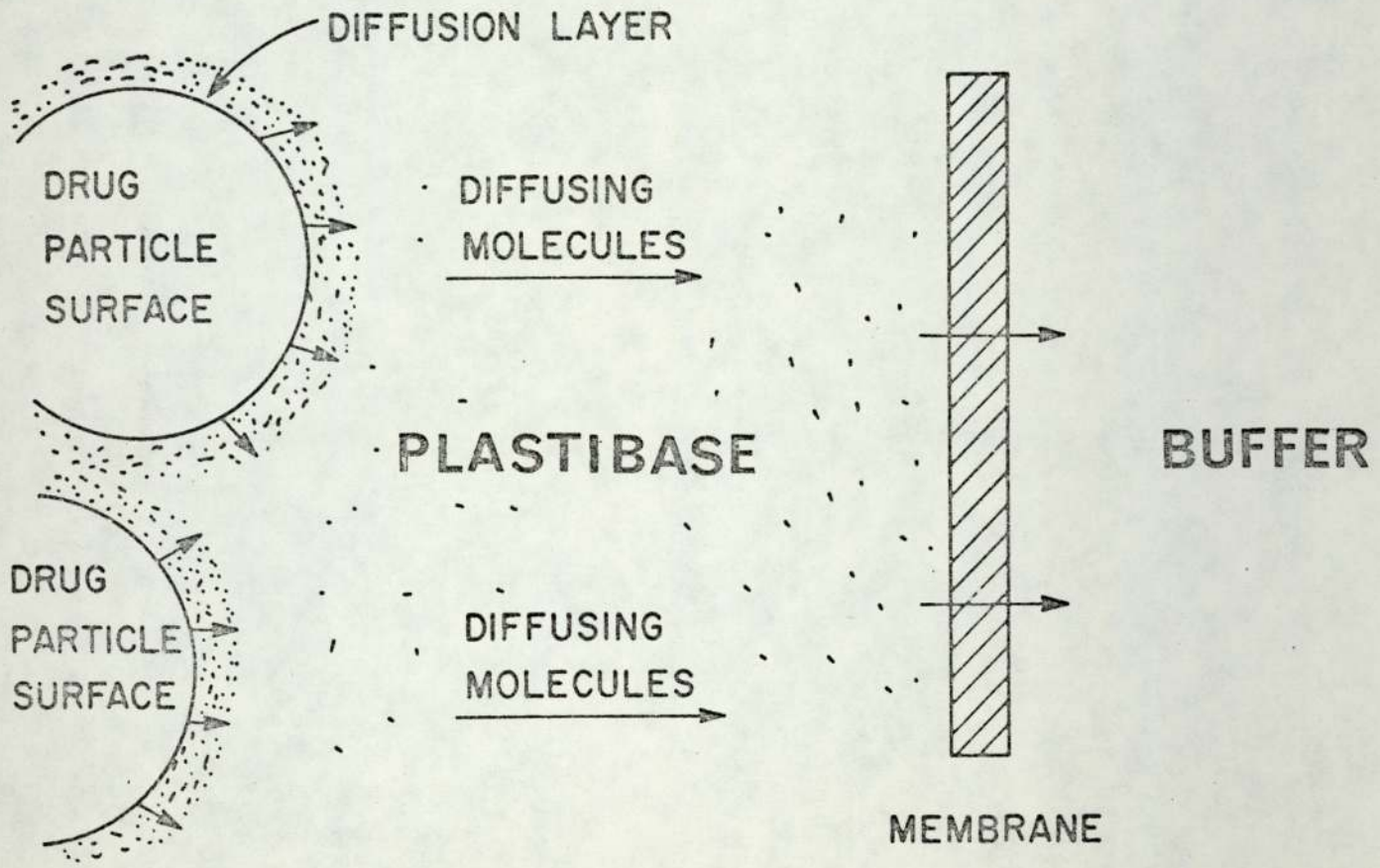

Figures 81 (b) and 82 (b). Similar findings have been reported from *in vitro* (328) and *in vivo* (126, 332 - 3) studies by several workers and would appear to be in keeping with the positive penetrative effects of increasing concentration as predicted by Fick's law. As only the dissolved drug is capable of diffusion from the semisolid to the receptor phase however, this finding is somewhat surprising in the case of salicylic acid where a large reservoir of the undissolved drug is present in the form of a suspension even at the 2% concentration. Whitworth & Asker (328) consider that the increase in the release of salicylic acid due to increased concentration reflects a solubility effect. A possible explanation of this behaviour is that increase in the concentration of salicylic acid leads to an increase in the available surface area for dissolution. This helps to speed up the replacement of the depleted dissolved drug resulting in a proportional increase in the rate of release. A large increase in the concentration of the drug however can hinder its own diffusion. This situation is seen in the case of 5% and 10% ointments which have similar but smaller diffusion coefficients that the 2% ointments. In these cases the reduction in diffusion coefficients results due to the possible increase in the collision interaction between the diffusing molecules. While the diffusion coefficient for methyl salicylate in Plastibase is smaller than the diffusion coefficient for salicylic acid in Plastibase, a considerably larger quantity of methyl salicylate is released into the receptor phase over a similar time period. The explanation for this lies in the relative solubilities of the drugs in Plastibase. Increases in the solubility of a drug undoubtedly leads to a greater release and penetration of the drug (132, 334 - 7) owing to a greater molar density and concentration gradient of the dissolved drug available for diffusion.

Plots of raw data for salicylic acid release from the five grades of Plastibase show a more or less linear relationship between drug release (measured in absorbance units) and $1/\eta_{app}$ or log $(1/\eta')$, Figures 89 and 90. This finding is further confirmed by plots of diffusion coefficients versus $1/\eta_{app}$ or log $(1/\eta')$, Figures 91 and 92. The release of methyl and ethyl salicylate on the other hand appears to be unaffected by rheological properties. This behaviour is explained as follows. Due to the fact that methyl and ethyl salicylate are in solution in Plastibase, the rate limiting step in the transport of these drugs appears to be passage through the membrane. In the case of salicylic acid however, due to the poor solubility of salicylic acid in Plastibase, the dissolution of the drug in the base plays an important part in the drug release mechanism. Thus the release rate is considerably affected by the properties of the base. Earlier experiments on concentration effects and the difference in the diffusion coefficients and release rates for salicylic acid and methyl salicylate would tend to support this theory. It is proposed that the processes in the drug release mechanisms may be ranked, as it were, according to their capacity to rate limit the release process i.e. dissolution > membrane transport > diffusion. Further studies on dissolution in Plastibase, diffusion through Plastibase and membrane transport are necessary to confirm this view.

The relationship between the microviscosity of the rheological environment as seen by the diffusing drug molecule, the measured rheological parameters and drug release is of particular interest in this study. In order to derive the microviscosity values for the Plastibases, the classical Stokes-Einstein equation relating diffusion

FIGURE 89

RELEASE OF SALICYLIC ACID FROM PLASTIBASES CORRELATED WITH THE APPARENT VISCOSITY VALUES DERIVED FROM CONTINUOUS SHEAR EXPERIMENTS

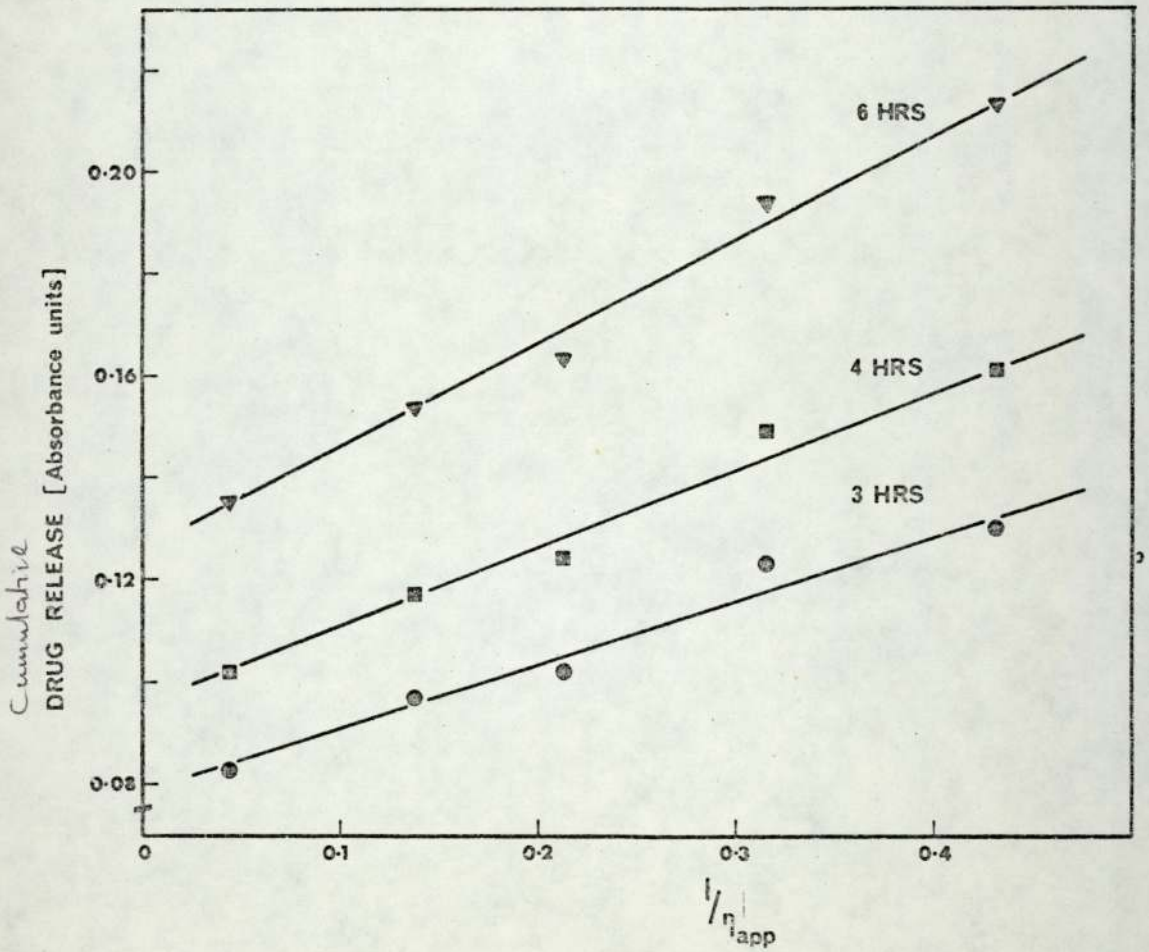

FIGURE 90

RELEASE OF SALICYLIC ACID FROM PLASTIBASES CORRELATED WITH THE DYNAMIC VISCOSITY VALUES DERIVED FROM OSCILLATORY TESTING OF THE VEHICLES

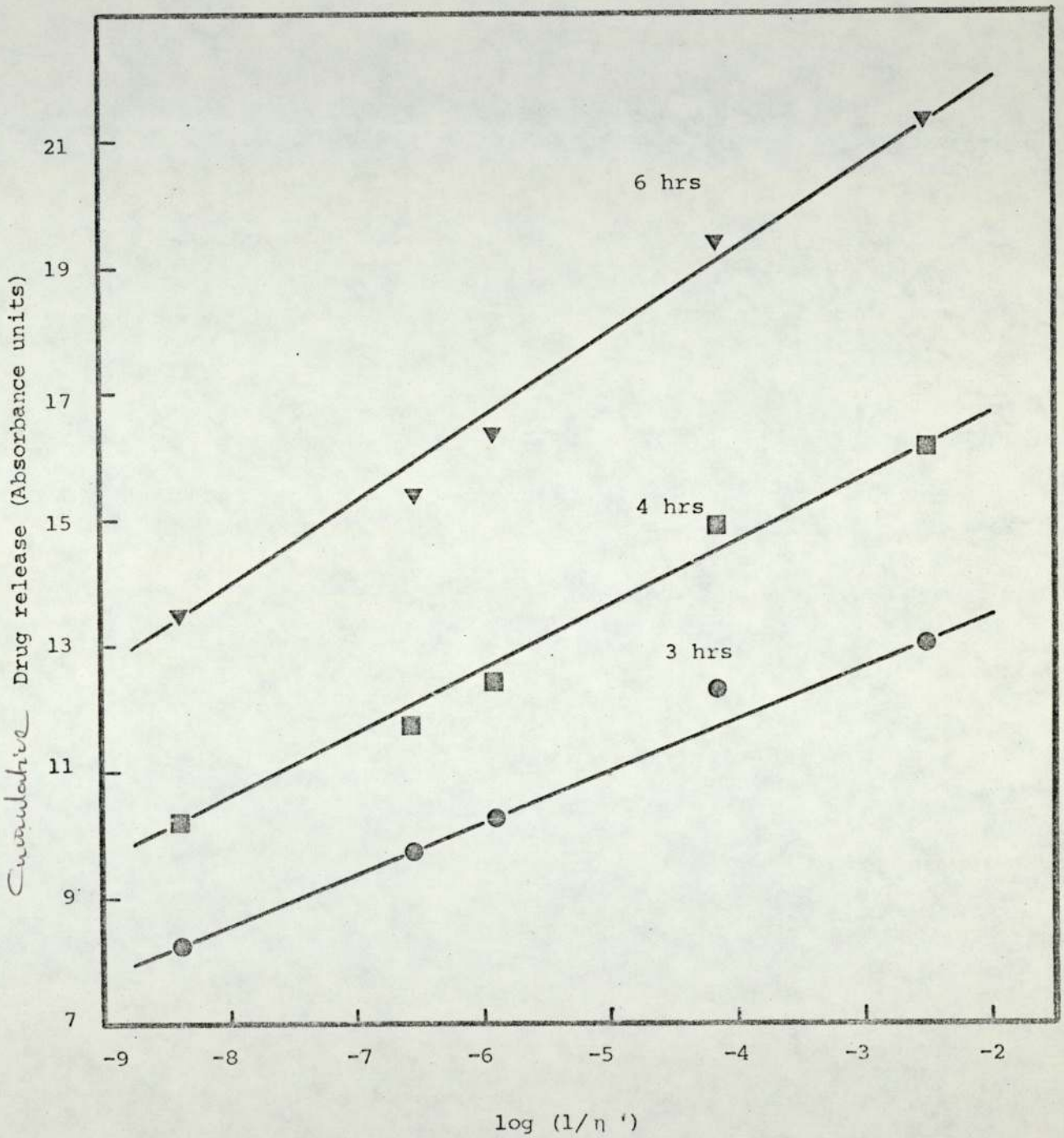

FIGURE 91

PLOTS OF APPARENT DIFFUSION COEFFICIENTS OF SALICYLIC ACID IN PLASTIBASES VERSUS INVERSE APPARENT VISCOSITY

(measured in Poise)

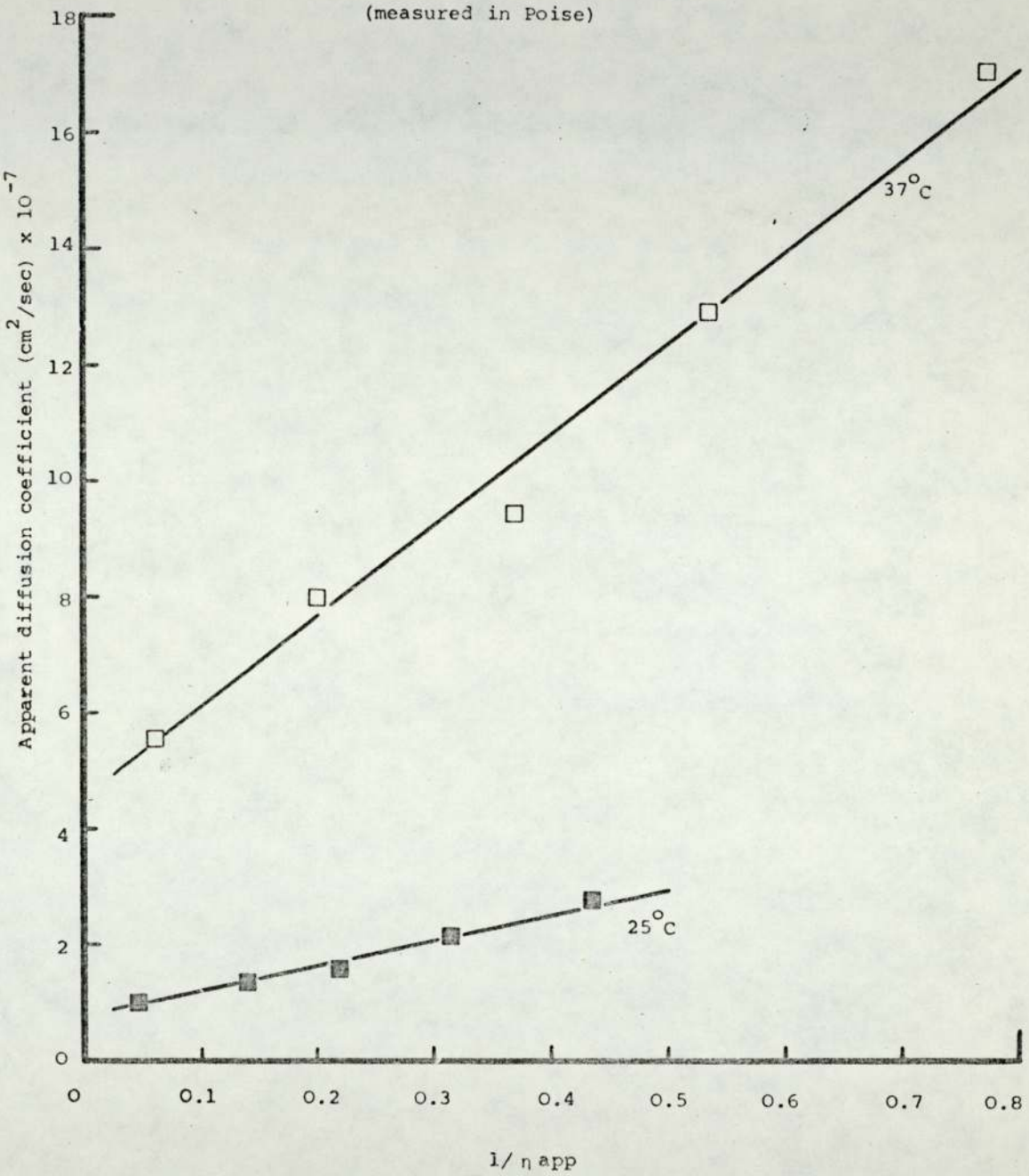

FIGURE 92

PLOTS OF APPARENT DIFFUSION COEFFICIENTS OF SALICYLIC ACID IN PLASTIBASES VERSUS LOG INVERSE DYNAMIC VISCOSITY

(measured in Poise)

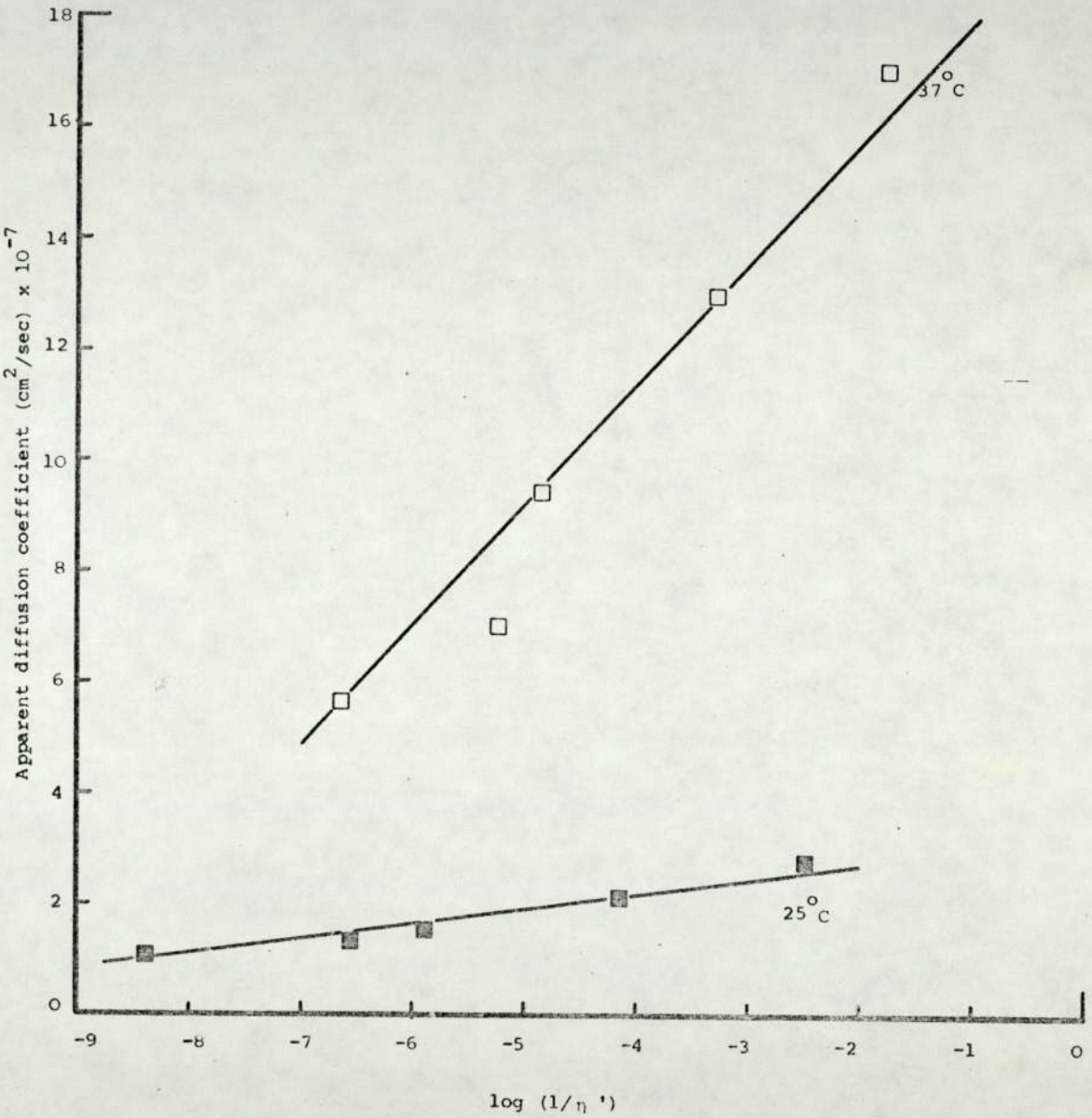

coefficients to viscosity was employed assuming r to be equal to 3.4×10^{-10} m (338).

$$D = \frac{kT}{6\pi\eta r} \qquad \ldots (61)$$

The microviscosity values derived for the five Plastibases at 25°C and 37°C, listed in Table 42, are considerably smaller than the measured macroviscosity values. Several workers have reported a similar discrepancy in their work. For instance, Florence et. al. (339, 340) reported that the microscopic viscosity values derived from diffusion coefficients of sodium chloride and potassium chloride in polyethylene glycol and polyrinylpyrrolidone using the Stokes-Einstein equation were smaller than the relative bulk viscosities. Block & Lamy (33) also reported observing a difference between the bulk viscosity and that apparently experienced by a diffusant. Frang & Nelson (341) showed that for the diffusion of salicylate in Sodium Carboxymethylcellulose solutions, the Stokes-Einstein equation does not hold since the relative viscosity increases over a hundredfold while the diffusion coefficient decreases less than 10%.

These discrepancies arising out of the use of the Stokes-Einstein equation may be explained as resulting from limitations of the equation.

Stokes-Einstein equation is derived by combining the Einstein (301) and Sutherland (342) equation,

$$D = \frac{kT}{\zeta} \qquad \ldots (91)$$

TABLE 42

COMPARISON OF MACRO AND MICRO VISCOSITY VALUES FOR THE FIVE GRADES OF PLASTIBASE AND LIQUID PARAFFIN

Plastibase Grade	Viscosity Values in Poise						
	η microscopic		η apparent		η'		η REL
	25°C	37°C	25°C	37°C	25°C	37°C	25°C
50W	0.59	0.12	23.06	17.02	2.49×10^{8}	4.47×10^{6}	23.07
30W	0.49	0.096	7.29	4.99	3.60×10^{6}	1.86×10^{5}	19.15
20W	0.42	0.071	4.57	2.72	8.64×10^{5}	7.59×10^{4}	16.41
10W	0.31	0.052	3.18	1.88	1.43×10^{4}	2.14×10^{3}	11.97
5W	0.23	0.039	2.32	1.30	3.26×10^{2}	6.33×10^{1}	9.08
Liquid Paraffin	0.025	-	1.572		1.572		1.0

where ξ is the viscous resistance per molecule, with Stokes' calculation (343) for the force acting on a spherical particle, radius r, moving in a continuous medium of viscosity η .

$$\xi = 6\pi\eta r \frac{1 + 2\eta/\beta r}{1 + 3\eta/\beta r} \qquad \ldots (92)$$

where β is the coefficient of sliding friction between the diffusing particle and its surroundings. The two limiting cases for Stokes' calculation are:- a large spherical solute molecule moving amongst smaller solvent molecules where

$$\beta = \infty , \qquad \xi = 6\pi\eta r \qquad \ldots (93)$$

and a small solute molecules moving amongst larger solvent molecules where

$$\beta = 0 , \qquad \xi = 4\pi\eta r \qquad (94)$$

Lamm (344) has found coefficients in the denominator of the equation to be of the order of 1.64π and 4.5π from other theories. Thus it is apparent that the value of the coefficient in the denominator of the Stokes-Einstein equation depending on the relative size of the solvent and solute molecule may affect the derived values of the diffusion coefficients or viscosity.

The shape of the molecule is also important. Stokes' calculation is based on the assumption that the diffusing molecule is spherical. As this is rarely the case, the shape of the molecule

will influence the numerical coefficient and hence ξ. Stokes' calculation does not take into account the migration of the solute molecules into holes in the solvent (as predicted by the hole theory of diffusion) nor does it consider the finite thickness of the solvent layers which flow round a moving solute molecule (345). It also does not take into account self diffusion of the solvent. Thus it is apparent that even in a continuous medium, Stokes-Einstein equation does not adequately describe the diffusional process of a solute.

In the case of gels, 'viscosity' is affected by long range entanglements, while diffusion is controlled by short range interactions (346). Thus the diffusivity of a solute in these systems is lowered from that of the solvent for the gel but not to the extent one might expect from the consistency of these materials. It is reasoned that a low concentration of a polymer can produce a substantial increase in the macroviscosity of a gel however the microscopic environment of a diffusion species is largely solvent and only infrequently does the diffusant encounter a polymer segment along its diffusion path (341). This diffusion in these systems does not comply with the Stokes-Einstein behaviour and the microscopic viscosity derived using the equation does not bear any direct relationship with the macroscopic viscosity.

The microviscosity values derived for the five Plastibases using the Stokes-Einstein equation can however be usefully employed in deriving an arbitrary relationship between the macro and the micro viscosity. Such relationships can be employed in the prediction of a macroviscosity corresponding to a particular diffusion coefficient or vice versa. Figure 93 shows plots of η_{micro} versus η_{app}.

FIGURE 93

RELATIONSHIP BETWEEN THE MICROSCOPIC VISCOSITY VALUES DERIVED USING THE STOKES-EINSTEIN EQUATION AND THE APPARENT VISCOSITY VALUES DERIVED FROM CONTINUOUS SHEAR TESTS

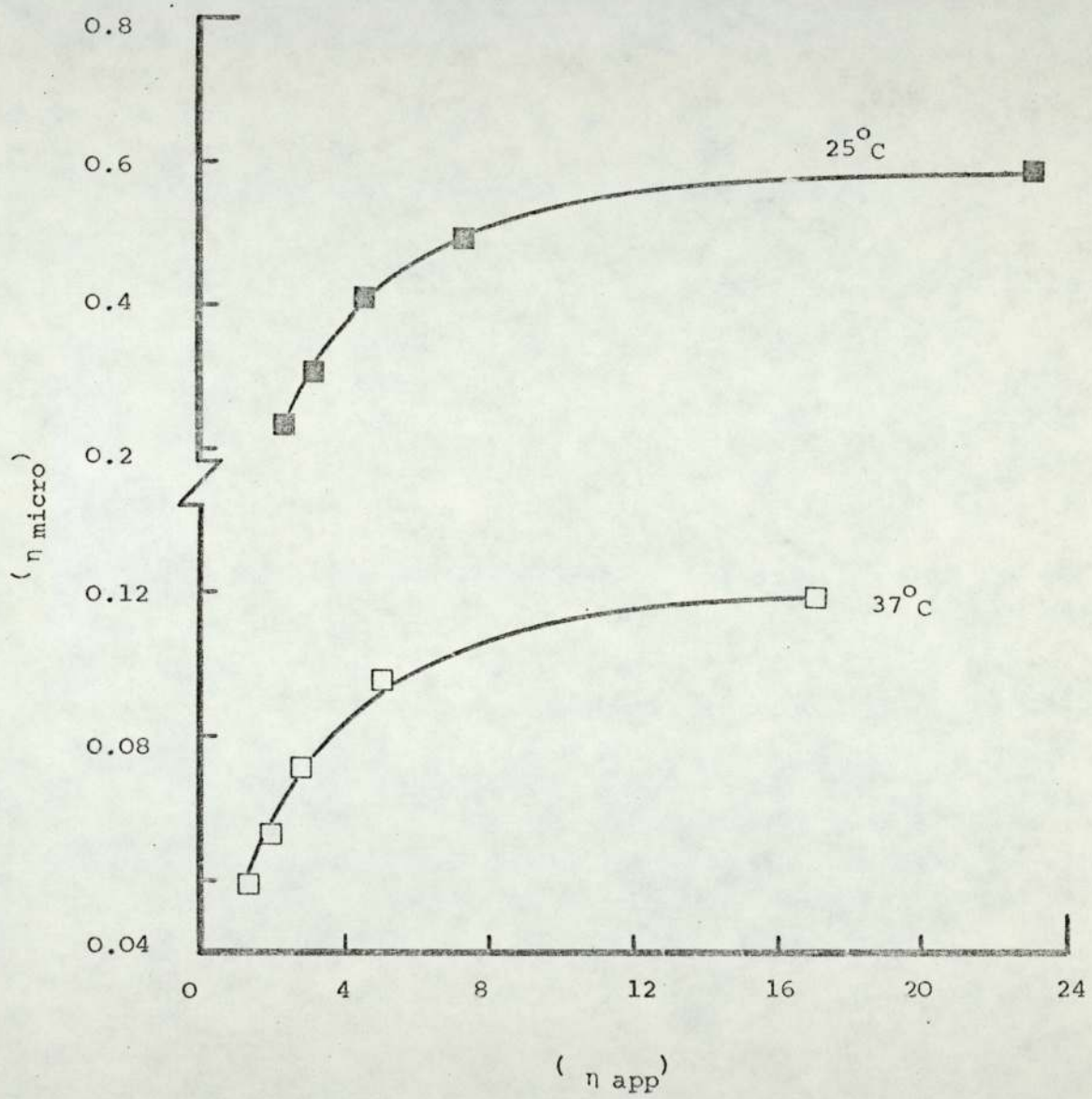

The curvilinear relationship between these two may be represented by the following polynomial equation at 25°C:

$$\eta_{micro} = -0.1276 + 0.1932\ (\eta_{app}) - 0.01848\ (\eta_{app})^2 + 0.0004649\ (\eta_{app})^3 \quad \ldots (95)$$

and at 37°C:

$$\eta_{micro} = -0.004 + 0.03806\ (\eta_{app}) - 0.004354\ (\eta_{app})^2 + 0.0001496\ (\eta_{app})^3 \quad \ldots (96)$$

Figure 94 shows a plot of η_{micro} versus log (η'). The linear relationship between these two may be represented by the following equation at 25°C:

$$\eta_{micro} = 0.06192 + 0.06280\ (\log\ \eta') \quad \ldots (97)$$

and at 37°C:

$$\eta_{micro} = 0.01439 + 0.0169\ (\log\ \eta') \quad \ldots (98)$$

Florence et al. (340) have suggested that at low bulk viscosity, the effective (relative) viscosity as defined below is more useful.

$$\frac{D_o}{D} = \frac{\eta}{\eta_o} = \eta_{REL} \quad \ldots (99)$$

FIGURE 94

RELATIONSHIP BETWEEN THE MICROSCOPIC VISCOSITY VALUES DERIVED USING THE STOKES-EINSTEIN EQUATION AND THE DYNAMIC VISCOSITY VALUES DERIVED FROM OSCILLATORY TESTS

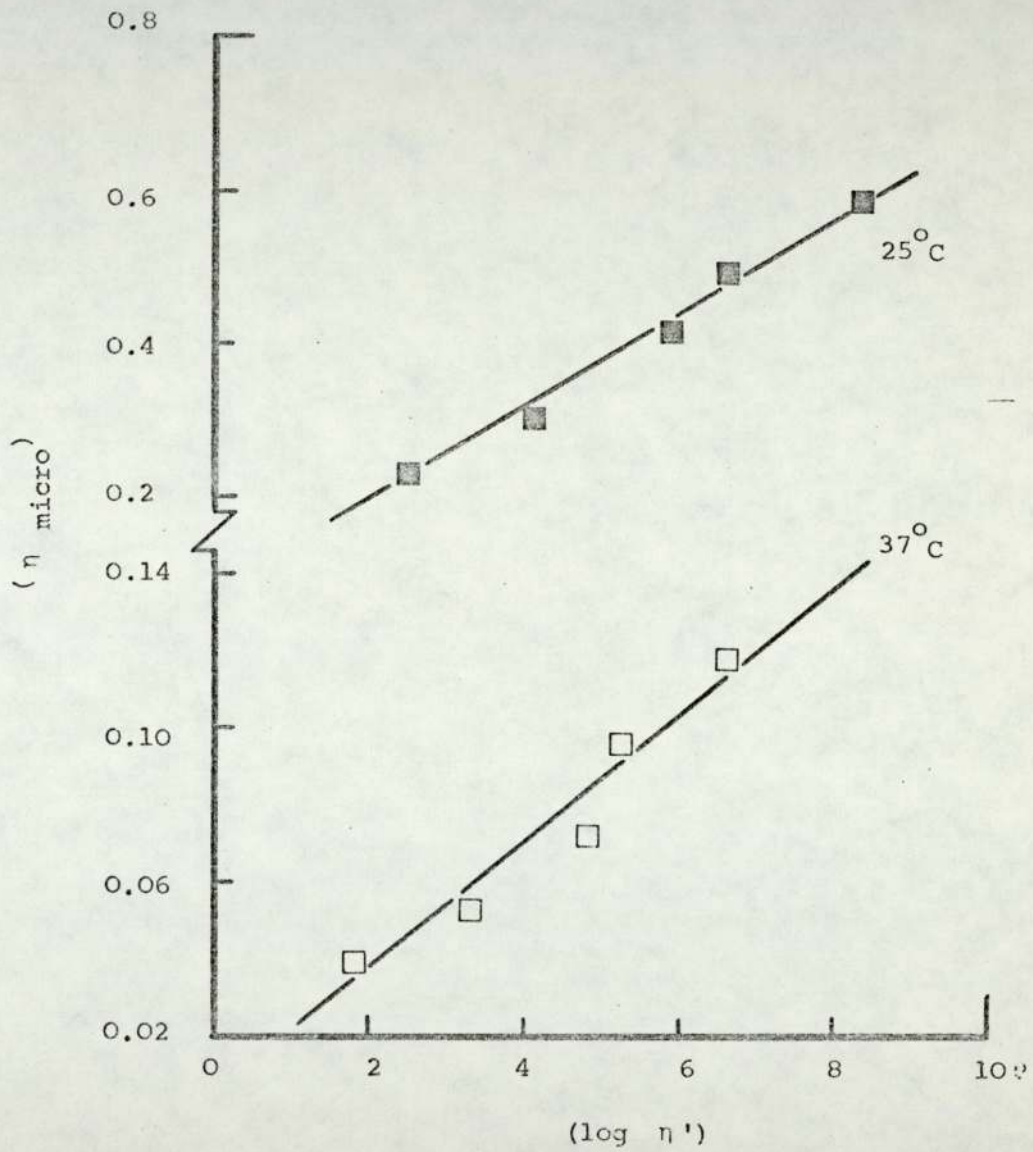

where D_o and D are the diffusion coefficients in the solvent and the gel (or solution) respectively, η_o and η are the 'viscosities' of the solvent and the gel (or solution) and η_{REL} is the effective viscosity. This would appear to be a more sensible adoption of the Stokes-Einstein equation in that the 'viscosity' values for the gels are normalised according to a known solvent viscosity. Viscosity values derived using this method are listed in Table 42.

The mechanical blockage of diffusion in polymer solutions or gels is related to the volume fraction of polymer (341). Mackie & Meares (347) have proposed the following equation to calculate the mobility of an ion, U, in a polymer matrix:

$$U = U_o \left(\frac{1 - V_p}{1 + V_p} \right)^2 \qquad \ldots (100)$$

where U_o is the mobility of the ion in water and V_p is the volume fraction of the polymer. Similarly Wang (348) has developed an equation for self diffusion of water in a protein solution.

$$D = D_o (1 - \alpha V_p) \qquad \ldots \qquad \ldots (101)$$

where α is the shape factor of protein.

Using any one of the methods described above, it is possible to derive a range of values of diffusion coefficients or viscosities for each gel system however none of these values can be directly related to the measured diffusion coefficients or measured viscosities respectively and thus arbitrary relationships have to be drawn up as shown earlier between the measured and derived parameters for prediction purposes.

It has been stated before that temperature is a relatively unimportant consideration in percutaneous absorption studies as penetration *in vivo* occurs only within a narrow temperature range. *In vitro* experiments however may be conducted over a wide range of temperatures thus allowing a study of the change in the rheological properties of a material with temperature and its effect on drug release.

Increase in temperature, through its effect on rheological properties was thus seen to promote an increase in the rate of release of salicylic acid from Plastibase. As before, the release of methyl salicylate appears to be somewhat unaffected by the rheological changes brought about by increase in temperature. The plots of apparent diffusion coefficients for salicylic acid release from Plastibase 50W versus $1/\eta_{app}$ and $1/\eta_{o}$ are shown in Figures 95 and 96. Both plots show a discontinuity at 30°C. This discontinuity corresponds with the discontinuity observed in creep testing of Plastibases and confirms that the phenomena is a function of the structural-rheological property of the material.

Arrhenius type plot of apparent diffusion coefficient versus $1/T^{\circ}K$, Figure 97, also showed a discontinuity at 30°C. Brown & Chitumbo (349) have reported a similar change in slope occurring at 25°C for glucose diffusion in various gels. These workers have reported that the apparent activation energy in the low temperature interval may be regarded as reflecting the small scale segmental motion of the polymer and in the higher temperature interval, the energy associated with the dynamic motion of large segments of polymer chains. Similar discontinuities in Arrhenius type plots have been reported and discussed

FIGURE 95

PLOT OF APPARENT DIFFUSION COEFFICIENT OF SALICYLIC ACID IN PLASTIBASE 50W DETERMINED OVER A RANGE OF TEMPERATURES VERSUS INVERSE APPARENT VISCOSITY

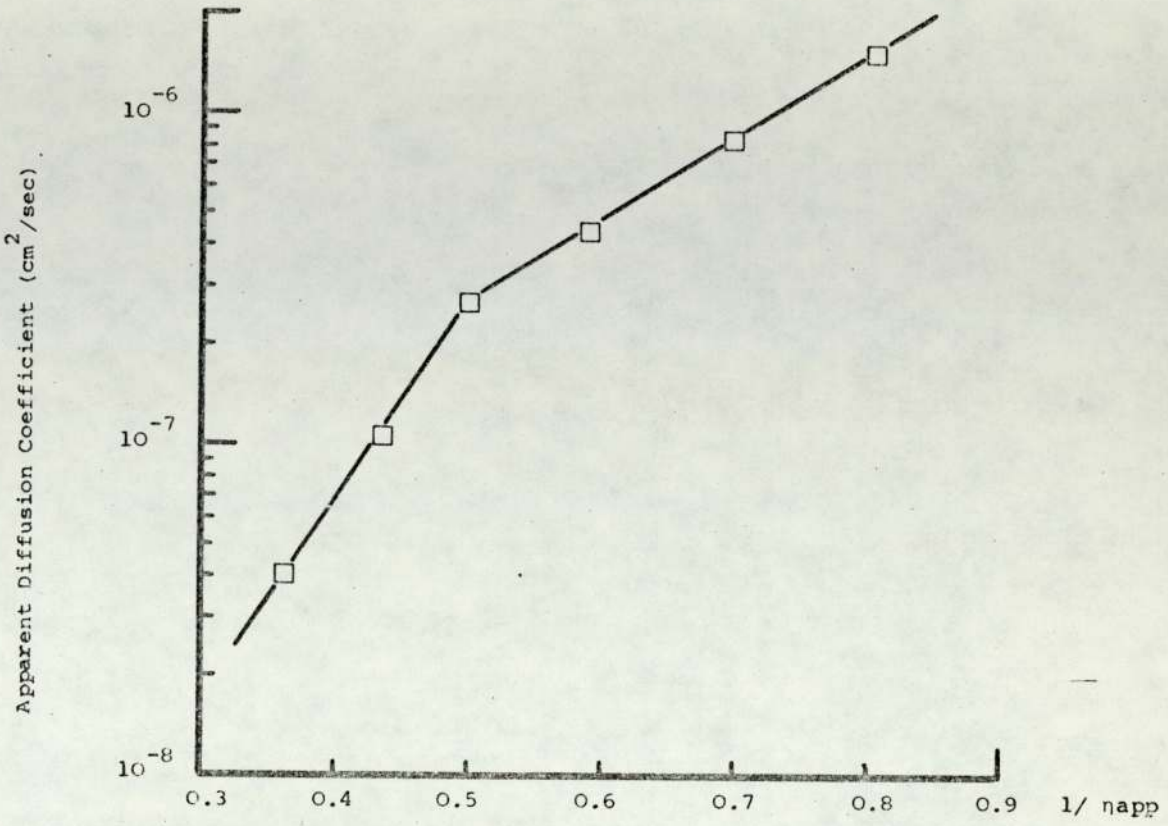

FIGURE 96

PLOT OF APPARENT DIFFUSION COEFFICIENT OF SALICYLIC ACID IN PLASTIBASE 50W DETERMINED OVER A RANGE OF TEMPERATURES VERSUS INVERSE RESIDUAL VISCOSITY

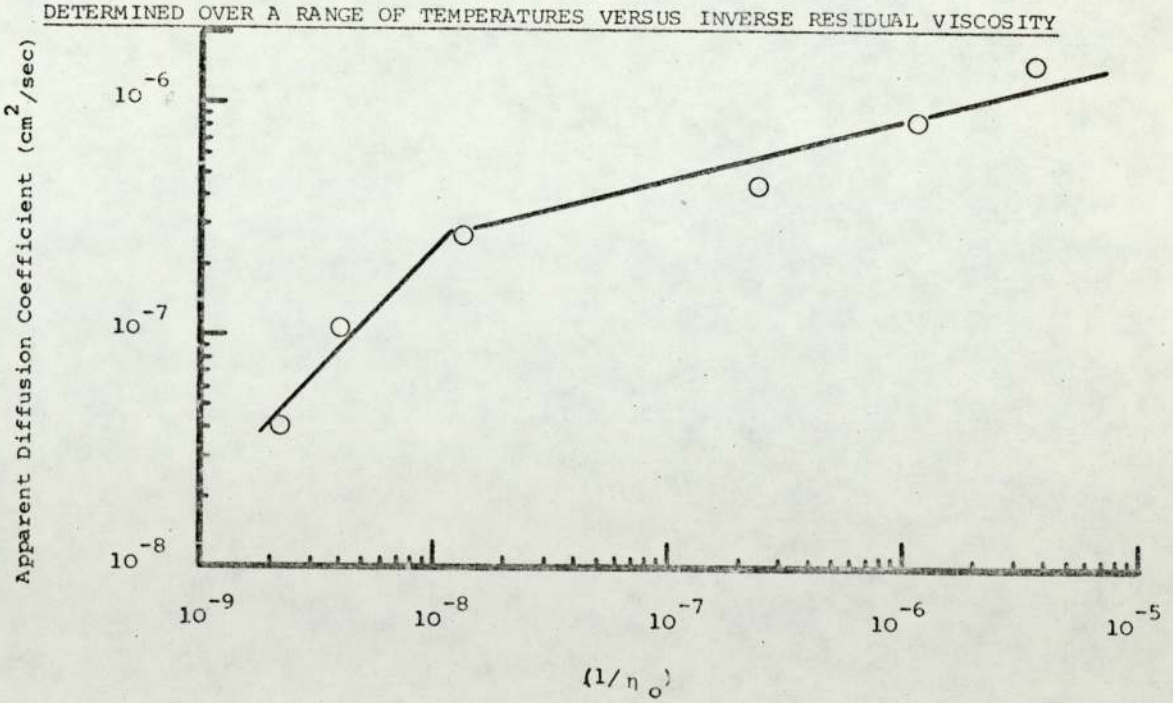

FIGURE 97

ARRHENIUS TYPE PLOT OF APPARENT DIFFUSION COEFFICIENTS OF SALICYLIC ACID IN PLASTIBASE 50W AT VARIOUS TEMPERATURES VERSUS INVERSE ABSOLUTE TEMPERATURE

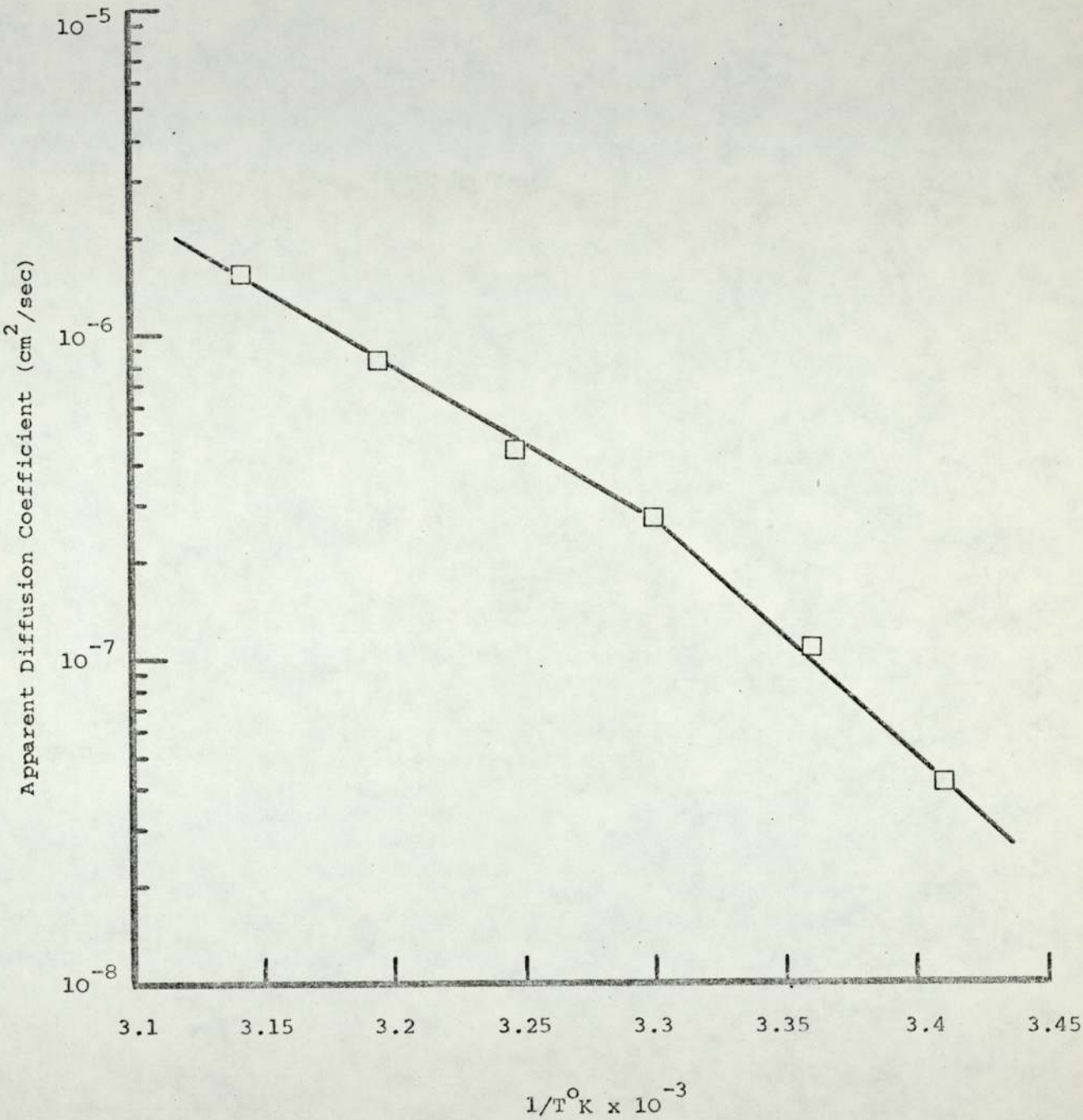

by other workers (350 - 2). The apparent activation energy from the shallow portion of the Arrhenius plot was derived to be 80.3 $kJmol^{-1}$. Similar high activation energy value has been reported by Amin (353) for methyl salicylate transport across human callus.

The Stokes-Einstein equation was employed as before bearing in mind the limitations of the equation to calculate the microviscosity of the rheological environment experienced by the diffusing salicylic acid. These data are listed in Table 43 and the relationship of the microviscosity with the macroviscosity values is illustrated in Figures 98 and 99. These plots again indicate the structural-rheological change occurring in Plastibase 50W at 30°C.

TABLE 43

COMPARISON OF MACRO AND MICRO VISCOSITY VALUES FOR

PLASTIBASE 50W OVER A RANGE OF TEMPERATURES

	20°C	25°C	30°C	35°C	40°C	45°C
η micro	1.55	0.59	0.24	0.15	0.080	0.045
η app	27.96	23.06	20.04	17.02	14.41	12.49
η_o	456×10^6	252.9×10^6	75.9×10^6	4.3×10^6	0.91×10^6	0.29×10^6

FIGURE 98

ILLUSTRATION OF THE RELATIONSHIP BETWEEN MICRO AND MACRO VISCOSITY VALUES

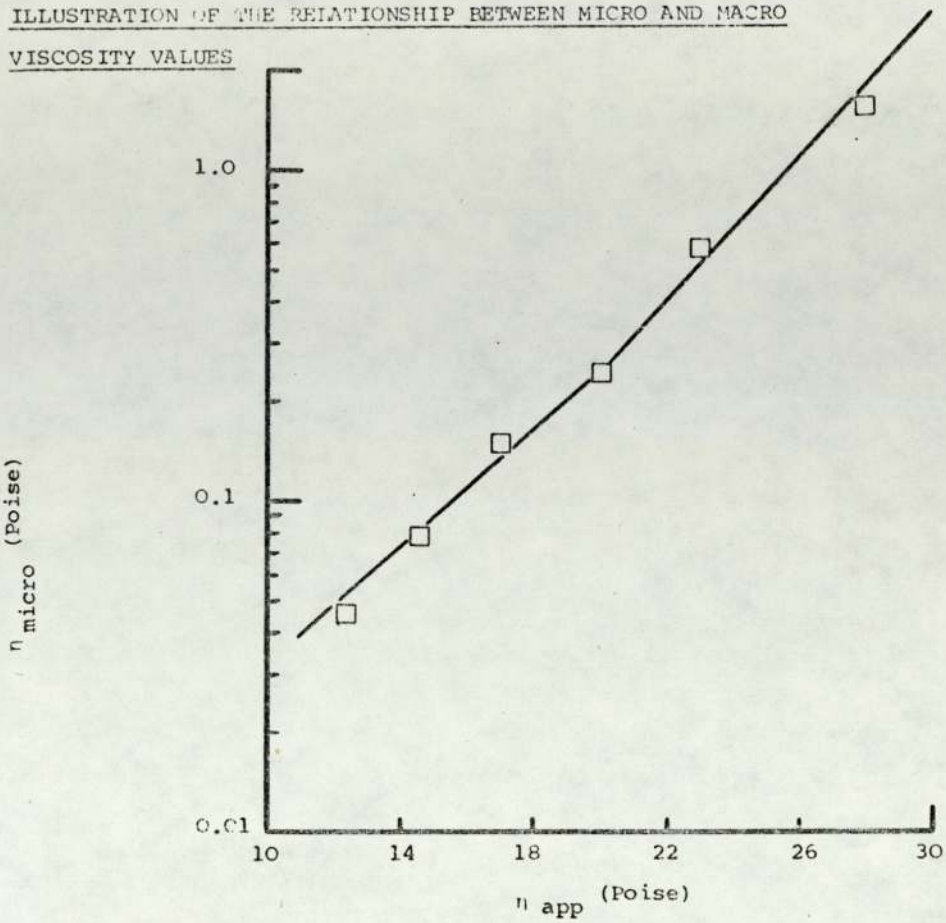

FIGURE 99

ILLUSTRATION OF THE RELATIONSHIP BETWEEN MICRO AND MACRO VISCOSITY VALUES

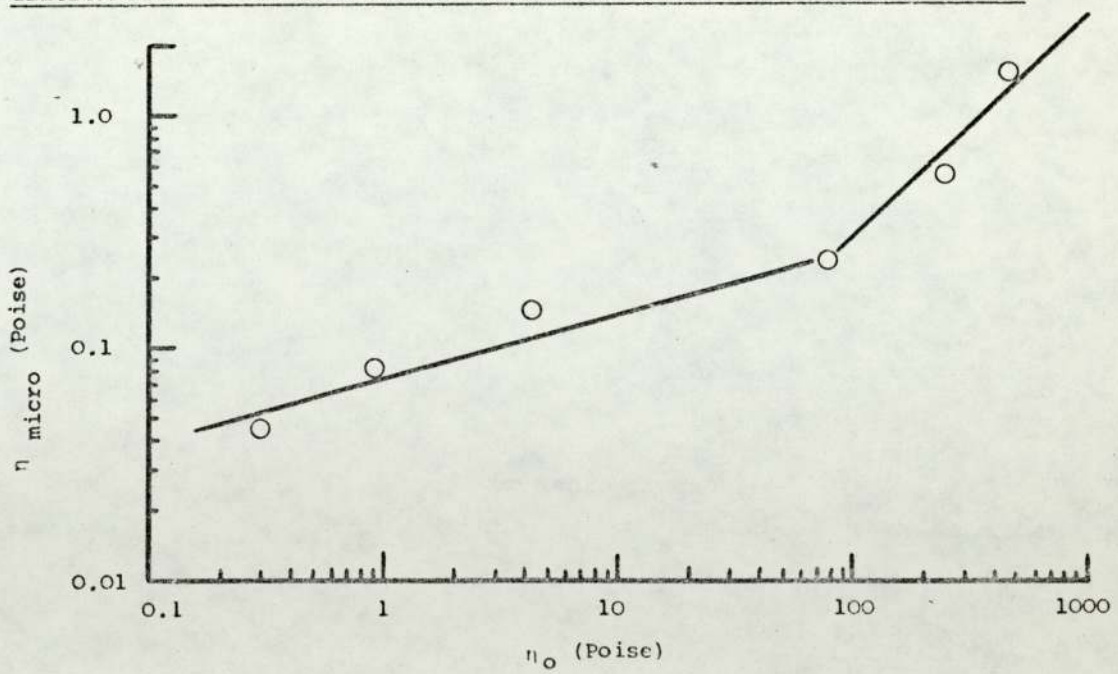

3 IN VIVO DRUG RELEASE FROM PLASTIBASES

3.1 Introduction

In vivo release and absorption of salicylates from topical vehicles has been shown to occur by many workers (98, 126, 311 - 2, 333, 354 - 7). The histologic changes in the skin after the application of salicylic acid were described by Gans (358) in 1925. Washitake et. al. (332) have recently shown that absorption into the skin leads to the formation of a cutaneous reservoir of the drug. Hlynka et. al. (333) have measured and compared intracutaneous and systemic absorption of salicylic acid as a function of rest time and concentration following topical application of the drug. Salicylate toxicity resulting from repeated topical application of salicylic acid to large areas of the body has also been reported (357, 359). Though several studies have been reported concerning elucidation of the physico-chemical factors which affect percutaneous absorption of salicylates (98, 311 - 2, 356), there is limited information in literature concerning the influence in vivo of rheological factors on drug absorption.

The purpose of the work reported in this section was to determine in vivo the topical release and absorption of salicylic acid and methyl salicylate from the five grades of Plastibase and thereby determine what influence the measured rheological properties of Plastibases have on drug release.

Two methods were adopted for this work:-

(i) the release on to and absorption by the skin was quantified from the keratolytic action of salicylic acid as judged from

an erythema response.

(ii) The systemic absorption of salicylic acid and methyl salicylate following release from the five Plastibases was determined from urinary excretion studies.

3.2 Assessment of drug release from keratolytic action of salicylic acid

3.2.1 Introduction

The keratolytic action of salicylic acid on the skin is well known and indeed salicylic acid is used for this reason in various formulations for the treatment of corns, callosities and warts. Histologic changes in the skin on application of salicylic acid have been described by Gans (358) and Strakosch (355). The latter reported that there is a direct relationship between concentration of salicylic acid and the time necessary to produce the same keratolytic action. Moncorps (354) was among the first workers to use the beginning of keratolysis as an end point to determine the release characteristics of different bases. Polano et. al. (360) developed a patch test method based on the irritant action of various drugs for determining the relative efficacy of various ointment bases. The above method was adopted by Robinson (228 - 9) for determining the relative efficacy of Plastibase and Plastibase Hydrophilic when compared with other vehicles. In this work salicylic acid release from Plastibase 50W, 20W and 5W was measured using a modification of the method proposed by Polano et. al. (360). Methyl salicylate induced hypermia is not as easily quantifiable as the keratolytic action of salicylic acid and thus this method cannot be employed for evaluating methyl salicylate release from Plastibases.

3.2.2 Materials

Plastibase 50W Batch Number 2363

Plastibase 20W Batch Number 2363

Plastibase 5W Batch Number 2363

Analytical grade of salicylic acid (B.D.H.) sieved through No 85 sieve.

27mm diameter Translet colostomy plasters (Macarthy's).

"Parafilm". Blenderm tape (3M).

3.2.3 Procedure

Plastibase 50W, 20W and 5W ointments were prepared containing 10% salicylic acid twenty four hours prior to commencing the study. Ten volunteers were selected for this study without reference to their sex. Tests for salicylate sensitivity were not carried out however the subjects confirmed verbally that they had never reacted adversely to salicylate administration.

As the consistency of the ointments varied from semisolid to mobile liquid, these could not be applied in the form of a patch and a reservoir had to be devised to hold the ointments in place. "Translet" colostomy plasters were thus employed for this prupose. These plasters have a wide circular ring which helps with the positioning of the colostomy bag round the stoma, and in this work helped to form the reservoir for the ointments.

Three such plasters were affixed on the flexor surface of the left forearm and one plaster on the flexor surface of the right forearm of each subject. The three reservoirs on the left forearm were filled

with Plastibase 20W, 5W and 50W ointments respectively. The reservoir on the right forearm was filled with Plastibase 50W which served as the control. The reservoirs were next covered with a strip of "Parafilm" which was secured with a rubber band and finally sealed with Blenderm tape, Figures 100 and 101. Ten volunteers thus produced a total of forty treatment areas. The plaster were left in place for twenty four hours after which they were removed and the forearms cleaned. Three to four hours after the removal of the plasters, the treatment areas were assessed by an independent observer according to a score system based on preliminary experiments on subjects who did not participate in this study. To avoid any confusion on the part of the observer resulting from dermatological terminology, the scoring system was simply based on the extent and severity of the erythema judged from the reddening of the skin. Every reddening was seen as a positive reaction. The following scoring system was employed:-

0 - Normal skin or no reaction

1 - Slight reddening in patches round circle

2 - Circle partially covered with light reddening

3 - Circle wholly or almost completely covered with light reddening

4 - Circle completely covered with even reddening

5 - Circle covered with intense reddening

6 - Circle covered with intense reddening and scaling

Reading of the test sites was repeated twenty four hours after the initial reading by the same observer. The observer was instructed that where there was some doubt about the allocation of a particular score, then an alternative score be given alongside the

FIGURE 100

ILLUSTRATION OF THE TEST APPLICATION TO THE FLEXOR SURFACE OF THE RIGHT FOREARM

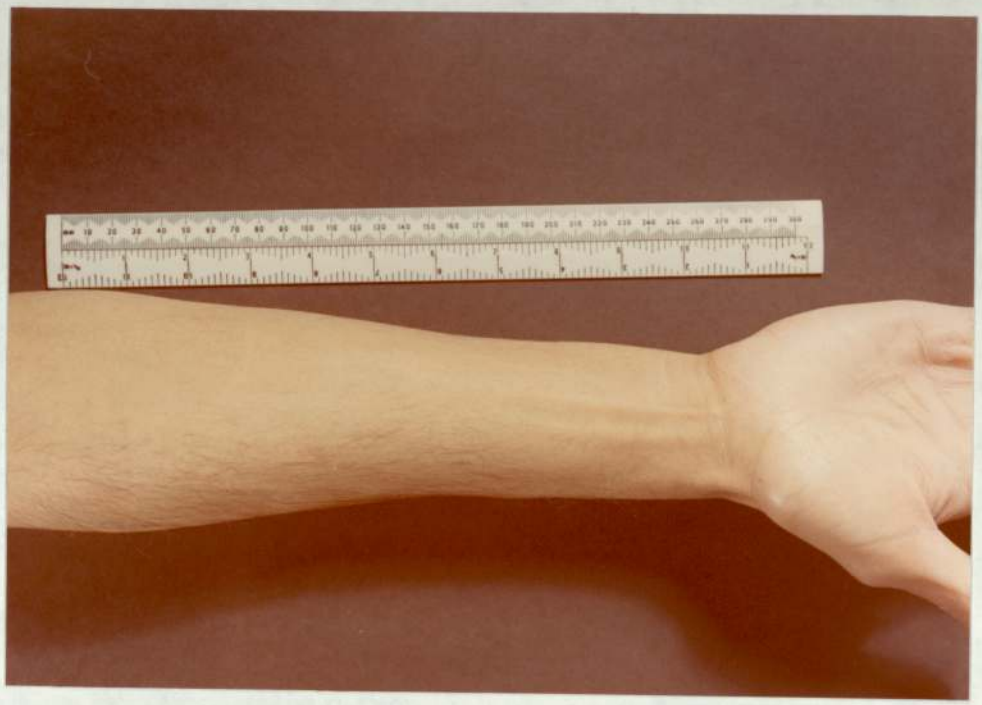

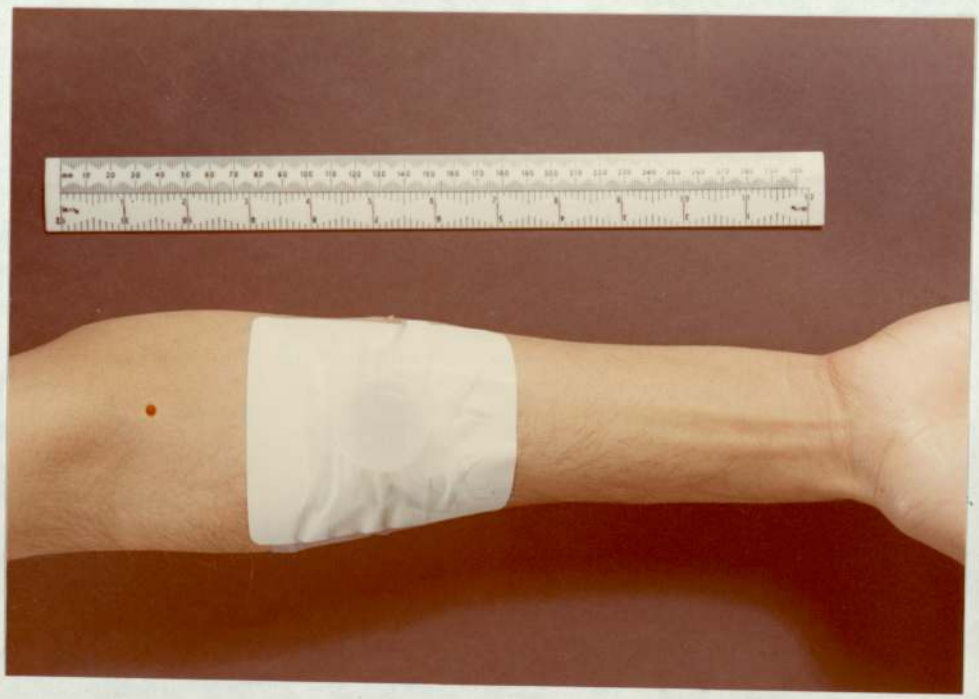

FIGURE 101

ILLUSTRATION OF THE TEST APPLICATION TO THE FLEXOR SURFACE OF THE LEFT FOREARM

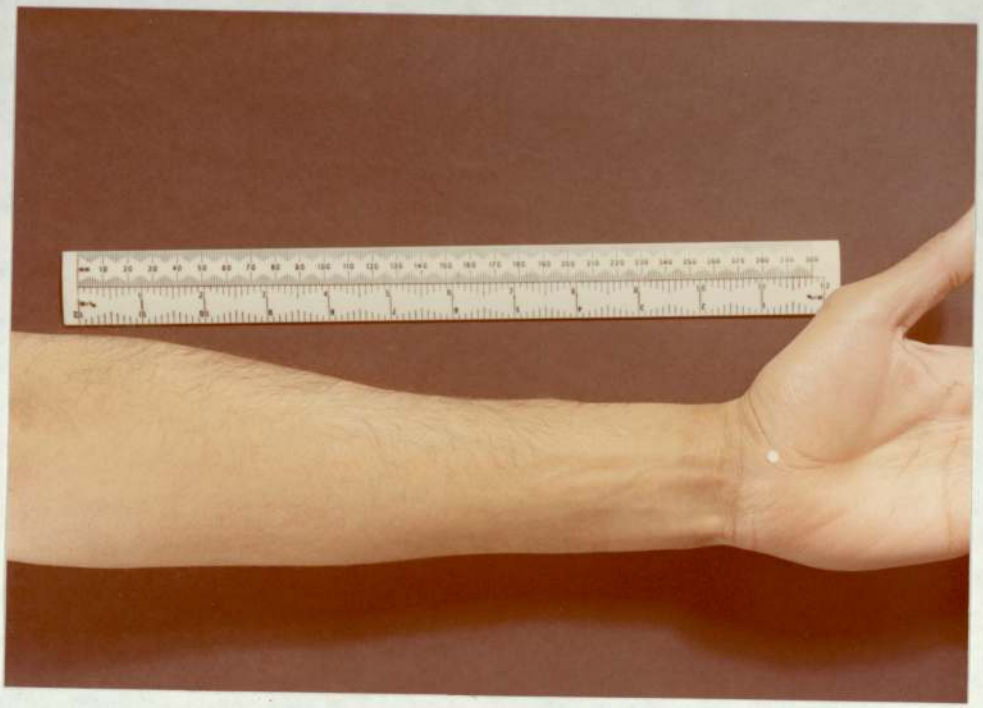

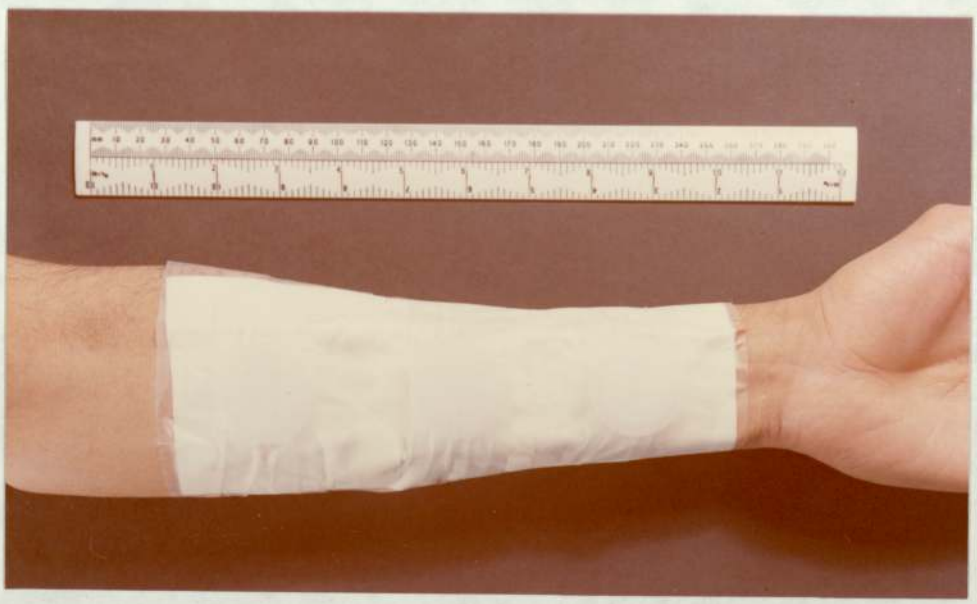

original score, e.g. 2 or 3. This was subsequently interpreted in the analysis of results as 2.5.

3.2.4 Results

An example of the application of test materials and the type of results obtained is illustrated in Figures 100 to 102. The scores recorded on two consecutive days for the ten volunteers are given in Table 44 and illustrated in Figures 103 and 104.

It was found that proper lighting was necessary for adequate discernment of erythema. Kligman & Wooding (361) have confirmed this finding and reported that certain fluorescent light sources, especially those rich in the blue and poor in the red end of the spectrum, are truly handicapping. In this work it was found that the test sites were best assessed in natural daylight.

Various forms of statistical analysis, e.g. variance analysis, probit transformations, etc., have been used in the interpretation of results of similar studies on vasoconstriction. In this work it was felt unnecessary to resort to extensive analysis of the results for two main reasons. Firstly, the total number of test sites does not justify the use of these methods and secondly, the large differences in the reactions obtained using the three formulations was adequate in itself to show that these formulations were significantly different in their drug release characteristics. Thus the results in this work were only analysed in order to derive the mean score, total score per formulation and the total score as a percentage of the total possible score.

FIGURE 102

ILLUSTRATION OF THE ERYTHEMA PRODUCED FOLLOWING THE APPLICATION OF OINTMENTS COMPARED WITH THE PLASTIBASE 50W CONTROL

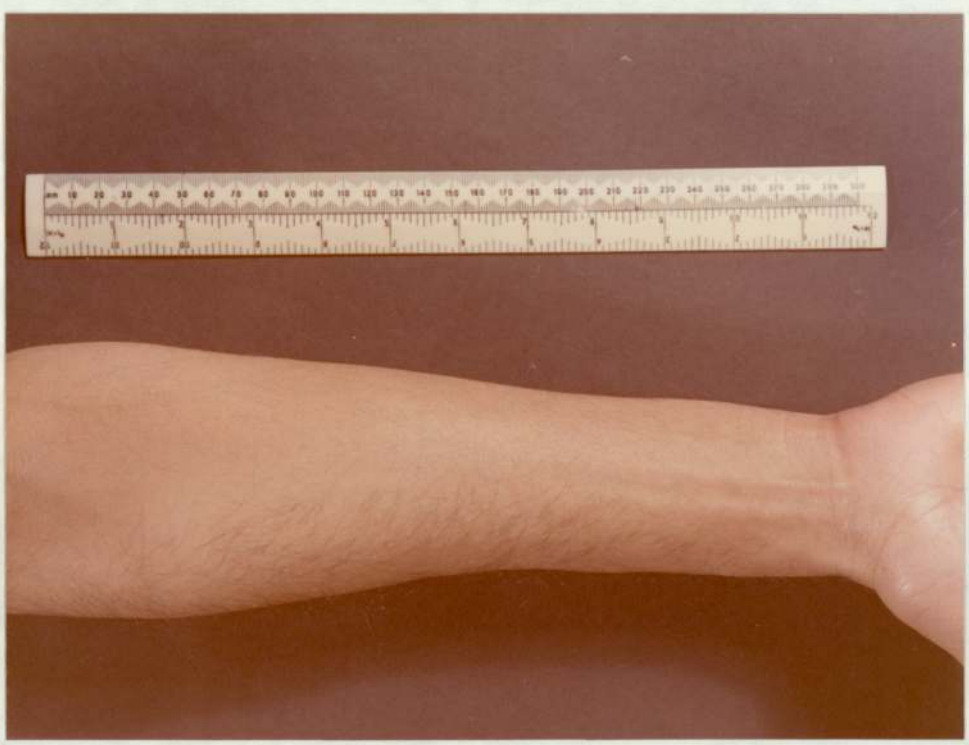

TABLE 44

DETAILS OF TEST SITE ASSESSMENT IN TEN VOLUNTEERS

FORMULATION APPLIED TO TEST SITE	Score assessed for 10 subjects										Mean Score	Total Score	Total score as % of total possible score
	1	2	3	4	5	6	7	8	9	10			
	DAY 1												
PLASTIBASE 50W CONTROL	0.0	0.0	0.0	0.0	0.0	0.0	0.0	0.0	0.0	0.0	0.0	0.0	0.0
PLASTIBASE 50W OINTMENT	0.5	1.0	1.0	1.0	0.5	2.0	1.0	1.0	0.5	1.0	0.95	9.5	15.8
PLASTIBASE 20W OINTMENT	1.0	2.0	3.0	2.0	2.0	3.0	2.0	2.0	2.0	3.0	2.2	22	36.7
PLASTIBASE 5W OINTMENT	2.0	3.5	5.5	4.0	3.0	5.0	3.0	5.0	4.0	5.5	4.05	40.5	67.5

Continued/.....

TABLE 44 (continued)

FORMULATION APPLIED TO TEST SITE	Score assessed for 10 subjects										Mean Score	Total Score	Total score as % of total possible score
	1	2	3	4	5	6	7	8	9	10			
	DAY II												
PLASTIBASE 50W CONTROL	0.0	0.0	0.0	0.0	0.0	0.0	0.0	0.0	0.0	0.0	0.0	0.0	0.0
PLASTIBASE 50W OINTMENT	1.0	0.5	1.0	1.0	0.5	1.0	0.5	2.0	0.5	0.5	0.85	8.5	14.2
PLASTIBASE 20W OINTMENT	1.0	1.5	2.0	2.5	1.0	2.0	2.0	1.0	1.5	3.0	1.75	17.5	29.2
PLASTIBASE 5W OINTMENT	3.0	3.0	3.0	4.0	3.5	4.5	3.0	2.0	3.5	5.0	3.45	34.5	57.5

FIGURE 103

PLOT OF MEAN SCORE VERSUS NUMBER OF APPLICATIONS OF THE PLASTIBASE 50W, 20W AND 5W OINTMENTS

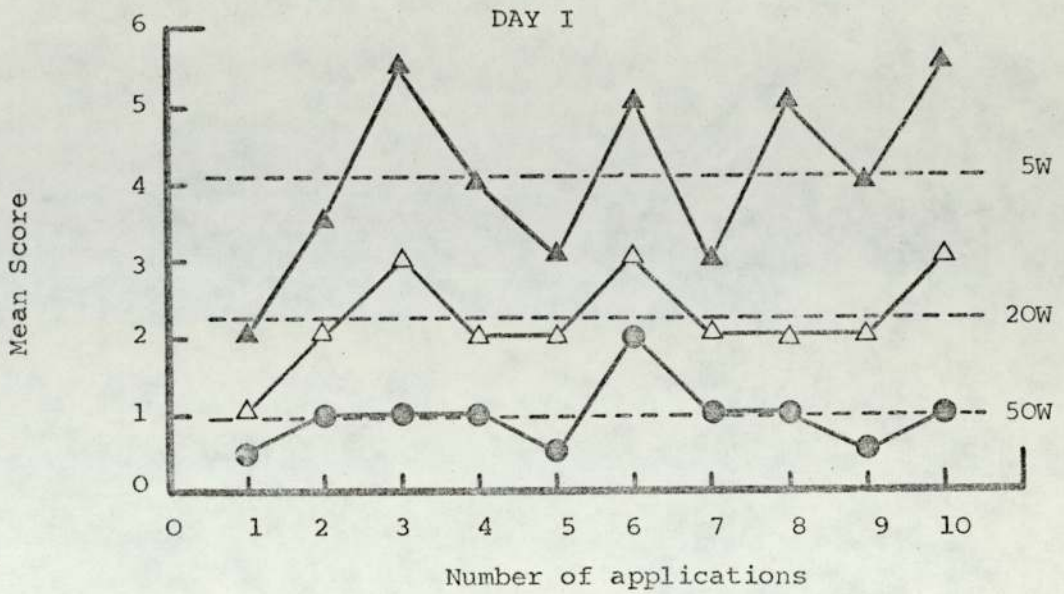

FIGURE 104

PLOT OF MEAN SCORE VERSUS NUMBER OF APPLICATIONS OF THE PLASTIBASE 50W, 20W AND 5W OINTMENTS

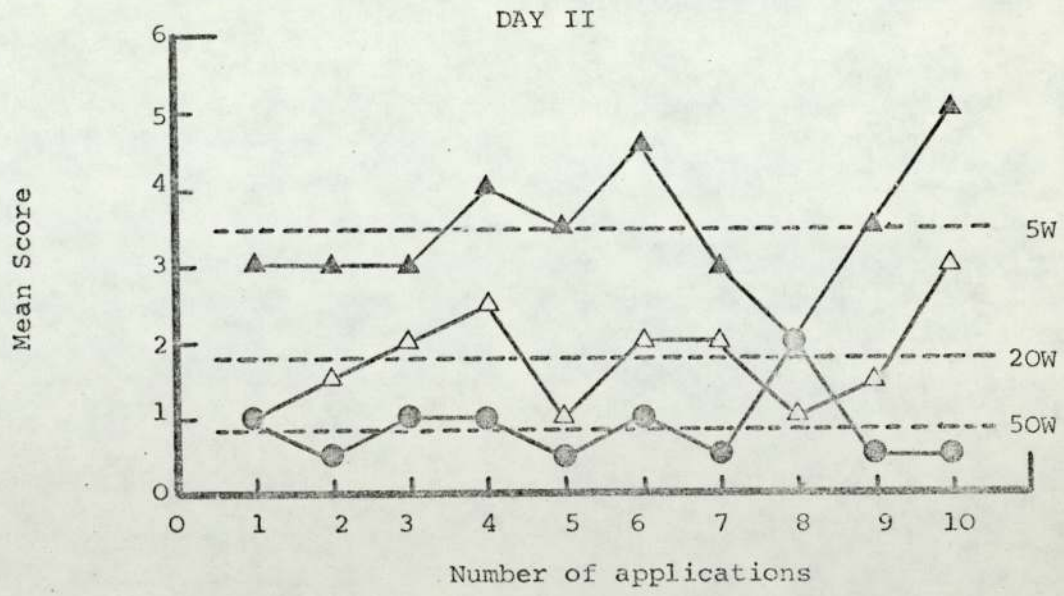

3.2.5 Discussion

The erythema or irritative reaction assessed following the application of salicylic acid ointments reflects the release from Plastibases and the absorption of the drug into the skin. While it is known that salicylic acid is absorbed and reserved into the stratum corneum (332), it is the penetration of the compound into the lower layers of the skin which promotes the keratolytic reaction assessed in this work.

The large area of application of the ointments (27mm diameter) helped in the evaluation of the test sites and enabled a wider range of score system to be used (0 to 6 instead of the 0 to 4 usually adopted in vasoconstrictor studies). The method suffers somewhat from the relatively few sites per person that the ointments can be tested upon and thus for statistically significant work a large number of volunteers would be required. Furthermore, the relative mobilities of the ointments restricted somewhat the position in which they could be applied, even on the forearm. In this work Plastibase 50W ointment was applied on the wrist end, Plastibase 5W ointment in the middle of the forearm and Plastibase 20W ointment on the elbow end. As this arrangement had to be adhered to on all the volunteers in order to prevent any leakages, a double blind trial was not possible and inevitably imposed a bias in the assessment of test sites. It is considered that in future trials, a quantal method based on the all or none principle may perhaps prove more useful in that it may not only reduce the scoring errors but may also enable the application quantities to be reduced and the number of test sites to be increased per person. It is recognised that while an intersubject variation in response is

inevitable in such studies, standardisation in procedures would lead to a greater control over such trials and would enable small differences in release rates to be distinguished. It must be emphasised however that in this work due to the large differences in the release characteristics of the three ointments tested, scoring of test sites or analysis of results posed no problem.

It was seen that Plastibase 5W produced by far the greatest irritative response in all individuals, followed by Plastibase 20W ointment. Plastibase 50W produced the smallest response. These results were largely confirmed on the second day when the test sites were re-evaluated though the mean scores were smaller on the second day. The only exception was subject number 8. It was not possible to determine the cause of the unusual reaction shown by the subject on the second day.

Plots of mean score of response for the three formulations versus $1/\eta_{app}$ and log $(1/\eta')$ for both days are linear, Figures 105 and 106, indicating that though the macroviscosity values do not necessarily reflect the microviscosity environment seen by the diffusing drug molecule, these values as determined by the volume fraction of the polymer in the gels are having a considerable influence on the release of salicylic acid as predicted by the equations of Mackie & Meares (347) and Wang (348).

A linear correlation was obtained between *in vivo* and *in vitro* results, further confirming the observations of Nakano & Patel (181) concerning the suitability of a silastic membrane for investigating drug release from diverse bases.

FIGURE 105

PLOT OF MEAN SCORE VERSUS INVERSE APPARENT VISCOSITY

DERIVED FROM CONTINUOUS SHEAR TESTS

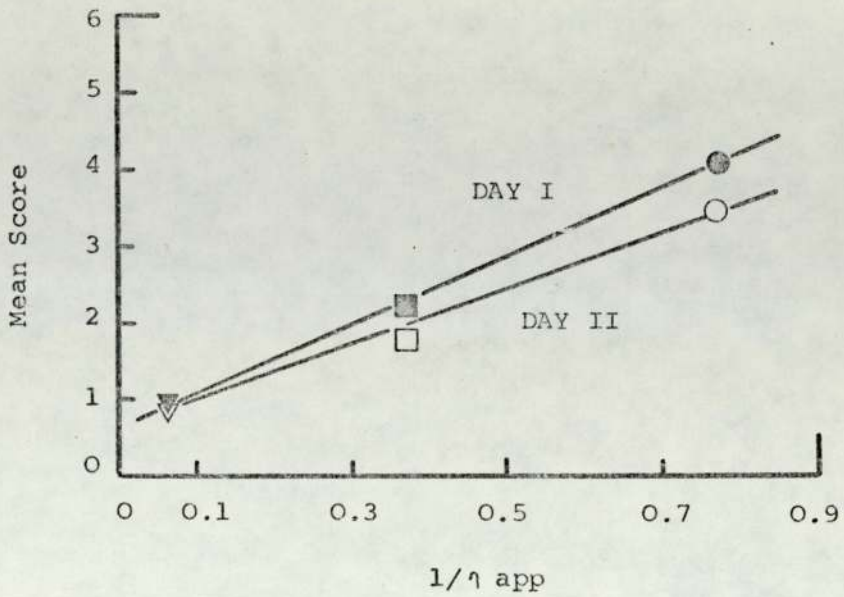

FIGURE 106

PLOT OF MEAN SCORE VERSUS LOG INVERSE DYNAMIC VISCOSITY

DERIVED FROM OSCILLATORY TESTS

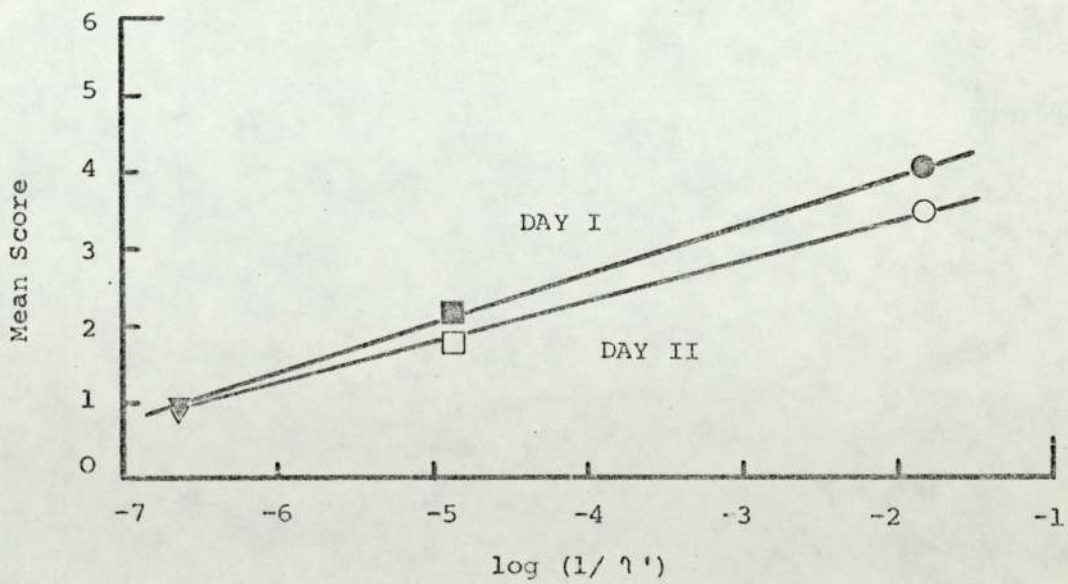

FIGURE 107

CORRELATION OF IN VIVO AND IN VITRO DATA

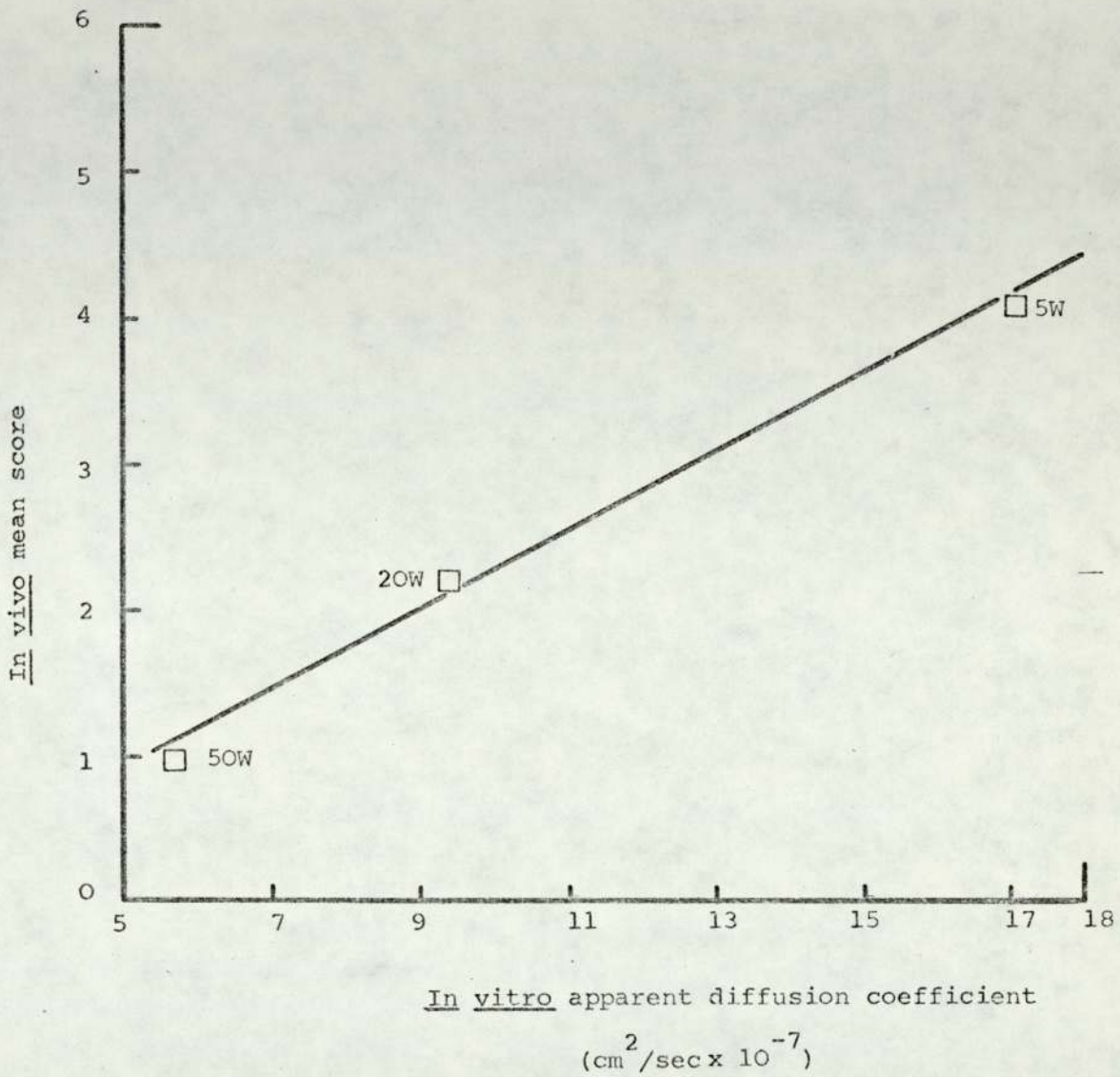

3.3 Assessment of salicylate absorption from urinary excretion following topical application of Plastibase ointments

3.3.1 Introduction

Urinary excretion studies have been adopted by several workers for studying the percutaneous absorption of salicylates (98, 311 - 2, 354, 355, 357). The assumption that has been made in these studies is that the rate of excretion of the drug parallels the skin absorption and the blood level of the drug. Though several reservations have been expressed concerning this assumption (13, 76), this type of studies has proved useful in the evaluation of physicochemical factors affecting percutaneous absorption (98).

Previous work (Section 3.2) has shown that Plastibase consistency affected the release from ointments and absorption by the skin of salicylic acid. As a result, it was of particular interest in this work to know the subsequent effect on the systemic absorption of the drug due to the consistency of these preparations. The object of this part of the work was thus to determine from urinary excretion studies the influence of rheological properties of Plastibase ointments on the systemic absorption of salicylic acid and methyl salicylate.

3.3.2 Materials

Plastibase 50W Batch Number 2363

Plastibase 20W Batch Number Not given

Plastibase 5W Batch Number 1280

Salicylic acid and methyl salicylate were of analytical grades (B.D.H.). Salicylic acid was sieved through a No. 85 sieve. Other materials were

as described below. All reagents were of analytical grade.

3.3.3 Experimental

(a) Assay of Salicylates

Acetylsalicylic acid and methyl salicylate absorbed into the body are rapidly hydrolysed to salicylic acid which in turn is conjugated in part with glycine to form salicyluric acid and with glucuronic acid to form acyl and phenolic glucuronides as is shown in Table 45. A small fraction of salicylic acid is hydroxylated to gentisic acid and several other metabolites (314). Free salicylic acid and its metabolites comprising 75% - 90% of the orally administered dose are eliminated from the body by renal excretion (362). The assay of salicylate excretion in urine must thus take into account not only free salicylic acid but also the major metabolites.

Such a method used in this work for total salicylate assay in urine was based on that of Chiou & Melukwe (363). This method is a modification of the methods of Trinder (364) and Levy (365) and overcomes under or over estimation of salicylate excretion resulting from a variation in the urinary blank contribution or under-reaction of the metabolites with the reagent. The analytical procedure employed was as follows.

2ml concentrated hydrochloric acid was added to 3ml of urine sample in a 15ml screw-top glass blood sample vial. After sealing the vials with plastic tops, they were incubated in an oven at 100^{o}C for seventeen hours. After cooling, 0.5ml of approximately 6N hydrochloric acid (prepared by dilution of concentrated hydrochloric

TABLE 45

THE BIOTRANSFORMATION OF ASPIRIN IN MAN (314)

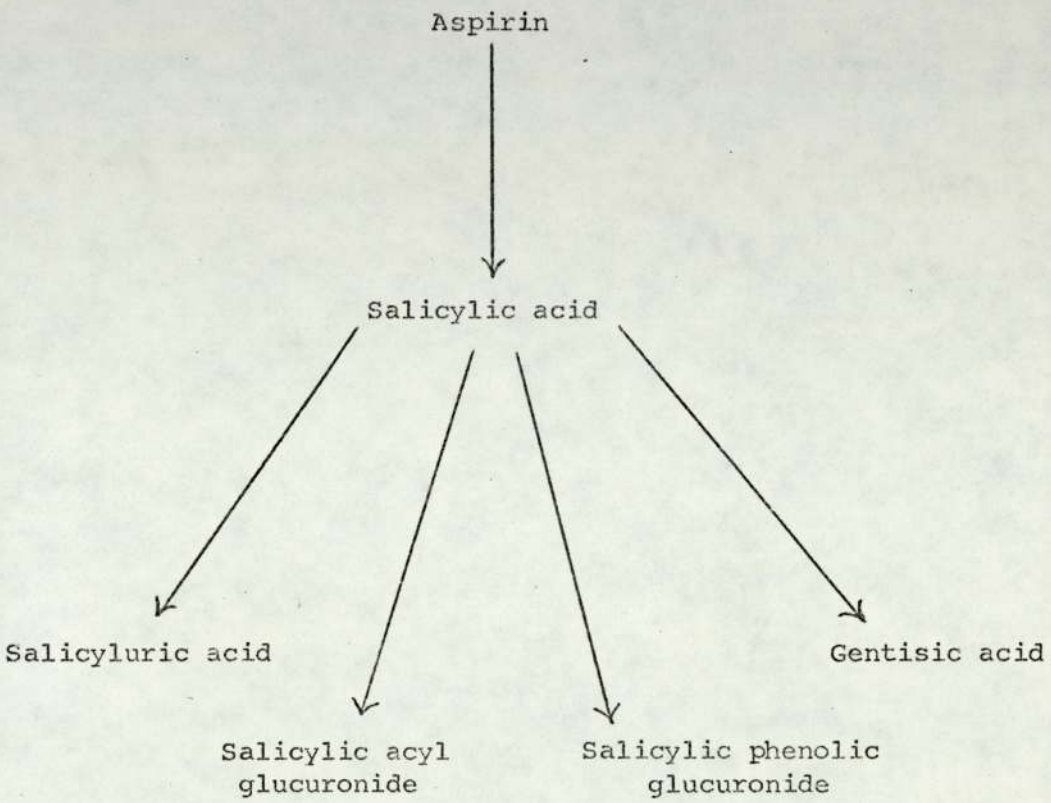

acid with an equal volume of distilled water) and 6ml of chloroform were added. The tubes were shaken for ten minutes. They were then centrifuged for five minutes in a laboratory centrifuge and the aqueous phase was aspirated. 3ml of the chloroform layer was then accurately transferred to another blood sample vial. 6ml of Trinder's reagent (364) without mercuric chloride was added. The tubes were shaken for ten minutes and centrifuged. The chloroform phase was aspirated and the absorbance of the aqueous layer was measured at 540nm (Pye Unichem SP500). Trinder's reagent without mercuric chloride was used as the blank. To calculate the concentration of total salicylate in urine specimens, a standard curve was constructed using known concentrations of salicylic acid in distilled water and following the same incubation and extraction procedure, Figure 108. All assays were run in duplicate and the average of two readings was taken as the true reading.

(b) Procedure employed in salicylate absorption study

Healthy male subjects, age 22 - 27 years, were chosen for this study. No attempt was made to control diet or liquid intake except that no drug, other than that under test, was taken for a week before the trial. No alcoholic beverages were allowed a day before and during the trial. The trial was usually commenced between 8.00 a.m. and 9.00 a.m. in the morning.

Previous work on salicylates has shown that the excretion of the drugs is highly dependent on the pH of the urine (314, 366 - 8). The urinary pH in a healthy subject fluctuates throughout the day and exhibits a circadian rhythm (369). Such fluctuations would be

FIGURE 108

STANDARD CURVE FOR SALICYLATE EXCRETION IN URINE

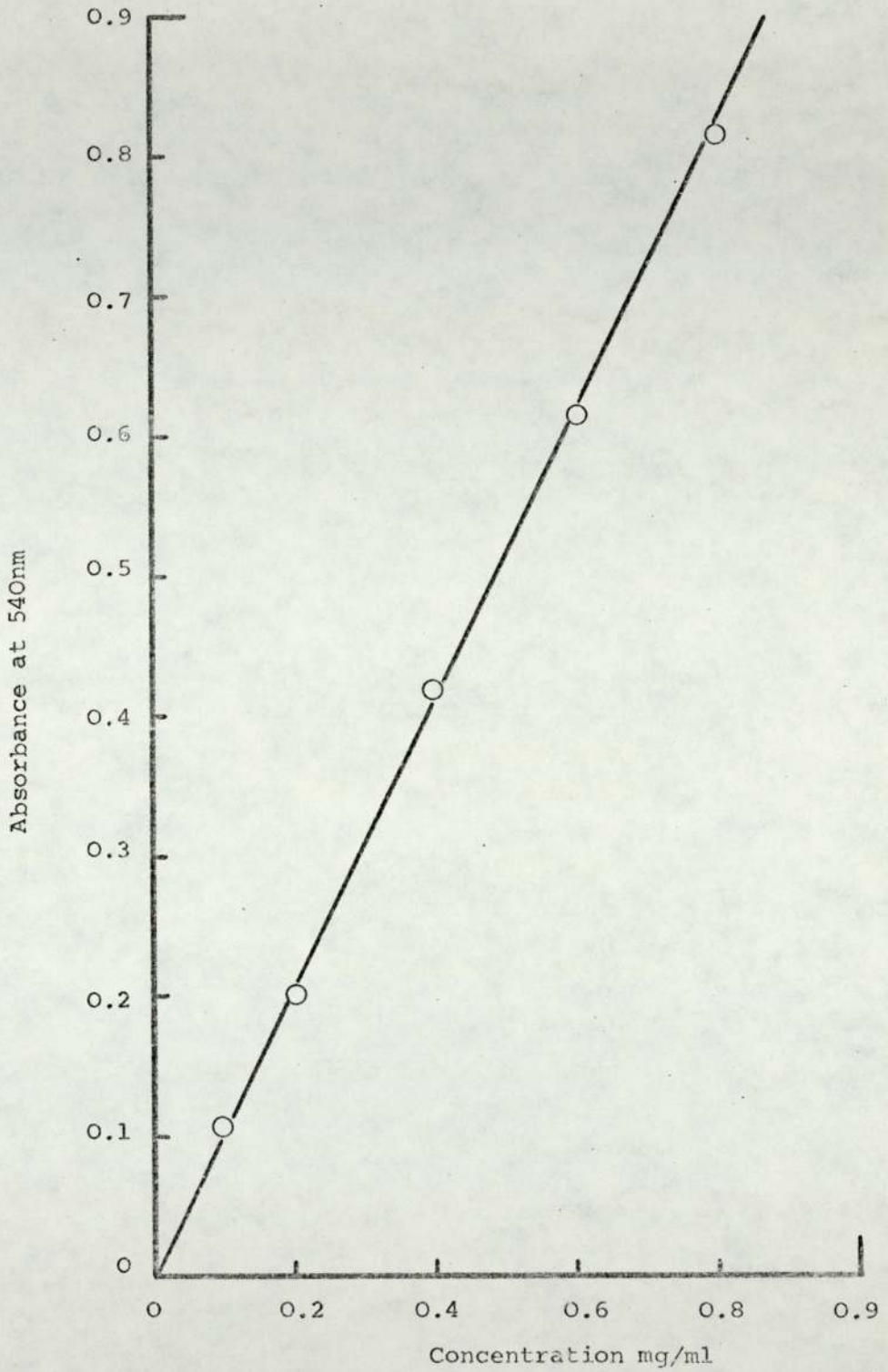

reflected in the excretion rate of free salicylate in the urine. In order to be able to relate the urinary excretion of salicylate to the relative absorption of the drug, it was necessary to control the urine pH in each subject throughout the trial. Smith et. al. (370) have shown that alkalinisation of the urine to a pH of 7.4 maximises the renal clearance of free salicylate. The following regimen for inducing alkaline urine was adopted in this work.

Initially 100ml of sodium bicarbonate solution (5% w/v) was administered one hour prior to commencing the trial followed by 20ml of the solution every hour for ten hours. Urine was collected at the time of application or administration of the medication and then at predetermined intervals. The total volume of the urine was measured and samples were retained for analysis and pH measurement.

Adult size, large Translet colostomy plasters (57mm diameter) were used for the topical application of the ointments. These reservoirs were filled and sealed as described previously (Section 3.2.3). 10% salicylic acid and 10% methyl salicylate ointments made with Plastibase 50W, 20W and 5W were used in this work. The ointment to be tested was prepared twenty four hours prior to commencing a trial. The following trials were conducted:-

(i) For control and comparative purposes, the urinary excretion of salicylates following oral administration of Aspirin (600 mg) was studied in two subjects.

(ii) The absorption of salicylic acid via the skin was studied from urinary excretion data following topical application of Plastibase ointments (50W, 20W and 5W) containing 10% of the

drug. The above three trials were repeated on the same subject in order to determine reproducibility and evaluate intrasubject variation.

(iii) The absorption of methyl salicylate via the skin was studied from urinary excretion data following topical application of Plastibase ointments (50W, 20W and 5W) containing 10% of the drug. The above three trials were repeated on the same subject in order to determine reproducibility and evaluate intrasubject variation.

3.3.4 Results

The results of the oral drug absorption trials are shown in Figures 109 and 110. In both subjects, the excretion of Aspirin reached a maximum two to four hours after administration of the drug and then decreased exponentially. Cumulative plots of excretion for both subjects showed that 74% and 78% of the drug was excreted in twenty four hours respectively by the two subjects. The excretion rate does not appear to be greatly influenced by urinary output. Small fluctuations were recorded in the urine pH in the alkaline range however these too do not appear to influence the rate of excretion.

The results of topical drug absorption trials with salicylic acid ointments are shown in Figures 111 to 113. All the three trials show a gradual increase in the excretion rate leading to an almost steady state of excretion. This is further indicated by cumulutaive plots of excretion which are almost linear. The fluctuations in the excretion of salicylates cannot be correlated with the urinary output or the urinary

FIGURE 109

URINARY EXCRETION OF SALICYLATE WITH CORRESPONDING URINARY pH AND URINE OUTPUT AFTER ORAL ADMINISTRATION OF 600mg OF ASPIRIN

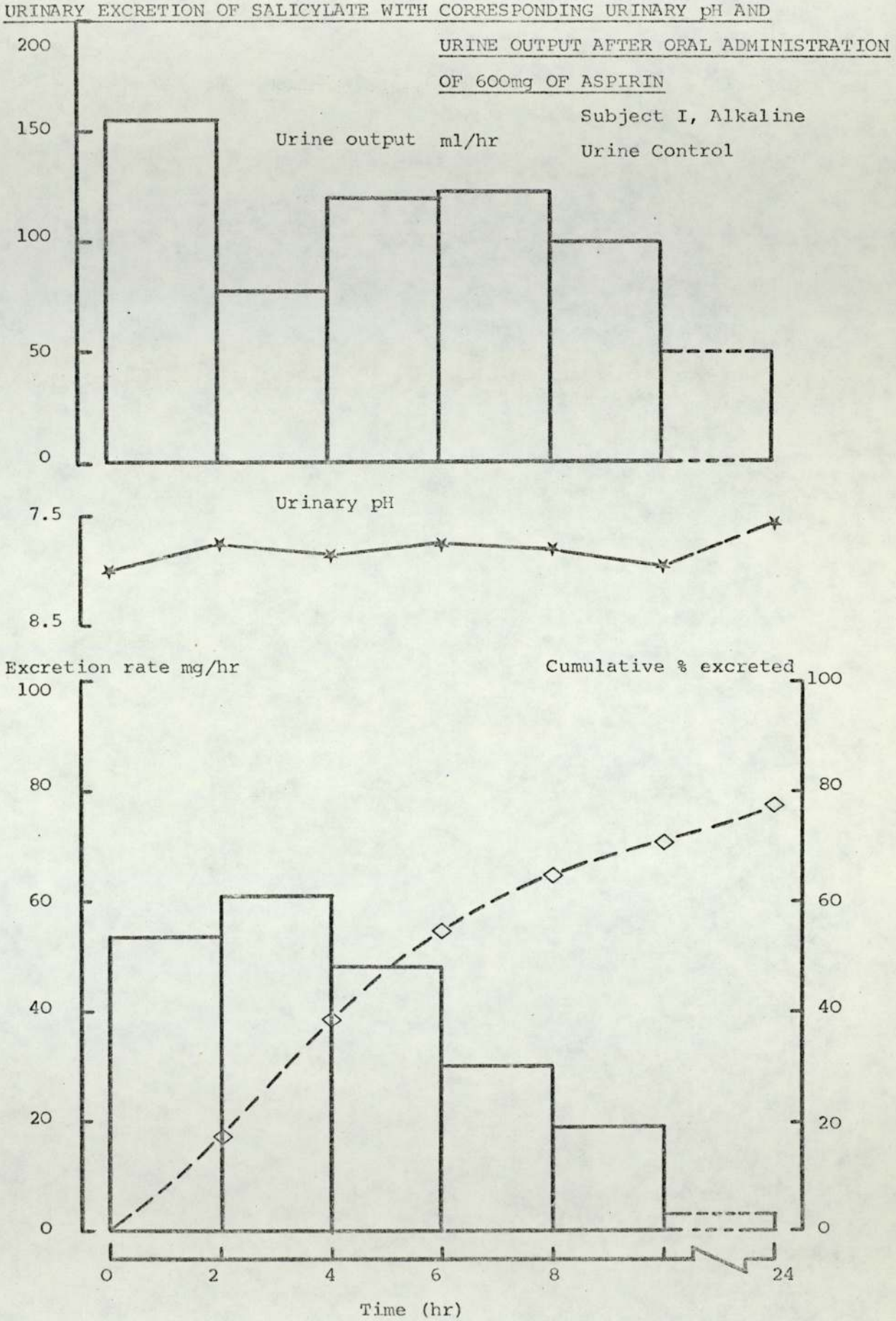

FIGURE 110

URINARY EXCRETION OF SALICYLATE WITH CORRESPONDING URINARY pH AND URINE OUTPUT AFTER ORAL ADMINISTRATION OF 600mg OF ASPIRIN

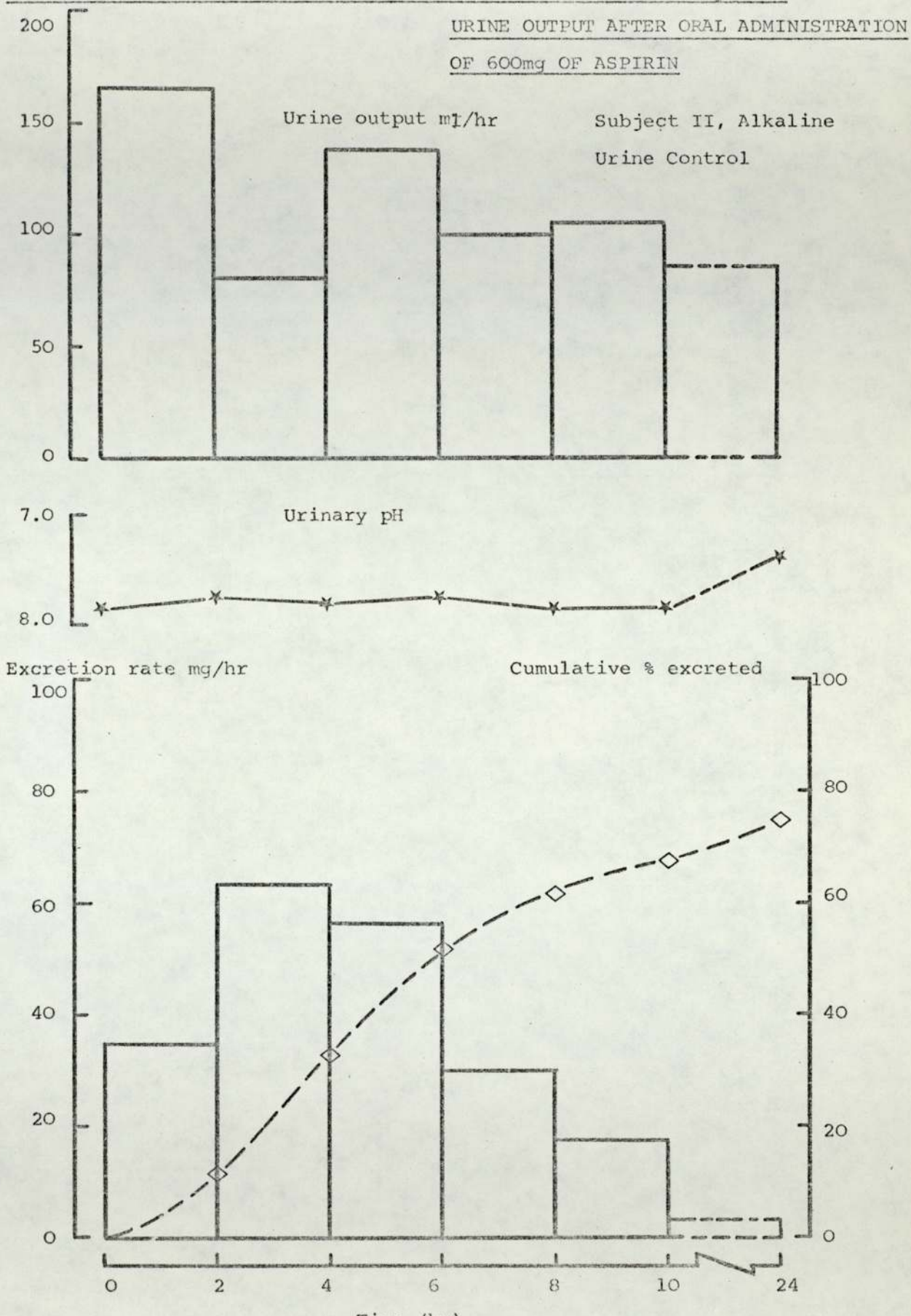

FIGURE 111

URINARY EXCRETION OF SALICYLATE WITH CORRESPONDING URINARY pH AND URINE OUTPUT AFTER TOPICAL APPLICATION OF PLASTIBASE 50W OINTMENT CONTAINING 10% SALICYLIC ACID

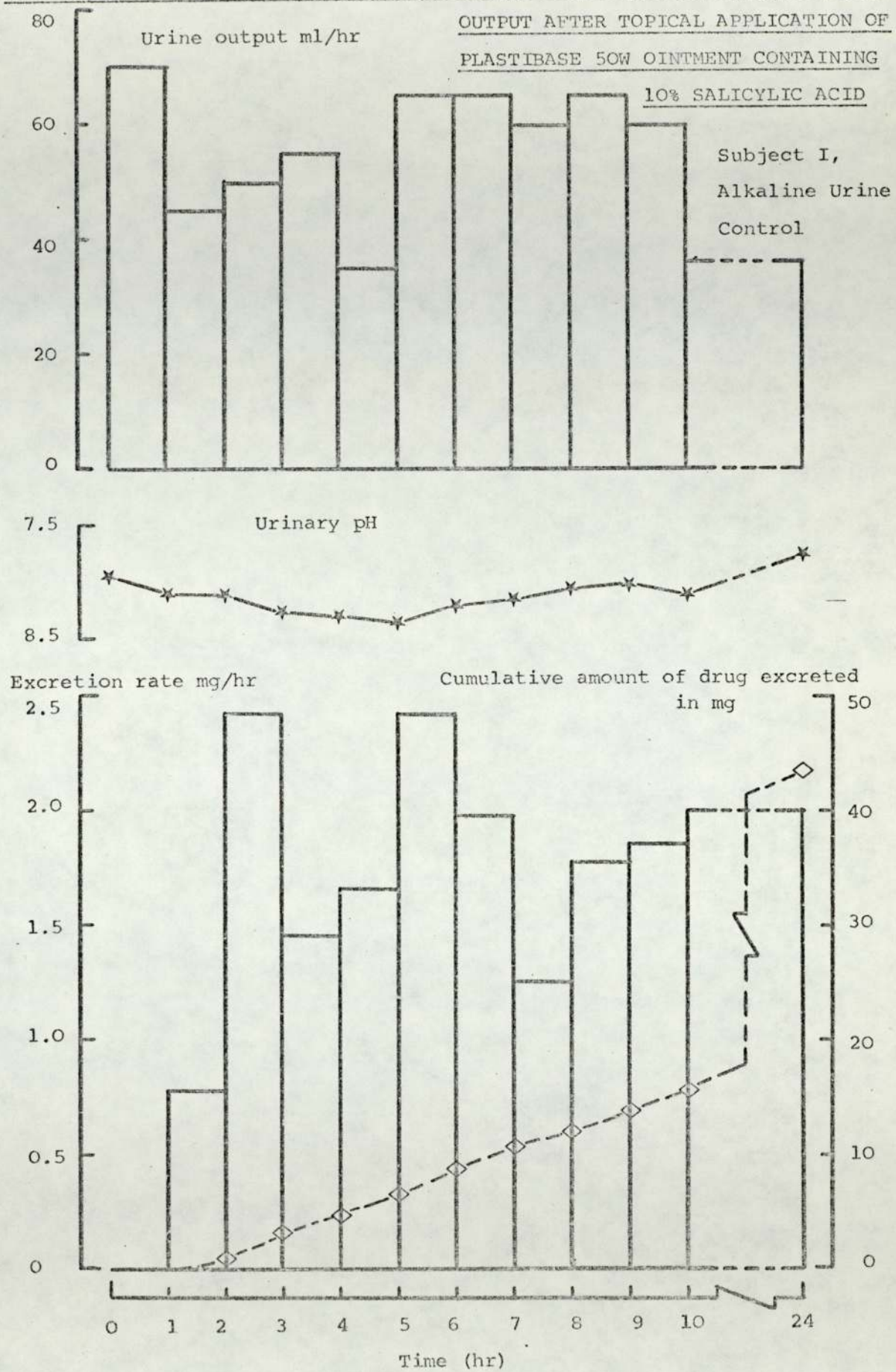

FIGURE 112

URINARY EXCRETION OF SALICYLATE WITH CORRESPONDING URINARY pH AND URINE OUTPUT AFTER TOPICAL APPLICATION OF PLASTIBASE 20W OINTMENT CONTAINING 10% SALICYLIC ACID

Subject 1, Alkaline Urine Control

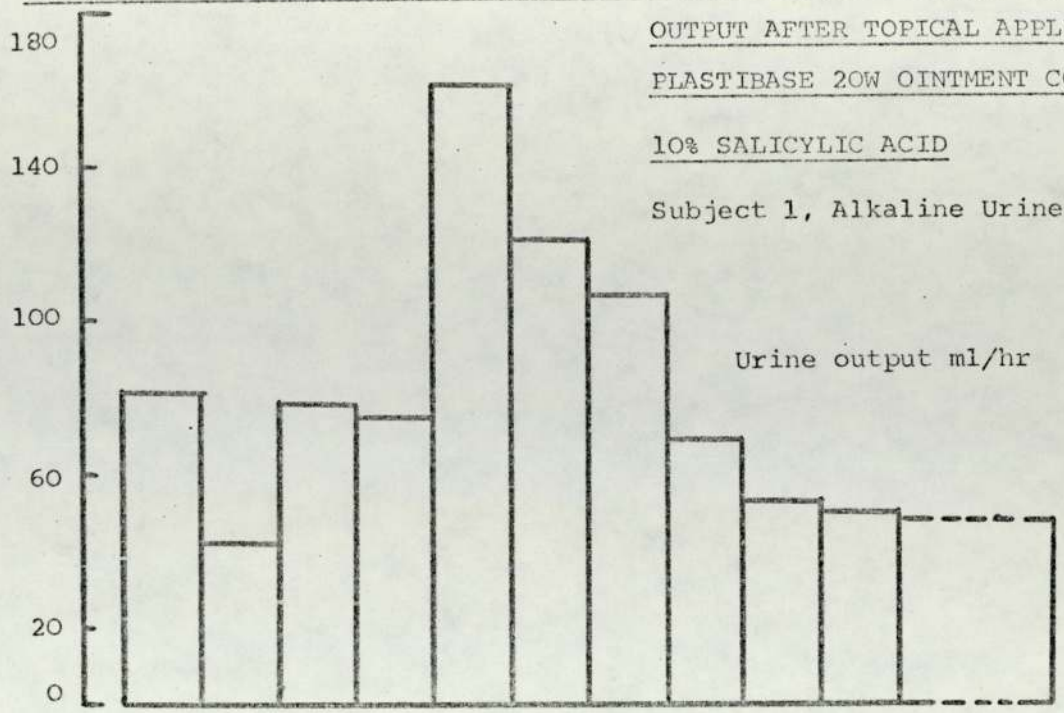

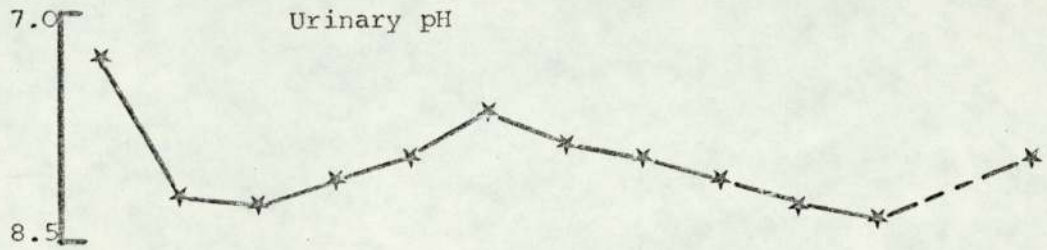

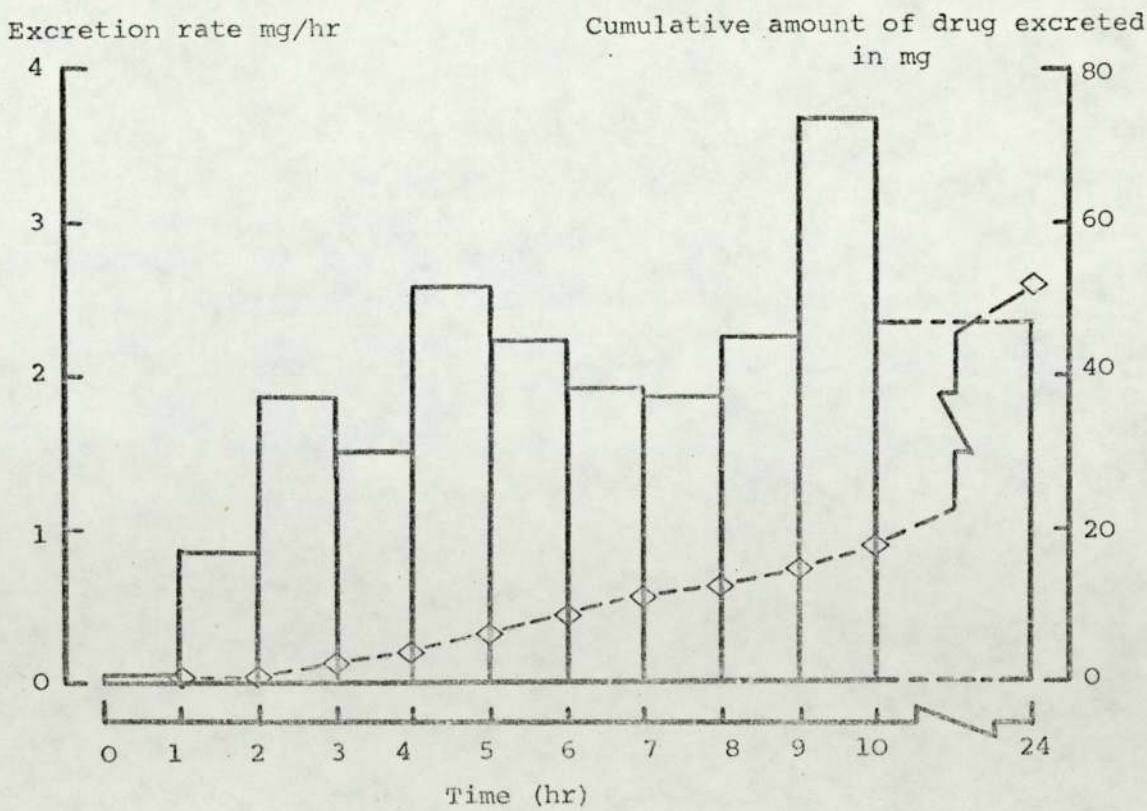

FIGURE 113

URINARY EXCRETION OF SALICYLATE WITH CORRESPONDING URINARY pH AND URINE OUTPUT AFTER TOPICAL APPLICATION OF PLASTIBASE 5W OINTMENT CONTAINING 10% SALICYLIC ACID

Subject I, Alkaline Urine Control

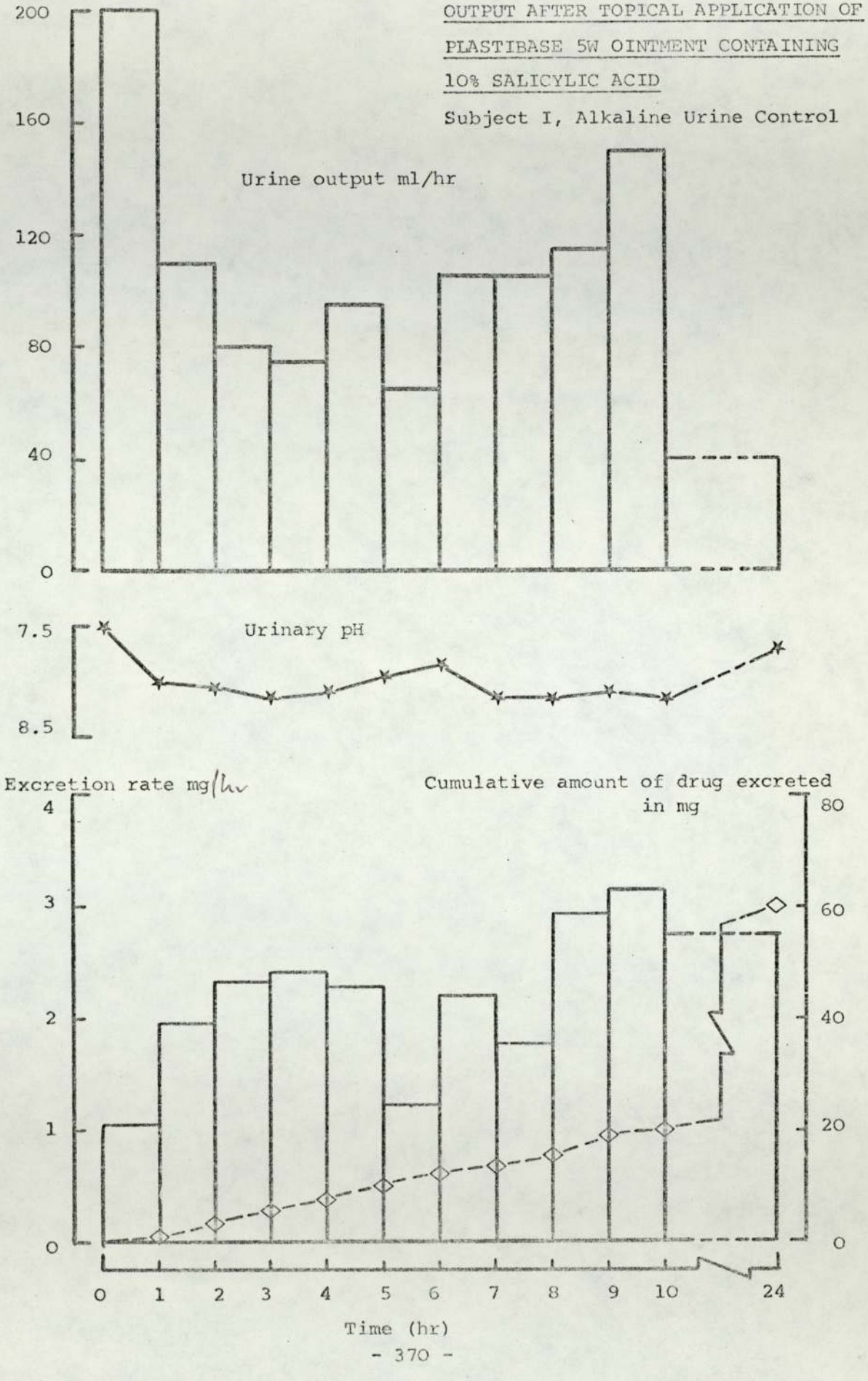

pH. Accumulated totals of drug excreted in twenty four hours show that following topical application of Plastibase 5W ointment, the largest quantity of drug was excreted. This was followed by Plastibase 20W. The smallest amount of drug was excreted following the application of Plastibase 50W. These results together with the cumulative results for the above three trials repeated are shown in Table 46.

The results of topical drug absorption trials with methyl salicylate ointments are shown in Figures 114 to 116. As with salicylic acid trials, there appears to be no apparent correlation between the fluctuations in excretion of salicylate and the urine output and urinary pH. Similar cumulative excretion plots show that excretion rates are not greatly affected by the properties of the vehicle. Results of these and cumulative results of the above three trials repeated are given in Table 47.

3.3.5 Discussion

Urinary excretion studies have an advantage over plasma or serum analysis in that sampling is particularly easy. Furthermore Wilkinson (371) has suggested that for drugs which are largely distributed in the extracellular fluid, and this would appear to be the case for salicylates (357), urinary excretion studies may be the only practical means of evaluating *in vivo* absorption of the drug from the dosage form. The elimination of an absorbed drug via the renal route is considerably influenced by urinary pH and in the case of salicylates, it has been shown that the optimal pH for maximal renal clearance of free salicylate is 7.4 (370). It has, moreover, been shown that urinary

TABLE 46

TOTAL URINARY EXCRETION OF SALICYLATES TWENTY FOUR HOURS AFTER APPLICATION OF PLASTIBASE OINTMENTS CONTAINING 10% SALICYLIC ACID UNDER ALKALINE URINE CONTROL. SUBJECT I.

Ointment	Initial Trials	Repeat Trials
Plastibase 50W	43.64 mg	42.58 mg
Plastibase 20W	51.63 mg	50.13 mg
Plastibase 5W	60.10 mg	58.95 mg

TABLE 47

TOTAL URINARY EXCRETION OF SALICYLATES TWENTY FOUR HOURS AFTER APPLICATION OF PLASTIBASE OINTMENTS CONTAINING 10% METHYL SALICYLATE UNDER ALKALINE URINE CONTROL. SUBJECT I.

Ointment	Initial Trials	Repeat Trials
Plastibase 50W	55.27 mg	53.32 mg
Plastibase 20W	52.50 mg	53.02 mg
Plastibase 5W	53.12 mg	55.10 mg

FIGURE 114

URINARY EXCRETION OF SALICYLATE WITH CORRESPONDING URINARY pH AND URINE OUTPUT AFTER TOPICAL APPLICATION OF PLASTIBASE 50W OINTMENT CONTAINING 10% METHYL SALICYLATE

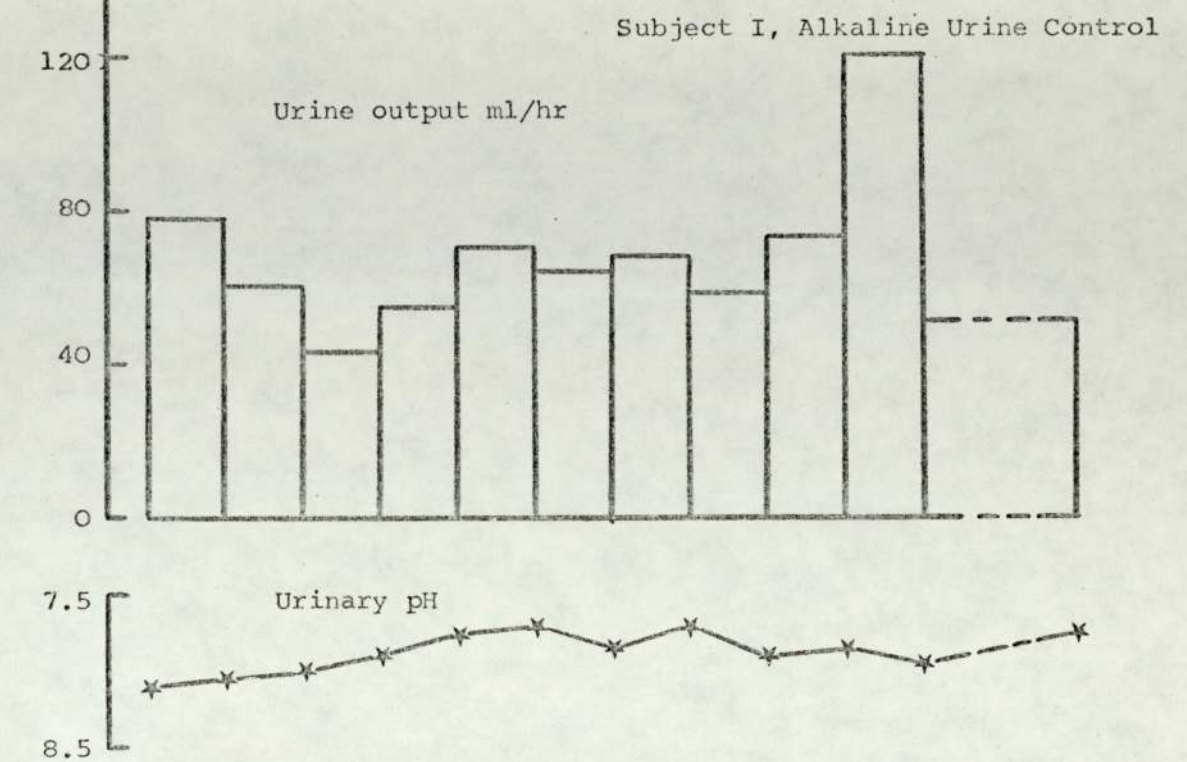

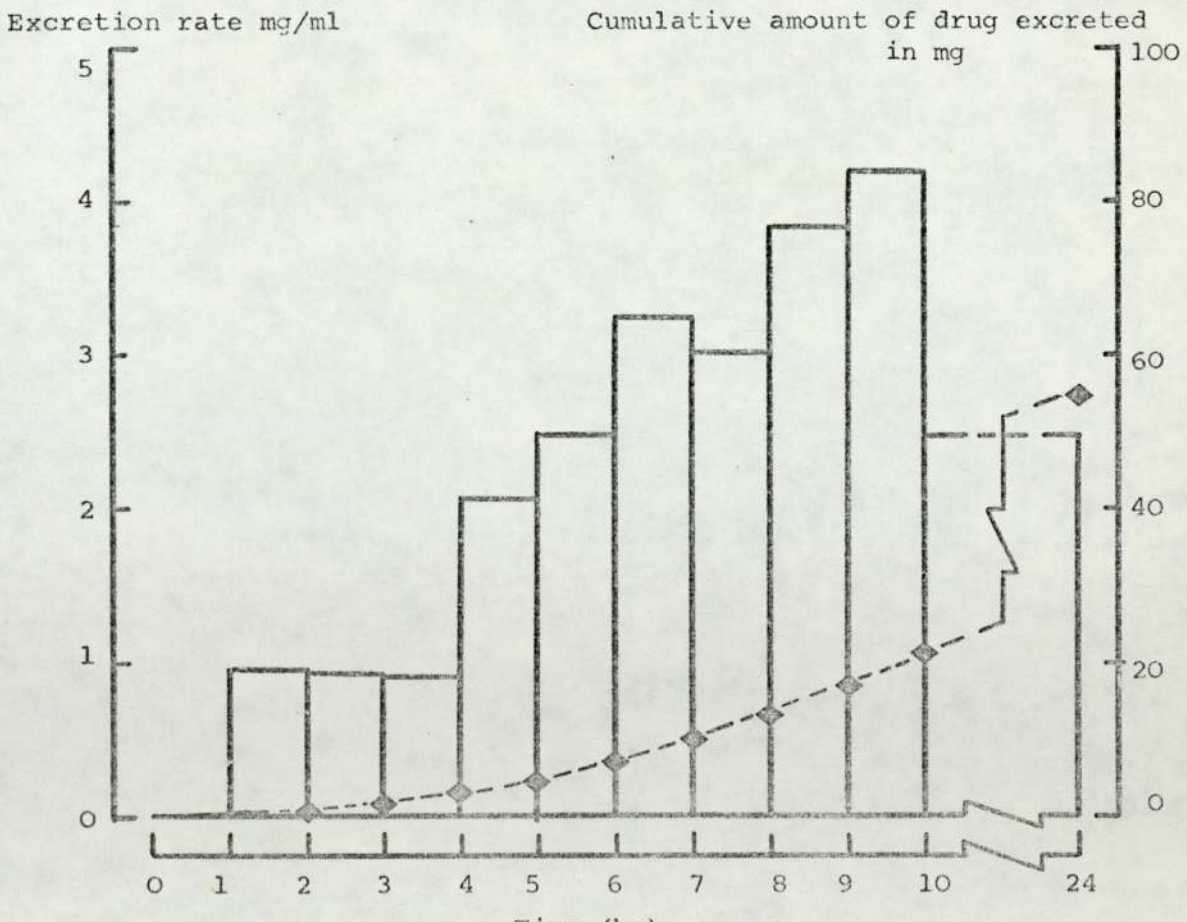

FIGURE 115

URINARY EXCRETION OF SALICYLATE WITH CORRESPONDING URINARY pH AND URINE OUTPUT AFTER TOPICAL APPLICATION OF PLASTIBASE 20W OINTMENT CONTAINING 10% METHYL SALICYLATE

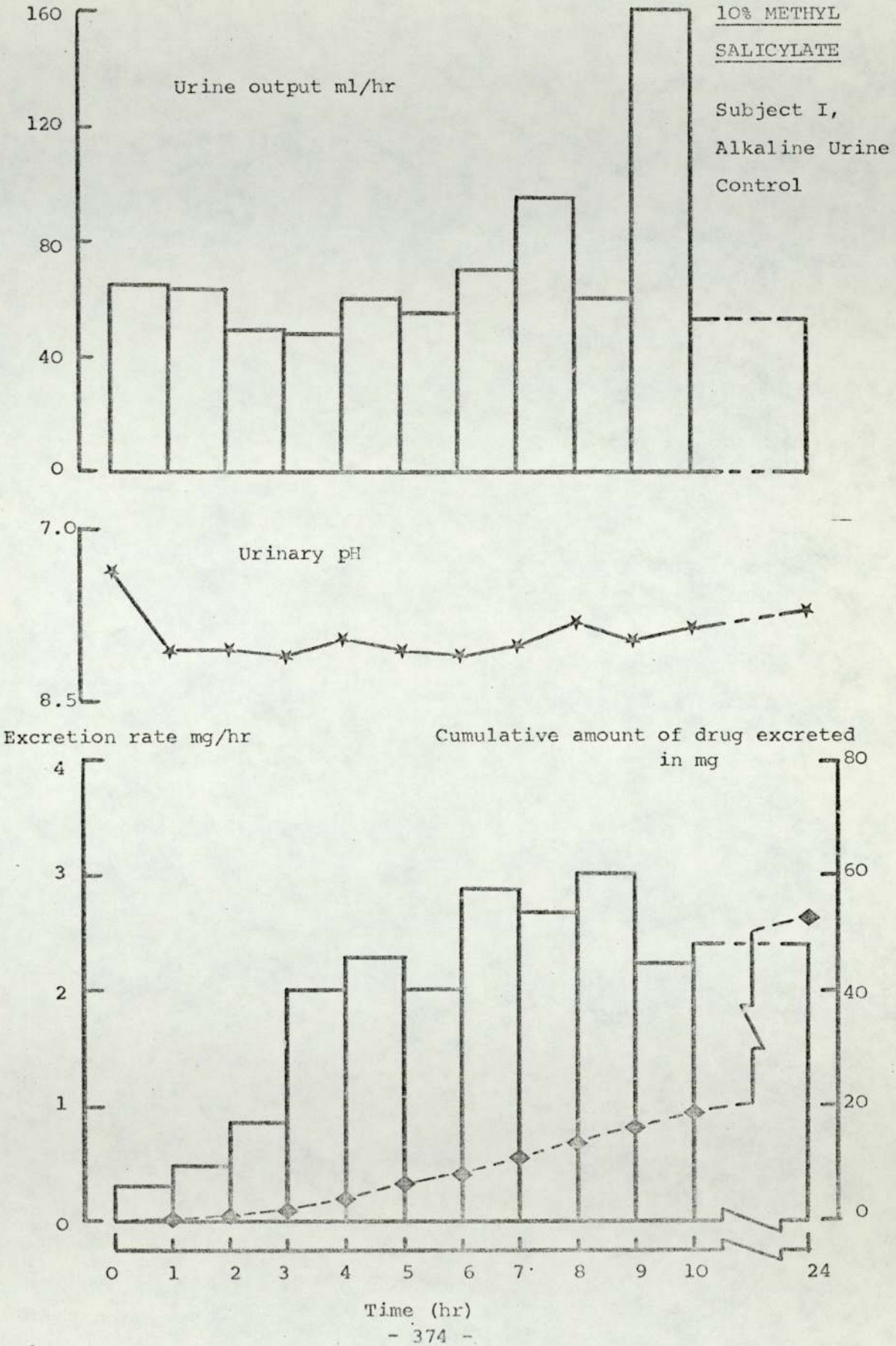

FIGURE 116

URINARY EXCRETION OF SALICYLATE WITH CORRESPONDING URINARY pH AND URINE OUTPUT AFTER TOPICAL APPLICATION OF PLASTIBASE 5W OINTMENT CONTAINING 10% METHYL SALICYLATE

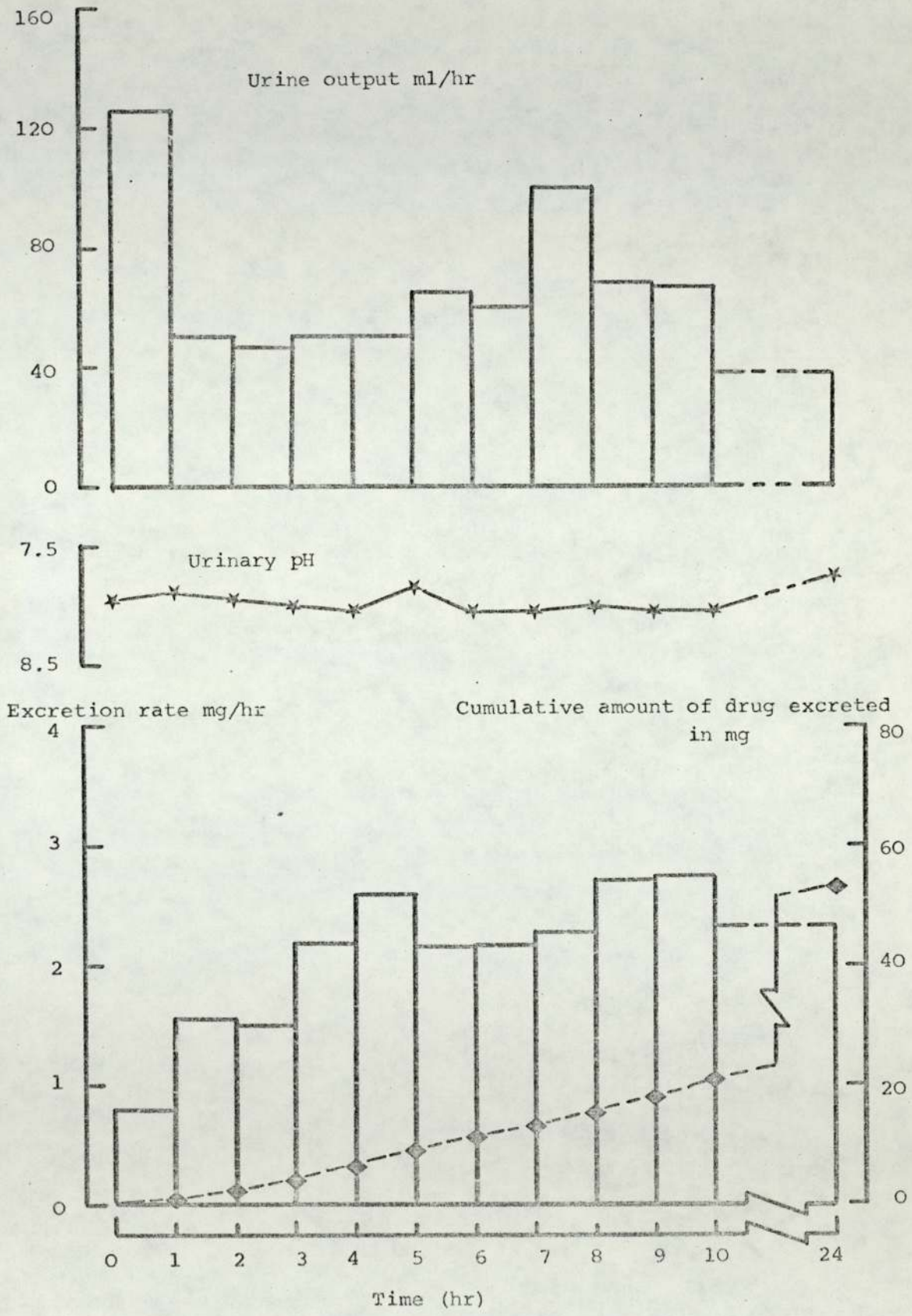

excretion of salicylates may be related to the plasma levels of the drug (372). Thus in this work, using alkaline urine control, it was possible to relate the excretion of the drug to the absorption of the drug via the oral and topical route.

Oral absorption of 600mg Aspirin in two subjects showed little intersubject variation. One of the subjects excreted 74% and the other excreted 78% of the administered drug within twenty four hours. These figures compare well with the urinary elimination figures quoted by other workers (362, 373). From these trials, though it was seen that intersubject variation was small, in order to reduce this variation further, topical drug absorption studies were carried out in one individual only.

There is no comparison between the oral and the topical dosage form. The quantity of drug absorbed via the topical route is considerably smaller than the oral route. It is recognised that a major contributing factor in this difference may be due to the difference in the administered and applied drug concentration via the two routes respectively. While it can be assumed that all of the orally administered drug is available for absorption, this does not apply in the case of a semisolid topical reservoir. Due to the low diffusivity of the drug in the vehicle, it is only the drug in the layer near the skin which may be available for absorption and thus it is somewhat difficult to predict the cumulative percentage of the absorbed drug that is excreted. Since the applied concentration of the drug in the ointments used is kept the same, the rate of excretion of the drug should reflect an adequate measure of rate of absorption. The

differences in the drug excretion profiles via the two routes indicates an interesting difference in the drug absorption. In the case of oral absorption the lag phase is small and most of the drug is absorbed in the first two to four hours. In the case of topical absorption however, the skin barrier prevents rapid absorption of the drug and the lag time is considerably longer. A steady state of excretion of the drug after twenty four hours indicates that the drug is still being absorbed.

Topical drug absorption trials with salicylic acid ointments showed a consistent increase in the excretion of salicylate with a decrease in the measured consistency of the material. Similar trials with methyl salicylate however showed a lack of correlation between the urinary excretion data and the measured consistency parameters of Plastibases. These results thus further confirm the finding of the in vitro studies on the Plastibase ointments and may be explained as before. It would seem that for methyl salicylate absorption, the rate limiting step appears to be skin absorption and thus the physical properties of the vehicle are relatively unimportant in the transport process. It is thought that in the case of salicylic acid, it is the balance in the rate limiting capacity of the dissolution, diffusion and membrane transport processes which will determine drug absorption and thus the physical properties of the vehicle are important. Thus for topical absorption of salicylic acid, plots of total salicylate excreted in twenty four hours versus $1/\eta_{app}$ and $\log(1/\eta')$ were linear, Figures 117 and 118. A linear correlation was also obtained for salicylic acid ointments between the in vivo drug absorption as determined from urinary excretion studies and the in vitro diffusion coefficients for Plastibase 50W, 20W and 5W ointments, Figure 119.

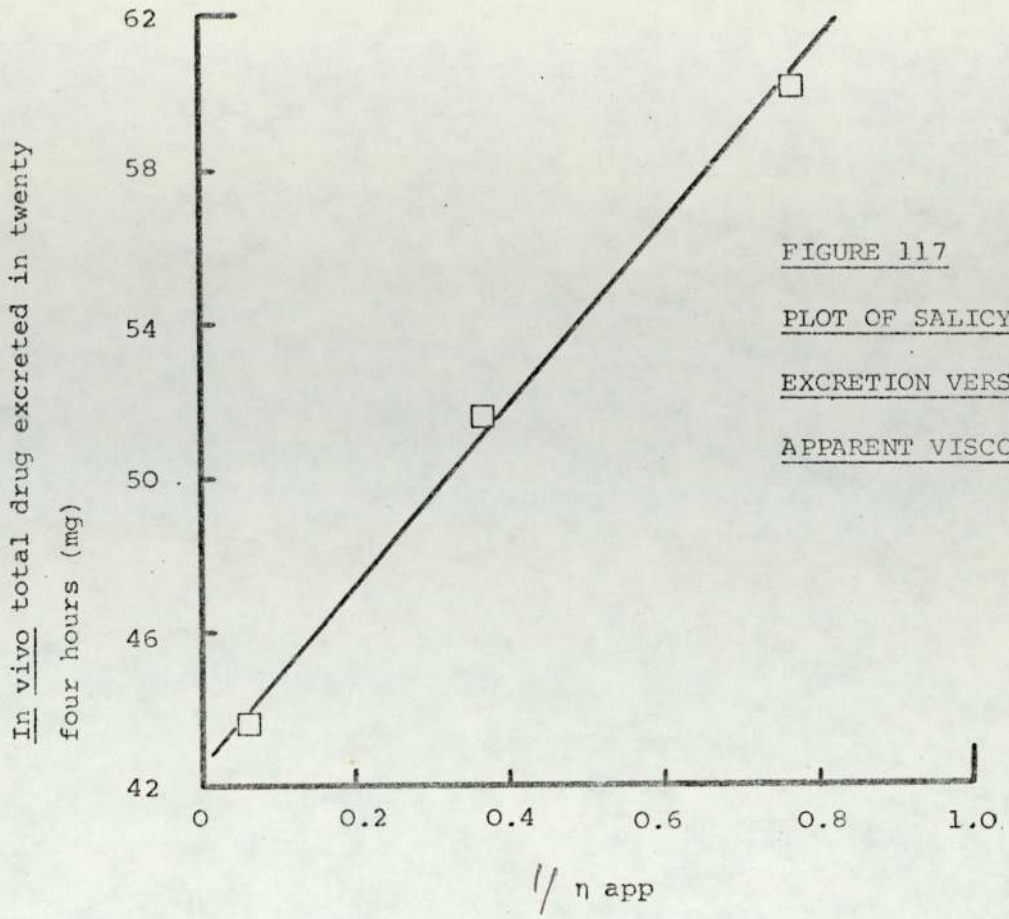

FIGURE 117

PLOT OF SALICYLATE EXCRETION VERSUS INVERSE APPARENT VISCOSITY

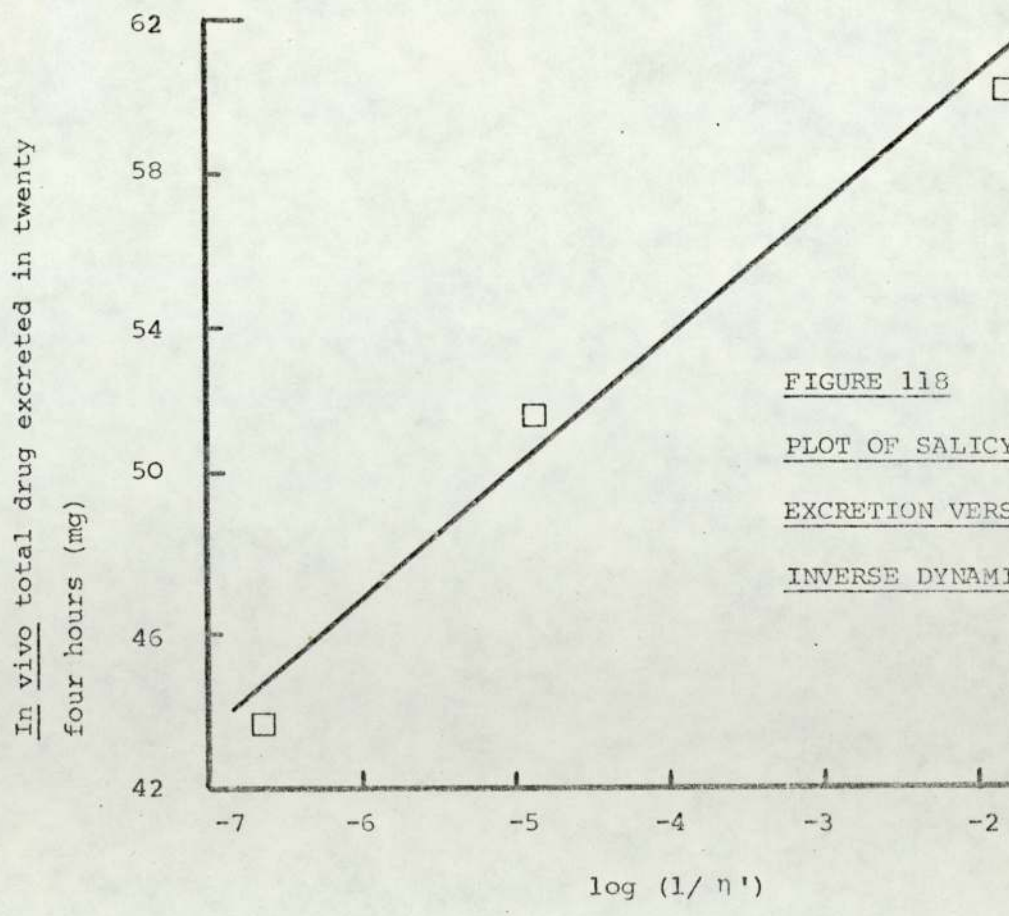

FIGURE 118

PLOT OF SALICYLATE EXCRETION VERSUS LOG INVERSE DYNAMIC VISCOSITY

FIGURE 119

CORRELATION OF IN VIVO URINARY EXCRETION DATA WITH

IN VITRO APPARENT DIFFUSION COEFFICIENTS

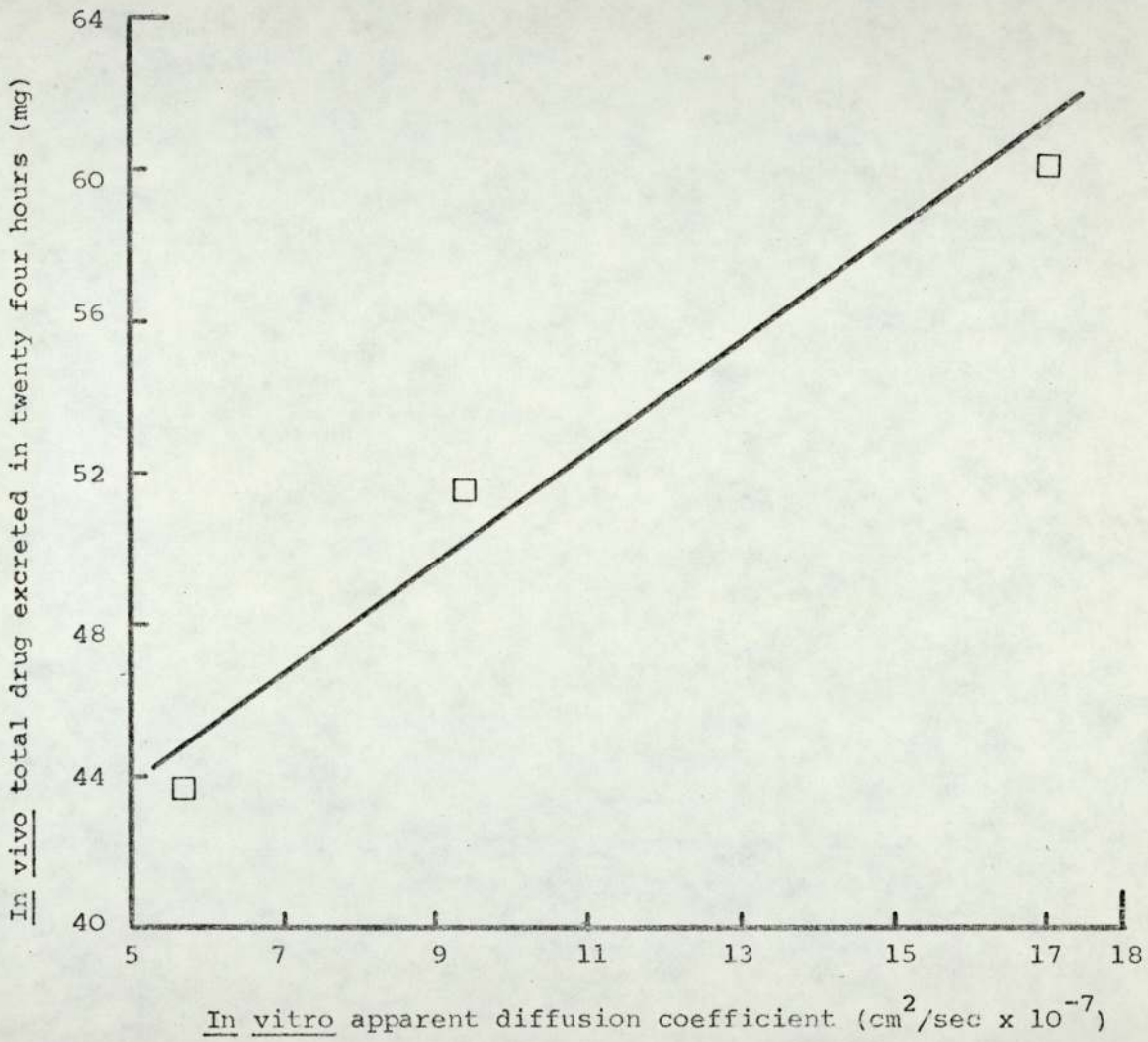

PART D

CONCLUSIONS AND

SUGGESTIONS FOR FURTHER WORK

1. CONCLUSION

The application of a transport theory to drug diffusion in semisolid pharmaceuticals requires a fundamental consideration of the viscous or frictional resistance experienced by a diffusing drug molecule. Although this fact has been recognised by several workers, few studies are reported to have been carried out in order to ascertain the extent of viscous influence on drug release. Unfortunately the complex nature of drug-vehicle systems used and the inappropriate choice of rheological and drug release test methods in these studies have lead to inconclusive results. The major problem however has been the difficulty in describing adequately the 'viscosity' of a semisolid. It was thus apparent that a more definitive approach was required in order to clarify this situation and this was the aim of this work.

The release of salicylic acid and methyl salicylate was investigated from Plastibases (polyethylene-mineral oil gels). Salicylic acid was chosen in this work due to its poor solubility in Plastibase. This allowed drug release from suspension ointments to be studied. Methyl salicylate was chosen because of its ready miscibility in Plastibases allowing release of a dissolved drug in an ointment to be studied. The inert nature of Plastibases ensured that the drug-ointment base interactions were kept to a minimum. As these vehicles are available in a range of consistencies, they were particularly useful as model systems in this work.

Rheological characterisation of the Plastibases was carried out using conventional (continuous shear) and fundamental (creep and

oscillatory) methods. Plastibases proved to be particularly good systems for continuous shear testing as none of the usual difficulties, e.g. shear fracture, etc., were encountered. Various relationships were derived between the apparent viscosity, limiting viscosity, static and dynamic yield stress and the percentage of polyethylene in the gels. Study of the temperature effect on the consistency of these gels showed the reported visco-static behaviour said to be exhibited by Plastibases, however creep tests were able to show that the effect is somewhat of an artifact. Arrhenius type plots of residual viscosity from creep studies and inverse absolute temperature showed a marked change in the consistency of these gels in the temperature region of 30°C. This change in the rheological properties of the gels was also reflected in a change in the in vitro salicylic acid release characteristics of these gels. Similar discontinuities are reported to occur in several polymeric systems. From further investigations in this work it was inferred that the temperature dependent structural changes in the 30°C temperature range were related to changes in the crystalline fraction of the gels. The conventional methods rely on the resistance offered to deformation and flow. It is reasoned that as the three dimensional gel network in Plastibase does not change markedly with temperature, these instruments are not able to detect the changes occuring in Plastibase leading to considerable changes in its consistency. However the creep method which does not rely on destructive testing is able to record the change. Oscillatory studies yielded fundamental parameters for all five Plastibases over a range of frequencies and were able to show that the Plastibase system behaves as a lightly cross-linked polymer of molecular weight 23,000. The latter finding is significant in that it helps to explain the elasticity exhibited by these systems and may further assist in explaining the visco-static behaviour of the

systems from continuous shear measurements. Relationships have been derived between the dynamic viscosity, storage modulus and percentage of polyethylene in the gels, and the parameters derived from conventional methods and fundamental methods of measurement have been compared.

Studies on vehicle design have shown that the range of model vehicles in this study may be extended using some well investigated formulation techniques. Investigation of work effects have drawn attention to the shear sensitivity of Plastibases. This is particularly significant on an industrial scale where high shear equipment is used in the manufacture of semisolid products. Dilution with liquid paraffin and irradiation of Plastibases showed the need for prior investigation of the effects of these practices. Emulsification of Plastibase 50W has shown that stable emulsions may be compounded at bench level.

A simple two compartment model with a membrane was used in this work for investigating the in vitro release of salicylates from Plastibases. Silastic membranes were used as transport through these membranes resembles skin transport. The release of salicylic acid and methyl salicylate into an aqueous sink were seen to comply with the "suspension" and "solution" models proposed by T Higuchi and W I Higuchi. Release of salicylic acid into saline was linearly related to the reciprocals of the apparent viscosity and the dynamic viscosity (at low test frequency). Release of methyl salicylate into saline was independent of the viscosity of the medium. The results of the in vitro studies were confirmed by in vivo determinations in human volunteers from skin irritation and urinary excretion data. The release of

salicylic acid from Plastibases and absorption of the drug by the skin as determined from skin irritiation response was linearly related to the reciprocal of the apparent viscosity and the dynamic viscosity (at low test frequency). A similar linear relationship was also derived for the systemic absorption of salicylic acid after topical application of the Plastibase ointments. The systemic absorption of methyl salicylate appears to be independent of the viscosity of the vehicle. It is concluded from these results that the viscosity of the base becomes an important factor when dissolution of the drug in the vehicle is a rate determining factor, e.g. as in the case of salicylic acid. In the case of methyl salicylate, transport through the skin appears to be the rate determining step and thus drug release is unaffected by the base viscosity. A linear correlation between the *in vitro* and *in vivo* drug release data confirmed the suitability of the silastic membrane and the *in vitro* model in mimicing the *in vivo* situation.

It was seen that the classical Stokes-Einstein equation is somewhat limited in its application to the hetrogenous gel systems, however the microviscosity values derived using the equation were related to the measured macroviscosity values by simple arbitrary relationships. These would be useful for *a priori* prediction of the measured viscosity or diffusion coefficients in formulation work.

2. SUGGESTIONS FOR FURTHER WORK

As a direct result of the above work, further studies are prompted in the following areas:-

(i) Rheological Testing

The low consistency Plastibases could not be characterised using the creep method. It is apparent that similar difficulties are also encountered in the creep testing of other materials of low consistency, e.g. water/oil emulsion (289). Suitable instrumentation would greatly facilitate rheological investigations of low consistency materials. Furthermore it would then also enable conversion and derivation of dynamic parameters in the low frequency region.

(ii) Mass Transport in Hetrogenous Media

The transport of a suspended drug in an ointment base involves dissolution, diffusion and membrane (or skin) transport. It is apparent that either one of these processes can rate limit the release and absorption of a drug. In order to be able to ascribe observed changes in drug release to any one of these processes, a fundamental study of each of these processes is required.

NOTATION

RHEOLOGICAL NOTATION

G	Shear modulus
G^*	complex shear modulus
$\|G^*\|$	Absolute shear modulus
G'	Storage shear modulus
G''	Loss shear modulus
G_o	Initial shear modulus (creep)
G_i	Shear modulus of ith Voigt element
I	Moment of inertia (oscillation)
J	Creep shear compliance
J^*	Complex shear compliance
$\|J^*\|$	Absolute shear compliance
J'	Storage shear compliance
J''	Loss shear compliance
J_o	Initial shear compliance (creep)
J_i	Shear compliance of ith Voigt element
J_N	Newtonian shear compliance (creep)
J_R	Retarded shear compliance (creep)
K	Constant for torsion bar (Rheogoniometer)
L	Retardation spectrum
N	Frequency of oscillation (cycles/sec. Dynamic)
R	Cone radius (the Ferranti Shirley Viscometer); Plate radius (the Rheogoniometer)
R_1	Radius of inner cylinder) (Concentric cylinder creep apparatus)
R_2	Radius of outer cylinder)
S	Stress parameter (Rheogoniometer)
T	Torque
Y_1	Static yield stress) (Continuous shear testing)
Y_2	Dynamic yield stress)

h	Height of inner cylinder (creep apparatus); distance between parallel plates (Rheogoniometer)
t	Time
α	Cone angle (cone and plate)
γ	Shear strain
γ^*	Complex shear strain
$\dot{\gamma}$	Shear rate
$\dot{\gamma}^*$	Complex shear rate
γ_o	Peak shear strain (oscillation)
$\dot{\gamma}_m$	Mean shear rate
δ	Phase angle
η	Coefficient of viscosity
η^*	Complex dynamic viscosity
$\lvert\eta^*\rvert$	Absolute viscosity
η'	Real component of complex dynamic viscosity, dynamic viscosity
η''	Imaginary component of dynamic viscosity
η_o	Residual Newtonian viscosity (creep)
η_i	Shear viscosity of ith Voigt element
η_{app}	Apparent viscosity)
η_{limit}	Limiting viscosity) (Continuous shear testing)
θ	Angular deflection of inner cylinder (creep apparatus)
ρ	Density
σ	Shear stress
σ^*	Complex shear stress
σ_o	Peak shear stress (oscillation)
σ_m	Mean shear stress
σ_i	Shear stress in the ith Voigt element
τ	Relaxation or retardation time
τ_i	Retardation time of ith Voigt element

υ	Amplitude ratio
ω	Frequency of oscillation (rad s^{-1})
Ω	Angular velocity (cone and plate)

DRUG RELEASE NOTATION

A	Effective cross-sectional area for diffusion
C_1	Concentration in Phase I
C_2	Concentration in Phase II
Co	Initial concentration of drug in ointment
Cs	Saturation solubility of drug
Cv	Concentration of drug dissolved in the vehicle
D	Diffusivity; diffusion coefficient
L	Lag time
PC	Partition coefficient
Q	Penetrant flux
T	Absolute temperature
h	Thickness of skin barrier, thickness of applied ointment
k	Boltzman's constant
r	Hydrodynamic radius
η	Viscosity coefficient

APPENDIX

MANUFACTURER'S SUGGESTED SPECIFICATIONS FOR PLASTIBASES

Property of Material	Formulation				
	5W	10W	20W	30W	50W
Appearance	Thick, hazy oil	Thick, hazy oil	Soft gel	Smooth, translucent, soft greaselike mass	Same as 30W
Colour	Colourless	Colourless	Colourless	Colourless within layers to white in bulk	Same as 30W
Odour	Practically odourless	Same as 5W	Same as 5W	Same as 5W	Practically odourless to slight
Texture	-	-	-	Free from particles perceptible to the touch	Same as 30W
pH	Neutral	Neutral	Neutral	Neutral	Neutral
Viscosity 25°C (Brookfield)	≈2500 cps	≈ 4100 cps	≈ 3200 cps	-	-
Consistency (Penetrometer)	-	-	-	≈ 325	≈ 300

MANUFACTURER'S SUGGESTED SPECIFICATIONS FOR PLASTIBASES (Continued)

Property of Material	Formulation				
	5W	10W	20W	30W	50W
Polyethylene (± 10%)	0.5%	1.0%	2.0%	3.0%	5.0%
Bleed Test	-	-	-	>0.1g at 45°C	>0.1g at 45°C
Heat Stability	-	-	-	Not more than slight curvature at 65°C	Same as 30W
Settling	-	-	Must show no evidence of settling after standing undisturbed for 24 hours	-	-

FERRANTI SHIRLEY VISCOMETER

Details of springs and cones.

Viscometer was fitted with a 2.15 gm cm/div spring.

Parameter	Large Cone	Medium Cone	Small Cone
Cone radius (cm)	3.5	2.0	0.997
Cone angle (rads)	0.01444	0.022824	0.0433151
Viscosity constant	3.24	27.45	408.0
Shear stress constant	23.5	126.0	1011.0
Shear rate constant	7.25	4.6	2.4

DATA FOR FIGURE 25

	Applied torque $Nm^{-2} \times 10^4$	Calibration with silicon oil of viscosity 1×10^{-4} $m^2 s^{-1}$ revs/min
1.	0.36	14.0
	1.04	40.5
	1.73	75.0
	2.42	98.0
	3.11	125.0
	3.79	147.5
		Calibration with silicon oil of viscosity 5×10^{-4} $m^2 s^{-1}$
2.	0.36	3.0
	1.04	7.5
	1.73	14.9
	2.42	20.0
	3.11	25.1
	3.79	30.5
	4.48	37.0
	5.17	42.5
	5.86	48.0
	6.54	53.6
	7.92	65.5
	9.29	76.5
	10.67	88.0
	12.04	99.0
	13.42	110.0
		Calibration with silicon oil of viscosity 1×10^{-3} $m^2 s^{-1}$
3.	1.04	2.9
	1.73	5.8
	2.42	7.8
	3.11	9.6
	3.79	12.0
	4.48	14.6
	5.17	16.6
	5.86	18.8
	6.54	20.9
	7.92	25.6
	9.29	30.5
	10.67	34.5
	12.04	39.0
	13.42	43.3
		Calibration with silicon oil of viscosity 1.25×10^{-2} $m^2 s^{-1}$
4.	3.11	1.03
	6.54	2.19
	9.98	3.38
	13.42	4.56

DATA FOR FIGURE 26

Asterisks indicate reconstituted data.

Time (sec)	Compliance ($N^{-1}m^2 \times 10^{-4}$)				
0	1.61	260	3.54*	520	4.50*
20	2.10*	280	3.62*	540	4.62
40	2.34*	300	3.72	560	4.63*
60	2.54	320	3.78*	580	4.70*
80	2.65*	340	3.85*	600	4.81
100	2.77*	360	3.97	620	4.83*
120	2.92	380	4.00*	660	3.13
140	2.99*	400	4.07*	720	3.02
160	3.09*	420	4.20	780	2.95
180	3.22	440	4.22*	840	2.90
200	3.28*	460	4.29*		
220	3.37*	480	4.42		
240	3.47	500	4.43*		

DATA FOR FIGURE 27

Time (sec)	Derived Compliance ($N^{-1} m^2 \times 10^{-5}$)
0	12.64
10	9.32
20	8.08
30	7.14
40	6.44
50	5.80
60	5.33
70	4.86
80	4.56
90	4.26
100	3.87
110	3.72
120	3.42
130	3.27
140	3.07
150	2.87
160	2.67
180	2.38
210	1.98
240	1.69
270	1.39
300	1.24
330	0.99
360	0.93
420	0.50

DATA FOR FIGURE 28

Time (sec)	Derived Compliance ($N^{-1} m^2 \times 10^{-5}$)
0	5.84
10	2.90
20	2.03
30	1.43
40	1.06
50	0.72
60	0.54
70	0.34
80	0.30
90	0.24
110	0.14
130	0.08
140	0.07
150	0.04

DATA FOR FIGURE 29

Time (sec)	Derived Compliance ($N^{-1} m^2 \times 10^{-6}$)
0	35.39
10	11.20
20	6.40
30	3.54
40	2.23
50	0.71
60	0.33

DATA FOR FIGURE 30

Time (sec)	Derived Compliance $N^{-1} m^2 \times 10^{-4}$	1st Order Retardation Spectra $(N^{-1} m^2 \times 10^{-6})$	Time (sec)	2nd Order Retardation Spectra $(N^{-1} m^2 \times 10^{-6})$
20	2.03	24.82	10	20.91
40	2.21	25.63	20	25.70
60	2.31	25.89	30	24.35
80	2.39	26.45	40	24.34
100	2.45	26.86	50	25.49
120	2.50	27.00	60	26.96
140	2.54	26.89	70	28.43
160	2.57	26.57	80	29.84
180	2.61	26.08	90	31.21
200	2.63	25.44	100	32.51
220	2.66	24.67	110	33.72
240	2.68	23.80	120	34.79
260	2.70	22.84	130	35.68
280	2.71	21.83	140	36.37
300	2.73	20.77	150	36.84
320	2.74	19.69	160	37.09
340	2.75	18.60	170	37.12
360	2.76	17.52	180	36.93
380	2.77	16.45	190	36.55
400	2.78	15.40	200	36.00
420	2.79	14.39	210	35.29
440	2.79	13.42	220	34.45
460	2.80	12.48	230	33.49
480	2.80	11.59	240	32.45
500	2.81	10.74	250	31.33
520	2.81	9.94	260	30.15
540	2.82	9.19	270	28.93
560	2.82	8.48	280	27.69
580	2.82	7.82	290	26.43
600	2.83	7.20	300	25.17
640	2.83	6.08	320	22.68
680	2.83	5.11	340	20.28
720	2.84	4.29	360	18.00
760	2.84	3.59	380	15.89
800	2.84	2.99	400	13.94

DATA FOR FIGURE 31

Temperature	Stress (Nm^{-2})	Strain x 10^{-3}
20°C	3.47	0.59
	7.36	1.36
	11.89	2.16
	15.88	3.00
	20.62	3.94
	24.19	4.59
	28.30	5.45
	30.71	5.97
	33.82	6.49
	38.02	7.28
25°C	3.58	0.71
	7.36	1.53
	11.78	2.40
	15.57	3.20
	20.41	4.23
	23.77	4.98
	28.19	5.92
	32.71	6.90
	35.97	7.61
	39.97	8.45
30°C	3.58	0.705
	7.36	1.66
	11.78	2.63
	15.57	3.53
	20.41	4.56
	24.19	5.46
	27.35	6.30
	31.56	7.19
	33.66	7.70
	38.71	8.93
35°C	3.58	0.85
	8.00	1.90
	11.78	2.82
	16.00	3.81
	20.41	4.93
	24.19	5.88
	28.61	7.05
	32.88	7.99
	35.55	8.79
	37.02	9.30
40°C	3.58	0.89
	8.20	2.11
	12.62	3.17
	15.99	4.04
	20.41	5.09
	24.19	6.14
	28.19	7.33
	33.24	8.84
	36.82	9.96

DATA FOR FIGURE 31 (Continued)

Temperature	Stress (Nm^{-2})	Strain x 10^{-3}
45°C	3.58	1.01
	8.00	2.26
	12.83	3.57
	16.62	4.77
	20.41	5.64
	24.19	6.77
	28.61	8.13
	32.61	9.40
	36.80	10.90

DATA FOR FIGURE 32

Temperature	Stress (Nm^{-2})	Strain x 10^{-3}
20°C	3.58	2.21
	8.41	5.08
	13.25	8.46
	17.88	11.65
	20.41	13.16
	24.19	15.98
25°C	3.58	2.44
	8.41	6.02
	13.25	9.40
	15.99	12.78
	20.41	19.74
	24.19	23.50
30°C	3.58	2.58
	8.00	6.58
	13.04	10.57
	15.99	15.50
	20.62	21.62
	24.19	30.07
35°C	3.58	3.29
	8.41	7.52
	11.99	10.34
	15.99	19.27
	20.41	27.25
40°C	4.63	4.23
	7.78	7.52
	11.78	12.22
	15.99	22.40
	20.41	31.07
45°C	3.58	3.76
	8.00	8.46
	12.47	17.86
	15.99	26.31

DATA FOR FIGURE 35

Time (sec)	Retardation Spectra ($Nm^{-1}m^2 \times 10^{-6}$)				
	10°C	15°C	20°C	25°C	30°C
10	7.18	6.09	5.93	8.32	10.76
20	5.66	6.42	7.83	9.55	14.02
30	5.51	7.48	9.31	11.43	12.29
40	6.01	7.23	9.28	11.78	11.23
50	6.55	6.49	8.75	11.72	11.70
60	6.87	5.79	8.30	11.83	13.08
70	6.95	5.34	8.16	12.23	14.76
80	6.87	5.17	8.31	12.87	16.37
90	6.71	5.24	8.70	13.64	17.73
100	6.53	5.47	9.23	14.41	18.78
120	6.37	6.20	10.41	15.71	19.96
140	6.11	7.01	11.47	16.46	20.07
160	6.14	7.74	12.25	16.63	19.36
180	6.28	8.33	12.71	16.30	18.10
200	6.46	8.75	12.88	15.59	16.50
250	6.86	9.15	12.30	12.89	12.09
300	6.95	8.82	10.82	9.82	8.16
400	6.22	7.02	7.18	4.88	3.19

Time (sec)	Retardation Spectra ($Nm^{-1}m^2 \times 10^{-6}$)		
	35°C	40°C	45°C
10	14.16	31.66	174.57
20	15.56	82.76	394.57
30	12.23	121.67	501.04
40	11.07	141.33	503.02
50	11.99	144.30	443.85
60	13.82	135.77	360.94
70	15.81	120.75	277.43
80	17.60	103.06	204.63
90	19.07	85.23	146.25
100	20.18	68.75	101.97
120	21.36	42.27	-
140	21.37	24.57	-
160	20.52	13.70	-
180	19.09	7.40	-
200	17.33	3.90	-

DATA FOR FIGURE 36

Time (sec)	Retardation Spectra ($N^{-1}m^2 \times 10^{-5}$)				
	10°C	15°C	20°C	25°C	30°C
10	2.79	3.38	5.83	8.29	7.04
20	4.36	5.66	8.05	7.72	16.63
30	6.87	6.57	8.03	6.72	22.10
40	9.81	7.51	8.54	7.72	23.22
50	12.68	8.85	9.86	9.69	21.43
60	15.19	10.43	11.60	11.84	18.23
70	17.23	12.06	13.37	13.83	14.66
80	18.75	13.57	14.98	15.55	11.31
90	19.78	14.88	16.34	16.95	8.46
100	20.35	15.95	17.40	18.03	6.17
120	20.35	17.36	18.67	19.26	3.10
140	19.23	17.86	18.93	19.45	1.47
160	17.45	17.63	18.43	18.85	0.67
180	15.33	16.87	17.38	17.70	0.30
200	13.15	15.75	15.99	16.21	0.13

Time (sec)	Retardation Spectra ($N^{-1}m^2 \times 10^{-5}$)		
	37°C	40°C	45°C
10	34.33	66.14	132.05
20	78.18	118.88	126.59
30	100.13	120.18	68.26
40	101.34	96.00	29.03
50	90.14	67.40	10.89
60	73.90	43.61	-
70	57.26	26.67	-
80	42.58	15.65	-
90	30.68	8.90	-
100	21.56	4.94	-

DATA USED FOR FIGURES 37 AND 38

Interbatch variation data for three batches of Plastibases.

Plastibase 50W Batch Number 2363

Temperature °C	Instantaneous Compliance ($N^{-1}m^2 \times 10^{-4}$)	Residual Viscosity Poise x 10^6
10	1.38	405.68
15	1.54	424.11
20	1.66	317.05
25	1.86	175.44
30	1.93	23.89
35	2.04	2.41
37	2.10	1.16
40	2.24	0.49
45	2.47	0.18

Plastibase 50W Batch Number 2298

10	1.01	434.22
15	1.09	391.41
20	1.24	341.63
25	1.34	203.37
30	1.48	13.80
37	1.59	1.97
40	1.61	0.76
45	1.73	0.78

Plastibase 50W Batch Number 2310

10	1.04	464.21
15	1.16	367.19
20	1.29	371.23
25	1.51	221.12
30	1.56	120.16
37	1.81	3.18
40	1.89	0.79
45	1.99	0.34

DATA FOR FIGURES 46 AND 47

η' in Poise and G' in Nm^{-2}

Frequency (Hz)	Plastibase 5W		Plastibase 10W		Plastibase 20W		Liquid Paraffin
	η'	G'	η'	G'	η'	G'	η'
0.0025	-	-	6.31×10^{3}	3.19×10^{1}	7.36×10^{4}	6.96×10^{2}	-
0.00791	1.36×10^{2}	2.70×10^{0}	1.48×10^{3}	3.53×10^{1}	1.16×10^{4}	7.90×10^{2}	-
0.025	3.63×10^{1}	3.22×10^{0}	3.41×10^{2}	3.46×10^{1}	-	6.85×10^{2}	1.930
0.0791	1.85×10^{1}	3.36×10^{0}	1.47×10^{2}	3.63×10^{1}	8.52×10^{2}	7.86×10^{2}	1.625
0.25	1.45×10^{1}	3.70×10^{0}	4.48×10^{1}	3.63×10^{1}	4.06×10^{2}	7.44×10^{2}	1.552
0.791	9.83×10^{0}	4.65×10^{0}	3.23×10^{1}	4.77×10^{1}	2.08×10^{2}	9.60×10^{2}	1.554
2.5	7.44×10^{0}	6.83×10^{0}	2.54×10^{1}	6.14×10^{1}	2.48×10^{2}	9.93×10^{2}	1.453
7.91	4.30×10^{0}	6.33×10^{0}	1.06×10^{1}	5.69×10^{1}	9.88×10^{1}	1.32×10^{3}	1.134
10.0	8.09×10^{-1}	1.79×10^{0}	2.15×10^{0}	1.02×10^{1}	5.40×10^{1}	-	0.196
12.6	2.20×10^{1}	8.69×10^{1}	3.26×10^{1}	3.89×10^{2}	6.55×10^{0}	1.22×10^{3}	6.172
15.8	9.99×10^{0}	3.07×10^{1}	1.91×10^{1}	1.64×10^{2}	2.67×10^{1}	1.41×10^{3}	2.807
19.9	7.71×10^{0}	3.97×10^{1}	1.50×10^{1}	1.53×10^{2}	3.78×10^{1}	1.35×10^{3}	2.494
25.0	6.66×10^{0}	4.56×10^{1}	1.28×10^{1}	1.61×10^{2}	4.56×10^{1}	1.10×10^{3}	2.276

DYNAMIC PARAMETERS FOR PLASTIBASES EMPLOYED IN PLOTTING FIGURES 48 TO 57

Viscosity values are given in Poise, modulus values in Nm^{-2} and compliances in $N^{-1}m^{2}$

Frequency (Hz)	η'	G'	η''	G"	J'	J"	Tan α
Plastibase 5W							
0.0791	1.53×10^{1}	3.13×10^{0}	3.96×10^{2}	1.21×10^{-1}	3.19×10^{-1}	1.24×10^{-2}	3.88×10^{-2}
0.250	1.02×10^{1}	3.01×10^{0}	1.20×10^{2}	2.55×10^{-1}	3.30×10^{-1}	2.80×10^{-2}	8.48×10^{-2}
0.791	7.09×10^{0}	4.26×10^{0}	5.39×10^{1}	5.61×10^{-1}	2.31×10^{-1}	3.04×10^{-2}	1.32×10^{-1}
2.500	4.96×10^{0}	5.76×10^{0}	2.30×10^{1}	1.24×10^{0}	1.66×10^{-1}	3.57×10^{-2}	2.15×10^{-1}
7.910	3.81×10^{0}	8.30×10^{0}	1.05×10^{1}	3.02×10^{0}	1.06×10^{-1}	3.87×10^{-2}	3.63×10^{-1}
25.000	3.68×10^{0}	-	-	9.19×10^{0}	-	1.07×10^{-1}	-
Plastibase 10W							
0.00791	6.82×10^{2}	3.46×10^{1}	4.38×10^{4}	5.40×10^{-1}	2.89×10^{-2}	4.50×10^{-4}	1.56×10^{-2}
0.0250	2.34×10^{2}	3.29×10^{1}	1.32×10^{4}	5.59×10^{-1}	3.04×10^{-2}	5.16×10^{-4}	1.70×10^{-2}
0.0791	8.73×10^{1}	3.47×10^{1}	4.39×10^{3}	6.91×10^{-1}	2.88×10^{-2}	5.72×10^{-4}	1.99×10^{-2}
0.2500	3.67×10^{1}	3.65×10^{1}	1.46×10^{3}	9.19×10^{-1}	2.74×10^{-2}	6.89×10^{-4}	2.52×10^{-2}
0.7910	2.14×10^{1}	3.80×10^{1}	4.81×10^{2}	1.69×10^{0}	2.62×10^{-2}	1.17×10^{-3}	4.45×10^{-2}
2.5000	1.42×10^{1}	4.27×10^{1}	1.71×10^{2}	3.55×10^{0}	2.33×10^{-2}	1.94×10^{-3}	8.32×10^{-2}
7.9100	9.99×10^{0}	5.23×10^{1}	6.61×10^{1}	7.90×10^{0}	1.87×10^{-2}	2.83×10^{-3}	1.51×10^{-1}
25.0000	7.46×10^{0}	3.18×10^{1}	1.27×10^{1}	1.87×10^{1}	2.34×10^{-2}	1.37×10^{-2}	5.86×10^{-1}

DATA FOR FIGURES 48 TO 57 (Continued)

Frequency (Hz)	η'	G'	η"	G"	J'	J"	Tan α
Plastibase 20W							
0.00250	3.46×10^{4}	4.18×10^{2}	1.67×10^{6}	8.66×10^{0}	2.39×10^{-3}	4.96×10^{-5}	2.07×10^{-2}
0.00791	9.69×10^{3}	4.16×10^{2}	5.26×10^{5}	7.66×10^{0}	2.40×10^{-3}	4.43×10^{-5}	1.84×10^{-2}
0.02500	3.11×10^{3}	4.10×10^{2}	1.64×10^{5}	7.77×10^{0}	2.44×10^{-3}	4.63×10^{-5}	1.90×10^{-2}
0.07910	1.09×10^{3}	4.06×10^{2}	5.13×10^{4}	8.59×10^{0}	2.46×10^{-3}	5.21×10^{-5}	2.12×10^{-2}
0.25000	3.44×10^{2}	4.15×10^{2}	1.66×10^{4}	8.59×10^{0}	2.41×10^{-3}	4.99×10^{-5}	2.07×10^{-2}
0.79100	1.51×10^{2}	4.83×10^{2}	6.10×10^{3}	1.20×10^{1}	2.07×10^{-3}	5.13×10^{-5}	2.48×10^{-2}
2.50000	7.31×10^{1}	5.02×10^{2}	2.01×10^{3}	1.83×10^{1}	1.99×10^{-3}	7.25×10^{-5}	3.64×10^{-2}
7.91000	4.24×10^{1}	5.59×10^{2}	7.07×10^{2}	3.36×10^{1}	1.78×10^{-3}	1.07×10^{-4}	6.01×10^{-2}
25.00000	2.75×10^{1}	6.23×10^{2}	2.49×10^{2}	6.88×10^{1}	1.59×10^{-3}	1.75×10^{-4}	1.11×10^{-1}
Plastibase 30W							
0.00250	9.87×10^{4}	1.03×10^{3}	4.14×10^{6}	2.47×10^{1}	9.66×10^{-4}	2.30×10^{-5}	2.39×10^{-2}
0.00791	3.28×10^{4}	1.05×10^{3}	1.33×10^{6}	2.60×10^{1}	9.50×10^{-4}	2.35×10^{-5}	2.47×10^{-2}
0.02500	8.68×10^{3}	1.06×10^{3}	4.25×10^{5}	2.17×10^{1}	9.41×10^{-4}	1.92×10^{-5}	2.04×10^{-2}
0.07910	2.69×10^{3}	1.07×10^{3}	1.36×10^{5}	2.13×10^{1}	9.32×10^{-4}	1.85×10^{-5}	1.98×10^{-2}
0.25000	9.86×10^{2}	1.08×10^{3}	4.33×10^{4}	2.46×10^{1}	9.23×10^{-4}	2.10×10^{-5}	2.28×10^{-2}
0.79100	3.97×10^{2}	1.23×10^{3}	1.56×10^{4}	3.14×10^{1}	8.10×10^{-4}	2.06×10^{-5}	2.54×10^{-2}
2.50000	1.90×10^{2}	1.30×10^{3}	5.22×10^{3}	4.75×10^{1}	7.66×10^{-4}	2.79×10^{-5}	3.64×10^{-2}
7.91000	1.01×10^{2}	1.45×10^{3}	1.84×10^{3}	7.98×10^{1}	6.87×10^{-4}	3.77×10^{-5}	5.50×10^{-2}
25.00000	6.54×10^{1}	1.56×10^{3}	6.26×10^{2}	1.64×10^{2}	6.32×10^{-4}	6.61×10^{-5}	1.65×10^{-1}

DATA FOR FIGURES 48 TO 57 (Continued)

Frequency (Hz)	η'	G'	η''	G"	J'	J"	Tan α
				Plastibase 50W			
0.00250	4.49×10^{5}	3.18×10^{3}	1.27×10^{7}	1.12×10^{2}	3.15×10^{-4}	1.11×10^{-5}	3.54×10^{-2}
0.00791	1.08×10^{5}	3.19×10^{3}	4.03×10^{6}	8.54×10^{1}	3.14×10^{-4}	8.40×10^{-6}	2.68×10^{-2}
0.02500	3.32×10^{4}	3.22×10^{3}	1.29×10^{6}	8.30×10^{1}	3.11×10^{-4}	8.01×10^{-6}	2.58×10^{-2}
0.07910	1.16×10^{4}	3.23×10^{3}	4.09×10^{5}	9.14×10^{1}	3.09×10^{-4}	8.74×10^{-6}	2.83×10^{-2}
0.25000	4.20×10^{3}	3.26×10^{3}	1.31×10^{5}	1.05×10^{2}	3.06×10^{-4}	9.86×10^{-6}	3.22×10^{-2}
0.79100	1.65×10^{3}	4.12×10^{3}	5.21×10^{4}	1.31×10^{2}	2.43×10^{-4}	7.70×10^{-6}	3.18×10^{-2}
2.50000	7.61×10^{2}	4.52×10^{3}	1.81×10^{4}	1.90×10^{2}	2.21×10^{-4}	9.31×10^{-6}	4.21×10^{-2}
7.91000	3.49×10^{2}	5.26×10^{3}	6.65×10^{3}	2.76×10^{2}	1.90×10^{-4}	9.96×10^{-6}	5.25×10^{-2}
25.00000	1.61×10^{2}	7.36×10^{3}	2.94×10^{3}	4.04×10^{2}	1.35×10^{-4}	7.43×10^{-6}	5.48×10^{-2}

DYNAMIC DATA FOR LIQUID PARAFFIN DILUTIONS OF PLASTIBASE 50W EMPLOYED IN PLOTTING FIGURES 48 AND 52

Viscosity values are given in Poise and modulus values in $Nm^{-2} \times 10^3$

Frequency (Hz)	4.79 PPE		4.59 PPE		4.41 PPE		4.25 PPE		4.09 PPE	
	η'	G'	η'	G'	η'	G'	η'	G'	η'	G'
0.00250	3.23×10^5	2.66	2.29×10^5	2.37	1.80×10^5	1.74	2.65×10^5	1.40	2.11×10^5	1.25
0.00791	9.04×10^4	2.66	5.02×10^4	2.11	5.85×10^4	1.81	6.10×10^4	1.54	4.71×10^4	1.29
0.02500	2.68×10^4	2.70	2.02×10^4	2.13	1.85×10^4	1.86	1.77×10^4	1.57	1.39×10^4	1.36
0.07910	1.05×10^4	2.72	7.29×10^3	2.20	6.78×10^3	1.87	5.93×10^3	1.57	4.61×10^3	1.40
0.25000	3.14×10^3	2.75	2.62×10^3	2.23	2.25×10^3	1.93	1.85×10^3	1.62	1.50×10^3	1.46
0.79100	1.50×10^3	3.45	9.42×10^2	2.80	9.01×10^2	2.30	9.22×10^2	1.96	6.65×10^2	1.64
2.50000	5.92×10^2	3.76	4.29×10^2	2.97	4.08×10^2	2.52	3.71×10^2	2.18	2.94×10^2	1.79
7.91000	2.88×10^2	4.46	1.99×10^2	2.42	2.00×10^2	2.94	1.67×10^2	2.49	1.12×10^2	2.13
25.00000	1.55×10^2	5.43	1.23×10^2	4.45	1.06×10^2	3.71	8.64×10^1	3.12	7.78×10^1	2.59

TRANSFORMED CREEP DATA EMPLOYED IN FIGURE 55

Time (sec)	Plastibase 30W		Plastibase 50W	
	η' (Poise)	G' (Nm^{-2})	η' (Poise)	G' (Nm^{-2})
20	1.29×10^{5}	1.46×10^{3}	1.85×10^{5}	4.94×10^{3}
40	2.77×10^{5}	1.20×10^{3}	3.70×10^{5}	4.75×10^{3}
60	4.28×10^{5}	1.01×10^{3}	5.55×10^{5}	4.64×10^{3}
80	5.62×10^{5}	8.64×10^{2}	7.43×10^{5}	4.56×10^{3}
100	6.80×10^{5}	7.54×10^{2}	9.33×10^{5}	4.48×10^{3}
400	1.75×10^{6}	2.26×10^{2}	3.64×10^{6}	4.10×10^{3}
1,000	2.28×10^{6}	5.23×10^{1}	1.17×10^{7}	3.89×10^{3}
4,000	2.46×10^{6}	3.60×10^{0}	8.26×10^{7}	2.58×10^{3}
10,000	2.48×10^{6}	5.66×10^{-1}	1.78×10^{8}	9.73×10^{2}
40,000	2.49×10^{6}	3.02×10^{-2}	2.37×10^{8}	8.44×10^{1}
100,000	2.49×10^{6}	3.11×10^{-3}	2.44×10^{8}	1.38×10^{1}
400,000	4.18×10^{6}	-	2.46×10^{8}	8.21×10^{-1}
1,000,000	4.18×10^{6}	-	2.46×10^{8}	1.15×10^{-1}
4,000,000	4.18×10^{6}	-	2.46×10^{8}	1.86×10^{-3}

POLYNOMIAL EQUATIONS DERIVED FOR PLOTS SHOWN IN FIGURE 56

All polynomials were of the form

$$y = a + bx - cx^2 + dx^3$$

where $y = \log \eta'$ and $x = PPE$

Plot at Frequency	a	b	-c	d
0.0025	0.24891	4.7733	1.5890	0.1702
0.00791	0.32502	3.5498	1.0359	0.10294
0.025	0.22773	2.8617	0.75579	0.071048
0.0791	0.17946	2.2965	0.54595	0.048383
0.25	0.19790	1.7385	0.35094	0.028036
0.791	0.19222	1.4230	0.26630	0.020529
2.5	0.18391	1.1526	0.19022	0.013507
7.91	0.17674	0.9459	0.13347	0.0077696
25.0	0.19590	0.7680	0.078628	0.0010872

DATA FOR FIGURE 58

Viscosity values are given in Poise and modulus values in $Nm^{-2} \times 10^3$

Frequency /Hz	BN 118		BN 2298		BN 1148		BN 2310	
	η'	G'	η'	G'	η'	G'	η'	G'
0.025	3.41×10^4	2.90	4.03×10^4	4.04	4.44×10^4	3.82	4.91×10^4	4.05
0.250	4.09×10^3	3.08	5.39×10^3	4.35	6.12×10^3	4.21	5.23×10^3	4.28
0.791	1.68×10^3	3.61	2.15×10^3	4.83	2.76×10^3	4.90	2.27×10^3	4.86
2.500	7.20×10^2	4.12	9.42×10^2	5.36	9.89×10^2	5.64	1.01×10^3	5.30
7.910	2.90×10^2	4.77	4.42×10^2	6.24	3.85×10^2	6.58	4.77×10^2	6.34
25.000	1.49×10^2	6.34	2.76×10^2	7.94	2.06×10^2	8.37	2.81×10^2	8.47

DATA FOR FIGURE 62

Time (sec)	Milled x 1 Retardation Spectra ($N^{-1} m^2 \times 10^{-5}$)	Milled x 2 Retardation Spectra ($N^{-1} m^2 \times 10^{-5}$)
10	1.69	1.25
20	2.71	2.11
30	2.72	2.18
40	2.55	2.06
50	2.54	2.03
60	2.71	2.17
70	3.01	2.43
80	3.35	2.76
90	3.69	3.12
100	4.00	3.49
120	4.48	4.17
140	4.76	4.72
160	4.86	5.14
180	4.80	5.43
200	4.62	5.59
250	3.89	5.54
300	3.02	5.06
400	1.56	3.63

Time (sec)	Milled x 4 Retardation Spectra ($N^{-1} m^2 \times 10^{-5}$)	Milled x 8 Retardation Spectra ($N^{-1} m^2 \times 10^{-5}$)
10	3.75	2.11
20	2.98	6.14
30	4.01	10.06
40	5.17	13.02
50	5.93	14.81
60	6.29	15.53
70	6.30	15.39
80	6.06	14.63
90	5.64	13.48
100	5.13	12.11
120	4.00	9.25
140	2.95	6.67
160	2.09	4.62
180	1.43	3.10
200	0.958	2.03
250	0.323	6.47
300	0.101	0.191
400	0.084	0.014

DATA FOR FIGURE 70(a)

Time (sec)	Retardation Spectra ($N^{-1}m^2 \times 10^{-5}$)			
	EM1	EM2	EM3	EM4
10	18.30	34.33	33.93	9.83
20	36.74	55.32	72.37	29.89
30	41.47	50.15	86.81	51.09
40	36.99	35.92	82.28	69.01
50	29.00	22.61	68.55	81.93
60	20.96	13.12	52.63	89.64
70	14.31	7.19	38.19	92.70
80	9.38	3.79	26.60	91.99
90	5.96	1.93	17.95	88.46
100	3.69	0.96	11.81	82.98
150	-	-	-	47.27

DATA FOR FIGURE 70(b)

Time (sec)	Retardation Spectra ($N^{-1}m^2 \times 10^{-5}$)			
	EM5	EM6	EM7	EM8
10	27.55	25.56	14.87	10.37
20	39.83	49.40	37.68	31.46
30	32.39	53.71	53.70	53.69
40	20.81	46.14	60.47	72.41
50	11.75	34.84	59.85	85.82
60	6.11	24.24	54.59	93.75
70	3.01	15.95	47.06	96.79
80	1.42	10.06	38.94	95.90
90	0.649	6.16	31.22	92.07
100	0.290	3.67	24.41	86.83
150	-	-	-	48.73

DATA FOR FIGURE 70(c)

Time (sec)	Retardation Spectra ($N^{-1}m^2 \times 10^{-5}$)			
	EM9	EM10	EM11	EM12
10	32.95	32.55	16.48	10.54
20	34.43	44.42	37.35	27.82
30	20.24	34.10	47.61	41.30
40	9.40	20.69	47.95	48.44
50	3.84	11.03	42.45	49.94
60	1.44	5.42	34.63	47.45
70	0.513	2.52	26.71	42.62
80	0.175	1.12	19.76	36.73
90	0.0579	0.484	14.17	30.67
100	0.0187	0.204	9.91	24.98
150	-	-	-	7.03

DATA FOR FIGURE 77

Concentration µg/ml	Absorbance
1.0	0.0254
2.0	0.0506
5.0	0.1260
10.0	0.2550
20.0	0.5100
50.0	1.2800

DATA FOR FIGURE 78

Concentration µg/ml	Absorbance
1.0	0.0246
2.0	0.0402
5.0	0.1230
10.0	0.2480
20.0	0.4900
50.0	1.2400

DATA FOR FIGURE 79

Concentration µg/ml	Absorbance
1.0	0.0236
2.0	0.0475
5.0	0.1190
10.0	0.2400
20.0	0.4800

DATA FOR FIGURE 81

Time (hr)	Drug release (µg/m) at 37°C from Plastibase 50W ointments containing 10% Salicylic acid	5% Salicylic acid	2% Salicylic acid
0	0.00	0.00	0.00
1	3.06	2.42	1.45
2	5.43	4.30	2.42
3	7.56	5.94	3.55
4	9.22	7.42	4.69
5	10.86	8.52	5.47
6	12.19	9.61	6.25
7	13.48	10.47	7.07
8	15.02	11.52	7.70
9	16.27	12.12	8.24

DATA FOR FIGURE 82

Time (hr)	Drug release (µg/ml) at 37°C from Plastibase 50W ointments containing 10% Methyl Salicylate	5% Methyl Salicylate	2% Methyl Salicylate
0	0.00	0.00	0.00
1	13.19	7.36	3.67
2	21.01	11.29	5.46
3	26.21	13.71	6.63
4	29.44	15.52	7.26
5	31.45	16.73	7.50
6	33.06	17.64	7.90
7	33.97	18.31	8.25
8	34.58	18.85	8.63
9	34.68	19.15	8.97

DATA FOR FIGURE 83

Time (hr)	Salicylic acid release (μ g/ml) at 25°C from ointments containing 10% of the drug					
	50W	30W	20W	10W	5W	Liquid Paraffin
0	0.00	0.00	0.00	0.00	0.00	0.00
0.25	0.72	0.78	0.86	1.00	0.96	0.88
0.50	1.07	1.19	1.47	1.50	1.54	1.74
0.75	1.35	1.50	1.78	1.93	2.05	2.64
1.00	1.56	1.84	2.11	2.30	2.36	3.55
1.50	1.99	2.36	2.54	2.97	3.13	5.23
2.00	2.52	2.91	3.05	3.61	3.81	6.93
3.00	3.22	3.77	4.00	4.80	5.08	10.18
4.00	3.98	4.57	4.88	5.82	6.31	13.48
5.00	4.67	5.31	5.59	6.74	7.42	17.70
6.00	5.27	5.94	6.37	7.58	8.36	19.84
7.00	5.98	6.60	7.07	8.42	9.30	22.81
8.00	6.48	7.21	7.81	9.22	10.23	25.59
9.00	7.03	7.81	8.28	9.96	11.09	28.52

DATA FOR FIGURE 84

Time (hr)	Salicylic acid release (μ g/ml) at 37°C from ointments containing 10% of the drug				
	50W	30W	20W	10W	5W
0	0.00	0.00	0.00	0.00	0.00
1	3.06	3.44	3.83	3.55	4.06
2	5.43	5.86	6.37	6.72	7.23
3	7.56	8.20	8.87	9.38	10.39
4	9.22	10.08	10.94	11.80	13.44
5	10.86	12.03	13.01	14.02	16.09
6	12.19	13.67	15.04	16.25	18.63
7	13.48	15.27	16.88	18.40	21.02
8	15.02	16.48	18.36	20.39	23.24
9	16.27	17.50	19.84	22.19	24.14

DATA FOR FIGURE 85

Methyl salicylate release (µg/ml) at 37°C from ointments containing 2% of the drug

Time (hr)	50W	30W	20W	10W	5W
0	0.00	0.00	0.00	0.00	0.00
1	3.67	3.65	3.39	3.23	3.59
2	5.46	5.54	5.22	5.00	5.48
3	6.63	6.65	6.37	6.23	6.65
4	7.26	7.30	6.98	7.06	7.74
5	7.50	7.36	7.38	7.82	8.43
6	7.90	7.72	7.78	8.27	8.99
7	8.25	8.08	8.15	8.71	9.40
8	8.63	8.55	8.59	9.07	9.72
9	8.87	9.01	8.87	9.44	10.02

Ethyl salicylate release (µg/ml) at 37°C from ointments containing 2% of the drug

Time (hr)	50W	30W	20W	10W	5W
0	0.00	0.00	0.00	0.00	0.00
1	1.00	1.19	1.35	1.48	1.38
2	1.63	1.67	1.56	2.06	1.90
3	2.13	2.25	2.04	2.23	2.33
4	2.58	2.73	2.42	2.69	2.33
5	2.92	3.08	2.73	3.00	2.63
6	3.15	3.23	3.02	3.29	2.88
7	3.40	3.48	3.23	3.54	3.58
8	3.58	3.67	3.44	3.77	4.10
9	3.73	3.92	3.65	4.02	4.25

DATA FOR FIGURE 86

Salicylic acid release (µg/ml) from Plastibase 50W ointment containing 10% of the drug

Time (hr)	20°C	25°C	30°C	35°C	40°C	45°C
0	0.00	0.00	0.00	0.00	0.00	0.00
0.25	0.43	0.72	0.86	0.78	1.76	1.19
0.50	0.57	1.07	1.27	1.39	2.97	2.73
0.75	0.78	1.35	1.64	2.38	3.85	3.91
1.00	0.98	1.56	2.01	2.99	4.47	5.00
1.50	1.25	1.99	2.70	4.10	6.45	7.03
2.00	1.54	2.52	3.32	5.16	7.60	8.91
3.00	2.15	3.22	4.65	7.11	10.14	12.52
4.00	2.62	3.98	5.74	8.82	11.99	15.63
5.00	3.09	4.67	6.76	9.82	13.93	17.73
6.00	3.61	5.27	7.75	11.13	15.61	20.70
7.00	3.93	5.98	8.65	12.46	17.27	22.30
8.00	4.23	6.48	9.61	13.59	19.06	24.60
9.00	4.51	7.03	10.55	14.82	21.26	26.50

DATA FOR FIGURE 87

Methyl salicylate release (µ g/ml) from Plastibase 50W ointment containing 2% of the drug

Time (hr)	20°C	25°C	30°C	35°C	40°C	45°C
0	0.00	0.00	0.00	0.00	0.00	0.00
1	2.66	3.27	2.96	3.29	3.85	3.71
2	4.07	4.92	4.52	5.02	5.54	5.44
3	4.94	6.05	5.62	6.23	6.63	6.37
4	5.65	6.73	6.31	7.02	7.26	6.94
5	6.07	7.26	6.83	7.58	7.78	7.18
6	6.45	7.64	7.22	8.06	8.10	7.42
7	6.75	7.96	7.54	8.53	8.37	7.50
8	7.04	8.19	7.82	8.87	8.57	7.58
9	7.34	8.47	8.04	9.19	8.75	7.62

DATA FOR FIGURE 108

Concentration mg/ml	Absorbance at 540nm
0.0	0.0000
0.1	0.1100
0.2	0.1990
0.4	0.4200
0.6	0.6100
0.8	0.8100

DATA FOR FIGURE 109

Time interval (hr)	Volume (ml)	pH	Amount excreted mg	Cumulative Total mg	% of Total administered
Control	-	8.00	0.00	0.00	0.00
0 - 2	310	7.75	106.95	106.95	17.83
2 - 4	155	7.85	123.23	230.18	38.36
4 - 6	240	7.75	96.25	326.43	54.33
6 - 8	245	7.80	60.03	386.46	64.41
8 - 10	200	7.95	38.00	424.45	70.74
10 - 24	700	7.55	42.00	466.45	77.74

DATA FOR FIGURE 110

Time Interval (hr)	Volume (ml)	pH	Amount excreted mg	Cumulative Total mg	% of Total administered
Control	-	7.85	0.00	0.00	0.00
0 - 2	330	7.75	69.30	69.30	11.55
2 - 4	160	7.80	126.40	195.70	32.62
4 - 6	275	7.75	112.75	308.45	51.41
6 - 8	200	7.85	60.00	368.45	61.41
8 - 10	210	7.85	35.70	404.15	67.24
10 - 24	1200	7.40	42.00	446.15	74.30

DATA FOR FIGURE 111

Time Interval (hr)	Volume (ml)	pH	Amount excreted mg	Cumulative Total mg
Control	-	7.95	0.00	0.00
0 - 1	70	8.10	0.00	0.00
1 - 2	45	8.10	0.79	0.79
2 - 3	50	8.25	2.43	3.22
3 - 4	55	8.30	1.46	4.68
4 - 5	35	8.35	1.65	6.33
5 - 6	65	8.20	2.42	8.75
6 - 7	65	8.15	1.98	10.73
7 - 8	60	8.05	1.26	11.99
8 - 9	65	8.00	1.79	13.78
9 - 10	60	8.10	1.86	15.64
10 - 24	500	7.75	28.00	43.64

DATA FOR FIGURE 112

Time Interval (hr)	Volume (ml)	pH	Amount excreted mg	Cumulative Total mg
Control	-	7.30	0.00	0.00
0 - 1	81	8.20	0.04	0.04
1 - 2	42	8.25	0.82	0.86
2 - 3	78	8.10	1.83	2.69
3 - 4	75	7.95	1.50	4.19
4 - 5	161	7.65	2.58	6.77
5 - 6	121	7.85	2.24	9.01
6 - 7	106	7.95	1.91	10.92
7 - 8	69	8.10	1.90	12.82
8 - 9	53	8.25	2.25	15.07
9 - 10	50	8.35	3.68	18.75
10 - 24	671	7.95	32.88	51.63

DATA FOR FIGURE 113

Time Interval (hr)	Volume (ml)	pH	Amount excreted mg	Cumulative Total mg
Control	-	7.50	0.00	0.00
0 - 1	200	8.00	1.05	1.05
1 - 2	110	8.05	1.95	3.00
2 - 3	80	8.15	2.32	5.32
3 - 4	75	8.10	2.40	7.72
4 - 5	95	7.95	2.28	10.00
5 - 6	65	7.85	1.24	11.24
6 - 7	105	8.15	2.21	13.45
7 - 8	105	8.15	1.79	15.24
8 - 9	115	8.10	2.93	18.17
9 - 10	150	8.15	3.15	21.32
10 - 24	550	7.70	38.78	60.10

DATA FOR FIGURE 114

Time Interval (hr)	Volume (ml)	pH	Amount excreted mg	Cumulative Total mg
Control	-	8.10	0.00	0.00
0 - 1	78	8.05	0.00	0.00
1 - 2	60	8.00	0.96	0.96
2 - 3	43	7.90	0.95	1.91
3 - 4	55	7.75	0.93	2.84
4 - 5	70	7.70	2.07	4.91
5 - 6	64	7.85	2.46	7.37
6 - 7	68	7.70	3.26	10.63
7 - 8	58	7.90	3.05	13.68
8 - 9	73	7.85	3.83	17.51
9 - 10	120	7.95	4.20	21.71
10 - 24	715	7.75	33.56	55.27

DATA FOR FIGURE 115

Time Interval (hr)	Volume (ml)	pH	Amount excreted mg	Cumulative Total mg
Control	-	7.35	0.00	0.00
0 - 1	65	8.05	0.31	0.31
1 - 2	64	8.05	0.50	0.81
2 - 3	49	8.10	0.87	1.68
3 - 4	48	7.95	2.00	3.68
4 - 5	60	8.05	2.30	5.98
5 - 6	58	8.10	2.02	8.00
6 - 7	70	8.00	2.89	10.89
7 - 8	95	7.80	2.69	13.58
8 - 9	60	7.95	3.02	16.60
9 - 10	160	7.85	2.24	18.84
10 - 24	720	7.70	33.66	52.50

DATA FOR FIGURE 116

Time Interval (hr)	Volume (ml)	pH	Amount excreted mg	Cumulative Total mg
Control	-	7.95	0.00	0.00
0 - 1	105	8.05	0.80	0.80
1 - 2	43	8.15	1.54	2.34
2 - 3	40	8.25	1.48	3.82
3 - 4	34	8.35	2.19	6.01
4 - 5	36	8.35	2.59	8.60
5 - 6	46	8.25	2.15	10.75
6 - 7	46	8.15	2.16	12.91
7 - 8	71	8.00	2.29	15.20
8 - 9	88	7.95	2.73	17.93
9 - 10	99	8.00	2.73	20.66
10 - 24	705	7.75	32.46	53.12

PRINTOUTS OF COMPUTER PROGRAMMES

COMPILED FOR THIS WORK

1. Creep Reconstitution Programme

2. Programme for the Calculation of Viscoelastic Functions from Dynamic Raw Data

3. Programme for Interconversion of Creep Data to Dynamic Data

1. CREEP RECONSTITUTION PROGRAMME

```
'BEGIN' 'COMMENT' CREEP DATA RECONSTITUTION MSK ;
'REAL' SUM,JAY,JO,ETA,FACTOR,CHART,DIFF,RT2,POWER,VALUE,SPEC1,SPEC2;
'INTEGER' I,T,N,TSTART,TFIN,TINT,M,ND;
'ARRAY' TAU,J[1:5];
M:=1;
ND:=READ;
L1:FACTOR:=READ;
ETA:=READ;
JO:=READ;
N:=READ;
TSTART:=READ;
TFIN:=READ;
TINT:=READ;
'FOR' I:=1 'STEP' 1 'UNTIL' N 'DO' 'BEGIN'
J[I]:=READ;
TAU[I]:=READ;
'END';
NEWLINE(1);
WRITETEXT('('CREEP%DATA%RECONSTITUTION%FOR%SET%NO%%%%')');
PRINT(M,2,0);
NEWLINE(2);
WRITETEXT('('FACTOR'('11S')'ETA'('13S')'JO'('15S')'N'('8S')'
TSTART'('5S')'TFIN'('7S')'TINT'('6S')'  ')');
NEWLINE(1);
PRINT(FACTOR,0,4);  SPACE(3);
PRINT(ETA,0,4); SPACE(3);
PRINT(JO,0,4);  SPACE(3);
PRINT(N,2,0);  SPACE(4);
PRINT(TSTART,5,0);  SPACE(3);
PRINT(TFIN,5,0);  SPACE(3);
PRINT(TINT,5,0);  SPACE(4);
NEWLINE(2);
WRITETEXT('('J[I]'('15S')'TAU[I]'('15S')'  ')');
NEWLINE(1);
'FOR'I:=1 'STEP' 1 'UNTIL' N 'DO' 'BEGIN'
PRINT(J[I],0,4);  SPACE(5);
PRINT(TAU[I],0,4);  SPACE(9);
NEWLINE(1);
'END';
NEWLINE(2);
WRITETEXT('('TIME%SEC'('5S')'J(T)'('12S')'CHART'('11S')'DIFF'('12S')
      SPEC1'('9S')'RT2'('6S')'SPEC2 ')');
'FOR'T:=TSTART 'STEP' TINT 'UNTIL' TFIN 'DO' 'BEGIN'
SUM:=0;
SPEC1:=0;
SPEC2:=0;
'FOR'I:=1 'STEP' 1 'UNTIL' N 'DO' 'BEGIN'
POWER:=T/TAU[I];
VALUE:=EXP(-POWER);
SUM:=SUM+J[I]*(1.0-VALUE);
SPEC1:=SPEC1+J[I]*POWER*VALUE;
SPEC2:=SPEC2+J[I]*POWER*POWER*VALUE;
RT2:=0.5*T;
'END';
```

```
JAY:=JO*SUM*T/ETA;
CHART:=JAY/FACTOR;
DIFF:=JO*SUM;
NEWLINE(1);
PRINT(T,4,0);
SPACE(5);
PRINT(JAY,0,4);
SPACE(3);
PRINT(CHART,0,4);
SPACE(3);
PRINT(DIFF,0,4);
SPACE(2);
PRINT(SPEC1,0,4);       SPACE(2);
PRINT(RT2,4,0);  SPACE(2);
PRINT(SPEC2,0,4);
'END';
M:=M+1;
'IF' (M=1) < ND 'THEN' 'GOTO' L1;
NEWLINE(1);
'END'
```

2. PROGRAMME FOR THE CALCULATION OF VISCOELASTIC FUNCTIONS FROM DYNAMIC RAW DATA

```
'BEGIN' 'COMMENT' SCHWARZL INTERCONVERSION TRANSIENT TO DYNAMIC MSK ;
'REAL' SUM,JO,ETA,JP,JDP,CONS,GP,GDP,EP,EDP,TANA,T;
'INTEGER' M,N,I,ND,K,TSTART,TFIN,TINT,TIME;
'ARRAY' J[1:5],TAU[1:5],A[1:11],B[1:11],JAY[1:14];
M:=1;
ND:=READ;
'FOR'I:=1 'STEP' 1 'UNTIL' 11 'DO' 'BEGIN'
A[I]:=READ;
'END';
'FOR'I:=1 'STEP' 1 'UNTIL' 11 'DO' 'BEGIN'
B[I]:=READ;
'END';
L1:ETA:=READ;
JO:=READ;
N:=READ;
TSTART:=READ;
TFIN:=READ;
TINT:=READ;
'FOR'I:=1 'STEP' 1 'UNTIL' N'DO' 'BEGIN'
J[I]:=READ;
TAU[I]:=READ;
'END';
NEWLINE(1);
WRITETEXT('('SCHWARZL%INTERCONVERSION%FOR%CREEP%DATA%SET%NO%%%')');
PRINT(M,2,0);
NEWLINE(2);
WRITETEXT('('ETA'('18S')'JO'('11S')'N'('11S')'TSTART'('5S')'TFIN'('10S
                                                    'TINT'('5S')'  ')');
NEWLINE(1);
PRINT(ETA,0,4); SPACE(3);
PRINT(JO,0,4);  SPACE(3);
PRINT(N,2,0);   SPACE(4);
PRINT(TSTART,5,0);  SPACE(6);
PRINT(TFIN,5,0);  SPACE(4);
PRINT(TINT,5,0);  SPACE(4);
NEWLINE(2);
WRITETEXT('('A[I]'('16S')'B[I]'('12S')'  ')');
NEWLINE(1);
'FOR'I:=1 'STEP' 1 'UNTIL' 11 'DO' 'BEGIN'
PRINT(A[I],0,6);  SPACE(4);
PRINT(B[I],0,6);  SPACE(4);
NEWLINE(1);
'END';
NEWLINE(2);
WRITETEXT('('J[I]'('14S')'TAU[I]'('10S')'  ')');
NEWLINE(1);
'FOR'I:=1 'STEP' 1 'UNTIL' N 'DO' 'BEGIN'
PRINT(J[I],0,4);  SPACE(4);
PRINT(TAU[I],0,4);  SPACE(4);
NEWLINE(1);
'END';
```

```
NEWLINE(2);
WRITETEXT('('TIME'('5S')'JP'('10S')'GP'('12S')'EP'('12S')'
     JDP'('11S')'GDP'('11S')'EDP'('10S')'TANA'('8S')'  ')');
NEWLINE(1);
'FOR' TIME:=TSTART 'STEP' TINT 'UNTIL' TFIN 'DO' 'BEGIN'
T:=32*TIME;
'FOR' K:=1 'STEP'  1 'UNTIL' 14 'DO' 'BEGIN'
SUM:=JO+T/ETA;
'FOR' I:=1 'STEP' 1 'UNTIL' N 'DO' 'BEGIN'
SUM:=SUM+J[I]*(1.0-EXP(-T/TAU[I]));
'END';
JAY[K]:=SUM;
T:=T*0.5;
'END';
JP:=0;
JDP:=0;
'FOR'I:=1'STEP'1'UNTIL'11'DO''BEGIN'
JDP:=JDP+B[I]*JAY[I+5];
JP:=JP+A[I]*JAY[I];
'END';
CONS:=JP↑2+JDP↑2;
GP:=JP/CONS;
GDP:=JDP/CONS;
EP:=GDP*TIME;
EDP:=GP*TIME;
TANA:=GDP/GP;
NEWLINE(1);
PRINT(TIME,2,0);
PRINT(JP,0,4);
PRINT(GP,0,4);
PRINT(EP,0,4);
PRINT(JDP,0,4);
PRINT(GDP,0,4);
PRINT(EDP,0,4);
PRINT(TANA,0,4);
NEWLINE(1);
'END';
M:=M+1;
'IF' (M=1) <ND 'THEN' 'GOTO' L1;
NEWLINE(1);
'END'
```

3. PROGRAMME FOR INTERCONVERSION OF CREEP DATA TO DYNAMIC DATA

```
'BEGIN' 'COMMENT' PARALLEL PLATES IN OSCILLATION RHEOGONIOMETER MSK;
'REAL' GAP,RAD,TORS,RES,DENS,U,G,Z,A,B,C,D,F;
'INTEGER' N,M,I;
'ARRAY' FREQ,X,AMP,PHASE,E,GO,GDP,JP,JDP,DPE,TANA[1:100];
M:=1;
L1:RES:=READ; 'COMMENT' RESONANT FERQUENCY(HERTZ);
'IF' RES>3000 'THEN' 'GOTO' L10;
RES:=1/(RES*RES);
GAP:=READ; 'COMMENT' GAP WIDTH(CM);
RAD:=READ; 'COMMENT' PLATE RADIUM (CM);
DENS:=READ; 'COMMENT' FLUID DENSITY;
TORS:=READ; 'COMMENT' TORSION BAR CONSTANT (DYNE CM PER RAD);
U:=TORS/(61.84*DENS*RAD*RAD*RAD*RAD*GAP);
N:=READ; 'COMMENT' NUMBER OF RESULTS;
'FOR' I:=1 'STEP' 1 'UNTIL' N 'DO' 'BEGIN'
FREQ[I]:=READ; 'COMMENT' TEST FREQUENCY;
G:=FREQ[I];
G:=1/(G*G);
G:=G-RES;
X[I]:=G*U;
AMP[I]:=READ; 'COMMENT' AMPLITUDE RATIO;
PHASE[I]:=READ; 'COMMENT' PHASE ANGLE IN DEGREES;
Z:=PHASE[I]*(3,14/180); 'COMMENT' PHASE ANGLE IN RADIANS;
A:=X[I]*GAP*GAP;
B:=AMP[I]*AMP[I]-2*AMP[I]*COS(Z)+1;
C:=2*3,14*FREQ[I];
D:=-C*DENS*A*AMP[I]*SIN(Z);
E[I]:=D/B;
D:=C*C*DENS*A*AMP[I]*( COS(Z)-AMP[I] );
GO[I]:=D/B;
DPE[I]:=GO[I]/FREQ[I];
GDP[I]:=E[I]*FREQ[I];
F:=(GO[I]*GO[I])+(GDP[I]*GDP[I]);
JP[I]:=GO[I]/F;
JDP[I]:= GDP[I]/F;
TANA[I]:=GDP[I]/GO[I];
'IF' I>1 'THEN' 'GOTO' L2;
NEWLINE(1);
WRITETEXT('('PARALLEL%PLATE%EXPERIMENT,CALCULATED%PARAMETERS%FOR%DAT
                                        SET%NO%     ')');
```

```
PRINT(M,2,0);
NEWLINE(2);
WRITETEXT('('FREQUENCY%%%%%STRESS%PAR%%%%%%EP%%%%%%%%%%GP%%%%%%%%%%
EDP%%%%%%%%%%GDP%%%%%%%%%%JP%%%%%%%%%%JDP%%%%%%%%%%TANA%    ')')
L2:NEWLINE(1);
PRINT(FREQ[I],0,4);
PRINT(X[I],0,4);
PRINT(E[I],0,4);
PRINT(GO[I],0,4);
PRINT(DPE[I],0,4);
PRINT(GDP[I],0,4);
PRINT(JP[I],0,4);
PRINT(JDP[I],0,4);
PRINT(TANA[I],0,4);
'END';
M:=M+1;
'GOTO' L1;
L10:NEWLINE(1);
'END'
```

REFERENCES

REFERENCES

1. Langenbucher, F. & Lange, B. (1969) Pharm. Acta. Helv., 45, 572.

2. Martin, A.N., Banker, G.S., Chun, A.H.C. (1964) In "Advances in Pharm. Sciences", Volume I, Chapter 1. Ed. by Bean, H.S., Beckett, A.H. & Carless, J.E., Academic Press, London.

3. Worthington, H.E.C. (1973) Acta Dermatovener (Stockholm) Suppl. 70, 53, 29.

4. Eros, I., et. al. (1970) Acta Pharm Hung., 40, 64.

5. Martin, A.N., Swarbrick, J., Cammarata, A., (1969) "Physical Pharmacy", Chapter 18. Lea & Febiger, Philadelphia.

6. Van Abbe, N.J. (1959) Pharm. J., pp 111.

7. Idson, B. (1971) J. Soc. Cosmet. Chem., 22, 615.

8. Van Abbe, N.J. (1969) "Pharmaceutical and Cosmetic Products for Topical Administration", pp 98, William Hinemann Medical Books Limited, London.

9. Skauen, D.M., et. al. (1949) J. Amer. Pharm. Assoc. (Sci). 38, 618.

10. Munzel, K. (1971) Pharm. Acta. Helv., 46, 513.

11. Higuchi, T. (1960) J. Soc. Cosmet. Chem., 11, 85.

12. Wurster, D.E. (1965) Amer. Perf. Cosmet., 80, 21.

13. Wagner, W.G. (1961) J. Pharm. Sci., 50, 379.

14. Gibaldi, M. "Introduction to Biopharmaceutics", pp 33. Lea & Febiger, Philadelphia.

15. Sherman, P. (1970) "Industrial Rheology", Chapter 1 & 5. Academic Press, London.

16. Larry, P. & Hymnimen, C.E. (1969) Drug Cosmet. Ind., 105, 40, 153.

17. Barr, M. (1962) J. Pharm. Sci., 51, 395.

18. Katz, M. & Poulsen, B. (1972) J. Soc. Cosmet. Chem., 23, 565.

19. Giroux, J. & Schrenzel, M. (1964) Pharm. Acta. Helv., 39, 615.

20. Brocades Limited (1972) Chem & Drug. p 762.

20(a). Arthur, M.B. (1975) Brocades Limited Personal Communication.

21. Nogami, H. & Hanamo, M. (1958) Chem. Pharm. Bull., 6, 249.

22. Wood, J.A., et. al. (1962) J. Pharm. Sci., 51, 668.

23. Khristov, K. (1964) Pharmazie, 19, 134.

24. Norn, M. (1964) Dan Tidsskr Farm, 38, 95.

25. Levy, G. & Jusko, W.J. (1965) J. Pharm. Sci., 54, 219.

26. Khristov, K. (1967) Pharmazie, 22, 251.

27. Khristov, K. & Draganova, L. (1967) Pharmazie, 22, 208.

28. Cid, E. (1968) Farmaco Pra, 23, 474.

29. Voigt, R. & Falk, G. (1968) Pharmazie, 23, 709.

30. Khristov, K., Gluzman M. & Levitskaya,I. (1969) Farmatsiya (Sofia), 19, 15.

31. Khristov, K. (1969) Farmacia (Romania), 17, 331.

32. Khristov, K. (1969) Farmatsiya (Sofia), 19, 1.

33. Block, L.H. & Lamy, P.P. (1969) Pharm. Acta. Helv., 44, 44.

34. Lamy, P.P. (1964) PhD Thesis - Philadelphia College of Pharmacy, Philadelphia, Pennsylvania.

35. Khristov, K., Gluzman, M., Todorova, P. & Daschevskaja, I. (1970) Pharmazie, 25, 344.

36. Baichwal, M.R. & Lohit, T. (1970) J. Pharm. Pharmac., 22, 427.

37. Popovicia, A. & Ionescu, M. (1970) Farmacia, 18, 545.

38. Short, M.P. & Rhodes, C.T. (1973) Pharmazie, 28/8, 509.

39. Whitworth, C.W. & Stephenson, R.E. (1971) J. Pharm. Sci., 60, 48.

40. Eros, I. & Kedvessy, G. (1972) Deutsche Apotheker-Zeitung, 112, 665.

41. Ritschel, W.A., et. al. (1974) Drug Res., 24, 907.

42. Whitworth, C.W. & Stephenson, R.E. (1975) Can. J. Pharm. Sci., 10, 89.

43. Barry, B.W. (1971) J. Soc. Cosmet. Chem., 22, 487.

44. Green, H. (1949) "Industrial Rheology and Rheological Structures", John Wiley & Sons Inc, New York.

45. Block, L.H. & Lamy, P.P. (1970) J. Soc. Cosmet. Chem., 21, 645.

46. Barry, B.W. (1974) In "Advances in Pharmaceutical Sciences", Vol. 4, Chapter 1. Ed. by Bean, H.S., Beckett, A.H. & Carless, I.E. Academic Press, London.

47. Barry, B.W. & Warburton, B. (1968) J. Soc. Cosmet. Chem., 19, 725.

48. Davis, S.S., et. al. (1968) J.Sci. Inst., Series 2, 1, 933.

49. McKennell, R. (1954) Proc. Int. Cong. Rheol., p 350 - 358. Ed. by Harrison, V.G.W. Butterworths, London.

50. McKennell, R. (1956) Anal. Chem., 28, 1710.

51. McKennell, R. (1960) "The Instrument Manual", 3rd Ed., p 284 - 328, United Trade Press, London.

52. Van Wazer, J.R., Lyons, J.W., Kim, K.Y. & Colwell, R.E. (1963) "Viscosity and Flow Measurement. A Laboratory Handbook of Rheology", Interscience, New York.

53. Grace, A.J. (1971) PhD Thesis, Portsmouth Polytechnic.

54. Hutton, J.F. (1963) Nature, 200, 646.

55. Davis, S.S., et. al. (1968) J. Pharm. Pharmac., 20, 157S.

56. Leaderman, H. (1958) In "Rheology, Theory and Applications", Vol II, pp 1 - 61, Ed. by Eirich, F.R., Academic Press, New York.

57. Ferry, J.D. (1970) "Viscoelastic Properties of Polymers", 2nd Ed. Chapters 1 - 4. John Wiley, New York.

58. Marvin, R.S. (1960) In "Viscoelasticity: Phenomenological Aspects", p 27 - 54, Ed. by Bergen, J.T. Academic Press, New York.

59. Reiner, M. (1975) "Selected Papers on Rheology", Elservier Scientific Publications, Amsterdam.

60. Alfrey, Jr., T.T. & Gurnee, E.F. (1956) In "Rheology, Theory and Applications", Vol I, Chapter 11, Ed. Eirich, F.R., Academic Press, New York.

61. Davis, S.S. (1970) Amer. Perf. Cosmet., 85, 45.

62. Warburton, B. & Barry, B.W. (1968) J. Pharm. Pharmac., 20, 255.

63. Davis, S.S. (1971) J. Pharm. Sci., 60, 1351.

64. Walters, K. (1968) "Basic Concepts and Formulae for the Rheogoniometer", Sangamo Controls Limited, Bognor Regis, England.

65. Poulsen, B.J. (1973) In "Drug Design", Vol. IV, Ed. by Ariens, E.J. Chapter 5. Academic Press, London.

66. The Pharmaceutical Journal October 27th, (1973) p 386.

67. The Pharmaceutical Journal May 11th, (1974) p 432.

68. Bylinsky, G. (1973) Fortune, June issue p 151.

69. Shaw, J., et. al. (1975) Paper presented at the British Pharmaceutical Conference, Norwich.

70. Stoughton, R.B. (1974) J. Invest. Derm., 63, 305.

71. Gaggi, R. & Del Mastro, S. (1972) Boll. Chim. Farm., 111, 434.

72. Beckett, A.H., et. al. (1972) J. Pharm. Pharmac., 24,

73. In "Guidelines for Biopharmaceutical Studies in Man", (1972) p 17. APhA Academy of Pharmaceutical Sciences, Washington, D.C.

74. Rothman, S. (1954) In "Physiology and Biochemistry of the Skin", p 27. University of Chicago Press, Chicago.

75. Hlynka, J.N., et. al. (1969) Can. J. Pharm. Sci., 4/4, 84.

76. Katz, M. & Poulsen, B.J. (1971) In "Handbuch der experimentellen Pharmakologie", Vol. 28. Ed. by Brodie, B.B. & Gillette, J.R. Part I Springer-Verlag, Berlin.

77. Katz, M. (1973) In "Drug Design", Vol. IV. Ed. by Ariens, E.J. Chapter 4. Academic Press, London.

78. Griesmer, R.D. (1960) J. Soc. Cosmet. Chem, 11, 79.

79. Kligman, A.M. (1964) In "The Epidermis" Ed. by Montagna, W. & Lobitz, W.C., Chapter 20. Academic Press, London.

80. Scheuplein, R.J. (1965) J. Invest. Derm., 45, 334.

81. Grasso, P. & Landsdown, A.B.G. (1972) J. Soc. Cosmet. Chem., 23, 481.

82. Marzulli, F.N. (1962) J. Invest. Derm., 39, 383.

83. Blank, I.H. & Scheuplein, R.J. (1964) In "Progress in Biological Sciences in relation to Dermatology", Vol. 2. Ed. by Rook, A. & Champion, R.H. p 245 - 261. Cambridge University Press, London.

84. McGreesh, A.H. (1965) Toxicol. Appl. Pharmacol., 7, 20.

85. Menczel, E. & Maibach, H.I. (1972) Acta Derm-Venereol., 52, 38.

86. Witter, V.H., et. al. (1951) J. Invest. Derm., 17, 311.

87. Mali, J.W.H. (1956) J. Invest. Derm., 27, 451.

88. Malkinson, F.D. (1964) In "The Epidermis", Ed. by Montagna, W. & Lobitz, W.C. Chapter 21. Academic Press, London.

89. Blank, I.H. (1964) J. Invest. Derm., 43, 415.

90. Scott, A. (1959) Brit. J. Derm., 71, 181.

91. Blank, I.H. (1953) J. Invest. Derm., 21, 259.

92. Treager, R.T. & Dirnhuber, P. (1962) J. Invest. Derm., 38, 375.

93. Idson, B. (1975) J. Pharm. Sci., 64, 901.

94. Feldmann, R.J. & Maibach, H.I. (1970) J. Invest. Derm., 54, 399.

95. Feiwal, M. (1969) Brit. J. Derm., 81, Suppl. 4, 113.

96. Vickers, C.F. (1966) In "Modern Trends in Dermatology", Vol. 3. Ed. by McKenna, R.B. Chapter 4. Butterworths, London.

97. Marzulli, F.N., et. al. (1969) Toxicol. Appl. Pharmacol., Suppl. 3, 76.

98. Wurster, D.E. & Kramer, S.F. (1961) J. Pharm. Sci., 50, 288.

99. Shelmire, J.B. (1960) Arch. Derm. Syph., 82, 24.

100. Fritsch, W.F. & Stoughton, R.B. (1963) J. Invest. Derm., 41, 307.

101. Stoughton, R.B. & Fritsch, W.F. (1964) Arch. Derm., 90, 512.

102. Cronin, E. & Stoughton, R.B. (1962) Brit. J. Derm., 74, 265.

103. Stoughton, R.B. (1965) Arch. Environ. Health, 11, 551.

104. Wildnauer, R.H., et. al. (1971) J. Invest. Derm., 56, 72.

105. Blank, I.H., et. al. (1967) J. Invest. Derm., 49, 582.

106. Arita, T., et. al. (1970) Chem. Pharm. Bull., 18, 1045.

107. Blank, I.H. (1964) In "The Evaluation of Therapeutic Agents and Cosmetics". Ed. by Sternberg, T.H. & Newcomer, V.D. Chapter 9. McGraw-Hill Book Co., New York.

108. Malkinson, F.D. (1964) ibid. Chapter 4.

109. Fredriksson, T. (1961) Acta Derm-Venereol., 41, 344.

110. Fredriksson, T. (1964) J. Invest. Derm., 42, 37.

111. Vickers, C.F.H. (1963) Arch. Derm., 88, 20.

112. Vickers, C.F.H. (1973) Trans. St. John's Hospital Derm. Soc., 59, 10.

113. Carr, R.D. & Tarnowski, W.M. (1966) Arch. Derm., 94, 639.

114. Scheuplein, R.J. & Ross, L.W. (1974) J. Invest. Derm., 62, 353.

115. Rothman, S. (1943) J. Lab. Clin. Med., 28, 1305.

116. McKenzie, A.W. (1972) Arch. Derm., 86, 611.

117. Katz, M. & Shaikh, Z. (1965) J. Pharm. Sci., 54, 591.

118. Idson, B. (1971) In "Topics in Medicinal Chemistry", Vol. 4. Ed. by Rabinowitz, J.L. & Myerson. R.M. p 181 - 233. Wiley, New York.

119. Blank, I.H. & Gould, E. (1959) J. Invest. Derm., 33, 327.

120. Treherne, J.E. (1956) J. Physiol. (London), 133, 171.

121. Stoughton, R.B., et. al. (1960) J. Invest. Derm., 35, 337.

122. Marzulli, F.M., et. al. (1965) J. Invest. Derm., 44, 339.

123. Scheuplein, R.J., et. al. (1969) J. Invest. Derm., 45, 334.

124. Feldmann, R.J. & Maibach, H.I. (1968) Proceed. Joint Conf. Cosmet. Sci., p 189. Toilet Goods Assn., Washington, D.C.

125. Christie, G.A. & Moore-Robinson, M. (1970) Brit. J. Derm., 82, Suppl. 6, 93.

126. Maibach, H.I. & Feldmann, R.J. (1969) J. Invest. Derm., 52, 382.

127. Skog, E. & Wahlberg, J.E. (1964) J. Invest. Derm., 43, 187.

128. Strakosch, E.A. & Clark, W.G. (1943) Amer. J. Med. Sci., 205, 518.

129. Macht, D.I. (1938) J. Amer. Med. Assn., 110, 409.

130. Schmid, G. (1937) Arch. Int. Pharmacodyn., 55, 318.

131. Treager, R.T. (1964) In "Progress in Biological Sciences in relation to Dermatology", Vol. 2. Ed. by Rook, A. & Champion, R.H. p 275. Cambridge University Press, London.

132. Barrett, C.W., et. al. (1965) Brit. J. Derm., 77, 576.

133. Haleblian, J. & McCrone, W. (1969) J. Pharm. Sci., 58, 911.

134. Sarkany, I. & Hadgraft, J.W. (1969) Brit. J. Derm., 81, 98.

135. Scheuplein, R.J. & Blank, I.H. (1971) Physiol. Review, 51/4, 702.

136. Wahlberg, J.E. & Skog, E. (1967) Acta Derm-Venereol., 47, 209.

137. Cortese, T.A. Jr. (1971) In "DMSO", Vol. I. Ed. by Jacob, S.E., Rosenbaum, E.E. & Wood, D.C. Chapter 13. Marcel Dekker, Inc., New York.

138. Reiss, F. (1966) Amer. J. Med. Sci., 252, 588.

139. Kligman, A.M. (1965) J. Amer. Med. Assn., 193, 796.

140. Stoughton, R.B. (1965) Arch.Derm., 91, 657.

141. Munro, D.D. (1969) Brit. J. Derm., 81, Suppl. 4, 92.

142. Sweeney, T.M., et. al. (1966) J. Invest. Derm., 46, 300.

143. Allenby, A.C., et. al. (1969) Brit. J. Derm., 81, Suppl. 4, 31.

144. Embery, G. & Dugard, P.H. (1969) ibid, 63.

145. Dugard, P.H. & Embery, G. (1969) ibid, 69.

146. Baker, H. (1968) J. Invest. Derm., 50, 283.

147. Tees, T.F.S. (1969) Brit, J. Derm., 81, Suppl. 4, 39.

148. Rammler, D.H. & Zaffaroni, A. (1967) Annls. N.Y. Acad. Sci., 141, Art 1, 13.

149. Vinson, L.J., et. al. (1965) Toxicol. Appl. Pharmac., 7, Suppl. 2, 7.

150. Montes, L.F., et. al. (1967) J. Invest. Derm., 48, 184.

151. Williams, D.I. (1969) Brit. J. Derm., 81, Suppl. 4, 74.

152. Elfbaum, S.G. & Laden,K. (1968) J. Soc. Cosmet. Chem., 19, 119, 163, 841.

153. Scheuplein, R.J. & Ross, L. (1970) J. Soc. Cosmet. Chem., 21, 853.

154. Barry, B.W. (1975) Paper presented at the British Pharmaceutical Conference, Norwich.

155. Bettley, F.R. (1965) Brit. J. Derm., 77, 98.

156. Sprott, W.E. (1965) Trans. St. John's Hospital Derm. Soc., 51, 186.

157. Koizumi, T. & Higuchi, W.I. (1968) J. Pharm. Sci., 57, 87.

158. Koizumi, T. & Higuchi, W.I. (1968) J. Pharm. Sci., 57, 93.

159. Coldman, M.F. et. al. (1969) J. Pharm. Sci., 58, 1098.

160. Barrer, R.M. (1951) "Diffusion In and Through Solids". Cambridge University Press, London.

161. Lueck, L.M. (1954) PhD Thesis, University of Wisconsin.

162. Jost (1952) In "Diffusion in Solids, Liquids, Gases". Academic Press Inc, New York.

163. Flynn, G.F. & Roseman, T.J. (1971) J. Pharm. Sci., 60, 1788.

164. Higuchi, W.I. (1962) J. Pharm. Sci., 51, 802.

165. Higuchi, T. (1961) J. Pharm. Sci., 50, 874.

166. Higuchi, W.I. & Higuchi, T. (1960) J. Pharm. Sci., 49, 598.

167. Ainsworth, M. (1960) J. Soc. Cosmet. Chem., 11, 69.

168. Gemmell, D.H.O. & Morrison, J.C. (1957) J. Pharm. Pharmac., 9, 641.

169. Stoughton, R.B. (1964) In "Progress in Biological Sciences in relation to Dermatology", Vol. 2. Ed. by Rook, A. & Champion, R.M. p 263 - 274. Cambridge University Press, London.

170. Blank, I.H. (1960) J. Soc. Cosmet. Chem., 11, 59.

171. Lockie, L.D. & Sprowls, J.B. (1949) J. Amer. Pharm. Assn. Sci. ed., 38, 222.

172. Patel, K.C., et. al. (1961) J. Pharm. Sci., 50, 300.

173. Schutz, E. (1957) Arch. Exp. Path. Pharmac., 232, 237.

174. Poulsen, B.J., et. al. (1968) J. Pharm. Sci., 57, 928.

175. Hadgraft, J.W. (1967) J. Mond. Pharm., 3, 76.

176. Aguiar, A.J. & Weiner, M.M. (1969) J. Pharm. Sci., 58, 210.

177. Garrett, E.R. & Chemburker, P.B. (1968) J. Pharm. Sci., 57, 944.

178. Scala, J., et. al. (1968) J. Invest. Derm., 50, 371.

179. Whitworth, C.W. & Becker, C.H. (1965) J. Pharm. Sci., 54, 569.

180. Olszewski, Z. & Kubis, A. (1969) Acta Polon. Pharm., 26, 440.

181. Nakano, M. & Patel, N.K. (1970) J. Pharm. Sci., 59, 985.

182. Roberts, M.S., et. al. (1974) Aus. J. Pharm. Sci., NS3, 81.

183. Wahlberg, J.E. (1965) Acta Derm-Venereol., 45, 397.

184. Mackee, G.M. (1944) J. Invest. Derm., 2 . 43.

185. McKenzie, A.W. & Stoughton, R.B. (1962) Arch. Derm., 86, 608.

186. Shelley, W.B. & Melton, F.M. (1949) J. Invest. Derm., 13, 61.

187. Brockmeyer, E. & Guth, E. (1955) J. Amer. Pharm. Assn., Sci. ed., 44, 706.

188. Gemmell, D.H.O. & Morrison, J.C. (1958) J. Pharm. Pharmac., 10, 167, 553.

189. Barry, B.W. & Woodford, R. (1974) Brit. J. Derm., 91, 323.

190. Barry, B.W. & Woodford, R. (1974) Curr. Therap. Res., 16, 338.

191. Barry, B.W. & Woodford, R. (1975) Brit. J. Derm., 93, 563.

192. Place, V.A., et. al. (1970) Arch. Derm. (Chicago), 101, 531.

193. Inman, P.M., et. al. (1956) Brit. Med. J., 2, 1202.

194. Blank, I.H. (1960) J. Occupat. Med., 2, 6.

195. "Extra Pharmacopoeia" Martindale (1967) 25th Ed. Edited by Todd, R.G. The Pharmaceutical Press, London.

196. Marcus, A. (1956) Drug Cosmet. Ind., 79, 456.

197. Meyer, E. (1950) "White Mineral Oil and Petrolatum". Chemical Publishing Co. Inc., Brooklyn, New York.

198. Mutimer, M.N., et. al. (1956) J. Amer. Pharm. Assn., Sci. Ed., 44, 101.

199. Gstirner, F. (1970) Ind. J. Pharm., 32, 73.

200. Barry, B.W. & Grace, A.J. (1971) J. Text. Studies, 2, 259.

201. Plastibase Trade mark registration (1955) No. 617, 115. U.S. Patents Office, Washington.

202. Plastibase Bulletin (1965) Pub. by E.R. Squibb & Sons, U.S.A.

203. Frohmader, S.H. & Archer, V.C. (1953) U.S. Patent 2, 627, 938.

204. Frohmader, S.H. & Shoemaker, M.J. (1953) U.S. Patent 2, 628, 187.

205. Shoemaker, M.J. (1953) U.S. Patent 2, 628, 205.

206. Jelene Trade mark registration (1955) No. 601, 549. U.S. Patents Office, Washington.

207. Schultz, K.E. & Kassem, M.A. (1963) Pharm. Acta. Helv., 38, 162.

208. Huttenrauch, R., et. al. (1972) Pharmazie, 27, 169.

209. Huttenrauch, R., et. al. (1972) Pharmazie, 27, 300.

210. Huttenrauch, R., et. al. (1973) Pharmazie, 28, 665.

211. Thau, P. & Fox, C. (1965) J. Soc. Cosmet. Chem., 16, 359.

212. Thau, P. & Fox, C. (1965) U.S. Patent 3, 215, 599.

213. Backer, A.L. (1973) Pharm. Week. Bl., 108, 969.

214. Foster, S., et. al. (1951) J. Amer. Pharm. Assn., Sci. Ed., 40, 123.

215. Schroeter, L.C. (1969) "Ingredient X", Chapter 2. Pergamon Press, New York.

216. Chun, A.H.C. (1956) M.S. Thesis, Purdue University.

217. Singiser, R.E. & Beal, H.M. (1958) J. Amer. Pharm. Assn., Sci. Ed., 47, 6.

218. Jones, E.R. & Lewicki, B. (1951) J. Amer. Pharm. Assn., Sci. Ed., 40, 509.

219. Schultz, K.E. & Kassem, M.A. (1963) Pharm. Acta. Helv., 38, 34.

220. Schultz, K.E. & Kassem, M.A. (1963) Pharm. Acta. Helv., 38, 86.

221. Davis, S.S. (1973) J. Texture Studies, 4, 15.

222. Mutimer, M.N., et. al. (1956) J. Amer. Pharm. Assn., Sci. Ed., 45, 212.

223. Huttenrauch, R., et. al. (1974) Pharmazie, 29, 192.

224. Leszczynska-Bakal, H., et. al. (1970) Diss. Pharm. Pharmac., 22, 55.

225. Jurgens, Jr., R.W. & Becker, C.H. (1974) J. Pharm. Sci., 63, 443.

226. Saeki, M. & Yasumori, S. (1972) Yakuzaigaku, 34, 182.

227. Saeki, M. & Yasumori, S. (1972) ibid, 32, 190.

228. Robinson, R.C.V. (1955) A.M.A. Arch. Derm., 72, 54.

229. Robinson, R.C.V. (1955) Bull. Sch. Med., Univ. Maryland, 40, 86.

230. Billups, N.F. & Sager, R.W. (1965) Amer. J. Pharm., 137, 57.

231. Kolstad, C.K. & Lee, C.O. (1955) J. Amer. Pharm. Assn., Sci. Ed., 44, 5.

232. Taub, A., et. al. (1954) J. Amer. Pharm. Assn., Sci. Ed., 43, 178.

233. Billups, N.F. & Patel, N.K. (1970) Amer. J. Pharm. Educ., 34, 190.

234. Golucki, Z. (1972) Diss. Pharm. Pharmac., 24, 407.

235. Grzesiczak, A. (1972) Acta. Polon. Pharm., 29, 181.

236. Ruggiero, J.S. & Skauen, D.M. (1962) J. Pharm. Sci., 51, 235.

237. Flesch, P., et. al. (1955) J. Invest. Derm., 25, 289.

238. Sheinaus, H., et. al. (1955) J. Amer. Pharm. Assn., Sci. Ed., 44, 483.

239. Pepler, A.F., et. al. (1971) Brit. J. Derm., 85, 171.

240. Blank, I.H. (1965) Ref. to in "Plastibase Bulletin". Published by E.R. Squibb & Sons, U.S.A.

241. Davis, S.S. (1973) Bull. Physio. Path. Resp., 9, 47.

242. Boardman, G. & Whitmore, R.L. (1961) Lab. Practice, November issue, p 782.

243. Glasstone, S., et. al. (1941) "Theory of Rate Processes," McGraw-Hill, New York.

244. Jobling, A. (1954) Proc. 2nd. Intern. Cong. Rheol., p 444. Ed. by Harrison, V.G.W., Butterworths Sci. Pub., London.

245. Bondi, A. (1951) "Physical Chemistry of Lubricating Oils," Reinhold Pub. Corp., New York.

246. Davis, S.S. (1969) J. Pharm. Sci., 58, 412.

247. Barry, B.W. & Grace, A.J. (1971) Rheol. Acta., 10, 113.

248. Glasstone, S. (1956) "Textbook of Physical Chemistry," p 449. McMillan Co., London.

249. Berneis, K. & Munzel, K. (1964) Pharm. Acta. Helv., 39, 88.

250. Barry, B.W. & Grace, A.J. (1970) J. Pharm. Pharmac., 22, 147S.

251. Davis, S.S. (1969) J. Sci. Inst., Series 2, 2, 102.

252. Barry, B.W. & Saunders, G.M. (1969) J. Pharm. Pharmac., 21, 607.

253. Dinsdale, A. & Moore, F. (1962) "Viscosity and Its Measurement," Chapter 3. Chapman & Hall, London.

254. Sherman, P. (1968) "Emulsion Science" Academic Press, London.

255. Inokuchi, K. (1955) Bull. Chem. Soc., 28, 453.

256. Davis, S.S. & Warburton, B. (1968) J. Pharm. Pharmac., 20, 836.

257. Alfrey, Jr., T.T. (1948) "Mechanical Behaviour of High Polymers" Interscience, New York.

258. Schwarzl, F. (1951) Physica, 17, 830.

259. Schwarzl, F. & Staverman, A.J. (1952) Physica, 18, 791.

260. Schwarzl, F. & Staverman, A.J. (1953) Appl. Sci. Res., A4, 127.

261. Williams, M.L. & Ferry, J.D. (1953) J. Polym. Sci., 11, 169.

262. Sherman, P. (1968) Paper presented at the 5th International Congress on Rheology, Kyoto, Japan.

263. Barry, B.W. & Grace, A.J. (1971) J. Pharm. Sci., 60, 815.

264. Barry, B.W. & Grace, A.J. (1971) J. Pharm. Sci., 60, 1198.

265. Barry, B.W. & Eccleston, G.M. (1973) J. Text. Studies, 4, 53.

266. Marriott, C., et. al. (1973) J. Physics E, Scientific Instr., 6, 200.

267. Kato, Y. & Saito, T. (1967) Arch. Pract. Pharm., 27, 127.

268. Haye, K. (1974) Personal Communication.

269. Moore, R.S. & Matsuoka, S. (1964) J. Poly. Sci., Part C, 5, 163.

270. Takayanagi, M., et. al. (1960) J. Poly. Sci., 46, 531.

271. Huseby, T.W. & Matsuoka, S. (1967) Mater. Sci. Eng., 1, 321.

272. Van Den Tempel, M. (1968) Discussion contributed to Brit. Soc. Rheol. S.C.I. Meeting on "Rheology and Texture of Foodstuffs". S.C.I. Monograph 27. p 263.

273. Haighton, A.J. (1959) J. Amer. Oil Chem. Soc., 36, 345.

274. Warburton, B. & Davis, S.S. (1969) Rheol. Acta., 8, 205.

275. Watson, J.D. (1969) Rheol. Acta., 8, 201.

276. "Frequency response analysis techniques for materials testing". Printed by Solatron Electronic Group Ltd., Farnborough, England.

277. Bogie, K. & Harris, J. (1966) Rheol. Acta., 5, 212.

278. Davis, S.S. (1972) Rheol. Acta., 11, 199.

279. Instrument Manual for the Weissenberg Rheogoniometer.

280. Hutton, J.F. (1973) Personal Communication.

281. Harris, J. & Wilkinson, W.L. (1969) Bull. Brit. Soc. Rheol., 1, 1.

282. Schwarzl, F.R. (1969) Rheol. Acta., 8, 6.

283. Ninomiya, K. & Ferry, J.D. (1959) J. Coll. Sci., 14, 36.

284. Schwarzl, F.R. (1969) Lecture presented at the 4th Micro-Symposium on Macromolecules, Prague.

285. Jones, T.E.R. & Walters, K. (1971) Rheol. Acta., 10, 365.

286. Davis, S.S. (1971) J. Pharm. Sci., 60, 1351.

287. "Alkathene" brand of polyethylene (1964) I.C.I. Publication. Welwyn Garden City, England.

288. Eccleston, G.M., et. al. (1973) J. Pharm. Sci., 62, 1954.

289. Komatsu, H. & Sherman, P. (1974) J. Text. Studies, 5, 97.

290. Scott Blair, G.W., & Burnett, J. (1957) Lab Practice, 6, 570.

291. Scott Blair, G.W. (1959) Brit. J. Appl. Phys., 10, 15, 97.

292. Boylan, J.C. (1966) J. Pharm. Sci., 55, 710.

293. Boylan, J.C. (1967) J. Pharm. Sci., 56, 1164.

294. Barry, B.W. (1969) J. Pharm. Pharmac., 21, 533.

295. Davis, S.S. (1969) J. Pharm. Sci., 58, 418.

296. Van Ooteghem, M. (1967) J. Pharm. elg., 22, 147.

297. Nelson, W.L. & Stewart, L.D. (1949) Ind. Eng. Chem., 41, 2231.

298. Kostenbauder, H.B. & Martin, A.M. (1954) J. Amer. Pharm. Assn., Sci. Ed., 43, 401.

299. Bernis, K., et. al. (1964) Pharm. Acta. Helv., 39, 604.

300. Barry, B.W., et. al. (1969) J. Pharm. Pharmac., 21, 397.

301. Einstein, A. (1906) Ann. Physik, 4/19, 289. From "Emulsions, Theory and Practice" by Becher, P. (1966) 2nd Ed. Reinhold Pub. Corp., New York.

302. Langner, H-J. & Ketelhohn, K. (1974) Drugs made in Germany, 17, 80.

303. Ruetz, H. (1974) Drugs made in Germany, 17, 90.

304. Hangay, G.Y., et. al. (1966) Conference on some aspects of physical chemistry. Vol. II, Chapter 3. Budapest.

305. Gunn, C. & Carter, S.J. (1967) "Dispensing for Pharmaceutical Students." Chapter 28. Pitman Medical Publishing Co. Ltd., London.

306. A.B.P.I. Report (1960) Report of a working party established by the Association of British Pharmaceutical Industry and others on the use of gamma radiation sources for sterilisation of pharmaceutical products. A.B.P.I., Tavistock Square, London, WC1.

307. Huttenrauch, R. & Keiner, I. (1974) Pharmazie, 29, 421.

308. Huttenrauch, R., et. al. (1974) Pharmazie, 29, 32.

309. Brydson, J.A. (1969) "Plastics Materials". Ed. by Dawson. Chapter 7. Iliffe Books Limited, London.

310. Charlesby, A. (1960) "Atomic Radiation and Polymers." Pergamon Press, London.

311. Brown, E.W. & Scott, W.O. (1934) J. Pharmacol. & Exper. Therap., 50, 32.

312. Brown, E.W. & Scott, W.O. (1934) ibid, 50, 373.

313. Gross, M. & Greenberg, L.A. (1948) "The Salicylates. A Critical Bibliographic Review". Interscience, New York.

314. Smith, M.J.H. & Smith, P.K. (1966) "The Salicylates. A Critical Bibliographic Review". Interscience, New York.

315. "British Pharmacopoeia" (1968) The Pharmaceutical Press, London.

316. Shinkai, H. (1969) Yakugaku Zasshi, 89, 365, 1283, 1700.

317. Coldman, M.F., et. al. (1971) Brit. J. Derm., 85, 457.

318. Wood, J.A. & Pawlovich, N.L. (1968) Can. J. Pharm. Sci., 3, 1.

319. Ayres, J.W. & Laskar, P.A. (1974) J. Pharm. Sci., 63, 1402.

320. Garrett, E.R. & Chemburkar, P.B. (1968) J. Pharm. Sci., 57, 949.

321. Flynn, G.L. & Smith, E.W. (1971) J. Pharm. Sci., 60, 1713.

322. Flynn, G.L. & Yalkowsky, S.H. (1972) ibid., 61, 838.

323. Lovering, E.G. & Black, D.B. (1973) ibid., 62, 602.

324. Stolar, M.E. et. al. (1960) J. Amer. Pharm. Assoc., Sci. Ed., 49, 144.

325. Most, C.F. (1970) J. Appl. Polymer. Sci., 14, 1019.

326. Spang-Brunner, B.H. & Speiser, P.P. (1976) J. Pharm. Pharmac., 28, 23.

327. Washitake, M. et. al. (1975) J. Pharm. Sci., 64, 397.

328. Whitworth, C.W. & Asker, A.F. (1974) J. Pharm. Sci., 63, 1618.

329. Hersey, J.A. & Cook, P.C. (1974) J. Pharm. Pharmac., 26, 126.

330. Chowhan, Z.T. & Pritchard, R. (1975) J. Pharm. Sci., 64, 754.

331. Bottari, F. (1974) J. Pharm. Sci., 63, 1779.

332. Washitake, M. et. al. (1972) Chem. Pharm. Bull., 20, 2429.

333. Hylnka, J.N. et al. (1969) Can. J. of Pharm. Sci., 4, 92.

334. Bagatell, F.K. et. al. (1974) Curr. Therap. Res., 16, 748.

335. Portnoy, B. (1965) Brit. J. Derm., 77, 579.

336. Whitworth, C.W. & Becker, C.M. (1965) J. Pharm. Sci., 54, 569.

337. Whitworth, C.W. (1968) ibid., 57, 1540.

338. "Encyclopedia of Chemical Technology" (1963) Vol. 6 & 17. Interscience, New York.

339. Florence, A.T. et. al. (1972) APLA Academy of Pharm. Sci., 2, 238.

340. Florence, A.T. et. al. (1973) J. Pharm. Pharmac., 25, 779.

341. Farng, K.F. & Nelson, K.G. (1973) J. Pharm. Sci., 62, 1435.

342. Sutherland, W. (1905) Phil. Mag., 9, 781.

343. Stokes, G.G. (1903) Mathematical and Physical Papers, 3, 1, 55. Cambridge University Press, London.

344. Lamm, O. (1938) Trans. Faraday Soc., 34, 1152.

345. Gierer, A. & Wirtz, K. (1953) Z. Naturf., 8a, 532.

346. Hiss, T.G. & Cussler, E.L. (1973) AICLE Journal, 19, 698.

347. Mackie, J.S. & Meares, P. (1955) Proc. Roy. Soc., Ser. C, 232, 498.

348. Wang, J.H. (1954) J. Amer. Chem. Soc., 76, 4755.

349. Brown, W. & Chitumbo, K. (1975) J. Chem. Soc., Faraday Transactions I, 71, 12.

350. Kumins, C.A. et. al. (1957) J. Phys. Chem., 61, 1290.

351. Stannett, V.T. & Williams, J.L. (1965) J. Polymer. Sci., C, 1965, 10, 45.

352. Tikhomirov, B.P. et. al. (1968) Makromol. Chem., 118, 177.

353. Amin, M. (1967) PhD Thesis, University of Wisconsin.

354. Moncorps, C. (1929) Arch. Expt. Path. & Pharmacol., 141, 50, 87.

355. Strakosch, E.A. (1943) Arch. Derm. Syph., 47, 16.

356. Cotty, V.F. et. al. (1960) J. Soc. Cosmet. Chem., 11, 97.

357. Taylor, J.R. & Halprin, K.M. (1975) Arch. Derm., 111, 740.

358. Gans, O. (1925) "Histologie der Hautkrankheiten", Vol. 1, Julius Springer, Berlin.

359. Latvshkina, N.V. (1971) Vestn. Dermatol. Ven., 45, 54.

360. Polano, M.K. et. al. (1950) Dermatologica, 101, 69.

361. Kligman, A.M. & Wooding, W.M. (1967) J. Invest. Derm., 49, 78.

362. Smith, P.K. (1953) J. Pharm. Pharmac., 5, 81.

363. Chiou, W.L. & Melukwe, I.O. (1974) J. Pharm. Sci., 63, 630.

364. Trinder, D. (1954) Biochem. J., 57, 301.

365. Levy, G. & Hollister, L.E. (1964) N.Y. State Med. J., 64, 3002.

366. MacPherson, C.R. et. al. (1955) Brit. J. Pharmac., 10, 484.

367. Gutman, A.B. et. al. (1955) J. Clin. Invest., 34, 711.

368. Levy, G. & Leonards, J.R. (1911) J.A.M.A., 217, 81.

369. Elliott, J.S. et. al. (1959) J. Urol., 81, 339.

370. Smith, P.K. et. al. (1946) J. Pharmac., 87, 237.

371. Wilkinson, G.R. (1966) PhD Thesis, University of London.

372. Nelson, E. & Levy, G. (1963) Nature, 197, 1269.

373. Parrott, E.L. (1971) J. Pharm. Sci., 60, 867.

AN INVESTIGATION OF THE INFLUENCE OF RHEOLOGICAL FACTORS ON THE RELEASE OF DRUGS FROM PHARMACEUTICAL SEMISOLIDS

by

MADHUSUDAN SAVCHAND KHANDERIA

A Thesis submitted for the Degree of Doctor of Philosophy

in the Department of Pharmacy of

The University of Aston in Birmingham

CORRIGENDA FOR SECTION ON REFERENCES

Reference No	Substitute
4.	Eros, I., Mihaly, K. & Gyorgy, K. (1970) Acta Pharm Hung., 40, 64.
9.	Skauen, D.M., Cyr, G.N., Christian, J.E. & Lee, C.O. (1949) J. Amer. Pharm. Assn., Sci. Ed., 38, 618.
22.	Wood, J.A., Wait Rising, L. & Hall, N.A. (1962) J. Pharm. Sci., 51, 668.
41.	Ritschel, W.A., Siegel, E.G. & Ring, P.E. (1974) Drug Res., 24, 907.
48.	Davis, S.S., Deer, T.J. & Warburton, B. (1968) J. Sci. Inst., Series 2, 1, 933.
55.	Davis, S.S., Shotton, E. & Warburton, B. (1968) J. Pharm. Pharmac., 20, 157S.
69.	Shaw, J.E., Chandrasekaran, S.K. & Taskovich, L. (1975) Paper presented at the British Pharmaceutical Conference, Norwich.
72.	Beckett, A.H., Gorrod, J.W. & Taylor, D.C. (1972) J. Pharm. Pharmac., 24.
75.	Hlynka, J.N., Anderson, A.J. & Riedel, B.E. (1969) Can. J. Pharm. Sci., 4, 84.

Reference No	Substitute
86.	Witten, V.H., Ross, M.S., Oshry, E. & Hyman (1951) J. Invest. Derm., 17, 311.
97.	Marzulli, F.N., Brown, D.W.C. & Maibach, H.I. (1969) Toxicol. Appl. Pharmacol., Suppl. 3, 76.
104.	Wildnauer, R.H., Bothwell, J.W. & Douglass, A.B. (1971) J. Invest. Derm., 56, 72.
105.	Blank, I.H., Scheuplein, R.J. & MacFarlane, D.J. (1967) J. Invest. Derm., 49, 582.
106.	Arita, T., Hori, R., Anmo, T., Washitake, M., Akatsu, M. & Yajima, T. (1970) Chem. Pharm. Bull., 18, 1045.
121.	Stoughton, R.B., Clendenning, W.B. & Kruse, D. (1960) J. Invest. Derm., 35, 337.
122.	Marzulli, F.N., Callahan, J.F. & Brown, D.W.C. (1965) J. Invest. Derm., 44, 339.
123.	Scheuplein, R.J. Blank, I.H., Brauner, G.J. & MacFarlane, D.J. (1969) J. Invest. Derm., 52, 63.
132.	Barrett, C.W., Hadgraft, J.W., Caron, G.A. & Sarkany, I. (1965) Brit. J. Derm., 77, 576.
142.	Sweeney, T.M., Downes, A.H. & Matoltsy, A.G. (1966) J. Invest. Derm., 46, 300.
143.	Allenby, A.C., Creasey, N.H., Edgington, J.A.G., Fletcher, J.A. & Schoek, C. (1969) Brit. J. Derm., 81, Suppl. 4., 47.
149.	Vinson, J.L., Singer, E.J., Koehler, W.R., Lehman, M.D. & Masurat, T. (1965) Toxicol. Appl. Pharmacol., 7, Suppl. 2, 7.
150.	Montes, L.F., Day, J.L., Wand, C.J. & Kennedy, L. (1967) J. Invest. Derm., 48, 184.
159.	Coldman, M.F., Poulsen, B.J. & Higuchi, T. (1969) J. Pharm. Sci., 58, 1098.
172.	Patel, K.C., Banker, G.S. & DeKay, H.G. (1961) J. Pharm. Sci., 50, 300.
174.	Poulsen, B.J., Young, E., Coquilla, V. & Katz, M. (1968) J. Pharm. Sci., 57, 928.
178.	Scala, J. McOsker, D.E. & Reller, H.H. (1968) J. Invest. Derm., 50, 371.

Reference No	Substitute
182.	Roberts, M.S., Shorey, C.D., Arnold, R. & Anderson, R.A. (1974) Aus. J. Pharm. Sci., NS3, 81.
192.	Place, V.A., Velazquez, J.G., Burdick, K.H. (1970) Arch. Derm., (Chicago), 101, 531.
193.	Inman, P.M., Gordon, B. & Trinder, E. (1956) Brit. Med. J., 2, 1202.
198.	Mutimer, M.N., Riffkin, C., Hill, J.A. & Cyr, G.N. (1956) J. Amer. Pharm. Assn., Sci. Ed., 44, 101.
208.	Huttenrauch, R., Suss, W. & Schmeiss, U. (1972) Pharmazie, 27, 169.
209.	Huttenrauch, R., Suss, W. & Schmeiss, U. (1972) Pharmazie, 27, 300.
210.	Huttenrauch, R., Suss, W. & Schmeiss, U. (1973) Pharmazie, 28, 665.
214.	Foster, S., Wurster, D.E., Higuchi, T. & Busse, L.W. (1951) J. Amer. Pharm. Assn., Sci. Ed., 40, 123.
222.	Mutimer, M.N., Riffkin, C., Hill, J.A., Glickman, M.E. & Cyr, G.N. (1956) J. Amer. Pharm. Assn., Sci. Ed., 45, 212.
223.	Huttenrauch, R., Suss, W. & Schmeiss, U. (1974) Pharmazie, 29, 192.
224.	Leszczynska-Bakal, H., Surowiecki, J. & Elsner, Z. (1970) Diss. Pharm. Pharmac., 22, 55.
232.	Taub, A., Hart, F. & Kassimir, S. (1954) J. Amer. Pharm. Assn., Sci. Ed., 43, 178.
237.	Flesch, P., Satanove, A. & Brown, C.S. (1955) J. Invest. Derm., 25, 289.
238.	Sheinaus, H., Christian, J.E. & Sperandio, G.J. (1955) J. Amer. Pharm. Assn., Sci. Ed., 44, 483.
239.	Pepler, A.F., Woodford, R. & Morrison, J.C. (1971) Brit. J. Derm., 85, 171.
243.	Glasstone, S., Laidler, K.J. & Eyring, H. (1941) "Theory of Rate Processes" McGraw Hill, New York.
266.	Marriott, C., Irons, L.I. & Harris, E.R. (1973) J. Physics E., Sci. Inst., 6, 200.
270.	Takayanagi, M., Anamaki, T., Yoshino, M. & Hoashi, H. (1960) J. Polymer Sci., 46, 531.

Reference No	Substitute
288.	Eccleston, G.M., Barry, B.W. & Davis, S.S. (1973) J. Pharm. Sci., 62, 1954.
299.	Bernis, K., Munzel, K. & Waaler, T. (1964) Pharm. Acta. Helv., 39, 604.
300.	Barry, B.W., Grace, A.J. & Sherman, P. (1969) J. Pharm. Pharmac., 21, 369.
304.	Hangay, G., Hortobagyi, G., Haraszti, M., Czen, K., Kovach, G. & Zarandy, A. (1966) Conference on some aspects of physical chemistry. Vol II, Chapter 3, Budapest.
308.	Huttenrauch, R., Suss, W. & Schmeiss, U. (1974) Pharmazie, 29, 32.
317.	Coldman, M.F., Kalinovsky, T. & Poulsen, B.J. (1971) Brit. J. Derm., 85, 457.
324.	Stolar, M.E., Rossi, G.V. & Barr, M. (1960) J. Amer. Pharm. Assn., Sci. Ed., 49, 144.
327.	Washitake, M., Anmo, T., Tanaka, I., Arita, T. & Nakano, M. (1975) J. Pharm. Sci., 64, 397.
331.	Bottari, F., Colo, G.D., Nannipieri, E., Saettone, M.F. & Serafini, M.F. (1974) J. Pharm. Sci., 63, 1779.
332.	Washitake, M., Yajima, T., Anmo, T., Arita, T. & Hori, R. (1972) Chem. Pharm. Bull., 20, 2429.
333.	Hylnka, J.N., Anderson, A.J. & Riedel, B.E. (1969) Can. J. Pharm. Sci., 4, 92.
334.	Bagatell, F.K. & Augustine, M.E. (1974) Curr. Therap. Res., 16, 748.
339.	Florence, A.T., Elworthy, P.H. & Rahman, A. (1972) APHA Academy of Pharm. Sci., 2, 238.
340.	Florence, A.T., Elworthy, P.H. & Rahman, A. (1973) J. Pharm. Pharmac., 25, 779.
350.	Kumins, C.A., Rolle, C.J. & Roteman, J. (1957) J. Phys. Chem., 61, 1290.
352.	Tikhomirov, B.P., Hopfenberg, H.B., Stannett, V.T. & Williams, J.L. (1968) Makromol. Chem., 118, 177.
356.	Cotty, V.F., Skerpac, J., Ederma, H.M., Zurzola, F. & Kuna, M. (1960) J. Soc. Cosmet. Chem., 11, 97.

Reference No	Substitute
360.	Polano, M.K., Bonsel, J. & Van Der Meer, B.J. (1950) Dermatologica, 101, 69.
366.	MacPherson, C.R., Milne, M.D. & Evans, B.M. (1955) Brit. J. Pharmacol., 10, 484 - 489.
367.	Gutman, A.B., Yu, T.F. & Sirota, J.H. (1955) J. Clin. Invest., 34, 711.
369.	Elliott, J.S., Sharp, R.S. & Lewis, L. (1959) J. Urol., 81, 339.
370.	Smith, P.K., Gleason, H.L., Stoll, C.G. & Ogorzalek, S. (1946) J. Pharmac., 87, 237.